Advanced Invasive Neurophysiological Methods to Aid Decision Making in Paediatric Epilepsy Surgery

Birgit Pimpel
Developmental Neurosciences
Great Ormond Street Institute of Child Health
University College London

Supervisors: Prof Torsten Baldeweg
                      Dr Friederike Moeller
                      Prof J Helen Cross
                      Dr Ronit Pressler

August 2021 | This dissertation is submitted for the degree of
                           Doctor of Philosophy in Cognitive Neuroscience and
                           Neuropsychiatry

DECLARATION

I, Birgit Pimpel, confirm that the work presented in this thesis is my own. Where information has been derived from other sources, I confirm that this has been indicated in the thesis.

The work presented in this thesis reflects the contributions of a team of researchers including colleagues from the Developmental Neurosciences Programme, Great Ormond Street Institute of Child Health, the team of the Great Ormond Street Neurophysiology Department as well as close collaborators from the Jean Gotman Lab, Montreal Neurological Institute. My individual contribution for the scientific studies included in this thesis is outlined below.

The work presented in chapter 2 was completed whilst on a fellowship at the Montreal Neurological Institute. The data was collected by Jean Gotman and his team. I selected the data based on the inclusion and exclusion criteria, performed pre-processing of all data and data analyses. For data analyses, the Matlab scripts of Dr Shennan Weiss were used with his permission. I performed statistical analyses and produced all figures and graphical presentation of the data shown in this chapter. All results and interpretations were presented by myself and were developed based on discussions with colleagues and at regular supervision meetings.

The work presented in chapter 3 was done in close collaboration with the GOSH Neurophysiology Department, especially Dr Friederike Moeller. I was responsible for transfer, re-montaging and pre-processing of the EEG data from the GOSH neurophysiology system and clinical PAC system. I again used the scripts for analyses from Dr Shennan Weiss. Dr Richard Rosch, UCL Wellcome Trust Clinical PhD Fellow wrote a script to fix certain artefacts only observed in some of the included paediatric data and supported me throughout this project with his programming expertise. I performed all statistical analyses and produced all figures and graphical presentation of the data shown in these chapters. All results and interpretations were presented by myself and were developed based on discussions with colleagues and at regular supervision meetings.

The work presented in chapter's 4 and 5 was done in close collaboration with the GOSH Neurophysiology Department. Alan Worley supported me with his technical expertise throughout this project and built a SynAmps Signal Processing Unit used in this work to record verbal responses time-locked to the ongoing EEG data. I was responsible for developing and recording some of the language tasks. The Panda Games used in these studies were developed by Dr Louise Weiss-Croft and implemented with her permission. I was further

responsible for recruiting patients, conducting language testing, recording data, transferring, re-montaging and pre-processing EEG data from the GOSH neurophysiology system and clinical PAC system. I performed all statistical analyses and produced all the figures and graphical presentation of the data shown in these chapters. All results and interpretations were presented by myself and were developed based on discussions with colleagues and at regular supervision meetings.

Dr Birgit Pimpel

August 2021

ACKNOWLEDGEMENTS

IMPACT STATEMENT

The goal of this research is to further our understanding of invasive neurophysiological biomarkers and thus to improve pre-surgical planning for children and adolescents with drug-resistant epilepsy. With 1% of affected children and adolescents, epilepsy is one of the most common neurological diseases in the paediatric population. About a quarter of these patients become drug-resistant and continue to have regular seizures. Epilepsy and its recurrent seizures can have major implications, especially in the paediatric population, as the brain is still developing and in a vulnerable state.

The field of epilepsy surgery as one pillar of therapy is growing and pre-surgical methods to delineate resection margins are constantly advancing. There is increasing use of stereotactically implanted depth electrodes to capture the epileptic network—including the onset and propagation of the seizure in all planes of the intracranial space. However, resection of the presumed seizure onset does not always lead to seizure freedom or even a seizure improvement. In addition, eloquent functions like language are at risk of getting impaired during surgery.

This thesis studies a rare cohort of adult and paediatric patients with drug-resistant epilepsy who underwent stereo-EEG investigations for pre-surgical assessment. Using advanced invasive neurophysiological methods, it contributes to existing research in two key ways.

First, it investigates biomarkers of epileptogenicity, to improve accurate and automatic localization of the extent of the ictally involved brain areas. The aim is to support surgical decision-making. This work includes the first study to replicate research that demonstrated the superiority of a new neurophysiological biomarker. It will help inform future research of its methodology implementation. In addition, this work investigated further biomarkers of

epileptogenic tissue, which have proven reliable in previous studies. It provides new insights from a different patient cohort.

Second, findings presented in this thesis contribute to language localisation research. In addition to delineating pathological tissue, it is of great importance to localise eloquent areas for pre-surgical planning and to prevent post-surgical cognitive decline. This work includes the first study to investigate language areas involved in speech perception, comprehension and production using invasive neurophysiological measures—event-related potentials and frequency changes––in children and adolescents with stereo-EEG implantations. The findings contribute to an improvement in the use of magnetoencephalography measures for non-invasive language mapping.

Findings presented in this thesis have been disseminated within the wider scientific community through presentations at several national and international conferences and meetings. Ultimately, this line of research will help to delineate epileptic and eloquent brain areas in pre-surgical evaluation. It will thus contribute to improving post-surgical seizure and cognitive outcomes for epilepsy patients.

ABSTRACT

For patients with drug-resistant focal epilepsy, surgery is the most effective treatment to attain seizure freedom. Intracranial electroencephalogram investigations succeed in defining the seizure onset zone (SOZ) where non-invasive methods fail to identify a single seizure generator. However, resection of the SOZ does not always lead to a surgical benefit and, in addition, eloquent functions like language might be compromised. The aim of this thesis was to use advanced invasive neurophysiological methods to improve pre-surgical planning in two ways.

The first aim was to improve delineation of the pathological tissue, the SOZ using novel quantitative neurophysiological biomarkers: high gamma activity (80–150Hz) phase-locked to low frequency iEEG discharges (phase-locked high gamma, PLHG) and high frequency oscillations called fast ripples (FR, 250–500Hz). Resection of contacts containing these markers were recently reported to lead to an improved seizure outcome. The current work shows the first replication of the PLHG metric in a small adult pilot study and a larger paediatric cohort. Furthermore, I tested whether surgical removal of PLHG- and/or FR-generating brain areas resulted in better outcome compared to the current clinical SOZ delineation.

The second aim of this work was to aid delineation of eloquent language cortex. Invasive event-related potentials (iERP) and spectral changes in the beta and gamma frequency bands were used to determine cortical dynamics during speech perception and production across widespread brain regions. Furthermore, the relationship between these cortical dynamics and the relationship to electrical stimulation responses was explored.

For delineation of pathological tissue, the combination of FRs and SOZ proved to be a promising biomarker. Localising language cortex showed the highest

level of activity around the perisylvian brain regions with a significantly higher occurrence rate of iERPs compared to spectral changes. Concerning electrical stimulation mapping beta and high gamma frequency bands represented the most promising markers.

CONTENTS

LIST OF FIGURES

13

14

LIST OF TABLES

LIST OF ABBREVIATIONS

ADHD   Attention deficit hyperactivity disorder
AED   Antiepileptic drug
AF   Arcuate fascile
AMY   Amygdala
AUROC   Area under the receiver operating characteristics
BA   Broadmann area
BP   Bereitschaftspotential
BOLD   Blood-oxygen-level-dependent
CING   Cingulate gyrus
EC   Early component
ECFS   Extreme capsule fiber system
ECoG   Electrocorticography
EEG   Electroencephalogram
EMG   Electromyogram
ERD   Event-related desynchronization
ERP   Event-related potential
ERS   Event-related synchronisation
ESI   Electrical source imaging
EZ   Epileptogenic zone
FC   Frontal cortex
FCD   Focal cortical dysplasia
FFG   Fusiform gyrus
FIR   Finite impulse response
fMRI   Functional MRI
FOP   Frontal operculum
fpMP   Frontal peak of motor potential
FR   Fast ripple
FRO   FR/Resection overlap
GABA   Gamma-aminobutyric acid
GOF   Goodness of fit
HC   Hippocampal abnormality
HFA   High frequency activity
HFO   High frequency oscillation
HG   Heschl's gyrus
HIP   Hippocampus
Hz   Hertz
ICA   Independent component analysis
IED   Interictal epileptiform discharge
iEEG   Invasive electroencephalogram/intracranial EEG
iERP   Invasive event-related potential
IFG   Inferior frontal gyrus
IFOF   Inferior-fronto-occipital fascile
ILAE   International League Against Epilepsy

INS_A	Anterior insula
INS_P	Posterior insula
IPL	Inferior parietal lobule
IPSP	Inhibitory post-synaptic potential
ITG	Inferior temporal gyrus
ITS	Inferior temporal sulcus
MEG	Magnetoencephalography
MFG	Middle frontal gyrus
MMN	Mismatch negativity
MP	Motor potential
MRI	Magnet resonance imaging
MSI	MEG source imaging
MTG_A	Anterior medial temporal gyrus
MTG_P	Posterior medial temporal gyrus
NMDA	N-methyl-D-aspartate receptor
nTMS	Navigated transcranial magnetic stimulation
NPV	Negative predictive value
NREM	Non-rapid eye movement
OCC	Occipital lobe
OFC	Orbital frontal cortex
PAC	Phase amplitude coupling
PaC	Parietal cortex
PC	Primary component
PET	Positron emission tomography
PLHG	Phase-locked high gamma
PLV	Phase-locking value
PMC	Premotor cortex
PPV	Positive predictive value
postC	Postcentral gyrus
postC_2	Dorsal postcentral gyrus
preC	Precentral gyrus
preC_2	Dorsal precentral gyrus
PRP	PLHG/Resection overlap
PSO	PLHG/SOZ overlap
ROC	Receiver operating characteristics
RP	Readiness potential
SD	Standard deviation
SEEG	Stereotactic electroencephalogram
SFG	Superior frontal gyrus
SLF	Superior longitudinal fascile
SMG	Supramarginal gyrus
SNR	Signal to noise ratio
SOZ	Seizure onset zone
SPECT	Single photon emission computed tomography
SPL	Superior parietal lobule
SPO	SOZ/PLHG overlap

SRO	SOZ/Resection overlap
STG_A	Anterior superior temporal gyrus
STG_P	Posterior superior temporal gyrus
STS	Superior temporal sulcus
TC	Temporal cortex
TS	Tuberous sclerosis
OC	Occipital cortex
UF	Uncinate fascile
VEEG	Video EEG
VHFO	Very high frequency oscillations

I INTRODUCTION

1 An introduction to the pre-surgical evaluation of paediatric patients with refractory epilepsy

1.1 Paediatric Epilepsies: clinical overview

1.1.1 Definition & Prevalence

Epilepsy is a common neurological condition characterized by recurrent epileptic seizures. An epileptic seizure is defined as "a transient occurrence of signs and/or symptoms due to abnormal, excessive or synchronous neuronal activity in the brain" (R. S. Fisher et al., 2014). Over 65 million people worldwide are estimated to suffer from epilepsy (Ngugi, Bottomley, Kleinschmidt, Sander, & Newton, 2010), including about 1 in 220 children and adolescents in the UK (JEC, 2011). The International League Against Epilepsy (ILAE) consider epilepsy to be a disease of the brain defined by (i) at least two unprovoked seizures over 24 hours apart, (ii) one unprovoked seizure and an over 60% chance of further seizures in the next 10 years, or (iii) an epilepsy syndrome diagnosis (R. S. Fisher et al., 2014).

Seizure incidence is highest in infants and children with a second peak of onset in the elderly (Bowman, Dudek, & Spitz, 2012). There are many different types of seizures. Seizures can have a focal onset within networks restricted to one hemisphere, which can be localized to a discrete area or involving a wider network. The seizure onset can also be generalised, involving bilaterally distributed networks or it can be unknown (Berg et al., 2010; R. S. Fisher et al., 2017). Furthermore, a patient's awareness can be retained or impaired during a seizure and seizures can be accompanied by motor symptoms (R. S. Fisher et al., 2017).

ILAE recently updated their seizure classification (Figure 1), where seizures are classified according to their onset – "focal", "generalised" or "unknown". Focal onset seizures can be differentiated according to the presence or absence of

impaired awareness, whereas a generalised onset implies altered awareness from the start. If a seizure does not fall into another category or there is insufficient information, it is unclassified.

ILAE 2017 Classification of Seizure Types Expanded Version [1]

Focal Onset	Generalized Onset	Unknown Onset
Aware / **Impaired Awareness**	**Motor** tonic–clonic clonic tonic myoclonic myoclonic–tonic–clonic myoclonic–atonic atonic epileptic spasms	**Motor** tonic–clonic epileptic spasms **Nonmotor** behavior arrest
Motor Onset automatisms atonic [2] clonic epileptic spasms [2] hyperkinetic myoclonic tonic **Nonmotor Onset** autonomic behavior arrest cognitive emotional sensory	**Nonmotor (absence)** typical atypical myoclonic eyelid myoclonia	**Unclassified [3]**
focal to bilateral tonic–clonic		

Figure 1. ILAE classification of seizure types. [1]Definitions, other seizure types and descriptors are listed in the accompanying paper and glossary of terms; [2]Degree of awareness usually is not specified; [3]Due to inadequate information or inability to place in other categories. Adapted from (Fisher et al., 2017).

Similarly, epilepsies can be divided into "focal", "generalised", "combined generalised and focal" and unknown types. Epilepsy is not a single condition, but a diverse family of disorders and its cause can be genetic, structural, metabolic, immune, infectious or unknown (Scheffer et al., 2017).

1.1.2   Treatment

The goals of epilepsy treatment are to stop seizures from occurring or reduce seizure frequency and to minimise adverse effects (Tomson & Steinhoff, 2012). Furthermore, social and/or vocational rehabilitation and lifestyle adjustments, including sleep optimising, stress reduction and medication compliance is a crucial aspect of epilepsy management (Stafstrom & Carmant, 2015; Sung, Muller, Jones, & Chan, 2014).

The mainstay of treatment for most patients with epilepsy is antiepileptic drug (AED) therapy. AEDs aim to reduce excessive electrical activity targeting different mechanisms. The main groups of mechanisms include sodium and calcium channel blockers, GABA enhancers, drugs reducing neurotransmitter release, NMDA receptor blockers, and blockers of unique binding sites (Sills, 2013).

However, studies have shown that in about 25–30% patients fail to respond to antiepileptic drugs or other treatments and continue to have regular seizures (Dichter & Brodie, 1996; Picot, Baldy-Moulinier, Daurès, Dujols, & Crespel, 2008). Once two adequately chosen and tolerated AED regimes (monotherapy or combination) fail to lead to seizure freedom the term drug-resistant epilepsy is used (Kwan et al., 2010). In these cases, it needs to be decided whether to trial a new line of medication or to refer the patient for pre-surgical evaluation as in a select group of these patients with drug-resistant epilepsy the chances of becoming seizure-free with properly planned epilepsy surgery is high (Jerome Engel et al., 2012; Wiebe, Blume, Girvin, & Eliasziw, 2001).

Especially in the paediatric population as the brain is developing and in a vulnerable state epilepsy and its recurrent seizures can have major implications. Poorly controlled epilepsy is associated with memory impairment, learning disabilities, ADHD, behavioural problems and poor academic achievement (Berg, Zelko, Levy, & Testa, 2012; Cormack et al., 2007; Gascoigne et al., 2018; Hermann et al., 2007; Parkinson, 2002). To minimise progression of these

problems, early intervention is crucial as these problems can increase by longer duration of epilepsy, hence, recurrent seizures and AED therapy (Hermann et al., 2006; Ijff & Aldenkamp, 2013; Vingerhoets, 2006).

The chance of achieving seizure freedom by starting subsequent drug regimens after unsuccessful use of two AEDs has been shown to be less than 10% (Brodie & Kwan, 2002; Mohanraj & Brodie, 2006). Therefore, non-pharmacological approaches need to be considered in these drug-resistant children. Epilepsy surgery is an option in patients with focal onset epilepsy, where the brain area responsible for generating seizures can be removed which can be curative or palliative, leading to reduced seizure frequency and need for AEDs. Considering clinical, neurophysiological and imaging data early referral to surgical evaluation is key (J. H. Cross et al., 2006). Furthermore, delay from epilepsy onset to surgery needs to be considered as currently waiting time still exceeds 10 years on average (Baud et al., 2018). Post-operatively, seizure freedom can be achieved in 48–86% of cases, depending on the surgical procedure (D'Argenzio et al., 2012; Lettori et al., 2008; Pulsifer et al., 2004; Skirrow et al., 2011; Téllez-Zenteno, Ronquillo, Moien-Afshari, & Wiebe, 2010; Terra-Bustamante et al., 2007). In recent years it has been recognized that the gain of epilepsy surgery may not only be complete seizure freedom, but also improved cognitive outcome and social development, especially in children, resulting in an overall increase of quality of life (Ryvlin, Cross, & Rheims, 2014; Skirrow et al., 2011, 2015; Van Schooneveld & Braun, 2013).

1.1.3   Pre-surgical evaluation – the role of invasive EEG

Surgical treatment is a multidisciplinary effort, considering results from seizure semiology, neuropsychological, neurodevelopmental, neuro-psychiatric evaluation and noninvasive techniques including video-electroencephalography telemetry (VEEG), MRI, positron-emission tomography (PET) and magnetoencephalography (MEG). The goal of pre-surgical evaluation is to define the brain areas responsible for generating seizures and to determine

whether this area can be resected without compromising eloquent functions like language, memory or movement (Luders, 2008). When non-invasive methods fail to localize an epileptogenic focus, intracranial electroencephalographic (iEEG) investigations are used to identify the epileptogenic zone (Diehl and Luders, 2000). The epileptogenic zone (EZ) is a theoretical cortical area, which is essential for generating seizures and which is defined as "the minimum amount of cortex that must be resected (inactivated or completely disconnected) to produce seizure freedom (H. O. Lüders, Najm, Nair, Widdess-Walsh, & Bingman, 2006). This concept of the epileptogenic zone defined by Lüders and colleagues becomes meaningful only when considering the definition of the five cortical zones proposed for pre-surgical evaluation (Figure 2).

		Diagnstic tools
Irritative zone	Cortical area generating epileptiform activity, defined by interictal spikes and sharp waves	EEG, MEG, EEG-fMRI
Eloquent cortex	Brain area in which a defined clinical function is located, e.g. language, movement, or vision	Neurological & neuropsychological examination, fMRI
Seizure onset zone	Cortical area that initiates seizures	EEG, ictal SPECT, lesser degree fMRI & MEG
Symptomatogenic zone	Cortical area, once activated, produces inital ictal symptoms	Initial seizure symptoms
Epileptogenic lesion	Abnormal neuroradiological brain tissue that has a relation to the epilepsy	MRI

Figure 2. Cortical zones and diagnostic tools used for pre-surgical evaluation. Adapted from (Rosenow & Lüders, 2001)

These cortical zones as well as the tests to define each of them clearly overlap, which implicates that the resection of any single zone would not lead to a satisfactory postsurgical outcome. In addition, no single diagnostic test allows measurement of the epileptogenic zone.

Currently the identification of the seizure onset zone and interictal spikes are used to delineate epileptic tissue but still 30–40% of patients remain to have seizures after surgical resection (Spencer and Huh, 2008).

1.1.3.1   Delineating the seizure onset zone
Non-invasive methods

To pursue the route of pre-surgical evaluation the working hypothesis must be one of a focal onset of epilepsy. The definition of focal seizures changed over time. The most recent definition tried to incorporate all discussed aspects: focal seizures are defined as "originating within networks limited to one hemisphere. They may be discretely localised or more widely distributed. Focal seizures may originate in subcortical structures. For each seizure type, ictal onset is consistent from one seizure to another, with preferential propagation patterns that can involve the contralateral hemisphere. In some cases, however, there is more than one network, and more than one seizure type, but each individual seizure type has a consistent site of onset (Berg et al., 2010).

First, seizure semiology, the clinical presentation of the patient during a seizure, gives valuable information about the possible origin concerning lateralisation and localisation (H. J. Cross, 2016). For further investigation scalp EEG in combination with video-recording is pivotal. Surface EEG is a non-invasive neuroimaging technique that measures the electrical activity of the brain with electrodes placed on the scalp. The epileptic basis of recurring paroxysmal events can only be confirmed with VEEG. However, scalp EEG is spatially limited and differentiating the primary seizure focus from propagation often poses a challenge (Jayakar, Nordli, & Snead, 2016). In addition, functional brain imaging techniques focussing on ictal information aid delineation of the seizure

onset zone (SOZ). Ictal single photon emission computed tomography (ictal SPECT) for one is a nuclear radiology study that measures the blood flow functional changes in the brain during seizures in a routine clinical setting. Furthermore, functional MRI (fMRI) and the simultaneous scalp EEG and fMRI (EEG-fMRI) can also be used for imaging complex patterns of the blood-oxygen-level-dependent (BOLD) changes during a seizure. In addition to localising the irritative zone, Yamazoe and group (2019) showed that using EEG-fMRI and interictal epilpetiform discharges (IED) aid localisation of the presumed SOZ, arguing that number of IEDs and a larger spatial extent of IEDs are more likely to locate the SOZ accurately. Similarly, MEG, which detects magnetic instead of electric fields produced by neuronal currents could be used for capturing ictal sources. However, these imaging tools are often impractical due to the low probability to record a seizure during their acquisition or due to patient movement during most types of seizures. Another tool for estimating the seizure source is electrical source imaging (ESI), which mainly uses interictal data though also ictal localisation by ESI is reported in a few cases. It seems to be imperative to apply ESI directly at ictal onset to avoid seizure propagation information and muscular artefacts (Koessler et al., 2010; Yang, Wilke, Brinkmann, Worrell, & He, 2011). Promising results were published by Pellegrino and colleagues showing that ictal MEG source imaging (MSI) combined with ictal ESI were concordant with clinical-SOZ in 81% of seizures, with MSI showing 90% compared to ESI showing 64% (2016). Overall, these additional imaging tools aid delineation of the epileptogenic zone rather than of the SOZ. Interictal MEG, fMRI or MSI/ESI results and their combination with VEEG information led to an increased localisation accuracy of focal epileptic activities (Stefan & Trinka, 2017).

Invasive methods
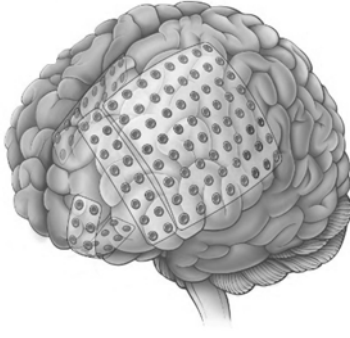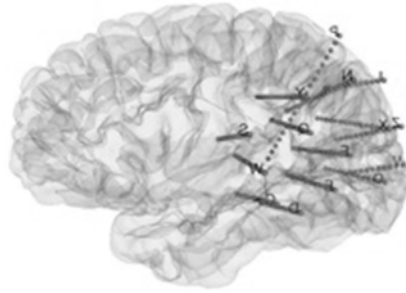
Following these non-invasive methods for SOZ localisation, next invasive methods are summarised. Intracranial EEG is the most direct way to record electrical activity from brain tissue. The obvious advantage over scalp EEG is its

direct recording of local field potentials from cortical tissue without distortion due to overlying media like cerebrospinal fluid, dura matter, cranium, muscle and skin. Hence, intracranial recordings are much less artefactual. Several methods are used to record iEEG depending on the patient characteristics and the expertise of the centre.

Extra-operative invasive recordings following surgical implantation of electrodes aim to gather ictal activity and activity from awake and alert periods and from sleep. Electrodes can either be placed on the surface of the brain or be implanted into the depth of the brain. Surface electrodes are called subdural electrodes. They are placed on brain regions where the epileptic focus is thought to reside and are left there for several days. They are arranged in grids and strips allowing sampling of a more extensive brain surface area. Furthermore, they permit delineation of the surface distribution of the SOZ. However, sampling of deep structures is not possible. Depth electrodes, however, can be inserted into the brain parenchyma or within lesional tissue to give information from deep structures such as hippocampus and amygdala. A complementary combination of subdural and depth electrodes is widely used.

Stereotactic EEG (SEEG) is a different method using stereotactically placed intracerebral electrodes, which aims to investigate all planes of the intracranial space. This is a method developed by Talairach and Bancaud (1973, 1974) that solely uses depth electrodes. Compared to the combined implantation method explained above, where depth electrodes are complementary and are implanted into a few specific targets, the SEEG method uses multiple electrodes. Electrode placement is different as it aims to capture network distribution involved in seizure generation and propagation (Cossu et al., 2006; Tassi, Jayakar, Pieper, & Kahane, 2016). Therefore, the selection of brain structures to be explored is tailored to each individual case. Hence, prior to implantation one or more hypotheses of SOZ location and pathways of seizure spread are formulated. Table 1 summarizes advantages and disadvantages of each technique.

30

Table 1. Advantages & disadvantages of subdural grids and strips versus SEEG (Podkorytova, Hoes, & Lega, 2016; Tassi et al., 2016).

	Subdural grid/strip	SEEG
Location	Subdural (on brain surface)	In brain tissue
Advantages	· Excellent cortical surface coverage · Accurate anatomic/functional mapping - for all ages · Generally well tolerated · Limitations can largely be overcome by concomitant depth electrode placement	· Minimally invasive approach, electrodes inserted through burr holes · Reaches deeper brain targets · Can be placed bilaterally · Improved mapping of functional networks · Lessened wound healing morbidity
Disadvantages	· More invasive – craniotomy · Samples only brain surface · Difficulty sampling interhemispheric targets · Higher rate of morbidity/ complication: infectious consequences, haemorrhage, cerebral oedema, if following previous surgery potential for adhesions and difficult dissection · Optimal contact over uneven cortical surfaces possible · Implantation challenging in children who have undergone prior surgery · Surgery has to be performed at the end of the intracranial monitoring	· Limited cortical surface coverage · Functional mapping restricted · Can be more difficult to perform in younger children due to technical reasons, i.e., thickness of the skull or the lower tolerance of long-term monitoring

Once electrodes are implanted the aim is to record interictal discharges and spontaneous seizures. Invasive EEG has a very high spatial resolution as the implanted electrodes can be close to or within the source which makes it a very

precise tool. However, only small areas of brain tissue can be sampled by each electrode.

Electrical Stimulation

To further define critical cortex electrical stimulation, another invasive method, is used. It is performed once spontaneous seizure data is recorded and is used to reproduce the patient's ictal clinical signs and EEG discharges. However, it has some limitations in particular in its application to children (Sinai et al., 2005). Electrical stimulation can induce discomfort or seizures and can lead to remote effects, which can be falsely localising. Electrical stimulation is a time- and resource-intensive procedure as many individual pairs of electrodes have to be tested sequentially.

1.1.3.2 Delineating eloquent cortex

In epilepsy patients, because of chronic pathological electrical activity and a possible reorganisation of functional anatomy to other areas, it is especially important to localise eloquent cortex prior to surgery (Marla J. Hamberger, 2007). The risk of producing new deficits post-surgery needs to be considered when planning surgery as it may affect the surgical approach and the patient's overall outcome.

In addition to defining the SOZ, electrical stimulation is the gold standard method to determine the relationship of the SOZ and the eloquent cortex (G a Ojemann, 1979; Sanai, Mirzadeh, & Berger, 2008). This so called functional mapping can result in the production of positive phenomena such as tonic or clonic movements and special sensations, or can inhibit function producing negative responses such as speech arrest or arrest of motor function (Tassi et al., 2016; Tuxhorn, 2010). It might predict which functions will be disturbed if the stimulated cortex were to be removed and hence, which areas should be spared during surgery. It requires a certain amount of cooperation, which is a limiting factor in some children with behavioural difficulties. Another shortcoming is the variation of methods used for iEEG between centres and therefore for electrical

stimulation of eloquent areas which makes comparison more difficult. Electrical stimulation when using subdural electrodes results in a two-dimensional map of areas, which were found positive/negative for language and motor function. Compared to that when using SEEG seizures are rather interpreted in neural networks; therefore, it is argued that because electrical stimulation is interrupting a network rather than a focal area, methodological factors like stimulation parameters and cognitive tasks used should be taken into account when interpreting results. When applying SEEG it seems important to evaluate the overlap of the epileptogenic network and the functional network (Trébuchon & Chauvel, 2016).

Another invasive method is Wada's test, also known as the intracarotid sodium amobarbital procedure, which is used to determine cerebral dominance of language and memory functions prior to neurosurgery (Wada & Rasmussen, 1960). Each hemisphere is selectively anesthetized to allow the function of the other hemisphere to be tested (Detre, 2004). In many hospitals Wada's test is partially replaced by non-invasive methods like fMRI and MEG, which map language, motor or memory function and hence aid surgical planning. Functional MRI uses blood oxygen level-dependent contrast, which theoretically reflects the increased oxygenated blood delivery to a particular cerebral area involved during specific tasks (Ogawa et al., 1993). Language lateralization results from fMRI and MEG or combined analyses concurs with Wada's test in 75–100% of patients (Arora et al., 2009; Janecek et al., 2013; Kamada et al., 2007). Concordance between investigated measures is greatest for right temporal lobe epilepsy patients with left language dominance and lowest for left temporal lobe epilepsy patients with left language dominance (Benke et al., 2006).

Another increasingly used non-invasive technique for functional mapping is navigated transcranial magnetic stimulation (nTMS). It delivers single short strong magnetic field pulses, which induce an electric field within the cortex. Moreover, with the appropriate stimulus intensity, it activates cortical motoneurons of the corticospinal tract and motor-evoked potentials are detected and mapped. First clinical evidence of its neurosurgical benefit for preoperative

localisation of eloquent cortex was shown for motor cortex in tumour patients (Forster et al., 2011; Krieg et al., 2014; Takahashi, Vajkoczy, & Picht, 2013). For language mapping repetitive TMS pulses are used (Pascual-Leone, GAtes, & Dhuna, 1991). Like for electrical stimulation language tasks are implemented and disruption of speech or hesitation is measured (Devlin & Watkins, 2007; Vigliocco, Vinson, Druks, Barber, & Cappa, 2011). nTMS results for language mapping imply high sensitivity but low specificity for detecting language sites (Ille et al., 2015; Rösler et al., 2014; Tarapore et al., 2013). A recent study, however, which included a paediatric cohort of typical surgical patients with ictal-onset areas or structural abnormalities near or within presumed language areas and patients with frequent seizures concluded that nTMS language mapping is clinically useful and safe. They furthermore stated that like in previous work their study showed mapping reliability is highest in frontal regions (Lehtinen et al., 2018).

1.2 High frequency oscillations (HFOs) as a new electrophysiological biomarker of epileptogenic tissue

1.2.1   What are HFOs?

In 1924, Hans Berger, a German psychiatrist, pioneered the recording of electrical activity from human brains using what he called the 'Electroenkephalogram'. By the time he published his findings in 1929, Berger had described the different brain rhythms, such as alpha waves, which were later referred to as "Berger's waves" (Berger, 1929). By 1939, he had described the main characteristics of the normal and abnormal EEG, including EEG changes in sleep and states of diminished consciousness (Berger, 1969).

Until recently, neurophysiologists largely focused on activity in the Berger bands (1–25 Hz) (Gloor, 1975). However, recent technological advances made it

possible to record electrophysiological signals beyond traditional low-pass filtered EEG and today, given the right equipment, frequencies as high as 500 Hz and beyond can be measured easily. This has led to an increasing number of research groups using iEEG recordings to study the neural bases of human cognition. Furthermore, the use of iEEG in humans is mainly restricted to patients undergoing resective surgery for medically refractory epilepsy, in whom it has been used most often to map the cortical networks responsible for seizures. In the last decade, HFOs in the frequency range between 80 and 500 Hz were proposed as new biomarkers for epileptogenic tissue (Bragin, Mody, Wilson, & Engel, 2002; Fujiwara et al., 2012; Jacobs et al., 2008; Wu et al., 2010; Zijlmans et al., 2012).

HFOs are defined as brief transient oscillatory EEG events (20–100ms), which are generated over small brain areas (1mm^3), persist for at least four oscillations and clearly stand out from the background activity. They are subdivided into ripples (80–250Hz) and fast ripples (FRs; >250Hz), although definitions of HFOs vary in the literature (Bragin et al., 2002; Jerome Engel, Bragin, Staba, & Mody, 2009; Grenier, Timofeev, & Steriade, 2001, 2003; Traub, 2003; Urrestarazu, Jirsch, LeVan, Hall, & Gotman, 2006). Recently, epileptic very-high-frequency oscillations (VHFOs; >1,000Hz) have been added to the spectrum (Usui et al., 2010). Figure 3 shows an example of an invasive recording with spikes, ripples, FRs and VHFOs.
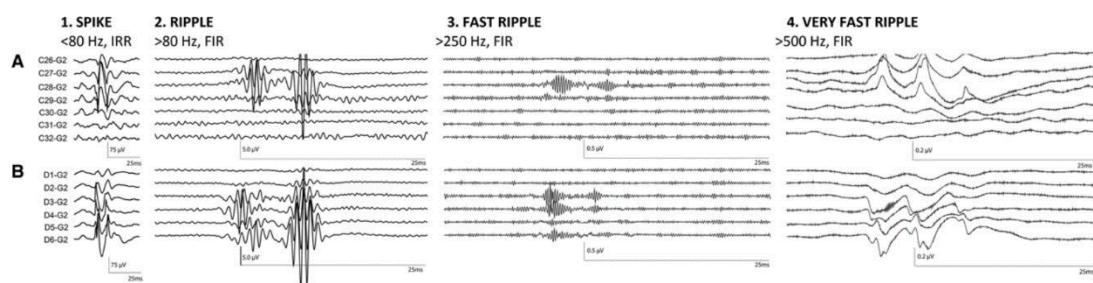
Figure 3. Examples of HFOs. (A) long-term ECoG recording showing two spikes with simultaneous ripples and fast ripples; **(B)** simultaneous long-term depth recording showing ripples and fast ripples that precede the cortical surface ripples and fast ripples slightly and very HFOs that can be recognized on one depth electrode channel (Zijlmans et al., 2017).

HFOs have been observed in both micro- and macroelectrode recordings, they can occur between seizures (interictal), at seizure onset and during seizures (ictal) and are seen most often during non-REM sleep (Bagshaw, Jacobs, Levan, Dubeau, & Gotman, 2009).

Detection of HFOs can be done visually or automatically. Drawbacks of visual identification are that it is highly time-consuming, as it lasts about ten hours to visually analyse HFOs in a 10-channel 10-min recording (Zelmann, Jacobs, Zijlmans, Dubeau, & Gotman, 2012). Furthermore, at least two reviewers are needed to separately mark the recording to achieve better reliability and the reviewers need have a certain level of experience to achieve reliable results (Jacobs et al., 2010a). Automatic detection on the other hand is promising and crucial to facilitate the clinical use of HFOs. Using automation, the time problem is solved. However, there is an abundance of articles reporting new automated detectors and their advantages. Zelmann and colleagues (2012) tested four detectors which were all based on different energy functions and built for different recordings and with different aims. They showed that all of them improved performance and that the main variation in results were observed in very active channels. Furthermore, the group recommended optimizing configuration settings for the data on hand instead of using standard settings.

The differentiation between physiological and pathological events is still challenging even with the implementation of automated detection. Patients studied mostly suffer from epilepsy and therefore more or less pathologically altered tissue is investigated (Jerome Engel et al., 2009).

1.2.2   Physiological and pathological HFOs and their mechanisms

Physiological HFOs were first described in the frequency range of 80-200Hz in animal studies and termed ripples. They were found in CA1 (Buzsáki, Horváth, Urioste, Hetke, & Wise, 1992), CA3, subiculum and entorhinal cortex (Chrobak & Buzsáki, 1996; Csicsvari, Hirase, Czurko, Mamiya, & Buzsaki, 1999) of the normal rat hippocampus during awake immobility and slow-wave sleep and reflect summated inhibitory post-synaptic potentials (IPSPs).

Ripples were later detected in the human mesial temporal structures and are thought to be involved in information processing and memory encoding, consolidation and recall (Axmacher, Elger, & Fell, 2008; Buzsáki, 2006; Buzsaki, Penttonen, Nadasdy, & Bragin, 1996; Siapas & Wilson, 1998). However, ripples are not limited to mesial temporal structures. Recent studies suggest that they can be stimulus-evoked by visual (Nagasawa, Juhász, Rothermel, Hoechstetter, Sood, & Asano, 2012) and somatosensory stimuli (Hashimoto, 2000) and hence also occur over occipital and central areas (Alkawadri et al., 2014; Nagasawa, Juhász, Rothermel, Hoechstetter, Sood, Asano, et al., 2012; Nonoda et al., 2016).

In contrast to physiologic HFOs, pathological HFOs are historically linked to FRs, which were first recorded in the dentate gyrus of epileptic rats and the hippocampus of temporal lobe epilepsy patients (Bragin et al., 1999). They generally contain power from 250 up to 800 Hz (Jerome Engel et al., 2009). HFOs, especially FRs, have been shown to be more correlated with the SOZ than interictal epileptiform discharges such as spikes (Bragin et al., 2002; Jacobs et al., 2008; Urrestarazu, Chander, Dubeau, & Gotman, 2007; Wu et al., 2010; Zijlmans et al., 2012). Ripples, too, seem to be linked to epileptogenicity as they are more frequent in SOZ areas than non-SOZ areas, although to a lesser degree than FRs (Jacobs et al., 2009). Raising the question whether different lesion types, and hence pathologically changed tissue, leads to increased intrinsic epileptogenic activity in SOZ areas, Jacobs and colleagues (2009) showed that

HFOs and especially FRs, are closely linked to seizure onset areas, but seem to be relatively independent of lesional changes. According to animal studies by Bragin and colleagues (1999; 2003), however, FRs were only recorded on the side of the lesion and ripples more often on the less affected side. In healthy tissue FRs have only been found after electrical stimulation while spontaneous FRs have not yet been described (Curio et al., 1997; Staba et al., 2004).

A decade after their discovery, the nature and mechanisms of pathological HFOs remain actively investigated. It is clear from the literature that multiple mechanisms are involved in the generation of HFOs. The main hypothesis is that pathological HFOs reflect population spikes of synchronously firing principle cells (Bragin, Wilson, & Engel, 2000; Dzhala, 2004). However, the action potential firing rate is often limited to <300Hz (Ibarz, Foffani, Cid, Inostroza, & Menendez de la Prida, 2010). Hence, the genesis of FRs whose frequency can be much higher, cannot be explained by this mechanism alone. A phase delay of different neuronal subpopulations is the currently accepted theory. Principle cells fire with lower frequency with a time delay, that can lead to a doubling of the frequency measured extracellularly as FRs. Network mechanisms proposed responsible for that phase delay are neuronal loss (Staba et al., 2007), disconnected neural populations, asymmetric firing, reduced spike-time-variability delayed activation and functional clustering of neurons (Bikson, Fox, & Jefferys, 2003; Foffani, Uzcategui, Gal, & Menendez de la Prida, 2007; Ibarz et al., 2010).

The distinction between physiological and pathological HFOs is not as simple as previously suggested. Until now, many studies have shown that epileptic oscillations also occur in the ripple frequency range (Crépon et al., 2010; Jacobs et al., 2008) and have demonstrated that physiologic and pathologic HFOs have a large frequency overlap and therefore, cannot be separated by frequency alone (Jerome Engel et al., 2009; Matsumoto et al., 2013).

To aid understanding of the distribution of physiological intracranial EEG activity Frauscher and colleagues (2018) developed the first atlas of region-

specific normative values for physiological HFOs and high frequency activity (HFA) in a common stereotactic space, which is freely available via an open web resource. They showed that physiological ripples were particularly frequent in the occipital cortex, medial and basal temporal region, transverse temporal gyrus and planum temporale, pre- and postcentral gyri, and medial parietal lobe. In contrast, physiological FRs and HFA were very rare, even in eloquent cortex. Thus, they argued, that FRs are better candidates for defining the epileptogenic zone (Frauscher, von Ellenrieder, Zelmann, Doležalová, et al., 2018; Frauscher, von Ellenrieder, Zelmann, Rogers, et al., 2018). Other means of distinguishing between physiological and pathological activity are reported by Kerber and colleagues (2014), who found that HFOs occurring in an oscillatory background activity might be suggestive of physiological activity compared to those on a flat background which reflect epileptic activity. Other methods of differentiation are analysing the co-occurrence of HFOs with physiologic phenomena like sleep slow-wave or sleep spindles to identify physiologic activity (Bruder et al., 2017) and investigating the co-occurrence of HFOs with epileptic spikes to identify pathologic HFOs (S. Wang et al., 2013; S. A. Weiss et al., 2016).

1.2.3   HFOs in epilepsy surgery

HFOs are a biomarker of epileptogenic tissue and studied in relation to surgical resection and post-surgical outcome in epileptic patients. As previously mentioned, HFOs can be observed during ictal and interictal periods. Most research in this field of epilepsy surgery is done using interictal HFOs and the role of ictal HFOs in epilepsy surgery is less well defined. Interictal periods are less noisy and non-REM sleep was shown to be best suited for observing HFOs (Bagshaw et al., 2009). For pre-surgical evaluation, ictal and interictal HFOs, independent of the type of epilepsy and its localization, were found to be successful in identifying the SOZ (Crépon et al., 2010; Jacobs et al., 2010b; Worrell et al., 2004). Most previous studies used electrocorticography (ECoG) and depth electrode recordings showed increased seizure freedom when a higher

number of contacts with ictal HFOs (Fujiwara et al., 2012) or inter-ictal HFOs were resected (Akiyama et al., 2011; Haegelen et al., 2013; Jacobs et al., 2010a; Wu et al., 2010). Furthermore, it was shown that postsurgical outcome increased when pre-surgically identified brain areas with high HFO rates were resected compared to resecting areas exhibiting low HFO rates (Cho et al., 2014). A meta-analysis by Höller and colleagues (2015) summarised the existing evidence for the relationship between resecting HFO-generating regions and post-surgical outcome. They related outcome to resection ratio, which they defined as the ratio of the number of channels showing HFOs that were inside the resection area to the number of channels on which HFOs were detected. They concluded that for ripples and FR resection ratio was significantly higher in seizure-free patients compared to non-seizure-free patients. The total effect-size however was small. The majority of research discussed was of retrospective nature. Only a few articles were prospective. Recently, however, Jacobs and colleagues (2018) reported results of their prospective multicentre trial investigating the predictive value of removing HFO-generating regions and seizure outcome. They observed a correlation between the removal of HFOs and seizure freedom; however, only on a group level for all patients but not for the centre-specific analysis.

Furthermore, the Utrecht group are studying HFOs during intraoperative electrocorticography, analysing HFOs before and after resection. They reported that HFOs measured after resection were superior in predicting seizure outcome highlighting the importance of disconnecting HFO networks (van 't Klooster et al., 2015, 2017). They are currently working on the first randomized controlled trial ("The HFO Trial") investigating the feasibility and safety of using HFOs during intra-operative tailoring of epilepsy surgery. Results are planned to be presented in due course.

1.3 The role of electrophysiological methods in localising language areas

As described above, in epilepsy patients the cortical anatomy as well as functional networks can vary due to pathological changes during development (George Ojemann, Ojemann, Lettich, & Berger, 2008; Sanai et al., 2008; Steinmetz, Furst, & Freund, 1990). Hence, when considering neurosurgery the anatomical relationship between eloquent areas and areas intended for surgical resection needs to be delineated.

In the following, first, I would like to summarise pathways essential for language processing and production discussed in the literature and second introduce EEG driven neurophysiological methods crucial for this work, which aid localisation of eloquent areas, in particular language areas.

1.3.1 Language network

The advances in non-invasive imaging techniques in the last twenty years and the interconnection of various fields of research, like cognitive neuroscience, linguistics, computational science and medicine propelled language research. Nowadays, language is perceived as a unified network of separated, yet intertwined sub-components rather than a modular model of expressive and receptive language, which were described by Broca and Wernicke in the 19th century (Broca, 1865; Wernicke, 1874).

The neural network consists of two main pathways connecting perisylvian language areas: the dorsal and ventral streams, similar to the visual system (Hickok, 2009; Poeppel, Emmorey, Hickok, & Pylkkänen, 2012; Poeppel & Hickok, 2004; Saur et al., 2008) (Figure 4). Each of the two pathways consists of at least two fibre tracts each (Figure 5).
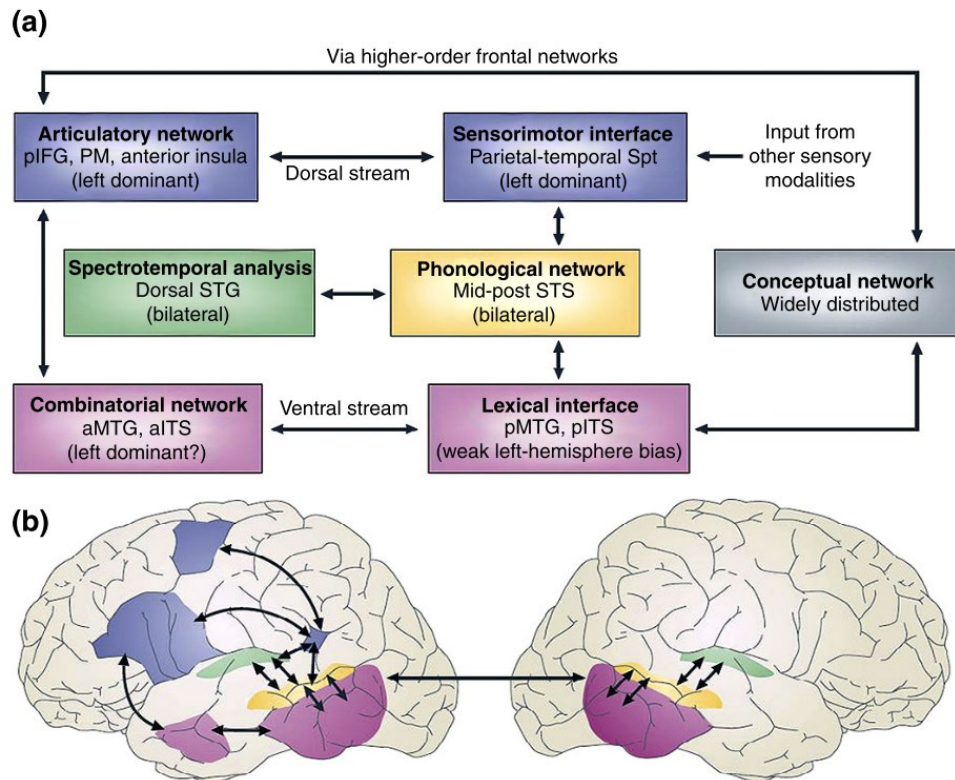
Figure 4. The Dual Stream Model of language (Hickok & Poeppel, 2007). Abbreviations: pIFG = posterior inferior frontal gyrus, PM = premotor cortex, STS = superior temporal sulcus, aMTG = anterior medial temporal gyrus, pMTG = posterior medial temporal gyrus, pITS = posterior inferior temporal sulcus

The dorsal pathway ("what" stream) supports auditory-to-motor mapping. Its two long-range fibre bundles are first, arcuate fascile (AF) which directly connects Broca's and Wernicke's area running from posterior and middle superior temporal gyrus (STG) to the posterior portion of Broca's area (BA 44, pars opercularis) (Frey, Campbell, Pike, & Petrides, 2008; Saur et al., 2008). It supports the processing of syntactically complex sentences (Friederici, 2012; Friederici & Gierhan, 2013). Second, parts of the superior longitudinal fascile (SLF) that indirectly connects middle temporal gyrus (MTG) or STG with the dorsal premotor cortex (PMC, in the service of speech output) via the parietal cortex (PaC, known to support phonological working memory) are relevant for word repetition (Friederici, 2012; Friederici & Gierhan, 2013; Galantucci et al., 2011). Furthermore, MTG also seems to be involved in lexical-semantic and

conceptual semantic aspects in particular (Lau, Phillips, & Poeppel, 2008; Patterson, Nestor, & Rogers, 2007).

In addition, the ventral pathway ("where" stream) supports auditory-to-meaning mapping. Its two fibre bundles discussed in the literature are first, the uncinate fascile (UF) that connects the anterior temporal cortex (TC) with the anterior inferior frontal cortex (FC) (Anwander, Tittgemeyer, Von Cramon, Friederici, & Knösche, 2007; Friederici, Bahlmann, Heim, Schubotz, & Anwander, 2006; Hua et al., 2009) and subserves local syntactic processes (Friederici & Gierhan, 2013). Second, the inferior-fronto-occipital fascile (IFOF) also called the extreme capsule fiber system (ECFS) that runs through the extreme capsule connecting the posterior TC, the occipital cortex (OC) and the PaC with the FC (Martino et al., 2011; Sarubbo, De Benedictis, Maldonado, Basso, & Duffau, 2013) and supports semantic processes and comprehension (Friederici & Gierhan, 2013; Galantucci et al., 2011).
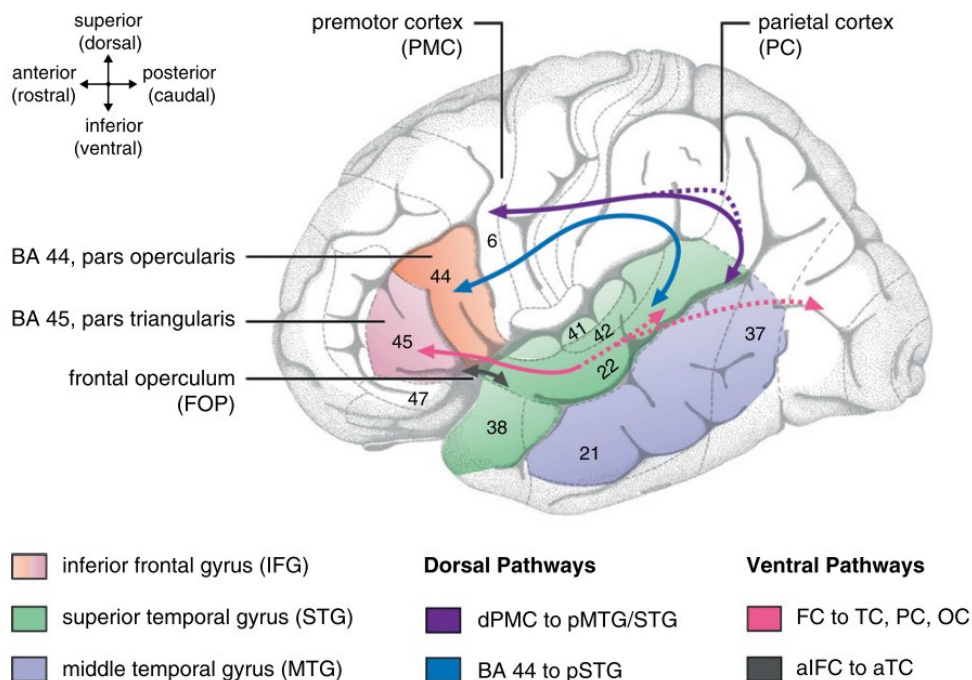
Figure 5. Language-relevant brain regions and connecting fiber tracts. schematic view of left hemisphere). Abbreviations: FC = frontal cortex, TC = temporal cortex, PC = parietal cortex, OC = occipital cortex, dPMC = dorsal PMC, pSTG = posterior STG, aIFC = anterior inferior FC; (Friederici & Gierhan, 2013)

43

The dorsal pathway has specifically been associated with expressive language (Catani, Jones, & Ffytche, 2005) and the ventral pathway with receptive language due to its role in semantic processing. However, rather than two separate streams, the these two pathways form a loop system for processing naturalistic language (Weiller, Musso, Rijntjes, & Saur, 2009). The brain areas discussed here are located around the Sylvian fissure and are called the perisylvian language areas. They are critical to perceiving, integrating and producing language and speech (Catani et al., 2005).

In patients with epilepsy localisation of classical language areas often differ from healthy children and adolescents due to neuroplastic changes in response to cortical insult, lesions or abnormal electric circuitry. Patients with early left-hemispheric epilepsy have a higher chance of right hemisphere lateralisation for language compared to the general population (Helmstaedter, Kurthen, Linke, & Elger, 1997; Liégeois et al., 2004). Furthermore, besides recruitment of right hemispheric regions, preserved language function can be observed in intact regions of the left hemisphere or bilaterally (Liégeois et al., 2004). Those results agree with earlier findings arguing that the developing brain has great capacity for reorganization of functional areas (Vargha-Khadem, O'Gorman, & Watters, 1985; Woods, Dodrill, & Ojemann, 1988). However, these possible reorganisation patterns lead to challenges in epilepsy surgery as localising this complex language network requires careful mapping of eloquent areas and the networks between them. This is an essential step during pre-surgical evaluation to avoid surgically induced language deficits.

1.3.2 Neurophysiological measures to localise language-related brain areas

Clinical investigations to determine the dominant hemisphere for language or localise language areas are discussed in Section 2.1.3.2. Here, I focus on neurophysiological measures to aid localisation of language areas. Invasive EEG monitoring is advantageous as it provides an invasive signal, which is a direct

measure of the neural activity on either the brain surface when using subdural electrodes or the depth of the brain when using depth electrodes or SEEG. Two measures of neuro-electrical activity are discussed in the literature, evoked responses, called event-related potentials (ERPs) and induced responses, so called spectral changes. Both are well-established methods to study cognitive processes (Davis, 1939; Davis et al., 1939; Cooper et al., 1965).

The following sections will summarise these two EEG based approaches, first event-related potentials and second event-related desynchronization (ERD) or event-related synchronization (ERS).

1.3.2.1 Event-related potentials

ERPs are averages of EEG data that are tightly time- and phase-locked to a stimulus that can be extracted from the ongoing EEG (Luck, 2014). They are also known as evoked responses (Tallon-Baudry & Bertrand, 1999). ERPs are mostly recorded using scalp EEG and represent the synchronous activation of groups of neurons during cognitive processing (Taylor & Baldeweg, 2002). ERPs are commonly used to examine typical and atypical responses of a variety of cognitive processes ranging from attention (Astheimer, Janus, Moreno, & Bialystok, 2014) and memory (Maratos, Allan, & Rugg, 2000) to language (Sullivan, Janus, Moreno, Astheimer, & Bialystok, 2014) and social processing (De Haan & Carver, 2013). ERPs have a unique temporal resolution (in ms) allowing precise timing of different information processing stages. Basic processing stages can be delineated by distinct ERP patterns that follow a hierarchy arising from sensory cortices extending to multimodal, association and premotor cortices illustrated in Figure 6 (Halgren & Marinkovic, 1995).

Brain regions implicated in generating specific ERP components are outlined schematically in the corresponding colour

1. *Sensory* ERP components (P1, N1, P2) are generated in primary (light blue) and secondary sensory cortices.

2. An *orienting* complex, consisting of N2 (or MMN), P3a and slow wave is generated in medial (cingulate gyrus) and lateral frontal and posterior parietal cortices (dark blue).

3. Endogenous N4 and P3b components, associated with *event integration*, are generated in the hippocampus, amygdala (shaded red) and associated inferotemporal and lateral orbitofrontal cortices (red).

4. The response-locked readiness potential during *response preparation* can be recorded in central gyrus and associated supplementary and premotor cortices (green).

5. ERP components correlated with *performance monitoring, such as the error-related negativity* are generated in the anterior cingulate cortex (broken green line). ERPs are shown here with negativity upward.

Figure 6. Hierarchical processing stages characterized by distinct ERP patterns. From (Halgren et al., 1995) and adapted by (Baldeweg & Boyd, 2007).

Intracranial ERPs (iERPs) are extracted from the iEEG in much the same way as from scalp EEG, except that their voltage is much larger (up to 150µV). Advantages of iEEG are that it can provide precise spatial resolution and that the signal is barely contaminated by electro-myographic artefacts. However, these investigations are limited to special circumstances, like epilepsy (Anaïs Llorens,

Trébuchon, Liégeois-Chauvel, & Alario, 2011). Trébuchon and colleagues (2013a) studied the dual-stream pathways in patients with epilepsy and invasive EEG monitoring using language tasks. They measured ERPs along the ventral stream (fusiform gyrus, inferior temporal gyrus and middle temporal gyrus) predominantly during their lexical-semantic task (adjective-noun pairs) and along the dorsal stream (left supramarginal gyrus) mainly during the phonological task (phoneme task on pairs of pseudo words). Their results showed strong left lateralization of typical ERP components.

Movement-related ERPs

Movement-related ERPs are for example the Bereitschaftspotential (BP) and the motor potential (MP). These are two of the potentials obtained from recording EEG and electromyogram (EMG) signals simultaneously while the participant is repeating a voluntary muscle movement, like finger tapping or wrist extension. BP and MP are illustrated below in Figure 7 showing each component in a scalp EEG recording (international 10–20 System) in relationship to the start of the EMG signal.

The Bereitschaftspotential, also called readiness potential (RP), is a negative cortical potential which starts about 2.0 s prior to the movement onset. BP has two components, the early pre-movement negativity (early BP) which starts about 1.2s to 0.5s before the EMG onset and the later negative slope (late BP) which starts 0.5s to shortly before the EMG onset (Shibasaki & Hallett, 2006). Motor potential or N10 is a negative peak localized at the contralateral central area (C2 of the International 10–20 System) and occurs immediately before the movement onset. It is well localized to a small area of the contralateral central scalp, precisely corresponding to the movement site. Another negative peak occurring shortly after N10 is localized over the midline frontal region and corresponds to N+50 or the frontal peak of motor potential (fpMP) (Shibasaki & Hallett, 2006).
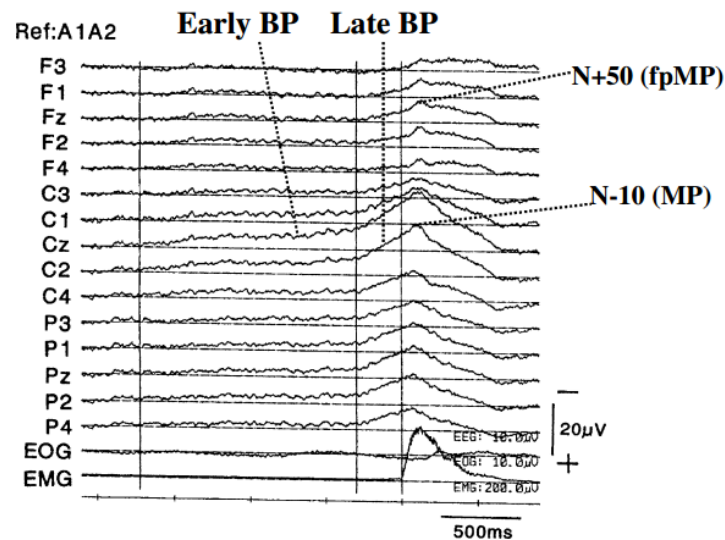
Figure 7. Movement-related cortical potential.

1.3.2.2 Event-related synchronisation (ERS) and event-related desynchronization (ERD)

Both phenomena are time-locked, but compared to ERPs are not perfectly phase-locked as they reflect systematic changes in the EEG (Pfurtscheller & Lopes, 1999). They occur with a jitter in latency from one trial to the next (Tallon-Baudry & Bertrand, 1999). ERS/ERD are frequency-band specific and are referred to as induced responses (Tallon-Baudry & Bertrand, 1999). ERD is an event-related suppression of spectral power in the alpha (8–13Hz) and beta (15–25Hz) frequency band during tasks activating sensorimotor cortex. ERS is an increase of spectral power in the gamma activity range (≥30Hz) (Pfurtscheller & Aranibar, 1979). Spatial mapping of ERS/ERD is used to study the dynamics of cortical patterns (Pfurtscheller, 2001).

Due to advances in computational analysis and the increased application of invasive ECoG investigations in neurosurgery, the implementation of time-frequency domain approaches to assess such induced task-related spectral power modulations in intracranial recordings increased. Regarding cognitive neuroscience, most work was done investigating gamma-band activity. Gamma-band modulation was studied analysing memory processing (Axmacher et al., 2008; Fell, Ludowig, Rosburg, Axmacher, & Elger, 2008; J. Jung et al., 2008),

speech perception and production (N. E. Crone et al., 2001), reading (Mainy et al., 2008), attention (J. Jung et al., 2008; Ray, Niebur, Hsiao, Sinai, & Crone, 2008) and auditory (Edwards, Soltani, Deouell, Berger, & Knight, 2005) and somatosensory processing (Aoki, Fetz, Shupe, Lettich, & Ojemann, 1999). In addition, time-frequency analysis of iEEG data has revealed robust task-related response patterns in lower frequency bands, mostly in the theta (4–7 Hz), alpha (7–14 Hz) and beta (15–30 Hz) bands (N. E. Crone, Miglioretti, Gordon, Sieracki, et al., 1998).

II IDENTIFICATION OF THE SEIZURE ONSET ZONE USING QUANTITATIVE STEREO-EEG

2 Phase-Locked High Gamma (PLHG) as an Electrophysiological Biomarker for Seizure Onset Zone Detection – MNI study

2.1 Introduction

Patients with medication-resistant focal epilepsy may be considered for neurosurgical treatment. Epilepsy surgery requires accurate identification of the epileptogenic zone (see Section 1.1.3 for a definition). In some patients, non-invasive methods fail to identify a single focal seizure generator. In those cases, intracranial electroencephalographic investigations are indicated (Diehl & Lüders, 2000) and used to define the SOZ (Rosenow & Lüders, 2001). The standard method for SOZ localization is visual inspection of initial ictal intracranial EEG changes (Rosenow & Lüders, 2001). However, increasing computational power and the development of quantitative EEG analysis methods led to the investigation of specific features within EEG data which might provide additional valuable information to aid seizure onset localisation (Zijlmans et al., 2017).

In the following, I will first lay out the rationale for exploring ictal phase-locked high gamma (80–150Hz; PLHG), present the aims of this study before describing the two methods I used to analyse the data and finally summarise the results of this project.

2.1.1 Rational for exploring PLHG

As previously described (Section 1.1.3) the SOZ defines the cortical area from which seizures arise while the EZ is a theoretical concept and describes the cortical area, which is essential for seizure generation and once removed leads to seizure freedom. The two zones do not necessarily correspond, the EZ can be smaller or bigger than the SOZ (Rosenow & Lüders, 2001).

For SOZ localisation EEG investigation is employed. Using scalp electrodes allows for a broad coverage of the brain surface. However, due to their large distance to generators and the many different layers (like scalp, dura mater etc.) scalp recordings show a low sensitivity for SOZ location, especially for seizure generators localized deep in the brain. Therefore, intracranial EEG (iEEG) recordings are implemented which eliminate the distance problem, as—if the preimplantation hypothesis of the SOZ is correct—electrodes are implanted close to the presumed seizure onset (Rosenow & Lüders, 2001). Hence, iEEG provides information about seizure onset and propagation. Besides interictal epileptiform discharges during interictal periods, epileptologists visually review ictal iEEG recordings for characteristics like low-voltage fast activity, rhythmic spiking, spike waves, rhythmically evolving theta, delta or alpha frequencies or an electrodecremental pattern to narrow down the SOZ (R. S. Fisher, 2014). Depending on the number and types of electrodes implanted, a various number of contacts has to be visually inspected, typically at least 50–100 contacts (Lesser, Crone, & Webber, 2011). This leads to long EEG reviewing and reporting hours which pose a major drawback of this investigation (Ganesan, Appleton, & Tedman, 2006; Keenan & Sadlier, 2015).

Hence, there is a need to identify biomarkers that can accurately and automatically localize the extent of the ictally involved brain areas, and thereby aid visual identification of the SOZ.

Weiss and colleagues (Schevon et al., 2012; S. A. Weiss et al., 2015) argued that conventional visual inspection might estimate a too extensive SOZ. They showed that cortical territories recruited during a seizure can be distinguished based on neurophysiological characteristics into the "ictal core" and the "ictal penumbra" (Figure 8). Using microelectrode arrays together with standard clinical subdural electrodes they demonstrated spatial patterns of hypersynchronous (multiunit) neural activity in human clinical seizures (Schevon et al., 2012). Schevon and colleagues (2012) suggested that the ictal core describes an area of intense rhythmic burst firing which is fully recruited to

the seizure. Low level, desynchronized firing located on the periphery of the core area represents the so called ictal 'penumbra'. The concept of distinction between ictal core and penumbra is based on multi-unit activity in microelectrode recordings; however, such microelectrodes are not routinely used clinically.
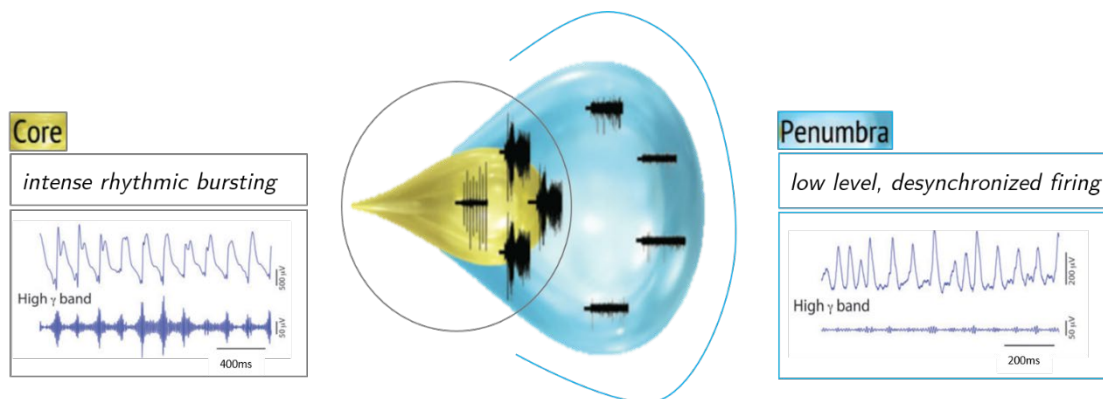
Figure 8. Neurophysiological signatures of ictal core & ictal penumbra. The ictal core (yellow, left) shows intense rhythmic high frequency firing modulated by low frequency burst activity and the penumbra (blue, right) exhibits main low frequency, desynchronized firing. Adapted from (S. A. Weiss et al., 2013).

Low frequency (1–30Hz) ictal signals, on which clinicians rely on to determine the ictal EEG onset, are not only seen in the seizure core territory but also in the penumbral region. Hence, both areas cannot reliably be distinguished using standard visual EEG inspection (Schevon et al., 2012; Trevelyan, Sussillo, Watson, & Yuste, 2006). This may lead to different estimates of seizure initiation and spread and may contribute to a poor surgical outcome (S. A. Weiss et al., 2013).

Weiss and colleagues (2013) proposed the co-occurrence of repetitive high gamma (80–150 Hz) activity in multi-unit recordings to be an indicator of the seizure-generating sites ('seizure core'). Using a computational approach they demonstrated that high gamma (80–150Hz) activity phase-locked to low frequency EEG discharges, detected in clinical subdural recordings, corresponds to ictal core high-frequency multi-unit activity in microelectrodes. This measure is termed the 'phase-locked high gamma' (PLHG) metric.

Cross-frequency phase-locking (also termed nested oscillation or phase-amplitude coupling (PAC)) describes the phenomenon of coupling between the amplitude of a fast rhythm and the phase of a slower rhythm (Penny, Duzel, Miller, & Ojemann, 2008). It was shown to occur across a range of frequencies and brain regions. Low frequency oscillations are thought to control information transfer between brain areas by modulating excitability of local neuronal ensembles (Fries, 2005; von Stein & Sarnthein, 2000). In addition, their phase influences rhythmic high frequency activity and spiking probability of individual neurons (Canolty & Knight, 2010). PAC seems to facilitate effective coordination of neural connectivity and its efficiency is taken as a measure of functional connectivity between the various neuronal ensembles (Canolty & Knight, 2010; Jensen & Colgin, 2007).

Weiss and colleagues (2015) observed this PAC phenomenon in epileptic foci and showed that only in the ictal core, but not in the penumbral region the peaks of ictal low frequency discharges coincide with both the multi-unit burst firing and the transient increases in high gamma amplitude (Figure 9).
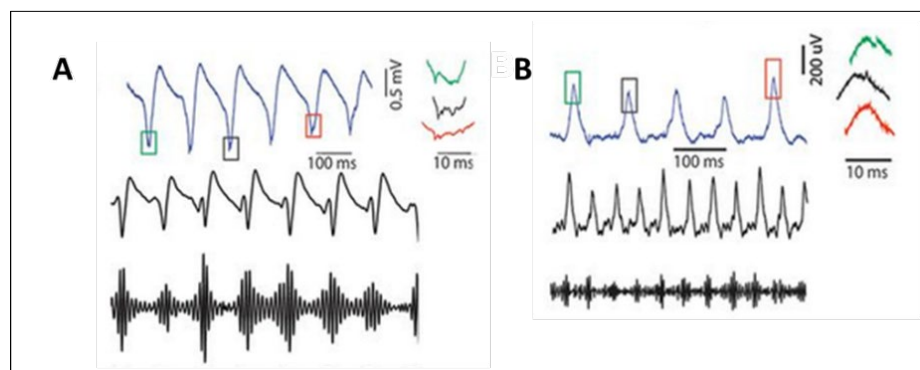
Figure 9. **Phase-locked high gamma amplitude differentiates seizure core from penumbra. A**. Ictal core electrode activity. Top: Ictal microelectrode recording illustrating high gamma (right) at the negative peak of the low-frequency rhythm (coloured squares). Middle: Simultaneous subdural recording. Bottom: High gamma (80–150Hz) filtered subdural recording. **B**. Same tracings for a penumbral electrode. Adapted from (Weiss et al., 2013).

A subsequent study by Weiss and colleagues (2015) retrospectively analysed subdural grid and depth electrode data of 45 surgical patients and computed the correlation of resection of PLHG-generating sites and clinically defined SOZ in

relation to postoperative seizure control. They showed that the temporal dynamics of PLHG recruitment was of importance. Recruitment of the first four PLHG channels, which identified the region invaded first by the seizure, was most informative and superior to late-appearing PLHG channels as outcome. Their results showed that patients with good post-surgical outcomes had significantly greater proportions of the first 4 PLHG sites resected compared to patients with bad surgical outcome (72.7%±5.1% and 45.4%±8.6%, respectively). They further added that SOZ resection is an effective seizure outcome classifier and emphasized the improved outcome classification when combining the SOZ and early PLHG sites information (Figure 10).
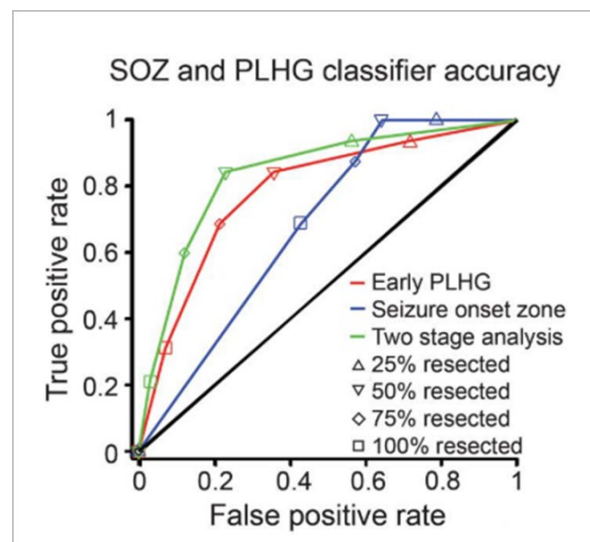
Figure 10. Receiver operating characteristics (ROC) curves. Sensitivity and specificity of seizure outcome classification illustrated by ROC curves. SOZ (blue), early PLHG (red), a 2-stage analysis using both measures (green) and random performance (AUROC of 0.5, black) are illustrated. Adapted from (Weiss et al., 2015).

Using the area under the receiver operating characteristic curve they illustrated that among the patients with at least 75% of SOZ resected, 78% of patients (n=30) had good outcomes. When adding at least 75% of early PLHG resection 91% of patients (n=22) showed good outcomes.

2.1.2 Study aims

According to Weiss and colleagues (2015) PLHG could be a valuable biomarker to improve SOZ delineation and seizure outcome, however, these results have not yet been replicated. They presented results based on mainly subdural electrode implantations, and the usefulness of this metric for SEEG has not been evaluated. The present study, therefore, aims to investigate PLHG as a metric for automated detection of SOZ in a cohort of patients with SEEG implantations and a clinically defined focal SOZ. Furthermore, I aimed to study the temporal and spatial relationships between PLHG recruitment, the clinically defined SOZ and occurrence of sharp activity. Sharp activity was compared to PLHG as it is a visible marker in iEEG and used in clinical SOZ delineation. It was identified using an automated detection metric to demonstrate results of a second quantitative measure. This project therefore aimed to answer four main questions:

1. Can PLHG recruitment be reproduced in a cohort of adult patients with SEEG implantation and a clinically defined focal SOZ?

2. How reproducible is PLHG recruitment across seizures in each patient?

3. What is the temporal and spatial relationship of PLHG recruitment and sharp activity?

4. Is the overlap of PLHG recruited channels with SOZ channels predictive of the post-surgical Engel outcome?

2.2 Methods

2.2.1 Patient selection

I retrospectively identified adult patients with a diagnosis of medically intractable epilepsy who underwent SEEG investigations at the Montreal Neurological Institute and Hospital between July 2006 and April 2015. The hospital ethical review board gave permission for this study. All SEEG recordings included had 2000Hz sampling rate compared to Weiss et al. who described using recordings with 500Hz and 1000Hz sampling rate. Inclusion criteria are summarised in Table 2.

Table 2. Seizure related and technical inclusion criteria.

Seizure criteria	Clinical or/and electrographic seizures
	Seizure duration ≥35s
	3 seizures of the same seizure type per patient
Technical criteria	Minimal artefacts in EEG recording
	MRI/CT images available to determine electrode location inside the brain

The duration of the seizure ≥35s, the second inclusion criterion, was suggested to me by Weiss, who did not describe a minimum seizure duration in his published work (S. A. Weiss et al., 2015). It was chosen generously to ensure that every seizure shows at least the early PLHG recruited channels (first 4 channels). Weiss and colleagues (2015) described that their average time of earliest recruitment was 14.2±2.4s from clinical seizure onset. All clinical data was drawn from the patient's records and postsurgical follow-up notes.

2.2.2 Clinical information

The following information was gathered: demographics, age at onset of epilepsy, duration of epilepsy, age at SEEG, neurophysiological findings including SOZ definitions, surgical resection plan and post-surgical seizure outcome. Post-operative seizure outcome was classified using the Engel scale (J. Engel, 1993b) with good outcomes defined as Engel class I or II (seizure-free and rare disabling seizures, respectively) and poor outcomes as class III or IV (worthwhile improvement or no improvement, respectively) (S. A. Weiss et al., 2015).

2.2.3 Intracerebral EEG recordings

Depth electrode placement for each patient was individually tailored and was based on clinical history, seizure semiology, results of surface EEG, neuroimaging and neuropsychological testing. iEEGs were sampled at 2000Hz and recorded using the Harmonie monitoring system (Stellate, Montreal, Canada). Electrode types used were MNH electrodes (9 contacts, length 40mm; manufactured on site) and DIXI electrodes with 10 contacts (33.5mm), 14 contacts (47.5mm) and 15 contacts (51mm) (manufactured in Besançon, France). Two contacts located in white matter were chosen as ground and reference. All EEG traces were referenced against the same common reference.

2.2.4 Data preparation

For each patient three seizure recordings plus three baseline recordings were gathered according to the inclusion criteria described above (Table 2). The seizure onset was determined by visual SEEG review by an experienced epileptologist (Dr F. Dubeau). Baseline recordings were 30s interictal segments clipped prior to the seizure. A relatively silent epoch with a limited number of interictal discharges was used and ideally, each seizure had its own baseline recording.

Recording blocks with excessive artefacts were excluded. If only single channels showed artefacts and these channels were not recording from the seizure onset zone only these artefactual channels were excluded.

2.2.5 Quantitative EEG methods

PLHG metric

To calculate PLHG, I used a set of Matlab scripts developed by Weiss named the 'PLHG metric' (S. A. Weiss et al., 2013, 2015). He shared his scripts with me and gave me permission to use them for my projects.

PLHG computation is based on measuring cross-frequency coupling using a phase-locking value (PLV). It is based on instantaneous phase and amplitude calculated from the Hilbert transform. The PLV is a measure of phase correlation, which can take a value from 0 to 1, where one means perfect phase-locking and zero signifies no locking. It is defined as:

$$PLV = \left| \frac{1}{N} \sum_{n=1}^{N} \exp(i(\phi_{4-30Hz}[n] - \phi_{a(80-150Hz)}[n])) \right|$$

Where N is the number of trials and $\phi_{(4-30Hz)}$ represents the instantaneous low-frequency (4–30Hz) phase and $\phi_{a(80-150Hz)}$ the instantaneous high-frequency (80–150Hz) phase amplitude for signal i in trial trial n.

For the PLHG calculation,

$$PLHG = \left| \frac{1}{N} \sum_{n=1}^{N} a_{norm(80-150Hz)} \exp(i(\phi_{4-30Hz}[n] - \phi_{a(80-150Hz)}[n])) \right|$$

$a_{norm(80-150Hz)}$ the instantaneous high gamma (80–150Hz) amplitude normalized to a pre-ictal or interictal baseline segment of 30s duration is added to the PLV, which adds the weight of the instantaneous high gamma (80–150Hz) amplitude.

PLV and PLHG were calculated over 3s sliding windows advanced in 333ms increments. All amplitudes and phases were determined using the Hilbert Transform. Data analysis was completed using MATLAB R2015b.

iEEG data was pre-processed before running through the PLHG metric. Table 3 illustrates the pre-processing and PLHG detection pipeline.

Table 3. PLHG pre-processing and analysis pipeline.

Data preparation
- Reject recordings with extensive artefacts
- Delete artefactual channels
- Select baseline recording (30s)
- Select seizure recordings

Bandpass filter (80–150Hz)

Detect early PLHG channels
- Compute PLHG values
- Determine PLHG threshold for each seizure

One patient (ID10) showed Herald spikes in all three seizures, which resulted in a late recruitment time for the patient's seizures compared to other patients. Herald spikes are interictal spikes, which announce the onset of electrographic seizures (Figure 11). Weiss and colleagues (2015) suggested to exclude Herald spikes from the seizure and the pre-ictal baseline for PLHG recruitment analysis. I followed their suggestion in the current study.
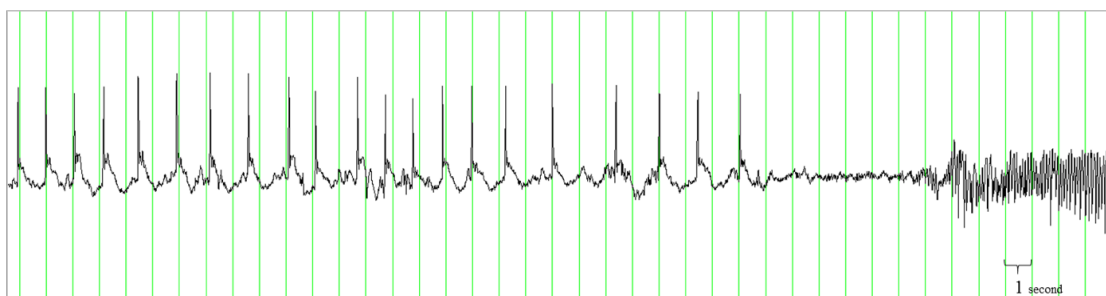
Figure 11. Herald Spikes. Example seizure showing herald spikes in one seizure onset channel of patient 10 with a recording sensitivity of 50 µV/mm.

The PLHG metric detects when a channel shows transient increases in high gamma amplitude phase-locked to low frequency EEG background. However, a channel only is considered as 'PLHG recruited' once a certain threshold is reached. This threshold is determined for each seizure independently, based on the PLHG value distribution, which is fixed to a mixed Gaussian model with one or two Gaussians. Positive goodness of fit values (GOF) reflect adequate fit.

The distribution of PLHG value could either be unimodal or bimodal. A unimodal distribution suggests sampling of mostly one type of PLHG population (e.g. ictal core electrodes or electrodes not involved in the seizure). The threshold here is defined as three coefficients of variation over the mean. A bimodal distribution suggests that two independent PLHG populations are represented in the PLHG data (with a clear separation between core and penumbra activity). In this case, the threshold is calculated as half of the coefficient of variation less than the mean of the higher-valued distribution (S. A. Weiss et al., 2015). This is an automated process implemented in the Matlab script.

The following Figure 12 presents an example seizure with a good model fit, showing the goodness of model fit across time points for both models. Furthermore, the PLHG values for all channels of this seizure and the automatically selected threshold generated by the model are illustrated.

A

B
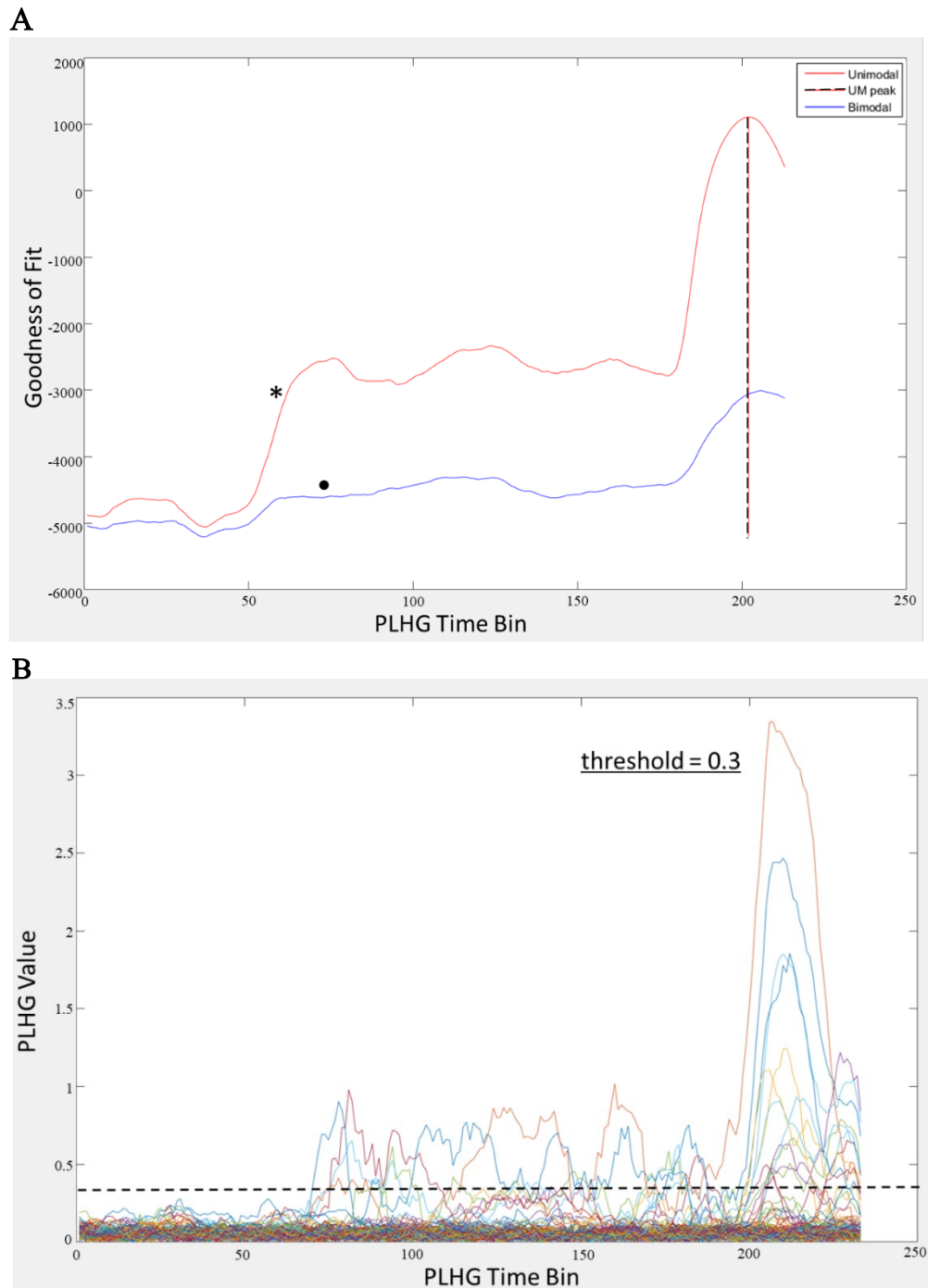
Figure 12. Sample seizure: Goodness of fit & PLHG values per channel. A. Goodness of fit model plot for unimodal (red, *) and bimodal (blue, ●) Gaussian models. The unimodal model shows a better fit as a local maximum was found for the unimodal fit at bin 204 (black dashed line). **B.** PLHG values per channel across time bins are illustrated and the automatically determined critical PLHG threshold of 0.3 (black dashed line). Every channel exceeding this threshold was regarded as a PLHG recruited channel.

Data output of these Matlab scripts identify the PLHG recruited channels and the time (from seizure onset, i.e., t=0s) of their recruitment.

Sharp activity detector

In a next step the seizure detection algorithm of Amiri and colleagues (Amiri, Lina, Pizzo, & Gotman, 2016) was implemented to detect sharp activity in these same three seizures of each patient using Matlab scripts developed by Dr M. Amiri. This employed the second derivative method (Carrie, 1972) to detect sharp events and parameters of the algorithm were chosen so that less than 10% of visually marked events were missed. The same seizure and baseline SEEG recordings chosen for the PLHG metric were used for the sharp activity detection. Time of occurrence of sharp events were inserted into the EEG recording.

An illustration of the automatic sharp activity detection (Amiri et al., 2016) is shown in Figure 13.

Bipolar montage   Time line interval: 1.0 s   Sensitivity 50uV/mm   1 second
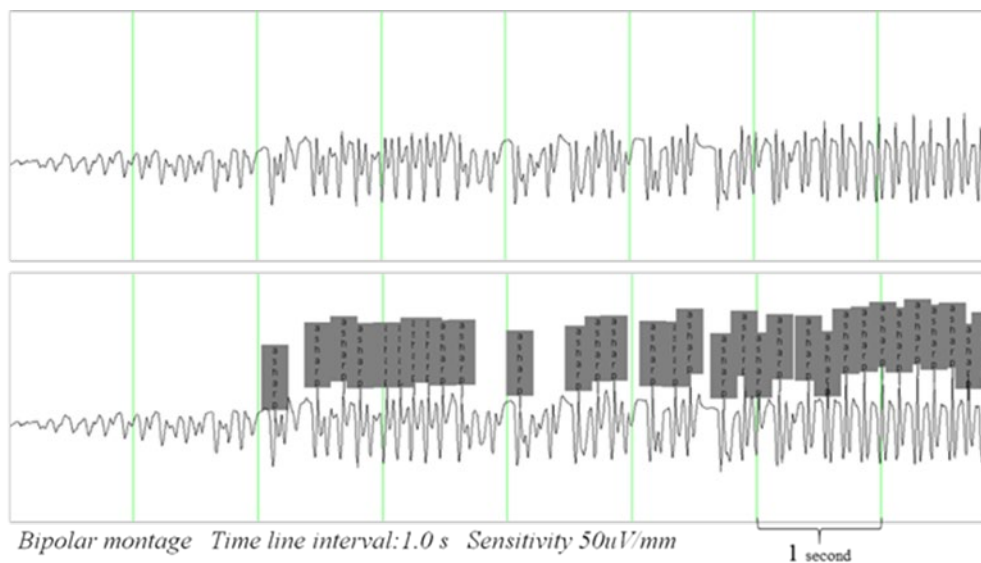
Figure 13. Example clipping of sharp events. A section of a seizure recording is shown twice: on top the unmarked recording and on the bottom, the recording showing sharp events (grey).

2.3 Statistical analysis

Differences in PLHG recruitment patterns were examined and the reproducibility of PLHG recruitment across the three seizures of each patient is shown by stating the proportion of PLHG recruited channels per seizure and patient. Reliability statistics of PLHG recruitment between seizures was calculated using Cronbach's alpha.

Next, to show PLHG recruitment and its relationship to another quantitative marker—sharp activity, occurrence of sharp activity before PLHG recruitment was analysed for the first 4 (early) and the first 8 (late) PLHG channels. These two groups (first 4 and first 8 PLHG channels) were chosen according to Weiss and colleagues (2015) stating that this distinction was quite arbitrary and that it was mainly based on the average SOZ size of 4.8±0.4 channels. The predictive relationship of sharp activity and PLHG recruitment was next investigated. Sensitivity, specificity, positive predictive value (PPV) and negative predictive value (NPV) were determined for sharp activity predicting PLHG recruitment.

Lastly, the overlap of PLHG channels with SOZ channels is analysed. The SOZ/PLHG overlap (SPO) is the proportion of PLHG channels included in the SOZ. This overlap is not only analysed for PLHG 4 and PLHG 8 as Weiss and colleagues (2015) presented, but for PLHG1–10. For example, PLHG1 means that only the first PLHG recruited channel for each seizure was included, which could add up to three channels. PLHG8 therefore included all channels recruited of all three seizures ≤PLHG8, meaning PLHG1 to PLHG8. The difference in SPO of the different numbers of PLHG recruited channels for good versus poor Engel outcome was tested using Wilcoxon rank sum test. Two approaches were used to analyse the difference in SPO in patients with good and poor Engel outcome. First, PLHG recruited channels were included without any restriction of occurrence in all three seizures of each patient (PLHG_a). Second, I included PLHG recruited channels, which were identified in at least two of the three seizures (PLHG_b).

2.4 Results

From 73 adult SEEG patients with medication-resistant epilepsy screened, 10 patients (mean age=34.5±10 years, range=24–53, 5 females) matched inclusion criteria and their SEEG recordings were included. Thirty spontaneous seizures lasting between 35–180s (mean 86.03±42.38s) were analysed. The number of depth electrodes implanted varied from 4–9 electrodes per patient (mean 7.1±1.6). iEEG was recorded from a total of 563 channels (mean 56.3±18.2 channels, range 25–85). Channels located in grey and white matter were included, but those located outside of the brain were excluded. Demographic information for the included patients is available in Table 4.

Table 4. Demographic details of SEEG patients.

ID	Age	Sex	Onset	MRI	Electrodes	hemi		Electrodes Location	Surgery	Engel
						R	L			
1	48	f	40	L H atrophy	8	4	4	RA, Ha, Hp, Insula & LA, Ha, Hp, I	L T neocort	III
2	24	m	3	PNH R trigone	5	5		RA, Hi, Hp, AN, PN	R SAH	II
3	53	f	28	normal	8		8	LA, H, Hp, ENT, T, OF, Ca, Cp	LSAH	I
4	44	m	adult	normal	6	3	3	RA, Ha, Hp and LA, Ha, Hp	L SAH	I
5	41	m	22	normal	8	6	2	RH, OF, SMAa, SMAp, Cp, I, LSMAa, SMAp.	no	
6	26	f	14	normal	9	9		RA, H, Hp, Im, OF, Ca, Cm, SMAa, SMAp	R OF	I
7	41	f	15	normal	4		4	LA, H, Hp, OF	L SAH	I
8	30	m	1.5	L supramarginal FCD	8	3	5	ROF, Ca, SMA and LOF, Ca, SMA, Pi, Tp	L F-T	III-IV
9	39	f	34	L post fusiform, para H cystic lesion	7		7	LA, Ha, Hp, LE, LEa, LL, Cp	L SAH	I
10	29	m		L inf F convexity PMG; L MTS	8		8	LA, Ha, Hp, Fp, OF, LEa, LEp, Ca	no	

Age & Onset: presented in years; MRI: lesion location on report; Electrodes: number of implanted electrodes; hemi = number of electrodes right vs left; Surgery: surgical resection performed; Engel: surgical outcome according to Engel classification (1993), Abbreviations: f = female; m = male; R = Right; L = Left; I = insula; Im = mid insula; H = Hippocampus; Ha = anterior hippocampus; Hp = posterior hippocampus; OF = Orbitofrontal; A = Amygdala; Ca = anterior cingulate; Cm = middle cingulate; Cp = posterior cingulate; SMAa = anterior SMA; SMAp = posterior SMA; Pi = inferior parietal; T = temporal lobe; Tp = posterior temporal; ENT = entorhinal cortex; LE = lesion; Lea = anterior of lesion; LEp = posterior of lesion; LL = lingual gyrus; F-T = fronto-temporal; Fp = frontal polar; PH = parahippocampus; PNH = periventricular nodular heterotopia; FF = fusiform gyrus; SAH = selective amygdalo-hippocampectomy.

2.4.1 PLHG recruitment in a cohort of SEEG patients and across their three seizures

In all 10 patients and their 30 seizures PLHG recruited channels were identified. Out of 1689 channels, 714 channels (42.3%) were PLHG recruited at some point during a seizure. Figure 14 illustrates the percentage of PLHG recruited channels versus not recruited channels for all 30 seizures. In 6 of these 30 seizures (20.0%) PLHG recruitment reached between 90–100%, which means that these seizures were presumably more widespread. The rest of the seizures showed a more focal PLHG recruitment. The average number of recruited PLHG channels per patient was 23.8±9.4 by seizure termination (range=6–54).
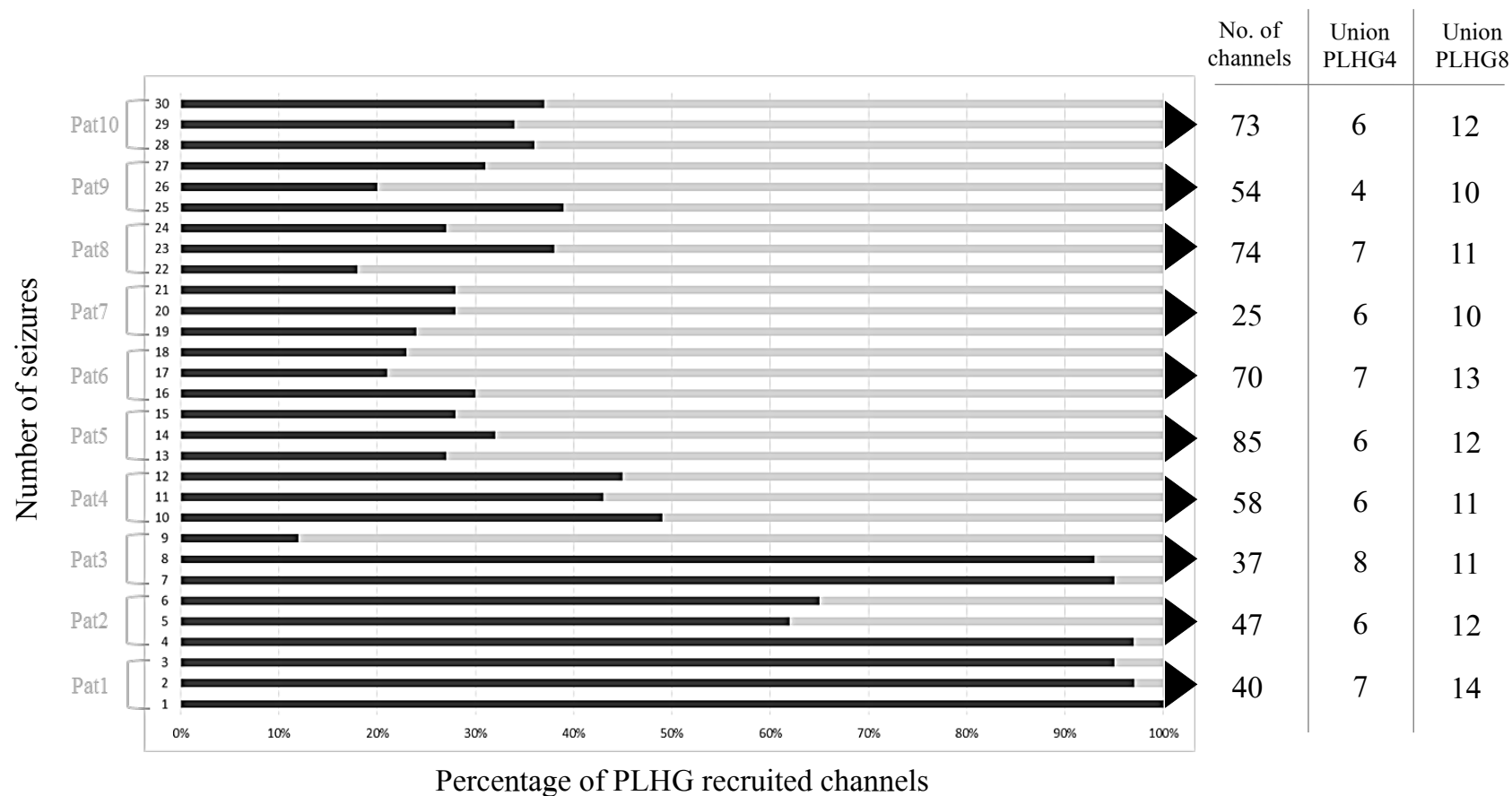
Figure 14. Proportion of PLHG recruited channels per seizure and patient. On the right the total channel number, the set union (= consists of all PLHG recruited channels, which are contained in either one, two or all three seizures) of PLHG recruited channels over all three seizures per patient for first 4 PLHG and first 8 PLHG is shown in grey.

Overall, there was good agreement (Cronbach's alpha=0.86) across the three seizures, but a few exceptions were noted. Two patients (Patient 2 and Patient 3) showed a different overall number of PLHG channels in one of their seizures. The first seizure of Patient 2 exhibited 12% of channels PLHG recruited compared to the other two seizures with 93% and 95% of PLHG recruited channels. The first seizure of Patient 3 showed 97% of PLHG channels compared to the other two seizures with 62% and 65% PLHG channels. To illustrate how many different PLHG recruited channels occur over all three seizures of a patient the set union is shown. The average set union for the cohort for 4 PLHG was 6.3±1.0 and for 8 PLHG 11.6±1.2. Patient 1, who has poor Engel outcome, shows the highest set union of recruited channels of all patients (see Figure 14).

2.4.2 Temporal and spatial relationship between sharp activity and PLHG recruitment

To investigate the relationship between PLHG recruited channels and channels showing sharp activity this section presents the occurrence of sharp activity before channels get PLHG recruited. The occurrence of sharp activity before the first 4 and the first 8 PLHG recruited channels is shown. Furthermore, sensitivity, specificity and predictive values explore how well sharp activity predicts PLHG recruitment in a temporal and spatial manner measured over all channels at seizure onset. For this analysis, I considered PLHG recruitment as the gold standard measure. Table 5 summarises results analysing all channels until the first 4 PLHG recruited channels and Table 6 sums up the results for the first 8 PLHG recruited channels.

Table 5. Predictive relationship of sharp activity and first 4 PLHG channel recruitment.

	4 PLHG	Not recruited	Total	Sensitivity	Specificity	PPV	NPV
Sharp activity	112	208	320				
No sharp activity	13	1356	1369	89.6%	86.7%	35.0%	99.1%
Total	125	1564	1689				

Table 6. Predictive relationship of sharp activity and first 8 PLHG channel recruitment.

	8 PLHG	Not recruited	Total	Sensitivity	Specificity	PPV	NPV
Sharp activity	196	241	437				
No sharp activity	39	1213	1252	83.4%	83.4%	44.9%	96.9%
Total	235	1454	1689				

The majority of PLHG recruited channels showed sharp activity before PLHG recruitment (PLHG4=89.6%, PLHG8=83.4%, all PLHG=56.7%). However, this proportion declines with a greater number of PLHG recruited channels considered, suggesting a greater accordance of these two measures at the beginning of a seizure.

Sensitivity and specificity of sharp activity predicting PLHG recruitment was high when including the first 4 and 8 PLHG channels. However, the positive predictive value (PPV) was low in both cases, indicating more widespread occurrence of sharp activity in relation to the PLHG defined seizure core. Nevertheless, the absence of sharp activity was a good predictor (high NPV) of lack of subsequent PLHG recruitment in a given channel.

2.4.3   Difference in SOZ/PLHG overlap (SPO) between good and poor Engel Outcome

In the following analysis, I accept the PLHG metric as the gold standard method to determine the resection area. I aimed to evaluate whether resected channels matched PLHG recruited ones and how this overlap differed between good and poor Engel outcome post-surgery. As the actual resection details were not available (no post-operative MRI co-registered with SEEG electrodes available to me), the working assumption here is that clinically defined SOZ channels were resected. Weiss and colleagues (2015) defined the first 4 PLHG channels as the most important ones in respect of resection and hence Engel outcome. He stated that his definition was quite arbitrary and that he mainly based it on the average SOZ size of 4.8±0.4 channels. Table 7 presents each patients' Engel outcome, the number of clinically defined SOZ channels, the mean time of recruitment for each patient and the percentage SOZ/PLHG overlap for recruited PLHG channels from 1–10. In order to estimate the potential dependence of the SOZ estimation from the temporal recruitment of PLHG channels, I included PLHG1–10 in my analysis, not only PLHG4 and PLHG8 as Weiss and colleagues suggested. I aimed to test which PLHG value best predicts post-surgical outcome and did not restrict my analysis to the arbitrary chosen values of 4 and 8. First, results of the set union approach of PLHG recruited channels (PLHG_a) is presented, which included PLHG recruited channels without any restriction of occurrence in all three seizures of each patient.

Table 7. Percentage of SOZ/PLHG overlap (SPO) and mean time of PLHG recruitment for each patient.(PLHG_a = PLHG recruited channels without any restriction of occurrence in all three seizures were included)

ID	Engel	SOZ	4 PLHG time	8 PLHG time	SOZ/PLHG overlap (SPO, %)									
					PLHG 1	PLHG 2	PLHG 3	PLHG 4	PLHG 5	PLHG 6	PLHG 7	PLHG 8	PLHG 9	PLHG 10
1	III	3	12.2±3.6	18.5±2.5	**50.0**	20.0	14.3	12.5	11.0	9.1	8.3	7.7	7.7	7.1
2	II	18	8.7±2.2	11.1±3.6	**100.0**	**100.0**	**100.0**	**83.3**	63.0	62.5	50.0	50.0	50.0	46.2
3	I	12	8.3±1.4	26.8±1.8	66.7	**80.0**	**80.0**	**80.0**	57.1	50.0	40.0	40.0	40.0	33.3
4	I	15	8.5±0.4	19.5±5.2	**100.0**	66.7	**80.0**	**80.0**	**71.4**	55.6.	50.0	38.5	35.7	35.7
5		27	4.7±1.0	9.2±2.6	-	-	-	-	-	-	-	-	-	-
6	I	12	16.1±7.9	34.6±10.1	50.0	50.0	50.0	57.1	50.0	36.4	33.3	28.6	28.6	26.7
7	I	6	13.7±5.6	44.3±12.5	**100.0**	**75.0**	**80.0**	**80.0**	57.1	44.4	44.4	40.0	40.0	40.0
8	III-IV	15	4.6±0.5	7.7±2.6	0.0	0.0	20.0	20.0	30.0	27.3	27.3	30.8	30.8	28.6
9	I	27	13.2±1.3	26.2±4.3	**100.0**	**100.0**	**100.0**	**100.0**	**83.3**	**77.8**	**70.0**	**72.7**	66.7	69.2
10		9	90.5±33.5	99.1±27.4	-	-	-	-	-	-	-	-	-	-

Engel: post-operative surgical outcome (J. Engel et al., 1993); SOZ: total number of clinically defined SOZ channels; 4 PLHG time: mean time in seconds until first 4 PLHG recruitment ± SD in seconds; 8 PLHG time: mean time in seconds until first 8 PLHG recruitment ± SD in seconds.

From the ten included patients, eight underwent surgery and had an Engel outcome documented. Six of these patients presented with good surgical outcome (Engel I & II), compared to two patients showing poor outcome (Engel III & IV). The average time of early PLHG recruitment after seizure onset was 10.0s (SD±5.3, range=3.3–19.2) and of late PLHG recruitment 29.7s (SD±27.7s, range=5.7–134.4) excluding Patient 10 who exhibited herald spikes and showed an average time of 90.5s and 99.1s, respectively. The number of clinically defined SOZ channels varied from 3–27 channels. There was no difference in the average time until PLHG4 and PLHG8 between patients with good and poor Engel outcome (n=8, p>0.1, Wilcoxon rank sum test).

To assess whether there is a difference between SPO in patients with good and poor Engel Wilcoxon rank sum test was performed. The boxplot below shows percentage of SPO for the first 10 PLHG recruited channels for patients with good and poor Engel outcome (Figure 15).
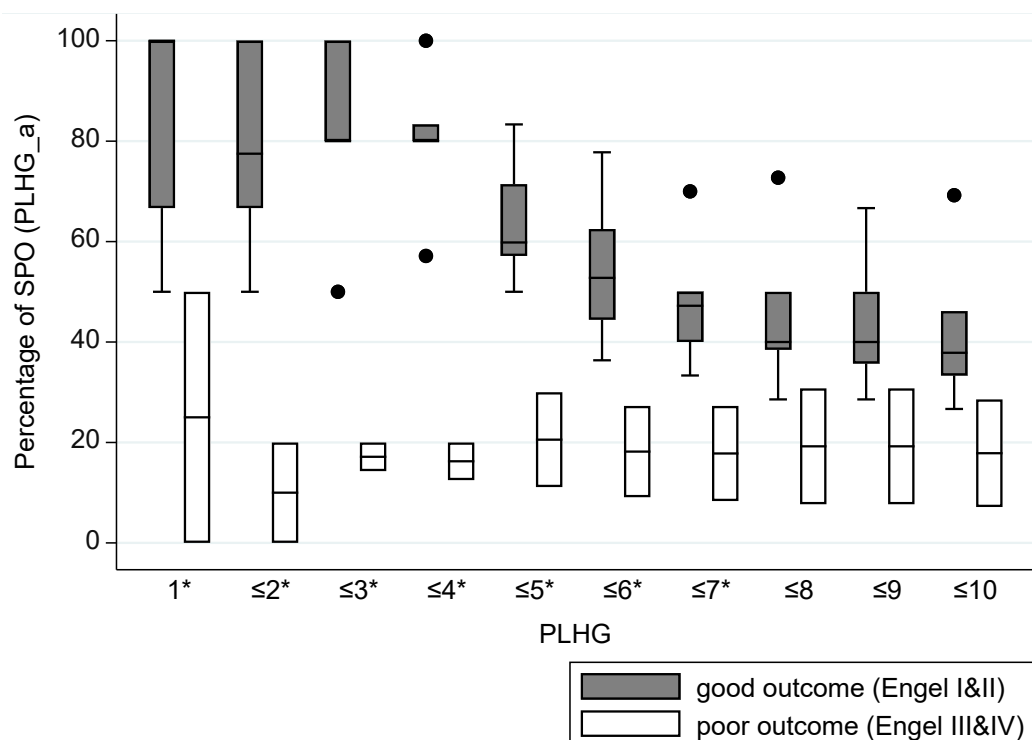
Figure 15. SPO for PLHG_a. Boxplot presenting percentage of SPO for patients with good versus poor Engel outcome for PLHG recruited channels 1–10 of PLHG_a. Significant difference with p<0.05 is marked with *.

Percentage of SPO of PLHG_a was significantly different between good and poor Engel outcome for PLHG1–7 (Figure 15, n=8, p<0.05, Wilcoxon rank sum test).

Significant differences according to seizure outcome was also observed for the second approach, PLHG_b (PLHG recruitment in at least two of the three seizures), including PLHG3–8. (see Appendix p.407–409, Figure 114 and Table 47, n=8, p<0.05, Wilcoxon rank sum test).

Weiss and colleagues (2015) repeated the analysis using a time-based criterion of PLHG identification, where all PLHG channels recruited within 30s after seizure onset were included. Next, I am replicating this analysis by analysing the overlap of PLHG recruited channels fulfilling the time criterion and fulfilling the criterion of being classified as SOZ channels (Table 8).

Table 8. Percentage of SPOtime and Engel outcome for each patient.

ID	1	2	3	4	5	6	7	8	9	10
Engel	III	I	I	I	-	I	I	III-IV	I	-
SPO_{time} (%)	100	100	75.0	100	44.4	100	100	100	55.6	100

Engel: post-operative surgical Engel outcome; SPO_{time} (%): PLHG recruited channels fulfilling the time criterion of 30s and overlapping SOZ.

This analysis showed no difference between patients with good and poor Engel outcome in respect of SOZ/PLHG$_{time}$ overlap (Table 8, n=8, p>0.05, Wilcoxon rank sum test).

2.4.4 Case studies

Here, I will present two patients in more detail. They represent the opposite ends of the seizure outcome spectrum: Case 1 showed good overlap between the PLHG metric and clinical assessment compared to Case 2, which showed poor overlap.

Case 1 (Patient 7)

Case 1 presents a 41-year-old right-handed woman whose seizures started at the age of 15. Her seizures manifested without an aura, with arrest of activity, mostly nocturnal, staring, intense chewing and postictal amnesia. She had no risk factors and her MRI was reported as normal. The ictal scalp EEG showed bilateral temporal rhythmic slow waves, more so on the left and no conspicuous interictal activity.

For SEEG investigation four electrodes were implanted in the left hemisphere. Brain areas implanted were the left amygdala (LA), anterior and posterior hippocampus (LH and LHp, respectively) and orbital frontal region (LOF). In total, fifteen seizures were captured. The seizures presented with a similar ictal onset, originating simultaneously from the hippocampal formation and amygdala, with a maximum in the anterior hippocampus.

The following Figure 16 illustrates the first 4 and 8 PLHG recruited channels, channels showing sharp activity during all three seizures and clinically defined SOZ channels.
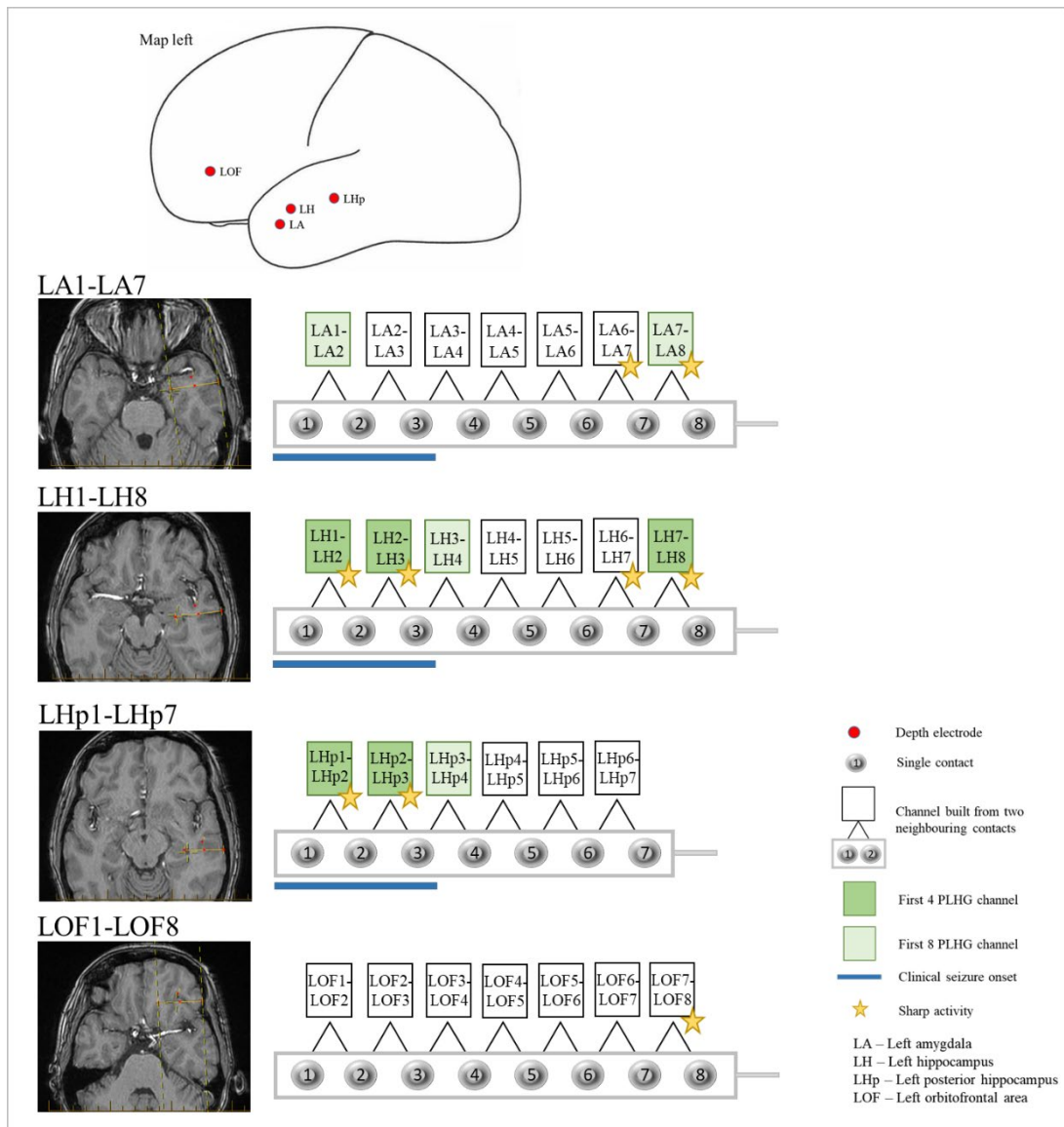
Figure 16. Case 1 summary. Patient with good post-surgical outcome is presented showing the left hemisphere with early and late PLHG recruitment, sharp activity and SOZ.

The main channels involved in the three seizures were the deepest contacts of the left anterior hippocampus electrode (LH1–3), to a lesser extent the deepest contacts of the left posterior hippocampus electrode (LHp1–3) and the deepest contacts of the left amygdala electrode (LA1–3). This patient underwent a left selective amygdalo-hippocampectomy, which led to an Engel class I outcome. Four of the five earliest PLHG recruited channels were defined in the clinical SOZ. Late recruitment overlapped with three more SOZ channels. The overlap of SOZ and PLHG recruited channels ranged from 40%–100%. Sharp activity, as automatically detected using a sharp detector, was more widespread and

activity overlapped with 100.0% of early PLHG channels and with 66.6% of late PLHG channels. This case illustrates an example where PLHG results pinpointed to the epileptogenic zone.

Case 2 (Patient 1)

Case 2 presents a 48-year-old woman, whose seizures started when she was 40 years old. Her seizures manifested with arrest of activity, oral and manual automatisms and vocalizations, post-ictal confusion, amnesia and no auras. The question of left hippocampal atrophy was raised by the MRI report. From scalp EEG the clinician described bilateral temporal interictal and left temporal ictal activity.

The patient had eight electrodes implanted for the SEEG monitoring, three in the right hemisphere and four in the left hemisphere. Brain areas targeted were the right and left amygdala, anterior and posterior hippocampus and insula. The SEEG investigation confirmed the presence of bilateral temporal lobe epileptogenicity. All seizures recorded, however, came from the left temporal lobe and showed a focal onset in the left posterior hippocampus (deepest contacts of electrode LP, LP1–LP2).

The following Figure 17 illustrates PLHG4 and PLHG8 recruited channels during all three seizures, the clinically defined SOZ channels and channels showing sharp activity.
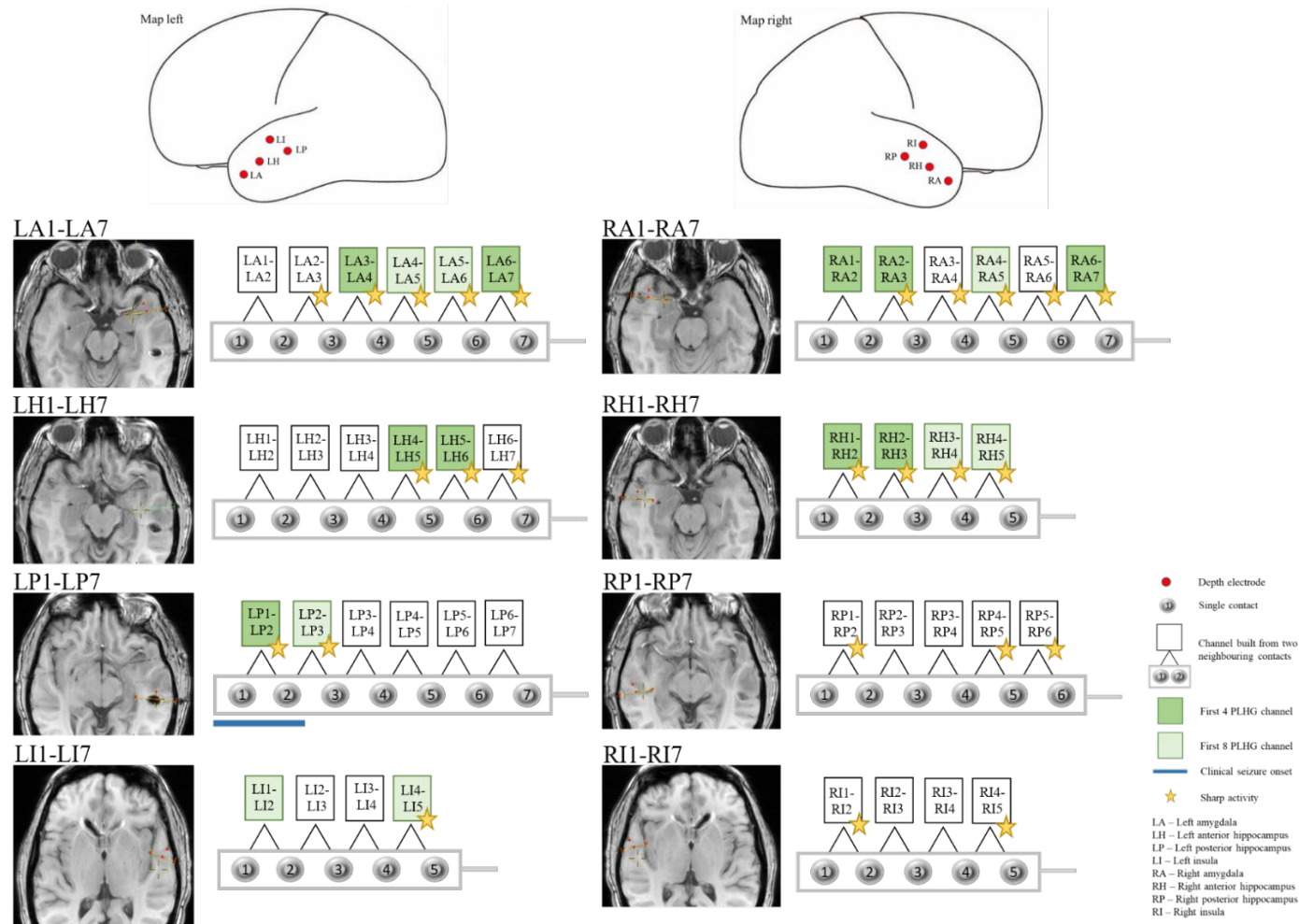
Figure 17. Case 2 summary. Patient with poor post-surgical outcome is presented showing implanted brain areas of left & right hemisphere, early and late PLHG recruitment, sharp activity and SOZ.

The surgical intervention was described as left temporal neocortical resection. No reasoning was reported to why this approach was chosen. After surgery, this patient showed Engel class III outcome. The agreement between the clinically defined SOZ and the detected PLHG channels was low (33%). Only, in one of the three seizures the PLHG metric marked the LP1–LP2 channel as one of the first 4 PLHG recruited channels. The rest of the PLHG recruited cannels did not fit with clinical assessment. They rather indicated lateral channels of left anterior hippocampus and amygdala electrodes and right amygdala and anterior hippocampus channels. A clinical decision was made to offer a second surgery. The second surgery took place one year later. This time a left selective amygdalo-hippocampectomy was chosen, which lead to an Engel class I outcome at 12 months post-surgery. This surgical resection did not show high agreement with the PLHG metric results either, as only lateral channels of these electrodes were PLHG recruited but not mesial ones. Sharp activity, as automatically detected using a sharp detector, was more widespread and activity overlapped with 90.0% of early PLHG channels and with 88.8% of late PLHG channels. This case illustrates an example where PLHG results did not pinpoint to the epileptogenic zone.

2.5 Discussion

The current study is the first to replicate the PLHG results published by Weiss et al. (2015). Weiss et al. argued that their PLHG metric could potentially improve SOZ localisation and hence surgical outcome.

The reasons for replicating the work of Weiss et al. are manifold. First, their study used HFO analysis. For the last twenty years, HFOs have been studied intensely and they are described as a promising biomarker for SOZ localisation (Akiyama et al., 2011; Haegelen et al., 2013; Jacobs, Zijlmans, Zelmann, Chatillon, Hall, Olivier, et al., 2010; Modur, Zhang, & Vitaz, 2011). Second, combining invasive HFOs with an advanced marker that emerged from testing neural firing patterns in microelectrode arrays is a promising approach. The combination of clinical iEEG and microelectrode arrays is mostly used in research and is not available in clinical practice. Hence, studying this combination of biomarkers with the outlook of facilitating clinical SOZ delineation was a motivator. Third, Weiss et al. offered to share their PLHG metric Matlab script. In today's data science era, it is important to independently replicate newly developed algorithms and test computational tools assisting the delineation of the EZ. The present work, unlike Weiss et al. (2015), used solely adult SEEG data and demonstrates that results from Weiss et al. (2015) can be replicated with these data, albeit in a small and selected sample. An analysis of the reliability of the PLHG metric suggests that there is a similar PLHG recruitment patterns across all three seizures. The measure can thus be considered reliable. By studying a second quantitative biomarker, sharp activity, which is used in clinical practice for SOZ identification, the study showed that these biomarkers show distinct temporal and spatial patterns in relation to the SOZ. The findings from this small sample are in line with the findings of Weiss et al. (2015), that resection of PLHG sites correlates with surgical outcome.

2.5.1 Reproducibility

Addressing Question 1: *Can PLHG recruitment be reproduced in a cohort of adult patients with SEEG implantation and a clinically defined focal SOZ?*

The design of this study differs in some respects from Weiss et al. (2015) with regard to the iEEG data used. Weiss and colleagues include patients with subdural grids and depth electrodes, but do not provide any information on their distribution. All their reported exemplary cases show subdural grid implantations. In contrast, the current study included depth electrodes only. Despite the likely different invasive evaluation methods used, results show that the PLHG metric shows similar characteristics of recruitment when using SEEG recordings. This is of interest as SEEG shows different coverage of the brain compared to subdural grids, it samples from deeper sources and covers limited gyral surface (Katz, Abel, & Abel, 2019; Podkorytova et al., 2016). Additionally, there is a widespread shift in practice with an increase in SEEG implantations (Gholipour, Koubeissi, & Shields, 2020), hence it is important to replicate the results of Weiss et al. (2015) in a cohort with SEEG recordings.

In all 30 seizures considered in this study, PLHG recruitment was detected using the PLHG metric developed by Weiss and group (Schevon et al., 2012; S. A. Weiss et al., 2013, 2015). Weiss et al. (2015) detected PLHG recruitment in all but two patients. Those two patients showed Engel outcome IV. The average number of PLHG recruited channels in this study is 23.8 compared to 21.0 described in Weiss et al. (2015). The average time of earliest recruitment in this study is 10.0 seconds after seizure onset compared to 14.2 seconds (S. A. Weiss et al., 2015). My findings indicate, though, that no association is observable between a longer lead in time and Engel outcome. There does not appear to be a consensus in the literature regarding seizure propagation times and outcome. One study is in agreement with the current results showing no association between slower seizure propagation times and better outcome (Spanedda, Cendes, & Gotman, 1997), while a few other studies assessing seizure

propagation found an association (W. Jung, Pacia, & Devinsky, 1999; Kim et al., 2010; Kutsy, Farrell, & Ojemann, 1999).

Addressing Question 2: *How reproducible is PLHG recruitment across seizures in each patient?*

With regard to reproducibility across seizures, like Weiss et al. (2015), I analysed three seizures in each patient. Only seizures with similar clinically defined onsets were considered for further analysis. This approach differs from Weiss and colleagues who included the first three consecutive seizures, including atypical seizures. In addition, in my study only seizures with a clinically defined focal seizure onset were included to ensure SOZ is clearly delineated. The reason for deviating from the strategy of Weiss et al. was to test whether the PLHG metric is stable and whether it results in similar recruitment patterns across seizures.

My results showed PLHG recruitment patterns with good agreement in all three seizures. Although the number of PLHG recruited channels might differ somewhat between seizures, nevertheless the overall PLHG pattern remained consistent. Even patients with poor Engel outcome showed similar PLHG recruitment patterns. It was thus shown that in adults the PLHG metric is stable across seizures of a specific type. These results allow proceeding to the next stage of testing seizures of different seizure types in future studies.

To sum up, although the design of the current study deviates in some respects from the original study set up by Weiss et al. (2015), it can be considered a design sufficiently similar to make replication plausible.

2.5.2   Temporal and spatial relationship of PLHG recruitment and sharp activity

Addressing Question 3: *What is the temporal and spatial relationship of PLHG recruitment and sharp activity?*

Ictal sharp activity was investigated together with PLHG recruitment as ictal biomarker for the SOZ as sharp activity is used to visually delineate the SOZ in clinical practice. Special interest lies in the co-occurrence of these two markers to evaluate whether PLHG recruitment can add information for SOZ delineation. Concerning the question of occurrence of sharp activity prior to PLHG recruitment, the results suggest that in all three analyses (first 4, first 8 and all PLHG channels) sharps were detected before the channel was PLHG recruited. This proportion declined with the number of PLHG recruited channels considered, suggesting a greater accordance of these two measures at the beginning of a seizure.

I conducted tests of sensitivity and specificity to evaluate the value of sharp activity preceding PLHG in predicting PLHG recruitment across all channels and seizures. This analysis showed that both sensitivity and specificity were high for sharp activity in predicting the early and late PLHG recruited channels. However, if we assume only having information about the occurrence of sharp activity to identify the seizure core (as defined here by PLHG recruitment) the results are less predictive. This was due to the low positive predictive value. Sharp activity was more widespread compared to PLHG recruitment. This is in line with previous work by Roehri and colleagues (Roehri et al., 2017) who demonstrated that the spatial extent of interictal epileptic discharges (IEDs), also called the irritative zone (Rosenow & Lüders, 2001), was typically more widespread and hence considered a poor marker of the epileptogenic zone. In their early work Penfield and Jasper (1954) already noted, that IEDs propagate from generating regions and that reliably differentiating the onset from the propagated IEDs seems impossible and needs further research. A similar conclusion was reached by Conrad and colleagues (2020) recently showing

significant spatial fluctuation of spike occurrence. While they could demonstrate that spikes localize seizure onset better than predicted by chance, they highlighted that temporal fluctuations in spike spatial distribution, particularly sleep and post-ictal related, can confound localization. They further argue that a longer IED sampling of at least 12 consecutive hours is commended, as this time was required to capture 80% of the variability in spike spatial distribution. My data, furthermore, suggest that channels free of sharp activity are unlikely to play any role in PLHG recruitment as indicated by a high negative predictive value.

In summary, while there is a close relationship between occurrence of sharp activity at seizure onset and PLHG recruitment, both metrics arguably capture different aspects of seizure evolution. This aspect would benefit from further study in the future.

2.5.3 Difference in SOZ/PLHG overlap between good and poor Engel outcome

Addressing Question 4: *Is the overlap of PLHG recruited channels with SOZ channels predictive of the post-surgical Engel outcome?*

In their final analysis, Weiss et al. (2015) focused on the early (first 4) PLHG sites because they had found that resection of such channels was superior as an outcome classifier to late-appearing PLHG. However, as their approach of choosing PLHG4 and PLHG8 was essentially arbitrary, I investigated not only these two time points but also the whole temporal spectrum of PLHG recruitment, ranging from 1 to 10. Furthermore, in addition to replicating Weiss' et al. (2015) criterion of including PLHG without any restriction of occurrence in all three seizures, I added one stricter criterion for SPO analysis to investigate whether this might add information and might show different predictiveness of surgical outcome. PLHG recruited channels were included, which occurred in at least two of the three seizures.

Despite the relatively small number of patients included in this cohort, both approaches show significant results, consistent across PLHG 3–7. The current findings thus partly confirm results shown by Weiss et al.: (i) they support that PLHG 4 is of particular—though not exclusive—importance. SPO is significantly different between good and poor Engel outcome in the expected direction. (ii) In addition, my findings show that PLHG 3 and 5–7 are superior to late appearing PLHG. This supports the concept that the region initially invaded by the seizure, the core area, is of greatest interest for epilepsy surgery compared to late invaded regions. (iii) Introducing the stricter criterion, including channels, which show the same recruitment in at least two seizures, does not lead to a narrower PLHG recruitment pattern.

To check the adequacy of their arbitrarily chosen definition of early PLHG, Weiss et al. (2015) repeated their analysis using a time-based criterion of PLHG identification. This was set within 30s after seizure onset. Unlike Weiss et al. (2015), I could not find significant correlation of this time-based criterion with outcome. This might be due to the fact that my results showed not only PLHG 4, like Weiss et al. (2015) but PLHG 4–7 as being most predictive for good outcome.

Overall, including PLHG recruitment information could benefit surgical decision-making, however, the SPO results should be interpreted in light of a difference in design of the current study and that of Weiss et al. (2015). For my study, postsurgical MRI coregistration of resected channels was not available. Therefore, SOZ and PLHG overlap (SPO) was investigated and SOZ channels (identified by an experienced epileptologist) were treated as a proxy of resected channels. In contrast, Weiss et al. (2015) analysed the overlap of PLHG contacts and the resection cavity delineated in postoperative MRI. The SPO approach taken in the current study seems justifiable as SOZ channels are generally considered essential for seizure initiation and are identified for the sole purpose of resection. In some cases, though, SOZ channels may not be resected: for example, if SOZ channels are located in eloquent areas and cannot be resected

without leading to functional loss. In cases such as this, in which resection would impact functional outcome, the surgical team might decide to leave SOZ-identified areas in the brain.

The following Chapter 3 will show that in a different sample of (paediatric) patients, the overlap between SOZ and resection was 81.2%, meaning 81.2% of channels that were clinically defined as SOZ were surgically removed. I would assume that the corresponding overlap in this current adult sample is higher, as the paediatric cohort included more complex epilepsy cases. To sum up, this study used SPO as a proxy of resection. This could have led to an underestimated predictiveness of PLHG with regard to the surgical outcome, meaning that PLHG might be even more predictive of the outcome had it been calculated based on data from actual resections.

2.5.4   Reflections on the methodology

Addressing artefact removal: Artefacts were identified by visual analysis in a bipolar montage with the support of an experienced scientist. In contrast, Weiss and colleagues (2013, 2015) used Independent Component Analysis (ICA) to eliminate artefacts. ICA is a method for identifying underlying components in a set of signals and for separating signals into spatially and temporally distinguishable components (Tharwat, 2018). It is frequently used in EEG research to decompose EEG signal from artefacts.

For this study, I also incorporated ICA using the EEGLAB software and toolbox (Delorme et al., 2011) on our data, however, after careful consideration decided to not use it, but instead use visual artefact detection using a bipolar montage. The reason for not using ICA was the uncertainty of whether identified ICA components would only contain artefacts or would also contain physiological signals. In some EEG recordings it was obvious which components had to be deleted to eliminate artefacts from the recording while in some EEGs it was very difficult to rule out that deleted ICA components would also contain seizure

related information (see Appendix p.398–406, Figure 106 to Figure 113 for details). It was thus advisable to err on the side of caution. It should be mentioned that there is not one correct or gold standard way to reject artefacts. Artefact rejection ranges from manual rejection and discarding entire EEG segments to automated artefact elimination via image processing algorithms (Radüntz, Scouten, Hochmuth, & Meffert, 2015). Both ICA and manual classification require the rater to have experience and knowledge for decision making. Furthermore, in some cases, due to very active interictal recordings only two or sometimes even one baseline segment could be found and was used as reference for the PLHG analysis of all three seizures. It was observed during pre-processing and analysis that the baseline segment used had a considerable effect on PLHG recruitment. A rather active baseline segment could lead to less PLHG recruitment and vice versa. This is an important factor to consider when using the PLHG metric and might warrant further investigation in the future.

In summary, the different artefact rejection method used compared to Weiss et al. (2015) did most likely not have any substantial effects on the results of this current work. However, caution should be taken when choosing the baseline segments for PLHG recruitment analysis.

2.6 Limitations and future consideration

The results of the current study should be interpreted in light of some limitations discussed in the following section.

The retrospective nature and the small sample size are the main limitations. Patients were carefully selected according to technical criteria and availability of seizures with similar onset patterns. To ensure that the SOZ was clinically well defined and that the PLHG recruitment patterns were comparable only focal seizure onsets where included compared to widespread seizure onsets. This study only analysed seizures of the same type. It might be important to include more than one seizure or seizure type for each patient, and to obtain PLHG information

for the whole range of seizure types. Not including all seizure types of a patient and taking only a few seizures of a patient into consideration is a general issue faced in SOZ localisation, leading to a selection bias, and hence makes it difficult to draw conclusions (Mehvari-Habibabadi et al., 2017). The relatively small sample size means that statistical tests could be biased towards the null hypothesis, e.g., the failure to replicate the significant relationship between Weiss' et al. time-based criterion of PLHG and outcome.

In addition, this cohort only included SEEG patients; hence, a comparison of implantation methods (grids versus depth electrodes) could not be incorporated. This might be a worthwhile endeavour for future studies.

Due to being a visiting researcher at the MNI, I was not granted full access to all clinical data, like surgical details and post-operative imaging. Therefore, information for resected contacts could not be verified by me. Here, SOZ data was thus used as proxy for resected channels. However, surgical resection data is important for discussing outcome data (Jacobs et al., 2018, 2010b; N. E. C. van Klink et al., 2014) and for making assumptions and drawing conclusions about the correlation of the extent of resected PLHG channels and channels showing spikes and the patient's Engel outcome. Hence, for the subsequent study (see Chapter 3) it was essential to have access to surgical resection data.

A further limitation was that channels located in white matter were not excluded from my analysis. This may have led to inflated values of specificity and NPV as the number of channels without sharp events and without PLHG recruitment might have been higher than the current results lead to believe. However, in terms of PLHG recruitment and sharp activity per se including white matter channels did not lead to any biased results, as no brain activity is recorded from contacts located in white matter.

To conclude, this was the first study aiming to replicate results from Weiss and colleagues (2015) using their PLHG metric. Furthermore, this was also the first study to investigate PLHG recruitment in a cohort of patients with exclusively

SEEG implantation. I showed that the PLHG metric is a potentially valuable quantitative method in identifying the seizure onset zone. However, it is not yet known if this also applies to paediatric patients with a different range of underlying pathologies. In the next chapter, I will examine this issue in a larger cohort of paediatric patients, with a focus on whether PLHG recruitment is a predictor of postoperative seizure outcome.

3 Phase-Locked High Gamma for Seizure Onset Zone Detection in a Paediatric Cohort - GOSH study

3.1 Introduction

The approach to epilepsy surgery differs in children compared to adults not only in the type of surgery offered but also in the number of each procedure carried out and the pathologies patients present. Neuronal migrational disorders, epilepsy syndromes and extratemporal epileptogenic foci are more common in children than in adults, with malformations of cortical development (39.3%), tumours (27.2%), and hippocampal sclerosis (15%) being the most frequent paediatric pathologies for epilepsy surgery (Blumcke et al., 2017). A European survey on trends in epilepsy surgery between 2008 and 2015 showed that extratemporal surgeries increased over time and in 2015 were the most common procedures performed. Hemispheric and multilobar surgeries remained stable over time and unilobar temporal surgeries significantly decreased (Barba et al., 2020). In contrast, in adults temporal lobe epilepsy is the most common type of medically intractable epilepsy and hence, temporal lobe resection the leading procedure (Téllez-Zenteno & Hernández-Ronquillo, 2012). As pathologies, complexity of epilepsy and resection volumes differ from the adult population the question whether surgical outcome results from adult research are applicable to the paediatric population has to be raised.

In the following, I will first lay out the rationale for exploring ictal phase-locked high gamma (80–150Hz; PLHG) in the paediatric population, next the rational for focusing on fast ripples, present the aims of this study before describing the two methods I used to analyse the data and finally summarise the results of this project.

3.1.1　Rational for exploring PLHG in a paediatric cohort

In the paediatric population, achieving seizure freedom is critical to prevent developmental arrest or regression. In the paediatric cohort, like in the adult patient group discussed in the previous chapter, there is a need for identifying biomarkers aiding delineation of the epileptogenic zone. The implementation of the PLHG metric in an adult group with refractory epilepsy lead to an improved outcome classification and combining PLHG with SOZ information enhanced accuracy (S. A. Weiss et al., 2015). Galanopoulou and Moshé (2011) questioned the transferability of biomarkers identified in adults to a paediatric cohort, due to their immature brains and continuous evolvement until adulthood. As an example, they mentioned the evolving behavioural manifestations of early life seizures, which start as unique types of seizures (e.g. infantile spasms) and subsequently change into focal-onset or generalized seizures seen in older patients. To my knowledge, there are no studies reporting PLHG results in paediatric patients with medication-resistant epilepsy, nor are there any independent replications in adults, apart from my pilot study reported in Chapter 2. The aim of this study was to apply the PLHG metric on iEEG data of children and adolescents and investigate the use of this biomarker in a paediatric cohort. For a detailed synopsis of the PLHG metric and its background, I would like to refer to the previous chapter (Sections 2.1 and 2.2).

3.1.2　Rational for focusing on fast ripples

HFOs have been proposed as a promising biomarker of the EZ (Cho et al., 2014; Haegelen et al., 2013; Jacobs et al., 2012; Kerber et al., 2014; N. E. C. van Klink et al., 2014). The focus of this study on fast ripples (>250Hz) instead of both fast ripples and ripples (80–250Hz) derives from previous research. Ripples were shown to occur in both normal areas, where they are associated with memory processing (Axmacher et al., 2008) and pathologic brain regions of epilepsy patients, while FRs are believed to reflect neuronal substrates of epileptogenic cortex. Furthermore, FRs are closely linked to seizure onset areas (Akiyama et

al., 2011; Crépon et al., 2010; Usui et al., 2011; Wu et al., 2010), and in addition occur relatively independent of lesional changes (Jacobs et al., 2009). Especially, in patients with mesial temporal atrophy and nodular heterotopia results showed that FRs were more closely linked to the SOZ than to the lesion (Jacobs et al., 2009). When focussing on paediatric research, multiple studies linked resection of FR-generating cortex to good postoperative seizure outcome. Research on intraoperative HFOs has focused on FRs in ECoG, especially in pre-resection ECoG, and concluded that removal of tissue with FR is linked to seizure freedom (Hussain et al., 2017; Hussain, Mathern, Sankar, & Wu, 2016; van 't Klooster et al., 2015, 2017; Wu et al., 2010). The Utrecht group demonstrated that a higher rate of residual FRs occurred in patients with recurrent seizures than in patients who reached seizure freedom. This could not be shown for residual ripples, spikes or even ictal spike patterns (van 't Klooster et al., 2015). Furthermore, they showed that the best post-surgical outcome predictor is the presence or absence of FRs after resection, given the presence of FRs before resection (van 't Klooster et al., 2017). Hussain and colleagues (2017) compared FRs to other abnormalities observed during intraoperative ECoG, like focal slowing, paroxysmal fast activity, intermittent spike discharges, continuous epileptiform discharges, focal attenuation, and intraoperative seizures. In comparison with these other abnormalities, FRs appear to be superior biomarker of the EZ. Similarly, extraoperative ECoG studies showed that incomplete removal of HFOs, especially FRs, was strongly linked to poor surgical outcome (Akiyama et al., 2011; Hussain et al., 2016; Okanishi et al., 2014).

3.1.3　　　Study aims

1. Is the resection of the clinically defined SOZ predictive of post-surgical outcome?

2. Is the resection of brain areas exhibiting FRs predictive of post-surgical outcome?

3. Can PLHG recruitment be reproduced in a cohort of paediatric patients with either SEEG or subdural electrode implantation and a clinically defined focal SOZ?

4. How reproducible is PLHG recruitment across seizures in each patient?

5. Is resection of channels showing PLHG recruitment predictive of post-surgical Engel outcome?

6. Does the overlap of epileptogenic zone defined by SOZ, FR or PLHG with surgical resection better predict post-surgical outcome?

3.2　Methods

3.2.1　　　Patient selection

I retrospectively identified consecutive paediatric patients (≤18 years of age) with a diagnosis of medication resistant focal epilepsy who underwent pre-surgical invasive EEG monitoring at Great Ormond Street Hospital for Children (GOSH) as part of their clinical assessment between July 2012 and April 2018. The hospital ethical review board gave permission for this study. Cases were identified by searching the clinical neurophysiology databank for invasive patients and further looking through each patient's recorded intracranial EEGs to check if seizures matched set inclusion criteria. Inclusion criteria were defined as follows: 1) three clinical or/and electrographic seizures, 2) focal seizure onset 3) seizure duration ≥35s, 4) minimal artefacts in iEEG recording 5) neurosurgery. Sampling rate of the included recordings was up to 1000Hz. The current recommendation in HFO literature, which is derived from the Nyquist

sampling theorem, states that a sampling rate used for recording should be at least three times the upper frequency of interest in order to avoid aliasing (Zijlmans et al., 2017). Aliasing leads to a frequency misrepresentation of the recorded activity as the insufficient sampling rate leads to loss of data and to lower frequencies than the actual waveform (Lyons, 2011). Recordings with artefacts affecting all channels were excluded. If artefacts occurred in single channels, which were not included in the seizure onset, those recordings were included.

3.2.2   Clinical information

The following information from the medical notes was gathered for all patients included in this study: demographics, age at onset of epilepsy, clinical examination results, duration of epilepsy, previous surgical treatment information, type of iEEG (SEEG or subdural grids), age at iEEG, imaging findings, neurophysiological findings, where applicable, surgical resection details, post-surgical outcome and post-surgical MRI to confirm the extent of the resection.

3.2.3   Invasive EEG recordings

Like in the MNI study, electrode placement was individually planned and was based on clinical history, seizure semiology, results of surface EEG, neuroimaging and neuropsychological testing. Electrode configurations included both subdural grid electrodes (⌀ 4.0mm outer ring, ⌀ 2.3mm inner ring) with 10mm centre-to-centre spacing, and semi-rigid depth electrodes (⌀ 0.8mm and comprised 5, 8, 10, 12, 15 or 18 contacts per electrode of 2mm length, 3.5mm apart, Dixi, Besançon, France, number of contacts depending on the target region). The multidisciplinary SEEG team chose the invasive electrode positioning according the hypothesized origin of seizures.

Intracranial EEG was recorded using Xltek (Natus, USA) system, which allowed a simultaneous recording of maximum 256 channels. The iEEG was sampled at 1024Hz. For SEEG recordings two contacts located in white matter were chosen as ground and reference. For subdural grid recordings, the ground and reference channels were either two strip contacts placed further away from the main grid or two grid contacts.

3.2.4 Classification of contacts

Clinical neurophysiologists (Dr S. Boyd, Dr F. Moeller, Dr R. Thornton, Dr R. Pressler and Dr K. Das) defined the SOZ, the area showing the first ictal activity during iEEG recordings. SOZ localisation was determined for clinical purpose and independently from this study.

To define the position of implanted SEEG electrodes/contacts and resection cavity, preoperative T1 MRIs were co-registered to postoperative T1 MRIs using FSL (Oxford, UK). Images were manually reviewed by the neurosurgeon (Mr M. Tisdall) to identify contacts within the resection cavity (Greve & Fischl, 2009; Jenkinson, Bannister, Brady, & Smith, 2002; Jenkinson & Smith, 2001). For patients with subdural grids, intraoperative photographs, iEEG notes and reports were used to identify resected contacts.

3.2.5 PLHG metric

Data preparation

Like in the previous chapter (Section 2.2.1), for each patient three seizure recordings and three baseline recordings were used. The seizure onset was determined by visual video EEG review by the neurophysiologist reporting the invasive. Baseline recordings were 30s interictal segments clipped prior to the seizure. A relatively silent epoch with a limited number of interictal discharges was used. Ideally, each seizure had its own baseline recording.

Recording blocks with excessive artefacts were excluded. If single channels showed artefacts and these channels were not recording from the seizure onset zone only these artefactual channels were excluded.

Dealing with amplifier saturation artefacts

In some of the included EEG recordings a so-called saturation artefact occurred, a square cut like artefact that happens when the amplifiers are saturated, suggesting that a particular electrode is loose. These clipped waves appear as square topped waves with vertical sides of variable duration (Light et al., 2010). This artefact prevented the PLHG metric to run correctly. Hence, to smooth this artefact, I implemented a Matlab code written by Dr R. Rosch, called 'artefact_fix' (see Appendix p. 415).

The square cut like artefact leads to sharp edges between recorded neural oscillations and flat periods. To smooth these sharp edges a period of about ten seconds of EEG recording prior to the artefactual segment was taken, baseline corrected and used to replace the artefactual part. To avoid further artefact occurrence due to introducing new edges, a gradual passage from the original recording to the new signal is built, at both the beginning and the end of the new segment. The 'artefact-fix' code was used for one patient and all three seizures. None of the channels fixed where involved in the seizure onset.

Detection of PLHG recruited channels

For a detailed description of the PLHG metric developed by Dr S. Weiss (2013, 2015) see the previous chapter under Section 2.2.5.

Manual thresholding

As described in Section 2.2.5, in order to get information about PLHG recruited channels, the PLHG metric calculates high gamma thresholds for each seizure independently. This threshold is based on the PLHG value, which is fixed to a mixed Gaussian model with one or two Gaussians. Either PLHG value distribution could be unimodal or bimodal and positive goodness of fit values

(GOF) reflect adequate fit. The model fit is an automated process, run using the PLHG metric Matlab script. However, in case both models fit poorly, manual thresholding was implemented. Figure 12 in Section 2.2.5 illustrates an example for a good model fit. The following Figure 18 presents a sample seizure with a poor model fit and manual thresholding.

A

B
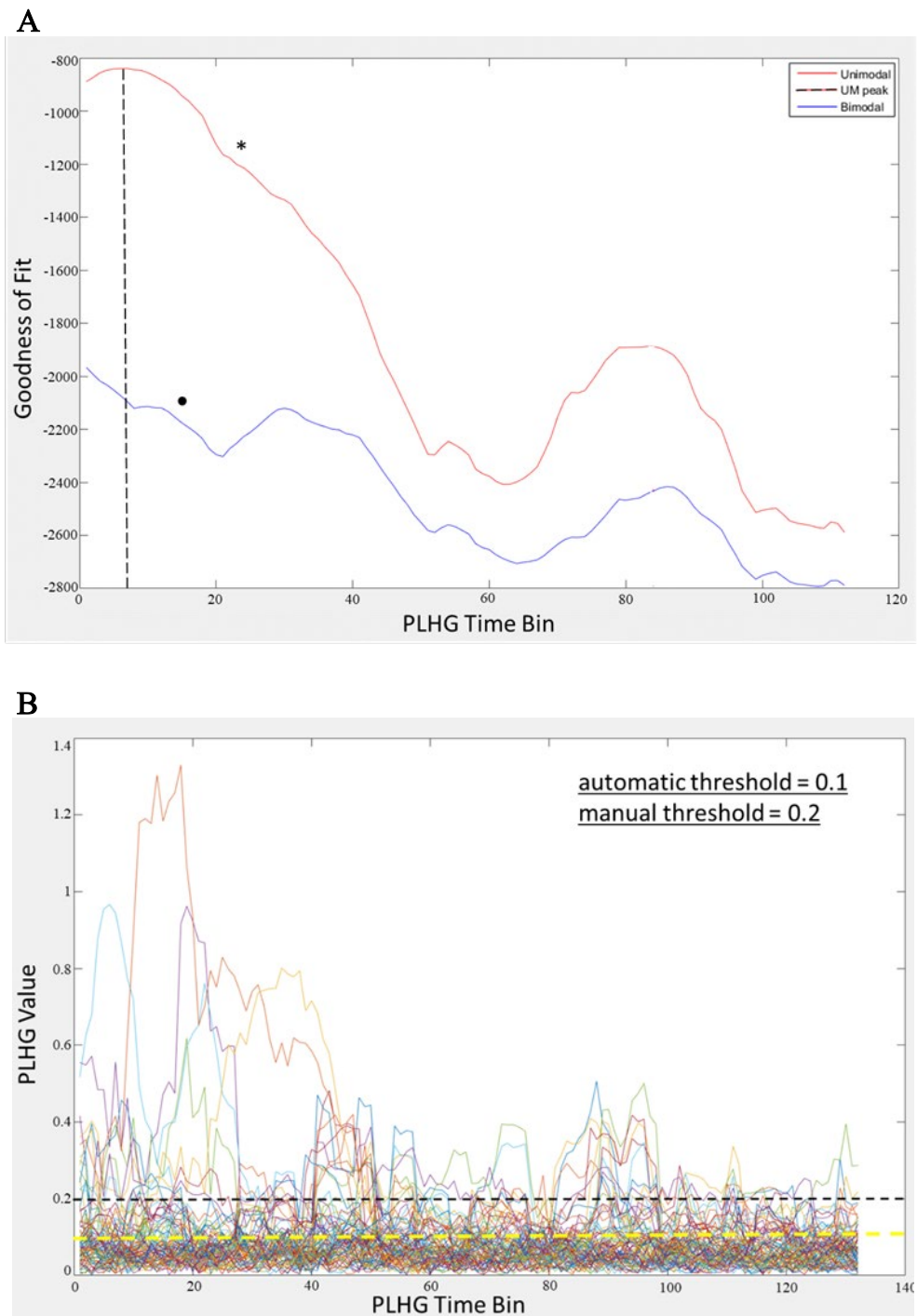
Figure 18. Sample seizure with poor model fit. A. Goodness of fit plot for unimodal (red, *) and bimodal (blue, ●) Gaussian model. Both models did not fit, as the local maximum is negative (at bin 17, green line). **B.** PLHG values for a seizure where both models failed and the threshold was selected manually. Automatic threshold (yellow dashed line) lies in PLHG value background activity and allows more channels to be recruited and recruitment time starts earlier. Manual thresholding is chosen as twice the automatic value (black dashed line) as suggested by Weiss et al (2015).

3.2.6 Automatic fast ripple detection

For the automatic detection of interictal HFOs, the detector developed by Akiyama and colleagues was used (Akiyama et al., 2011). This detector was built to extract ripples (80–200Hz) and fast ripples (200–300Hz). In this study, I focused on fast ripples (FR) only. First, a high-pass filter at 200Hz (16th order FIR) was implemented, followed by calculating the Hilbert transform, the envelope curve of the filtered EEG.

The period for FR detection in the invasive EEG was taken from slow-wave sleep, as highest rates of HFOs occurred in slow-wave sleep (Bagshaw et al., 2009; Staba et al., 2004). Sleep segments were chosen with the help of electromyography electrodes, recorded video and the Compressed Spectral Array channel. For each patient, FRs were detected during non-rapid-eye-movement (NREM) sleep using a bipolar montage. Ten epochs of 2-min interictal EEG during NREM sleep were chosen, remote from each other and from seizures by at least 1 hour (Akiyama et al., 2011). Furthermore, segments from the first night of invasive monitoring were avoided, which is standard procedure for marking interictal HFOs. The aim of using a higher number of shorter epochs compared to few long epochs is to ensure to capture the variability of the EEG during the recording period.

3.3 Statistical analysis

Good versus poor surgical outcome

Postoperative seizure outcome was determined according to Engel's classification (J. Engel, 1993b) at >12 months after surgery with good and poor outcome defined in two different ways for this study. First, like Weiss and colleagues (2015) Engel class I and II (seizure free and rare disabling seizures, respectively) was classified as good outcome and Engel class III and IV (worthwhile improvement or no improvement, respectively) as poor outcomes. In the following sections, this is referred to as 'analysis Engel A'. Second, for a more stringent criterion, only Engel class I was considered as favourable in contrast to all other outcomes (Engel class II-IV). This is further referred to as 'analysis Engel B'.

SOZ and surgical outcome

The decision of whether a channel was defined as SOZ channels was described above. In clinical practice, knowledge about the SOZ is usually used to predict surgical outcome. We calculated whether removing SOZ channels results in good outcome compared to not removing these channels. SOZ channels were classified as removed and non-removed regardless of factors like not removing channels due to e.g. being localised in eloquent areas or frequency of seizures generated from each SOZ in case of multiple SOZs in a patient.

The overlap of channels showing both SOZ association and surgical resection (SOZ/Resection overlap = SRO) was calculated and a Wilcoxon rank sum test was used to compare this percentage overlap between patients with good outcome versus patients with poor outcome.

FR and surgical outcome

To calculate whether the majority of FR-generating sites were removed during surgery, I used methods described by Jacobs and colleagues (Jacobs et al., 2018, 2010a). I calculated FR rates as the occurrence of FR per unit of time (average

of 10 x 2min segments) in removed and non-removed contacts, and the number of removed and non-removed contacts with FRs regardless of FR rates (i.e., the extent of tissue showing FRs). This will be explained in the following paragraphs.

I investigated whether high rates of HFOs are indicative of epileptic areas. Therefore, like Jacobs et al (2010a) I calculated a ratio between rates of FRs in removed contacts and FRs in non-removed contacts.

$$Ratio\ Rate_{FR} = \frac{\sum_{RemCh} Rate_{FR} - \sum_{NonRemCh} Rate_{FR}}{\sum_{[RemCh, NonRemCh]} Rate_{FR}}$$

where RemCh are the channels that were removed and NonRemCh are the channels that were not removed.

This ratio identifies the relationship between FR rates in removed contacts compared with FR rates in non-removed contacts. A value between 0.1 and 1.0 identifies patients in whom the majority of FRs have been removed, whereas a value between -0.1 and -1.0 indicates that the majority of FRs remained untouched. A value around zero indicates a similar total amount of FRs that were removed and that remained untouched. I expected patients with values around +1 for FRs to have good outcome and patients with values around -1 to have poor outcome.

Second, I analysed the extent of removed FR channels regardless of the rate, reflecting the spatial extent of the FR-generating area that was removed. I calculated the ratio between the number of removed and non-removed channels showing FRs as follows:

$$Ratio\ Channs_{FR} = \frac{\#ChannRem_{FR} - \#ChannNonRem_{FR}}{\#ChannRem_{FR} + \#ChannNonRem_{FR}}$$

Where #ChannRem is the number of removed channels with FRs and #ChannNonRem is the number of non-removed channels with FR.

Third, I calculated the association of resected areas showing FRs with post-surgical Engel outcome like Akiyama and colleagues (2011). Compared to the two previous FR analyses presented, channels were here only included if they showed high rate FR rate of >1/min. Resected channels showing FRs (FR/Resection Overlap = FRO) were included in the analyses.

A Wilcoxon rank sum test was used to compare the two ratios as well as percentage of FRO in patients with good versus patients with poor Engel outcome.

PLHG recruitment and surgical outcome

First, differences in PLHG recruitment patterns were examined and the reproducibility of PLHG recruitment across the three seizures of each patient is shown by stating the proportion of PLHG recruited channels per seizure and patient. Reliability statistics of PLHG recruitment between seizures was calculated using Cronbach's alpha.

The seizure stereotypy was further analysed using the Levenshtein distance, a measure of the difference in channel sequence (S. A. Weiss et al., 2015). The Levenshtein distance between two strings is the number of single character deletions, insertions, or substitutions required to transform one string into the other. Here, instead of individual characters, I am comparing whole strings (EEG contact labels). Levenshtein distance is then normalised by dividing through the maximum length of a sequence and this is further averaged. Next, a null distribution is generated for each patient where channels are selected randomly and compared using the Levenshtein distance. Z scores for both patient Levenshtein distance and normal distribution Levenshtein distance are calculated and a t-test is calculated for all patients against the null hypotheses (that the sequence of recruited channels is not stereotypical and normally distributed).

Second, I adopted similar measures as in the previous chapter (see Section 2.3), where no resection data was available and the PLHG metric was accepted as gold standard method to determine the resection area. The aim for this analyses as in the previous chapter was to evaluate the overlap of PLHG recruited channels with clinically defined SOZ channels (PLHG/SOZ overlap = PSO) and the association of this overlap with Engel outcome after surgery.

Third, the overlap of PLHG channels with the resection volume was analysed (PLHG/Resection overlap = PRO). PSO and PRO were not only analysed for early and late PLHG recruitment (PLHG 4 and PLHG 8, respectively). Like in the previous chapter, the overlap was analysed sequentially from bins PLHG1 to PLHG10. For example, bin PLHG1 means that only the first PLHG recruited channel for each of the three seizures was included, which could add up to at least three channels. At least three channels, because multiple recruited channels could show the same recruitment time and that led to including all of them into this bin. Bin PLHG2, therefore, means the first and the second channels recruited of all three seizures were included, meaning PLHG1 to PLHG2 ($\leq$PLHG2), and so on. The difference in the percentage overlap of PLHG recruited and SOZ channels (PSO) and PLHG recruited and resected channels (PRO) for the different numbers of PLHG recruited channels was tested for patients with good versus poor Engel outcome using the Wilcoxon rank sum test.

Two approaches were used to analyse the differences in percentage of PSO and PRO in patients with good and poor Engel outcome. First, PLHG recruited channels were included without any restriction of occurrence in all three seizures of each patient (PLHG$_{any}$). Second, I included only those PLHG recruited channels, which were identified in at least two of the three seizures (PLHG$_{two}$).

Two- and three-stage analyses

The surgical target zones investigated in this study were the SOZ (clinical gold standard), and as experimental measures the FR zone and the PLHG zone. They were used to test whether their resection or resecting a proportion of these zones was associated with good or poor postsurgical outcome. The sets of zones allowed several combinations, which are illustrated and defined in Figure 19.
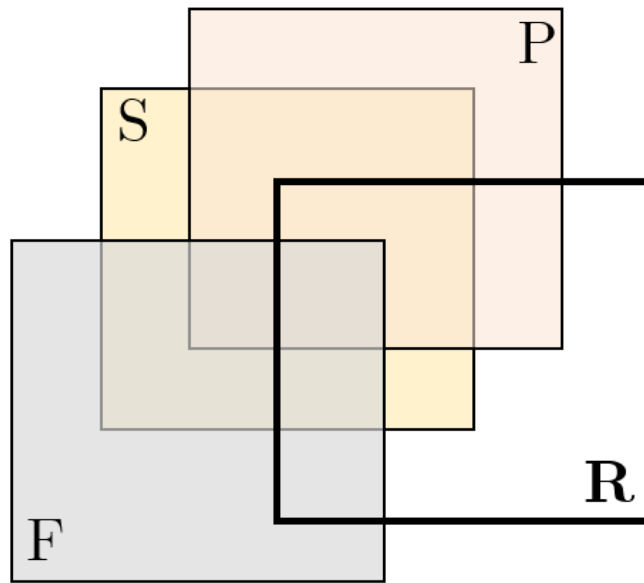
Figure 19. Introduction of investigated zones. S = channels defining the SOZ, P = PLHG recruited channels, F = channels showing fast ripples, R = resected channels, S∪F = resected channels that show SOZ and/or FR, S∪P = resected channels that show SOZ and/or PLHG, S∪P∪F = resected channels that show SOZ and/or PLHG and/or FR.

First, I tested whether the 2-stage analyses using the clinically defined SOZ and the two experimental measures individually would improve accuracy of post-surgical outcome classification. Hence, I asked whether combining SOZ and PLHG information and SOZ and FR information would improve outcome accuracy. A union approach was used to calculate the percentage overlap between these zones. This was done for SOZ and PLHG (S ∪ P) and SOZ and FR (S ∪ F). For S ∪ P resected channels showing PLHG and/or SOZ

association were included. For S $\cup$ F resected channels showing PLHG and/or FR association were included. These analyses, hence, included a broader area of channels.

Second, to combine all three biomarkers, a 3-stage analysis was done including resected channels showing PLHG and/or SOZ and/or FR association (S$\cup$P$\cup$F). Again, a union approach was used to calculate the percentage overlap between these three zones. The difference in the percentage overlap of all zone combinations was tested for patients with good versus poor Engel outcome using the Wilcoxon rank sum test.

Regarding FRs, for all analyses in this section (like Akiyama and colleagues (2011)), I included contacts with high-rate FRs, which were defined by a FR rate of >1/min (equivalent to >20 FRs per channel during 10x2min segments).

Again, two approaches were used to analyse the differences in percentage of overlap between the various zones for patients with good and poor Engel outcome. First, PLHG recruited channels were included without any restriction of occurrence in all three seizures of each patient (PLHG$_{any}$). Second, I included PLHG recruited channels, which were identified in at least two of the three seizures (PLHG$_{two}$).

Third, receiver operating characteristic (ROC) curves were constructed for the SOZ, FRs and area overlap tests for 25%, 50%, 75% and 100% resected cut-off values. True positives, defined as the proportion of patients with good outcomes with correctly classified contacts for each test were plotted against false positives, defined as the proportion of patients with poor outcomes with correctly classified contacts for each test. The quality of outcome classification was assessed using area under the ROC curve (AUROC).

3.4　Results

3.4.1　　Patients

From 89 patient records screened, 66 patients underwent surgery and from those 21 surgical patients were included in this study. A summary of demographic and clinical information of included patients is available in Table 9. The patients mean age was 11.2 years (±4.7, range=3.8–18.7 years, 10 females). Five patients had non-lesional and 16 patients had lesional epilepsy, which was based on MRI findings and not on post-surgical histology. The most prevalent abnormality was focal cortical dysplasia (FCD, 7 patients, 43.8%), followed by tuberos sclerosis (TS, 4 patients, 25.0%), hippocampal abnormality (HC, 2 patients, 12.5%) and subtle abnormalities (3 patients, 18.8%).

Six patients had subdural grids with or without additional depth electrodes or strips implanted and 15 patients had stereotactically implanted electrodes. All subdural grids used had 48 contacts. Furthermore, all grid patients had additional depth electrodes implanted, on average 1.5 electrodes (±0.5, range 1–2) with an average of 4.9 contacts (±1.5, range 4–8). Five grid patients (83.3%) had additional strips implanted, on average two strips (±0.7, range 1–3) with an average of 5.1 contacts (±1.8, range 2–8). SEEG was recorded from an average of 11.3 implanted electrodes (±3.9, range 4–17) and an average of 85.7±40.3 contacts per patient. Four patients underwent previous iEEG monitoring and surgery (ID3, ID6, ID7, ID22), and the data presented here relate to the second surgery.

Twelve of the surgical patients had Engel outcome class I (57.1%), three patients Engel class II (14.3%), three patients Engel class III (14.3%) and three patients Engel class IV (14.3%). The mean follow-up time post-surgery was 14.0 (±4.8, range 6–24) months. Figure 20 illustrates the screening process of iEEG patients considered for study inclusion.
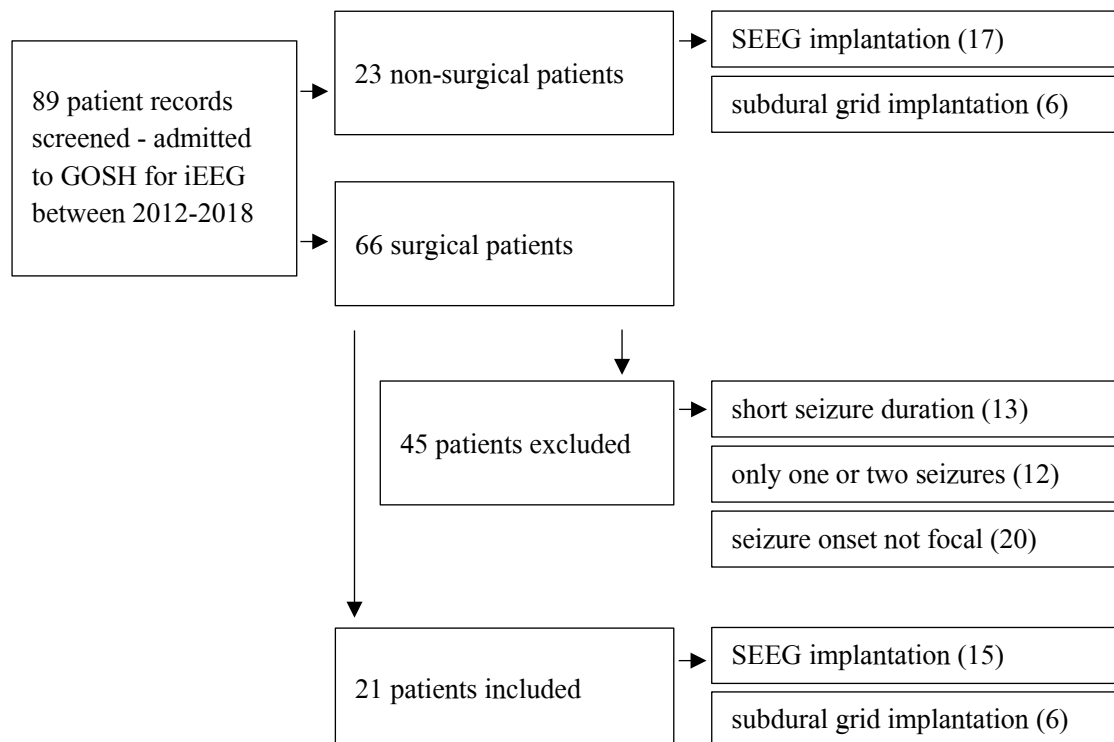
Figure 20. Patient inclusion tree.

In total, 63 spontaneous seizures lasting on average 96.6s (±50.8s; range 35–204s) were analysed. Contacts located in white matter and outside of the brain––as visualised on co-registered electrodes on MRI images using the imaging platform 3D slicer (https://www.slicer.org/) were excluded from further analysis (Fedorov et al., 2012).

Seizures included showed various types. Thirteen patients had only one habitual seizure type (61.9%) and hence this was included in further analyses. Six patients showed more than one seizure type (28.6%). In five of these patients, several seizure types were included while in one patient only one seizure type was used for analyses. Two patients presented with subtle clinical and a few electrographic seizures only (9.5%). Table 10 summarises seizure types of the included patients.

Table 9. Demographics & Clinical Information.

ID	Age	Sex	Onset	MRI	iEEG	Side	Surgery	Follow up	Engel
1	5.5	m	0.003	L F FCD	SEEG	L	Redo L F opercular and insula	12	IIIa
2	14.0	f	2	lesion negative	SEEG	R	R SM and insula resection	12	Ia
3	9.9	m	0.008	small R hemisphere, myelin immaturity	SEEG	R	R TPO disconnection, insular resection	12	IIb
4	14.3	m	4.42	L FCD	grid	L	L P F resection	12	II
5	7.6	m	3.41	lesion negative	SEEG	R	R P lesionectomy, ECOG motormapping	6	Ib
6	6.0	f	2.42	TS, multiple tuber	grid	R	R P tuber resection	12	IV
7	5.3	m	1	multiple tuber, TS	SEEG	L	L ant T lobe resection	12	Ia
8	18.4	f	1	L HC sclerosis, L P FCD	SEEG	L	L T lobe resection	12	Ia
9	18.6	f	7	lesion neg, possible L P abnorm sulcation	SEEG	L	L ant T lobectomy and AHE	14	IIb
10	9.2	f	0.12	L P extending to P Operculum FCD	SEEG	L	L P resection	12	Ia
11	17.2	f	7	lesion negative	SEEG	R	R ant lobe resection	12	Ia
12	14.9	m	2.5	bilateral HC sclerosis	SEEG	B	R ant T lobe resection	12	III
13	5.0	f	0.17	L STG FCD	SEEG	L	L T lesionectomy	12	Ia
14	7.6	m	5	subtle R temporal lobe abnormalities	SEEG	R	R ant T lobe resection	12	IIIa
15	12.5	f	0.67	TS, multiple tuber & L HC abnormality	SEEG	L	Resection of L F & P tubers	12	Ia
16	6.5	f	0.003	R FCD	SEEG	R	Redo R F lesionectomy	24	IVa

Continued

ID	Age	Sex	Onset	MRI	iEEG	Side	Surgery	Follow up	Engel
17	12.0	f	5	R FCD	grid	R	R CP cortical resection	24	IV
18	3.8	m	0.08	multiple tuber L P, TS	grid	L	L P tuber resection	24	Ia
19	10.7	m	0.15	lesion negative	SEEG	R	Thermocoagulation & Laser ablation	12	Ia
20	17.7	m	0.003	Gliotic changes L postC	grid	L	L postC gyrus lesion resection	12	Ia
21	16.1	f	12	L SFG FCD	grid	L	L SFG gyrus resection	21	Ia

Age & Onset: are presented in years; MRI: lesion location on MRI report, Side: hemisphere implanted; Surgery: surgical resection performed; Follow up: in months; Engel: post-operative surgical outcome according to Engel classification (Engel, 1993); Abbreviations: f = female, m = male, B = bilateral, L = left, R = right, P = parietal, T = temporal, F = frontal, postC = post central, SFG = superior frontal gyrus, STG = superior temporal gyrus, FCD = focal cortical dysplasia, TS = Tuberous sclerosis, HC = hippocampus.

Table 10. Different seizure types and number of patients.

Seizure types	No of patients (n=21)	IDs
Patients with habitual seizures	13	1,3,4,5,8,10,11,12,13,16,17,18,19
Patients with several seizure types - similar onset, different propagation	4	2,9,14,21
Patient with several seizure types, majority type used	1	15
Patient with several seizure types, only one had clinical features	1	20
Patients with subtle & electrographic seizures	2	6,7

3.4.2 Using SOZ for outcome prediction

For the SOZ analysis, all 21 surgical patients were included. These patients had a clinically defined SOZ, underwent epilepsy surgery and had an Engel outcome description (Table 11). The mean percentage of SOZ resection was 81.3% (range=16.7–100%).

Association of SOZ/Resection Overlap and Engel outcome

Here, I tested the association between SOZ/Resection overlap (SRO) and surgical outcome. The hypothesis was that surgical removal of SOZ contacts leads to good post-surgical outcome. Results however show that there was no significant difference between the percentage of SRO in patients with good (n=15) versus poor (n=6) surgical outcome (p>0.1, Wilcoxon rank sum test; Figure 21). SOZ and surgical resection information for each patient is summarised in Table 11.
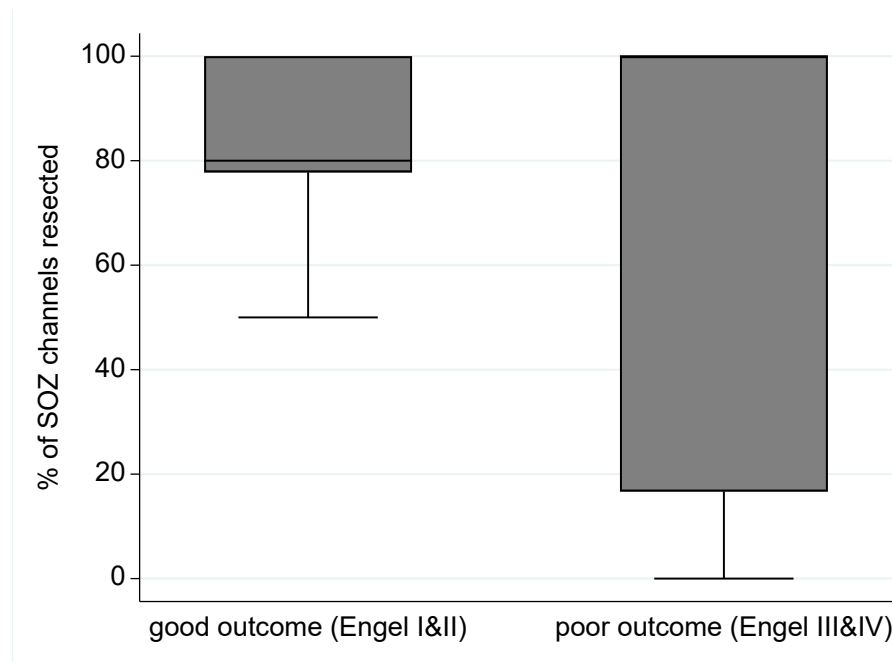
Figure 21. Boxplot of percentage of SRO for patients with good versus poor outcome.

110

Table 11. Patients with a clinically defined SOZ and epilepsy surgery.

ID	MRI	SOZ channels	SOZ resected	Surgery	Limitations	Engel
1	L F FCD	6	1	Redo L F opercular and insula	2nd surgery, motor	IIIa
2	lesion negative	10	8	R SM and insula resection		Ia
3	small R hemisphere, myelin immaturity	5	4	R TPO disconnection, insular resection	2nd surgery	IIb
4	L FCD	5	5	L P F resection	motor	II
5	lesion negative	5	5	R P lesionectomy, ECoG motor mapping	motor	Ib
6	TS	2	2	R P tuber resection	tuber network	IV
7	TS	10	5	L ant T lobe resection		Ia
8	L HC sclerosis & L P FCD	9	9	L T lobe resection		Ia
9	lesion neg, L P abnorm sulcation	12	11	L ant T lobectomy and AHE		IIb
10	L P extending to P operculum FCD	18	14	L P resection		Ia
11	lesion negative	2	2	R ant lobe resection		Ia
12	bilateral HC sclerosis	1	1	R ant T lobe resection	bilateral pathology	III
13	L STG FCD	4	4	L T lesionectomy		Ia
14	subtle R T lobe abnormalities	2	2	R ant T lobe resection		IIIa
15	TS & L HC abnormality	10	8	Resection of L F and P tubers	tuber network	Ia
16	R FCD	2	2	Redo R F lesionectomy	2ns surgery, motor	IVa
17	R FCD	1	0	R CP cortical resection	motor	IV
18	TS, multiple tuber L P	5	5	L P tuber resection		I
19	lesion negative	8	5	Thermocoagulation & Laser ablation		I
20	Gliotic changes L postC	4	3	L postC gyrus lesion resection		I
21	L SFG FCD	5	4	L SFG gyrus resection		I

MRI: lesion location on report; Surgery: resection details; Follow up: in months; Engel: surgical outcome according to Engel classification (J. Engel, 1993b); SOZ channels: from six patients with poor surgical outcome five showed a small SOZ area with 1–2 SOZ channels (83.3%). Patients with good outcome (n=15) only once showed a SOZ area comprising of less than four channels (6.0%). The maximum number of SOZ channels was 18 in this group. Abbreviations: f = female, m = male, R = right, L = left, P = parietal, T = temporal, F = frontal, CP = centroparietal, postC = post central, SFG = superior frontal gyrus, STG = superior temporal gyrus, FCD = focal cortical dysplasia, TS = Tuberous sclerosis, HC = hippocampus.

For analysis 'Engel B' results also did not show significant difference between SRO in patients with good (n=12) versus poor (n=9) surgical outcome (p>0.1, Wilcoxon rank sum test).

3.4.3 Fast ripples

Patient inclusion and surgical outcome

Nineteen of the 21 surgical patients were included in FR analysis. Two patients with subdural grids were excluded, because of low sampling rate (512Hz; ID20, 21). From the 19 included patients for FR analysis, two patients did not show any FRs (ID14, 19). From the 17 patients showing FRs, 15 had SEEG implantations and two had subdural grid electrode implantations. Clinical details are given in Table 11 and Figure 22 illustrates the inclusion and exclusion of patients for the FR analysis for this study.

Twelve of the surgical patients had good (Engel I&II) post-surgical outcome and five had poor (Engel III&IV) outcome. Both patients who did not exhibit FRs had SEEG implantations. One of them was lesion negative (ID19) and underwent thermocoagulation and laser ablation and showed a good post-surgical outcome with Engel class I. The second patient (ID14) had subtle right temporal lobe abnormalities, underwent a right anterior temporal lobe resection and showed poor outcome with Engel class IIIa. Both had a right-hemisphere implantation regime.
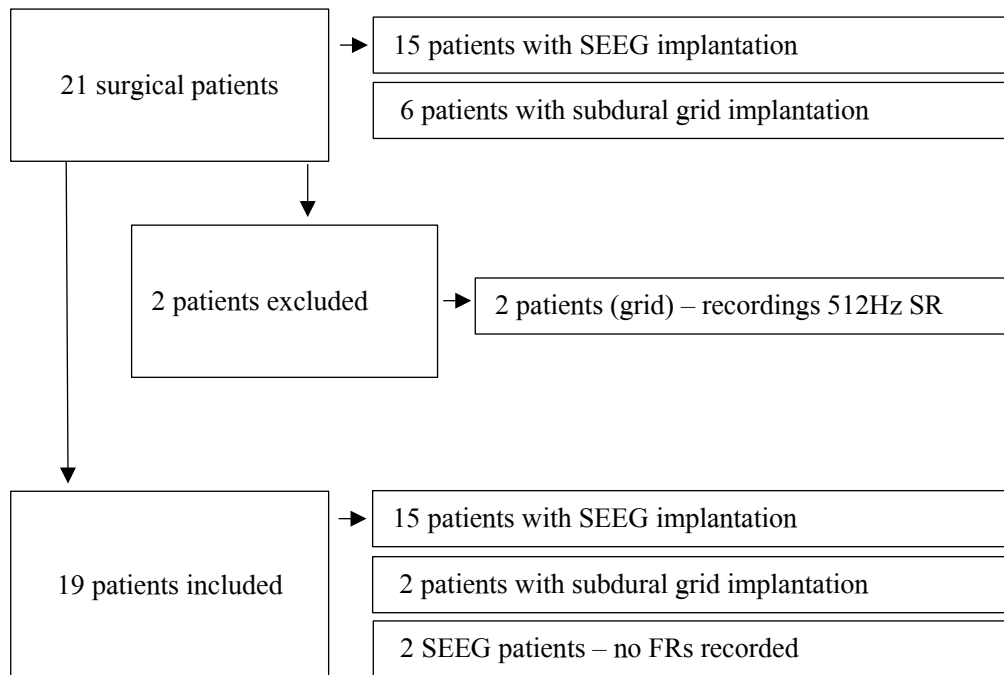
Figure 22. Inclusion tree of patients for the FR analysis. Abbreviation: SR = sampling rate

Association of FR rates and number of contacts showing FRs with Engel outcome

In a first step, I quantified FR rates in removed and non-removed contacts, and next the number of removed and non-removed contacts with FRs regardless of FR rates.

Table 12 presents patient's FR rates and number of channels with fast ripples in removed and non-removed channels, FR ratio rate and FR ratio channels as described in Section 3.3.

Table 12. FR Ratio Rate and Ratio of number of channels with FRs.

ID	FR Rate RemCh	FR Rate NonRemCh	No of RemCh$_{FR}$	No of NonRemCh$_{FR}$	FR Ratio Rate	FR Ratio Channs	Engel
1	0.34	4.99	0	1	-0.87	-1.00	3
2	44.33	40.71	6	9	0.04	-0.20	1
3	2.21	0.69	1	0	0.52	1.00	2.5
4	8.17	13.50	1	2	-0.25	-0.33	2
5	4.70	1.08	2	0	0.63	1.00	1.5
6	15.08	18.93	3	6	-0.11	-0.33	4
7	0.00	16.21	0	5	-1.00	-1.00	1
8	143.11	36.39	13	4	0.59	0.53	1
9	163.45	16.61	11	6	0.82	0.29	2.5
10	7.56	2.41	2	1	0.52	0.33	1
11	3.94	4.24	3	1	-0.04	0.50	1
12	9.33	0.69	2	0	0.86	1.00	3
13	172.76	7.18	7	2	0.92	0.56	1
14	-	-	-	-	-	-	3
15	6.85	30.27	2	5	-0.63	-0.43	1
16	537.16	406.19	14	11	0.14	0.12	4
17	4.68	9.33	2	2	-0.33	0.00	4
18	133.88	261.06	8	16	-0.32	-0.33	1
19	-	-	-	-	-	-	1

Abbreviations: RemCh = removed channels, NonRemCh = non-removed channels, RemCh$_{FR}$ = removed channels showing FRs, NonRemCha$_{FR}$ = non-removed channels showing FRs; Engel: 1 = class I; 1.5 = class Ib, 2 = class II, 2.5 = class IIb, 3 = class III, 4 = class IV.

Summaries for each individual patient and their total FR count including rejected and accepted FRs are summarised in the appendix (p.411–412; Figure 115 and Figure 116).

Next steps included testing the association between FR rates and ratio of FR channels in removed and non-removed contacts and surgical outcome. The hypothesis was that surgical removal of contacts with high FR rates and high FR channel ratio lead to good post-surgical outcome. Results show that there was evidence for a higher mean FR ratio (good: 0.15±0.58, poor: -0.06±0.57) and a higher mean FR channel ratio (good: 0.16±0.59, poor: -0.04±0.65) in patients

with good (n=12) compared to those with poor surgical outcome (n=5), however the difference was not significant (p>0.1; Figure 23).
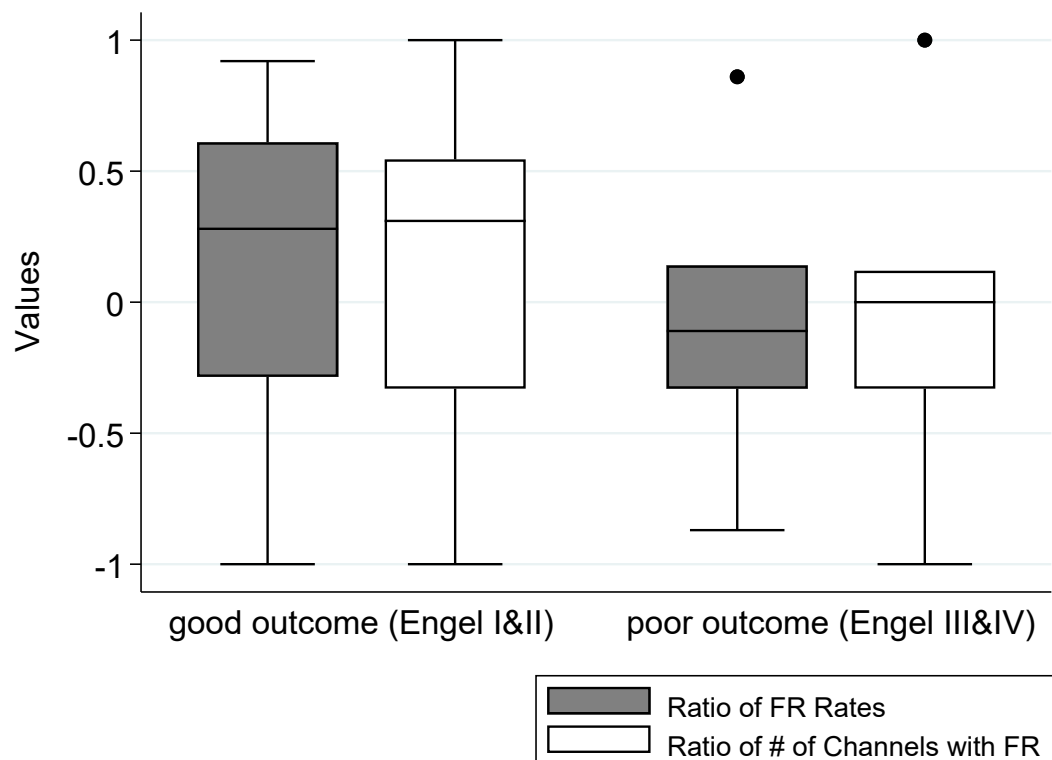
Figure 23. FR ratio & ratio of number of channels with FR in patients with good versus poor outcome.

The outlier in both analyses in the poor outcome group is ID12, who had a bilateral SEEG implantation regime and Engel outcome class III after a right anterior lobe resection. However, despite the poor Engel outcome the patient showed both a high ratio of FR rate (0.86) and a high ratio of number of channels with FRs (1.00). A year after the surgical intervention, the temporal lobe seizures decreased, however, the patient continued to have several vacant episodes almost daily. Auras were unchanged from pre-surgery, which in the preoperative invasive recording were shown to arise from either the right or left amygdala and still presented with repetitive swallowing, gulping or burping. This patient is further discussed in Section 3.4.8.

When excluding the outlier from the analysis results still showed no significant differences between good and poor outcome for both ratios (FR ratio: 0.15±0.58,

-0.30±0.37, respectively; FR channel ratio: 0.16±0.59, -0.30±0.44, respectively; p>0.1).

For analysis 'Engel B' results showed no significant differences for both ratios between patients with good versus poor surgical outcome (p>0.1). This was also true when excluding the outlier ID12 from the analyses (p>0.1).

Association of FR/Resection Overlap (FRO) and Engel outcome

Here, I calculated the association of resected areas showing FRs with post-surgical Engel outcome like Akiyama and colleagues (2011) to further analyse combinations of overlap which are presented later in Section 3.3 Figure 19. There was evidence for a higher percentage of FRO (good: 0.58±0.29, poor: 0.48±0.33) in patients with good (n=13) compared to those with poor surgical outcome (n=6), however, the differences were not significant (p>0.1; Wilcoxon rank sum test, Figure 24).
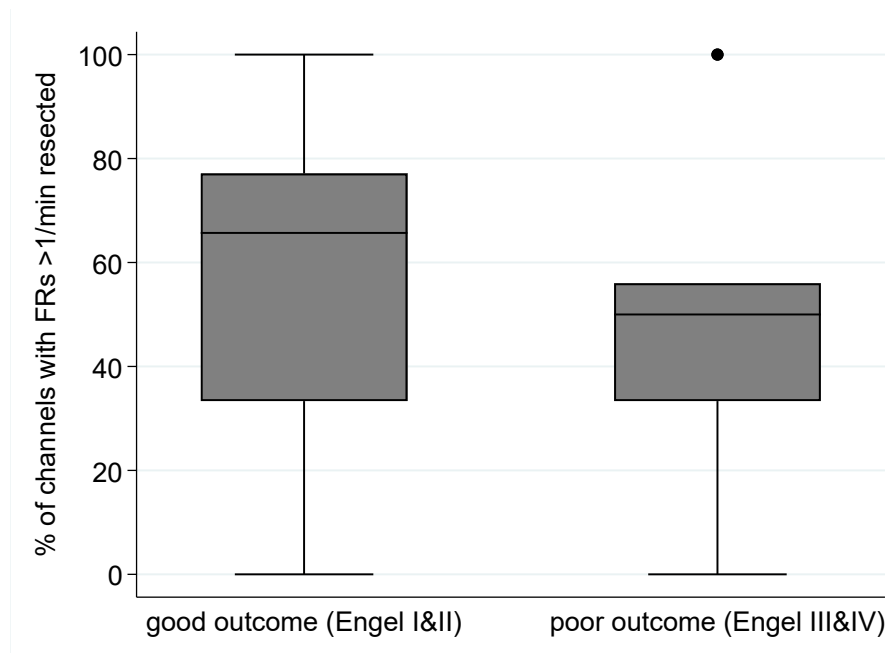
Figure 24. Percentage of resected channels with FRs >1/min comparing patients with good versus poor Engel outcome.

The outlier in the poor outcome group is again ID12 (see previous FR analysis). When excluding the outlier from the analysis results still show no significant differences between good and poor outcome for FRO (good: 0.58±0.29, poor: 0.35±0.22, respectively, p>0.1).

When using only Engel class, I as good post-surgical outcome results show no significant differences between patients with good versus poor surgical outcome (p>0.1). This is also true when excluding the outlier ID12 from the analyses (p>0.1).

3.4.4 PLHG metric and surgical outcome

Reproducibility of PLHG recruitment

PLHG recruitment was identified in all 21 patients. In total, 1726 channels were included. Three seizures of each patient were analysed and 1192 channels (23.0%, calculated for 3 x total channel number) were PLHG recruited at some point during a seizure. The average time of earliest PLHG recruitment was 15.6s after seizure onset (±14.1; range 3–51.0s). The average number of recruited channels was 23.1 (±20.5; range 1–80 channels). Figure 25 illustrates the percentage of PLHG recruited channels for all 21 patients and 63 seizures.
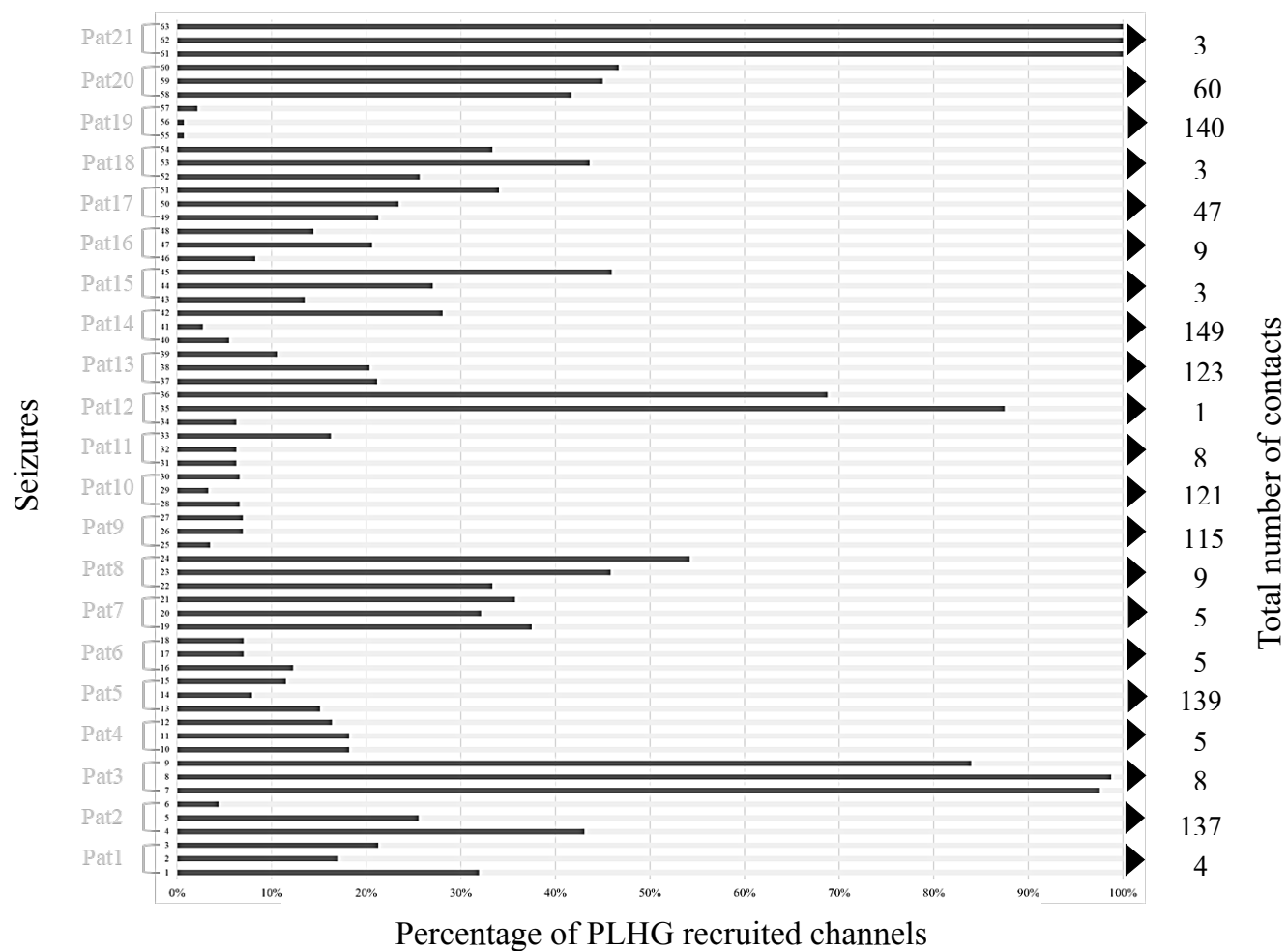
Figure 25. Percentage of PLHG recruited channels per seizure and patient, including the total number of contacts in grey matter recorded from for this study.

Overall, there was good agreement across the three seizures (Cronbach's alpha=0.93) and high stereotypy of seizures over all patients (Levenshtein distance, p<0.01, t-test). Nevertheless, as illustrated in Figure 8 different seizure patterns occurred across patients. Several patients showed a focal PLHG recruitment pattern (<20% of PLHG recruited channels) in all three seizures (ID4, 5, 6, 9, 10, 19). Contrary to those, two patients displayed a recruitment pattern, where almost all channels showed PLGH recruitment at some point during the seizure (ID3, 21). Another pattern was seen in a few patients (ID11, 12, 13, 14) where one seizure's PLHG recruitment pattern behaved differently compared to the other two seizures. The rest of the patients showed either a similar recruitment pattern between their three seizures (ID7, 20) or a variable pattern (ID1, 2, 8, 15, 16, 17 and 18).

Regarding included seizure types, Table 13 shows percentage of seizure types and percentage of PLHG recruitment pattern for patients in the good versus the poor outcome group. Both groups showed the same percentage of patients having habitual clinical seizures and showing more than one seizure type. Table 14 summarises each patients seizure types used for PLHG analyses and PLHG pattern descriptions.

Table 13. Percentage of seizure types and PLHG recruitment patterns comparing patient with good versus poor outcome.

		good outcome (n=15)	poor outcome (n=6)
Seizure types	habitual	66.70% (n=10)	66.70% (n=4)
	others	33.30% (n=5)	33.30% (n=2)
PLHG pattern	all	13.30% (n=2)	0.0% (n=0)
	focal	33.30% (n=5)	16.70% (n=1)
	variable	26.80%(n=4)	0.50% (n=3)
	one/two	13.30% (n=2)	33.30% (n=2)
	similar	13.30% (n=2)	0.0% (n=0)

Habitual = habitual clinical seizures, others = more than one seizure type, subtle seizures, electrographic seizures, focal = focal PLHG recruitment pattern, all = almost all channels showed PLGH recruitment, one/two = one seizure's PLHG recruitment pattern behaved differently compared to the other two seizures, similar = similar recruitment pattern, variable = variable pattern.

Table 14. Summary of seizure types used and PLHG description.

ID	Seizure types	PLHG pattern	Engel
1	Habitual seizures	different	IIIa
2	3 seizure types - one each chosen for study	different	Ia
3	Habitual & electrographic seizures - habitual ones used	all	IIb
4	Habitual & electrographic seizures - habitual ones used	focal	II
5	Habitual seizures	focal	Ib
6	Habitual & electrographic seizures - electrographic Type1 used	focal	IV
7	1 subtle seizure and 2 electrographic seizures, all used	similar	Ia
8	Habitual seizures	different	Ia
9	2 seizure types - chosen Type1 including one slightly atypical	focal	IIb
10	Habitual seizures	focal	Ia
11	Habitual seizures & auras - habitual seizures used	one/two	Ia
12	Habitual seizures & auras - habitual seizures used	one/two	III
13	Habitual & electrographic seizures - habitual seizures used	one/two	Ia
14	3 seizure types - one each chosen for study	one/two	IIIa
15	4 seizure types, Type1 (majority) used	different	Ia
16	Habitual seizures	different	IVa
17	Habitual seizures	different	IV
18	Habitual seizures	different	I
19	Habitual seizures	focal	I
20	3 seizure types, only Type1 had clinical features, type 1 used	similar	I
21	Habitual and electrographic seizures - habitual ones used	all	I

Focal = focal PLHG recruitment pattern, all = almost all channels showed PLGH recruitment, one/two = one seizure's PLHG recruitment pattern behaved differently compared to the other two seizures, similar = similar recruitment pattern, different = generally different pattern

A further PLHG characteristic, very early recruitment (under 4s) was found in several patients' seizures. This did not only affect single channels, in some seizures up to thirty channels were recruited so rapidly. In total, 6 patients (12 seizures) showed very early PLHG recruitment (Table 15, grey shading). It occurred in 11.1% of SEEG recordings and 38.9% of grid recordings. Not only very early recruitment, but also recruitment in the same time increment (e.g. 3s) was noticeable in these seizures. The average number of very early recruited channels was 12.9 (±11.6, range 1–37). Table 48 in the appendix presents

examples of PLHG recruitment for four patients with a seizure each, with two cases exhibiting very early recruitment.

Table 15. Summary of PLHG recruitment and its duration.

ID	iEEG	No of Contacts	Sz duration (s)			No of PLHG channels		
			Sz1	Sz2	Sz3	Sz1	Sz2	Sz3
1	SEEG	47	131	98	108	10	8	15
2	SEEG	137	261	67	65	6	35	59
3	SEEG	81	80	35	42	68	80	79
4	grid	55	35	45	40	9	10	10
5	SEEG	139	68	58	58	16	11	21
6	grid	57	88	59	128	4	4	7
7	SEEG	56	102	96	66	20	18	21
8	SEEG	96	128	193	182	52	44	32
9	SEEG	115	89	108	105	8	8	4
10	SEEG	121	40	43	50	8	4	8
11	SEEG	80	93	82	176	13	5	5
12	SEEG	16	109	202	92	11	14	1
13	SEEG	123	70	134	149	13	25	26
14	SEEG	146	130	122	111	41	4	8
15	SEEG	37	190	130	241	17	10	5
16	SEEG	97	36	46	55	14	20	8
17	grid	47	163	204	35	16	11	10
18	grid	39	97	108	108	13	17	10
19	SEEG	140	52	70	49	3	1	1
20	grid	60	94	121	90	28	27	25
21	grid	37	61	94	63	37	37	37

Contacts: number of contacts recorded from; Duration: seizure duration in seconds (s) for all three seizures; PLHG channels: number of PLHG recruited channels for all three seizures; seizures with very early recruitment (<4s) are shaded in grey; Sz = seizure

To compare patients with subdural grid implantation and SEEG implantation several characteristics were analysed. The mean number of contacts implanted in patients with grids (48.8±8.5) was significantly smaller than in those with SEEG implantations (95.4±40.0; p<0.01; Wilcoxon rank sum test). The mean number of channels showing PLHG recruitment was not different in patients

with grids (15.9±10.6) and SEEG patients (19.6±20.0, p>0.1; Wilcoxon rank sum test). The mean time of PLHG recruitment did not show a difference between the two groups of patients (grids 7.0s±5.4; SEEG 11.7s±15.3; p>0.1; Wilcoxon rank sum test).

Association of PLHG/SOZ overlap (PSO) with Engel Outcome

In this section, the overlap of PLHG recruited channels with clinically defined SOZ channels (PSO) was evaluated.

PSO was analysed for PLHG recruited channel bins 1–10 as above in two ways. Percentage of PSO of PLHG$_{two}$ (including channels with the same PLHG recruitment in at least two of the three seizures) was significantly higher in patients with good versus poor outcome for the PLHG3 bin (Figure 26, p<0.05, Wilcoxon rank sum test). Results show that there was evidence for a higher mean percentage of PSO for most of the remaining bins in patients with good compared to those with poor surgical outcome, however, the difference was not significant. Similar evidence for a higher mean percentage of PSO1–10 was seen for PLHG$_{any}$ (including all channels recruited in three seizures), albeit without any significant differences (at level p<0.05) in any of the bins.
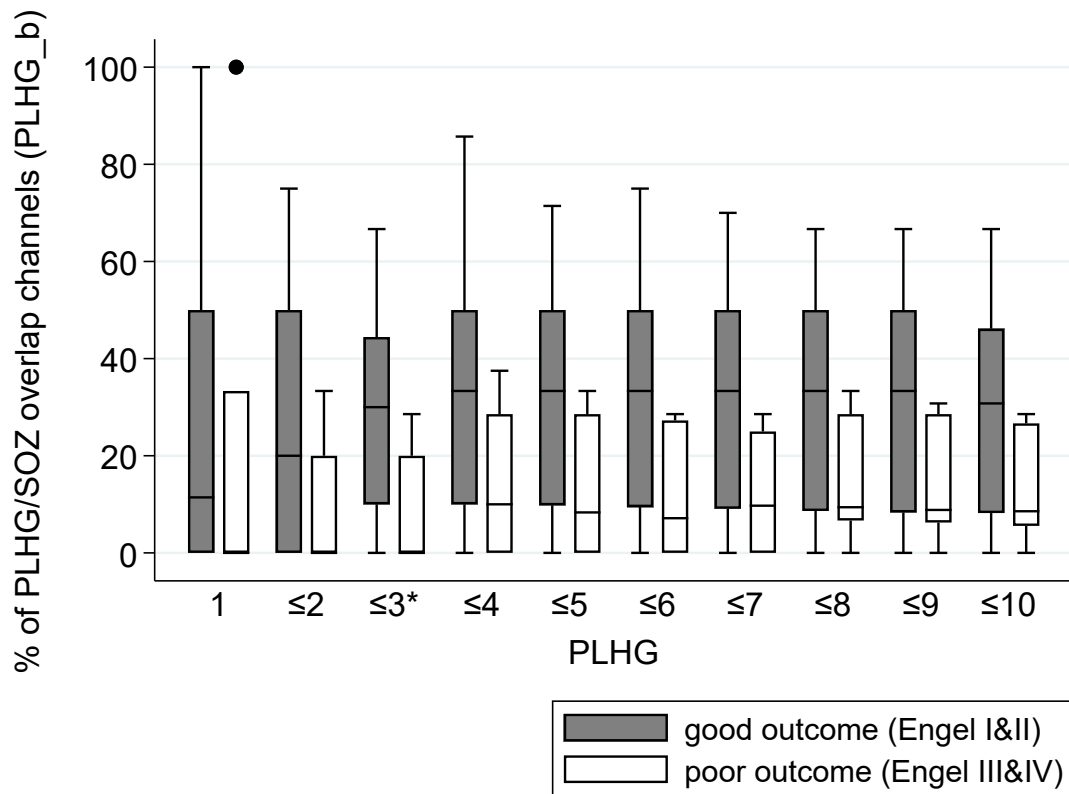
Figure 26. PSO for PLHG$_{two}$ good versus poor Engel outcome. Boxplot presenting percentage of channels showing PLHG/SOZ overlap for patients with good versus poor Engel outcome from PLHG 1–10 for the PLHG$_{two}$ approach. Significant difference with $p<0.05$ is marked with *.

To explore if pathology type mattered the mean percentage of PSO (for PLHG$_{any}$ and PLHG$_{two}$) was analysed for each patient (Table 16). Patients showing $\leqslant 10\%$ mean overlap in PSO had subtle pathologies (ID3, 11, 15; 100% of subtle abnormalities), or were lesion negative (ID2, 12; 40% of lesion negative patients), or had FCD (ID17, 18; 28.6% of FCD patients). Three of these patients showed poor Engel outcome (Engel class III&IV; ID15, 17, 18).

Table 16. Summary of mean percentage of PLHG/SOZ Overlap (PSO), pathology and Engel outcome for each patient.

ID	Engel	mean % PSO overlap		Pathologies
		PLHG$_{any}$	PLHG$_{two}$	
1	3.5	0.51	0.30	L F FCD
2	1	0.06	0.00	lesion negative
3	2.5	0.10	0.10	small R hemisphere, myelin immaturity
4	2	0.49	0.42	L FCD
5	1.5	0.43	0.32	lesion negative
6	4	0.27	0.20	TS, multiple tuber
7	1	0.54	0.48	TS, multiple tuber
8	1	0.90	0.59	L HC sclerosis
9	2.5	0.48	0.32	lesion negative, possible L P abnormal sulcation
10	1	0.82	0.51	L P extending to P Operculum FCD
11	1	0.05	0.00	Gliotic changes L posterior central to L P
12	1	0.00	0.00	lesion negative
13	3	0.25	0.25	bilateral HC sclerosis
14	1	0.23	0.14	L STG FCD
15	3	0.00	0.00	subtle R temporal lobe abnormalities
16	1	0.73	0.60	TS, multiple tuber and L HC abnormality
17	4	0.04	0.02	R FCD
18	4	0.06	0.03	R FCD
19	1	0.22	0.22	L SFG FCD
20	1	0.58	0.40	TS, multiple tuber L P
21	1	1.00	0.42	lesion negative

Abbreviations: R = right, L = left, P = parietal, T = temporal, F = frontal, SFG = superior frontal gyrus, STG = superior temporal gyrus, FCD = focal cortical dysplasia, TS = Tuberous sclerosis, HC = hippocampus.

The two overlap analyses (Percentage of PSO for PLHG$_{any}$ and PLHG$_{two}$) were also conducted using the second Engel outcome definition (Engel B), where good outcome is defined as Engel class I. Results for the two metrics, PLHG$_{any}$ and PLHG$_{two}$, did not show any difference in the percentage of PSO between Engel outcome groups (PLHG1–10 $p > 0.1$, Wilcoxon rank sum test).

Association of PLHG/Resection Overlap (PRO) with Engel Outcome

First, PLHG/Resection overlap (PRO) was analysed and its difference between patients with good and poor Engel outcome examined. This was done for PLHG recruited channels 1–10. The analyses was done using two approaches. First, results for the set union approach of PLHG recruited channels (PLHG$_{any}$), comparing patients with good and poor Engel outcome, is presented. Here, included PLHG recruited channels did not have to be reproducible across the three seizures. Channels recruited across any seizure were included. Percentage of PRO of PLHG$_{any}$ was not different between patients with good and poor Engel outcome for all ten PLHG channel recruitment bins (Figure 27, n=21, all PLHG bins: p>0.1, Wilcoxon rank sum test).
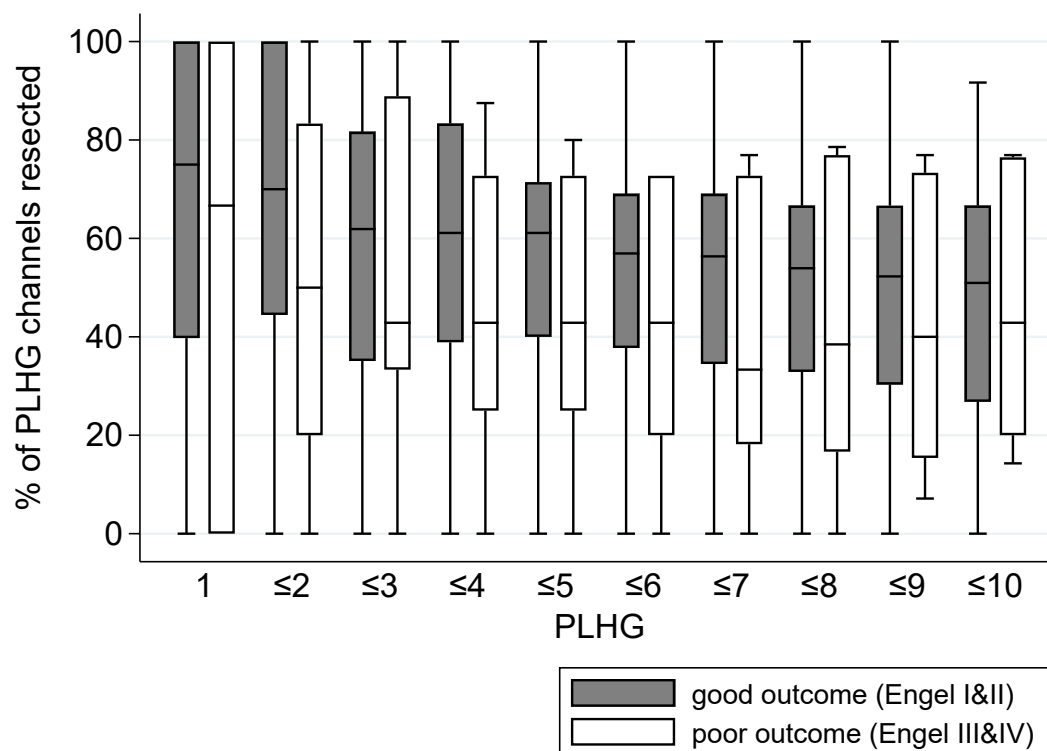
Figure 27. Proportion of PLHG channels resected (PRO for PLHGany metric) in the Engel outcome groups. Boxplots presenting percentage of channels showing PLHG1–10/Resection overlap (PRO1–10) for patients with good (n=15) versus poor (n=6) Engel outcome for the PLHG$_{any}$ approach.

Second, analyses of PLHG recruited channels, which were identified in at least two of the three seizures (PLHG$_{two}$) was conducted. Results show that the percentage of PRO was also not different between outcome groups for all ten

125

PLHG channel recruitment bins tested (PLHG1-10 p>0.1, Wilcoxon rank sum test).

The same results were obtained when using Engel class I as good outcome only (PLHG1–10 p>0.1, Wilcoxon rank sum test).

Like in Weiss et al (2015) the classification analysis was repeated using a time-based criterion of PLHG identification within 30 seconds after seizure onset, and again found no significant results (good outcome group: mean time (s) 39.9±27.2, min = 6.1s, max = 126.3s, poor outcome group: mean time (s) 39.4±19.9, min = 9.5s, max = 74.0s, p>0.1, Wilcoxon rank sum test).

3.4.5   Two-stage analyses

Next, I asked whether 2-stage testing using clinically defined SOZ in combination with PLHG recruitment 1–10 and FRs would improve accuracy of outcome classification.

Association of two-stage SOZ and FR testing with Engel outcome (S ∪ F)

First, I tested whether combining SOZ and FRs (S ∪ F) would lead to an improved outcome classification. This analysis included SOZ channels and channels with high rate FR>1/min. Results show that there was evidence for a higher percentage of resected SOZ/FR channels (good: 0.64±0.25, poor: 0.51±0.25) in patients with good (n=12) compared to those with poor surgical outcome (n=5), however the differences were not significant (p>0.1; Wilcoxon rank sum test, Figure 28).
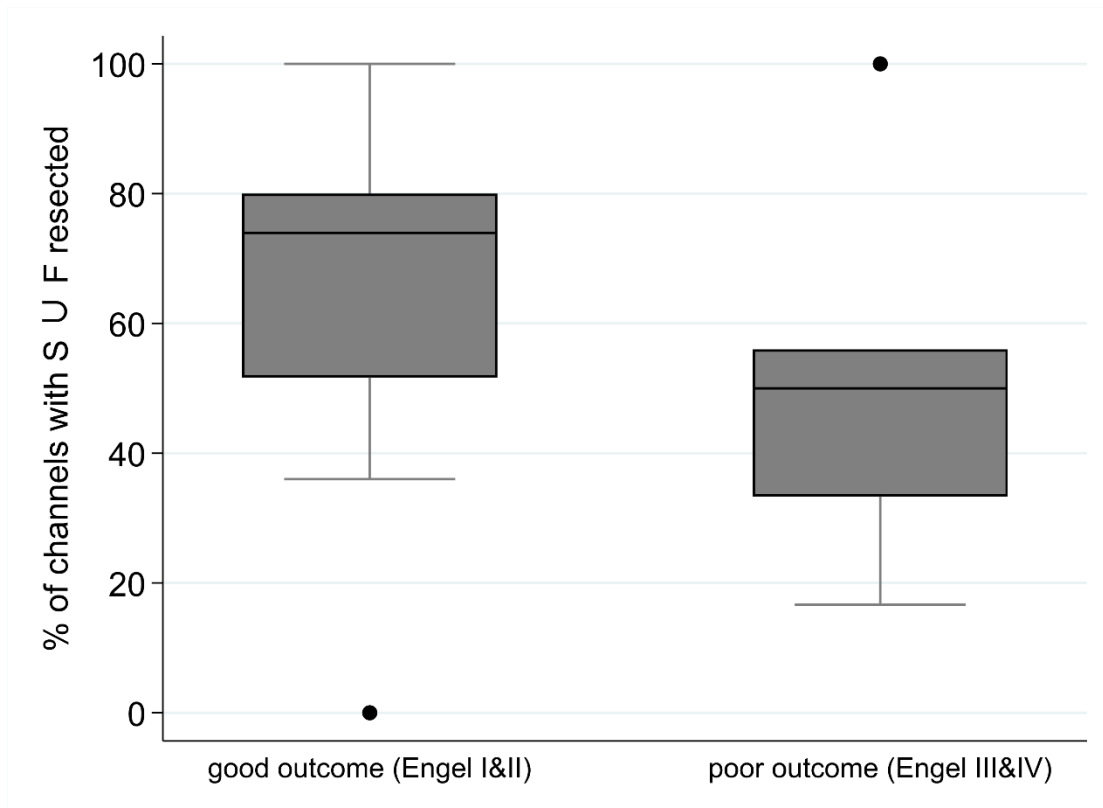
Figure 28. Percentage of channels showing S ∪ F resected for patients with good versus poor outcome.

The outlier in the poor outcome group is again ID17 (see previous FR analysis). The outlier in the good outcome group is ID12. This patient had tuberous sclerosis and a left hemisphere SEEG implantation with electrodes implanted in all nine tubers. After a left anterior temporal lobe resection the patient showed Engel outcome class I. Despite stopping medication only one very subtle clinical event was recorded, which seemed to be a very subtle version of the habitual vacant episodes recorded in telemetry previously. The ictal activity recorded during SEEG monitoring was deriving from two tubers in the temporal lobe. FRs were only seen in one of these two tubers, the more posterior one. Anterior temporal lobe resection, however, included only resection of the anterior tuber, which did not show FRs.

When excluding the outlier ID17 results still show no significant differences between good and poor outcome for channels showing S ∪ F (good: 0.70 ± 0.17, poor: 0.51 ± 0.28 respectively; p>0.1). However, when also excluding ID12 from

the analysis SOZ $\cup$ FRs results show a significantly higher percentage of resected channels showing S $\cup$ F in patients with good outcome compared to poor outcome (p<0.05, Wilcoxon rank sum test).

When using only Engel class I as good post-surgical outcome results show no significant differences for any of the analyses between patients with good versus poor surgical outcome (p>0.1). This is also true when excluding the outliers ID17 and ID12 from the analyses (p>0.1).

Association of 2-stage SOZ and PLHG testing with Engel Outcome (S $\cup$ P)

In the following analysis, I aimed to evaluate whether channels showing both SOZ association and/or PLHG recruitment (S $\cup$ P), were resected and if this 2-stage testing improved the accuracy of the outcome classification. Again, I am plotting this measure across all PLHG bins 1–10, investigating which extent threshold of recruitment shows the strongest association with Engel outcome.

SOZ and PLHG 2-stage testing did not improve outcome classification. This was true for all bins for both approaches (PLHG1–10, PLHG$_{any}$ and PLHG$_{two}$) and for results using the second outcome classification (Engel B; p>0.1, Wilcoxon rank sum test). Figure 29 illustrates results for PLHG$_{any}$ approach.
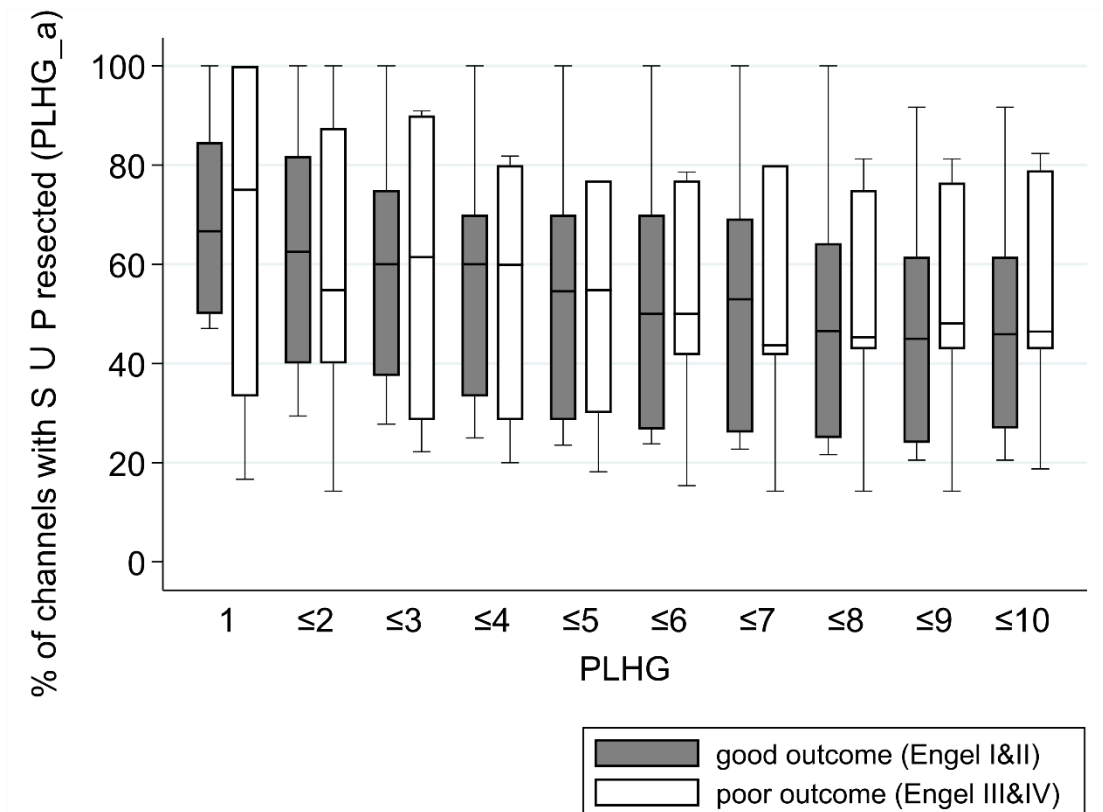
Figure 29. Association of resected S ∪ P channels with Engel outcome (PLHGany). Boxplot presenting percentage of resected channels showing S ∪ P for patients with good (n=15) versus poor (n=6) Engel outcome from PLHG 1–10 for the PLHG$_{any}$ approach. No significant differences were found.

3.4.6   Three-stage analysis

Association of 3-stage SOZ, PLHG and FR testing and Engel Outcome (S ∪ P ∪ F)

In the following analysis, I aimed to evaluate whether channels showing all three characteristics: PLHG recruitment, SOZ association and FRs (S ∪ P ∪ F) were resected, and if this 3-stage testing improved outcome classification. Again, I am analysing both approaches (PLHG$_{any}$ and PLHG$_{two}$) for PLHG1–10.

Three-stage testing of S ∪ P ∪ F did not improve outcome classification. This was true for all bins (PLHG1–10) for both approaches (PLHG$_{any}$ and PLHG$_{two}$) and for results using the second outcome classification (Engel B; p>0.1, Wilcoxon rank sum test).

3.4.7   Summary of overlap results

To sum up, results of all analyses can be found in the following Table 17. It shows results of differences in the various area combinations between patients with good and poor Engel outcome. Next, Figure 30 illustrates the percentage of resected channels for different zones.

Table 17. Differences in percentage of zone overlaps between good and poor Engel outcome.

		Engel A (good = Engel I&II, poor = Engel III&IV)										Engel B (good = Engel I, poor = Engel II-IV)									
FRO	(without ID12,17)	1.57										0.99									
S ∪ F		2.30**										1.34									
PLHG		1	2	3	4	5	6	7	8	9	10	1	2	3	4	5	6	7	8	9	10
PSO$_{any}$		-0.93	**-1.73***	**-1.84***	**-1.84***	**-1.68***	**-1.67***	-1.64	-1.60	**-1.68***	**-1.75***	-1.00	-1.58	**-1.75***	-1.54	-1.32	-1.10	-1.07	-1.03	-1.14	-1.17
PSO$_{two}$		-0.63	-1.65	**-2.06****	-1.62	-1.73	**-1.81***	**-1.77***	-1.45	-1.53	-1.52	0.15	-1.39	-1.49	-1.55	-1.26	-1.40	-1.15	-0.89	-0.86	-0.79
PRO$_{any}$		0.08	0.08	0.08	0.08	0.08	0.08	0.08	0.08	0.08	0.08	-0.42	-0.22	0.43	0.07	0.32	0.53	0.43	0.75	0.82	0.64
PRO$_{two}$		0.58	0.58*	0.58	0.58	0.58	0.58	0.58	0.58	0.58	0.58	0.20	-1.04	-1.54	-1.30	-1.01	-1.23	-1.23	-0.93	-0.86	-0.86
S ∪ P$_a$		0.16	0.27	-0.08	0.20	-0.23	-0.04	-0.08	-0.27	-0.43	-0.23	-0.18	-1.032	-0.14	0.11	-0.36	-0.32	-0.43	-0.68	-0.71	-0.71
S ∪ P$_b$		-0.41	0.20	-0.08	0.43	0.51	0.51	0.20	0.16	-0.078	-0.27	-0.15	0.25	-0.15	0.14	0.36	0.46	-0.11	-0.25	-0.75	-0.78
S ∪ P ∪ F$_a$		0.55	0.51	0.00	0.00	0.00	0.00	0.16	-0.16	-0.55	-0.12	-0.07	0.14	-0.14	-0.14	-0.28	-0.28	-0.21	-0.71	-0.93	-0.75
S ∪ P ∪ F$_b$		0.62	0.62	0.43	0.74	1.05	1.25	1.05	1.01	0.78	0.23	-0.04	-0.21	-0.32	-0.04	0.25	0.50	0.36	0.18	-0.25	-0.64

PLHG 1-10 lists z (Wilcoxon rank sum test) scores and significance levels for both Engel outcome groupings (A, B); ** significance level p<0.05, * significance level p<0.1; $_{any}$ = including PLHG recruited channels without any restriction of occurrence in all three seizures of each patient); $_{two}$ = including PLHG recruited channels with the same PLHG recruitment in at least two of the three seizures; PSO = PLHG/SOZ overlap; PRO = PLHG/Resection overlap; FRO = FR Resection overlap; S ∪ F = union of resected channels showing SOZ and/or FRs; S ∪ P = union of resected channels showing SOZ and/or PLHG recruitment; S ∪ P ∪ F = union of resected channels showing SOZ and/or PLHG and/or FRs;.

131
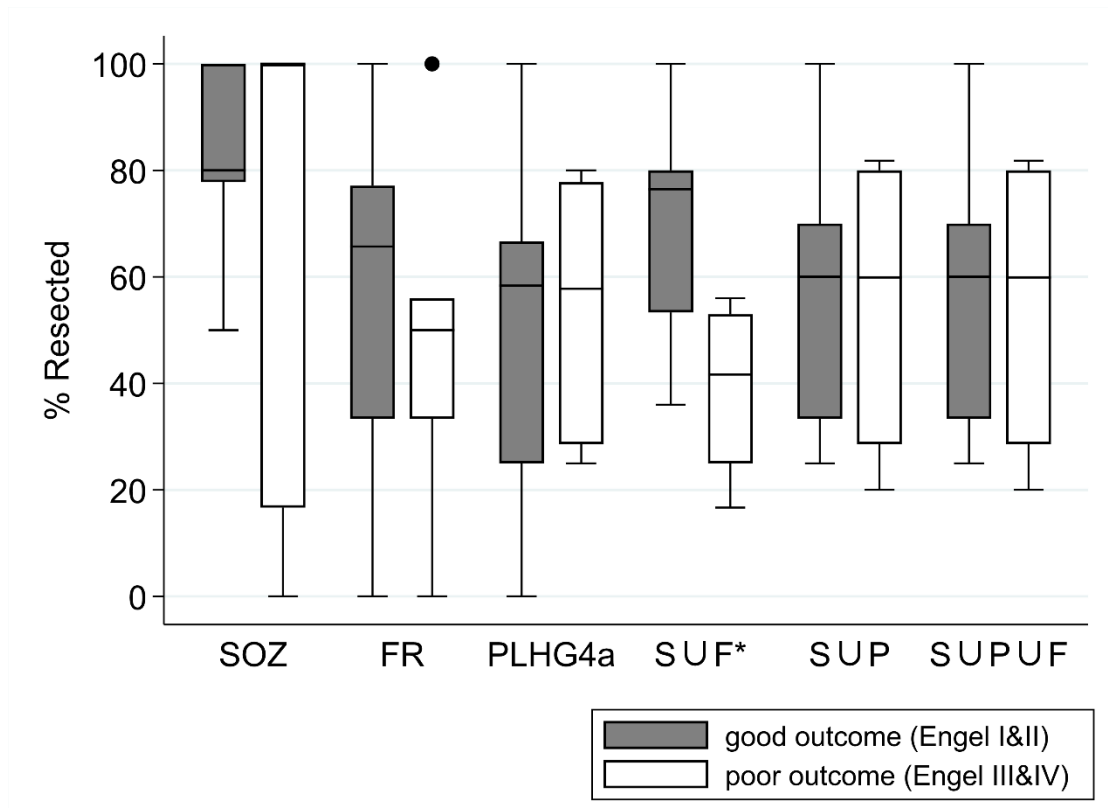
Figure 30. Surgical outcome classification by extent of SOZ, FR, early PLHG and 2- and 3-stage analyses. Boxplots showing percentage of resected channels according to surgical outcome for the SOZ, FRs, early and (PLHG4$_{any}$) and overlapping areas S∪P, S∪F and S∪P ∪F. Significant difference is marked with *.

First, SOZ, FR, PLHG4a are shown, which do not show a difference in the proportion of resection between patients with good versus poor Engel outcome. PLHG4 is presented, as early recruitment was described as most predictive in Weiss et al (2015). Significant difference is shown in the proportion of S∪F resection between patients with good (Engel class I&II) and poor outcome (Engel class III&IV) with a higher proportion of S∪F channels resected in patients with good outcome. This difference was not evident for any other zone combinations.

Next, I asked whether 2-stage and 3-stage testing using the different zone overlaps would improve the accuracy of outcome prediction (see Figure 31).
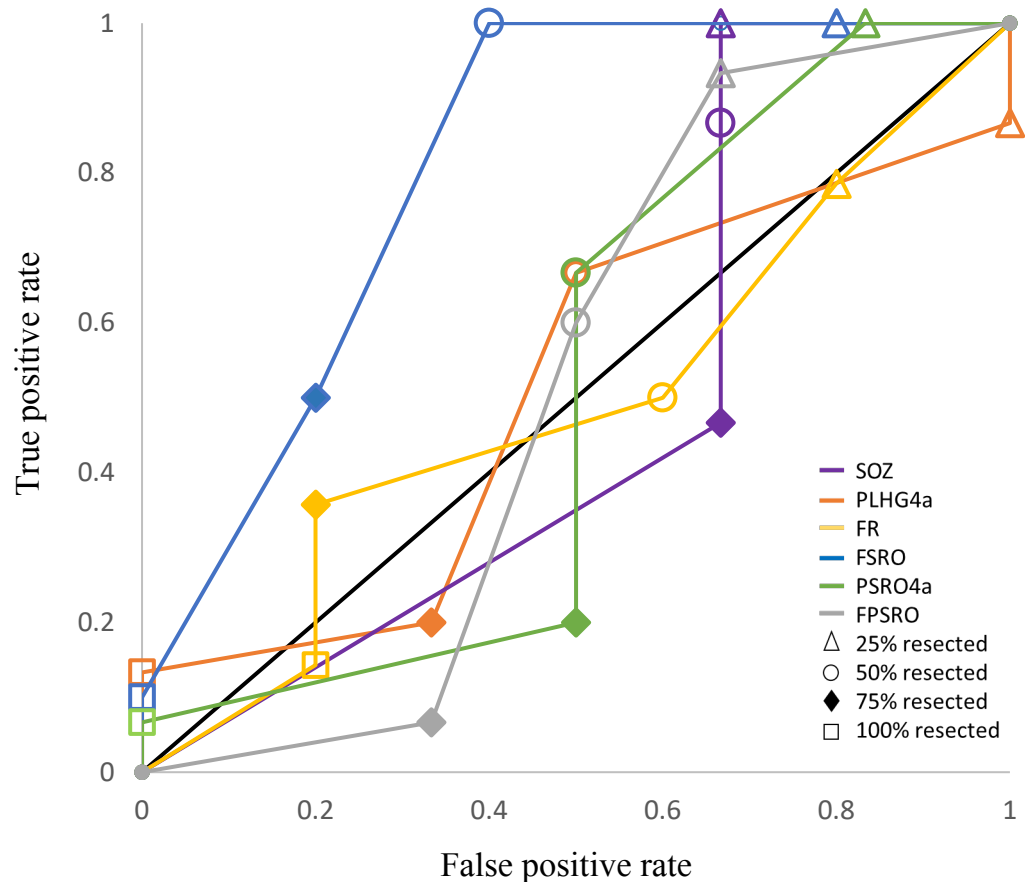
Figure 31. Outcome accuracy using SOZ, FR, PLHG and 2- and 3-stage testing. Receiver operating characteristic curve comparing sensitivity and specificity of seizure outcome classification using SOZ (yellow), FR (red), PSO4a (blue) and PSO3b (green). Results at each data point were based on resections exceeding the corresponding cutoff proportion for each measure.

The solid black line in Figure 31 indicates random performance, with an AUROC of 0.50. The only analyses improving outcome classification was using SOZ and FR (S ∪ F), which improved AUROC to 0.81 (Figure 31 blue line). The remaining zones and zone overlap combinations did not show any improvement in accuracy of outcome classification. They all showed close to random performances. Of the five patients meeting the 75% cut-off value of contacts resected for both SOZ and FRs (n=15) 100% showed good outcomes. Three of these patients (60%) became seizure free (Engel class I).

3.4.8　　　Case Studies

The following patients were chosen as both present the opposite ends of the post-surgical outcome classification. The first patient was a curative case compared to the second patient where a palliative approach was taken.

Case 1 (ID13, Figure 32)

A 5-year-old, right-handed female presenting with focal seizures. Her birth history showed an uncomplicated pregnancy and full-term birth without perinatal concerns and a normal development. Her first seizure occurred at eight weeks of age, characterised by brief elevation of the left arm and eye deviation to the left, lasting only a few seconds. Her subsequent events were subtle, occurred from sleep and were characterised by arousal, restlessness, vocalisation, trembling movements and posturing of the right arm/automatism of the left hand. She verbalised during the events but her voice was "shaky". Seizures lasted between 30 seconds and 2 minutes. In some of her events she complained of hearing a noise ("what's that noise?", "it was buzzy") or her head felt fuzzy.

The MRI scan showed an area of signal abnormality in the posterior part of the inferior portion of the left superior temporal gyrus, suggestive of focal cortical dysplasia. Previous EEG localised to temporal regions, mostly left and post-ictal slowing consistently lateralised to the left. Clinical features suggested left lateral temporal lobe epilepsy.

She underwent a left hemispheric SEEG implantation with 14 electrodes covering the temporal, parietal and occipital lobe and the insula (Figure 32). The patient had seven habitual seizures, all from sleep and numerous (>100) electrical seizures with similar EEG features. Her intracranial EEG findings suggested involvement of middle contacts of the electrode implanted in the anterior part of the lesion (F/STG_A) and the deepest contacts of the electrode I the posterior part of the lesion (G/STG_P). Lateral contacts of the electrode implanted in the temporo-parieto-occipital junction, which was part of the lesion

134

(L/TPO), was involved later and might have indicated the posterior-superior boundary. The deep contacts of (H/P_MTG) possibly indicated the inferior extent. Clinically, she stirred, had jittery movements of the hands (R>L) and looked to the left. She appeared confused and scared, whimpered, but did not usually speak. No auditory symptoms were reported. Seizure stimulation showed similar EEG pattern as for her habitual seizures and language testing did not lead to any obvious interruption of language (electrodes tested were L/TPO, F/STG_A, G/STG_P, H/P_MTG, K/SMG). After multidisciplinary discussion, it was decided to perform a lesionectomy resecting the lesion including electrodes F and G. Her 12-months post-surgery follow up showed Engel class I outcome.

The PLHG metric marked all areas that were involved in the ictal onset and spread (Figure 33). The overlap between the PLHG recruited channels and resection area was around 50% for PLHG bins 1–10. Channels with FRs, as automatically detected using a FR detector, showed a more localised distribution. Channels with FRs were resected in 77.8%. This case suggests that PLHG1–10 recruited channels and FR could aid delineating epileptogenic tissue.
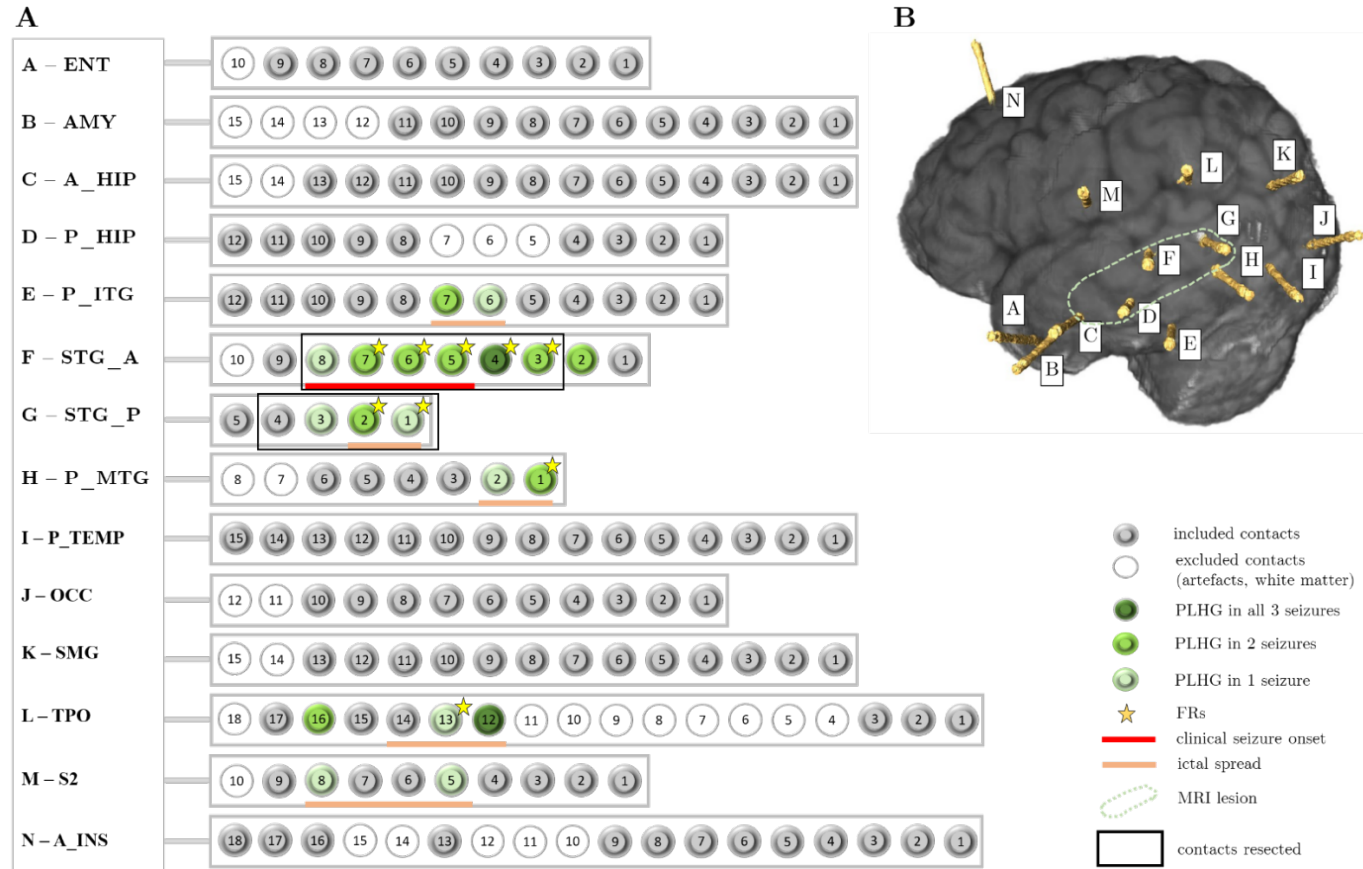
Figure 32. Summary Case 1 (ID13). A. presents clinical seizure onset and spread and first 10 PLHG recruited channels for all three seizures, FR activity and resection area. **B.** illustrates implantation regime including a schematic illustration of the MRI lesion. ENT = entorhinal cortex, AMY = amygdala, A_HIP = anterior hippocampus, P_HIP = posterior hippocampus, P_ITG = posterior inferior temporal gyrus, STG_A = anterior to lesion, STG_P = posterior to lesion, P_MTG = posterior middle temporal gyrus, P_TEMP = posterior temporal gyrus, OCC = occipital lobe, SMG = supramarginal gyrus, TPO = temporo-parieto-occipital junction, S2 = secondary somatosensory cortex, A_INS = anterior insula
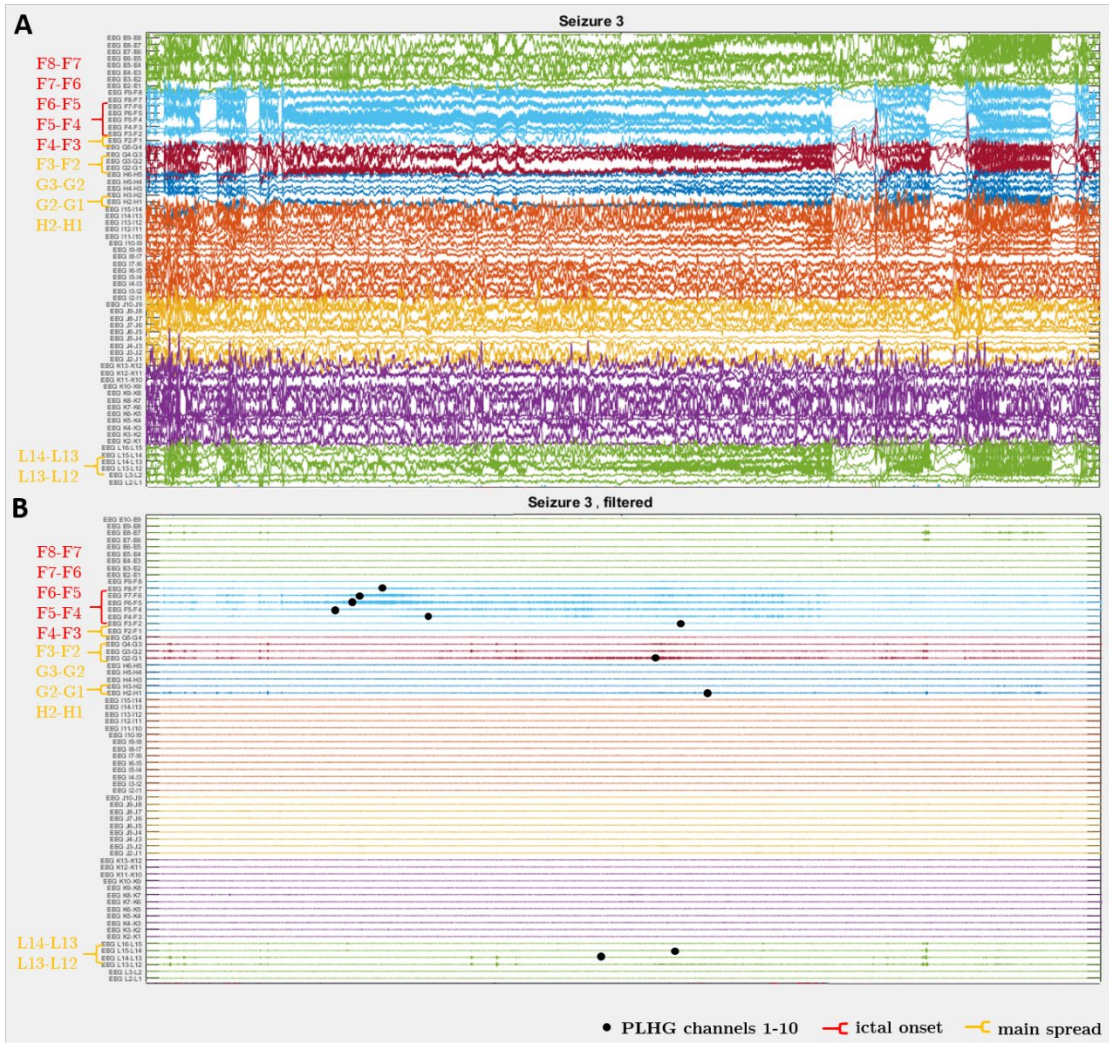
Figure 33. Example seizure Case 1 (ID13): PLHG recruitment bins 1–10. A. illustrates ID13's seizure 3 and its ictal onset and spread. For better visualisation only electrodes E-L are shown here as they involve the clinically defined ictal onset (red brackets) and ictal spread (yellow brackets). Each implanted electrode is shown in a different colour. **B.** shows the filtered seizure 3 with the first 10 PLHG recruited channels marked with black circles.

Case 2 (ID12, Figure 34)

A 14-year-old male presenting with focal seizures. He is the first born of twins from IVF with an uneventful pregnancy and development until age 2½ with his first seizure as he was falling asleep. His eyes rolled up, he was stiff and unresponsive with jerking of the whole body, mum reports this lasted 2.5 hours. His second seizure occurred six months later from sleep with no associated fever. Two more seizures were noticed in the next two months. After that, he was seizure free on Valproate. Age nine years he began to have episodes of 'stomach churning' behavioural arrest with lips going blue, and difficulty with comprehension lasting a few seconds. Age ten years he had two episodes of left-sided tonic-clonic seizures with secondary generalisation lasting about 15 minutes. Carbamazepine was started. Age eleven years he presented with focal seizures about five times a day consisting of unresponsiveness, head and eye deviation to the left, stiffening and jerking of the left arm and leg, partially aware and slurred speech lasting 2–3 minutes with sleep following. These could occur from sleep. They could be preceded by a rising sensation, but he had other episodes of odd sensations, which were not associated with focal seizures. He had two event types: first, numerous aura types with feeling scared, gusts of wind and feelings of things coming up in his stomach and chest, smells and tastes. His second type began with fear, fumbling, shivering and twitching of the left side of the body, all lasting less than five minutes and sometimes secondary generalisation occurred. They happened about six times a day.

The MRI showed bilateral hippocampal sclerosis left more than right. In addition, poor grey-white matter differentiation in the right temporal lobe, which also appeared smaller in volume than the left. Previous EEG monitoring resulted in an ictal onset localised in the right anterior quadrant of the temporal lobe, auras occasionally showed left rhythmic theta. This is in keeping with his MRI results and his semiology. fMRI results showed left lateralisation for language functions.

He underwent a bilateral anterior temporal lobe SEEG implantation with four electrodes covering the right and left amygdala and hippocampus (Figure 34B). The patient had nine habitual focal seizures and numerous auras. The SEEG monitoring results showed an onset of focal seizures always from the right, but with a spread to the left and often a more pronounced spiking over the left towards the end of the seizure. Most auras started from the right amygdala, however, with about 30% of auras showing an onset from the left amygdala or not clearly discernible. After discussion, a right sided temporal lobectomy was suggested. The estimated prognosis was seizure freedom for focal seizures 50 % and for auras 10%. Significant seizure reduction for focal seizures 70% and for auras 40%. The patient's 12-months post-surgery follow up showed Engel class III outcome.

For PLHG recruitment, solely his habitual focal seizure recordings were used, not the aura recordings, as they were too short. In all three seizures the most mesial amygdala channel (RAD1–2) was always the first to be PLHG recruited (Figure 35). Only with a time-delay of about 20–30s later the rest of the channels were recruited. Out of the three seizures used, one seizure showed only one PLHG recruited channel, RAD1–2. The sequence of the PLHG recruited channels of the other two seizures, apart from RAD1–2 being the first one, was variable. They included the right amygdala, the right hippocampus and the left amygdala. The overlap between the PLHG recruited channels and resection area varied from 40%–100% for the sequence of recruited PLHG channels analysed (1–10). Only one channels, RAD1–2 showed FR activity. Both PLHG recruitment and FRs pointed to the main onset channel, the RAD1–2 channel. Like the EEG, which showed the right hippocampus and left amygdala and hippocampus involved in seizure spread, the PLHG recruitment also suggested that the left side was involved. A caveat here is that the short aura recordings could not be analysed using the PLHG metric. The surgical resection focused on the right hemisphere only as resection cannot involve both amygdalae and hippocampi, accepting not achieving seizure freedom. In this case, clinically defined seizure onset, PLHG recruitment and FR activity pointed to similar areas

of epileptogenicity. Due to surgical restriction, only one hemisphere was operated on and, hence, this is likely to have led to a poor post-surgical Engel outcome—albeit significant improvement according to the patient and his parents.
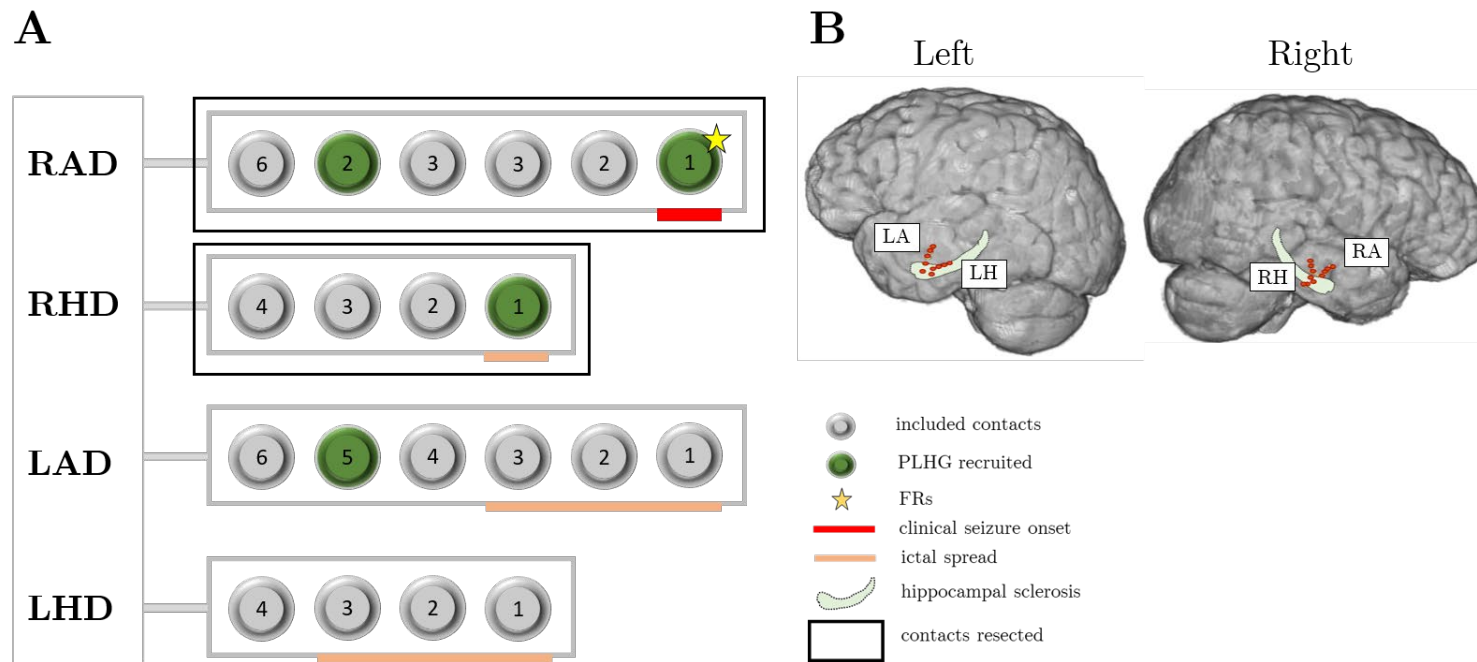
Figure 34. Summary Case 2 (ID12). A. Summary presents clinical seizure onset and spread of habitual seizures, first 4 PLHG recruited channels, FR activity and resection area; **B.** illustrates implantation regime including schematic illustration of pathology: bilateral hippocampal sclerosis; RAD = right amygdala depth electrode, RHD = right hippocampus, LAD = left amygdala, LHD = left hippocampus.
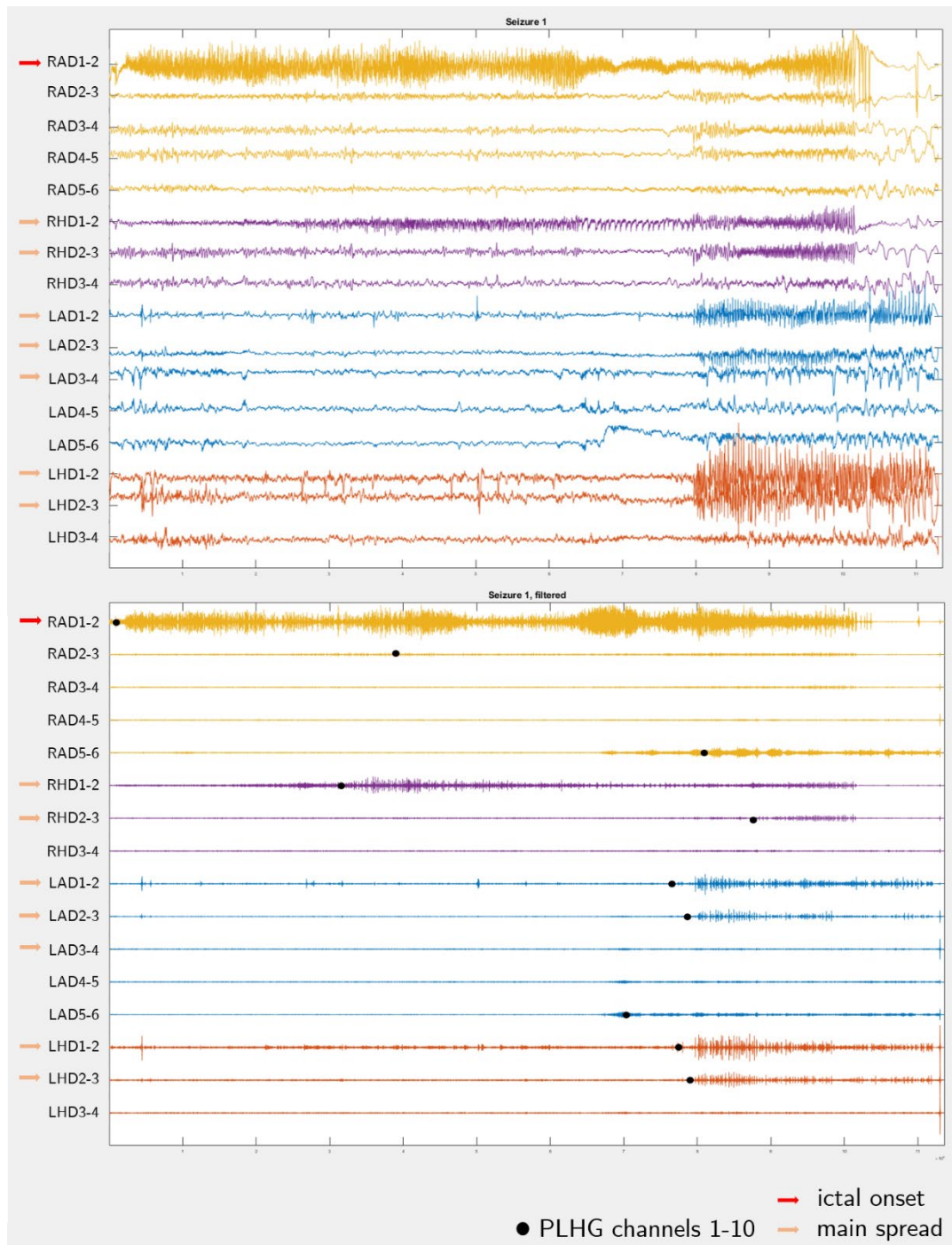
Figure 35. Example seizure Case 2 (ID12): PLHG recruitment bins 1–10. A. illustrates ID12's seizure 1 and the ictal seizure onset and progression. The recording of each implanted electrode is shown in a different colour for better visualisation. The various coloured arrows on the left depict the clinically defined ictal onset, ictal spread and late spread. **B.** shows the filtered seizure 1 with the first 10 PLHG recruited channels marked with black circles.

3.5   Discussion

The aim of this study was to implement two biomarkers for epileptogenic tissue, PLHG and FRs, and study their predictive value for post-surgical outcome. The current study is the first to implement the PLHG metric developed by Weiss and colleagues (2015) in a paediatric cohort with medication-resistant epilepsy and invasive EEG monitoring during pre-surgical evaluation. Results of their group, showing an improvement in surgical outcome when implementing PLHG information could not be replicated in this paediatric cohort. However, the second biomarker investigated, FRs, showed some promising outcome prediction results when combining it with clinical SOZ information.

Addressing Question 1: *Is the resection of the clinically defined SOZ predictive of post-surgical outcome?*

The minimum of cortical area that needs to be resected to render a patient seizure free is the so-called epileptogenic zone. This zone, however, is a theoretical framework, which cannot be delineated using a single method and is currently only known by post-surgical outcome (H. O. Lüders et al., 2006). Invasive EEG is the gold standard to delineate the SOZ, the cortical area that initiates seizures (Diehl & Lüders, 2000). In contrast to Weiss and colleagues (2015), however, in line with reports from other groups (Haegelen et al., 2013; Jacobs et al., 2010a) the current study found that removal of the SOZ is not an effective classifier of post-surgical outcome. Some patients continued to have seizures even when the contacts that signified the SOZ were removed (e.g., ID3, 4, 9). The smaller sample size of this study and some differences in clinical methodology including patient selection may have contributed to the negative finding. Weiss and group (2015) reported a high rate of incomplete SOZ resection (39%), discussing this being an important factor limiting post-surgical outcomes. However, in the present study the rate of incomplete SOZ resection was even lower (18.7%), suggesting other contributing factors. I observed that all but one patient with poor outcome had a small SOZ area with only 1–2 clinically defined SOZ

channels. On the contrary, all but one patient with good outcome never showed less than four and maximum 18 SOZ channels. A possible explanation might be the spatially limited sampling of intracranial investigations (Prasad, Pacia, Vazquez, Doyle, & Devinsky, 2003). On the contrary, some patients in whom part of the SOZ was not resected showed good post-surgical outcome (ID2, 7, 10, 20, 21). Also Malmgren & Edelvik (2017) reported that using the SOZ for surgical decision-making resulted in unfavourable outcomes in 40–50% of well-selected patients. Hence, there is clinical need for further biomarkers supporting delineation of the EZ.

3.5.1 Interictal fast ripples (FR) as biomarker of epileptogenic tissue

Addressing Question 2: *Is the resection of brain areas exhibiting FRs predictive of post-surgical outcome?*

Interictal FRs, especially at high occurrence rates, have previously been reported to be reliable markers of epileptogenic tissue (Akiyama et al., 2011; Crépon et al., 2010; Usui et al., 2011; Wu et al., 2010). This was shown by detecting HFOs in seizure-generating brain tissue. The link to the SOZ had already been established by microelectrode studies (Bragin, Engel, Wilson, Fried, & Mathern, 1999; Bragin et al., 2002; Staba, Wilson, Bragin, & Fried, 2002) and was later confirmed with clinical electrodes (Crépon et al., 2010; Jacobs et al., 2008; Urrestarazu et al., 2007). Previous retrospective reports (Höller et al., 2015; Jacobs et al., 2012) and one prospective study (Hussain et al., 2016) suggested an association between resection of HFO-generating tissue and post-surgical seizure outcome. The current study only showed that there was evidence for a higher mean FR ratio and a higher mean FR channel ratio in patients with good compared to those with poor surgical outcome; however, the difference was not significant. Recently favourably HFO results were challenged by results of a multi-centre study of Jacobs and colleagues (2018) who showed a correlation between the removal of HFO-generating regions and seizure-free outcome only

at the group level, including three centres, but not at an individual centre-specific level. In two of the three centres, HFOs did not reliably predict postsurgical outcome. The group discussed possible confounding factors like their approach of marking HFOs. All three centres used a hybrid approach, combining visual and automatic HFO detection and they argued that their visually marked HFO segment might have been too short to build the automatic detection on. Furthermore, the extent of HFO generating areas and the HFO types differed between centres. This might have been different between centres due to using different implantation methods and recording not only pathological but also physiological HFOs. Furthermore, one centre acquired data under general anaesthesia, which probably led to fewer physiological HFOs being included in the FR measure. In addition, resections were planned differently. Two centres used SOZ definition compared to the third centre, which relied on interictal EEG data and performed larger resections if interictal activity was visible. This study showed that methodological factors are likely to account for differences in results.

3.5.2   PLHG recruitment as a biomarker for epileptogenic tissue

Replication of findings and reproducibility of PLHG patterns across seizures

The aim of this study was to replicate results of Weiss and colleagues (2015) using the PLHG metric. They showed that implementing PLHG metric information of an adult group with refractory epilepsy lead to an improved surgical outcome classification and furthermore the combination of PLHG recruitment and SOZ information enhanced outcome accuracy (S. A. Weiss et al., 2015). I could show similar results in a cohort of adult patients with medication-resistant epilepsy using recordings of SEEG implantations compared to Weiss and colleagues (2015) who used subdural grid implantations. Here, I am implementing their PLHG metric in a paediatric patient population with

either SEEG or subdural grid implantation. Furthermore, like in the previous study with the adult population, I am investigating within-subject reproducibility in PLHG recruitment.

Addressing Question 3: *Can PLHG recruitment be reproduced in a cohort of paediatric patients with SEEG and subdural electrode implantation and a clinically defined focal SOZ?*

All 87 seizures considered in this study showed PLHG recruitment detected using the PLHG metric developed by Weiss and group (2012; 2013, 2015). In comparison, Weiss et al. (2015) detected PLHG recruitment in all but two patients with Engel class IV outcome. The average number of PLHG recruited channels in this study is 24.6 compared to 21.0 described in Weiss et al. (2015). In both adult and paediatric patients with drug-resistant focal epilepsy, surgery is the most effective intervention to achieve long-term seizure freedom. Therefore, a promising biomarker developed and tested in an adult cohort needs to be analysed for its transferability into a paediatric cohort. It is a quite common approach that biomarkers that are tested on adults first are then investigated for their use in children and adolescents (Goldman, Becker, Jones, Clements, & Leeder, 2011). Furthermore, in contrast to Weiss and colleagues (2015) this study included both patients with SEEG and patients with subdural implantations. Despite testing children and adolescents and including different implantation methods, results showed similar PLHG recruitment characteristics. It is also of importance to replicate PLHG metric results using SEEG recordings, as an increasing proportion of stereotactic studies targeting deep and extra-temporal areas is performed (Baud et al., 2018).

A PLHG characteristic observed in this study, which was not reported by Weiss and colleagues (2015) was very early recruitment (under 4s), which occurred in seizures of several patients. Up to thirty channels could be PLHG recruited that quickly. This should be seen in light of the temporal filtering in PLHG computation (for a detailed summary see Section 2.2.5). The phase-locking value and PLHG were calculated over a 3s sliding window advanced in 333ms

increments. Hence, the first possible time bin of PLHG recruitment could only be the 3s bin. Additionally, PLHG recruitment in the same time increment (e.g. 3s) was observed. I inspected a possible technical issue with clipping the seizure recordings by including or producing sharp activity at the very beginning of the clipped epoch. I repeated analyses with slightly different clipped versions of these affected recordings. However, the resulting very early recruitment and the same recruiting times could not be avoided; hence, the clipping time did not seem to be the issue.

There was not a leading pathology in these patients, nor did their EEGs show any differences or abnormalities. Very early recruitment occurred more frequently in subdural grid than SEEG recordings. This might be associated with different seizure spread patterns depending on implantation method. However, Weiss and colleagues did not report this very early recruitment although they mostly used grid recordings. Nevertheless, it is not clear, if they did not observe this phenomenon in their data or if they did not report it.

Overall, I was able to use the PLHG metric in a paediatric cohort with different invasive implantation methods and replicated essential characteristics of PLHG recruitment.

Addressing Question 4: *How reproducible is PLHG recruitment across seizures in each patient?*

Unlike Weiss and colleagues (2015), who chose the first three consecutive seizures, including atypical seizures, I chose slightly different inclusion criteria as I added the question of reproducibility of PLHG recruitment to this study. I included patients if three seizures with a clinically defined focal seizure onset were available. Most children presented with habitual clinical seizures. However, when children presented with several seizure types, mostly showing a similar seizure onset but a different seizure spread pattern, these were included as well. The primary aim was to test whether the PLHG metric is stable and

whether it results in similar recruitment patterns across seizures. Although the number of PLHG recruited channels seemed to differ somewhat between seizures, reproducibility testing showed PLHG recruitment patterns with good agreement in all three seizures. Furthermore, on a group level my data showed that seizures where stereotyped. Hence, it could be shown that the PLHG metric is stable across chosen seizures and in future studies all seizure types of a patient should be included, as well as atypical seizures or seizures with insidious onsets to ensure a comprehensive analysis as many pre-surgical patients do not present with a clear localised focal seizure onset.

To sum up, despite the differences in the study design of the current study, including a different patient cohort and a second implantation method, this study's design can be considered sufficiently similar to make replication plausible.

3.5.3   PLHG classifier and FR classifier accuracy

Addressing Question 5: *Is resection of channels showing PLHG recruitment predictive of post-surgical Engel outcome?*

Like in the previous chapter, I explored the temporal spectrum of PLHG recruitment, ranging from PLHG1 to 10, while Weiss and colleagues (2015) focused on PLHG4 and PLHG8 for apparently arbitrary reasons. In addition, I implemented a stricter criterion for PRO (=PLHG/Resection overlap) analysis to investigate whether this approach might add information and might show different predictive power of surgical outcome. Besides PLHG without any restriction of occurrence in all three seizures, PLHG recruited channels, which occurred in at least two of the three seizures were analysed. Contrary to the findings of Weiss and colleagues (2015) the results of the current paediatric study did not show an improved outcome classification using PLHG1–10 recruitment. Neither the regions that were invaded early by the seizure, nor those that were late, were shown to be of importance for the purposes of epilepsy

surgery. This was true for both approaches (PLHG$_{any}$ & PLHG$_{two}$) tested. In comparison to Weiss and colleagues (2015) who included consecutive seizures (typical plus atypical ones), the majority of the patients included in this study showed habitual clinical seizures (66.7%) with similar seizure onsets. Not every possible seizure type could be included for each patient. However, a few patients also showed different seizure types, subclinical seizures or atypical seizures. Hence, this could not have led to the discrepancy in PLHG results of the two studies.

Addressing Question 6: *Does the overlap of epileptogenic zone defined by SOZ, FR or PLHG with surgical resection predict post-surgical outcome?*

Furthermore, I hypothesized that combining the two investigated biomarkers and clinical SOZ information might be more predictive of seizure outcome.

The first combination I would like to highlight is the PSO (=PLHG/SOZ overlap). I investigated PSO, because for the previous adult MNI study, no resection data was available and SOZ data was used as a proxy for likely resection region. The current study could show, like the adult MNI study, that early PSO (PLHG3) alone was predictive of post-surgical outcome. For most of the remaining PLHG bins a higher mean percentage of patients with good compared to those with poor surgical outcome was seen, however, not significantly so on bin-wise testing. This shows that PLHG information might be of importance to include in principle. Furthermore, I could reproduce PSO findings of the adult MNI study (Section 2.4.3), strengthening the argument of potentially needing to include PLHG information, yet further research here is needed. However, when including resection information, for SOZ alone (SRO = Seizure/resection overlap), for PRO alone or for combining the two, S ∪ P (= SOZ association and/or PLHG recruitment), no improvement in prediction accuracy could be shown. The reason might be that resection not always included exactly the SOZ channels defined clinically as some resections were much more extensive than the SOZ would have suggested. This is due to the nature of some

surgical resection procedures. Furthermore, in some patients with tuberous sclerosis for example, more than those tubers showing the ictal onset were resected if they were in close proximity to each other. In some cases however, resection was limited by eloquent areas in proximity to the ictal onset areas, hence some SOZ channels needed to be spared to prevent language or motor deficit.

Next, I would like to discuss findings on the combination of SOZ and FR information (S $\cup$ F). FRs are proposed as biomarkers of the EZ, believed to reflect a propensity for high frequency neuronal discharges within epileptogenic cortex (Akiyama et al., 2011; Crépon et al., 2010; Usui et al., 2011; Wu et al., 2010). Resection of a combination of these two measures resulted in an improvement in accuracy when comparing patients with good and poor Engel outcome. However, resection of FR contacts alone (FRO = FR/Resection overlap) did not lead to any improvement. It seems to be critical to use FR information in a two-stage approach with SOZ association to improve outcome classification. However, this needs to be tested in a bigger patient cohort, as these results could only be achieved by excluding two outlier cases. Interestingly, the three-stage approach, including a combination of both biomarkers and SOZ information did not result in any prediction accuracy improvement.

3.5.4   Reflections on the methodology

There were technical issues like artefact removal and sampling rate and clinical and sample related issues that need to be addressed.

First, artefact removal was discussed in the previous chapter. As the same methods were used in this study, I would like to refer to Section 2.5.4 of Chapter 2 for further discussion.

Second, for this study, EEG recordings with a sampling rate of 1024Hz were used. This sampling rate is sufficient when exploring high gamma activity, however, when investigating fast ripples this sampling rate is low compared to

some previous studies (Urrestarazu et al., 2007; Zelmann et al., 2009; Zijlmans et al., 2009). The recommended sampling rate for FR identification is >2000Hz (Zijlmans et al., 2017). However, the data was recorded for clinical purposes and from 2012 onwards, before any such HFO recommendations were available. Nevertheless, this might result in limited recording of HFOs in the fast ripple range, although there is evidence that HFOs at frequencies below 300 Hz (sampled at <1024 Hz) are specific for areas of seizure onset (Crepon et al., 2010; Ochi et al., 2007; Worrell et al., 2008).

Third, paediatric patients included here were a heterogeneous group, however typical for patients selected for this procedure. Children and adolescents with prior surgeries were included. Patients who show recurrence of seizures in the short-term are more likely to remain intractable as seizure-generating networks still remain (De Tisi et al., 2011; Najm et al., 2013; Thom, Mathern, Cross, & Bertram, 2010). Furthermore, patients were included in whom the main surgical strategy was not curative but palliative, like in TS patients where the aim often is a temporary seizure freedom or reduction of seizure burden by resecting the dominant tuber.

Fourth, regarding defining the Engel outcome the current recommendation is using Engel class I outcome as good and Engel class II-IV outcomes as poor (Jacobs et al., 2018). Weiss and colleagues (2015) used a different definition where good outcome was defined as Engel class I&II and poor outcome as Engel class III&IV. Results of this current study only showed significant results when using the outcome group definition of Weiss and colleagues (2015) compared to the one adopted by Jacobs and colleagues (2018).

Fifth, sample size in this study was smaller compared to the study of Weiss et al (2015). He included 46 patients compared to 21 patients in this study. Sample size difference might have led to different results. Nevertheless, both studies included a similar percentage of patients with good versus poor outcome (Weiss et al: good = 71.1%, poor = 28.3%; current study: good = 71.4%, poor = 28.6%). Concerning studies investigating HFOs, the sample size here was similar to

previous published work (Jacobs et al., 2016, 2018; N. van Klink, Frauscher, Zijlmans, & Gotman, 2016; Wu et al., 2010).

3.6 Limitations and consideration

The results of the current study should be interpreted in light of some limitations discussed in the following section.

First, limitations regarding seizure types and implantation methods please see the previous chapter Section 2.6.

Second, implementing code from a different group posed some challenges. Written instructions were available, but scarce. During analysing adult MNI data using the PLHG metric did not lead to difficulties. Only when analysing GOSH paediatric data obstacles were encountered. Some patients SEEG recordings were continuously active, making it hard to detect segments for baseline recordings. Baseline recordings were used to subtract activity from ictal recordings, which hence could have led to distortion of some recruitment patterns.

Third, the threshold for classifying a PLHG site was determined for each seizure independently, based on the PLHG value distribution. As explained in Section 2.2.5 the distribution could be bimodal, unimodal, or the threshold could be set manually. In the work of Weiss and colleagues (S. A. Weiss et al., 2013, 2015) manual thresholding was not described, however, information about manual thresholding in relation to their study was given in person. No further details about the use of manual thresholding were provided in the work of Weiss and colleagues (2015) and how this may have affected their data. In this study, I used manual thresholding for seven patients (33.3%). In two of these patients in only one seizure and in five of these patients in all three seizures. Asking whether this approach mattered for the occurrence of very early recruitment, results showed that in three of the patients with very early recruitment manual thresholding was applied and for the other three patients it was not used.

Fourth, one inclusion criterion was the duration of a seizure needing to be at least 35s long. This was decided upon due to a personal recommendation of Dr Weiss as he argued that often early PLHG was seen only very late. Nevertheless, this inclusion criterion is restrictive as the average time of earliest PLHG recruitment was 15.6s in this study and 14.2s in Weiss et al. (2015). Further PLHG research should incorporate shorter seizures, as in the current study many patients had to be excluded because of seizure durations around 20s. This restriction also limited the sample and power of this study and should be considered in further research.

Fifth, seizure outcome was measured using the Engel classification. Although this is a simply classification it is still used and interpreted differently by various groups. Adhering to the grouping of Weiss an colleagues (2015) where good outcome was defined as Engel I and II and poor outcome as Engel III and IV led to significant differences. In contrary, the classification of Jacobs and colleagues (2018), where good outcome was defined as Engel I and poor outcome as Engel II-IV did not lead to significant results. Furthermore, seizure outcome is one-sided, as it only focuses on seizure freedom, while improvement of cognitive skills or quality of life was not taken into account. There is a lack of classification systems for cognitive outcome, like Engel or ILAE for seizure outcome, which made comparison of post-surgical language or memory outcomes more difficult. Furthermore, the paediatric cohort highlighted that aims can be at least twofold, curative and palliative. For both patient groups the same seizure outcome classification system was used, although it was known in a few patients before surgery that complete seizure freedom won't be achieved. A classification system comprising outcomes concerning seizure freedom, cognition and quality of life might be useful.

To conclude, this was the first study aiming to replicate results from Weiss and colleagues (2015) using their PLHG metric in a paediatric cohort with medication-resistant focal epilepsy. However, I could not show that the PLHG information alone, nor a combination of PLHG and SOZ are valuable in

predicting post-surgical outcome, keeping in mind that my sample was much smaller than the one of Weiss and colleagues (2015). However, results showed that combining SOZ and FR information might be a potentially useful marker for improving predictive accuracy of surgical outcome in this paediatric cohort.

III Invasive Electrophysiological Mapping of the Language Cortex in Children with Focal Epilepsy

4 Principal Methods

This chapter describes the context and the general methodology underlying the two studies described in subsequent Chapters 5 and Chapter 6.

4.1 Participant recruitment

All patients approached were aged between 5 and 17 years at the time of testing and had a diagnosis of medication resistant focal epilepsy. The prospective cohort was recruited from amongst those admitted to invasive pre-surgical EEG monitoring at Great Ormond Street Hospital for Children (GOSH). The direct care team in conjunction with the clinical research team initiated contact with potential families while they were admitted to Koala ward. Families were informed about the study and information leaflets for parents and age-appropriate ones for the child or adolescent were handed to them. At the earliest they were approached again the next day and questions were answered. If participants and parents/guardians were happy to take part in the study a consent/assent form was signed. Patients without a basic understanding of English were excluded from the study.

4.2 Ethical approval

The study was allocated to and approved by the North East - Newcastle & North Tyneside 1 Research Ethics Committee (Reference 16/NE/0036) and is registered with the Research and Development Office of GOSH.

4.3 Clinical information

Prior to invasive EEG monitoring, a detailed clinical evaluation was performed for each patient by the treating clinicians. Demographics, age at onset of epilepsy, clinical examination results, imaging findings, neuropsychological test scores (IQ, language, memory, academic attainments, handedness), previous

surgical treatment information and neurophysiological findings were recorded for this study. In addition, implantation plan and neurophysiological findings from the invasive monitoring admission, surgical resection details and outcome information from a subsequent surgical intervention were recorded.

4.4 Language Tasks, Stimuli Design and Stimuli Presentation

For language testing six different tasks were developed. For three of these tasks stimulus material from the 'Panda Games' was used, which are an fMRI task battery designed by Dr Louise Weiss-Croft (Croft, 2014). The other three comprised of auditory language tasks designed for this study.

4.4.1 Panda Games

These 'Panda Games' were built on the functional neuroanatomical model of language proposed by Price and colleagues (Price, 2012). This model is based on the most consistent structure-function mappings evident from the last 20 years of fMRI and PET investigations of language. It is based on converging evidence for neural networks for heard speech, speech production and reading, which interact with sensory and motor processes localized to specific structures and with distributed activation shared across several functions (see Figure 36).

Figure 36. Language processing stages and their anatomical locations (A) of the functional neuroanatomical model of language (B) proposed by Price and colleagues (Price, 2012); **C.** represents the most consistent structure-function mappings in adults using fMRI. Processing stages are colour coded, and anatomical regions are labelled. This figure is taken from Price 2012.

In essence, the 'Panda Games' comprise tasks for auditory comprehension, reading comprehension, word retrieval and sentence formulation and engage receptive and expressive language skills. These auditory and picture stimuli are suitable for children, having been validated on healthy children and piloted on children with epilepsy in the same age range as of the current study. The 'Panda Games' also include baseline tasks for each main task which is vital for fMRI research to ensure the delineation of critical linguistic function in addition to basic sensorimotor function.

Originally, the Panda Games were grouped into four difficulty levels according to these age groups (children with verbal abilities in the normal range: 5–7 year olds to level 1, 8–10 year olds to level 2, 11–13 year olds to level 3 and 14–16 year olds to level 4; children with verbal abilities outside the normal range were assigned a level according to their age-equivalent level of functioning as determined by performance on neuropsychological assessments) (Croft, 2014). Each task comprised of 24 stimuli. As this study cohort was expected to include children from as young as 5 years, with learning difficulties and/or developmental delay only a few stimuli from difficulty Level 4 were included. For this study, a subset of the Panda Games was used and adapted for ERP recording: auditory sentence comprehension, picture naming and sensorimotor control condition.

Picture Naming (PN)

This task was used to induce word retrieval from visual input and articulation. Participants were asked to name 50 colour pictures depicting objects and animals. They were asked to name items as quickly as possible, and to say the first thing that "popped into their head". Image sizes were 350x350 pixels. Example pictures are shown in Figure 37a.

Colour Naming with words (CNw)

This task was used to induce semantically shallow word retrieval from visual input, and articulation. Participants were instructed to name the colour of the

square border (5 pixels) around a 350x350 pixel meaningless coloured pattern. The meaningless pattern was a visually warped version of PN stimuli, matched for visual complexity. Stimulus order matched the PN task. Example pictures, which match the PN stimuli, are shown in Figure 37b.
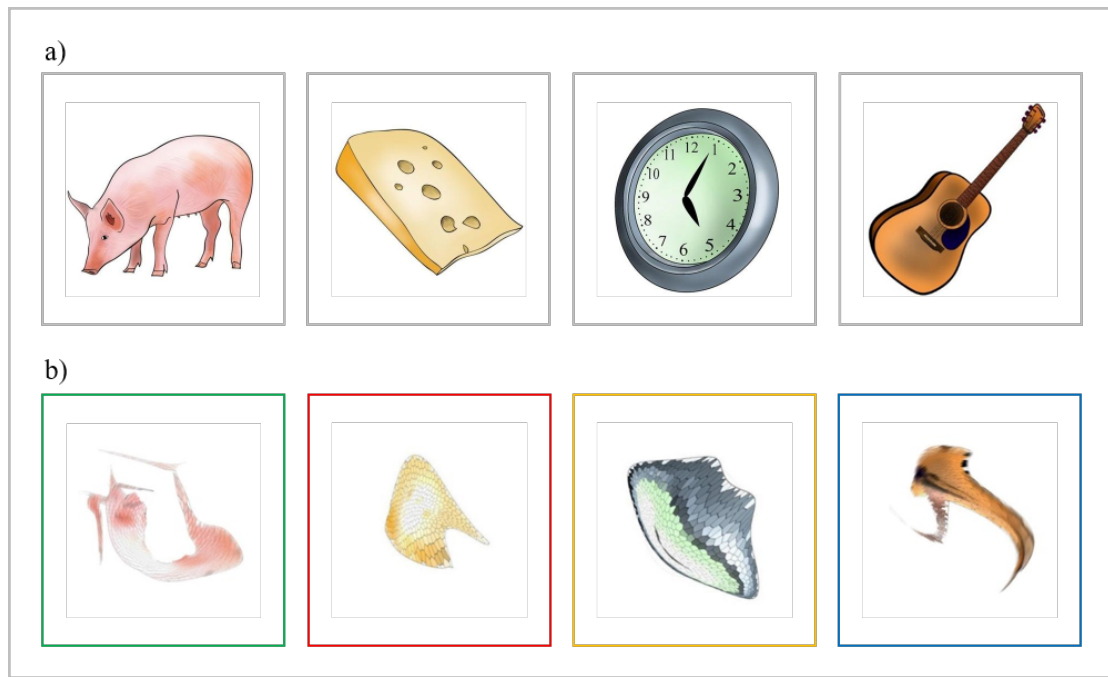
Figure 37. Example pictures of the Picture Naming and Colour Naming with Words tasks.

Processes involved in generating words involved in picture and colour naming plus their anatomical location (Price, 2012) are summarised in Table 18.

Table 18. Processes involved in generating words in response to a visual stimulus (PN, CNw) and their anatomical location.

Processes involved in PN and CNw	Anatomical location
Visual processing	occipital and ventral occipito-temporal cortex
Accessing semantics	left posterior MTG/ITG
Semantic associations	left anterior STS/MTG/ITG and ventral occipital-temporal cortex
Word retrieval	left MFG/SFG
Relevant articulatory associations are then accessed, including: · action selection · orofacial motor planning · sequencing of motor plans	bilateral premotor cortex, left dorsal premotor cortex left ventral Pars Opercularis (BA 44) and premotor cortex left dorsal Pars Opercularis (BA 44) and preSMA
A response is then either initiated or suppressed	Anterior cingulate (ACC)
Response initiation leads to: · motor execution · orofacial motor activity · timing control over motor output · breathing	SMA and ACC bilateral pre- and postcentral gyri left putamen and cerebellum ventral thalamus and left anterior insula
Expected and actual speech output are associated with · further auditory processing · articulatory recoding · supported by short term memory	STG/STS and Planum Temporale (PT) left Pars Opercularis (BA 44) & ventral premotor cortex Pars Opercularis (BA 44), PT, SMG

Listen and Name (LN)

This task was used to induce sentence level semantic and syntactic processing from phonological input, word retrieval and articulation. Participants were asked to listen to sentence-level auditory descriptions of objects and animals and saying the name of the item being described out loud. Sentences had been recorded by a female native English speaker in a sound proof room using prorec software (http://www.phon.ucl.ac.uk/resource/prorec/). Example sentences are illustrated in Figure 38.

A long orange vegetable

An animal that gives milk

An object in the bathroom that flushes

A musical instrument played by strumming it's strings
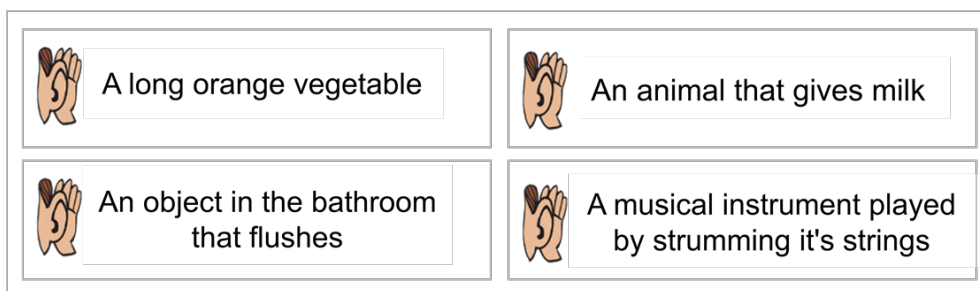
Figure 38. Example sentences of the Listen and Name task.

Language processes involved in the Listen and Name task plus their anatomical location are summarised in Table 19.

Table 19. Processes involved in generating words in response to auditory stimuli (VG, LN) and their anatomical location (Price, 2012).

Processes involved in VG and LN	Anatomical location
Auditory processing	bilateral STG left posterior STS
Semantic access	left posterior MTG/ITG
Semantic processing of the heard signal: · semantic associations · multimodal integration · semantic retrieval	left anterior STS/MTG/ITG and ventral occipito-temporal cortex pSTS left Pars Triangularis (BA45), Pars Orbitalis (BA47), left SFG and bilateral Angular G
Selection of lexical response	left MFG
Obtaining articulatory associations & sequences	left Pars Opercularis (BA44), bilateral premotor cortex (BA6), left primary motor cortex (BA4) and SMA
Motor output	bilateral primary and pre-motor cortex, SMA, ACC, left putamen, anterior insula and thalamus
Any articulatory recoding that is required (e.g. due to an error) supported by short-term memory	left Pars Opercularis (BA44) and ventral premotor cortex (BA6) left Pars Opercularis (BA44), PT, temporo-parietal junction/SMG

Auditory stimuli for this task required further processing as they were originally pre-processed for an fMRI paradigm. For an ERP paradigm the exact onset of the stimulus is crucially important. Stimuli were further processed using audio editing software (Goldwave Version 6.12, GoldWave Inc, 2015) to insert trigger points to permit accurate subsequent ERP analysis, e.g. averaging. Triggers (cues) were manually inserted at the beginning of each word of the sentence (Figure 39).
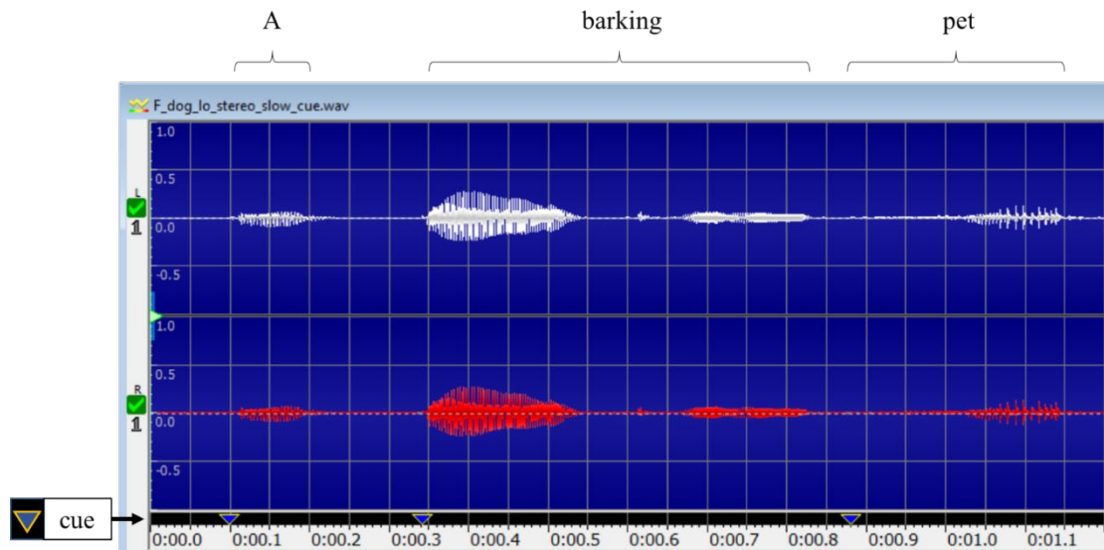
Figure 39. This shows an example sentence from the LN task with cues inserted at each word's sound onset.

After testing the first few patients with this task, it became obvious that the speed of the sentences during the LN task was too fast. Although, this task was developed for patients with epilepsy and stimuli from the hardest Level 4 were avoided participants struggled to understand some of the sentences. Therefore, the speed of the stimuli was reduced by 15% using 2.2.0 of Audacity® recording and editing software (Audacity Team, 2018).

4.4.2   Additional auditory stimuli

In addition to the 'Panda Games', three more auditory language tasks were designed for this study. Tasks chosen were Verb Generation, Word Repetition and listening to reversed words (Baseline Listen).

Verb Generation (VG)

This task was used to induce word-level semantic processing from phonological input, word retrieval and articulation. Participants were presented with a common noun and instructed to say a single verb associated with each noun ("a doing word that goes with it"). Example words used for the VG tasks are shown

in Figure 40 and language processes involved in the verb generation task and their anatomical location (Price 2012) are summarised in Table 19.

Word Repetition (WR)

This task was used to observe effects of phonological input, mapping auditory inputs to articulatory activity and to observe articulatory processing. Participants were presented with a common noun and instructed to repeat the word they just heard. Processing steps involved in word repetition and their anatomical location (Price 2012) are summarised in Table 20 and example words used for the WR tasks are shown in Figure 40.

Table 20. Processes involved in word repetition and their anatomical location (Hope et al., 2014; Price, 2012).

Processes involved in WR	Anatomical location
Auditory processing	bilateral STG, including Heschl's gyri & PT
Accessing semantics/ associations	left posterior MTG & posterior ITG
Semantic input to articulation	left MFG
Motor control to overt speech	preCentral, postCentral, Cerebellum, anterior Insula, Putamen, thalamus
Auditory feedback	bilateral STG, including Heschl's gyri & PT

Baseline Listen (BL)

This passive listening task was used to induce auditory processing and word level semantic processing. Participants were instructed to solely listen to "funny sounding" non-words. They were allowed to occupy themselves with e.g. drawing during this task. Example words used for the BL tasks are shown in Figure 40.

Figure 40. Example words for Verb Generation, Word Repetition and Baseline Listen tasks.

Verb Generation is the current gold standard language task at GOSH to identify the language dominant hemisphere in surgical candidates. Word stimuli for the tasks were chosen from existing lists already in use for pre-surgical fMRI scanning at GOSH (Liégeois et al., 2004, 2002).

All stimuli chosen from that existing list of words were newly recorded and further processed using 2.2.0 Audacity® software. They were spoken by a female native English speaker and recorded in stereo. Each stimulus was cut at the very onset and offset of the speech oscillation. Further processing steps included pitch change, noise reduction and normalising peak amplitude.

In addition, for the Baseline Listen task words were reversed using 2.2.0 of Audacity® software. Figure 41 illustrates oscillations from the original word and the reversed version.
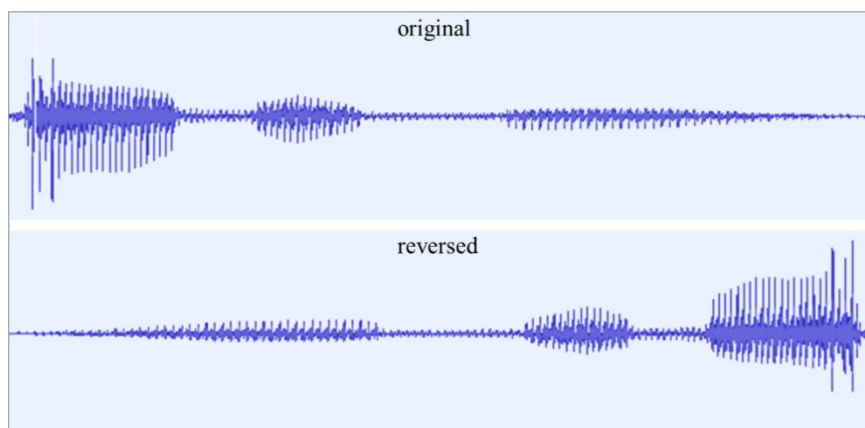
Figure 41. Example of original and reversed word sound waveform.

166

4.4.3 Stimuli presentation

Presentation® software was used to present stimuli to participants in an automated way (©2017 Neurobehavioral Systems, Inc).

All necessary equipment for stimuli presentation and ERP recording was kept on a trolley and placed at the patient's bedside (see Figure 42). Intracranial EEG recording and stimulation equipment is described in detail in Section 5.7.
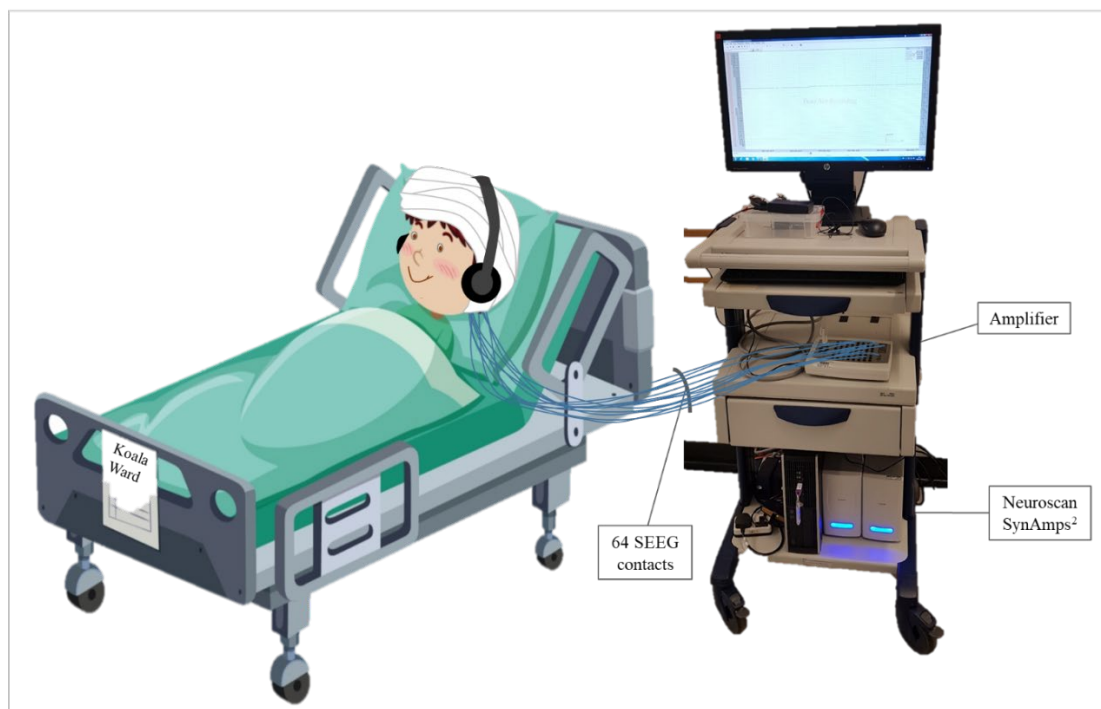
Figure 42. Illustration representing recording and stimulation equipment and setup for stimuli presentation.

Auditory stimuli were presented through portable speakers (M-Audio® AV 30) placed next to the bed of the participant (distance approximately 1 meter) at the beginning of the study period for the first three participants and later on through headphones (SONY) to minimise external noise level during task presentation. Audio levels were adjusted to a comfortable level for each participant prior to the auditory presentation.

Picture stimuli were presented sequentially on a 24–inch LED monitor placed on the ERP trolley at the patient's bedside (maximum distance to participant 1.5 meter). Picture stimuli consisted of colourful child friendly pictures sized 16.2cm

in height and width, presented at the centre of the monitor on a black background. Participants were instructed to overtly name objects presented in the picture naming tasks.

The inter-stimulus interval for all tasks (auditory and visual) was not set to a specific time. A button press initiated presentation of the next stimulus. The sequence of the stimuli delivery had already been pre-programmed. The button press was controlled by the researcher. This setting was chosen as it allowed a flexible presentation mode, with the possibility to pause experimental run at any time. This method of stimuli delivery seemed most appropriate after a trial run with a 5-year-old participant.

4.5 Testing environment

Participants underwent their individual clinical assessment during their stay at Koala ward. This was the main purpose of their stay. Hence, all ERP testing took place once clinical assessment was completed and before participants were called for electrode deplantation.

If participants underwent electrical stimulation for language mapping during clinical assessment, identical language tasks were prioritised during the language iERP testing session.

All ERP testing took place within the same day in the patient's room on Koala Ward at GOSH. Participants were comfortably seated in their bed.

4.6 Language iERP testing session

Participants underwent one language testing session where they were presented with both auditory and visual language tasks. The number of tasks completed during this session was dependent on the participants' attention, cognitive skills and the available time to test. The duration of testing varied from 15–90 minutes. Breaks were taken if needed. Prior to starting the ERP recording participants

were presented with a practice trial consisting of four stimuli. If participants did not perform the task correctly during the practice session, task instructions were repeated and the practice trial was re-started. Practice stimuli were repeated until the participant was familiar with the task. Three participants (18.75%) trialled the VG trial stimuli twice and four participants (36.40%) played the LN trial stimuli twice. Each task consisted of a total of 50 stimuli, which were presented sequentially and in a pre-determined order.

4.7 Intracranial EEG recording

4.7.1   Clinical data acquisition

Electrode configurations included subdural grid electrodes (⌀ 4.0mm) with 10mm centre-to-centre spacing, and semi-rigid depth electrodes (⌀ 0.8mm and comprised 5, 8, 10, 12, 15 or 18 contacts per electrode of 2mm length, 3.5mm apart (Dixi, Besançon, France), depending on the target region. Electrode positioning was chosen by the treating clinicians based solely on clinical considerations and no electrodes were placed for the purposes of this study.

Intracranial EEG (iEEG) was recorded using Xltek IP Video EEG (Natus, USA) system, which permitted simultaneous recording of up to a maximum of 256 EEG channels. The sampling frequency was 1024Hz with an acquisition filter band-passed 0.1–343Hz. Two contacts located in white matter were chosen as ground and reference.

4.7.2   Anatomical definition of depth electrode positioning

The anatomical position and trajectory of the implanted electrodes was post-operatively determined by co-registering a post-implantation CT and a pre-implantation MRI image, typically a T_1- or $T_{2\text{-weighted}}$ fluid-attenuated inversion recovery (FLAIR) image using 3D Slicer software.

3D Slicers is a free open source software for medical image computing and visualization (Fedorov et al., 2012). At GOSH slicer is implemented as a surgical planning tool.

To determine the position of individual electrode contacts in specific brain regions the 3D Slicer extension module, Brain Zone Detector, was used which localizes the neuroanatomical sources of the recorded activity by automatically determining each contact position within a volumetric brain atlas (Narizzano et al., 2017). With the help of this tool, and confirmation via visual inspection, it was possible to assign contacts to different brain regions.

4.7.3 Study data acquisition

For this study iEEG was recorded continuously using Neuroscan SynAmps[2] 64-channel amplifier from Compumedics (El Paso, TX). Data was sampled at 5000Hz (apart from four patients: ID2 and ID3—1000Hz, ID9—2000Hz and ID100—500Hz sampling rate), with an acquisition filter setting from DC-1000Hz, with a resolution of 24bits and with a notch filter applied (50Hz). Ground and reference used for clinical recording were chosen in this study.

Neuroscan SynAmps[2] was used as it permitted stimulus lines to input time-locked digital trigger pulses which was essential for this study design. The Neuroscan setup for this study recorded from 64 channels compared to the clinical EEG system which could record up to 256 channels. Hence, for this study only a sub selection of the contacts used for the clinical iEEG could be used. The electrodes selected for the ERP recording where selected depending on their proximity to the language cortex. Additionally, all contacts used for clinical electrical language stimulation were also included in the final contact selection for this study. White matter contacts and artefactual contacts were excluded.

In addition to the iEEG, data from a microphone was recorded in a separate channel to identify verbal responses from participants. It was important that the verbal responses were time-locked to the on-going EEG data. This was made

possible with the help of Alan Worley, principal clinical scientist at GOSH Clinical Neurophysiology Department, who built a SynAmps Signal Processing Unit, which is illustrated and explained in detail in the Appendix p.415 (Figure 117). Data from the microphone was band-pass filtered from 10–1000Hz and a notch (50 Hz) filter was applied.

4.8 ERP analysis

4.8.1 Stimulus-locked analysis

EEG data was processed using BrainVision Analyzer 2.1 software (Brain Products GmbH, Gilching, Germany). EEG recordings were visually checked for artefacts. Channels found to be artefactual throughout the recording were excluded from further processing (see Figure 43). Data was then re-referenced to a common average reference, filtered using a high pass filter (HPF; 0.1Hz, 2nd order) to reduce DC drift, and subsequently segmented from 500ms before stimulus onset to 2000ms post stimulus for VG, WR, BL, PN and CNw tasks. For the LN task a window from 2000ms prior to stimulus onset to 7000ms post stimulus was chosen. This long window was selected as the LN task comprised sentences of different word counts and length. The minimum number of words in a sentence was three and the maximum was 12 words. The average duration of a sentence was 3.1s for trials with 15% reduced speed (SD = 0.9s, min = 1.4s, max = 5.5s) and 2.7s for trials with original speed (SD = 0.7s, min = 1.2s, max = 4.7s). Data was further subjected to baseline correction (from 500ms pre-stimulus to 0ms). Artefact correction and rejection settings were decided on an individual basis. Intracranial EEG tends to be significantly less affected by artefacts compared to scalp EEG. The main artefacts in scalp EEG where artefact correction is essential are ocular and muscle artefacts which are however of no concern in intracranial recordings. An EEG recording from an electrode in close proximity to the seizure focus could show a more active recording or interictal activity compared to recordings of electrodes further away. However, when

rejecting an epoch due to satisfying artefact correction settings in one electrode only, information from all other electrodes gets lost as all channels in that epoch are rejected. Artefact correction settings checked for each data set were (a) Gradient: maximum allowed voltage difference between two data points, (b) Max-Min: maximum allowed absolute voltage difference, (c) Amplitude: minimal and maximal amplitude and (d) Low Activity: Lowest allowed activity in microvolts. These criteria could be set for specific time intervals (specified in milliseconds) within the epoch. If interictal activity occurred in all channels, like a burst of generalized spike-wave complexes, individual channel mode of artefact rejection was used. Examples of common EEG artefacts are presented in Figure 44. In 75.6% of study datasets no artefact correction was used and in 24.4% of data sets individual channel mode of artefact rejection was used. Finally, 40–50 trials per subjects were averaged for subsequent analyses.
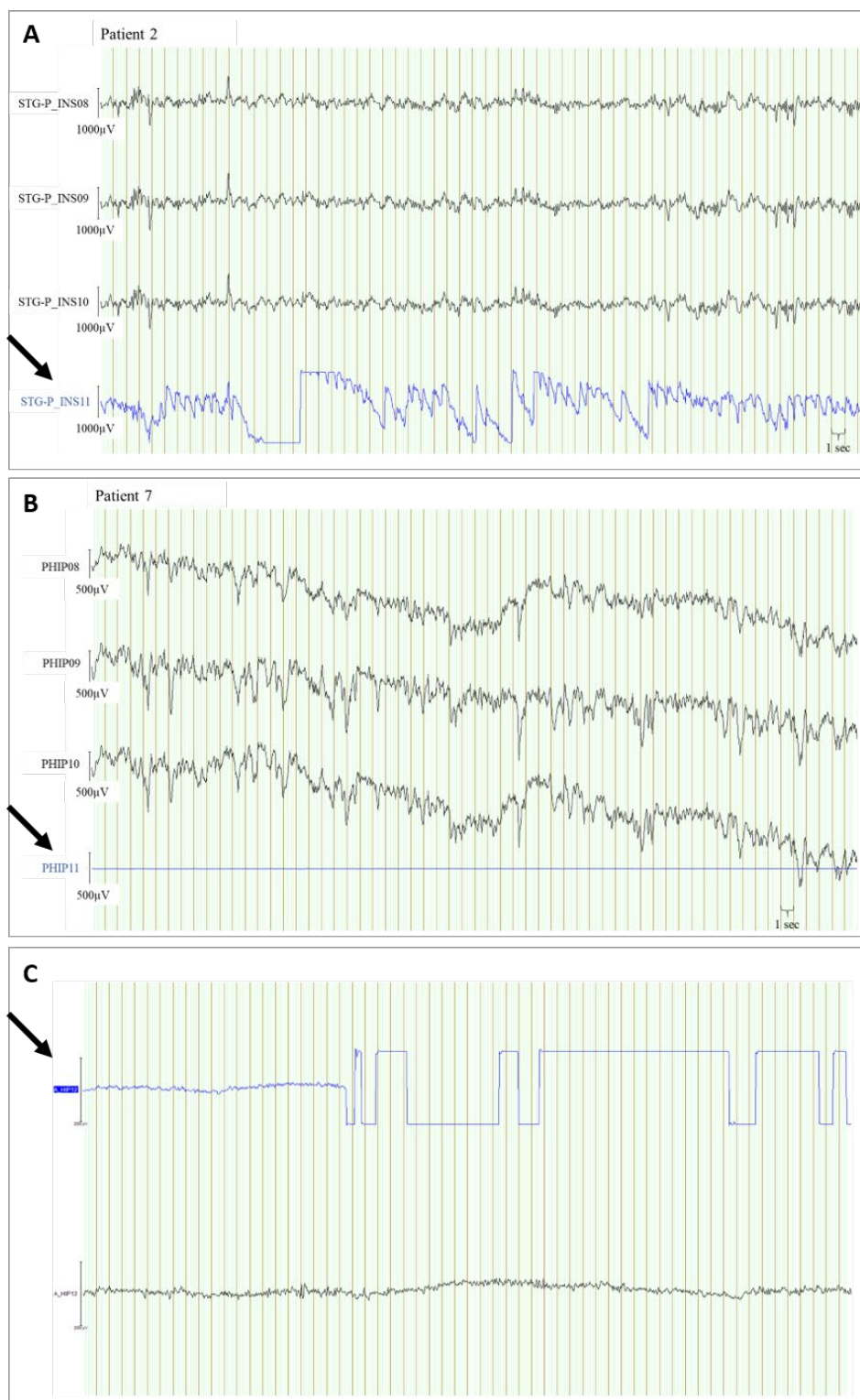
Figure 43. Examples of artefacts occurring throughout the EEG recording and which were excluded from further processing. Artefactual channels are shown in blue/marked with an arrow (A-C).
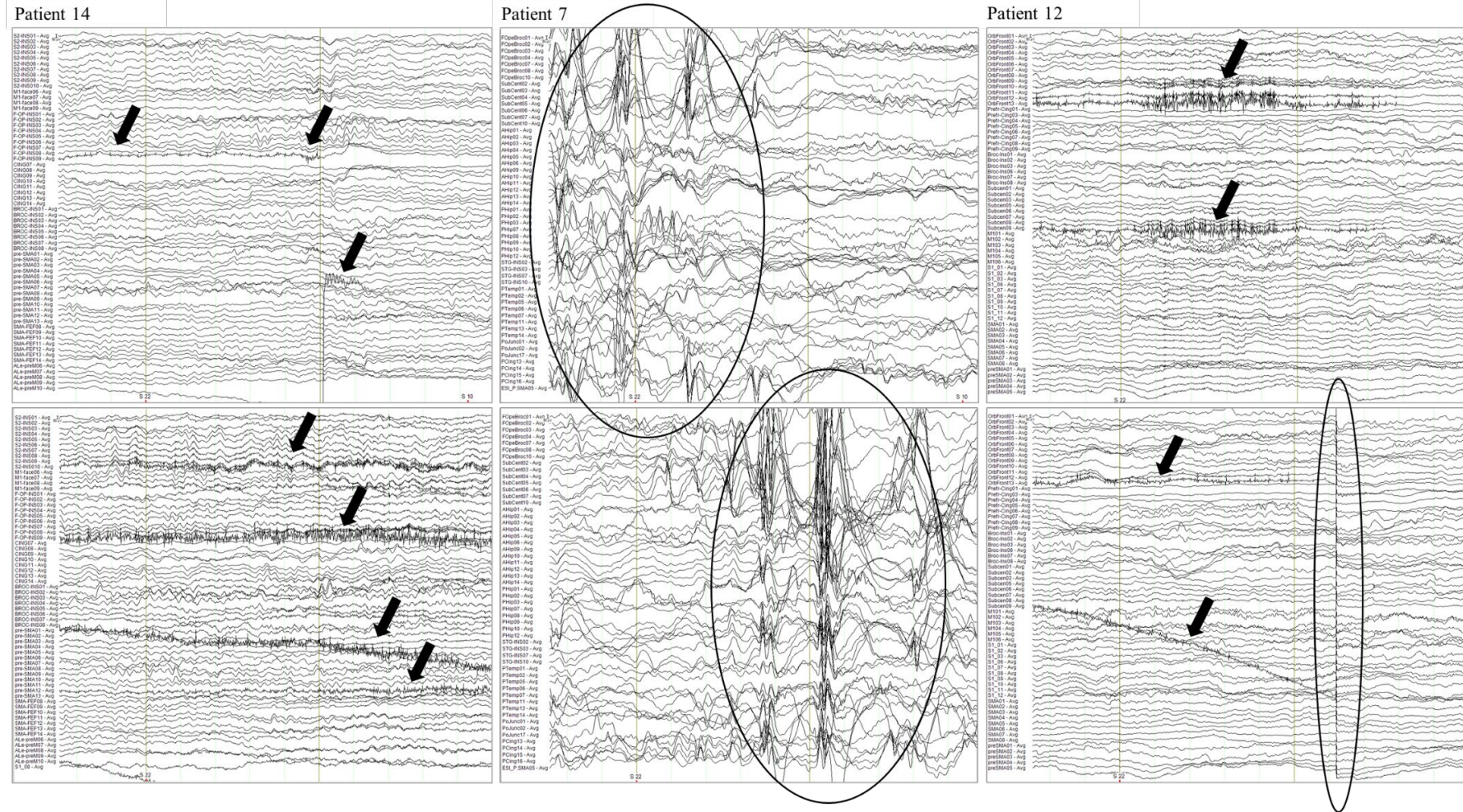
Figure 44. Examples of artefacts detected and eliminated using individual artefact mode. For each of the three patients presented here two examples of artefacts are shown.

4.8.2   Response-locked analysis

To be able to analyse response-locked neural processes, markers for speech-response onset were inserted manually. This was done using the 'Edit Marker' option of the BrainVision Analyzer software. Figure 45 shows the speech-response marker channel, which recorded speech responses of participants and an example speech response oscillation.
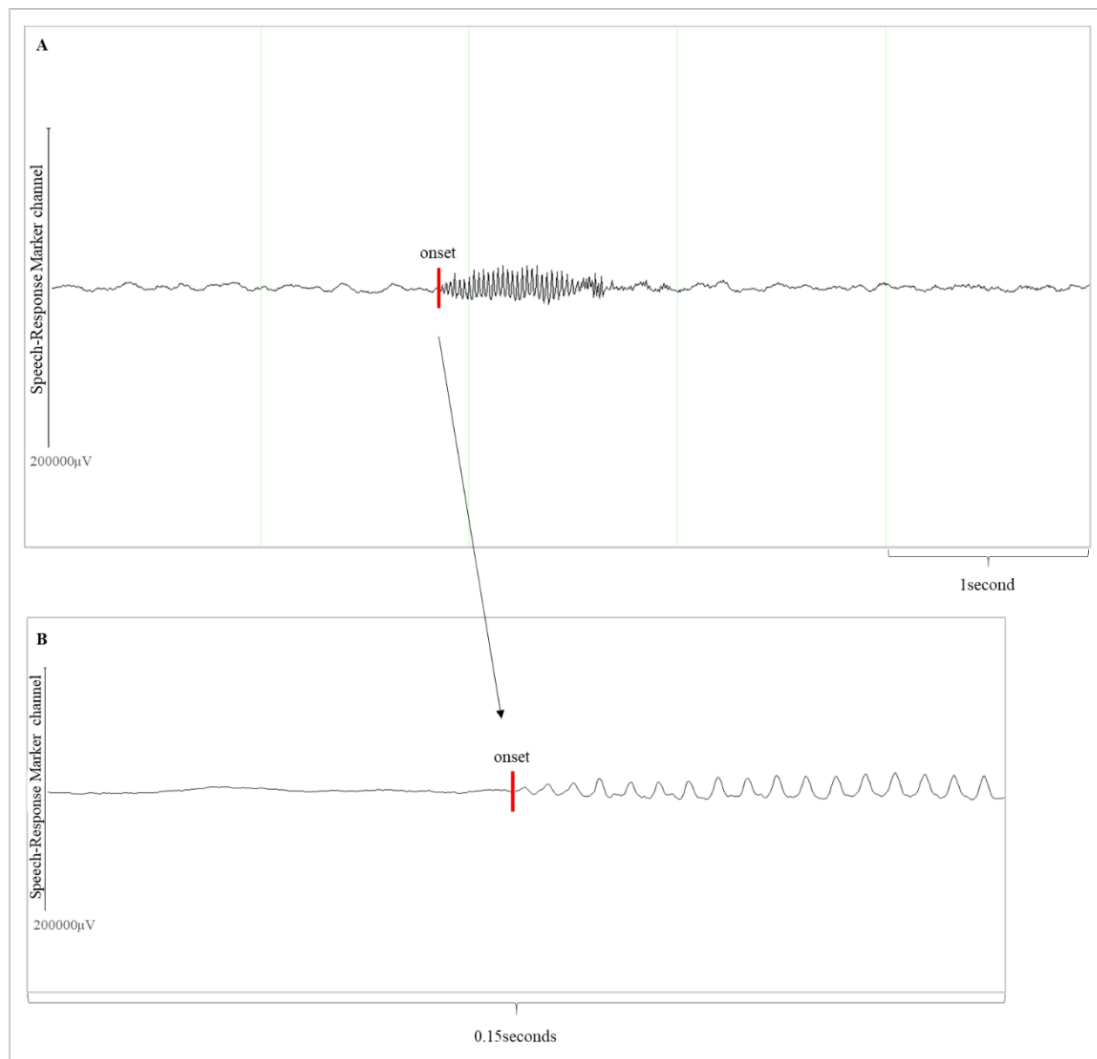
Figure 45. Example of manual marking of speech-response onset in iEEG recording. A illustrates example speech-response oscillations (time scale = 1s) with onset marked in red. **B** shows speech-response onset marker with a time scale of 0.15 seconds to emphasize marker were set with due diligence. These markers were then used for further processing.

The next pre-processing steps were the same as described above in Section 6.8.1. The only exception was the window chosen for segmenting the EEG recording,

175

which was set from 1000ms prior to response onset to 1000ms post response onset. This is due to the change of focus when it comes to response-locked analysis. Here, it is of interest to also investigate a longer pre-response time window to assess whether a preparatory activity is seen before the actual response is given.

Also here, 40–50 trials per subjects were averaged for subsequent ERP analyses.

In most published articles, ERP waveforms are shown as grand averages, where averaged waveforms of individual participants were put together to form an average across the whole subject group using a standardised scalp electrode montage. In contrast to this approach, in the current thesis each participant had a unique and individual implantation regime and hence grand averages were not the primary choice for analysis. Individual averages were used for further analysis as detailed in the following sections. Nevertheless, a grand average across patients was attempted (described in 6.4.11) where one contact per brain region per patient showing a robust iERP was chosen to stand in as individual average. These individual brain regions' averaged waveforms where then subjected to a grand average to compare morphology of waveforms in left and right hemisphere implanted patients.

4.8.3 Control marker analysis

To control for background activity 'control marker' were inserted manually during offline processing of the recording, when no stimulation had been carried out. Control marker were added into the same EEG recordings which contained the stimulus marker. They could be set into the EEG recording during resting conditions where no tasks were carried out. Such resting conditions for example could be, when the recording was already running but the language testing had not started yet, or after testing ended but the recording was still running. These control markers could also be set at times of breaks during stimulus presentation.

The purpose of these so-called control marker was to generate control waveforms to the stimulus-locked waveforms from the same recording period. This step was necessary to determine whether the averaged iERP was different from the level of background activity that would be present in any randomly chosen epoch (Akatsuka, Wasaka, Nakata, Kida, & Kakigi, 2007). Control marker were pre-processed identically to the stimulus marker, as described above and they matched the number of stimulus marker.

4.8.4 Visual iERP analysis

The first question that had to be answered was whether or not a robust iERP waveform was present. Therefore, averaged waveforms for each contact, each task and each patient were visually analysed. To aid decision making of the robustness of an iERP a set of essential processing steps was determined and incorporated. This set of processing steps included inspecting stimulus- and response-locked waveforms, control-marker-locked waveforms, standard deviation (SD) and split half reproducibility which was assessed by averaging odd and even stimulus trials separately. Each condition had to be satisfied in order to classify a waveform as a robust iERP.

Stimulus-locked and response-locked averaged waveforms were visually analysed and compared to control marker waveforms. Figure 46 (a, b) illustrates stimulus- versus control marker-locked waveforms and its classification as a robust iERP. The next processing step implemented was inspecting the standard deviation (SD) for each data point for the averaged epochs (see examples in Figure 46 (c, d)). Lastly, for the assessment of split-half reproducibility ERP averages based on odd and even trial numbers were computed for each task condition and their waveforms visually compared for reproducibility (Figure 46 (e, f)).
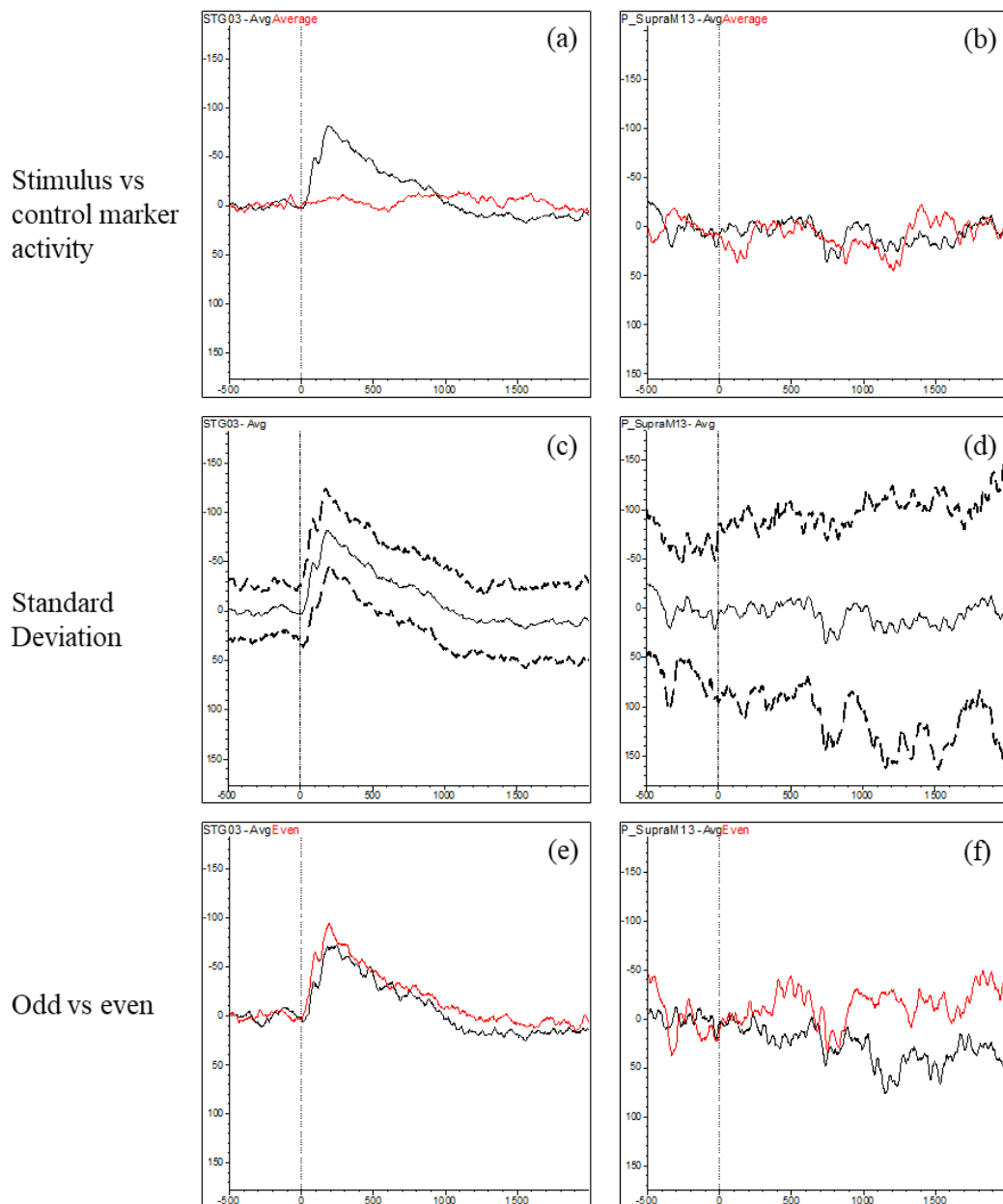
Figure 46. Examples of processing steps showing criteria for classifying a waveform as a robust iERP or not. . (a) illustrates a robust iERP (black) compared to the control marker waveform (red); (b) shows an example where no difference was seen between stimulus- and control marker-locked waveform, leading to no iERP; two different types of SD encountered are illustrated in (c, d) - (c) shows an example of an ideal SD (dashed lines) while (d) illustrates an example of an SD which was much larger: the waveform was therefore rejected for further analysis; (e) illustrates an example split-half reproducibility where odd (black) and even (red) waveform averages match well compared to (f) where odd (black) and even (red) show poor replicability.

Only individual subject iERP averages, where the three conditions of robustness were met, further quantification of ERP parameters (peak latency and amplitudes, etc.) was performed.

178

4.8.5　　　Additional ERP analysis

As described before, visual analysis was implemented and a first selection of iERPs was made. To add a more quantitative evaluation of robustness with respect to background activity a paired t-test against zero analysis was implemented for each task average. This analysis comprised of a data point by data point comparison between the iERP wave and zero in the same subject. Only waveforms surviving this test were counted as robust.

To decide on a valid significance level, first the control marker averages were taken and a paired t-test against zero for each data point was performed. This was done to get an overview of the ongoing activity in the EEG which is unrelated to the stimulus. The maximum negative and positive amplitude t-values were noted and after analysing all individual subject data a t-test threshold for the significance level of the task average defined. The value +/-3 was chosen as the significance threshold.

Next, the stimulus average waveforms and the control marker average waveforms were again visually compared. With the help of the t-test significance of the stimulus averages overlaid a decision was made whether the waveform was classified as a robust iERP or not. Only significant differences which were present over 20 consecutive time points for each component were taken into consideration (Molholm et al., 2006; Trébuchon, Démonet, Chauvel, & Liégeois-Chauvel, 2013b). Some of the waveforms encountered where not easily classified as robust iERPs. Figure 47 gives some examples of waveforms to illustrate how a waveform can look like a robust iERP in cases were for example SNR is small, however, with using the significance level these ERP-like waveforms could be rejected.
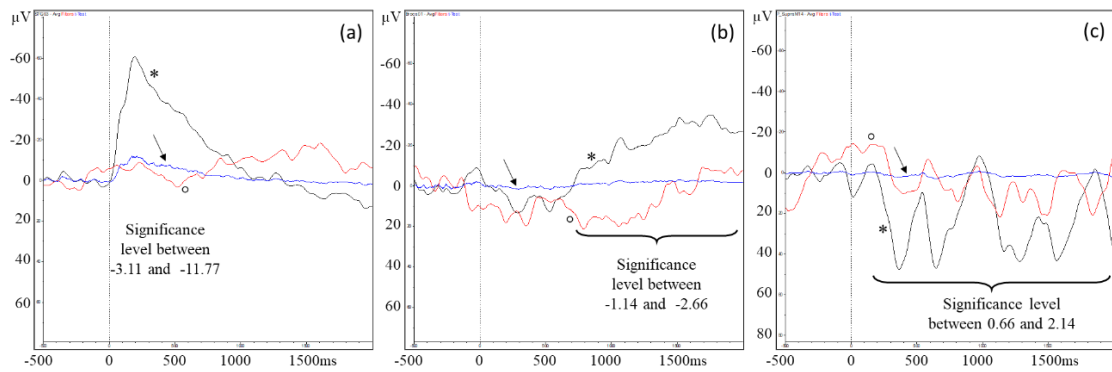
Figure 47. Classification of robust iERPs aided by t-test significance level. (a) illustrates a robust iERP (black line/*) with the overlaid control marker waveform in red (°). The blue line (arrow) represents the significance level which was very high during this ERP (maximum -11.77); (b) shows a waveform looking like a late ERP, however the significance level only showed a maximum of -2.66 here, therefore this was not classified as an ERP; and (c) depicts a waveform which already looks like ongoing noise and not like a robust ERP. This could be confirmed using the significance level (maximum 2.14).

4.8.6 iERP component definition

The time window chosen for iERP averaging was -500 to 2000ms. During processing and analysing iERPs four main morphological characteristics were obvious regarding the onset an duration of the measured evoked response. This classification enabled comparisons between patients. The four components were defined based on four time windows for inspection:

· Primary component (PC): peak latency ≤100ms
· Early component (EC) peak latency between 100–200ms
· Middle latency component (MLC): peak between 200–700ms and wave ending before the 1500ms mark
· Long latency component (LLC): start time between 0–700ms and a duration between 800–>1500ms

700ms was chosen as a margin as it was the average length of word stimuli used for language paradigms. This classification agrees with observations Kojima and colleagues (2012) made when measuring gamma-oscillations during an auditory sentence task.

4.9 Event-related Synchronization and Desynchronization (ERS/ERD) analysis

Compared to ERPs, ERS/ERD are also time-locked but not phase-locked to the event and reflect systematic changes in oscillatory activity within a specified frequency range. Furthermore, they are frequency-band specific and are referred to as induced responses (Pfurtscheller, 1977; Pfurtscheller & Aranibar, 1977). ERD is a short-lasting and localized event-related amplitude decrease and ERS an amplitude increase (Pfurtscheller & Aranibar, 1977). A classic example of ERD is the blocking of occipital alpha rhythm after visual stimulation (Pfurtscheller, 1992) and of ERS, the enhancement of mu rhythms during visual stimulation (Koshino & Niedermeyer, 1975).

Pre-processing of raw EEG data for ERS/ERD analysis was identical to the ERP pre-processing pipeline described in 5.8, apart from one different setting. For ERS/ERD analysis of response-locked epochs the reference interval taken was from 700ms prior response onset to 500ms prior response onset (duration of 200ms). For a reference interval one looks for an interval with baseline activity rather than a task-active interval. Hence, this interval was chosen as it proved to be less active than other intervals (Pfurtscheller, 2001; Pfurtscheller & Aranibar, 1979). Next, sampling rate was down sampled to 1000Hz. Data was filtered before down sampling with 450Hz, 24dB, 4th order. The conversion was based on a spline interpolation between data points. ERS/ERD transform was implemented using BrainVision Analyzer2. This transform was used to analyse the event-related course of individual frequency bands in the EEG. The classical power method (Pfurtscheller, 2001) was applied here. EEG power (in percentage) of the activity period (A) is presented relative to the preceding reference interval (R) which is a pre-defined period of a few hundred milliseconds before the event. ERD or ERS is defined as the percentage of power decrease or increase, respectively, according to the expression ERD% = (A – R)/R*100. ERS/ERD is computed by bandpass filtering each event-related trial, squaring the amplitude samples in each trial and averaging over N trials (Kalcher

& Pfurtscheller, 1995). A separate data set for point-to-point significance was also generated. This is computed using the following sign test:

$$p_{(j)} = (0.5)^N \sum_{i=1}^{k_{(j)}} \binom{N}{i}$$

Using BrainVision Analyzer Significance Node the value P(j) is multiplied by 100%, hence, the range is between 0 and 100%. It allows to assess how probable the increase (ERS) or decrease (ERD) is with respect to the baseline (reference) according to the above sign test. This measure is used as an indication of significance (Kalcher & Pfurtscheller, 1995).

Three different frequency bands were chosen which are the most frequently investigated bands in the last 20 years on the subject of language mapping and invasive EEG and MEG (Arya et al., 2017, 2015; Cervenka, Corines, et al., 2013; N. E. Crone, Sinai, & Korzeniewska, 2006; Tierney et al., 2018). They were defined as: first, beta ERD with a central frequency of 20Hz and a bandwidth of 10Hz; second, low gamma ERS with a central frequency of 50Hz and a bandwidth of 20Hz; and third, high gamma ERS with a central frequency of 90Hz and a bandwidth of 20Hz.

A significance level was determined similarly to iERP analysis using the significance level of the control marker condition using a t-test against zero. The maximum negative and positive amplitude t-values were noted and, after analysing all data, a t-test threshold for the significance level of the task average was defined. The value of +/-30 was chosen as the significance threshold. Only significant differences which were present over 20 consecutive time points for each component were taken into consideration (Molholm et al., 2006; Trébuchon et al., 2013b).

Next, data was visually analysed using the set threshold and classified as robust ERS/ERD or not. Figure 48 illustrates the classification of robust ERS and ERD.
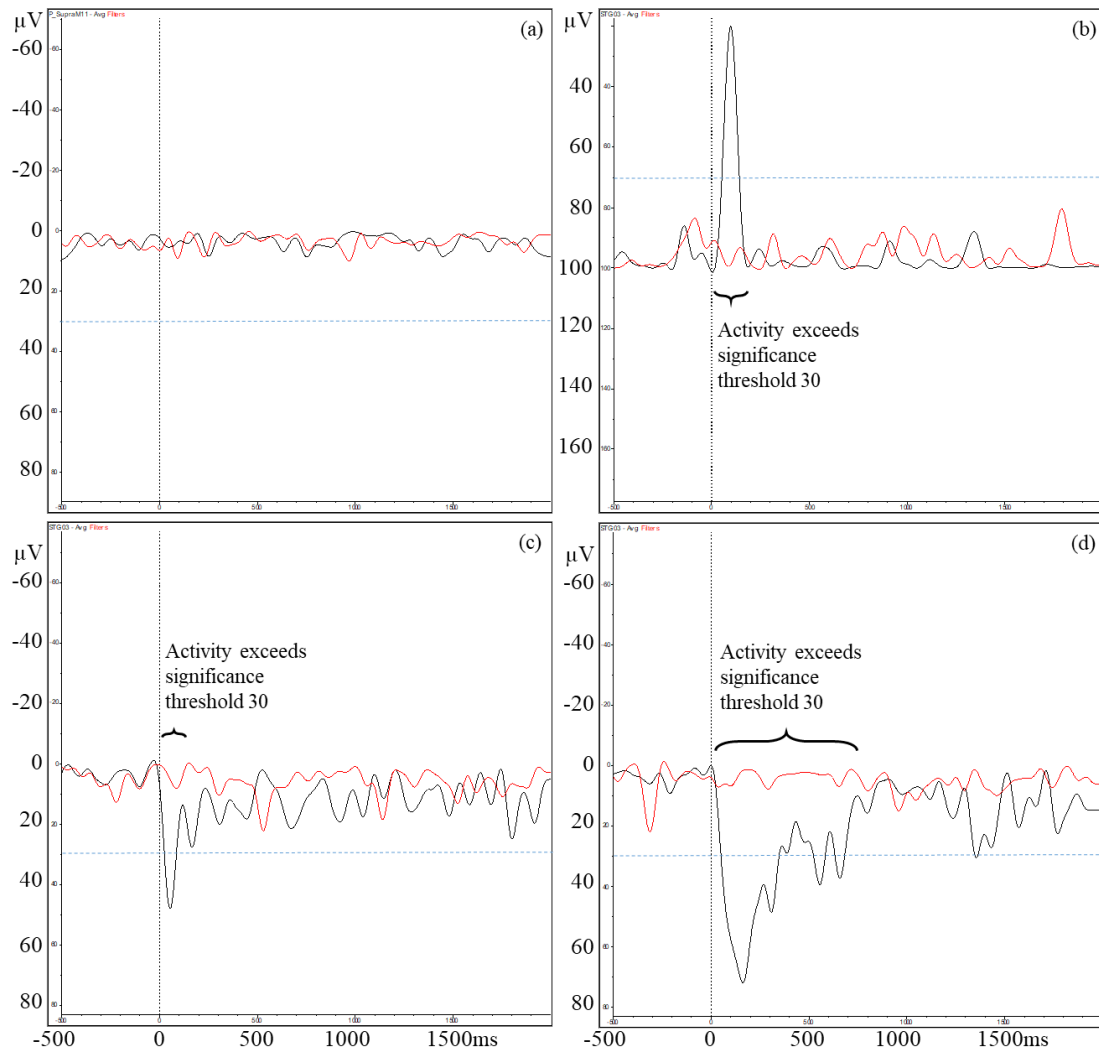
Figure 48. Classification of robust ERS/ERD aided by t-test significance level. (a) shows ERS/ERD activity, neither in the stimulus-locked (black line) nor in the control-marker-locked recording (red line). The dashed blue line represents the significance level 30; (b) illustrates robust stimulus-evoked beta ERD; (c) illustrates low gamma ERS and (d) shows high gamma ERS.

5 Topography and Morphology of language-related iERPs

5.1 Introduction

5.1.1 Rational for exploring the use of iERPs

Language organisation is complex and besides the well-known cortical areas, like Broca's area for language production and Wernicke's area for language comprehension, it involves several further brain regions and white matter tracts for connecting those areas. Chronic neurological diseases like epilepsy can alter brain processing which can lead to atypical language dominance or atypical language distribution pattern (Adcock, Wise, Oxbury, Oxbury, & Matthews, 2003; Brázdil et al., 2005; Liégeois et al., 2004).

Epilepsy surgery candidates undergo invasive EEG monitoring in order to localise the seizure onset zone and eloquent areas. Optimal post-surgical outcome depends on delineating those brain regions and completely resect the epileptogenic zone while maintaining functionally important brain areas (J. Engel, 1993a). Once a patient presents with semiology involving language or motor functions and it is believed that surgery put eloquent functions at risk the method of choice to localise functional areas is electrical stimulation. This is the gold-standard method to localise cortical areas essential for language or movement. However, it carries several limitations. It is time- and staff-intensive, increases risk of inducing seizures, leads to false positives, is suboptimal for the use with young children as compliance is an important factor. Furthermore, it is insufficiently standardised for clinical practice when it comes to patient selection, language tasks and stimulation settings (Aungaroon et al., 2017; Marla J. Hamberger, Williams, & Schevon, 2014; Karakis et al., 2015; Nakai et al., 2017). Sakpichaisakul and colleagues (2020) argued that at present the decision for pre-surgical language mapping is often empirical and that patients with a

SOZ outside of typical language areas often do not undergo electrical stimulation mapping. However, they recommend a wider use of pre-surgical language ESM in order to prevent neuropsychological deficits post-surgery.

The invasive nature of iEEG, whether using subdural grid or SEEG monitoring, allows for directly measuring brain activity and offers an opportunity to extend cognitive neuroscience research. Event-related potentials, discharges from large populations of neurons that are stimulus-locked to cognitive events are an alternative method used to study various cognitive processes. Like with scalp EEG, ERPs can be extracted from iEEG. Resulting iERPs show a higher voltage and a higher spatial resolution ($3.5–4mm^2$) than with scalp EEG (Miller, Sorensen, Ojemann, & Nijs, 2007; Taylor & Baldeweg, 2002; Urrestarazu et al., 2007).

As early as 1981 neurosurgical patients were tested during awake surgery and slow electrical cortical activation in response to speech perception and production was measured in perisylvian areas in the dominant hemisphere (Fried, Ojemann, & Fetz, 1981). Using microelectrode recordings from the lateral temporal lobe Creutzfeldt and colleagues (1989a, 1989b) were able to record single neuron responses to speech stimuli from the superior, middle and inferior temporal gyrus with varying activation pattern depending on listening to spoken words and sentences compared to overt speaking. In addition, several studies reported that generators of cognitive iERPs during auditory stimuli showed a widespread distribution, including cortical and subcortical regions. (Bares & Rektor, 2001; Halgren et al., 1995; Halgren, Marinkovic, & Chauvel, 1998). Liégeois-Chauvel and colleagues described at least six auditory areas within the superior temporal gyrus using auditory evoked potentials recorded from invasively monitored patients. These auditory areas are the primary auditory cortex located in the medial and intermediate part of Heschl's gyrus (HG), the secondary auditory cortex located in the lateral part of HG, the planum temporale, an area located in the posterior STG, an area in front of HG, the anterior STG and the posterior insula (Liégeois-Chauvel, Trébuchon-Dafonseca,

Marquis, & Chauvel, 2003). Furthermore, iERPs were also used to differentiate the dorsal and ventral language streams. The left supramarginal gyrus, belonging to the dorsal stream, was mainly activated during phonological information processing while the anterior and middle temporal gyrus and fusiform gyrus belonging to the ventral stream showed activation during lexicosemantic information processing. Their similar iERP latencies suggested parallel processing along both streams (Trébuchon et al., 2013a).

Besides cortical information, SEEG also permits recording from subcortical structures, like the basal ganglia (Bares & Rektor, 2001; Rektor et al., 2003), the amygdala (Corsi-Cabrera et al., 2016) and the hippocampus, which are often target structures for surgical resection. iERP language research recently revealed reliable hippocampal activity during a picture naming task, modulated by repetition priming and semantic context. The authors argued that this activity is related to implicit learning (A. Llorens et al., 2016). Besides speech sound perception, it is feasible to record ERP activity associated with production of speech. Llorens and colleagues (2011) showed that activity was not only measured with response onset, but prior to response onset and that in both time periods perisylvian regions were activated. The inferior frontal gyrus was involved more during pre-response activity compared to speech onset.

Pre-surgical invasive EEG monitoring provides a unique opportunity to combine epilepsy diagnostics and cognitive neurophysiology to study the functional organisation of speech and language with greater temporal resolution than fMRI and greater spatial resolution than scalp-recorded ERPs.

5.1.2 Study aims

I designed language paradigms and tested a representative sample of paediatric patients with medication-resistant epilepsy admitted to invasive EEG monitoring with the aim to determine cortical dynamics during speech perception and speech production and generate a language map using iERP measures across widespread brain regions. To my knowledge, there is no study investigating language areas involved in speech perception, comprehension and production using iERPs in children and adolescence with SEEG implantations yet. The aims of this chapter are to:

1. Characterise topography and morphology of stimulus-locked iERPs across the sample to establish:
   a. Region-specific task differences
   b. Region-task-specific differences
2. Characterise speech-response-locked iERP topography and morphology across the sample.
3. Characterise iERP activation differences between hemispheres.
4. Characterise iERP topography in a clinical context on an individual case basis.

5.2 Methods

5.2.1 Participants

I prospectively identified consecutive paediatric patients with a diagnosis of medication resistant focal epilepsy through the Great Ormond Street Hospital for Children (GOSH) epilepsy surgery list. They were admitted to GOSH for a pre-surgical invasive EEG monitoring as part of their clinical assessment between November 2016 and April 2018. The age span of 5–17 years was chosen as it was representative of patients requiring epilepsy surgery at GOSH. Furthermore, it was important that participants were able to complete several language tasks.

Patients without a basic understanding of English were excluded from the study. The ethical review board gave permission for this study.

5.2.2   Clinical information

This is described in Chapter 4, Section 4.3.

5.2.3   iEEG data acquisition and acquisition of 3D brain images

This is described in Chapter 4, Section 4.7.

5.2.4   Language iERP testing

As described in Chapter 4, Section 4.4–4.6 participants were presented with different language games. These were always carried out after all clinical assessments were completed.

5.2.5   iEEG quantitative analysis

These are detailed in Chapter 4, Section 4.8. After pre-processing, EEG data were subjected to visual and additional ERP analysis (detailed in Sections 4.8.4 and 4.8.5) and iERPs at each contact were classified in robust iERPs and no iERPs measured (detailed in Section 4.8.6).

5.3 Statistical analysis

The percentage of contacts with detectable iERP activity was calculated for each brain region per patient and a weighted average was taken across patients. A weighted average was chosen, because each patient had an individual implantation regime and hence patients had different numbers of contacts implanted into respective brain regions. The average was weighted by the number of contacts implanted into each brain region.

Wilcoxon rank sum tests were used to compare differences in the occurrence rate of contacts with iERPs between regions and tasks.

5.4 Results

5.4.1 Demographics

In total, I informed 24 patients and their parents about the study. Two families declined to participate. Of the 22 who consented, one was brought to theatre for explantation of electrodes before completing the testing and one patient refused to take part when approached on the day of iERP language testing. The final sample included 20 children and adolescents with drug-resistant focal epilepsy (aged 5–17 years). A summary of the numbers approached, consented and excluded can be found in Figure 49. At the beginning of the testing session, participants and parents/ guardians were explained all procedures again and reminded that participation was voluntary and that they could withdraw at any time. The clinical characteristics of the patient sample are summarised in Table 21.

HOSPITAL STAY

- Admission
- Electrode Implantation
- Back at Hospital Ward
- Five-day Window for Clinical Assessment
- Electrode Explantation
- Discharge

RECRUITMENT STEPS

25 families approached by primary care team and clinical research team with an invitation to participate in the study.

Information was given and study leaflets were left with family.

23 participants consented/assented

21 participants tested

20 participants in study to date

EXCLUSION AND DROP OUTS

not consented as they did not want to take part (n = 2)

consented but due to time restraints not tested (n = 1)

consented but on the day of testing patient refused (n = 1)

started testing, but participant's attention that day did not allow propper testing (n = 1)

Figure 49. Recruitment information. Number of participants approached, participants indicated an interest and participants recruited and tested are summarised. Different steps of hospital stay and reasons for dropout at each stage are provided.

Five patients (ID2, 8, 18, 20, 100) had fMRI testing and language lateralisation information was available.

For group analyses six patients were excluded. Two of them (ID3, 4) had prior epilepsy surgery with big resection areas, two other patients (ID10, 15) had a diagnosis of tuberous sclerosis and electrodes placed in cortical tubers, hence abnormally developed regions of brain tissue. One patient did not have an SEEG implantation like the other patients, but subdural grids implanted (ID17). Finally, one patient (ID101) did not meet formal inclusion criteria but was included. ID4, 10 and 101 are presented as case studies in Section 6.4.12.

Table 21. Patient demographics.

ID	AGE	ONSET	SEX	HAND	MRI	HISTO	SIDE	SURGERY	FOLLOW UP	SZ OUTCOME
2	9.2	0.1	F	R	L P/T	FCDIIB	L	Y	4	20 seizures /month
3	9.9	0.7	F	L	temporal lobe	FCDIIA	L	N		-
4	9.8	0.01	M	L	anterior to disconnection		R	Y	12	2 behavioural arrest
5	6.5	5	F	R	anterior R T lobe		R	Th	6	10–15 seizures/day
7	17.3	11	M	L	occipital poles		L	N		-
8	12.3	6	F	L	L hippocampus	MTS	L	Th	6	5–10 seizures/week
9	8.5	1.5	F	L	lesion negative		L	N		-
10	9.1	1.5	F	L	bilateral tubers	TS	L	Y	12	1–2 seizures/day
11	7.0	0.8	F	L	FCD Type II	FCDII	R	Y	6	no seizures
12	6.1	0.2	F	R	post. resection cavity-SFG	FCDIIA	L	N		-
13	10.9	0.5	M	L	FCD Type IIB	FCDIIB	R	Th	12	no seizures
14	6.4	0.8	F	L	left inf. frontal region	FCDIIB	L	Y	6	one event
15	8.1	0.2	F	L	bilateral tubers	TS	R	Y	8	absences, 2 seizures
16	14.0	0.8	F	L	R F & T region		R	N		-
17	7.6	1	F	L	L precentral gyrus	FCDIIB	L	Y	5	subtle seizures
18	7.6	4.4	M	L	R temporal pole		R	Y	6	15 auras/day
19	14.5	1.7	M	L	L temporal pole	FCD	L	Y	1	no seizures
20	14.3	11.1	M	L	lesion negative		L	N		-
100	5.3	0.2	F	R	L sup. temporal gyrus	FCD	L	Y	12	no seizures
101	7.3	1.9	F	R	abnormal cortex-L IFG	FCDIIB	B	Y	6	no seizures

Age and onset are presented in years; Hand: handedness; MRI: lesion location on MRI report; Side: implanted hemisphere; Follow up: is presented in months after surgery; Abbreviations: FCD = focal cortical dysplasia, MTS = mesial temporal sclerosis, TS = tuberous sclerosis, L = left, R = right, F = female, M = male, T = temporal, P = parietal, Y = surgery, N = no surgery, Th = thermocoagulation.

5.4.2   Task completion

In total, six language tasks were designed to present to each individual: Listen Baseline (BL), Word Repetition (WR), Verb Generation (VG), Listen Name (LN), Picture Naming (PN) and Colour Naming (CNw) (for more details see Section 5.4). Due to individual factors, like cognitive abilities, behavioural difficulties, seizure burden of the participant or time limits due to further clinical procedures, participants completed a varying number of tasks. First task presented to the patients were the auditory word tasks. I started with the easiest, the passive baseline task. Next followed the word repetition task, then verb generation and when possible the sentence task. Lastly the picture naming and colour naming tasks were played. Table 22 summarises the number of participants who completed the different language tasks. Seven patients were able to complete all six tasks (7/20). The task with least correct responses of 59% over all patients was LN followed by the VG task with 83%. The other four tasks show a similar mean percentage of correct responses ranging from 94–98%. Furthermore, it illustrates the percentage of correct responses for each participant and task.

In five participants the individual speech responses to task stimuli were recorded using a microphone for subsequent analysis of response-locked iERP, which are further referred to as WRr (n=5), VGr (n=5).

Table 22. Summary of tasks completed by each participant and percentage of correct responses.

ID	% of correct responses						Speech responses	
	VG	WR	BL	LN	PN	CNw	VGr	WRr
2	90%	100%	✓					
3	78%	98%	✓					
4	88%	100%	✓	85%				
5	72%	94%	✓	24%				
7	62%	98%	✓	67%	100%	100%		
8	62%	100%	✓	54%	98%	100%		
9	100%	100%	✓	73%	100%	100%		
10	70%	96%	✓					
11	72%	100%	✓					
12	86%	100%	✓	30%	84%	86%		
13	94%	100%	✓	89%	100%	100%	✓	✓
14	80%	100%	✓	44%	85%	94%	✓	✓
15		92%	✓		100%	100%		
16	96%	100%	✓	29%		98%		
17			✓					
18	88%	82%					✓	✓
19		72%			80%			✓
20	100%	100%	✓	95%	100%	100%	✓	✓
100	88%			60%				
Mean %	83%	96%		54%	94%	98%		
No of participants completing task	16	17	16	11	9	9	4	5

Summary of percentage of correct responses for each participant and task, except ID101. Tasks completed are shaded light grey. Furthermore, participants whose individual speech responses were recorded are marked with ✓. Mean percentage of correct responses per patient and total number of participants completing each task are presented.

5.4.3   Implantation regimes for each patient

Figure 50 and Figure 51 illustrate the different implantation regimes of all included patients. All but one were SEEG implantations and that one was a subdural grid investigation (ID17). One patient had a bilateral implantation regime (ID101).
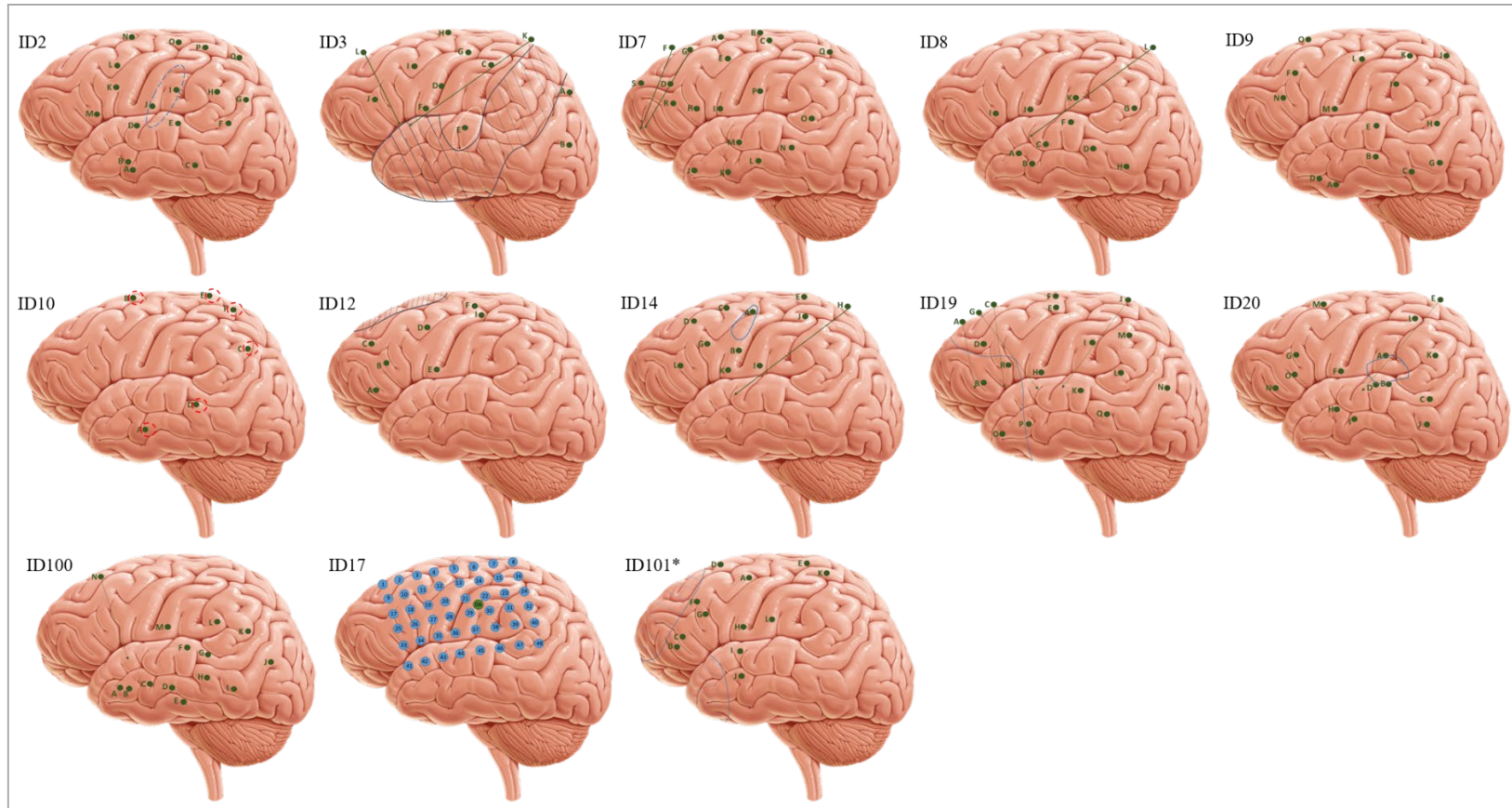
Figure 50. Overview of left-sided implantation regimes. Green dots mark depth electrodes insertion locations at the cortical surface; ID3 and ID12 show blue dashed areas which present resection areas of previous surgeries; ID10 shows red dashed circles which mark tubers; ID14, ID19 and ID20 have known lesions which are marked with a blue line; ID17 had an ECoG implantation where the blue circle represent the contacts of the 48-contact grid and the green circle represents the location of the depth electrode; ID101 is marked with an * as this was a bilateral SEEG implantation, left side is shown here.
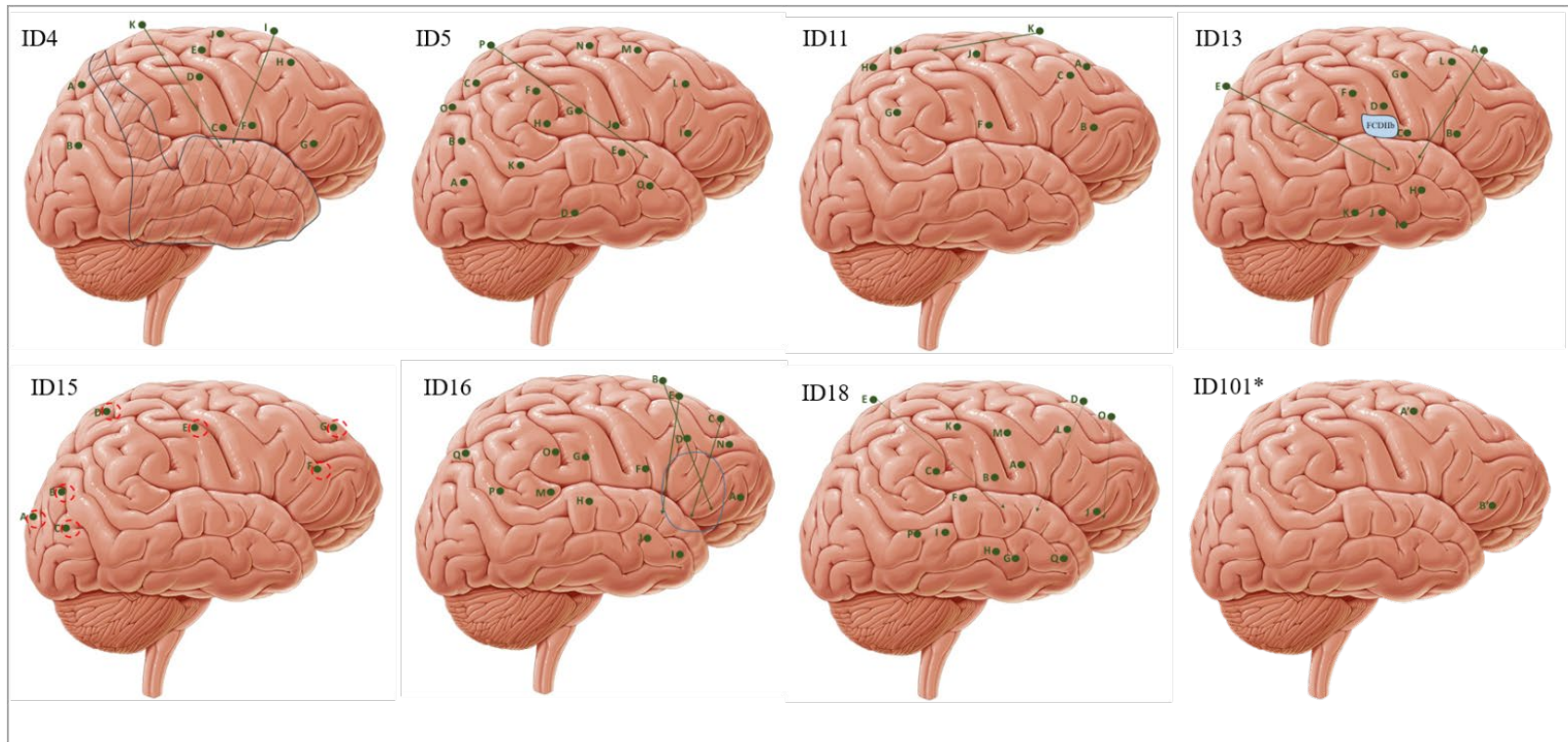
Figure 51. Overview of right-sided implantation regimes. Green dots mark depth electrodes insertion location; ID4 shows a blue dashed area which presents a resection area of a previous surgery; ID15 shows red dashed circles which mark tubers; ID13 and ID16 have known lesions marked in blue. ID101 is marked with an * as this was a bilateral SEEG implantation, right side is shown here.

5.4.4 Brain regions targeted by SEEG implantation

As described in Section 5.7.2 Slicer was used to assign SEEG contacts to different brain regions. In this and the following chapter the distinction between brain areas localized in the perisylvian language cortex and in additional brain areas will be made. The perisylvian language cortex consists of the regions around the lateral sulcus (Sylvian fissure) and is illustrated in Figure 52.
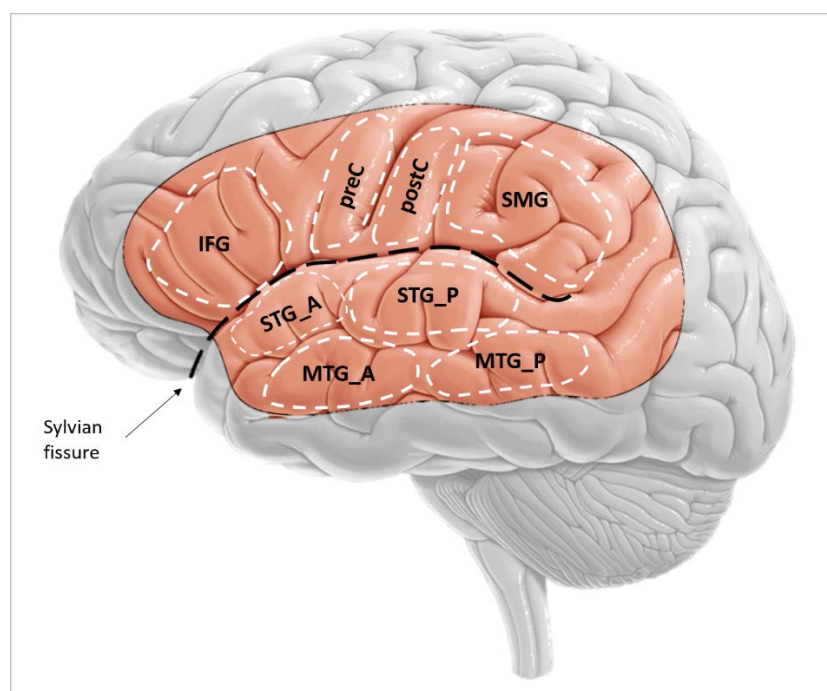
Figure 52. Perisylvian language cortex. Lateral view of the brain illustrating the Sylvian fissure (dashed black line) as well as distinguishing between perisylvian cortex (in pink) and its different areas (white dashed areas) and additional brain areas (in grey). Abbreviations: IFG = inferior frontal gyrus, preC = precentral gyrus, postC = postcentral gyrus, STG_P = posterior superior temporal gyrus, STG_A anterior superior temporal gyrus, MTG_A = anterior middle temporal gyrus, MTG_P = posterior middle temporal gyrus.

In this study, twenty-two brain regions were identified showing robust iERPs. Abbreviations used for brain regions are summarised in Table 23. This summary again distinguishes between regions lying in the perisylvian language cortex and additional brain regions.

Table 23. Brain regions and their abbreviations distinguishing perisylvian language cortex and additional brain regions.

	Abbr.	Brain areas	No. of patients included per task								
			VG	WR	BL	PN	CNw	LN	VGr	WGr	LNr
Perisylvian brain regions	INS_A	Anterior Insula	12	12	10	8	8	10	4	5	3
	INS_P	Posterior Insula	11	11	9	7	7	9	4	5	3
	IFG	Inferior Frontal Gyrus	8	9	7	9	8	7	4	5	3
	preC	Precentral Gyrus	9	10	8	6	6	7	3	4	2
	postC	Postcentral Gyrus	9	9	8	4	5	6	3	3	2
	SMG	Supramarginal Gyrus	11	11	9	7	7	8	3	4	2
	STG_P	Posterior Superior Temporal Gyrus	10	10	8	6	6	8	3	4	1
	STG_A	Anterior Superior Temporal Gyrus	3	2	2	1	1	2	0	1	1
	MTG_P	Posterior Middle Temporal Gyrus	7	7	6	5	5	6	2	2	1
	MTG_A	Anterior Middle Temporal Gyrus	6	6	5	5	4	5	1	3	2
Additional brain regions	HIP	Hippocampus	5	5	4	3	3	4	0	1	0
	CING	Cingulate	5	6	5	2	2	3	0	1	0
	AMY	Amygdala	1	1	1	0	0	1	0	0	0
	SFG	Superior Frontal Gyrus	3	3	2	3	3	2	2	2	1
	MFG	Middle Frontal Gyrus	8	9	8	4	5	4	3	3	2
	OFC	Orbital Frontal Cortex	2	2	2	1	2	2	0	0	0
	preC_2	Precentral Gyrus, dorsal part	5	6	4	2	1	2	0	0	0
	postC_2	Postcentral Gyrus, dorsal part	1	1	1	1	1	0	0	0	0
	IPL	Inferior Parietal Lobule, excl. SMG	4	3	3	2	2	3	0	0	0
	SPL	Superior Parietal Lobule	2	2	2	2	2	1	1	0	0
	OCC	Occipital Lobe	0	0	0	1	1	0	0	0	0
	ITG	Inferior Temporal Gyrus	6	6	5	2	3	4	1	0	1
	FFG	Fusiform Gyrus	1	1	1	1	1	2	1	1	1

In the following sections, I would like to describe topography and morphology of iERPs measured in this study. First, to give a quick overview of what the chapter comprises, I present example iERPs and their morphology recorded from perisylvian brain regions. Next, to emphasize brain regions involved in language processes, I am focusing on region-specific differences and summarise occurrence of iERPs and their morphological characteristics during auditory word and sentence tasks. Following that, I am addressing the question of task-

specific differences independent of region information and I will give an overview of iERP occurrence dependent on the various tasks presented. Furthermore, I will discuss morphological differences in iERP between tasks. Next, I will show results combining region and task information before presenting response-locked iERPs. Finally, I will compare iERPs recorded from the left and right hemisphere before ending with a few case presentations.

5.4.5   Overview of region-specific iERPs

First, as this study did not focus on investigating a certain iERP component, I would like to give a short illustrative overview of stimulus-locked iERPs in various brain regions of the perisylvian area measured in this study (Figure 53).
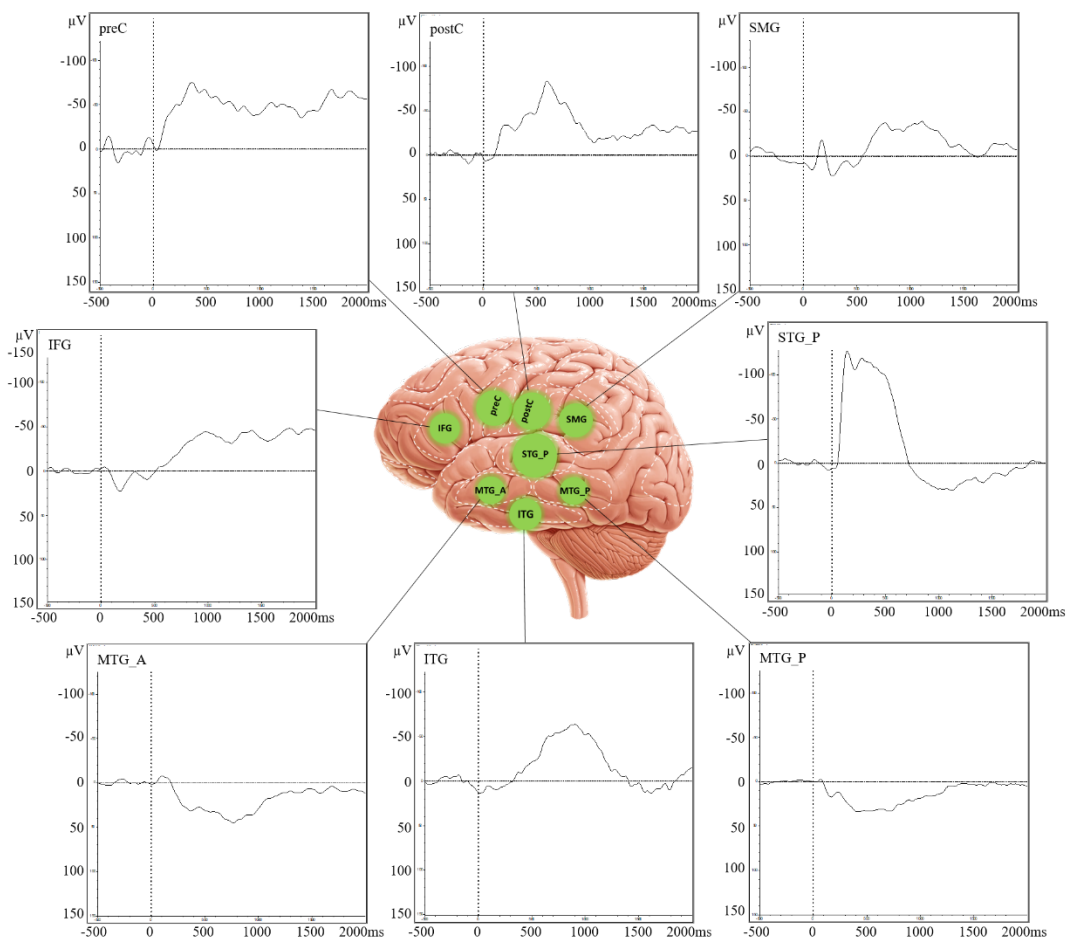
Figure 53. Indicative example iEPRs for each region located in the perisylvian cortex, including ITG. . These example iERPs are taken from the VG task of different patients to give an overview of the variability in ERP morphology in the different brain regions during this task.

5.4.6 Stimulus-locked iERPs during listening to auditory word stimuli

Topography of region-specific iERPs during auditory word tasks

For the auditory word tasks (BL, WR, VG; recorded in n=13 patients) areas of the perisylvian region exhibited a higher percentage of iERPs compared to additional brain regions. However, additional brain regions like superior frontal gyrus, hippocampus, fusiform gyrus and inferior temporal gyrus also showed iERP occurrence of more than 50%. Maximum iERP occurrence could be found in posterior STG (see Figure 54).
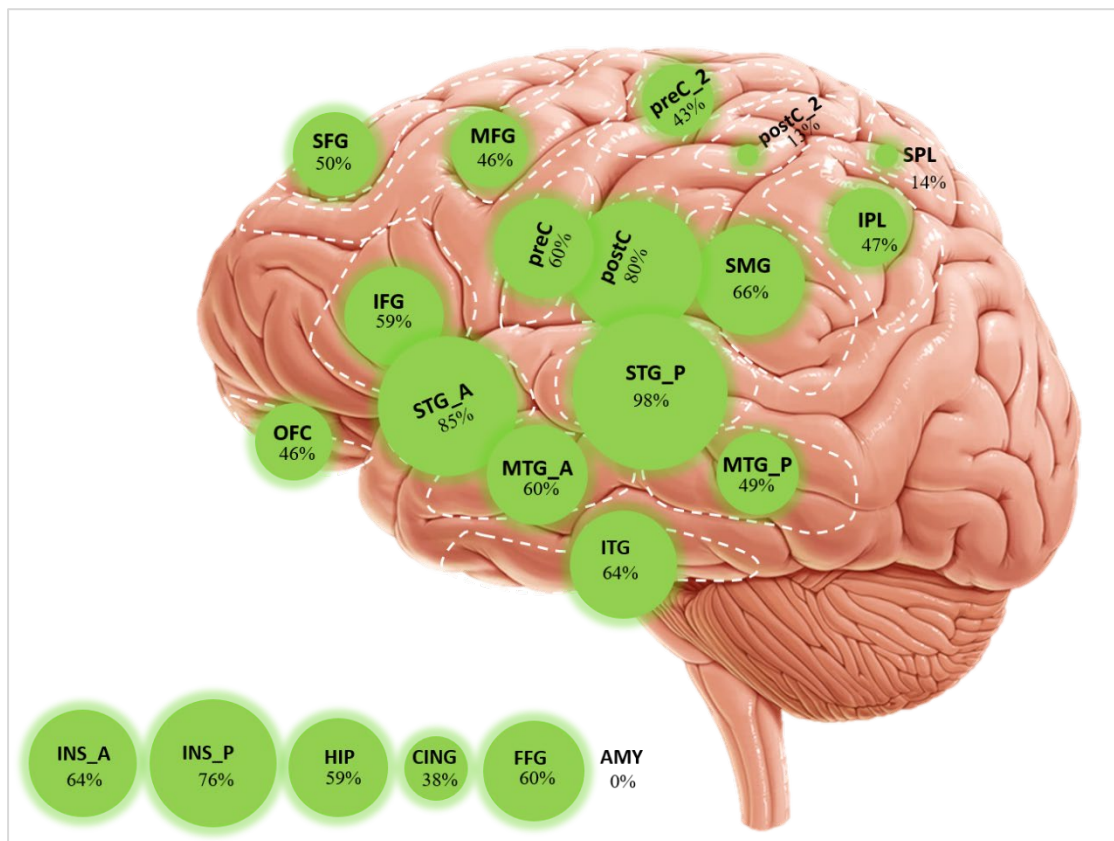
Figure 54. Overview of occurrence of iERPs during auditory word tasks in perisylvian and additional brain areas. It is worth mentioning again that the following brain regions were only recorded from in only one or two patients: SFG, postC_2, SPL, STG_A, and OFC)

Morphology of iERP components during auditory word tasks

a. *Primary component in posterior STG and insula*

Primary components were measured in five patients immediately after stimulus onset with a peak latency <100ms. Two brain areas were involved—the posterior insula (INS_P) and the posterior STG (STG_P). INS_P showed a mean peak latency of 76.3ms (SD±21.9ms; n=4 patients, 11 contacts, three tasks: BL, WR, VG) compared to the posterior STG of 75.6ms (SD±16.1ms; n=3 patients, 25 contacts, three tasks: BL, WR, VG; p>0.1, Wilcoxon rank sum test). Figure 55 illustrates examples of earliest components from the posterior insula and the posterior STG.
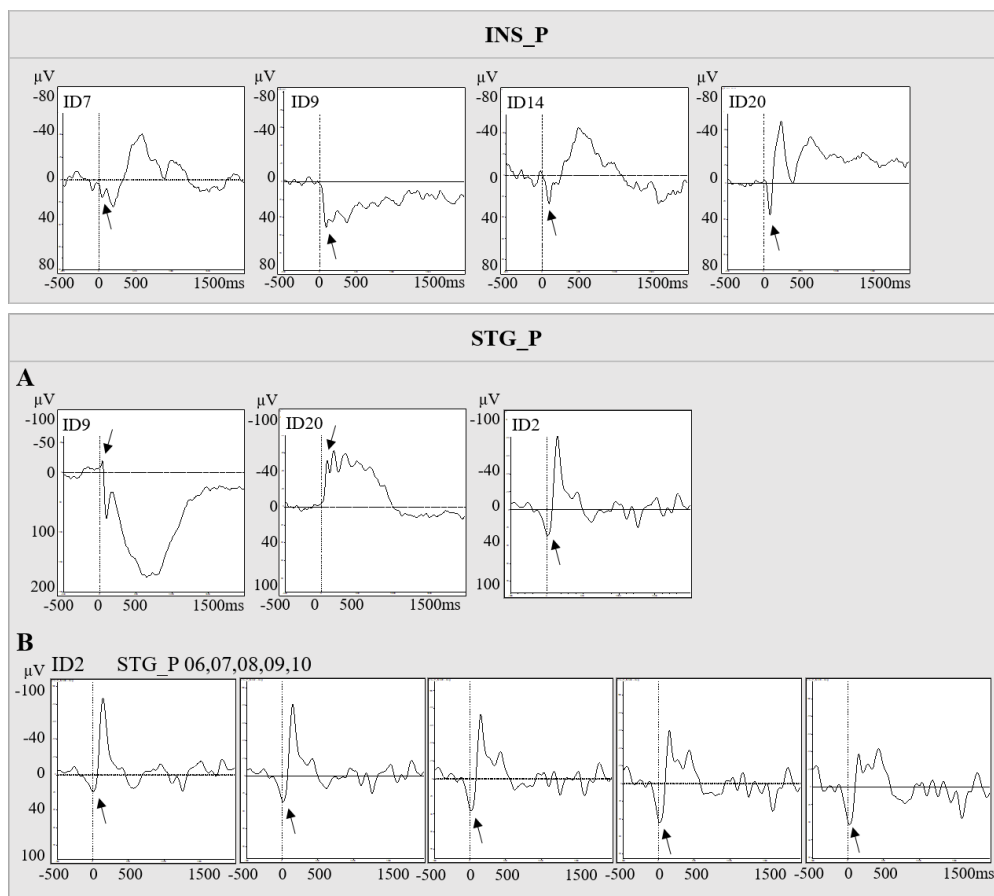
Figure 55. Example cases of earliest components from the posterior insula and the posterior STG. Earliest components in INS_P are shown for all four patients they were measured in (arrow marks earliest components). A) illustrates one example for each patient and B) depicts the progression of morphology build up in one patient (ID2) over neighbouring STG_P06–10 channels, going from medial to lateral. It shows a negative wave with decreasing amplitude and additional an early positive component with increasing negative amplitude.

201

b. Early component (EC)

Early components showed a peak between 100–200ms. They were mainly identified in the posterior part of the STG (STG_P; 61%). Examples of morphology observed in the posterior STG are illustrated in Figure 56 and an example case is presented in Figure 57. In general, the EC morphology in the posterior STG showed a negative peak between 100–200ms with varying shapes, in some cases an additional prior positive component or a following positive wave. The mean peak amplitude was -82.6µV (min=-35.7µV, max=-136.3µV, SD=30.5µV) and the mean latency 149.1ms (min=123.0ms, max=188.0ms, SD=18.4ms). Early components were also measured, however to a much lesser extent (3–29%), in eleven other brain areas. Compared to the mainly negative wave seen in the posterior STG the rest of the regions mostly exhibited an early positive component, apart from variants in the posterior insula, supramarginal gyrus and hippocampus, which showed early negative waves (Figure 58).

The mean positive peak amplitude was 37.9µV (min=6.1µV, max=98.1µV, SD=15.1µV) and the mean latency 143.1ms (min=100.0ms, max=200.0ms, SD=20.1ms). The mean negative peak amplitude was -48.0µV (min=-3.81µV, max=-218.1µV, SD=35.7µV) and the mean latency 153.5ms (min=109.0ms, max=190.0ms, SD=18.1ms). Regions where early components were measured including their morphological characteristics are summarised in Table 24.
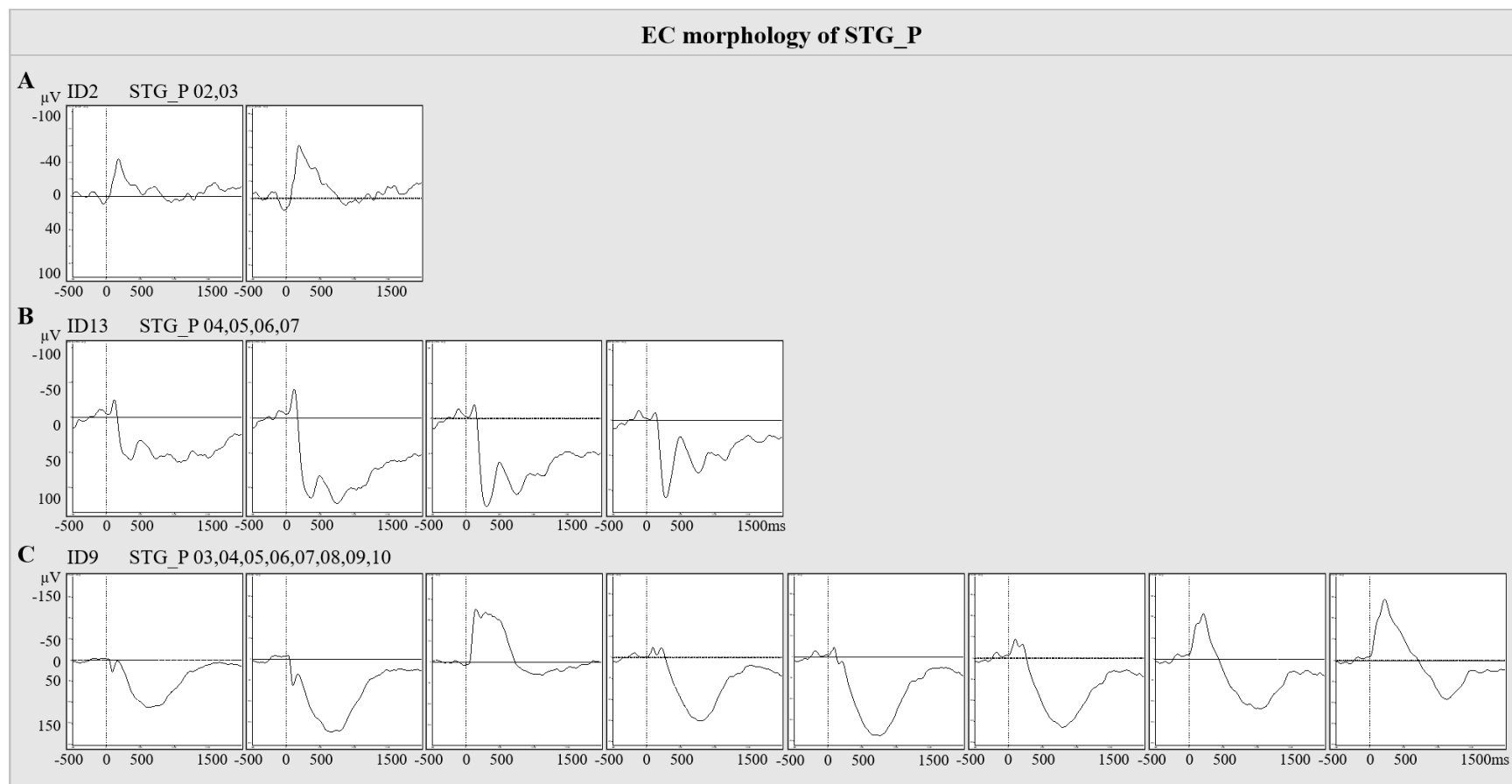
Figure 56. Example cases showing variability of EC morphology of STG_P. A) EC components measured in STG_P contacts of ID2. It shows a negative wave with increasing amplitude B) ECs of ID13 with a negative component with varying amplitude first and a following sustained positive wave; C) ID9 with a phase reversal between contact 04 and 05 and varying morphology within one electrode in general: from a positive component in contacts 03 and 04, to a negative one in 05 and a negative early wave with increasing amplitude and a following positive wave in 06–10.
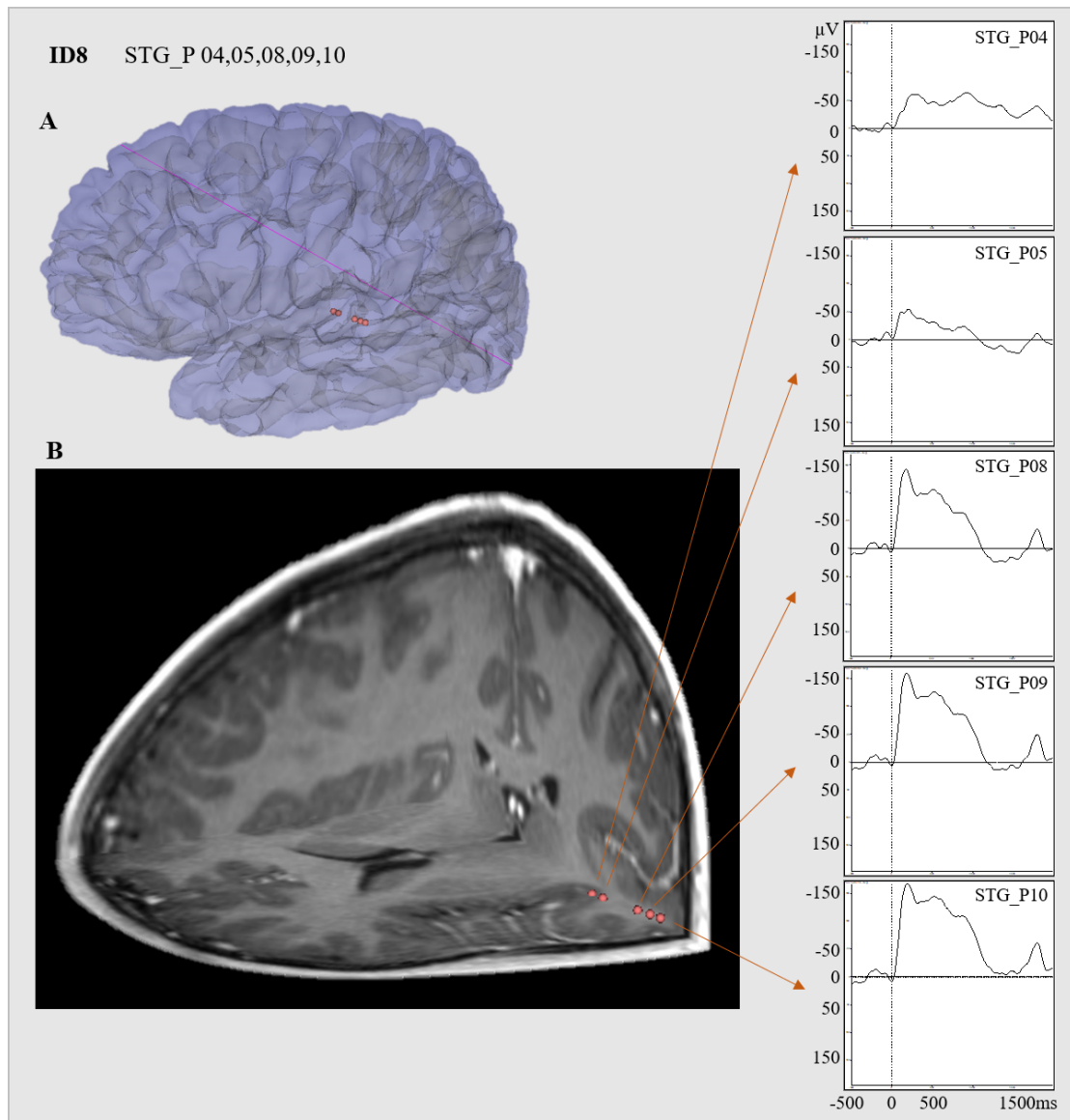
Figure 57. Example position of electrode in STG_P. Example case (ID8) illustrating representative ECs to the VG task recorded from the posterior STG. A) shows the patient's 3D brain view taken from slicer with the STG_P contacts recorded from marked in pink; B) presents the MRI localisation of the contacts with pink arrows pointing at each contact's iERP. STG_P04 is the most medial contact starting out with a negative component lasting until about 1500ms, STG_P05 shows an even lower amplitude than STG_04 and is shorter in duration, STG_08, STG_09 and STG_10, the three most lateral contacts exhibit an early sharp negative component, with an increasing amplitude the more lateral the contact is located and an overall duration of about 1250ms.
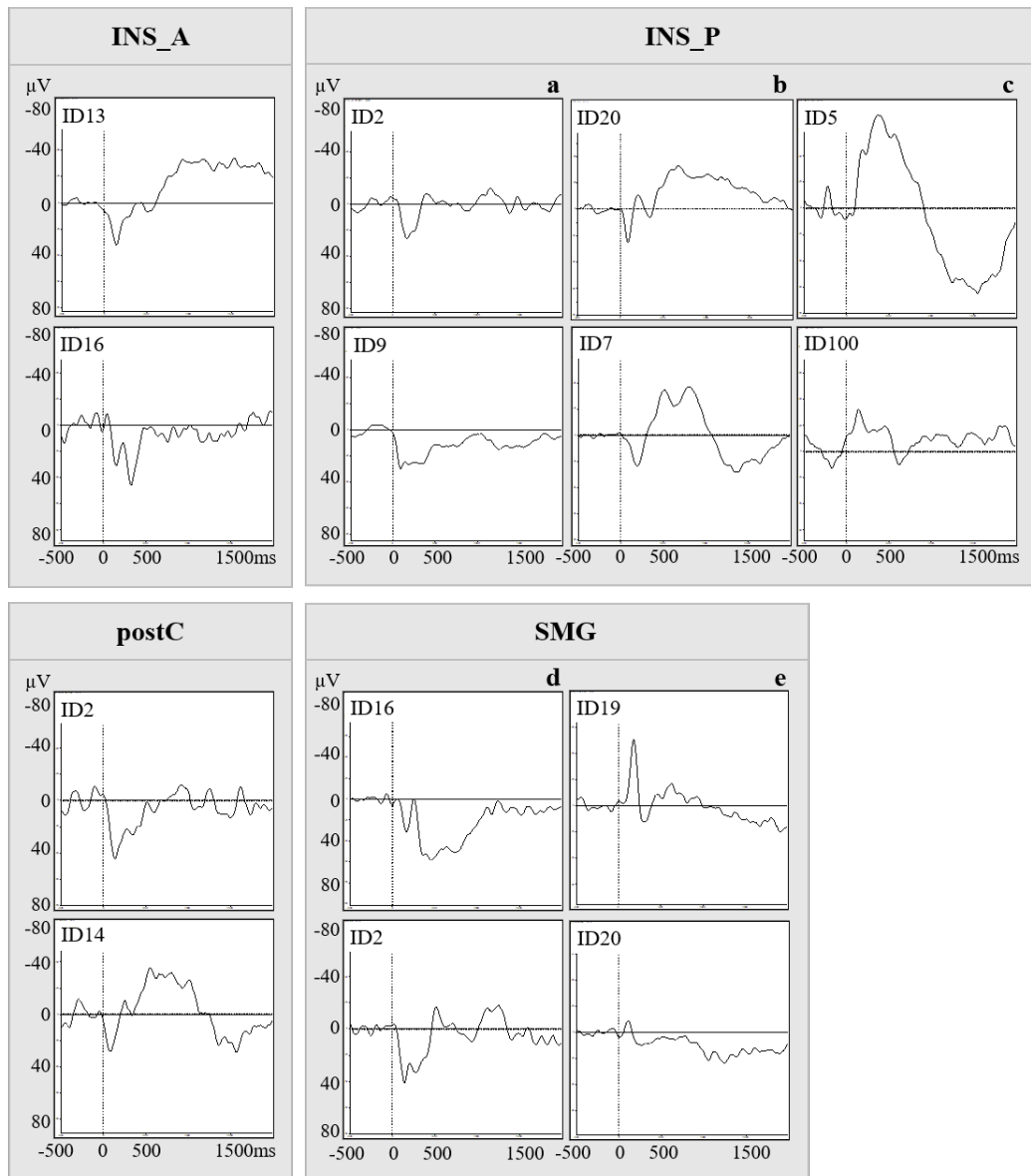
Figure 58. Summary of further brain areas exhibiting ECs and their morphology. INS_A presents with a positive wave and in some cases, this was followed by a positive component; INS_P exhibits three variations: **a.** a positive wave, **b.** a positive component with following negative component or **c.** a negative component; post C presented with a positive EC and sometimes this was followed by a negative component; SMG showed **d.** a positive component or **e.** a negative one with sometimes a positive component following.

Table 24. Summary of brain regions exhibiting ECs.

Brain Region	No. of patients	Morphology
STG_P	11	Ia) Negative component (ID7,8,16,20,100) Ib) Negative component plus an earlier positive component (ID2,18) II) First negative component followed by positive component (ID5,9,13,19)
INS_P	10	a) Early positive component of varying duration b) Early positive component with following negative component c) Negative component with or without late positive wave
SMG	6	a) Early positive component of varying duration with or without negative component b) Negative component
postC	4	Early positive component with or without late negative wave
INS_A	3	Early positive component with or without late negative wave
preC	2	Positive wave
STG_A	2	Early positive component, followed by negative component ≤200ms or negative component
IFG	2	Positive wave
preC_2	1	Positive wave
MTG_P	1	Positive wave
ITG	1	Positive wave
HIP	1	Negative wave

This includes the number of patients ECs were measured in plus their morphological characteristics. Brain Region = brain region of electrode placement.

Middle latency components (MLC)

The middle latency component was defined as a wave that peaked between 200–700ms and ended before 1500ms. Overall, in most brain regions this component presented with either a positive or a negative deflection. The mean positive peak amplitude was 31.4µV (min=4.1µV, max=134.3µV, SD=17.5µV), mean latency 333.8ms (min=87.3ms, max=1034.4ms, SD=190.8ms) and mean duration 994.2ms (min=150.1ms, max=1780.2ms, SD=269.5ms). The mean negative peak amplitude was -61.1µV (min=-14.4µV, max=-315.5µV, SD=52.5µV), mean latency 534.1ms (min=124.3ms, max=1481.1ms, SD=249.0ms) and mean duration 913.5ms (min=109.2ms, max=1796.4ms, SD=326.5ms). MLC in the posterior STG showed a very similar morphology to the EC with only the peak being measured >200ms. Figure 59 and Figure 60 illustrates example iERPs in regions and morphology where MLCs were measured.
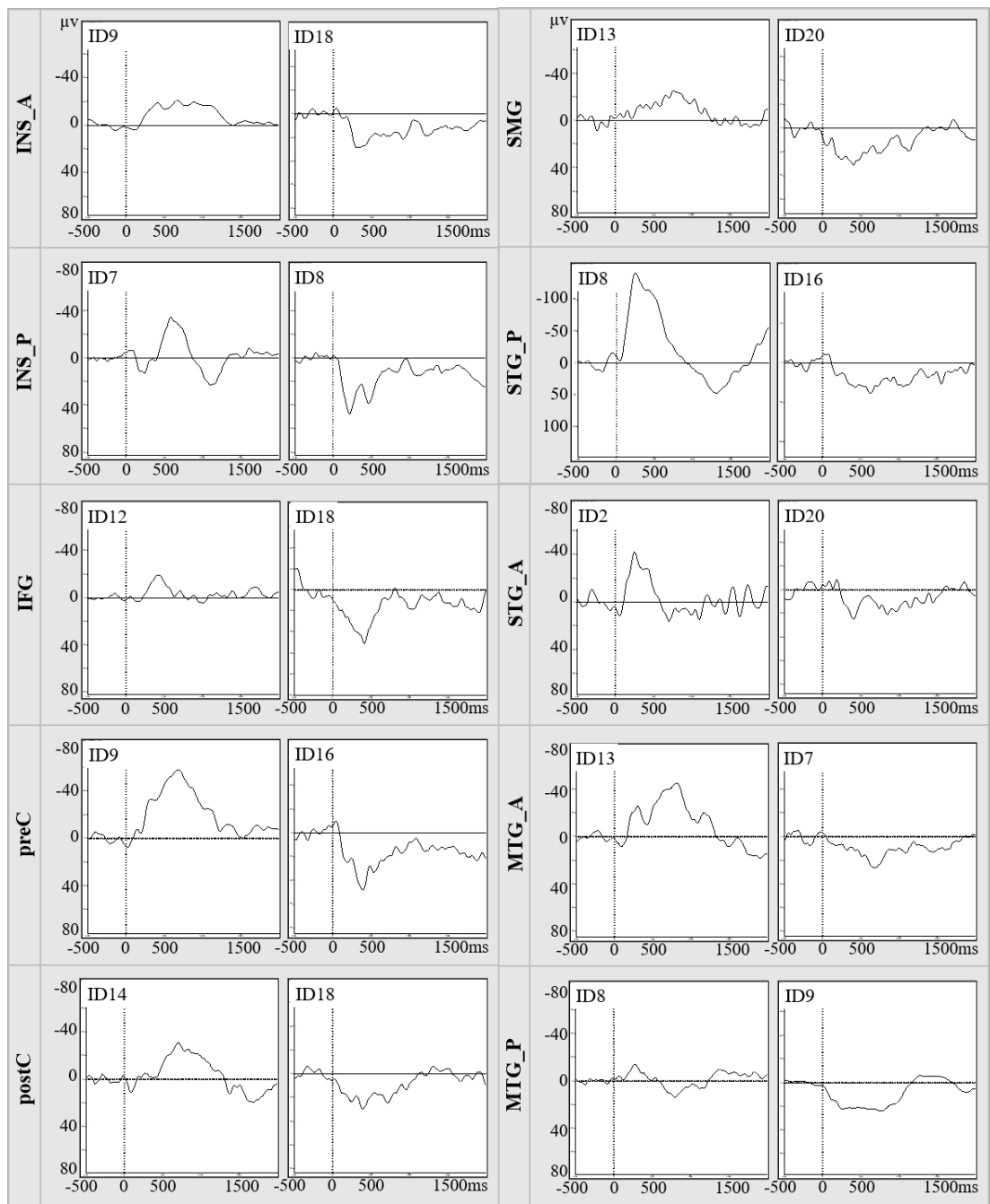
Figure 59. Summary of perisylvian brain areas showing MLCs and their morphology.
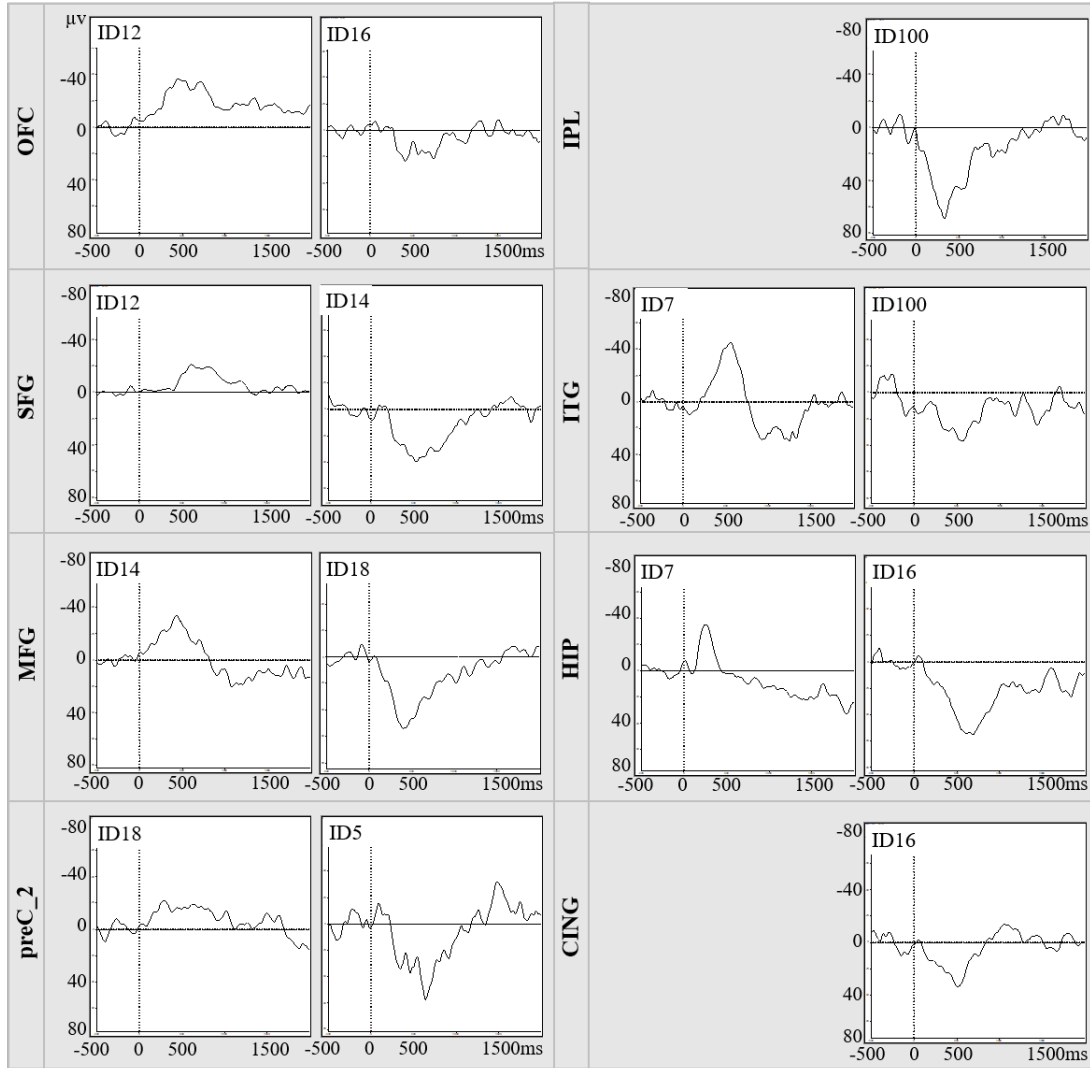
Figure 60. Summary of additional brain areas showing MLCs and their morphology.

c. Long latency component (LLC)

The LLC was defined as a wave which started between 0–700ms and lasted over the 1500ms mark. This component had two variations. It mostly presented as a long lasting wave, which started shortly after stimulus onset and showed either a positive or negative deflection, or it showed two waves, one in the first half of the window with either positive or negative amplitude changing to the opposite polarity in the second half of the time window (Figure 61). For the long lasting wave, the mean positive peak amplitude was 48.8μV (min=12.9μV, max=174.9μV, SD=26.4μV), mean peak latency 729.4ms (min=436.2ms,

max=1902.2ms, SD=436.2ms) and mean duration 1673.5ms (min =1206.1ms, max=1954.3ms, SD 235.0s). The mean negative peak amplitude was -56.0µV (min=-16.8µV, max=-243.5µV, SD=33.2µV), mean peak latency 850.9ms (min=164.5ms, max=1911.2ms, SD=401.9ms) and mean duration 1645.4ms (min=975.4ms, max=1986.4ms, SD=241.3ms).
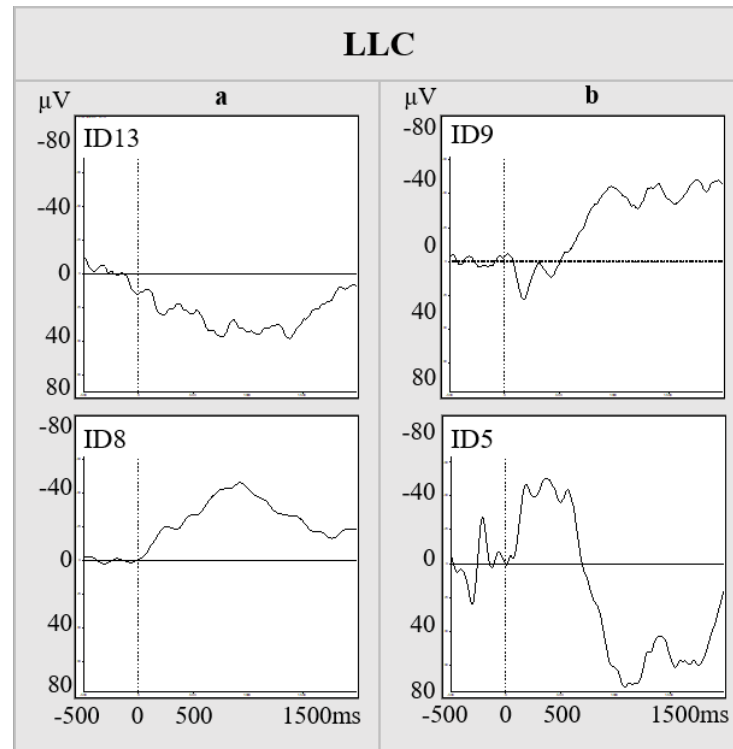
Figure 61. Summary of long latency components and their morphology.

In summary, bilateral posterior STG and posterior insula exhibited the earliest components, called primary components in this study. Their mean peak latency occurred around 75–80ms, hence <100ms and without a primary complex like those recorded in primary auditory cortex (Liégeois-Chauvel et al., 2003). The following component measured, the early component, occurred between 100–200ms, most frequently in the posterior STG. However, it was also measured in remote areas from the auditory cortex like anterior and posterior insula, supramarginal gyrus and postcentral gyrus. ECs were measured in a few more areas, however, less than two patients showed iERPs there: precentral gyrus, anterior STG, inferior frontal gyrus, posterior MTG, inferior temporal gyrus and

the hippocampus. Next component, middle latency component, in the posterior STG showed a very similar morphology to the EC measured in the posterior STG with only the peak being measured >200ms instead of between 100–200ms. MLCs in other areas had a similar morphology showing a prolonged wave with a peak. The last component, the long latency component, showed two variations. On the one hand a long lasting wave over the whole of the ERP window with either a positive or negative deflection. On the other hand, a split wave with a polarity change to the opposite polarity half time.

With regards to topography of these components the highest number of contacts showing ECs were measured in posterior STG and anterior STG, although only two patients had electrodes implanted in the anterior STG. However, also the rest of the perisylvian regions exhibited ECs, albeit with a lower percentage of occurrence and with a lower amplitude. MLC and LLC were distributed quite equally between perisylvian and additional brain regions. A summary of brain regions and the percentage of occurrence of iERPs is illustrated in Figure 62.
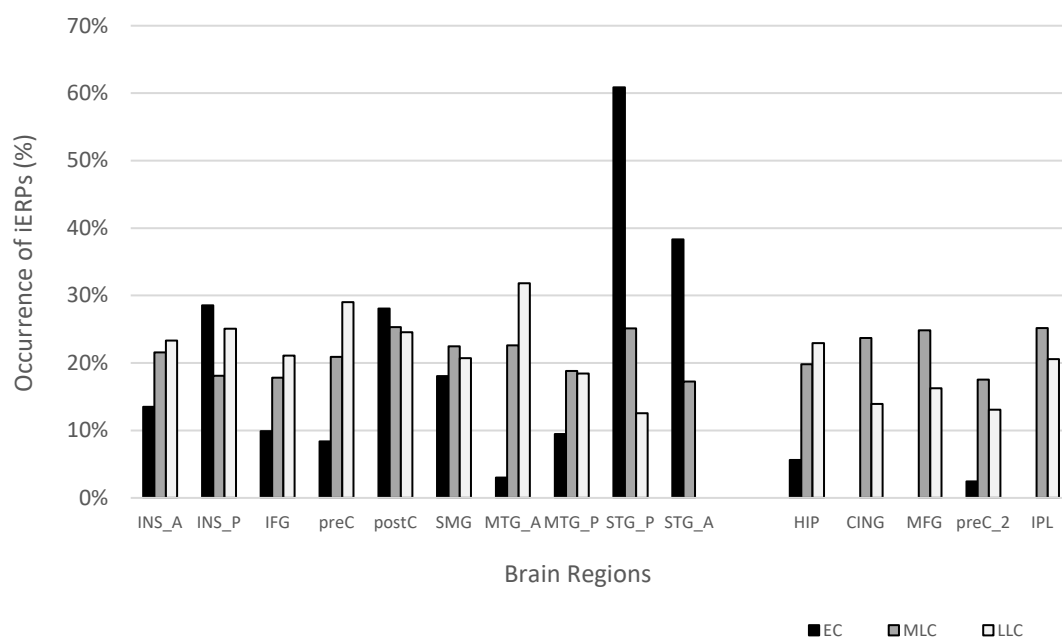
Figure 62. Distribution of iERP components during auditory word tasks. Brain regions showing EC, MLC and LLC components measured during auditory word tasks.

5.4.7 Stimulus-locked iERPs during listening to auditory sentence stimuli

Topography of region-specific iERPs during auditory sentence stimuli

For the LN task (in n=10 patients) areas of the perisylvian region exhibited a higher percentage of iERPs compared to additional brain regions. The inferior temporal gyrus also showed iERP occurrence of 50% (Figure 63). Table 25 summarises the number of patients with electrodes implanted in analysed brain regions.
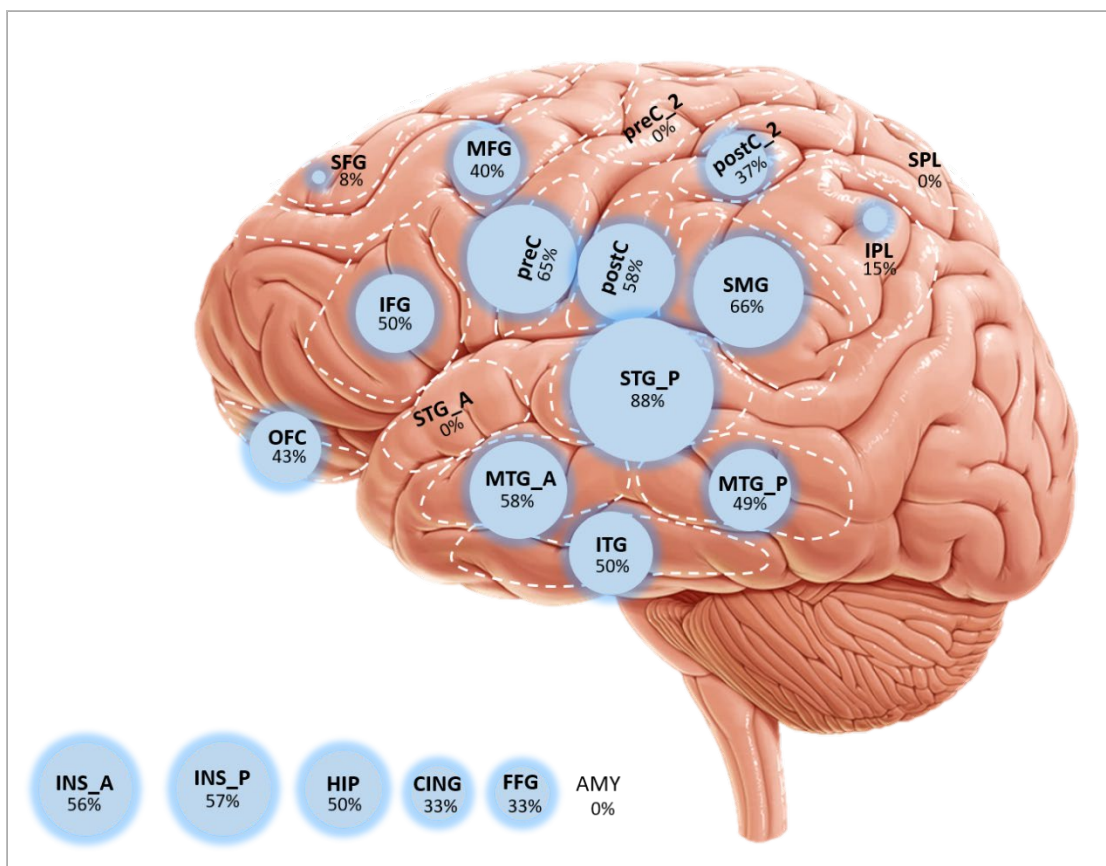
Figure 63. Overview of iERPs for the auditory sentence task. Maximum iERP occurrence was measured in STG_P with 88% and minimum iERP occurrence in SFG with 8%. No iERPs were measured in the amygdala, superior parietal lobule, dorsal precentral gyrus and anterior STG.

Table 25. Number of patients with electrodes implanted in brain regions used for analyses.

	INS_A	INS_P	HIP	CING	AMY	OFC	SFG	MFG
n	10	9	4	3	1	2	2	4

	IFG	preC	preC_2	postC	postC_2	SMG	IPL	SPL
n	7	7	2	6	2	8	3	1

	STG_P	STG_A	MTG_P	MTG_A	ITG	FFG
n	8	2	5	4	3	2

Compared to the topography of iERPs during auditory word tasks, the sentence task showed less activity in the superior frontal gyrus, dorsal precentral gyrus, postcentral gyrus, inferior parietal lobule and fusiform gyrus. All other areas, and in particular the perisylvian regions showed about the same percentage of iERPs in both the word and the sentence tasks. The anterior STG did not show any activity during the sentence task; however, the anterior STG was only sampled in two patients (ID20, 100). The performance of these two patients was better during word tasks compared to the sentence task although the difference was not significant ($p>0.1$, Wilcoxon rank sum test).

Morphology of region-specific iERPs during auditory sentence stimuli

For this analysis, only the morphology of primary and early components was analysed. Sentences varied in length (range 1.4–5.5s) hence, time windows for iERP analysis varied in length. Therefore, it was not possible to look at further components like MLC or LLC as were analysed for auditory single word tasks.

Primary components were elicited in five regions. Like during auditory word tasks described before, earliest mean peak latency was measured in the posterior STG compared to the rest of regions (66.8ms±21.4 and 80.2ms±11.4). Besides the posterior STG, PCs were observed with increasing mean peak latency in the following regions. As only a few contacts showed PCs the number of contacts and the number of patients sampled from is noted as well. STG_P (66.8ms±21.4, 13 contacts, 3 patients) < SMG (69.2ms±3.8, 8 contacts, 2 patients) < postC

(69.5ms±2.6, 4 contacts, 1 patient) < INS_P (82.3ms±2.5, 4 contacts, 2 patients) < MTG_P (82.5ms±10.7ms, 10 contacts, 2 patients) < IFG (88.0ms±14.0, 4 contacts, 1 patient). Waveform was similar in all regions with either a negative or a positive peak <100ms. The duration of the waves varied with the shortest component measuring 165.0ms compared to the longest duration of 6979.2ms.

Early components were elicited in seven regions with increasing mean peak latencies. SMG (118.0ms±16.4, 16 contacts, 4 patients) < MTG_P (119.7ms±34.2, 6 contacts, 1 patient) < INS_P (120.0ms±16.5, 14 contacts, 5 patients) < STG_P (126.3ms±16.1, 14 contacts, 5 patients) < postC (129.5ms±22.3ms, 14 contacts, 5 patients) < INS_A (136.6ms±22.2, 11 contacts, 2 patients) < preC (140.9±12.6, contacts 8, patients 2). EC morphology was similar in all regions with either a negative or a positive peak between 100–200ms. Mean peak latency, mean amplitude, mean iERP duration, minimum, and maximum for each category is summarised for PCs, ECs and for the rest of the iERPs in Table 26. iERPs and morphological details are divided into negative and positive going iERPs (Figure 64).

Table 26. Morphology of region-specific iERPs during auditory sentences.

PC	mean positive latency (ms)	76.6	SD	18.1	min	37.0	max	99.0
	mean positive amplitude (µV)	19.6	SD	4.3	min	10.3	max	27.3
	mean positive duration (ms)	4531.7	SD	2066.8	min	165.0	max	6979.2
	mean negative latency(ms)	76.9	SD	10.0	min	60.0	max	95.0
	mean negative amplitude (µV)	-13.2	SD	1.7	min	-8.9	max	-16.2
	mean negative duration(ms)	6130	SD	917.4	min	4565	max	6944.3

EC	mean positive latency (ms)	130.8	SD	25.2	min	101.0	max	196.0
	mean positive amplitude (µV)	92.3	SD	87.4	min	27.7	max	215.0
	mean positive duration (ms)	2143.0	SD	1817.6	min	186.0	max	6979.2
	mean negative latency(ms)	122.5	SD	15.8	min	100.0	max	151.7
	mean negative amplitude (µV)	-77.2	SD	65.0	min	-16.6	max	-274.6
	mean negative duration(ms)	2505.0	SD	1424.1	min	686	max	6944.3

Rest	mean positive latency (ms)	1501.6	SD	1377.6	min	213.2	max	5350.4
	mean positive amplitude (µV)	43.0	SD	27.4	min	9.6	max	137.5
	mean positive duration (ms)	2721.4	SD	1872.6	min	178.3	max	6944.7
	mean negative latency (ms)	1759.1	SD	1399.0	min	208.2	max	6249.2
	mean negative amplitude (µV)	-53.3	SD	39.7	min	-15.8	max	-270.1
	mean negative duration (ms)	3786.4	SD	1765.9	min	348.5	max	6955.0

Summary of mean latency, mean amplitude and mean duration of PCs, ECs and other iERPs elicited during LN task. Morphological details of PCs, ECs and other iERPs elicited during LN task. Rest = includes all other peaks measured besides PCs and ECs.
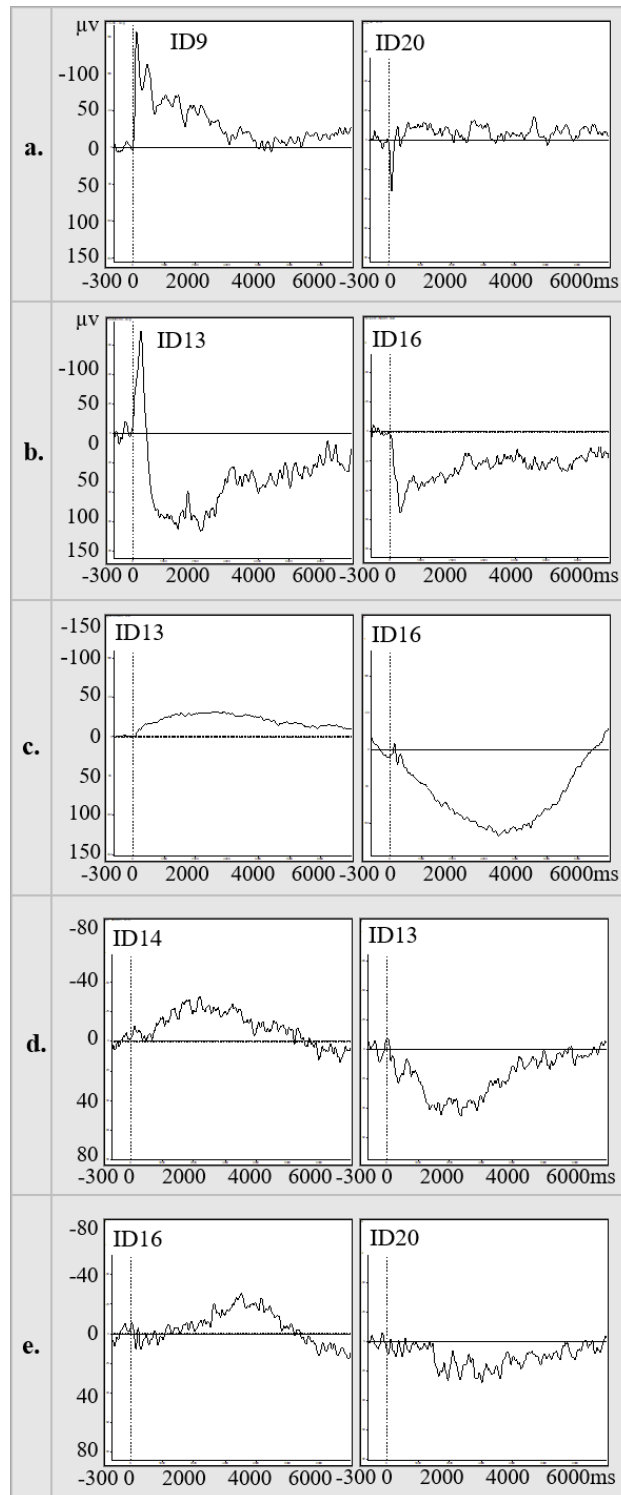
Figure 64. Examples of iERPs to auditory sentences, showing either negative or positive deflections. a. depicts an iERP example with a primary component; **b.** shows an iERP example with an early component; The following examples illustrate the three possible iERPs besides PC and EC. **c.** the wave starts very early after stimulus onset and lasts until the end of the time window; **d.** the wave starts early after stimulus onset and lasts until 4000–5000ms; **e.** the wave starts around 2000–3000ms after stimulus onset.

216

To sum up, Figure 65 illustrates brain regions sampled from which elicited robust iERPs. The perisylvian and additional brain areas and the insula, cingulate gyrus and hippocampus are shown. Regions highlighted in grey were only recorded from one or two patients. Furthermore, fusiform gyrus and amygdala were regions, which were only recorded from one or two patients, both showed iERPs, but are not illustrated here.
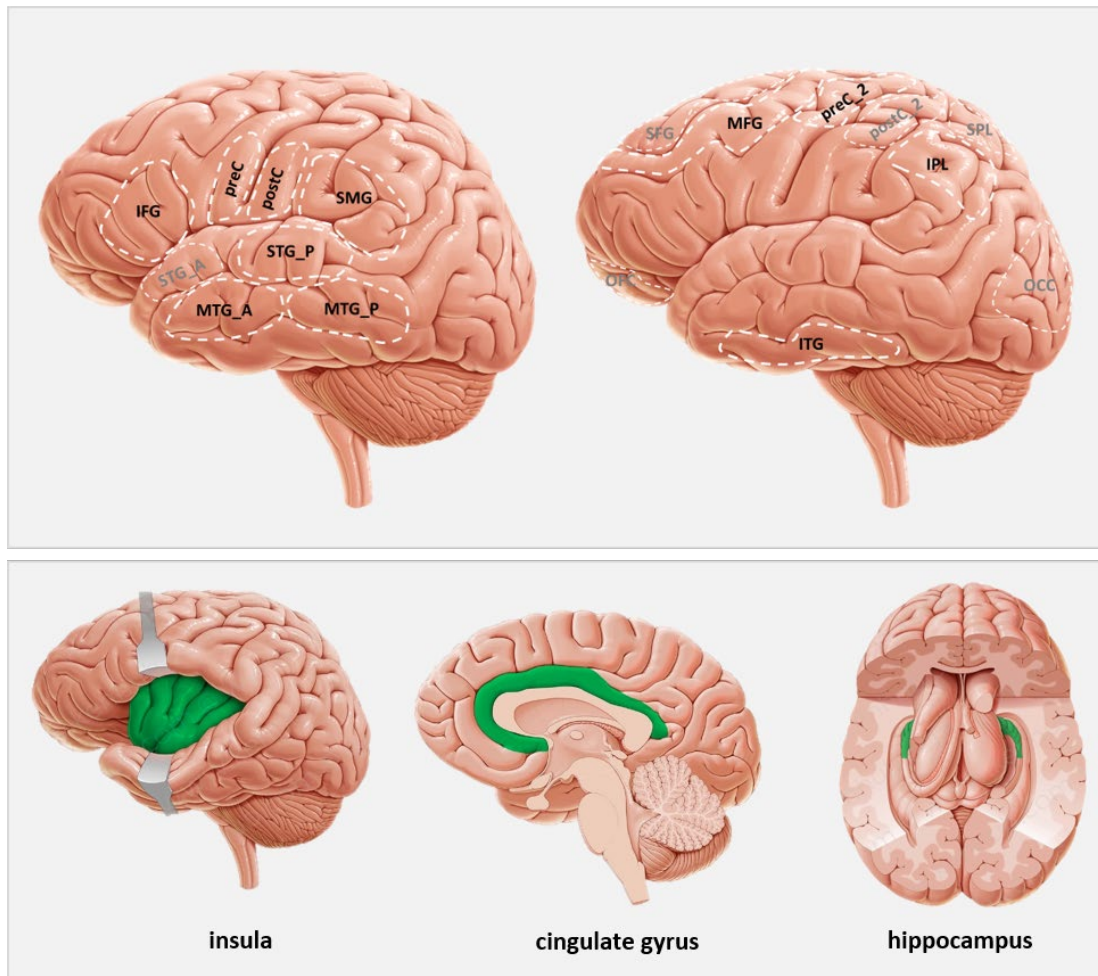
Figure 65. Cortical and subcortical brain regions showing robust iERPs. (areas marked in white dashed lines and in green, respectively). Abbreviations: IFG = inferior frontal gyrus, preC = precentral gyrus, postC = postcentral gyrus, SMG = supramarginal gyrus, STG_P = posterior superior temporal gyrus, STG_A = anterior STG, MTG_A = anterior medial temporal gyrus, MTG_P = posterior MTG, SFG = superior frontal gyrus, MFG = medial frontal gyrus, preC_2 = dorsal precentral gyrus, postC_2 = dorsal postcentral gyrus, SPL = superior parietal lobule, IPL = inferior parietal lobule without SMG, OCC = occipital lobe, ITG = inferior temporal gyrus. Brain illustrations are taken with permission from ©Kenhub (www.kenhub.com); Illustrator: Paul Kim.

5.4.8　Overview of task-specific iERP occurrence across all implanted brain regions

In total, six tasks were administered, hence six stimulus-locked iERP (BL, WR, VG, LN, PN, CNw) groups were formed. To address the question whether there were differences between stimulus-locked iERPs between different tasks the weighted average percentage of contacts with iERPs was analysed. Here, analysis was conducted across all brain regions sampled (Figure 66).
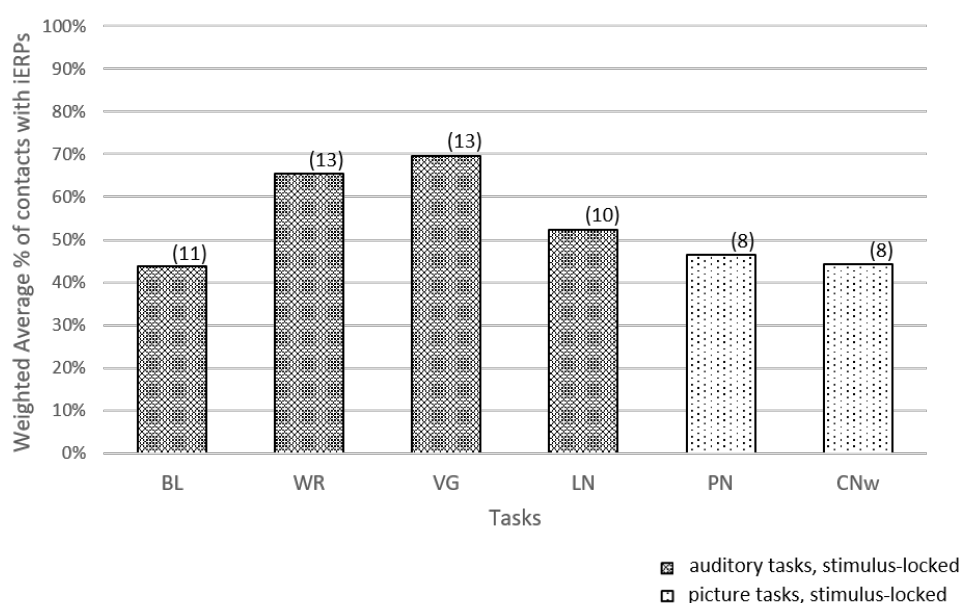
Figure 66. Weighted average percentage of contacts with iERPs for different tasks. Auditory, stimulus-locked tasks (BL, WR, VG, LN) are presented first, followed by picture and colour naming tasks (PN, CNw). The number of included patients for each task are shown in brackets on top of each bar.

A Wilcoxon rank sum test showed that occurrence was significantly enhanced during the active word tasks (VG, WR) compared to the passive baseline task (both $p<0.5$, n=11) and during the auditory verb generation task compared to the visual picture naming task ($p<0.5$, n=8).

Differences in waveform morphology between active and passive auditory word tasks (BL versus WR and VG)

A few morphological characteristics between iERPs of active versus passive tasks were observed, which are summarised in Figure 67. Morphological

differences measured between BL and WR/VG were similarly expressed across all regions where those iERP were observed.
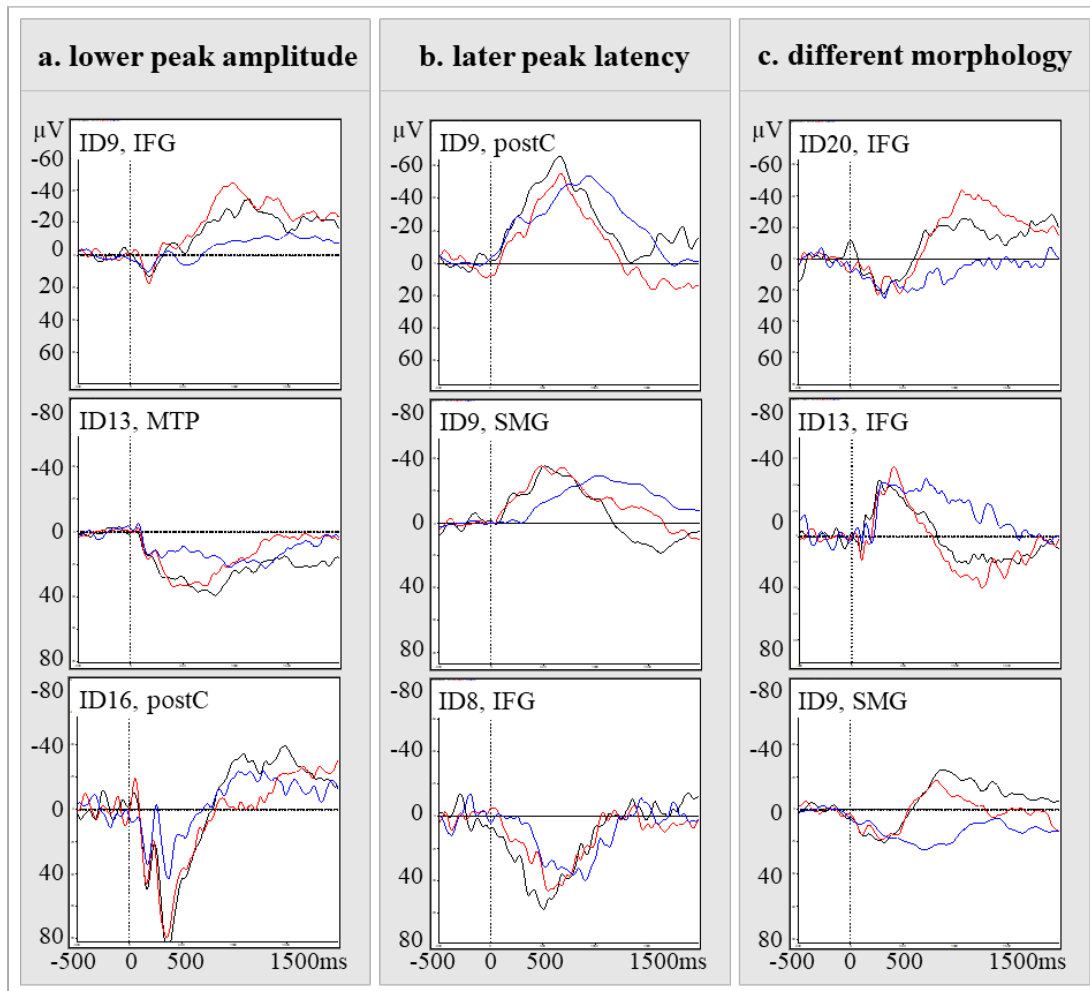
Figure 67. Examples of morphological characteristics between passive and active auditory word tasks. BL = blue, WR = black, VG = red. **a.** illustrates examples in three different patients and brain regions where the active tasks elicited iERPs with a higher peak amplitude compared to the passive task; **b.** shows example iERPs where an earlier peak latency can be found in the active tasks; **c.** presents iERPs where the active tasks elicited iERPs with a different morphology compared to BL task. While during WR and VG the iERPs seem to be composed of two components and a polarity change, iERPs during BL task are longer in duration and do not change polarity.

Differences in morphology between picture and colour naming

Morphological characteristics observed between iERPs elicited during picture versus colour naming tasks are illustrated in Figure 68 . No region-specific morphological changes were measured for these two tasks.
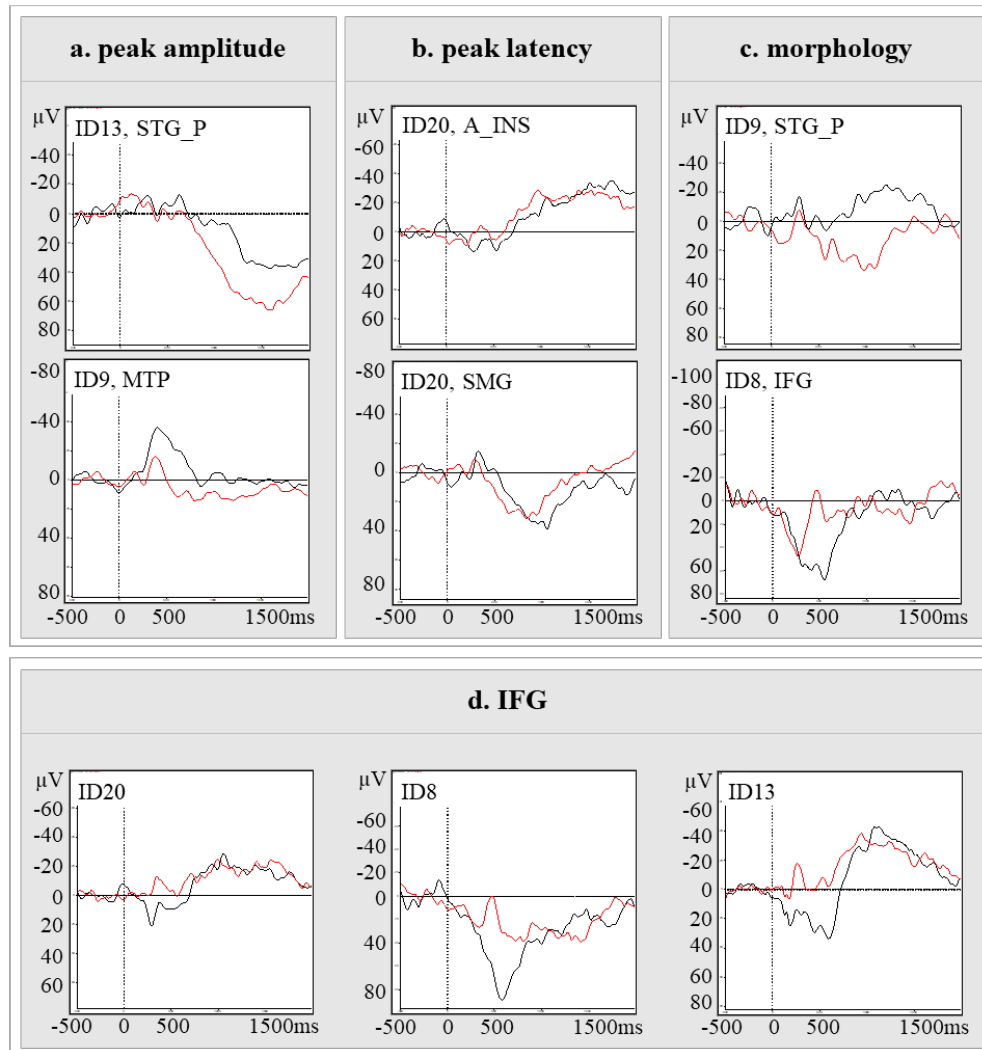
Figure 68. Examples of morphological characteristics between picture and colour naming tasks. PN = black, CNw = red. **a.** presents two patients and two brain regions where one of the tasks elicited an iERP with a higher peak amplitude compared to the other task. **b.** shows two examples where the colour naming task presented a slightly earlier peak latency compared to the picture naming task. **c.** illustrates two brain regions in two patients where both tasks elicited an iERP, however, both with a different morphology between tasks; **d.** summarises the three patients where iERPs were elicited in the same contacts during both tasks. In all cases iERPs elicited during the picture naming task show an early component, followed by a late component or lasting long compared to the colour naming task which elicited iERPs that showed no early but a late component.

5.4.9   Region- and task-specific occurrence of iERPs

Several distinct anatomical regions were identified, showing robust iERPs in temporal, parietal and frontal lobes in both hemispheres in response to passive and active auditory and picture naming stimuli.

Auditory tasks

The following Figure 69 illustrates the comparison of all auditory tasks depicting the mean percentage of contacts showing iERPs in perisylvian brain areas.
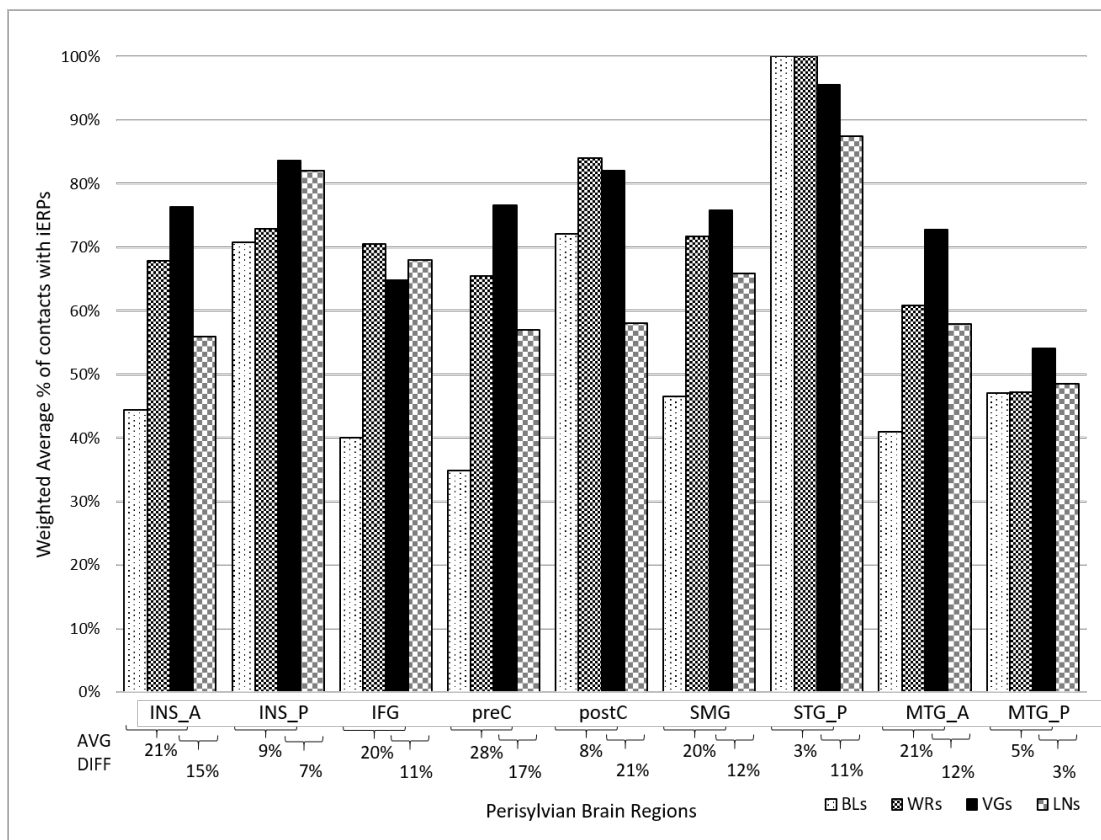
Figure 69. Mean percentage of contacts showing iERPs in perisylvian brain regions during different auditory word and sentence tasks (BL, WR, VG, LN). Mean percentage of contacts showing iERPs in perisylvian brain regions during different auditory word and sentence tasks (BL, WR, VG, LN). Average difference between the three-word tasks and the VG and LN tasks is shown at the bottom.

The passive auditory task (BL) elicited fewer iERPs in most perisylvian brain regions compared to the active tasks (WR, VG) except in the posterior insula, posterior STG and posterior middle temporal gyrus where BL and WR showed the same or a similar mean percentages of contacts with iERPs.

221

During the VG task, most iERPs were elicited in the anterior and posterior insula, precentral gyrus, supramarginal gyrus, and anterior and posterior middle temporal gyrus compared to BL and WR tasks. The biggest average difference between these three auditory word tasks was measured in the pre-central gyrus (28%), where the VG task elicited the highest number of iERPs.

During the WR task most contacts with iERPs were measured in the postcentral gyrus.

Listening to sentences elicited most activity in the posterior STG and the posterior insula. When comparing activity during LN to WR in the various brain regions little difference could be measured. However, the anterior insula showed significantly less iERPs during the LN task compared to the WR task. Furthermore, when comparing activity during the LN significantly fewer iERPs were measured compared to the VG task in the anterior and posterior insula, pre-central gyrus, posterior STG, supramarginal gyrus and anterior middle temporal gyrus.

Maximum mean difference between the LN and the auditory word tasks (BL, WR and VG) could be found in the post-central gyrus (21%), followed by the pre-central gyrus and anterior insula (17% and 17%, respectively). Least average difference showed the posterior middle temporal gyrus and posterior insula (3% and 7%, respectively).

Next, Figure 70 illustrates the comparison of all auditory tasks depicting the mean percentage of contacts showing iERPs in additional brain regions.
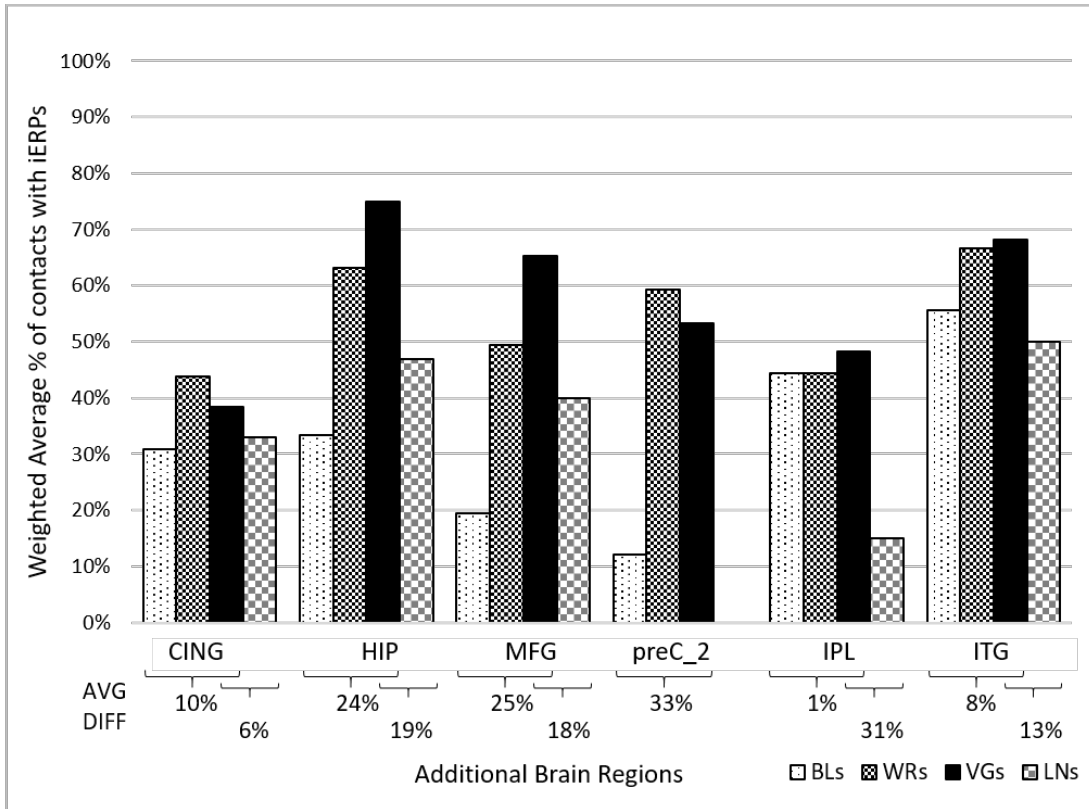
Figure 70. Mean percentage of contacts showing iERPs in additional brain regions comparing different auditory tasks.

Contacts in these non-perisylvian regions showed high activity during the active tasks (WR,VG) and in most regions much less activity during the passive baseline (BL) task. These differences were significant for the hippocampus (BL<VG, $p<0.05$), middle frontal gyrus (BL<VG, BL<WR, $p<0.01$), dorsal part of precentral gyrus (BL<VG, BL<WR, $p<0.01$) and inferior temporal gyrus (BL<VG, $p<0.05$). Only contacts in the inferior parietal lobule showed similar activity during passive and active tasks. While cingulate and dorsal precentral gyrus showed a significantly higher activity during the WR compared to the VG tasks ($p<0.1$ and $p<0.05$, respectively), the hippocampus and middle frontal gyrus elicited significantly less activity during WR compared to VG task ($p<0.05$ and $p<0.01$, respectively).

223

Visual tasks

Next, I present the distribution of iERPs during picture and colour (baseline) naming tasks in Figure 71 and the comparison of mean percentage of contacts showing iERPs comparing both visual naming tasks (Figure 72).
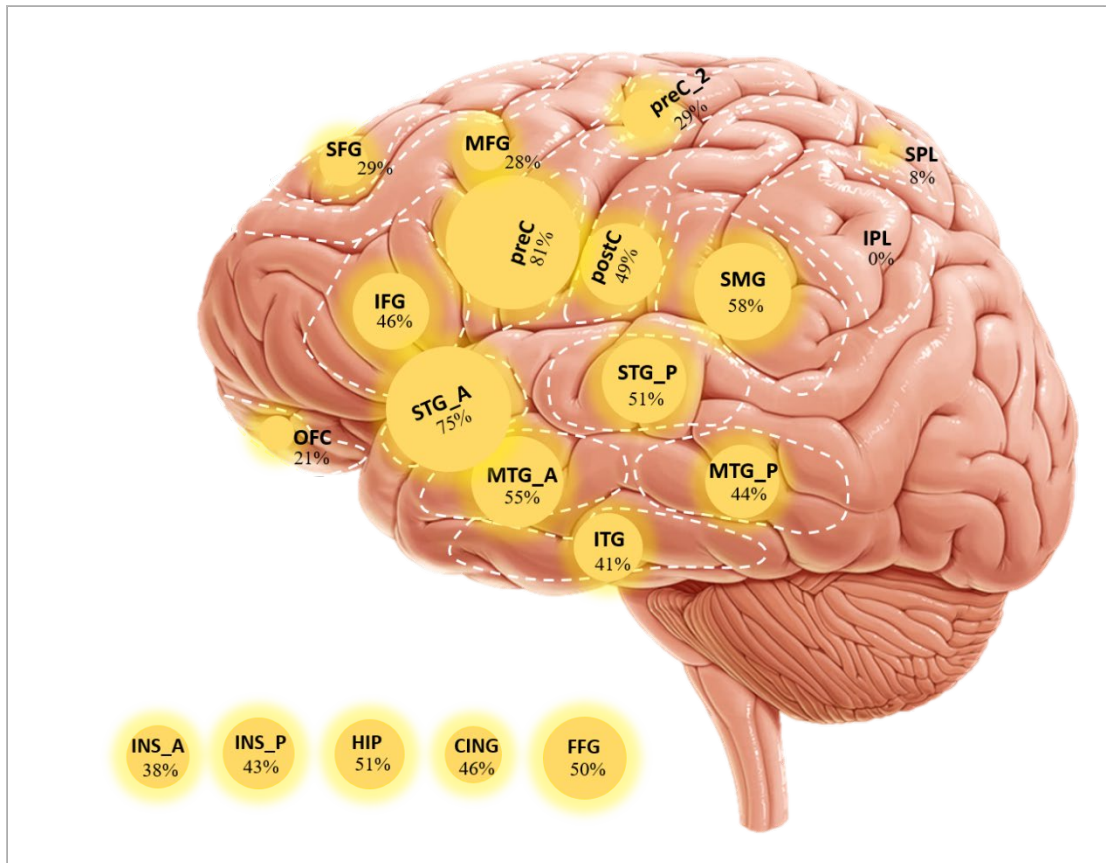
Figure 71. Overview of iERPs for the visual naming tasks—picture and colour naming. Maximum iERP occurrence was measured in precentral gyrus with 81% and minimum iERP occurrence in the superior parietal lobule with 8% and inferior parietal lobule with no activity.
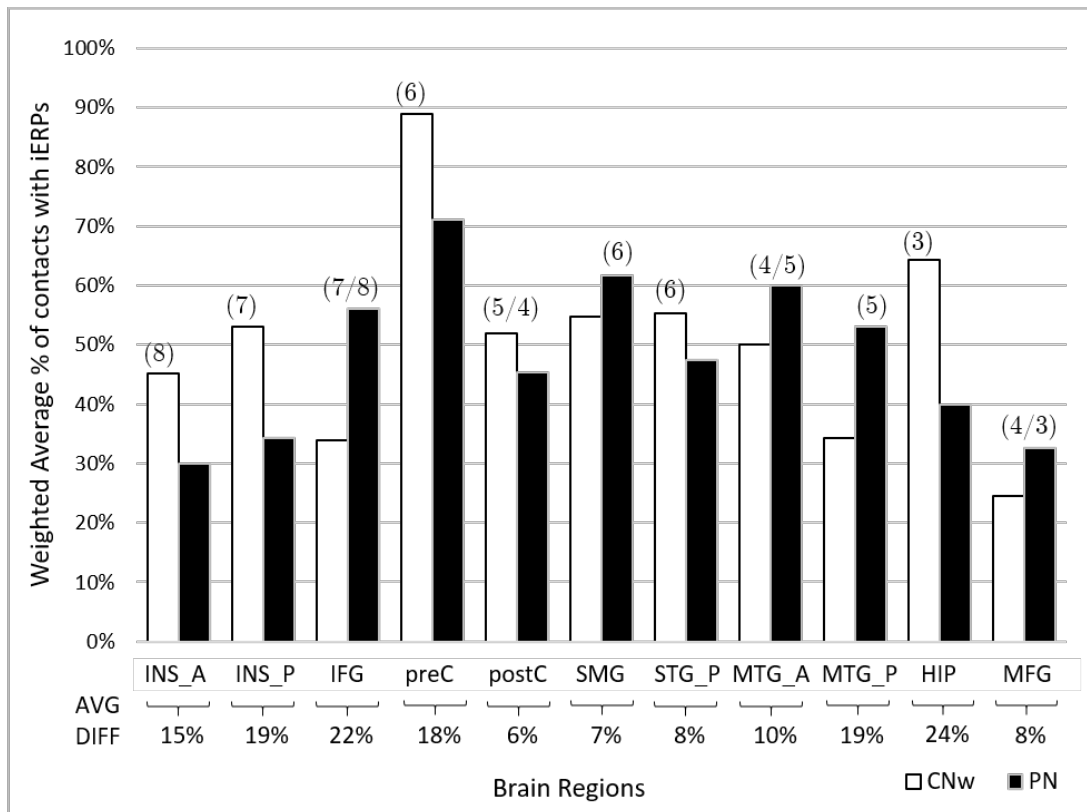
Figure 72. Mean percentage of contacts showing iERPs in perisylvian and additional brain regions during visual tasks comparing picture and colour naming tasks. Numbers in brackets refers to the number of patients implanted with electrodes used for this analysis.

Colour naming led to significantly higher activation compared to picture naming in the anterior and posterior insula. Picture naming elicited significantly higher activation in the inferior frontal gyrus, supramarginal gyrus, posterior medial temporal gyrus and medial frontal gyrus. A full summary of significant differences between all tasks can be found in Table 27.

225

Table 27. Wilcoxon rank sum test results for stimulus-locked auditory and picture naming tasks.

	BL-WR	BL-VG	WR-VG	PN-CNw	BL-LN	WR-LN	VG-LN
INS_A	Z=-5**	Z=-5**	Z=-1	Z=-2*	Z=-3**	Z=-2*	Z=-5**
INS_P	Z=-3**	Z=-4**	Z=-5**	Z=-4**	Z=-2*	Z=0	Z=-2*
IFG	Z=-5**	Z=-5**	Z=-1	Z=-3**	Z=-5**	Z=0	Z=-1
preC	Z=4**	Z=-4**	Z=0	Z=0	Z=-5**	Z=-1	Z=-2*
postC	Z=0	Z=-3**	Z=0	Z=0	Z=-2	Z=-2	Z=-2*
SMG	Z=-7**	Z=-7**	Z=-3*	Z=-7**	Z=-7**	Z=0	Z=-2*
STG_P	Z=0	Z=-3**	Z=-3**	Z=-1	Z=-7	Z=0	Z=-3
MTG_A	Z=-3**	Z=-3**	Z=0	Z=0	Z=-3**	Z=-1	Z=-3**
MTG_P	Z=-1	Z=0	Z=-3**	Z=-3**	Z=-3**	Z=-1	Z=0
CING	Z=-1	Z=0	Z=1*				
HIP	Z=0	Z=-3*	Z=-3**				
MFG	Z=-6**	Z=-7**	Z=-7**	Z=-6**	Z=-6**	Z=-7**	Z=-7**
preC_2	Z=-5**	Z=-4**	Z=-2**				
IPL	Z=0	Z=0	Z=0				
ITG	Z=0	Z=-2*	Z=-1				

The table summarises Z-scores and significance levels for the comparison of responses between tasks. ** shows a significance level $p<0.01$ and * $p<0.05$. Each auditory word task is compared to all other auditory word tasks and to the sentence tasks. The picture naming task is compared to the colour naming task. A negative Z-score shows that the first task of a pair exhibited less activity, e.g. BL-WR with Z=-5** means that BL task elicited significantly less ($p<0.01$) iERPs compared to the WR task. A positive Z-score means the opposite.

5.4.10   Response-locked iERPs

Topography and morphology of response-locked iERPs for auditory word tasks

From 18 brain regions implanted (n=5 patients), nine showed robust response-locked iERPs with the highest occurrence of activity measured in the precentral gyrus. For this summary only brain areas with iERP data from at least three participants were taken into account. The rest only occurred in one or two patients (CING, HIP, SFG, preC_2, SPL, STG_A, MTG_P, ITG, FFG). In CING, HIP and FFG no iERPs were measured and the rest of the regions showed iERP occurrence rate ranging from 7%–35%. Figure 73 illustrates the topography and the morphology of response-locked iERPs in response to auditory word tasks.
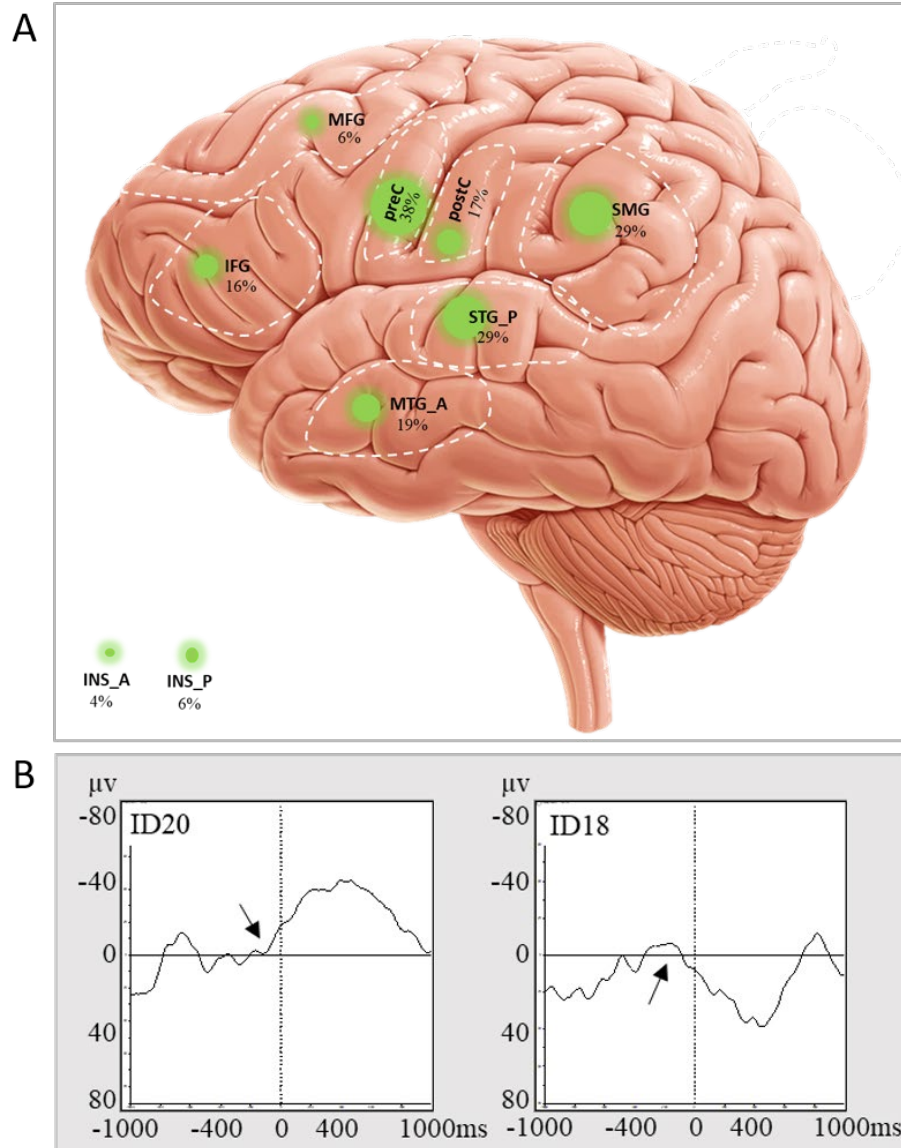
Figure 73. Response-locked iERP occurrence across brain regions for VG and WR tasks. A. depicts the topography of robust response-locked iERPs. **B.** illustrates their ramp-like morphology. 0 indicates the speech onset.

The morphology of these response-locked iERPs showed ramp-like waves starting very shortly before response onset (50–100ms), which could either have a positive and negative deflection. Brain regions did not differ in response morphology other than the polarity of the wave.

5.4.11 Comparison of left versus right hemisphere activation during auditory word tasks

The following section presents an attempt at performing a grand average analysis comparing iERP morphology from auditory word tasks from the left and the right hemispheres. For this grand average analysis iERPs were chosen manually for each patient and brain region, reflecting the patients most prominent and typical response for this region. This data reduction was necessary to obtain comparable responses from each subject. The limitations of this approach is inherent in the sparse but individualised sampling of regions using iERP.

Morphology of grand average iERPs for the perisylvian brain areas are described next. Figure 74 and Figure 75 illustrate grand average activity during auditory word tasks comparing left and right hemisphere.

iERPs from the left and right anterior insula showed similar magnitude, with varying polarity. The iERPs in the left anterior insula showed an earlier peak around 150–250ms, while the right anterior insula showed a peak around 300–500ms. Activity in the posterior insula was similar in morphology bilaterally for all three tasks. Left hemisphere iERPs showed an earlier positive peak of lower amplitude compared to the right side (left - peak: between 100–200ms, amplitude 20–30μV duration 500–700ms; right - peak: 150–300ms, 20–40μV, duration 700–1000ms). Activity in the precentral gyrus showed a different morphology comparing both hemispheres, with an early positive component in the left precentral gyrus and a prolonged wave with a peak latency of 400ms in the right precentral gyrus. Activity in the left precentral gyrus showed a different wave during BL task compared to WR and VG tasks. Finally, grand average iERPs in the postcentral gyrus behaved similarly, with a slightly later peak latency in the right hemisphere, however with a similar amplitude of -40μV (peak latency—left: 500–800ms; right: 700–1100ms). The right hemisphere showed an early positive component. All tasks behaved similarly.
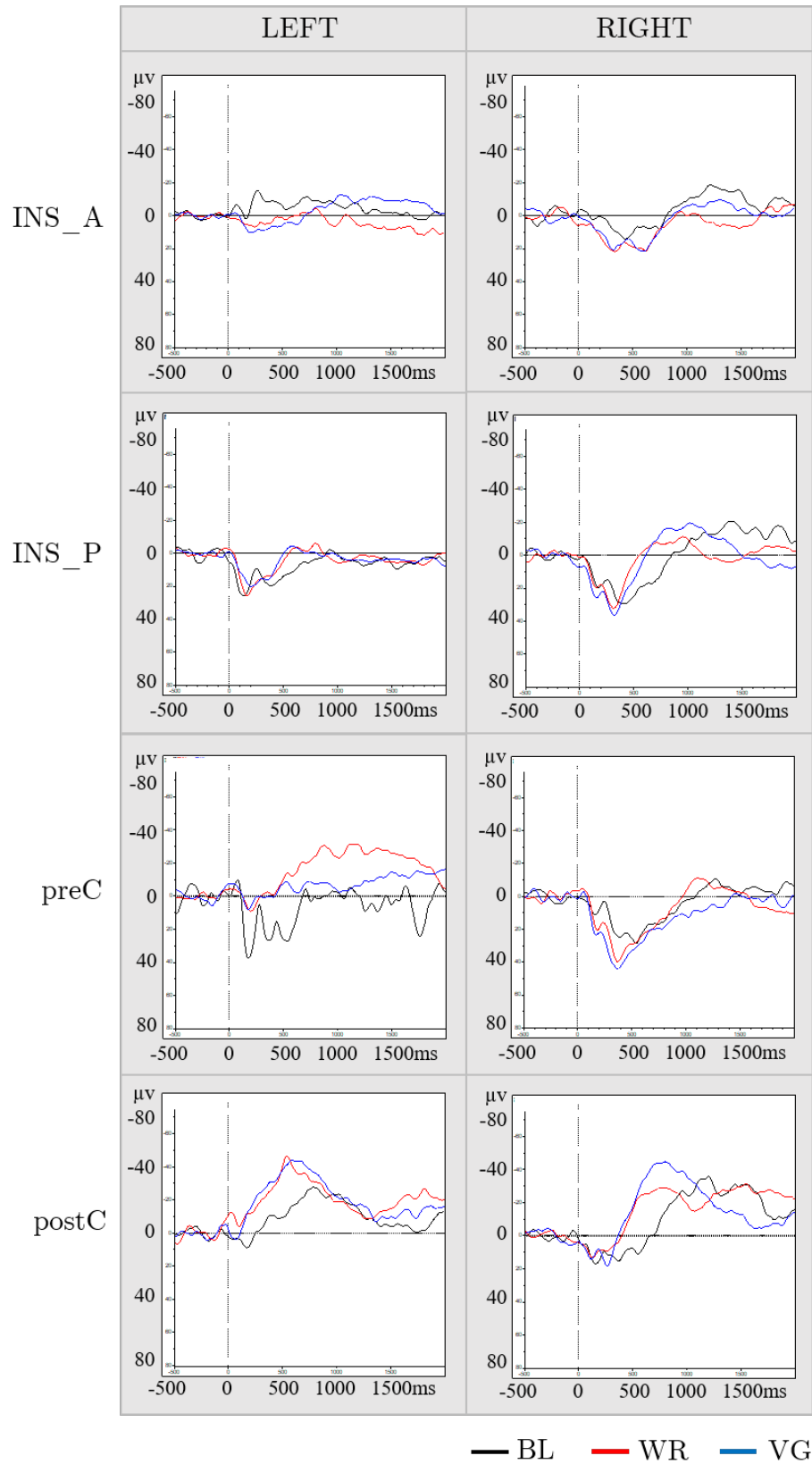
Figure 74. Grand average iERPs for auditory word tasks comparing left and right hemisphere implantation regimes.
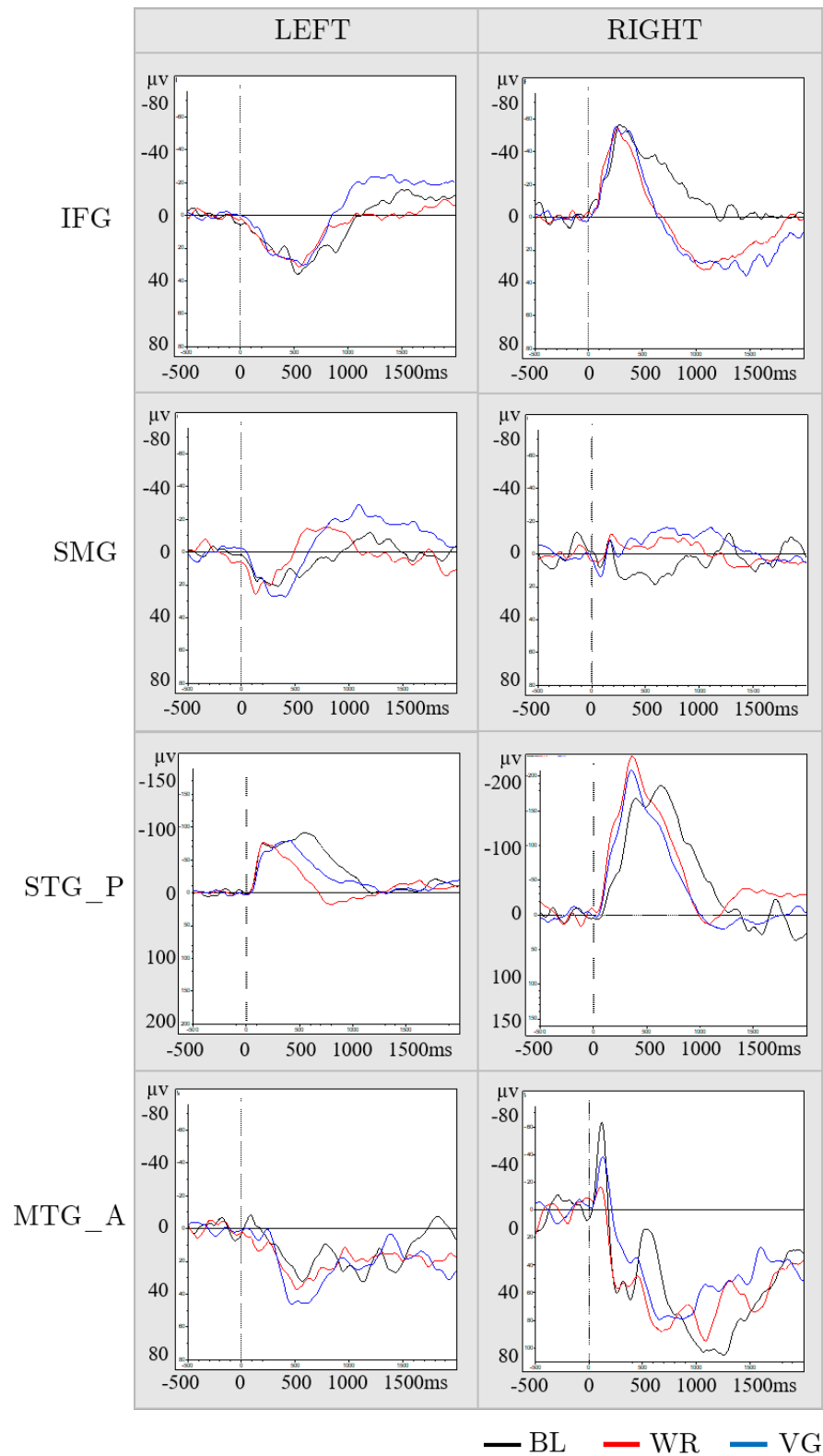
Figure 75. Grand average iERP analysis for auditory word tasks comparing left and right implantation regimes.

iERPs from the left IFG showed a late positivity (peak: 500–600ms, 30–40µV, duration: 900–1000ms), whereas iERPs from the right IFG showed an earlier negative peak (peak: 300–400ms, 60µV, duration: 900–1000ms) followed by late positive wave. All three tasks led to a similar wave morphology. Activity in the SMG showed similarities bilaterally with an early negative or positive peak at 150ms and amplitudes of 20–60µV. Activity from the posterior STG showed consistently a bilaterally early negative component (peak between 100–200ms) followed by a sustained negative component. This cluster showed the highest amplitudes overall (max. -230µV). Grand average iERPs in the left anterior MTG showed a long lasting positivity (peak: 400–600ms, 30–50µV, duration: 500–600ms) compared to the right side with an early negative component (peak between 100–200ms) followed by a sustained positive component.

The number of patients with contacts in the above described brain areas varied and is shown in Table 28.

Table 28. Number of patients included for each brain region presented in the grand average analysis.

	Left hemisphere			Right hemisphere		
	BL	WR	VG	BL	WR	VG
INS_A	7	8	8	4	5	5
INS_P	6	7	7	4	5	5
preC	6	6	6	4	5	5
postC	5	5	5	4	5	5
IFG	6	7	6	3	3	2
SMG	4	5	5	2	3	3
STG_P	5	6	6	2	3	3
MTG_A	3	3	4	2	2	2

In summary, activity in the anterior and posterior insula and the postcentral gyrus showed an earlier peak in the left hemisphere compared to the right. The morphology iERPs in the postcentral gyrus and the anterior middle temporal gyrus was different between left and right hemispheres. In the inferior frontal gyrus activity showed opposed polarity and the right IFG activity peaked earlier than the left. Similar morphological characteristics were found in the posterior STG and the SMG.

5.4.12   Case Studies

In the following, I am presenting three patients. The first case study summarises a typical SEEG patient with non-lesional epilepsy and an implantation regime involving the perisylvian regions. This case shows typical language-related iERPs measured in the perisylvian area in this study. The second case study presents a patient with tuberous sclerosis and electrodes implanted in pathological brain tissue. The aim with this case was to present language-related activity surrounding these tubers. Finally, the third case describes a patient who underwent previous neurosurgical resection and was admitted for a second invasive implantation as seizure persisted. The goal here was to show language-related activity in the remaining brain regions.

Case 1 (ID9)—Patient with SEEG implantation covering perisylvian regions

Patient ID9 was an 8½-year old girl with drug-resistant focal epilepsy, who experienced her first seizure at the age of 18 months. She lately presented with three different seizure types: nocturnal tonic seizures with secondary generalisation, forced head turning to the left during sleep and generalized tonic-clonic seizures.

Previous scalp EEG indicated that seizure semiology was likely to be of left temporal origin, although prominent interictal discharges were also noted parietally. Her MRI was lesion negative. Her parents reported deterioration at school, attention and concentration difficulties and disinhibited behaviour over the last year.

Patient ID9 was admitted to GOSH Koala ward for a left-sided SEEG implantation. In total 15 electrodes were implanted (Figure 76). From her invasive recording the seizure onset could not be clearly localised. From electrodes L (SMA) contacts 1–2 and from electrode K (S1, but functionally motor) contacts 5–7 were involved near the onset, however, unequivocal EEG features were not noted. This region was adjacent to the primary and supplementary motor areas, which was determined using electrical stimulation

mapping. Any resection in this area would have carried a significant risk of permanent or transient motor deficit. Therefore, surgery was not recommended.

Electrode type	Label	Contacts	Location
depth	A	1-15	amygdala
depth	B	1-12	anterior hippocampus
depth	C	1-12	posterior hippocampus
depth	D	1-12	entorhinal cortex
depth	E	1-12	superior temporal gyrus
depth	F	1-15	middle frontal gyrus - cingulate
depth	G	1-12	temporo-occipital junction
depth	H	1-15	angular gyrus
depth	I	1-18	supramarginal gyrus
depth	J	1-12	superior parietal lobule
depth	K	1-12	S1
depth	L	1-10	M1-SMA
depth	M	1-10	pars opercularis – insula
depth	N	1-10	frontal operculum – insula
depth	O	1-15	superior frontal gyrus

Figure 76. Case 1 (ID9) - Patient with SEEG implantation covering perisylvian regions. A. illustrates the labelled implanted electrodes of the left hemisphere; B. summarises the placement locations of implanted electrodes.

This patient was able to complete all six language tasks. She had no incorrect responses in all but one task. In the sentence task she responded correctly in 73% of the cases.

For this study, only seven of the fifteen electrodes could be included. Electrodes C, E, G, H, I, M, N were chosen (Figure 77A). Contacts involved in the seizure onset were not included in ERP recording.

Figure 77B to Figure 79 illustrate iERPs elicited during the auditory word task (BL, WR, VG).
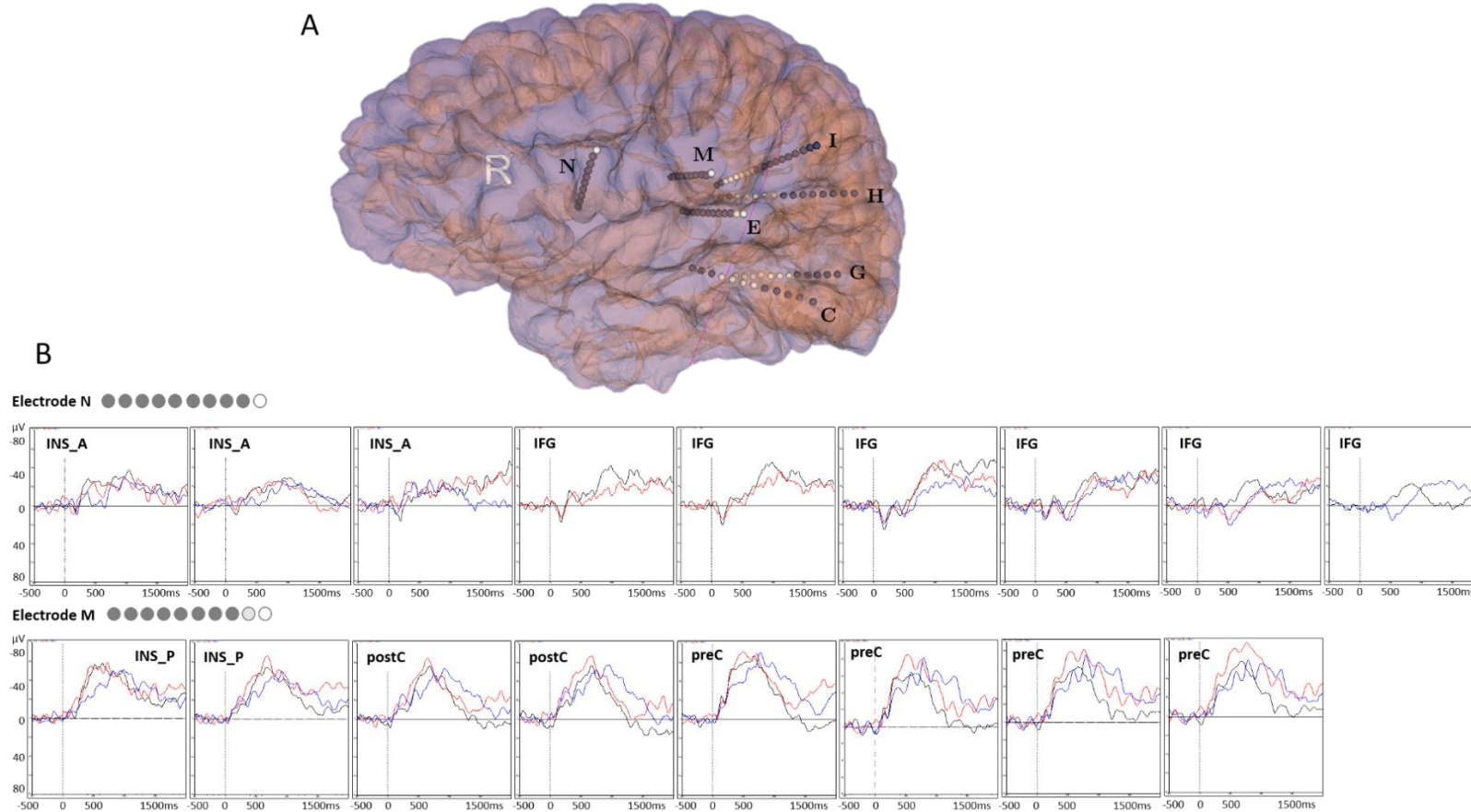
Figure 77. Case 1 (ID9)—robust iERPs (1). A. depicts the patients' brain image and electrodes included in iERP analysis. B. illustrates robust iERPs during auditory word tasks (BL–blue, WR–red, VG–black) for the first two electrodes. Electrode N: inserted in frontal operculum and aiming at anterior insula. Electrode M: inserted in pars opercularis and aiming at posterior insula. The circles depict the number of contacts inserted. Grey contacts recorded robust iERPs, light grey ones did not and white contacts were not included in iERP analysis. Each iERP box includes a corresponding region label, which names the region the contact was located in. iERP box most left shows the most mesial contact and the iERP box most right shows the most lateral contact.
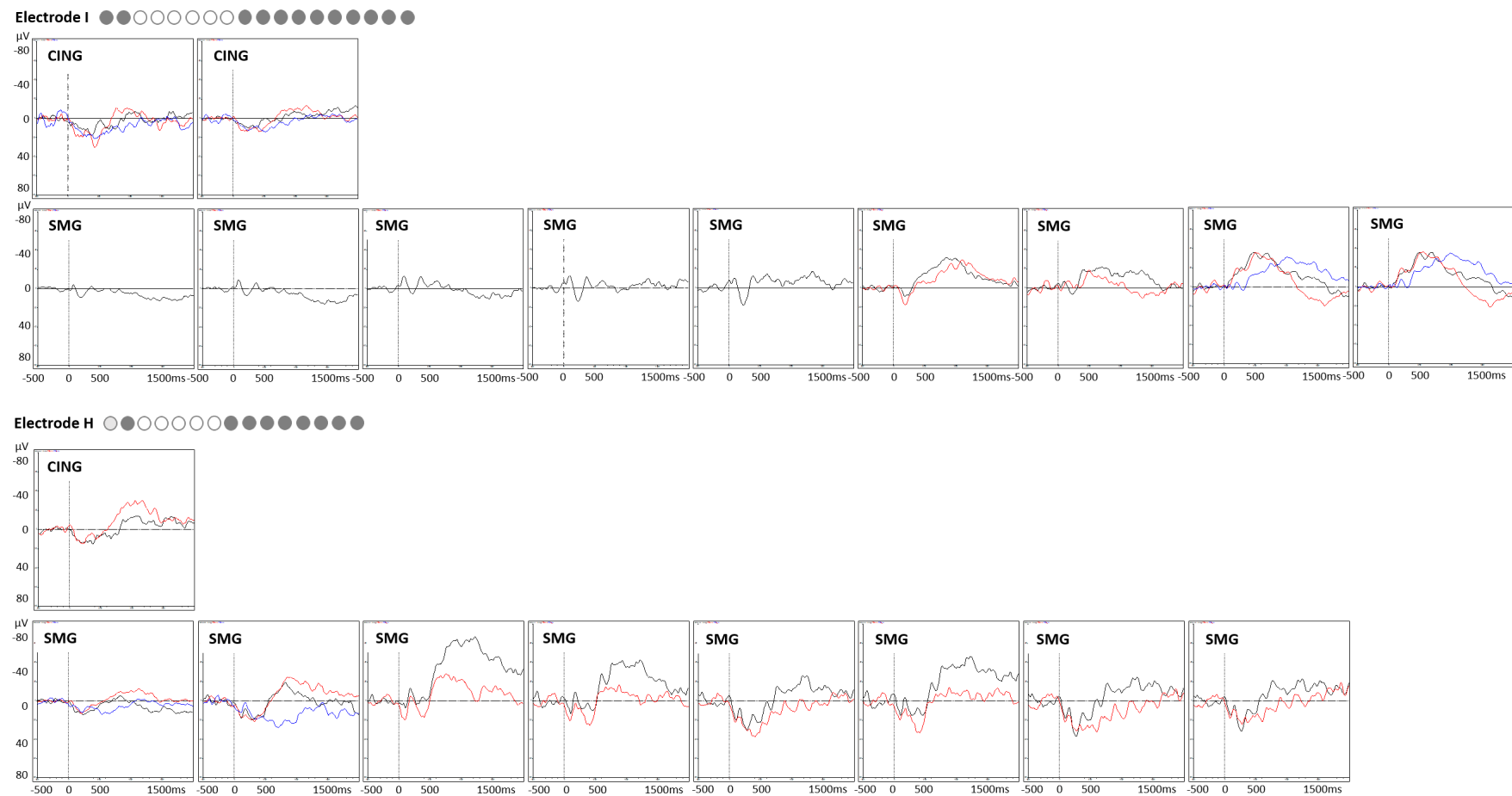
Figure 78. Case 1 (ID9)—robust iERPs (2). Robust iERPs during auditory word tasks (BL–blue, WR–red, VG–black) elicited in contacts of electrodes I (SMG) and H (angular gyrus) are illustrated. The circles depict the number of contacts inserted. Grey contacts recorded robust iERPs, light grey ones did not and white contacts were not included in iERP analysis. Each iERP box includes a corresponding region label, which names the region the contact was located in. First iERP box shows the most mesial contact and last iERP box the most lateral contact.
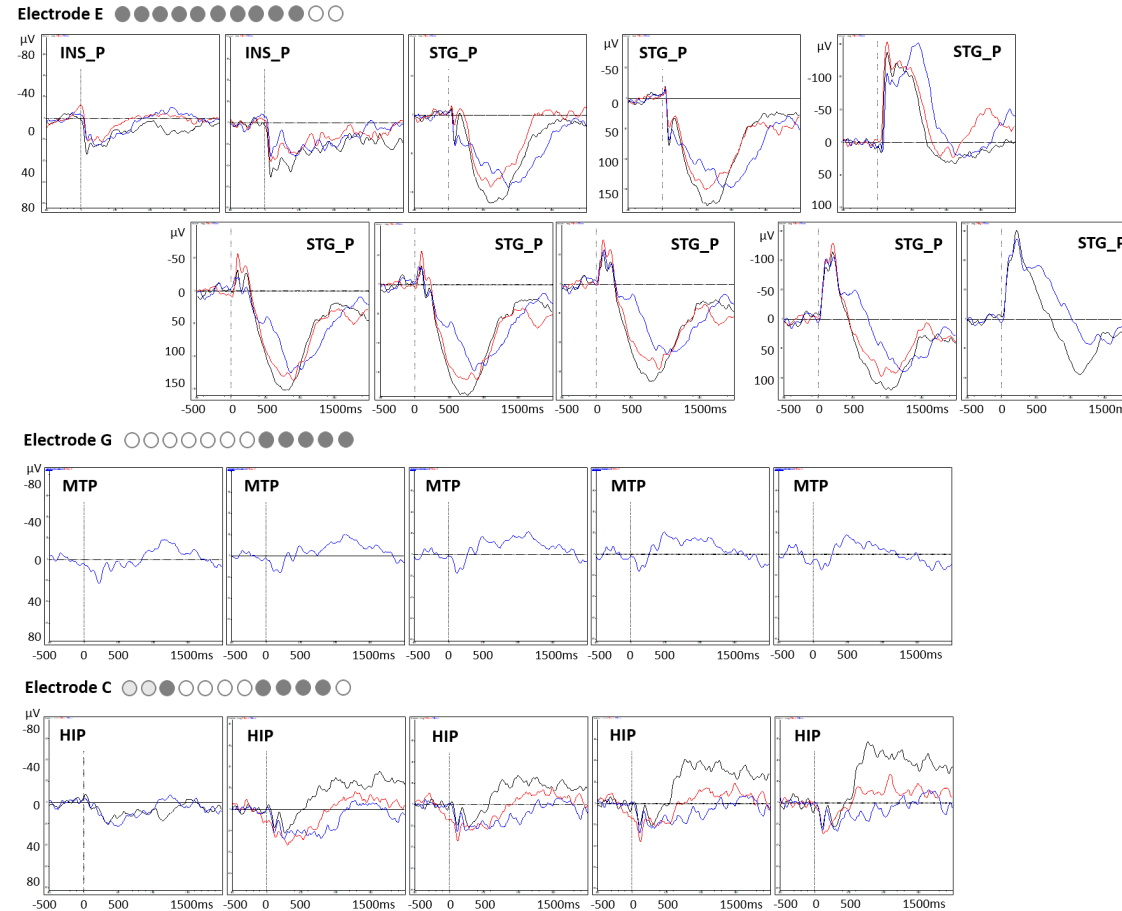
Figure 79. Case 1 (ID9)—robust iERPs (3). Robust iERPs during auditory word tasks (BL–blue, WR–red, VG–black) elicited in contacts of electrodes E (posterior STG to posterior insula), G (temporo-occipital junction) and C (posterior hippocampus) are illustrated. The circles depict the number of contacts inserted. Grey contacts recorded robust iERPs, light grey ones did not and white contacts were not included in iERP analysis. Each iERP box includes a corresponding region label, which names the region the contact was located in. First iERP box shows the most mesial contact and last iERP box the most lateral contact.

In total, 57 contacts (89.1%) showed robust iERPs. Typical pattern of primary auditory components were most prominent in the posterior STG and posterior insula and in addition occurred in the supramarginal gyrus. All perisylvian areas sampled from showed language-related activity measuring middle latency components (anterior insula, cingulate, hippocampus, IFG, posterior MTG and postcentral gyrus) or long latency components (anterior and posterior insula, IFG, posterior MTG, pre- and postcentral gyrus). A few of the sampled contacts were involved during interictal activity. Five of the interictally involved contacts (62.5%; N1, I1, M1, 2) I recorded from showed stimulus-locked activity.

Case 2 (ID10)—Patient with Tuberous Sclerosis Complex

Patient ID10 was a 9-year old, right-handed girl with Tuberous Sclerosis Complex (TSC1 mutation) and drug-resistant focal epilepsy. She experienced her first seizure at the age of 18 months. Her latest seizures occurred about twice a day and three different seizure types were observed: Type 1 started with behavioural arrest, head and eye deviation to the left, possible right eye twitching without a collapse. These were brief lasting typically less than 20 seconds; Type 2 started also with behavioural arrest, with gradual head drop and eyelid twitching, dribbles and fell to the floor, then showed generalised shaking. These lasted for approximately 30 seconds and sometimes post-ictal confusion occurred; During Type 3 the patient became flushed, unsettled, made dramatic movement of her arms and legs. She was unresponsive to questions during these episodes, which lasted up to several minutes.

The MRI showed multiple cortical tubers and subependymal nodules in both hemispheres. MEG investigation was suggestive of a multifocal irritative zone with two hot spots over the left dorsolateral prefrontal cortex and over the right opercular and superior temporal regions where cortical tubers were localised. Seizure onset zone was difficult to localize with scalp EEG and only partially overlapped with the interictal epileptic activity, which was seen almost

exclusively over left frontal-anterior temporal region. Only recently, difficulties at school were reported.

Patient ID10 was admitted to GOSH Koala ward for a left-sided SEEG implantation. In total, six electrodes were implanted in regions showing cortical tubers (Figure 80). She had 20 captured seizures during her admission. All three main seizure types and one additional variant were captured several times. From her invasive recording, the seizure onset was difficult to localise. However, the mesial parietal tuber (electrode F) was invariably involved initially. In addition deep contacts of electrode B (normal tissue of the cingulate) always preceded clearly recognisable clinical seizure manifestations (head bowing, facial asymmetry, head and/or eye deviation). A seizure was elicited from deep contacts of electrode F (1–2) during electrical stimulation. Resection of the mesial parietal tuber and lateral contacts of electrode F was proposed offering relatively good chance of seizure modification, but not necessarily seizure freedom. One year post surgery this patient presented with 1–2 seizures a day.

During language testing for this study the patient was able to complete three tasks (BL, WR and VG). She performed better during the word repetition task with 96% of correct responses compared to 70% during the verb generation task.

For this study, all the implanted electrodes could be included. Contacts involved in the seizure onset (F, B—deep contacts) were included in the iERP recording. Figure 80 illustrates iERPs elicited during the auditory word tasks.

Electrode	Label	Contacts	Location
depth	A	1-12	middle temporal gyrus-hippocampus
depth	B	1-10	preSMA - cingulate
depth	C	1-8	parietal
depth	D	1-8	posterior STG
depth	E	1-8	M1
depth	F	1-8	mesial parietal
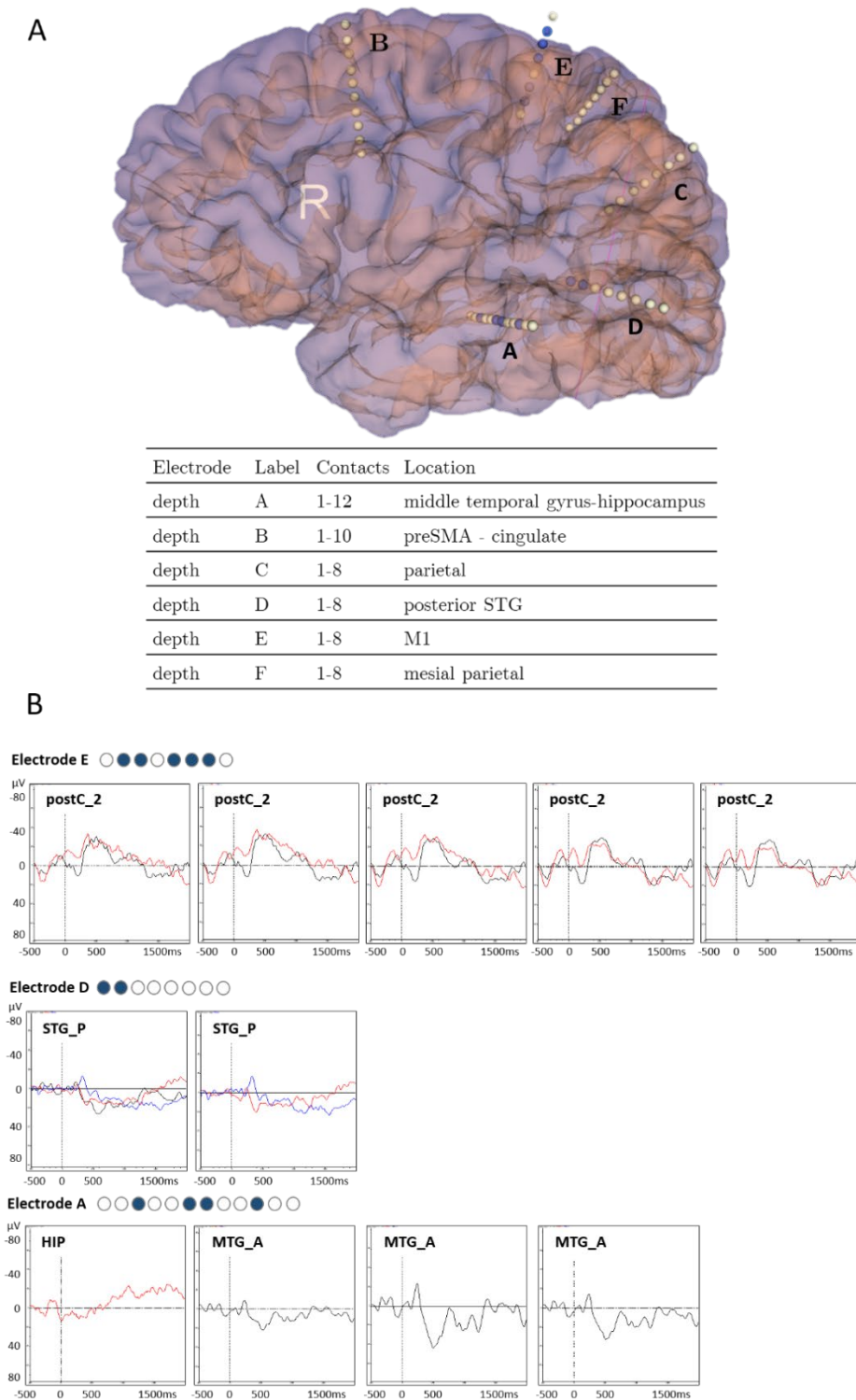
Figure 80. Case 2 (ID10)—Patient with Tuberous Sclerosis Complex and SEEG implantation regime. A. illustrates the patients' brain image and electrode placement of the left hemisphere. **B.** shows robust iERPs during auditory word tasks (BL–blue, WR–red, VG–black) elicited in a few contacts of electrodes E (M1), D (posterior STG) and A (MTG to hippocampus) are illustrated. The blue and white circles show the number of contacts of the electrode. The circles depict the number of contacts inserted. Blue contacts recorded robust iERPs and white contacts did not. Each iERP box includes a corresponding region label, which names the region the contact was located in. iERP box most left shows the most mesial contact and the iERP box most right shows the most lateral contact.

In total, 11 contacts (21.2%) showed robust iERPs. Long latency components were measured in contacts localised in the posterior STG and the hippocampus. Middle latency components were elicited in the anterior middle temporal gyrus and dorsal postcentral region. No primary and early components were measured. This patient showed less language-related iERPs, most probably because of the electrodes being implanted in tubers, hence pathological brain tissue. No iERPs were measured in contacts involved in the seizure onset. Contacts sampling from electrodes F(1–4), A(1–3, 12), C(6–8), B(1–4) and D(2–6) showed various interictal activity and two of these contacts, A3 and D2, sampling from the anterior middle temporal gyrus and from the posterior STG, respectively, showed stimulus-locked activity. The area showing reliable activity over all patients, the posterior STG, here showed little activity. Furthermore, activity measured in the posterior STG occurred later and the posterior STG did not elicit primary or early components. Still, despite recording from mostly contacts in pathological tissue, the dorsal postcentral gyrus, the anterior middle temporal gyrus and the hippocampus showed language-related activity, mostly middle latency activity.

Case 3 (ID4)—Patient with previous resection

Patient ID4 was a 9-year and 8 months old, left-handed boy with epilepsy characterised by left focal sensory-motor seizures. He already underwent a right temporal lobe resection and parieto-occipital disconnection when he was two years old. He experienced his first seizure at day three of life. Lately he presented with one type of seizure consisting of left-sided focal sensory-motor seizures (sometimes with pain) occurring daily. They were brief, lasting from a few seconds up to under two minutes or occurred in clusters with some seizure free days. During his seizures he stared, had jerky movements of the left arm and left leg, with or without drooling or he showed brief episodes resembling spasms, where his body was reported to curl to the left. Furthermore, he had non-epileptic sleep jerks. Mild developmental delay was reported.

The MRI showed a small and scarred right cerebral hemisphere with a small residual parieto-occipital connection. The scalp EEG activity was not well localised at onset, but was lateralised to the right and showed early involvement of the right anterior quadrant.

Patient ID4 was admitted to GOSH Koala ward for a right-sided SEEG implantation. In total, eleven electrodes were implanted. The electrical features of the seizures recorded suggested a seizure onset anterior to the previous disconnection and included the posterior part of the insula cortex and the posterior part of the medial parietal lobe (deepest contacts of electrodes C and D). Independent seizures were seen arising in the disconnected cortex, very occasionally seen at the same time as a habitual event. There was no convincing evidence of a residual connection. The patient underwent an elective redo right temporo-occipital disconnection and a right insular resection. One year post surgery he showed two episodes of behavioural arrest.

For this study, the patient was able to complete four language tasks (BL, WR, VG and LN). He performed best during the word repetition task with 100% of correct responses and during the verb generation and sentence tasks with 88% and 85%, respectively.

The clinical SEEG implantation regime is summarised in Figure 81. A subset of clinically implanted electrodes was included for this study recording. Contacts involved in the seizure onset (C, D—deep contacts) were included in the iERP recording. Figure 82, Figure 83 and Figure 84 illustrate iERPs elicited during the auditory word tasks (BL, WR and VG).

Electrode	Label	Contacts	Location
depth	A	1-10	Superior Parietal
depth	B	1-12	Inferior Parietal
depth	C	1-8	S2-Insula
depth	D	1-12	S1
depth	E	1-12	Posterior Middle Frontal Gyrus
depth	F	1-8	Frontal Operculum-Insula
depth	G	1-8	Inferior Frontal Gyrus
depth	H	1-12	Anterior Middle Frontal Gyrus
depth	I	1-18	Anterior Oblique-Insula
depth	J	1-10	Supplementary Motor Area
depth	K	1-15	Posterior Oblique-Insula
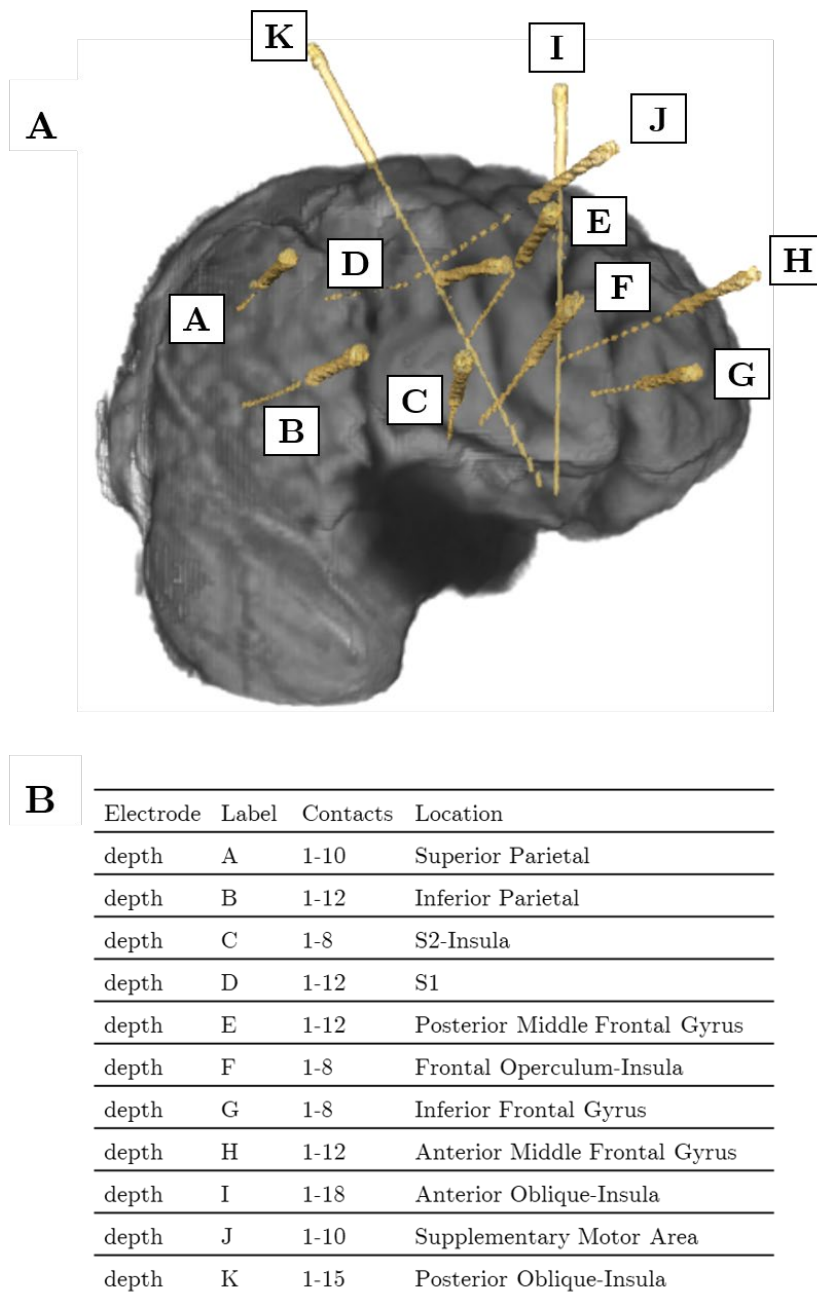
Figure 81. Case 3 (ID4)—SEEG patient with previous resection. A. illustrates the labelled implanted electrodes of the right hemisphere; **B.** summarises the placement locations of implanted electrodes.
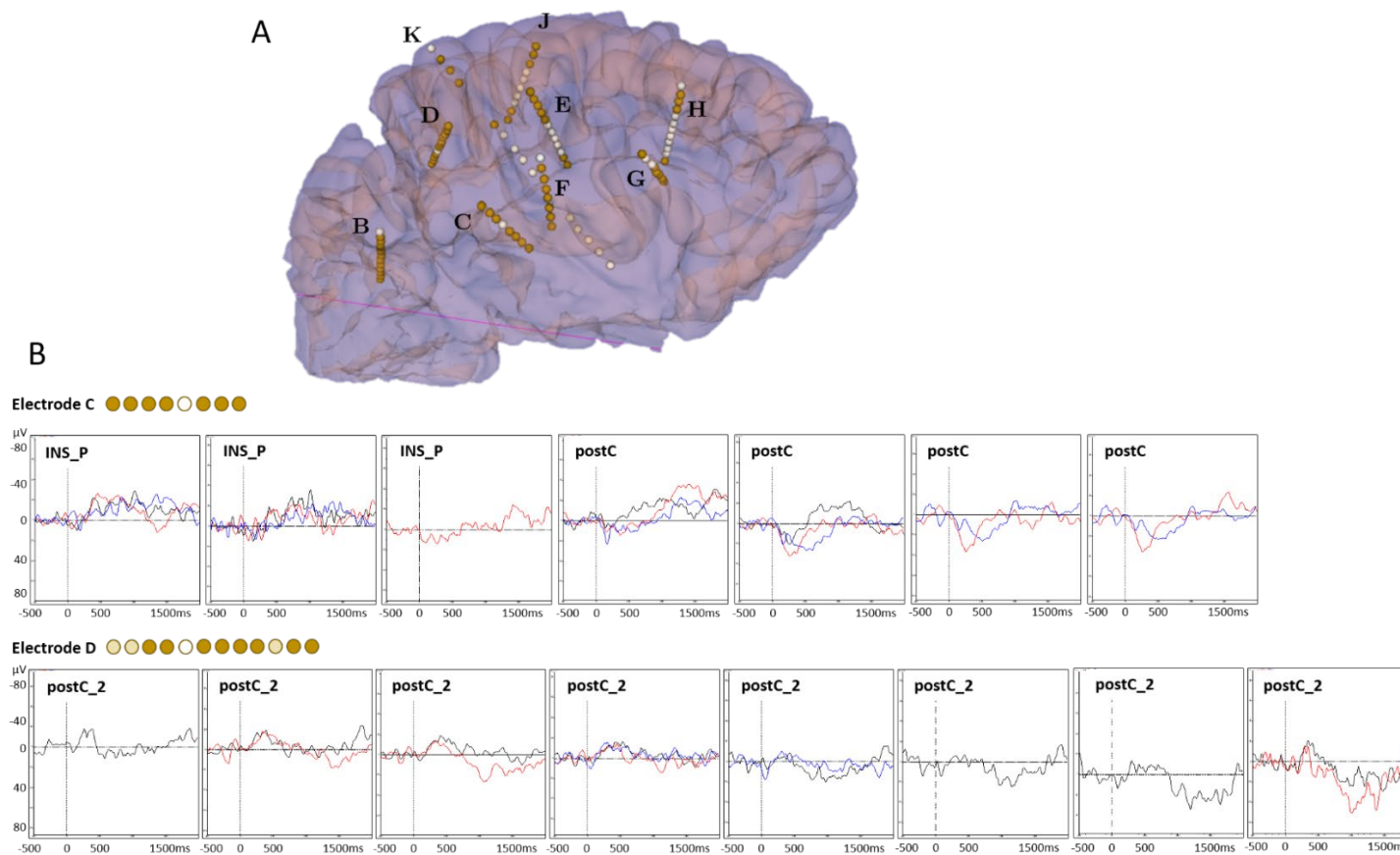
Figure 82. Case 3 (ID4)—SEEG patient with previous resection-robust iERPs. (1). **A.** depicts the patients' brain image and electrodes included in iERP analysis. **B.** illustrates robust iERPs during auditory word tasks (BL–blue, WR–red, VG–black) for the first two electrodes. Electrode C: inserted in secondary somatosensory cortex and aiming at posterior insula. Electrode D: inserted in primary somatosensory cortex. The circles depict the number of contacts inserted. The brown contacts recorded robust iERPs, the light brown contacts did not and the white contacts were not included in iERP analysis. Each iERP box includes a corresponding region label, which names the region the contact was located in. iERP box most left shows the most mesial contact and the iERP box most right shows the most lateral contact.

246
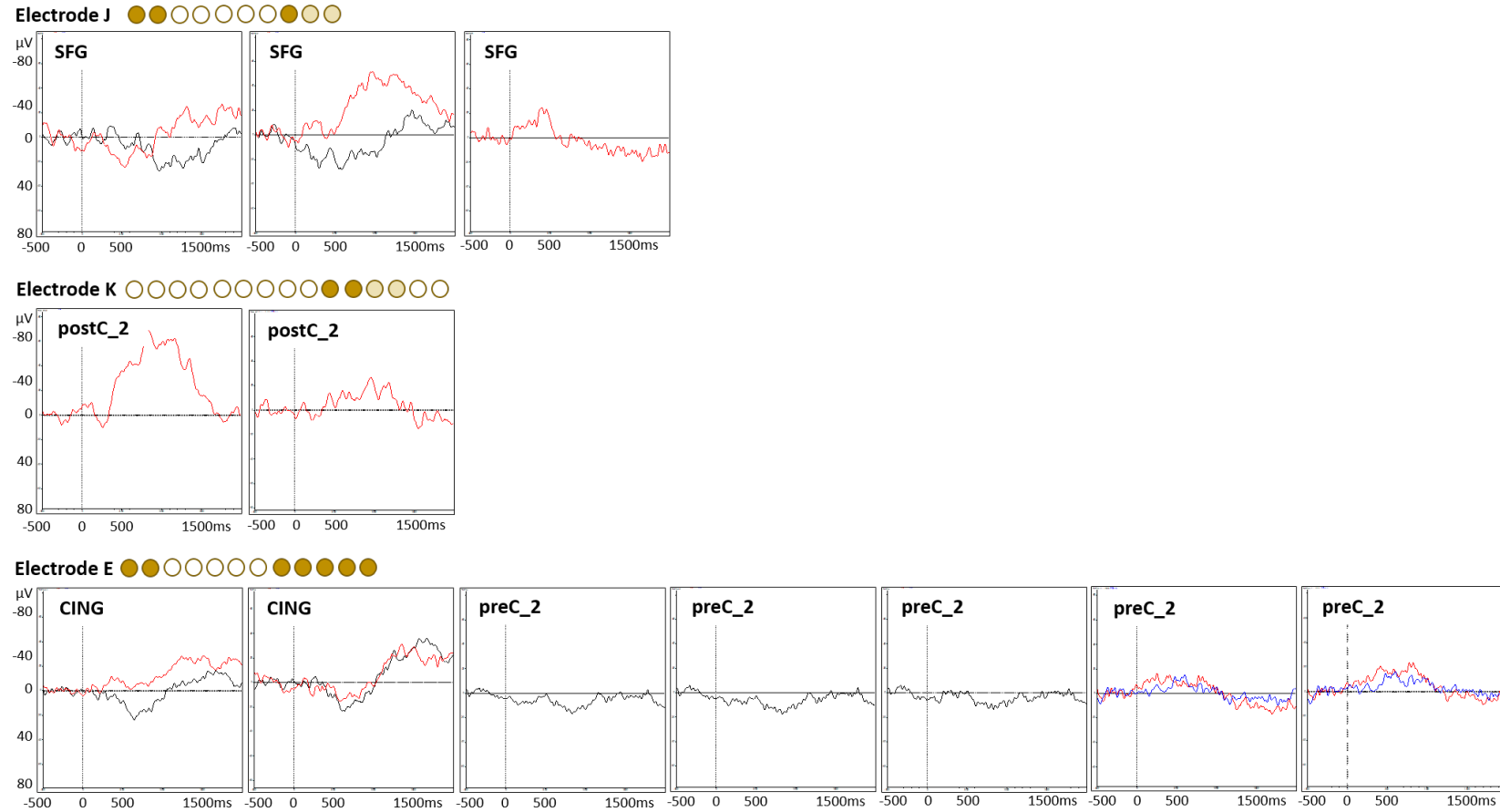
Figure 83. Case 3 (ID4)—SEEG patient with previous resection-robust iERPs (2). Robust iERPs during auditory word tasks (BL–blue, WR–red, VG–black) elicited in contacts of electrodes J (SMA), K (posterior oblique to insula), E (posterior middle frontal gyrus) are illustrated. The circles depict the number of contacts inserted. The brown contacts recorded robust iERPs, the light brown contacts did not and the white contacts were not included in iERP analysis. Each iERP box includes a corresponding region label, which names the region the contact was located in. iERP box most left shows the most mesial contact and the iERP box most right shows the most lateral contact.
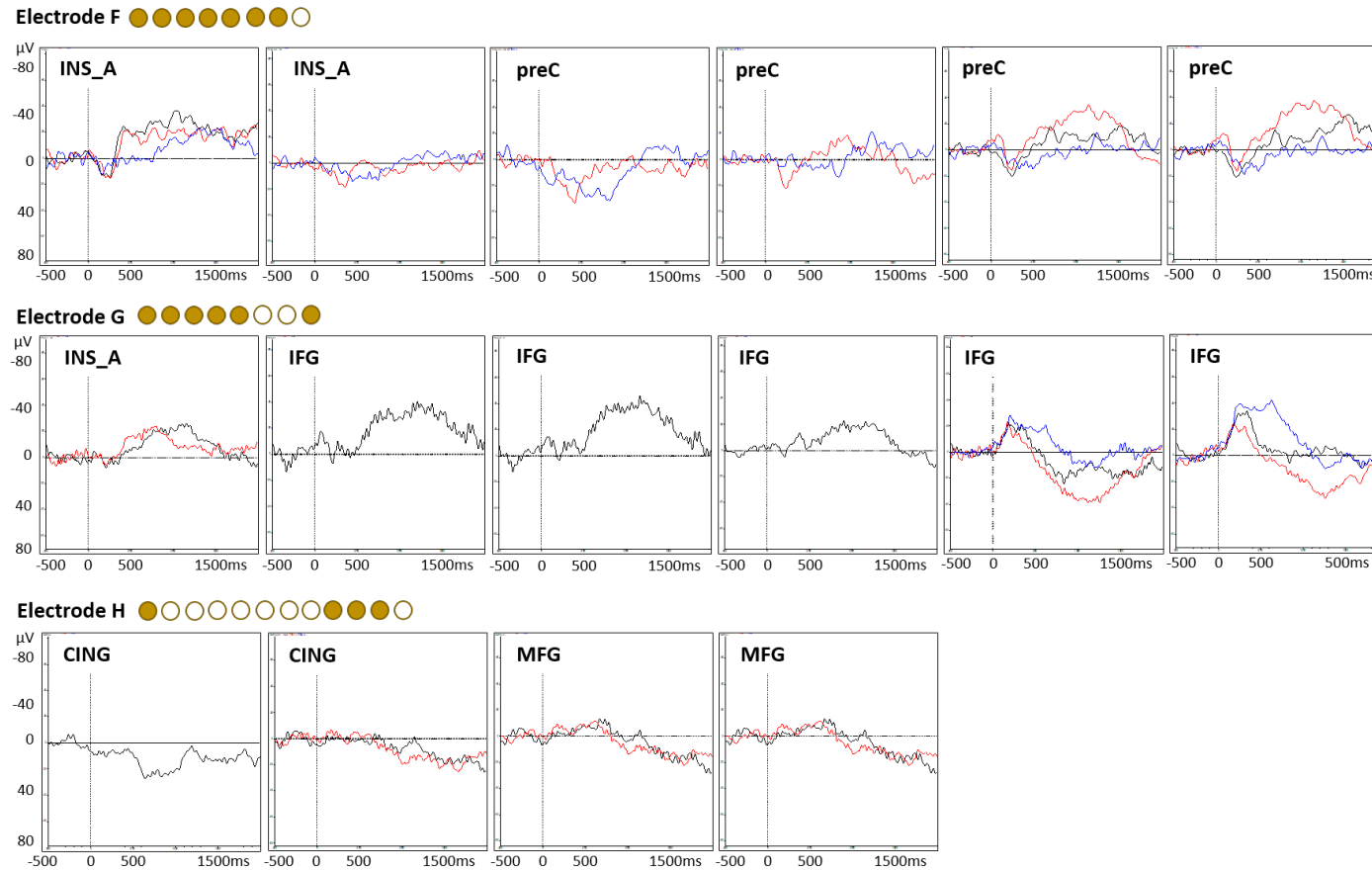
Figure 84. Case 3—SEEG patient with previous resection-robust iERPs (3). Robust iERPs during auditory word tasks (BL–blue, WR–red, VG–black) elicited in contacts of electrodes F (Frontal operculum to insula), G (inferior frontal gyrus), H (anterior middle frontal gyrus) are illustrated. The circles depict the number of contacts inserted. The brown contacts recorded robust iERPs and the white contacts were not included in iERP analysis. Each iERP box includes a corresponding region label, which names the region the contact was located in. iERP box most left shows the most mesial contact and the iERP box most right shows the most lateral contact.

248

In total, 92 contacts (48.7%) showed robust iERPs. Only a few contacts showed early components (4.3%). They were localised in the postcentral gyrus. The activity measured was mostly long latency components (54.4%) and middle latency components (41.3%). Electrode B, implanted into the inferior parietal lobule, did not show any iERPs. Some contacts involved in the seizure onset showed iERPs (contacts C1, C2 and D3) while did not show language-related activity (contacts D1, D2). Most of the contacts showing interictal activity (D3, D9, D11, D12, C1–8, and E1–2) showed iERPs while a few did not (D1–2, B, D10).

Case 4 (ID101)—Non-verbal patient with SEEG implantation

Patient ID101 was a seven year and four month old girl with pharmaco-resistant epilepsy secondary to left frontal cortical dysplasia. She underwent left frontal lobectomy, anterior temporal lobectomy and amygdalectomy at the age of five years and eight months. Histopathology showed FCD Type IIb. She showed developmental impairment and fluctuation in developmental skills depending on seizure frequency. She was right-handed, but initiated most tasks predominantly with her left hand. An intermittent hemi-neglect was noted. Movements were ataxic in quality with reduced fluency. She had an uneven profile of language skills, with a severe receptive and expressive language disorder. This patient was unable to cooperate behaviourally with electrical stimulation mapping, and the primary care team made a clinical referral for language iERP testing, in the absence of any other method of testing eloquence of the implanted left-sided brain regions.

The MRI showed no abnormality of the right hemisphere and a residual left inferior frontal lesion. The postoperative scalp EEG showed seizures arising posterior to the previous left frontal resection. However, changes were quite extensive and not clearly localised.

Patient ID101 was admitted to GOSH Koala ward for a bilateral SEEG implantation. In total 14 electrodes were implanted, twelve in the left hemisphere and two electrodes in the right hemisphere (Figure 85). During her invasive recording, a complex epileptic network with two electrographic onset types could be shown. First, a focal type, involving electrodes C, B, G and deep contacts of I. Second, a diffuse type, involving most contacts in the precentral region as well as the contralateral electrodes. Seizures were only simulated from orbitofrontal areas (B 7–6, 2–1, C2–1, 6–5). Motor was localised at E1–3 for right hand, and SMA response with stimulation of A1–8 and A'1–9. Suggested resection included all contacts of B and C and fronto-opercula contacts of electrode G and F electrode. The clinical team discussed concerns about language. It was believed that the chance of expressive language recurrence was extremely low considering her minimal language skills. Therefore, including Broca's area in the resection was unlikely to add deficit whereas seizure reduction was likely to improve quality of life.

In addition to the patient's severe language disorder, her main language was Russian. With the help of the patient's father, we translated and recorded all verb generation words and sentence stimuli into Russian and used these two tasks for language testing. The patient was not able to answer any task, however the stimuli were used as auditory language stimuli. The aim was to assess whether language-related activity could be recorded using the iERP method. The analysis showed a very active background recording and no robust iERPs could be measured. Figure 85 gives an overview of the SEEG implantation regime of both

hemispheres and illustrates electrodes used for recording language-related iERPs for this study.

Electrode	Label	Contacts	Location
Depth	C	12	Left Posterior Orbitofrontal
Depth	B	12	Left Anterior Orbitofrontal
Depth	F	12	Left MFG to Cingulate
Depth	G	08	Left Broca to Insula
Depth	J	12	Left Hippocampus
Depth	I	08	Left Temporal Operculum to Insula
Depth	H	08	Left Frontal Operculum
Depth	L	10	Left Parietal Operculum
Depth	A	12	Left Frontal Eye Field to SMA
Depth	K	12	Left S1
Depth	E	08	Left M1
Depth	D	08	Left pre SMA
Depth	A''	15	Right Fontal Eye Field to SMA
Depth	B''	12	Right Orbitofrontal

Figure 85. Case 4 (ID101)—Non-verbal SEEG patient. A. illustrates all labelled implanted electrodes of both hemisphere and summarises their placement locations. B. depicts the left and right hemispheres with circled electrodes used in this study.

To give an example of activity measured in this patient's contacts during the verb generation task, Figure 86 illustrates activity from electrode G, which was implanted in the inferior frontal gyrus and anterior insula.
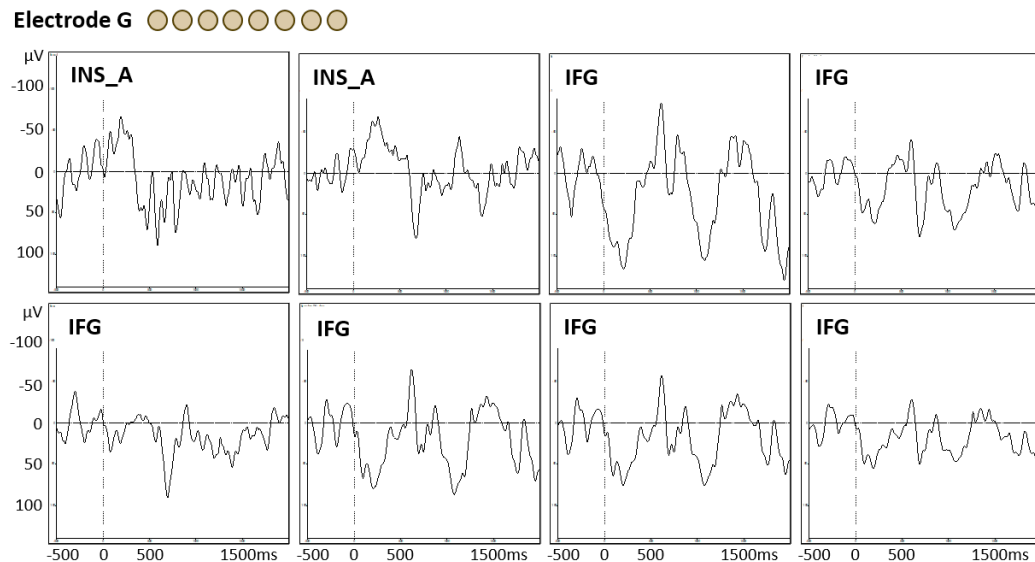
Figure 86. Case 4 (ID101)—Non-verbal SEEG patient—no robust iERPs measured. Stimulus-locked activity in contacts of electrode G (inferior frontal gyrus to insula). Examples depict active background activity and no robust iERPs were measured in these contacts (shown in brown). Each box includes a corresponding region label, which names the region the contact was located in (INS_A = anterior insula, IFG= inferior frontal gyrus). The box most left shows the most mesial contact and the iERP box most right shows the most lateral contact.

The activity measured was very active and no robust stimulus-locked activity was discernible. Whether this was due to the epileptic network being located in these regions or that there was no language-related brain areas there cannot be distinguished with certainty.

A left frontal basal and insula resection was done six months post surgery the patient did not experience any seizures. It was reported that possible absence events occurred since one month. No notes were made about her language skills post-surgery.

5.5 Discussion

Depending on the localisation of the seizure onset and its relation to eloquent cortex, certain pre-surgical assessments need to be undertaken prior to surgical resection to minimise risk of neurological and cognitive deficits post-surgery. As clinical routine showed that for paediatric patients, especially for very young patients and patients with cognitive impairment, an fMRI study for assessing language lateralisation is not an optimal procedure. However, the MRI scanner environment and lying still for extended testing sessions is challenging for many children. This lead to the idea to study language- and speech-related activation using ERPs recorded during invasive EEG monitoring. This method turned out to be easy to administer on the patient's bedside and the language tasks used were interesting for patients, and they were motivated to take part. Robust iERPs were elicited from perisylvian as well as additional brain regions and their morphology was not region specific, however, in some cases region- and task-specific. Analysing hemispheric differences was a first attempt and it was shown that in addition to the well known left-hemisphere language processing regions, the right hemisphere is involved in language processing quite actively.

In the following sections, I will discuss the functional anatomy of auditory and visual naming processing in context of this study's iERP findings from the point of view of information flow.

5.5.1   Region-specific differences of activation

Addressing Aim 1a: Characterise topography and morphology of stimulus-locked iERPs across the sample - Region-specific differences

Auditory word processing

As expected, highest activation during speech comprehension is focused around the perisylvian brain regions compared to additional brain regions. Nevertheless, in agreement with our results, earlier work showed widely distributed generators of auditory ERPs beyond the perisylvian language areas. ERPs were elicited in frontal, temporal, and parietal cortices and in addition in mesial temporal regions and the basal ganglia (Halgren et al. 1995, 1998; Bares and Rektor 2001). Like in the current study, several intracranial studies measured highest activation in response to auditory stimuli from the bilateral posterior STG (Boatman, Lesser, & Gordon, 1995; Howard et al., 2000; Liebenthal, Binder, Spitzer, Possing, & Medler, 2005). These regions are part of the wider 'Wernicke's area' and play an important role in higher-auditory processing of speech sounds. Activation measured in the posterior STG did not differ depending on the type of auditory stimuli used here (word repetition, verb generation, listening to non-meaningful word). These observations are in agreement with fMRI studies that demonstrated bilateral activation of the superior temporal gyrus using both speech and non-speech sounds. Furthermore, activation was not modulated by semantic content, neither by meaningful nor not meaningful stimuli (Binder et al., 1997; Price, 2012). Contacts labelled as posterior STG showed primary components bilaterally with a mean peak latency of 76ms. This cluster of contacts included all contacts localised in this anatomical region. I did not further distinguish between Heschl's gyrus, planum temporal, superior temporal sulcus, etc. In terms of temporal and spatial resolution, auditory evoked potentials can be measured with precision and components are described as early as 8ms post-stimulus. Auditory stimuli for these studies are clicks or tones (Steinschneider, Liegeois-Chauvel, & Brugge, 2011). The generator for such early components is the most posteromedial part of the Heschl's gyrus (Liégeois-Chauvel, Musolino,

Badier, Marquis, & Chauvel, 1994). In this current study, word stimuli with variable onset slopes were used and iERPs did not show primary complexes typical for the primary auditory cortex. Hence, the assumption is that these iERPs were elicited in secondary and higher auditory cortices (Liégeois-Chauvel et al., 1994, 2003). From these regions, the information flow continues in parallel to the posterior and anterior parts of the STG. In the posterior STG results showed early components with a mostly negative peak between 100–200ms with varying shapes. In some cases, an additional prior positive component or a following positive wave were observed. There was variability between the waveforms and peak latencies, which is likely due to different electrode placements and inter-subject variability. The iERPs in these areas partially persisted for several hundred milliseconds after onset of the stimulus (Howard et al., 2000). Regarding the anterior STG, this region had electrodes implanted in only two patients. Nevertheless, these areas showed early components with an early positive followed by negative component ≤200ms or a negative component only.

Interestingly, the posterior insula was activated with latencies comparable to primary auditory information processing. This region elicited similarly early waves as the posterior STG with a mean peak latency of 76ms for the primary component. Liégeois-Chauvel and colleagues (2003) presented similar results for the insular gyrus with a peak latency between 72–75ms, showing activation in the posterior insular cortex about 10ms prior to activation in the anterior insula. Anatomically, the Heschl's gyrus borders the insular cortex medially (Moerel, De Martino, & Formisano, 2014) and the auditory cortex, including primary auditory cortex, sends projections to the insula (Morán, Mufson, & Mesulam, 1987; Remedios, Logothetis, & Kayser, 2009). Compared to the posterior insula, the anterior insula showed later activation with early positive components between 100–200ms. According to lesion studies and PET and fMRI studies the anterior insula was shown to be involved in articulatory coding and motor programming of speech (Price, 2012).

Besides the posterior STG and the insula several other brain regions showed early components as early as 100–200ms peak latency. These early component results can be interpreted in view of the current proposed framework of language processing with a dorsal and a ventral pathway being responsible for auditory-motor mapping and sound-meaning mapping, respectively (Poeppel & Hickok, 2004). As a first instance, the bilateral STG is involved in speech perception. Then, the two processing streams diverge. Further early activity (100–200ms) is measured in the supramarginal and postcentral gyrus and decreasing early activity in the precentral and inferior frontal gyrus. These areas represent the dorsal stream, which in a later processing stage all show middle and long latency components, suggesting their involvement in higher-auditory processing. The supramarginal gyrus is engaged in phonological retrieval and temporal aspects of word recognition (Prpić, 2015). The postcentral gyrus, especially the ventral part is representing tongue and mouth somatosensory activation while precentral activation reflects distinct motor representation. Hope and colleagues (2014) interpreted activation of the left ventral premotor cortex during a word repetition task as evidence that this area plays a role in articulatory sequencing.

Along the second, parallel pathway, the ventral stream, auditory input is projected to the middle temporal gyrus, anterior parts of the superior and inferior temporal gyrus and fusiform gyrus (Trébuchon et al., 2013b). This route showed high early activation (100–200ms) in the anterior STG, although only implanted in two patients, and showed lower early activation in anterior and posterior MTG. Middle and late latency components were measured in all areas, comparable to the dorsal stream, apart from the anterior STG, where no long latency component was found. Trébuchon and colleagues (2013a) presented results of their intracranial EEG study analysing an ERP component, the N400, which is considered to be an index of lexical and semantic processing. Using this ERP component, they tried to distinguish the ventral and dorsal stream by presenting a lexical-semantic (words) and a phonological (pseudo-words) tasks to adult drug-resistant epilepsy patients. The dorsal stream predominantly

processed phonological information, especially in the left supra-marginal gyrus and the ventral stream, especially the anterior and middle temporal and fusiform gyri processed and lexico-semantic information. They furthermore suggested that the inferior frontal gyrus might be a common endpoint for both pathways, as the late N400 did not show significant difference between both tasks.

Auditory sentence processing

Interestingly the sentence comprehension task in this study led to fewer overall contacts being activated, although language-processing demands increased compared to auditory word tasks. In addition to auditory language comprehension processing steps and brain regions discussed before, sentential level processing involves similar brain regions, however with a different emphasis (Friederici, 2012). With increasing complexity of auditory input, going from phoneme to word and then to phrase processing a posterior to anterior-directed processing gradient from the posterior STG to middle STG and lastly to anterior STG is described (DeWitt & Rauschecker, 2013a). MEG studies confirmed that so called phrase structure building processes needed for sentence comprehension were localized in anterior STG/superior temporal sulcus (Friederici, Wang, Herrmann, Maess, & Oertel, 2000; Herrmann, Maess, Hahne, Schröger, & Friederici, 2011). Semantic processes during sentence comprehension are described to involve the middle temporal gyrus, the anterior temporal lobe and the anterior part of the inferior frontal gyrus. The current study did not confirm results regarding the anterior STG region. This area did not show any activity during the sentence task, while during the word tasks activity was observed. A contributing factor for the negative finding could be that the anterior STG was only sampled in two patients and these patients did not perform as well during the sentence task compared to the word tasks. During testing it was obvious with some of the children that when tasks difficulty increased, especially with the sentence task, their attention shifted and response time was slower. This was solely an observation as response time was not measured. However, varying attentional control from stimulus to stimulus within subjects is described in the

literature and influences the efficiency of processing, leading to longer reaction times, decreased response accuracy and to some extend variation in the measured signal when not focussing on the task accordingly (Schomaker & Talsma, 2009). Furthermore, another factor for measuring less iERPs during the sentence task might have been due to stimulus-locking and the different sentence length and time windows used for iERP analysis. When averaging the time-locked activity during sentence comprehension, only in the early window averaging (about 500–700ms) led to robust iERPs and the rest of the time window might have had contributions from endogenous processes that are not strictly stimulus-locked, hence invisible to the ERP waveform.

The rest of the perisylvian regions showed a similar activation in the ventral and dorsal pathways of language processing during sentence comprehension like during the word tasks.

5.5.2   Region-task-specific differences of activation

Addressing Aim 1b: Characterise topography and morphology of stimulus-locked iERPs across sample - Region-task-specific differences

Auditory tasks

The three tasks used to study auditory word processing all activated the perisylvian areas, with the baseline task - listening to time-reversed words, hence non-meaningful, generally eliciting the least activity. The difference between the passive (baseline) versus the active tasks can also be observed in the morphology of waves elicited. The baseline task apart from the primary and early components generally showed different features regarding peak amplitude, peak latency or shape differences. Those variations were not region specific, as discussed before: iERP components (early, middle long) were distributed over all regions without a specific maximal focus. Morphology of iERPs measured during word repetition and verb generation tasks did not differ in that way. Word repetition

258

seems to be a simple task, as it involves an auditory input that solely needs to be translated into an auditory output that matches the heard word. However, as research showed, a complex cascade of responses is involved with multiple brain regions being recruited during this task (Cheng, Schafer, & Riddel, 2014; R. J. Cooper, Atkinson, Clark, & Michie, 2013; Hope et al., 2014). My findings are in accordance with previous results showing that perisylvian regions and in addition superior and medial frontal regions, inferior parietal and inferior temporal areas including fusiform gyrus were recruited during word repetition. Furthermore, the insula and subcortical areas were involved. The cingulate gyrus was more activated during the word repetition task compared to the verb generation task. This finding is contrary to previous work showing that cingulate gyrus activity increases with task demand (Fu et al., 2002). The cingulate region is involved in modulating control functions, being associated with initiation, inhibition, attention, and selection during various tasks. Whitney and colleagues (2009) studied cortical activation using different verbal fluency and association tasks. They concluded that the cingulate gyrus plays a role as a modulator in its interaction with executive brain regions in the prefrontal cortex and adjusts to the different tasks rather than being involved in word selection processes.

A second subcortical region being highly active was the hippocampus with its involvement during the verb generation task more so than during the repetition task. The hippocampus was shown to play a role in associative and semantic binding between a stimulus and the following verbal response during speech production (Whitney, C., Weis, S., Krings, T., Huber, W., Grossman, M., & Kircher, 2009). The task demand and hence the increased retrieved semantic information during verb generation might explain this behaviour between the two tasks.

Visual tasks

Picture naming is probably the most frequently used task during functional language mapping. This might be due to its easy administration and implementation in clinical practice. This task appears simple, however, it

involves a series of processing stages starting with visual processing, including semantic access, word retrieval, articulatory associations and further motor planning and response initiation until a word is spoken out loud that best matches the picture seen (Price, 2012). However, previous work showed that sparing visual naming regions did not prevent post-surgical language deficits completely (Cervenka, Boatman-Reich, Ward, Franaszczuk, & Crone, 2011; Kojima et al., 2012; Towle et al., 2008). Recently, Binder and colleagues (2020) provided a statistical map of left temporal lobe regions essential for naming visual objects. They argued that the fusiform gyrus about 4–6 cm posterior to the temporal tip was mainly involved and that this area could be avoided during temporal lobe resection.

The panda games picture and colour naming used in this study were developed for different paediatric age groups offering stimulating stimuli material (Croft, 2014). The patients managed to maintain focus during both tasks. Presented stimuli were rarely too difficult to name correctly and hence motivation was high during playing these games. Response accuracy was high for both tasks (PN: 94%, CNw: 98%). In the current study both tasks yielded similar brain activation, measuring almost the same mean percentage of contacts with iERPs overall. The tasks were originally designed for an fMRI paradigm with the goal to subtract activity measured during the colour naming task from the picture naming task to study brain regions involved in semantic access and association during picture naming (Croft, 2014). Using the iERP setup showed that all perisylvian regions and in addition frontal regions and medial and inferior temporal regions were recruited during visual naming. This studies results are in agreement with previous findings from electrical stimulation mapping, nTMS and fMRI studies (Haglund, Berger, Shamseldin, Lettich, & Ojemann, 1994; Krieg et al., 2016; G a Ojemann, 1979; Price, 2012). My findings further suggest regional differences between the two tasks, where colour naming led to significantly higher activation in the anterior and posterior insula compared to picture naming. As the insula is involved in motor control of speech production (Oh, Duerden, & Pang, 2014) the

increased recruitment during colour naming might be explained by its quick involvement during colour naming where semantics do not have to be accessed in the same high level as during picture naming. Furthermore, picture naming elicited significantly higher iERPs in the posterior medial temporal gyrus, medial frontal gyrus, inferior frontal gyrus and supramarginal gyrus. These regions were shown to play key roles during picture naming for accessing semantics, retrieving words and accessing articulatory associations in previous work (Price, 2012).

Both auditory and visual naming tasks showed robust activity in the anterior STG. This result is not consistent with published data by Cervenka and colleages (2013). Their frequency results in the gamma band showed that activation was higher in the dominant anterior temporal and anterior frontal neocortex more often during auditory than visual naming. Furthermore, electrical stimulation mapping results agreed with their results, showing more patients with post-surgical language deficit when basal or lateral temporal sites, which showed language involvement, were resected (M. J. Hamberger, Seidel, Mckhann, Perrine, & Goodman, 2005; Krauss et al., 1996).

5.5.3   Response-locked activation

Addressing Aim 2: Characterise speech-response-locked iERP topography and morphology across sample

Previous language studies suggest that processes involved in speech production (e.g. lexical selection, articulatory preparation) following auditory or visual naming tasks happen in a 600ms time window before the onset of speech (Indefrey, 2011; Anaïs Llorens et al., 2011). Hence, for this part of the study a time window of 1000ms before and after speech onset was chosen. Response activity included in this analysis was the so-called readiness potential (or Bereitschaftspotential), a subcomponent of movement-related cortical

261

potentials. The highest activity was measured in the precentral gyrus followed by the supramarginal gyrus and the posterior STG, which is in agreement with previous literature (Edwards et al., 2010; Towle et al., 2008). The network comprising of the posterior STG and inferior rolandic gyri was already discussed being involved in speech perception and overt speech production. The activity measured in the posterior STG was due to listening to speech of the participant articulating the response (Fukuda et al., 2010). Hope and colleagues (2014) found the left ventral premotor cortex and left anterior putamen to be activated by phonological inputs during speech production. The medial part of SMG, bordering the posterior temporal region is called the Sylvian parietal-temporal area (area Spt). This area is thought to be the linking region of auditory speech and motor programming (Hickok, 2009). Lesions there caused speech repetition deficits, similar to conduction aphasia in adults (Northam et al., 2018). Furthermore, fMRI data suggests SMG recruitment with phonological processes (Démonet, Thierry, & Cardebat, 2005; Vigneau et al., 2006).

5.5.4   Left versus right activation

Addressing Aim 3: *Characterise activation differences between hemispheres*

The section analysing and discussing interhemispheric differences is rather an observational attempt and description of hemispheric language activation as the language lateralization information was only available for five patients. The rest of the patients did not show semiology relevant for suspecting the involvement of language areas in the seizure onset or propagation area; hence, there was no clinical need for an fMRI to determine language lateralization. Therefore, for most of the children I did not know the language dominant hemisphere. I therefore assumed that those patients had a typical lateralization pattern, with language being left-lateralised.

Most language literature focuses on the left hemisphere, as it has consistently been shown to be dominant for language. Nevertheless, Ries and colleagues

(2016) reported that fMRI results yielded that the right hemisphere is activated during word retrieval tasks, however often to a lesser degree and less robustly than the left hemisphere. My hemisphere analysis results are not in line with previous results as left and right brain regions showed similar iERP occurrence and wave morphology. Some differences, like the reversed polarity of the waves in the inferior frontal gyrus were not discussed in previous literature. It is not clear yet, whether iERPs show distinct polarity features like during scalp EEG. The polarity of a wave is dependent on the location of the contact towards the source. The closer a contact is to the generator the higher the amplitude and as using SEEG electrodes, the location varies between patients (Wendling, Badier, Chauvel, & Coatrieux, 1997). There are no similar studies yet. Furthermore, the anterior middle temporal gyrus showed a negative early high amplitude component followed by a long lasting positive component in the right hemisphere compared to only a long positive component in the left hemisphere. There was hardly any task dependent iERP variability between both hemispheres. Deciphering left and right hemisphere involvement needs further research, a larger sample of right hemisphere implanted patients and more comprehensive information about individual language lateralisation as well as the inclusion of patients with typical and atypical language dominance.

5.6 Limitations and consideration

The results of the current study should be interpreted in light of some limitations and practical issues discussed in the following section.

First, for this study Neuroscan SynAmps^2 was used with a setup of 64 channels to record from. The clinical EEG system had the capacity to record from up to 256 channels. Hence, for this study only a sub selection of the clinically chosen contacts could be used. When I needed to choose, I decided to include electrodes closest to the supposed language areas. Therefore, perisylvian areas where sampled more frequently. Furthermore, some brain regions were implanted quite rarely and therefore there was an imbalance of numbers of contacts placed for

the different areas. Considering the individual numbers of contacts implanted the weighted average for statistical analysis. Despite the issue with gathering information from only 64 channels, there was also some practical issues. For the study recordings, each contact had to be disconnected from the clinical system and plugged into the Neuroscan headbox. This was only possible once the clinical investigations were over. Hence, due to this limitation, I was dependent on having enough time left before explantation of electrodes and furthermore, this procedure was staff- and time-intensive. Exploring the options of the clinical EEG system for future projects would be an important step.

Second, most studies investigating language functions have access to language lateralisation information in order to know whether the hemisphere investigated is the dominant one for language or not (Arya et al., 2017; Flinker et al., 2015; Fonseca et al., 2009). For this study, due to clinical reasons only five patients underwent fMRI for language lateralisation. Therefore, for grand average results comparing right versus left hemisphere activation this must be taken into account. The number of patients with right implantations was lower and hence, for grand average analysis only a few right hemisphere patients could be included.

Third, the general recommendation for studying language processing in patients with epilepsy is to record spatially distant from pathological tissue and temporally distant from seizures to avoid noise (Llorens et al., 2011). Studying delineation of eloquent and pathological tissue, however, implies a close proximity of the targeted functional brain areas and the epileptogenic brain areas. Therefore, for this study the spatial distance recommendation was not adhered to and hence, it cannot be ruled out that eloquent areas sampled are affected by noise and bias occurrence rates of language-related activity. Halgren and group (1998) noted, that epileptogenic tissue can lead to both attenuated and hyper-responsive cognitive potentials; however, that normal cognitive responses can be measured.

Fourth, all patients admitted to Koala ward during the period of this study were invited to take part. This was a very heterogeneous group as their age ranged from five to seventeen years of age. There are age-dependent variations in cortical and subcortical recruitment during language processing (Weiss-Croft & Baldeweg, 2015). Age-dependent differences were not investigated here.

To conclude, this study aimed to map cortical dynamics during speech perception and speech production and to generate language maps using iERPs measured in children and adolescents with invasive monitoring (SEEG and subdural grids). Like previous studies, I could show that generators of language iERPs during auditory and visual stimuli showed a widespread distribution, including cortical and subcortical regions (Bares & Rektor, 2001; Halgren et al., 1995, 1998). Most activation was observed in the perisylvian regions, with the posterior STG and posterior insula showing the highest occurrence of iERPs and earliest activation. Information processing followed the dorsal and ventral streams. Comparing passive and active tasks showed the least activity during the passive baseline task and morphological characteristics were different compared to word repetition and verb generation. During sentence processing compared to word processing less overall activation was observed and in addition the anterior STG was not involved. This finding was not in line with previous study results. The two visual tasks used yielded similar brain activation. During speech production, the highest activity was observed in the precentral and supramarginal gyrus and the posterior STG.

6 Concordance of language-related iERPs with spectral power changes

6.1 Introduction

Around the period of 1980–1990, the implementation of ECoG investigations for seizure onset localisation increased across centres worldwide and an interest in using invasive EEG to study cognitive processes emerged. At that time, two paths were pursued as cognitive processes could be studied using different types of measures of neuro-electrical activity (N. E. Crone, Korzeniewska, & Franaszczuk, 2011; Pfurtscheller, 2001). On the one hand, time- and phase-locked activity (evoked) ERPs were investigated, a well-established method, which was used in cognitive neuroscience since around 1930 (R. Cooper, Winter, Crow, & Walter, 1965; H. Davis, Davis, Loomis, Hervey, & Hobart, 1939; P. A. Davis, 1939). On the other hand, spectral changes from the ongoing EEG that were time- but not phase-locked (induced), e.g. event-related synchronisation and desynchronization (ERS/D) were explored.

6.1.1 Rational for exploring the use of ERS/D

Pfurtscheller and colleagues introduced the terms ERS and ERD in the 1970 (1977; 1977) and at that time lower frequency ranges, especially in the alpha and beta bands (8–13Hz and 15–25Hz, respectively) were the main spectral changes studied (e.g. in response to movement) (Neuper & Pfurtscheller, 2001; Pfurtscheller, 1992; Pfurtscheller & Aranibar, 1977). With the emergence of invasive EEG monitoring in patients with focal epilepsy, the focus shifted to studying higher frequencies, mainly using subdural grid electrodes. Crone and colleagues (2001) presented subdural electrode results of low (35±50Hz) and high (75±100Hz) gamma band changes in response to auditory speech and non-speech stimuli (phonemes and tones, respectively). They showed that gamma ERS was more focused than the broader spatial distribution of alpha ERD and

that its onset overlapped with the N100, but peaked later and outlasted it. Compared to tones, phonemes produced greater gamma ERS. They suggested that gamma changes might be an index of cortical responses and that more complex cognitive tasks, like speech perception, required more cortical power and hence increased gamma ERS. Furthermore, several studies reported that speech- and language areas delineated by electrical stimulation mapping were concordant with language-related high gamma ERS and recommended its use in pre-surgical evaluation to gather additional information about eloquent areas (Arya et al., 2015; Kojima et al., 2012; Sinai et al., 2005; Y. Wang et al., 2016).

In addition, resection of contacts eliciting language-related high gamma changes and its predictive value for post-operative language deficits were studied. Kojima and colleagues (2013, 2012) showed in paediatric and adult patients that several brain regions were involved during auditory naming tasks. The left superior-temporal, inferior-frontal, dorsolateral-premotor, and inferior-rolandic sites elicited high gamma augmentation. Their results revealed that post-operative language deficit requiring speech therapy could be predicted by the number of resected sites with gamma-augmentation in these brain areas.

Besides high gamma augmentation, low gamma responses were studied concerning their role in language-related processes. Crone and group (2001) compared high and low gamma activity and their results yielded a more localised area in the posterior STG eliciting high gamma responses critical for auditory discrimination compared to low gamma activity. Furthermore, co-occurrence of high-gamma augmentation with beta-attenuation (15–30Hz) was reported in several studies (N. Crone, 1998; J.-P. Lachaux, Axmacher, Mormann, Halgren, & Crone, 2012; Miller, Shenoy, Miller, Rao, & Ojemann, 2007). Therefore, the present study incorporated these three frequency bands as a measure of cortical activation.

6.1.2 Rational for comparing these two types of changes in electrical activity

In the previous Chapter 5 language-related iERPs and their potential use in localising speech and language areas were discussed. When averaging EEG data for iERP analysis much of the dynamic information contained is discarded in the process to achieve a time- and phase-locked ERP responses. ERS/D result from dynamical changes of neural networks, which are also contained within individual trials, however, the variable phase component is preserved (Makeig, 1993). Llorens and colleagues (2011) argued that spectral changes are ideally suited to study language and linguistic processes, as language-related cortical activity shows sustained responses reflecting network interactions.

This group further reviewed articles reporting the use of intracranial EEG investigations to study gamma activity elicited by overt or covert language production tasks in adult participants. The majority of articles described the use of ECoG compared to only a few articles reporting results from multi-contact depth electrode investigations. They stated that the number of individuals tested in each article was relatively low (ranging from case studies to <4 to 10 patients) and that a great variety of tasks and theoretical approaches were used. Data from ECoG studies was summarised and they illustrated speech-related activity across patients and studies either triggered auditorily or visually (Figure 87) (Anaïs Llorens et al., 2011).
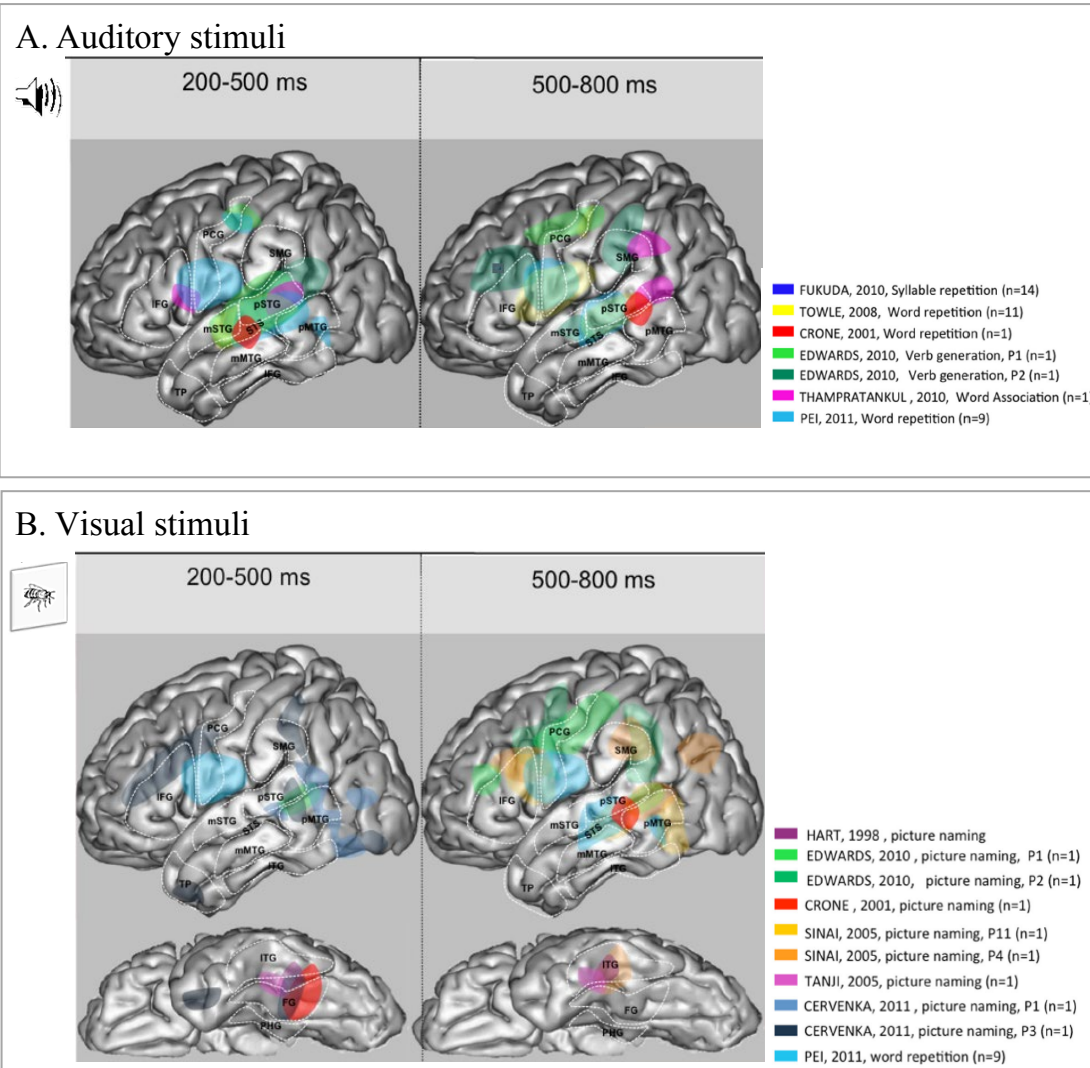
Figure 87. Speech-related activities across patients and studies (Llorens et al., 2011). A. illustrates auditorily triggered responses and **B.** summarises visually triggered responses. Brain activity results gathered from previous work is projected on a standardized left hemisphere. Results of each research group are shown in a different colour. Activity is shown for two different time period—200–500ms and 500–800ms after stimulus onset. Abbreviations: IFG = inferior frontal gyrus; STS = superior temporal sulcus; STG = superior temporal gyrus; SMG = supramarginal gyrus; pSTG = posterior part of the superior temporal gyrus; mSTG = middle part of the superior temporal gyrus; pMTG = posterior part of the middle temporal gyrus; mMTG = middle part of the middle temporal gyrus; PCG = pre central gyrus; TP = temporal pole; FG = fusiform gyrus; ITG = inferior temporal gyrus.

In light of the literature's focus on language-related frequency band modulation in epilepsy patients the question of the difference of the localising value between the two types of changes in electrical activity arose.

The functional relationship between evoked and induced responses in brain areas essential for cognitive processing, e.g. speech perception, remain poorly understood (Haenschel, Baldeweg, Croft, Whittington, & Gruzelier, 2000; Sinai et al., 2009). Tallon-Baudry and colleagues (1999) studied gamma activity and its role in object representation and distinguished between evoked and induced gamma activity. It has been proposed that early evoked potentials play a role in encoding modality specific stimulus properties, while induced gamma activity is involved in network mechanisms, binding together brain areas that are essential for representing the whole object, by linking all its features together (feature binding). Furthermore, Sinai and colleagues (2009) compared spatial distribution and magnitude of intracranial auditory responses elicited during electrical stimulation mapping with auditory evoked and induced responses. They found that auditory evoked responses showed a broader spatial distribution compared to spectral changes. Results showed that areas eliciting the largest evoked auditory responses and the largest spectral power increases were associated with sites that showed disruption of speech perception during electrical stimulation mapping.

Pre-surgical invasive EEG monitoring provides a unique window into brain–behaviour interactions to study the functional organisation of speech and language with greater temporal resolution than fMRI and greater spatial resolution than scalp-recorded EEG.

6.1.3   Study aims

I designed language paradigms and tested a representative sample of paediatric patients with medication-resistant epilepsy admitted to invasive EEG monitoring with the aim to determine cortical dynamics during speech perception and speech production. I generated a language map using iERP measures as presented in the previous Chapter 5, but also using spectral changes across widespread brain regions and frequencies. Furthermore, I am testing the relation between these cortical dynamics and positive electrical stimulation responses in a subset of patients. The aims of this chapter are to:

1. Characterise the topography of beta, low- and high-gamma frequency band activity across the sample to establish:
    a. Region-specific task differences
    b. Region-task-specific differences
2. Characterise the differences and concordance between evoked and induced activity.
3. Characterise speech-response ERS/D and demonstrate differences to iERP occurrence.
4. Characterise the relation between electrical stimulation responses and ERS/D and iERPs in a subgroup of patients undergoing electrical stimulation mapping for language.

6.2   Methods

6.2.1   Participants

For this chapter, I am using data of the same patients described in Chapter 5, Section 5.2.1. I included paediatric patients with medication resistant focal epilepsy who were admitted to GOSH for a pre-surgical invasive EEG monitoring. They were aged between 5–17 years of age, which is representative

of patients requiring epilepsy surgery as part of the Epilepsy Surgery Programme at GOSH. The ethical review board gave permission for this study.

6.2.2   Clinical information

This is described in Section 5.2.2.

6.2.3   iEEG data acquisition and acquisition of 3D brain images

This is described in Section 5.2.3.

6.2.4   Functional electrical stimulation

Extra-operative bipolar functional electrical stimulation was performed in a few patients as clinically required, using an OSIRIS NeuroStimulator (InoMed). The following settings were used: pulse frequency of 1Hz, pulse duration increasing from $500\mu s > 750\mu s > 1000\mu s > 1500\mu s$, stimulus duration of 5–7s and stimulus intensity of 1.5–3mA. Stimulus intensity was increased first, if no response was elicited duration was increased up to $2000\mu s$ and $3000\mu s$. The selection of electrode pairs was discussed in the multidisciplinary team and stimulation was performed by the treating neurophysiologist together with the paediatric neurologist. Word repetition, verb generation, picture naming and open conversation were used for clinical mapping, with a trial run carried out before electrical stimulation to help select appropriate stimuli for individual patients.

6.2.5   Language testing

As described in Chapter 4, Section 4.6 participants were presented with different language games. These were always carried out after all clinical assessments were completed.

6.2.6   iEEG quantitative analysis

These are detailed in Chapter 4, Section 4.9. After pre-processing EEG data were subjected to visual inspection for artefacts and additional ERS/D analysis in the three frequency bands: 1) beta ERD with a central frequency of 20Hz and a bandwidth of 10Hz; 2) low gamma ERS with a central frequency of 50Hz and a bandwidth of 20Hz; 3) and high gamma ERS with a central frequency of 90Hz and a bandwidth of 20Hz. ERS/D responses were then classified in robust and not robust activity.

6.2.7   Statistical analysis

The percentage of contacts with detectable ERS/D was calculated for each brain region per patient and a weighted average was taken across patients. A weighted average was chosen, because each patient had an individual implantation regime and hence patients had different numbers of contacts implanted into respective brain regions. The average was weighted by the number of contacts implanted into each brain region, as for the iERP analysis above.

Wilcoxon rank sum tests were used to compare differences in the occurrence rate of contacts with ERS/D between regions and tasks. Furthermore, the Wilcoxon rank sum test was used to compare differences between the occurrence rate of contacts showing iERPs and ERS/D.

For the analysis of the relationship between contacts testing positive when stimulated (ES+) and contacts showing spectral changes the following was accepted: contacts where electrical stimulation interfered with language or oral motor functions were regarded as ES+, whereas stimulated contacts which did not show any such responses were regarded as ES–, irrespective of their lobar location. Although electrical stimulation was performed at electrode pairs, each electrode was counted separately to allow comparison with spectral changes measured which was based on a common average montage. Contacts showing spectral changes were regarded as beta ERD+, low gamma ERS+ and high

gamma ERS + and contacts showing iERPs were regarded as iERP+. Chi-Square statistic was used for relationship testing.

6.3 Results

6.3.1 Demographics and further patient characteristics

The patient cohort was the same as described in the previous study. In short, the final sample included 20 children and adolescents with drug-resistant focal epilepsy aged 5–17 years. For the group analysis six patients were excluded, due to previous neurosurgical resection (ID3, 4), a diagnosis of tuberous sclerosis and hence abnormally developed tissue (ID10, 15), subdural grid implantation (ID17) and severe expressive and receptive language deficits (ID101). A detailed summary and a table with patient characteristics can be found in Chapter 5, Section 5.4.1 in Table 21.

Furthermore, information regarding task completion, implantation regimes and brain regions sampled is discussed in detail in 5.4.2–5.4.4.

6.3.2 Occurrence of induced and evoked responses

In the previous Chapter 5, I showed and discussed iERP topography and morphology results. In this section, I am comparing topography of iERPs to frequency band results, presenting results of concordance between contacts showing evoked responses with contacts showing induced responses. All three analysed frequency bands—beta ERD, low gamma ERS and high gamma ERS are shown together.

First, a general comparison of contacts showing iERPs versus contacts showing activity in the three frequency bands is shown, differentiating between auditory word tasks (BL, WR, and VG) and visual tasks (PN and CNw, see Figure 88).

274
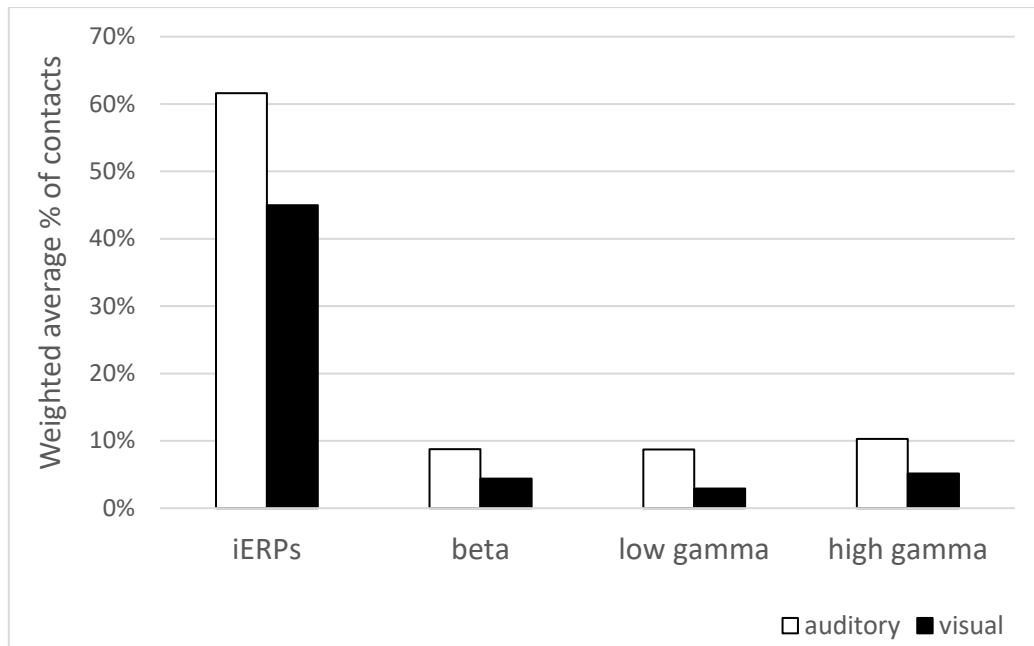
Figure 88. Comparing contacts with iERPS and frequency band activity. The mean percentage of contacts with iERPs versus contacts showing frequency band activity in the beta, low gamma and high gamma bands are illustrated. The graph differentiates between auditory and visual tasks.

For both auditory and visual task groups, significantly more contacts with robust iERPs were measured compared to contacts showing spectral power changes for all three frequency bands analysed ($p<0.01$, Wilcoxon rank sum test).

6.3.3   Region-specific spectral changes and comparison with iERPs

Auditory and visual tasks

Several distinct anatomical regions were identified showing beta ERD, low gamma ERS and/or high gamma ERS in the temporal, parietal and frontal lobes in both hemispheres in response to passive and active auditory and picture naming tasks. The following Figure 89 and Figure 90 illustrate the mean percentage of contacts showing spectral changes in the three chosen frequency bands first for the auditory word tasks and next for the visual tasks.
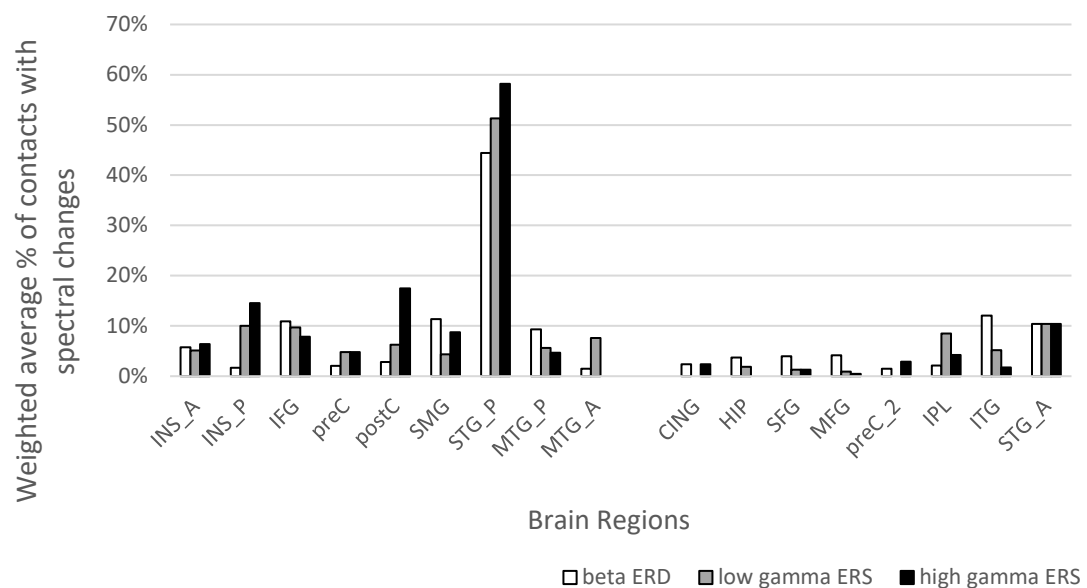
Figure 89. Region-specific spectral changes to auditory stimuli. The figure illustrates the mean percentage of contacts with beta ERD, low gamma ERS and high gamma ERS during auditory word tasks (BL, WR and VG) across the total sample. On the left side the perisylvian brain regions are summarised and on the right side the additional brain regions are shown. Areas with less than two patients with implantations are not shown here (amygdala, fusiform gyrus, orbital frontal gyrus, dorsal postcentral gyrus and superior parietal lobule).
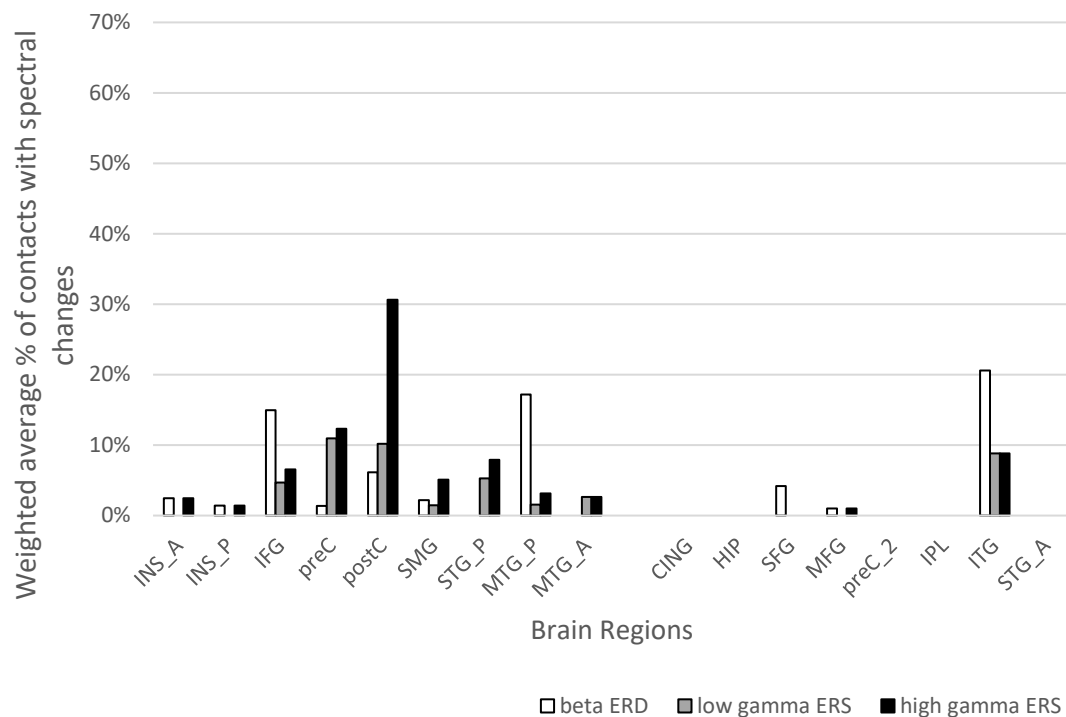
Figure 90. Region-specific spectral changes to visual stimuli. The figure illustrates the mean percentage of contacts with beta ERD, low gamma ERS and high gamma ERS during visual tasks (PN and CNw). On the left side of the graph perisylvian brain regions are summarised and on the right side additional brain regions are shown. Areas with less than two patients with implantations are not shown here (amygdala, fusiform gyrus, orbital frontal gyrus, dorsal postcentral gyrus and superior parietal lobule).

During auditory stimulus presentation, the most frequent occurrence in all three frequency bands was seen in the posterior STG, compared to the visual tasks where the postcentral gyrus and the inferior temporal gyrus showed highest activation. The average percentage of contacts with spectral changes between the three frequency bands was similar for auditory and visual analysis (auditory—beta: 6.6%±0.9%, low gamma: 6.1%±1.0%, high gamma: 6.7%±1.2%, p>0.1; visual: beta: 3.6%±0.6%, low gamma: 2.3%±0.3%, high gamma: 4.1%±0.7%, p>0.1, Wilcoxon rank sum test).

Next, I compared region-specific frequency band results with iERP results for auditory and visual tasks. In all regions, there was a significantly higher mean percentage of contacts showing iERPs compared to contacts showing either beta ERD, low gamma ERS or high gamma ERS for auditory tasks (p<0.01; Wilcoxon rank sum test). For visual tasks, most regions showed significantly

277

higher mean percentage of contacts with iERPs compared to contacts with spectral changes in all three frequency bands (see Appendix Table 49). However, no significant difference was found between contacts showing evoked and induced responses in the postcentral gyrus for all three frequency bands. Furthermore, no difference was observed in the posterior STG (iERP=high gamma ERS) and in the posterior middle temporal gyrus (iERP=beta ERD and iERP=high gamma ERS). Figure 91 and Figure 92 illustrate the comparison of iERPs and spectral changes measured in brain regions first during auditory word tasks and second during visual tasks.

A

iERPs

ERS/ERD
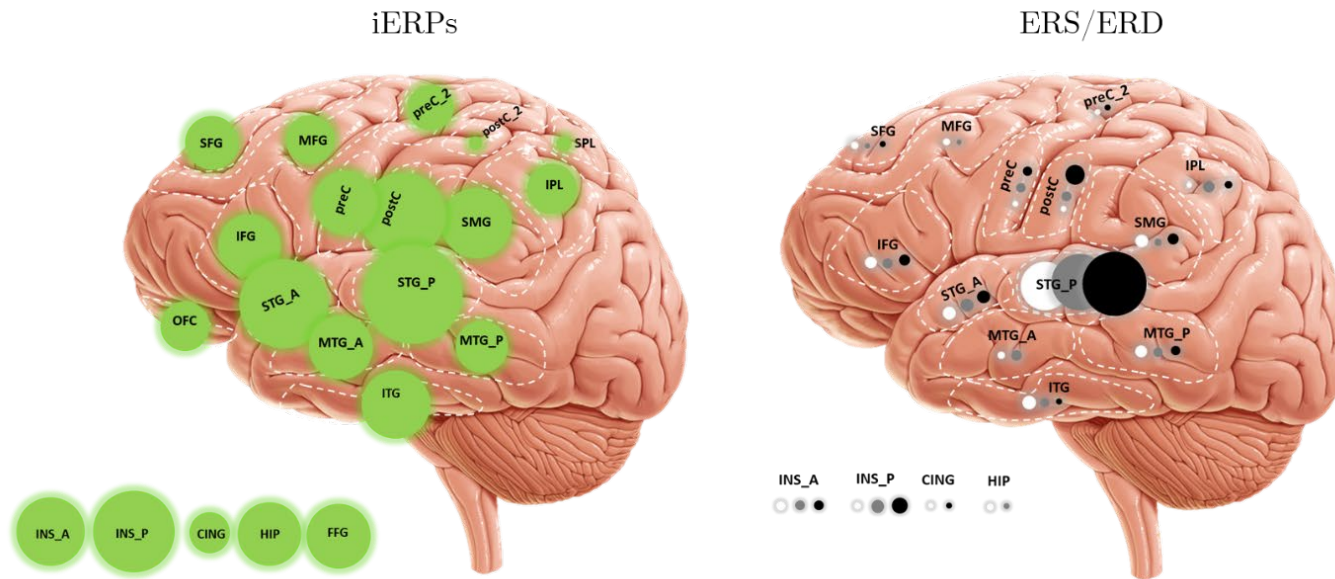
B

	iERP	Beta ERD	Low Gamma ERS	High Gamma ERS
INS_A	62.9%	5.8%	5.1%	6.4%
INS_P	75.8%	1.7%	10.1%	14.5%
IFG	58.4%	10.9%	9.7%	7.9%
preC	59.0%	2.1%	4.8%	4.8%
postC	79.4%	2.8%	6.3%	17.5%
SMG	64.7%	11.4%	4.4%	8.8%
STG_P	98.5%	44.4%	51.3%	58.2%
MTG_P	49.4%	27.8%	5.6%	4.7%
MTG_A	58.2%	1.5%	7.6%	0.0%
CING	37.7%	2.4%	0.0%	2.4%
HIP	57.2%	3.7%	1.9%	0.0%
SFG	49.8%	4.05%	1.3%	1.3%
MFG	44.7%	4.2%	0.9%	0.5%
preC_2	41.5%	1.5%	0.0%	2.9%
IPL	45.7%	2.1%	8.5%	4.3%
ITG	63.5%	12.1%	5.2%	1.7%
STG_A	85.3%	10.4%	10.4%	10.4%

Figure 91. Region-specific comparison of evoked versus induced activity in response to auditory speech stimuli. **A.** illustrates two schematic left hemispheres. However, data from left and right implantations was used. The left one shows iERP occurrence in the different brain regions in response to auditory word stimuli (BL, WR and VG). The differently sized green circles indicate iERP occurrence rates (as shown in B). The right brain illustrates the occurrence of beta ERD (white circles), low gamma ERS (grey circles) and high gamma ERS (black circles). Again, different circle sizes indicate different rates. **B.** summarises the mean percentage of contacts showing iERPs and spectral changes of the three frequency bands for the various perisylvian and additional brain regions.

	iERP	Beta ERD	Low Gamma ERS	High Gamma ERS
INS_A	37.8%	2.4%	0.0%	2.4%
INS_P	42.9%	1.4%	0.0%	1.4%
IFG	45.8%	15.0%	4.7%	6.5%
preC	80.8%	1.4%	11.0%	12.3%
postC	49.0%	6.1%	10.2%	30.6%
SMG	58.4%	2.2%	1.5%	5.1%
STG_P	51.3%	0.0%	5.3%	7.9%
MTG_P	43.8%	17.2%	1.6%	3.1%
MTG_A	55.3%	0.0%	2.6%	2.6%
CING	46.2%	0.0%	0.0%	0.0%
HIP	51.7%	0.0%	0.0%	0.0%
SFG	29.2%	4.2%	0.0%	0.0%
MFG	28.0%	1.0%	0.0%	1.0%
preC_2	28.6%	0.0%	0.0%	0.0%
IPL	0.0%	0.0%	0.0%	0.0%
ITG	41.2%	20.6%	8.8%	8.8%
STG_A	75.0%	0.0%	0.0%	0.0%
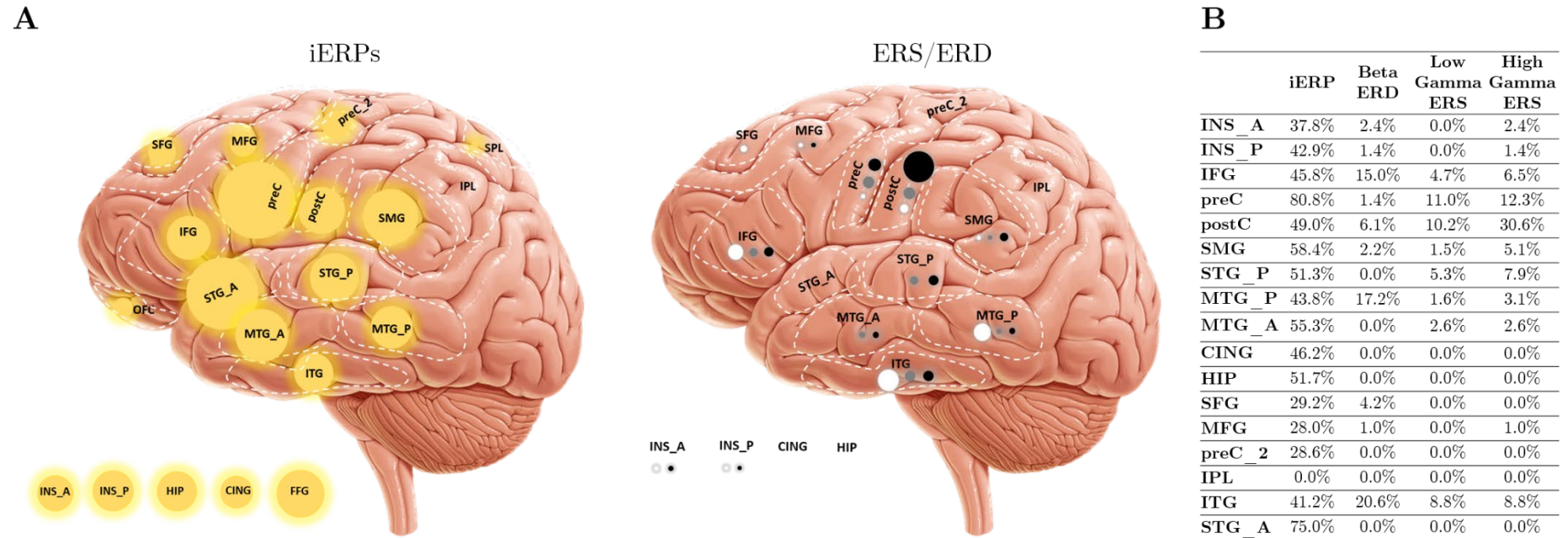
Figure 92. Region-specific comparison of evoked versus induced activity in response to visual stimuli. **A.** illustrates two schematic left hemispheres. However, data from left and right implantations was used. The left one shows iERP occurrence in the different brain regions in response to visual stimuli (PN, CNw). The different sized yellow circles indicate iERP rates. The right brain illustrates the occurrence of beta ERD (white circles), low gamma ERS (grey circles) and high gamma ERS (black circles). Again, different circle sizes indicate different rates. **B.** summarises the mean percentage of contacts showing iERPs and spectral changes of the three frequency bands for the various perisylvian and additional brain regions.

Next, I used the classification applied in the previous Chapter 5, grouping spectral changes in primary (peak <100ms), early (peak between 100–200ms), middle latency (peak between 200–700ms, activity ending before 1500ms) and long latency (wave starting between 0–700ms, lasting over 1500ms mark) activity.

Primary activity

Most contacts showing spectral changes during auditory word tasks peaking <100ms were located in the posterior STG. Compared to primary iERP components, which were found in only two brain regions, the posterior STG and posterior insula, primary frequency band activity was measured in more brain regions. Primary beta ERD was measured in six regions (STG_P, STG_A, SMG, preC, MTP, INS_A), primary low gamma ERS in three (STG_P, SMG, IFG) and primary high gamma ERS in two regions (STG_P, IFG). Unlike results of the iERP analysis, results of the frequency analysis did not show primary activity in any of the bands in the posterior insula. In the inferior frontal gyrus primary activity was measured in the two gamma bands, but not in the beta band. During picture naming tasks, no primary spectral changes were elicited. The number of contacts showing primary activity, the mean peak latency and standard deviation is summarised for all three frequency bands in Table 29.

Early activity

Early activity peaking between 100–200ms during auditory word tasks was mainly identified in the posterior STG in all three frequency bands, like for the iERP analysis. Early iERP components were measured in the anterior and posterior insula, supramarginal gyrus and postcentral gyrus, all of which showed spectral changes as well. Early beta ERD was measured in 11 brain regions, while early low and high gamma ERS were measured in six and five regions, respectively. Furthermore, besides the posterior STG, high early beta ERD activity was found in the inferior frontal gyrus, followed by the supramarginal gyrus and posterior middle temporal gyrus. During visual tasks, fewer brain

regions showed spectral changes in all frequency bands. As during auditory tasks most regions showed beta ERD, one brain region showed low gamma ERS and none showed high gamma ERS. The number of contacts showing early activity, the mean peak latency and standard deviation is summarised for all three frequency bands in Table 30 and Table 31.

Middle latency activity

The middle latency activity peaked between 200–700ms and ended before 1500ms. Only few contacts with middle latency activity were identified in the beta ERD band for both auditory and visual tasks. During auditory tasks middle latency low and high gamma ERS was mostly measured in the posterior STG, followed by the posterior insula and supramarginal gyrus. In comparison, middle latency iERP components were measured in almost all perisylvian and additional brain regions sampled from. During visual tasks middle and inferior temporal gyurs and inferior frontal gyrus showed low and/or high gamma ERS. The number of contacts showing middle latency activity, the mean peak latency and standard deviation is summarised for all three frequency bands in Table 32 and Table 33.

Long latency activity

The long latency activity started between 0–700ms and lasted over the 1500ms mark. This activity was rarely measured for any of the three bands during auditory word tasks. If measured, it occurred mostly in the posterior STG, followed by the supramarginal gyrus and precentral gyrus. In comparison, long latency iERP components occurred to a similar degree as the middle latency components and were measured in almost all brain regions. No spectral changes were measured during visual tasks. The number of contacts showing long latency activity, the mean peak latency and standard deviation is summarised for all three frequency bands in Table 34.

Late latency activity

Compared to the iERP analysis, here another activation pattern occurred. Activity starting later than 700ms and lasting until the end of the 2000ms time window. This was probably response-related activity. It was measured in all three frequency bands during auditory and visual tasks. During auditory tasks, low and high gamma ERS was highest in the pre- and postcentral gyrus, followed by inferior frontal gyrus and supramarginal gyrus for high gamma ERS. Middle frontal and inferior frontal gyrus and inferior temporal gyrus showed highest late latency beta ERD. During visual tasks, less activity was measured compared to auditory tasks. However, highest activity was measured in similar brain regions. The number of contacts showing late latency activity, the mean peak latency and standard deviation is summarised for all three frequency bands in Table 35 and Table 36.

To sum up, for all three frequency bands primary components were not as localised as primary iERP components, comprising several perisylvian regions. Furthermore, they did not occur in the posterior insula while primary iERP components did. Highest occurrence rate for primary, early and middle latency components was observed in the posterior STG. Occurrence of early components was high in the beta ERD band, while only a few middle latency components were observed in the beta band. The opposite was true for low and high gamma ERS components. Middle latency components occurred more often in the low and high gamma band while only a few early components were measured. Long latency components were rarely measured, while a new component was observed during the frequency analysis, the late latency component. This component was observed in several perisylvian regions and they occurred similarly in all three frequency bands.

Table 29. Region-specific primary activity for auditory word tasks for all frequency bands.

		STG_P	STG_A	SMG	preC	MTG_P	INS_A	IFG
Beta ERD	n (contacts)	32	1	12	1	1	1	
	mean peak latency (ms)	75.1	96.5	72.3	98	80	50	
	SD (ms)	14.3	1.5	17.2	0.0	0.0	0.0	
Low Gamma ERS	n (contacts)	18		2				4
	mean peak latency (ms)	67.3		80.0				84.0
	SD (ms)	11.0		0.0				4.1
High Gamma ERS	n (contacts)	5						1
	mean peak latency (ms)	70.4						98.0
	SD (ms)	28.6						0.0

Table 30. Region-specific early activity for auditory word tasks for all frequency bands.

		STG_P	STG_A	SMG	preC	MTG_P	INS_A	IFG	SPL	postC	INS_P	ITG
Beta ERD	n (contacts)	33	2	20	2	6	3	14	2	2	3	1
	mean peak latency (ms)	124.4	120.3	126.5	162.7	131.0	158.3	121.9	120.0	131.5	115.7	132.0
	SD (ms)	21.0	8.8	24.4	22.6	20.5	16.5	22.3	0.0	2.5	6.9	0.0
Low Gamma ERS	n (contacts)	5			2		1	4		1	2	
	mean peak latency (ms)	160.4			149.0		120.0	128.0		124.0	176.0	
	SD (ms)	29.9			1.0		0.0	39.5		0.0	9.0	
High Gamma ERS	n (contacts)	35			2			1		1	6	
	mean peak latency (ms)	132.5			178.5			102.0		189.0	141.3	
	SD (ms)	26.5			3.5			0.0		0.0	27.3	

Table 31. Region-specific early activity for visual tasks for all frequency bands.

		STG_P	STG_A	SMG	preC	MTG_P	INS_A	IFG	SPL	postC	INS_P	ITG
Beta ERD	n (contacts)			3		10	1	11		2	1	2
	mean peak latency (ms)			169.7		144.8	178.0	156.9		148.0	190.0	143.5
	SD (ms)			13.7		6.1	0.0	6.4		2.2	0.0	3.5
Low Gamma ERS	n (contacts)							2				
	mean peak latency (ms)							110.0				
	SD (ms)							0.0				
High Gamma ERS	n (contacts)											
	mean peak latency (ms)											
	SD (ms)											

Table 32. Region-specific middle latency activity for auditory word tasks for all frequency bands.

		STG_P	STG_A	SMG	preC	MTG_P	INS_A	IFG	postC	INS_P	ITG
Beta ERD	n (contacts)	2		2			1				
	mean peak latency (ms)	564.0		641.5			678.0				
	SD (ms)	0.0		91.5			0.0				
Low Gamma ERS	n (contacts)	47	3	1	1		3		1	8	1
	mean peak latency (ms)	446.5	312.2	741.0	492.0		402.7		512.0	371.9	230.0
	SD (ms)	130.0	36.2	0.0	0.0		179.8		0.0	180.9	0.0
High Gamma ERS	n (contacts)	39	3	14			3		1	14	
	mean peak latency (ms)	422.6	298.5	411.6			449.7		289.0	388.9	
	SD (ms)	229.4	40.5	128.8			260.2		0.0	112.3	

Table 33. Region-specific middle latency activity for visual tasks for all frequency bands.

		STG_P	STG_A	SMG	preC	MTG_P	INS_A	IFG	postC	INS_P	ITG
Beta ERD	n (contacts)								1		
	mean peak latency (ms)								597.0		
	SD (ms)								0.0		
Low Gamma ERS	n (contacts)					1		1			2
	mean peak latency (ms)					489.0		301.0			360.0
	SD (ms)					0.0		0.0			41.0
High Gamma ERS	n (contacts)					1					
	mean peak latency (ms)					349.0					
	SD (ms)					0.0					

Table 34. Region-specific long latency activity for auditory word tasks for all frequency bands.

		STG_P	SMG	preC	INS_A	postC
Beta ERD	n (contacts)	1	1			
	mean peak latency (ms)	676.0	1678.0			
	SD (ms)	0.0	0.0			
Low Gamma ERS	n (contacts)	3	1		1	
	mean peak latency (ms)	269.0	553.0		250.0	
	SD (ms)	0.0	0.0		0.0	
High Gamma ERS	n (contacts)		2	2		1
	mean peak latency (ms)		568.0	1490.0		1001.0
	SD (ms)		2.0	0.0		0.0

Table 35. Region-specific late latency activity for auditory word tasks for all frequency bands.

		STG_P	SMG	preC	MTG_P	INS_A	IFG	postC	INS_P	ITG
Beta ERD	n (contacts)	12	1			3	5	1		6
	mean peak latency (ms)	1250.6	1676.0			1342.0	1699.2	1189.0		1285.8
	SD (ms)	409.8	20.0			83.7	67.3	0		151.1
Low Gamma ERS	n (contacts)	1	6	4	2	3		12	1	2
	mean peak latency (ms)	1752.0	1681.0	1422.5	1870.0	1699.3		1194.8	978.0	1218.0
	SD (ms)	0.0	141.0	213.5	50.0	17.2		297.0	0.0	494.0
High Gamma ERS	n (contacts)	2	12	6	3	5	11	22	1	1
	mean peak latency (ms)	1312.0	1390.1	1533.8	1700.0	1523.6	1540.3	1452.9	1302.0	1589.0
	SD (ms)	288.0	300.0	111.1	81.6	218.4	231.7	326.5	0.0	0.0

		SFG	MTG_A	MFG	IPL	HIP
Beta ERD	n (contacts)	5	1	9	1	2
	mean peak latency (ms)	1456.0	1058.0	1085.7	1150.0	1635.5
	SD (ms)	288.6	0.0	115.7	0.0	50.5
Low Gamma ERS	n (contacts)	1	1	2	3	
	mean peak latency (ms)	987.0	1480.0	705.0	1746.0	
	SD (ms)	0.0	0.0	5.0	48.1	
High Gamma ERS	n (contacts)				2	
	mean peak latency (ms)				1780.0	
	SD (ms)				0.0	

Table 36. Region-specific late latency activity for visual tasks for all frequency bands.

		STG_P	SMG	preC	MTG_P	INS_A	IFG	postC	INS_P	ITG
Beta ERD	n (contacts)					1	4			3
	mean peak latency (ms)					1610.0	1590.0			1346.3
	SD (ms)					0.0	155.9			118.0
Low Gamma ERS	n (contacts)	1	2	8			2	5		
	mean peak latency (ms)	1490.0	1440.0	1317.0			1612.5	1023.8		
	SD (ms)	0.0	0.0	335.7			212.5	190.9		
High Gamma ERS	n (contacts)	6	5	8	1	2	6	15	1	3
	mean peak latency (ms)	1185.7	1142.2	1513.9	972.0	1247.0	1525.0	1083.1	1780.0	700.0
	SD (ms)	217.4	243.2	79.5	0.0	243.0	381.9	285.6	0.0	0.0

		SFG	MTG_A	MFG	IPL	HIP
Beta ERD	n (contacts)			1		
	mean peak latency (ms)			1598.0		
	SD (ms)			0.0		
Low Gamma ERS	n (contacts)		1	2		
	mean peak latency (ms)		999.0	705.0		
	SD (ms)		0.0	5.0		
High Gamma ERS	n (contacts)		1			
	mean peak latency (ms)		1020.0			
	SD (ms)		0.0			

6.3.4 Region- and task-specific spectral changes and comparison with iERPs

Several distinct anatomical regions were identified, showing ERS/D in temporal, parietal and frontal lobes in both hemispheres in response to passive and active auditory and picture naming stimuli.

Auditory word tasks

The following Figure 93 illustrates the comparison beta ERD, low gamma ERS and high gamma ERS in perisylvian brain regions during all auditory word tasks (BL, WR and VG).
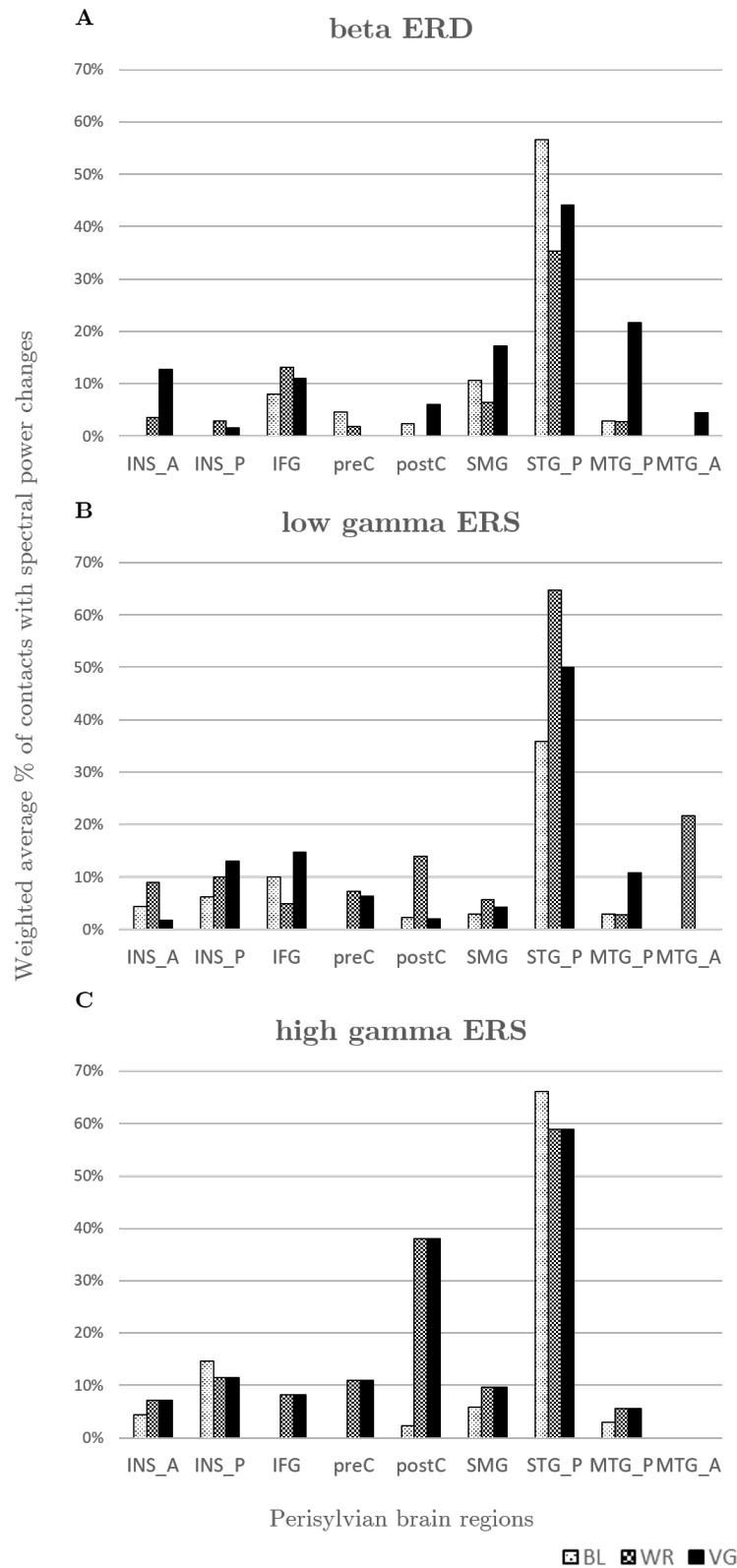
Figure 93. Region- and task-specific spectral changes during auditory word tasks. Mean percentage of contacts showing spectral changes in the beta, low gamma and high gamma bands in perisylvian brain regions during auditory word tasks (BL, WR and VG).

First, differences in the percentage of contacts showing spectral changes between the three auditory tasks (BL, WR and VG) in the various perisylvian brain regions were addressed. Overall, all brain regions showed similar activity during the three tasks concerning the frequency bands measured. The only brain regions showing significant differences between tasks were the anterior insula, measuring significantly less beta ERD during the BL task compared to the VG task and the posterior STG showing significantly less low gamma ERS during the BL task compared to the WR task (p=<0.05, Wilcoxon rank sum test, see Appendix Table 50).

Second, differences in the percentages of spectral power comparing the three frequency bands (beta ERD, low gamma ERS and high gamma ERS) in the various brain regions were analysed. The posterior insula showed significantly lower beta activity compared to high gamma activity. Significantly less beta activity compared to low gamma and high gamma activity was measured in the postcentral gyrus and significantly less beta activity compared to high gamma activity was measured in the posterior STG (p=<0.05, Wilcoxon rank sum test, see Appendix Table 51).

Visual tasks

Next, I present the comparison of mean percentage of contacts showing spectral changes during picture and colour (baseline) naming tasks in Figure 94.

A

beta ERD

B

low gamma ERS

C

high gamma ERS

Weighted average % of contacts with spectral power changes

Perisylvian brain regions

□ CNw ■ PN
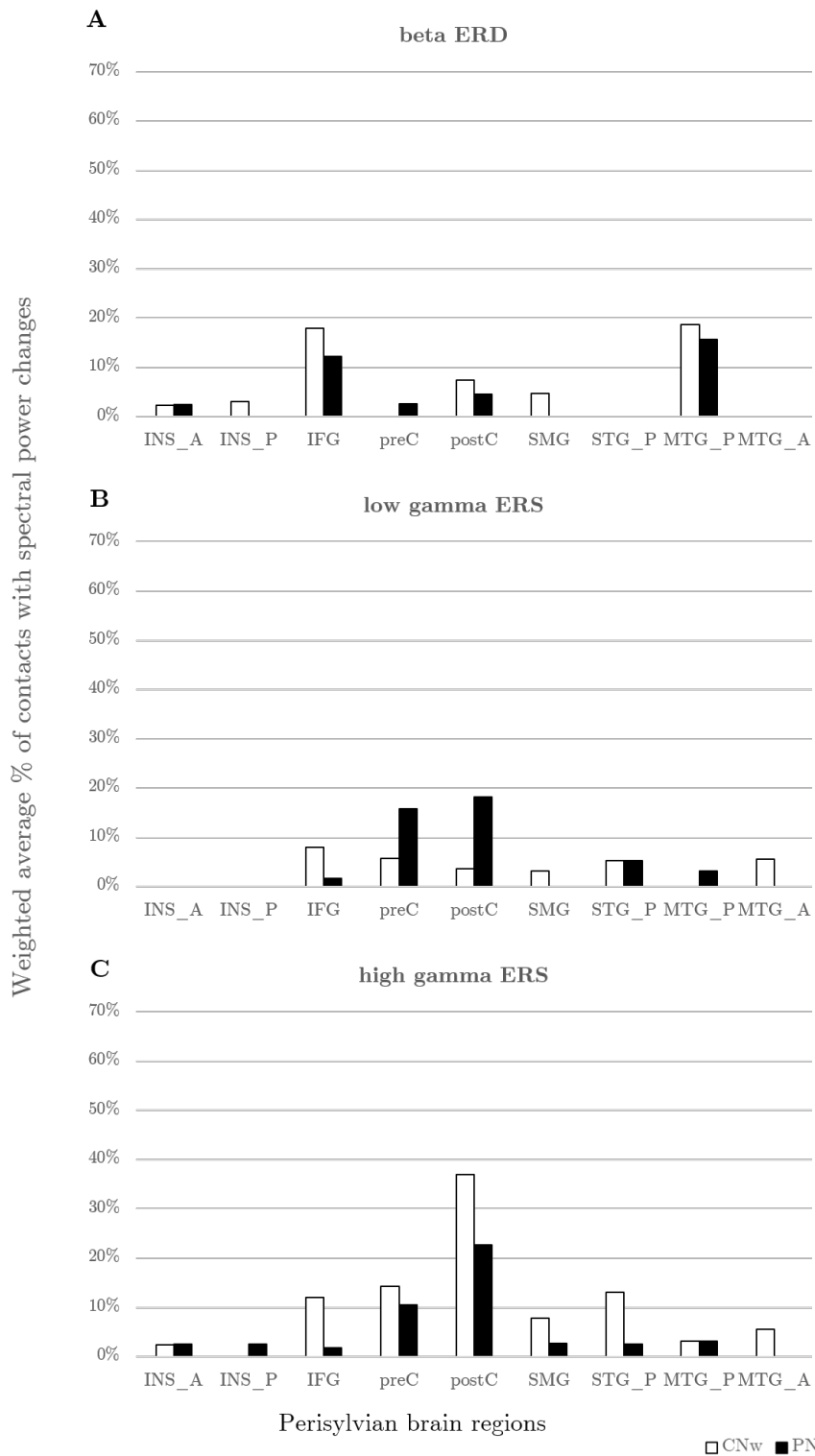
Figure 94. Region- and task-specific spectral changes during visual naming tasks. Mean percentage of contacts showing spectral changes in the beta, low gamma and high gamma bands in perisylvian brain regions during visual naming tasks (PN, CNw).

293

First, differences in the percentage of contacts showing spectral changes between the two visual tasks (PN, CNw) in the various perisylvian brain regions were addressed. Overall, all brain regions showed similar activity during these tasks and no significant differences were measured ($p=<0.05$, Wilcoxon rank sum test, see Appendix Table 50).

Second, differences in the percentages of spectral power comparing the three frequency bands (beta ERD, low gamma ERS and high gamma ERS) in the various brain regions were analysed. The posterior STG showed significantly lower beta activity compared to high gamma activity ($p=<0.05$, Wilcoxon rank sum test, see Appendix Table 52).

6.3.5 Concordance of region- and task-specific spectral changes and iERPs

In this section, to investigate whether evoked and induced activity occurred in the same contacts, I analysed the co-occurrence of iERPs with beta, low gamma and high gamma activity for each contact. As shown before, significantly more iERPs were elicited during auditory and visual tasks in most regions compared to spectral changes. Here, I am taking a closer look at the contacts showing spectral changes and whether these contacts also elicited iERPs. A contact showed either an iERP together with frequency activity, frequency activity alone, an iERP alone or no activity.

Results showed that most of the contacts eliciting ERS/D also showed iERPs (mean=6.4%±3.1%, range=1.4%–11.8%), only a few did not (mean=0.8%±0.6%, range = 0.0%–2.2%, see Appendix Table 53). Comparing frequency bands, a significantly higher percentage of contacts showed concordance of iERPs and low gamma ERS for all auditory task and concordance of iERPs and high gamma ERS for BL and WR task ($p<0.01$ and $p<0.05$, respectively; Wilcoxon rank sum test). For visual tasks, a significantly higher percentage of contacts showed concordance of iERPs and beta ERD

compared to low and high gamma ERS for which no significant results were observed (p<0.05, Wilcoxon rank sum test, Appendix Table 54). The following Figure 95, Figure 96 and Figure 97 illustrate concordance of iERPs and spectral changes for the three frequency bands, differentiating auditory and visual tasks.
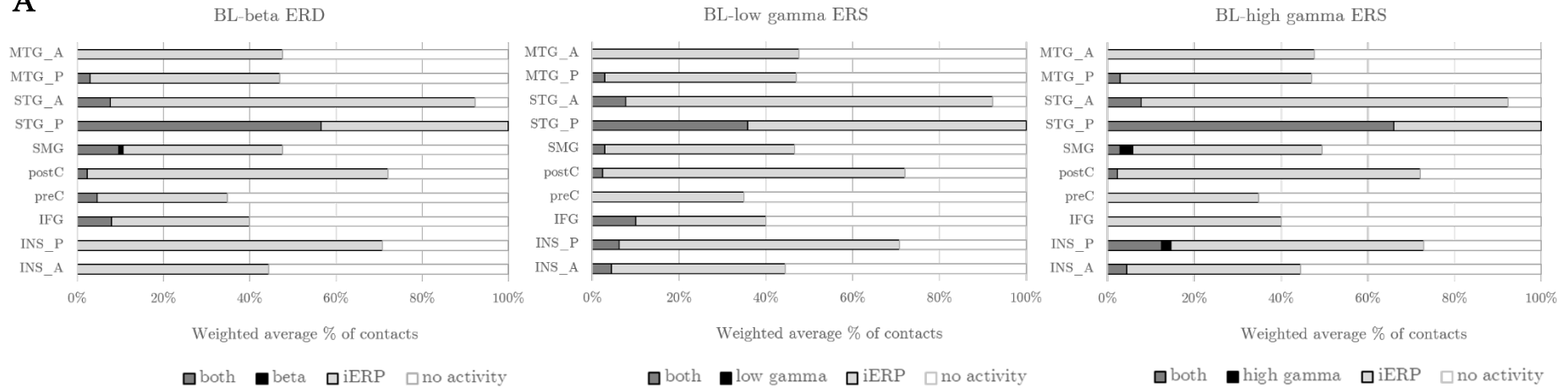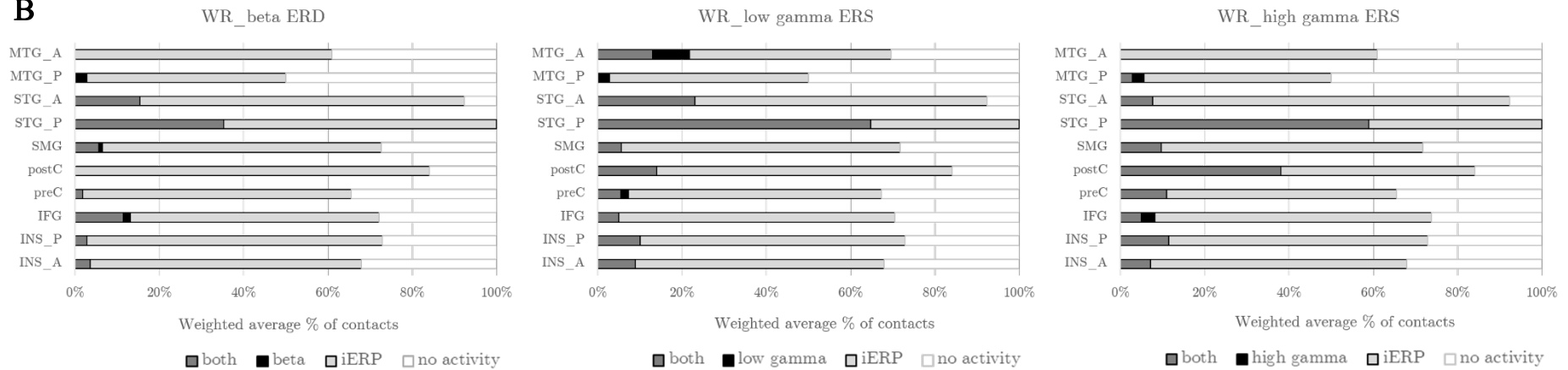
Figure 95. Concordance of region- and task-specific spectral changes and iERPs for Baseline (BL) and Word Repetition (WR) tasks (1). Each figure illustrates the mean percentage of contacts showing either spectral changes alone, spectral changes together with iERPs, iERPs alone or no activity for one of the three frequency bands analysed—beta ERD, low gamma ERS and high gamma ERS. **A.** shows results for the BL task and **B.** shows results for the WR task. Abbreviation: both = concordance of iERP and spectral changes in certain frequency band.
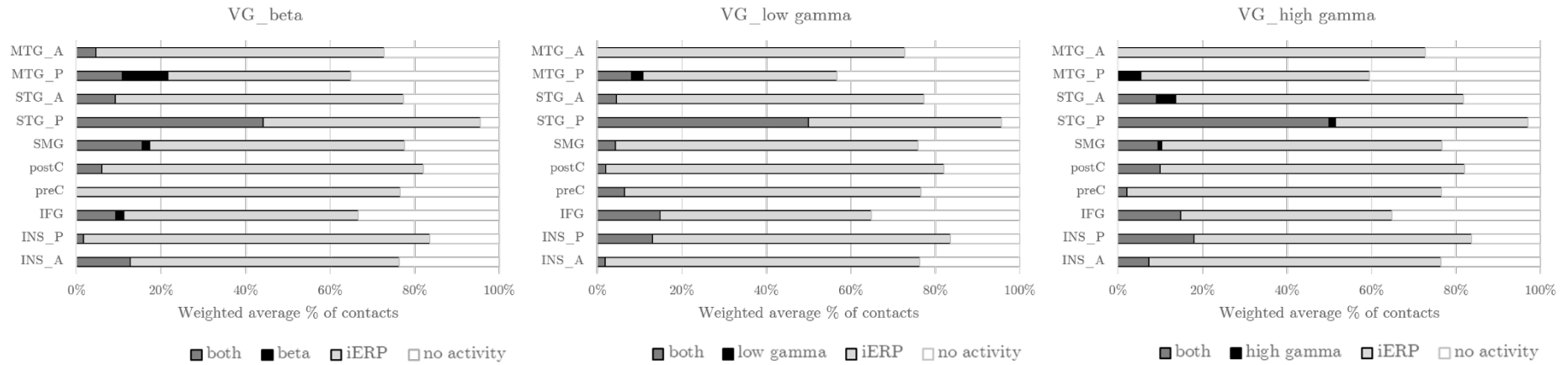
Figure 96. Concordance of region- and task-specific spectral changes and iERPs during the VG task (2). Each figure illustrates the mean percentage of contacts showing either spectral changes alone, spectral changes together with iERPs, iERPs alone or no activity for one of the three frequency bands analysed—beta ERD, low gamma ERS and high gamma ERS. Abbreviation: both = concordance of iERP and spectral changes in certain frequency band.
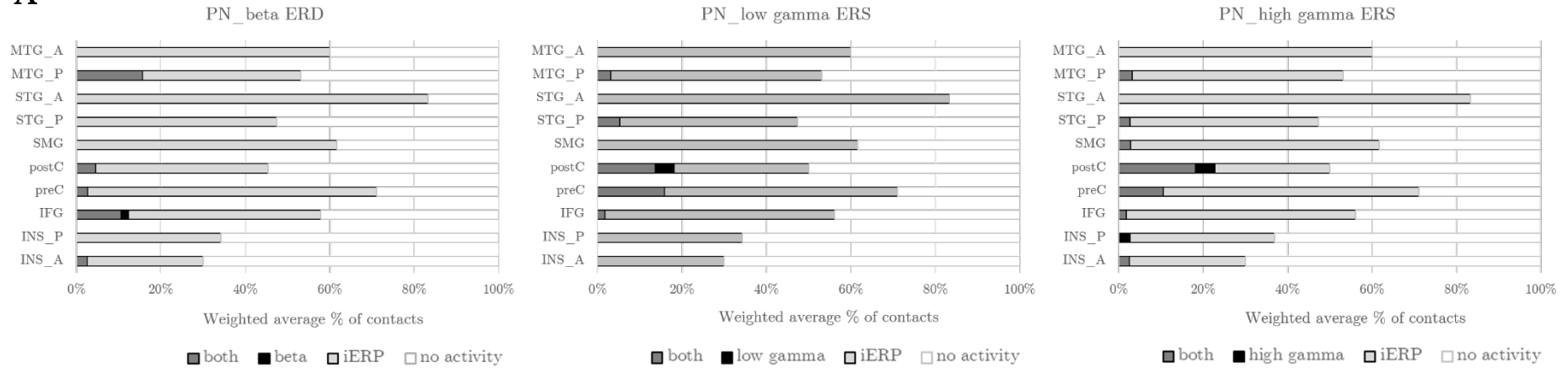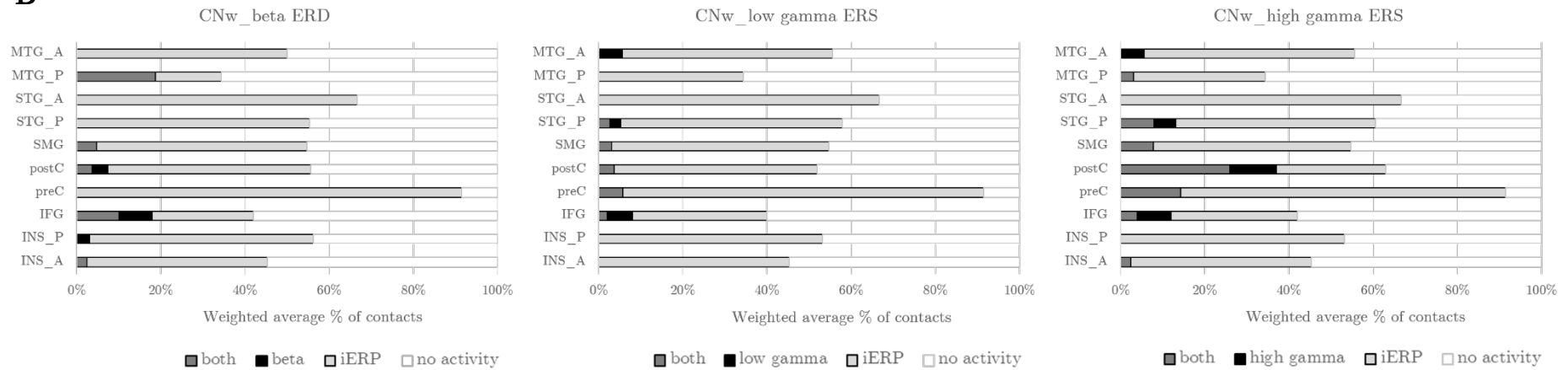
Figure 97. Concordance of region- and task-specific spectral changes and iERPs for the visual tasks (3). Each figure illustrates the mean percentage of contacts showing either spectral changes alone, spectral changes together with iERPs, iERPs alone or no activity for one of the three frequency bands analysed—beta ERD, low gamma ERS and high gamma ERS. **A.** shows results for the PN task and **B.** shows results for the CNw task. Abbreviation: both = concordance of iERP and spectral changes in certain frequency band.

Furthermore, the co-occurrence of the three frequency bands was analysed for each contact. Each frequency band was compared to the other two bands. A contact showed activity in either two frequency bands, one frequency band alone or did not show activity. Results showed that low and high gamma ERS co-occurred more frequently than beta ERD with low and high gamma ERS. No significant differences could be shown between the co-occurrence of low and high gamma and each of the activities alone (p>0.05, Wilcoxon rank sum test). On the contrary, beta ERD occurred significantly less often together with low and high gamma ERS (p<0.05, Wilcoxon rank sum test). This was true for auditory word tasks and visual naming tasks. Summary graphs can be found in the Appendix Figure 126 to Figure 128.

6.3.6 Response induced spectral changes

From 18 implanted brain regions (n=5 patients), eight showed speech response-induced activity. For this summary only brain areas with frequency activity data from at least three patients were taken into account. The rest only occurred in one or two patients (CING, HIP, preC_2, postC_2, SPL, STG_A, MTG_P, ITG and FFG). In CING, HIP, FFG, IPL, SPL no activity was measured in any of the studied frequency bands. The rest of the regions—preC_2, postC_2, STG_A, showed activity ranging from 8.3%–66.7%. Figure 98 illustrates the topography of speech-response induced activity in the beta, low gamma and high gamma band in response to auditory word tasks.
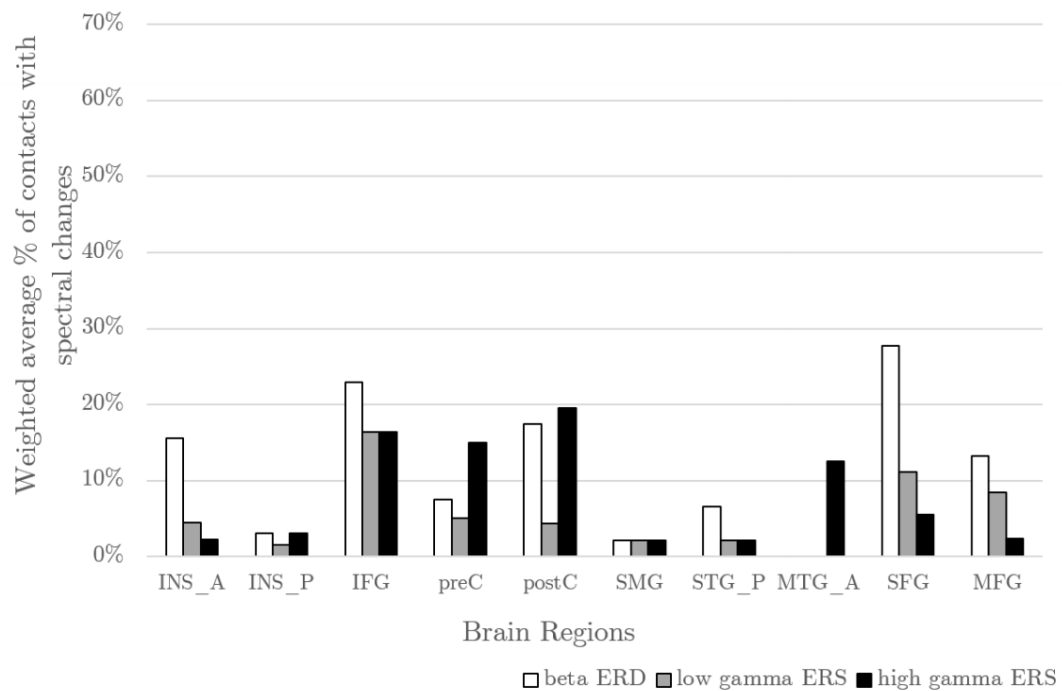
Figure 98. Speech-response induced ERS/D. A. illustrates the brain regions showing speech-response induced frequency band activity. **B.** and **C.** summarise and illustrate the mean percentage of contacts showing spectral changes in the beta, low gamma and high gamma band in various brain regions in response to auditory word tasks (WR and VG).

Differences in the percentages of spectral changes comparing the three frequency bands (beta ERD, low gamma ERS and high gamma ERS) in the various brain regions was analysed. The postcentral gyrus showed significantly higher high gamma ERS compared to low gamma ERS ($p=<0.05$, Wilcoxon rank sum test, see Appendix Table 55).

Next, I compared region-specific frequency band results with iERP results for speech response activity. All regions showed similar mean percentage of contacts with iERPs compared to contacts with either beta ERD, low gamma ERS or high gamma ERS ($p>0.1$; Wilcoxon rank sum test). Figure 99 illustrates the comparison of iERPs and spectral changes measured in brain regions during speech response to auditory word stimuli.
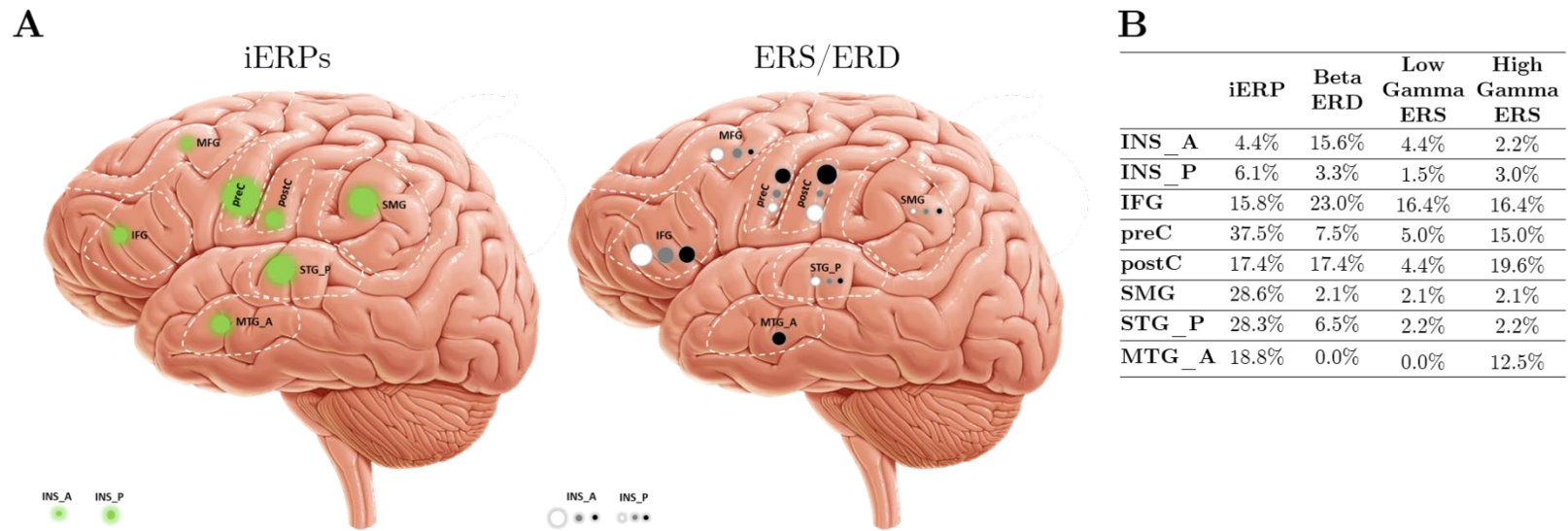
Figure 99. Region-specific comparison of evoked versus induced activity in response to speech production. A. illustrates two schematic left hemispheres. However, data from left and right implantations was used. The left one shows iERP occurrence in the different brain regions during speech response to auditory word stimuli. The different sized green circles indicate iERP rates. The right brain illustrates the occurrence of beta ERD (white circles), low gamma ERS (grey circles) and high gamma ERS (black circles). Different circle sizes indicate different rates. **B.** summarises the mean percentage of contacts showing iERPs and spectral changes of the three frequency bands for the various perisylvian brain regions.

	iERP	Beta ERD	Low Gamma ERS	High Gamma ERS
INS_A	4.4%	15.6%	4.4%	2.2%
INS_P	6.1%	3.3%	1.5%	3.0%
IFG	15.8%	23.0%	16.4%	16.4%
preC	37.5%	7.5%	5.0%	15.0%
postC	17.4%	17.4%	4.4%	19.6%
SMG	28.6%	2.1%	2.1%	2.1%
STG_P	28.3%	6.5%	2.2%	2.2%
MTG_A	18.8%	0.0%	0.0%	12.5%

6.3.7 Relation between spectral changes/iERPs and electrical stimulation responses

This section presents a comparison of the topography of spectral changes and iERPs during auditory word tasks with behavioural effects of clinical electrical stimulation on naming and oral motor function (positive responses). A sub-sample of this chapter's cohort was chosen for this analysis. I included seven patients, who were investigated for language lateralisation and language localisation as their seizure onset zone was located close to their suspected language relevant brain regions. All of them had electrical functional stimulation for clinical language assessment. All patients had left-sided SEEG implantation regimes. Table 37 summarises the patient characteristics and states the number of contacts showing positive and no (negative) responses when stimulated.

Table 37. Patient characteristics - language localisation cases.

ID	handedness	fMRI	Hemisphere	ES	ES+	ES –	Language tasks	Surgery
2	L	L	L	Y	0	17	LN	Left parietal opercular insula
3	L		L	Y	4	0	VG, PN	
8	R	L	L	Y	12	14	PN, LN, reading	Thermocoagulation
12	L		L	Y	0	3	VG, LN	
19	R		L	Y	0	6	WR, PN	Left frontal resection
20	R	B	L	Y	14	4	WR, PN	
100	R	L	L	Y	0	19	Conversation, object naming	Left temporal lesionectomy

Abbreviations: ES = electrical stimulation for language, ES+ = contacts showing positive responses (e.g. speech hesitation, dysphasia, dysarthria) when tested using ES, ES– = contacts showing no responses when tested using ES, LN = Listen&Name, VG = verb generation, WR = word repetition, PN = picture naming, L = left, R = right, B = both, Y = yes, N = no.

A total of 93 contacts were stimulated (range 3–28 contacts) in the seven patients. Three patients showed ES+ contacts, while in four patients no ES+ contacts were observed. In total, 30 contacts elicited responses during electrical stimulation.

A chi-square test across all patients and ES contacts was performed to examine the relation between spectral changes/iERPs and electrical stimulation responses. The three auditory tasks (BL, WR and VG) were analysed separately for each frequency band and for iERPs. In addition, an analysis merging WR and VG tasks was done for each frequency band and for the iERP analysis. Results showed a significant relation between electrical stimulation responses and beta ERD and for high gamma ERS (p<0.01 and p<0.05, respectively), as summarised in Table 38.

Table 38. Chi-Square results summary depicting the correlation between electrical stimulation responses and spectral changes/iERPs.

	Pearson chi^2		Pearson chi^2
iERP_BL	3.35	High gamma ERS_BL	0.96
iERP_WR	0.27	High gamma ERS_WR	0.66
iERP_VG	0.00	High gamma ERS_VG	4.95*
iERP_WR&VG	1.75	High gamma ERS_WR&VG	8.50**
Beta ERD_BL	9.47**	Low gamma ERS_BL	2.68
Beta ERD_WR	9.26**	Low gamma ERS_WR	1.68
Beta ERD_VG	9.54**	Low gamma ERS_VG	1.38
Beta ERD_WR&VG	9.20**	Low gamma ERS_WR&VG	1.12

The table shows iERP and the three spectral changes results (beta ERD, low gamma ERS, high gamma ERS) and further differentiates between the three auditory task. '_WR&VG' shows results when merging the two active auditory tasks into one analysis (N=93). Significance level ** p<0.01 and * p<0.05.

Results show that beta ERD was most predictive of electrical stimulation responses. The direction of correlation is of importance as shown in more detail in Table 39 where beta ERD for the VG task is presented.

Table 39. Correlation between ES responses and presence or absence of beta ERD for the VG task.

	betaERD_VG−	betaERD_VG+	Total
ES−	32	12	44
ES+	30	0	30
Total	62	12	74

For this analysis N=74. ID19 did not complete the VG tasks and therefore only six patients were included in this analysis.

None of the ES+ contacts showed beta ERD during VG. The same was true for the BL, WR and the combined '_WR&VG' analysis. Beta ERD was only observed in ES− contacts. This suggests that the absence of beta ERD is more predictive of ES+ contacts, however with a low specificity (63.2%) and no sensitivity (0%). The PPV and NPV were 0% and 44.4%, respectively.

Results for high gamma ERS for the VG task and the combined '_WR&VG' analysis were other predictive values besides beta ERD. Again, the direction of predictiveness is of importance. Table 40 illustrates the results for high gamma ERS_WR&VG in detail.

Table 40. Correlation between ES and high gamma ERS_WR&VG merged.

	highERS_WR&VG−	highERS_WR&VG+	Total
ES−	56	7	63
ES+	19	11	30
Total	75	18	93

ES+ contacts were almost twice as likely to be high gamma ERS negative than positive. Furthermore, in 75% of the cases where no high gamma ERS was observed (_any approach) contacts did not show responses when triggered using electrical stimulation. Results showed that high gamma ERS (_WR&VG) is a

specific (88.8%) but not a sensitive (36.7%) modality for language localization compared with electrical stimulation as the current clinical gold standard. The PPV and NPV were 61.1% and 74.7%, respectively.

To sum up, this preliminary exploration of the relationship between ES and ERS/D shows that there appears to be a weak positive correlation of high ERS– with ES+ and weak negative one with beta ERD+. This however needs to be interpreted in light of some limitations. First this analysis only included a subsample of contacts analysed for spectral changes. Many more SEEG contacts in this analysis did not show ERD/S. Second, language tasks used for electrical stimulation testing did not always overlap with tasks used for the study.

6.3.8 Case presentations

In the following section, I am presenting three patients who underwent electrical stimulation for clinical language localisation. These cases were chosen to be presented here, as none of them had prior epilepsy surgery and had several electrodes tested for language using electrical stimulation. The aim of these case presentations is to illustrate iERP and ERS/D topography, their co-occurrence and the relation between positive or negative electrical stimulation responses. Furthermore, all of these reported patients had additional fMRI testing for language lateralisation. Summaries of the other four patients can be found in the Appendix from p. 436–457.

Case 1 (ID2)

Patient ID2 was a 9-year and 2 months old, left-handed girl with medication-resistant epilepsy. Her first language was Maltese. She was able to communicate in English; however, she was not a native speaker. Her first seizure occurred with six weeks of age and the latest events presented as Type 1—Nocturnal events characterised by sudden awakening, arm abduction, dystonic posturing of the left arm, with cycling movements of the left leg, rapid eye blinking with facial flushing, hypersalivation, unresponsiveness and grimacing. These events lasted up to 50 seconds and occurred every other day. Type 2—were daytime events characterised by a sudden fall or leaning slowly to the left, loss of consciousness and eyelid twitching. She could be dysphasic and appeared confused for a few minutes afterwards. Those events were mainly provoked by an emotional upset like fear or panic. These seizures did not occur for four months at the time of invasive monitoring. She showed normal developmental milestones, however, she presented increasing difficulties with academic progress, concentration and retaining new information.

The MRI showed a region of abnormal cortical folding in the left parietal operculum, which was accompanied by some blurring of the grey-white matter junction. This was consistent with focal cortical dysplasia. The scalp EEG suggested focal seizures of left hemispheric origin; however, the onset was not

clear. The PET findings were suggestive of a focus in the left parietal cortex extending into the superior temporal gyrus, which supported the EEG findings.

Patient ID2 was admitted to GOSH Koala ward for a left-sided SEEG implantation. In total, 17 electrodes were implanted. The electrical features of the seizures recorded suggested a seizure onset from the electrode sampling from the lesion and PET hypometabolism (electrode I, maximum contacts 5–9) and from the posterior operculum and insula (electrode J). To gain information about language lateralisation an fMRI was done, which showed a left lateralisation for language. To decide whether functional brain areas were in close vicinity to the planned resection area, the patient underwent electrical stimulation mapping for language. None of the contacts stimulated were noted to be involved in language processes as no error or hesitancy during language tasks was observed. The patient underwent a left parietal operculum-insular resection. Due to technical difficulties, the surgery had to be terminated and resection was not completed. Post-surgery the patient presented with seizures occurring 20 times a month. Furthermore, she had a slight right facial weakness and showed receptive and expressive aphasia-type language deficits. She presented with difficulties understanding instructions, had word finding difficulties, and showed perseveration of topics, jargon and some speech sound errors. Speech and language therapy was recommended. About six month after the first surgery a second left-sided insula-opercular resection was performed. Since then the patient is seizure free. She is still receiving speech and language therapy. A right facial weakness post-surgery was very mild.

For this study, the patient was able to complete three language tasks (BL, WR and VG) in English. She performed best during the word repetition task with 100% accuracy followed by the verb generation task with 90%.

The clinical SEEG implantation regime is summarised in Figure 100. A subset of clinically implanted electrodes was included for this study recording. Contacts involved in the seizure onset (electrodes I and J—deep contacts) were also included in the iERP recording. The following Figure 101 illustrates the patient's

implantation regime, contacts stimulated during functional electrical stimulation, electrical stimulation responses, iERPs and spectral changes elicited during the auditory word tasks (BL, WR and VG).

Electrode	Label	Contacts	Location
Depth	A	1-12	Left Anterior Hippocampus
Depth	B	1-15	Left Amygdala
Depth	C	1-15	Left Posterior Hippocampus
Depth	D	1-10	Left STG to Anterior Insula
Depth	E	1-12	Left STG to Posterior Insula
Depth	F	1-18	Left Posterior Temporal
Depth	G	1-5	Left TPO
Depth	H	1-18	Left Angular
Depth	I	1-12	Left SMG
Depth	J	1-10	Left Parietal Operculum to Posterior Insula
Depth	K	1-8	Left Frontal Operculum to Mid Insula
Depth	L	1-15	Left MFG to Cingulate
Depth	M	1-12	Left IFG to Anterior Insula
Depth	N	1-8	Left SMA
Depth	O	1-5	Left M1
Depth	P	1-15	Left S1
Depth	Q	1-12	Left Posterior Parietal

Figure 100. Case 1 (ID2)—implantation regime summary. A. It illustrates all implanted SEEG electrodes, with the ones used for this study highlighted with pink letterboxes. Each blue dot presents a contact. Electrodes D, E, F and H show white dots in addition, which highlight contacts used for language stimulation during clinical assessment. **B.** The table summarises the electrode locations and their labels, circling the ones used for language stimulation. **C.** presents the language fMRI results of this patient during an overt verb generation task.
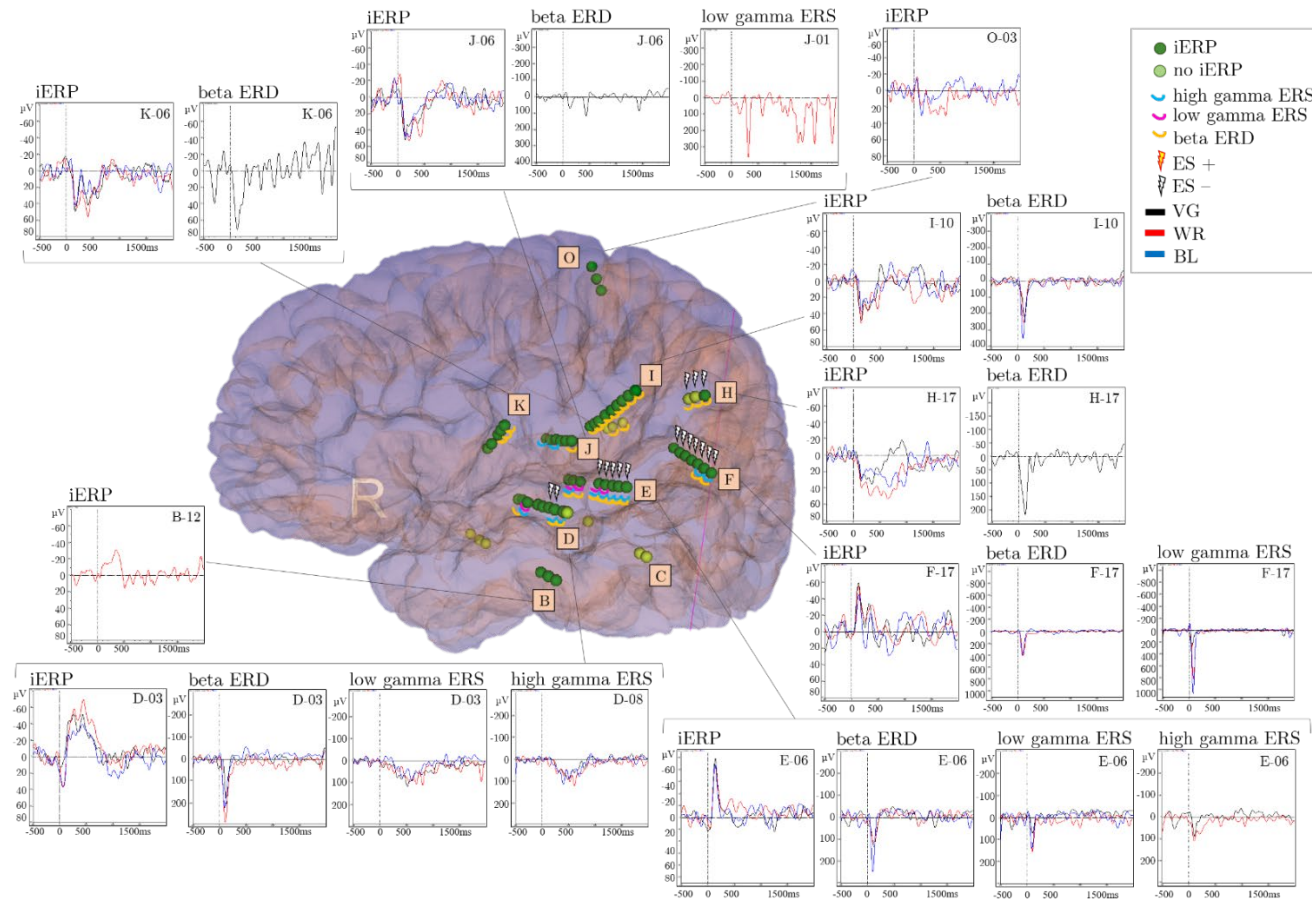
Figure 101. Case 1 (ID2)—Response summary. This summary includes the subset of contacts chosen for this study. Contacts showing iERPs are depicted in dark green and contacts without iERPs in light green. Contacts showing spectral changes are highlighted in either blue (high gamma ERS), pink (low gamma ERS) or yellow (beta ERD). Contacts showing a positive or negative response to electrical stimulation mapping are highlighted (red versus black). For each electrode, the maximum iERP and/or spectral changes are illustrated.

For this patient's recording 62 contacts were chosen. Reporting results of three tasks (BL, WR and VG) leads to a total number of 186 contacts. Like for the group results reported previously, a higher number of contacts with iERPs was observed compared to contacts showing spectral changes. Furthermore, iERPs were observed in a wider area, while spectral changes were more localised. For clinical electrical language stimulation testing 17 contacts were chosen for this study. The task used was an auditory listen and naming task. No responses were observed. Table 41 summarises the number of contacts showing iERPs and spectral changes and brain regions involved. This summarises activity, which was measured during at least one of the language tasks (see Appendix Figure 129 to Figure 131 for details).

Table 41. Overall occurrence of iERP, spectral changes and electrical stimulation responses during for case ID2.

	No of contacts (%)	No of ES– contacts	Brain regions
iERP	129 (68.3%)	15 (88.2%)	STG_P, STG_A, INS_P, INS_A, MTG_A, postC, preC, preC_2, SMG
High gamma ERS	11 (5.8%)	4 (23.5%)	STG_P, STG_A
Low gamma ERS	28 (14.8%)	11 (64.7%)	STG_P, STG_A, SMG, INS_P, postC
Beta ERD	56 (29.6%)	9 (52.9%)	SMG, STG_P, STG_A, INS_P, postC, preC

For this patient the sensitivity markers could not be tested as no positive responses to electrical stimulation were observed. High gamma ERS was most specific. Table 42 summarises sensitivity and specificity analysis for the two active tasks word repetition and verb generation. The baseline task was not included in the table as it was a passive listening. Nevertheless, analyses for the passive listening task showed similar results.

Table 42. Relation between ES and iERP/spectral changes—sensitivity and specificity analysis for WR&VG for case ID2.

	iERP	Beta ERD_any	Low gamma ERS_any	High gamma ERS_any
Sensitivity	-	-	-	-
Specificity	11.8%	41.2%	58.8%	76.8%
PPV	0.0%	0.0%	0.0%	0.0%
NPV	100%	100%	100%	100%

This summarises activity that was measured during at least one of the language tasks. Considering the patient's receptive and expressive language deficits post-surgery, I analysed the resected contacts for evoked and induced activity. From electrode I, contacts 5–12 and from electrode J, contacts 5–8 were resected (see Figure 100 and for more details Appendix Figure 132 and Figure 133). Contacts J7 and J8 were not included in the iERP analysis. The rest of the contacts showed robust iERPs (100%) and nine contacts showed beta ERD (90%). No low or high ERS was measured in these contacts.

The clinical assessments done showed a right-handed girl with left lateralisation for language and no language-related activity in the contacts stimulated. Contacts planned to resect were not tested for language function. Post-surgery the patient presented with receptive and expressive language deficits. Using language-related iERP and frequency analysis showed some areas of function, however, results did not concur with functional stimulation results. Nevertheless, electrodes I and J, which were resected showed robust iERPs and beta ERD and these results together with her post-opertaive language deficits suggest that iERP and beta ERD pointed towards language-essential brain areas. In this case, iERP and frequency analysis could have been used to check whether areas planned for resection showed language-related activity and electrical stimulation could have been done. This would have been mostly important for informing parents of post-surgical language outcome as in this case the possibility of seizure freedom outweighed functional deficits.

Case 2 (ID8)

Patient ID8 was a 12-year and 3 months old, right-handed girl with medication-resistant epilepsy. Her first language was Portuguese and her second English. Her first seizure occurred with six years of age and the latest events presented as Type 1 seizures, which began occasionally with her hearing voices. She then became frightened and ran to the toilet. She turned to the left and looked at or pulled her right hand. She also held or cleared her throat and had an unusual feeling in her mouth or down the right side of her body. On rare occasions, she talked gibberish and had possible clonic jerking of her shoulders. This lasted between 2–4 minutes and they occurred about 1–2 times per day. Type 2 events could occur after a Type 1 seizure or in isolation. Initially she stared and became unresponsive. If standing she fell to the floor and had jerking of all four limbs (most prominently in her shoulders), which typically lasted between 2–20 minutes. Seizures occurred 1–2 times per day. She went to a mainstream school and presented with severe anxiety.

The MRI showed left mesial temporal sclerosis with atrophy and increased hippocampal signal along with a dilated temporal horn of the left lateral ventricle. The PET was suggestive of a wider area of abnormality. The scalp EEG suggested a left anterior temporal onset. Her auditory hallucinations, early loss of speech and fearful look suggested the ictal changes involved a wider network than her mesial temporal structures alone. Therefore, invasive EEG was offered.

Patient ID8 was admitted to GOSH Koala ward for a left-sided SEEG implantation. In total, 11 electrodes were implanted. The electrical features of the seizures recorded suggested a seizure onset from electrode contacts in the insular cortex (deep contacts of F, L, J and K) with secondary activation of contacts in the frontal operculum (L), with a spread to lateral temporal lobe and hippocampus. Language fMRI showed some bilateral activation with a predominance on the left during a covert verb generation task. On a story comprehension task there was bilateral superior temporal lobe activation.

313

Functional electrical stimulation suggested motor areas in close vicinity to the ictal onset zone. Furthermore, language stimulation showed several contacts located in language-related areas, such as the posterior superior temporal gyrus, the subcentral area and the pars triangularis. The multidisciplinary team decided not to offer a surgical resection, as a wide resection of the dominant insula and frontal operculum would have been required. This would have put clinically meaningful risks to both motor and language function in the dominant hemisphere. However, thermocoagulation of insular and contacts involved in secondary activation of frontal operculum and hippocampus was offered and performed as a palliative procedure (K1–5; I1–6; F1–2; J1–3; L2–9, C1–3; D1–3). Seizures returned one month post thermocoagulation. Furthermore, the patient presented with progressive focal insular atrophy, which started further investigations that eventually indicated left sided Rasmussen's encephalitis.

For this study, the patient was able to complete six language tasks (BL, WR, VG, LN, PN, CNw) in English. She performed best during the word repetition and colour naming tasks with 100% of correct replies, followed by the picture-naming task with 98%, verb generation task with 62% and the sentence task with 54%.

A subset of clinically implanted electrodes was included for this study recording. Some contacts involved in the seizure onset were included in the iERP recording (J, K, L and D). For the case presentation below results for auditory word tasks (BL, WR and VG) are presented. Figure 102 summarises the clinical SEEG implantation regime presenting all electrodes implanted, contacts representing the ictal onset and language fMRI results. The following Figure 103 summarises the subset of contacts used in this study. It illustrates each electrode and contact included, it depicts an example response of the maximum iERP and spectral changes elicited during the auditory word tasks (BL, WR and VG) for each electrode that showed responses. Furthermore, it shows contacts chosen for clinical electrical language stimulation including their responses (positive or negative responses).

B.

Electrode	Label	Contacts	Location
Depth	A	1-12	Left Entorhinal
Depth	B	1-12	Left Amygdala
Depth	C	1-12	Left Anterior Hippocampus
Depth	D	1-12	Left Posterior Hippocampus
Depth	F	1-10	Left Posterior STG – Insula
Depth	G	1-8	Left Supramarginal Gyrus
Depth	H	1-12	Left Basal Temporal
Depth	I	1-10	Left Pars Triangularis – Insula
Depth	J	1-10	Left Subcentral – Insula
Depth	K	1-12	Left Parietal Operculum
Depth	L	1-18	Left Posterior Oblique Insula

Figure 102. Case 2—SEEG implantation regime summary and fMRI results. A. illustrates all SEEG electrodes implanted, with the ones used for this study highlighted with pink letterboxes. Each blue dot presents a contact. Electrode I, J, K and F show light blue contacts in addition, which highlight contacts used for language stimulation during clinical assessment. Contacts surrounded by red circles represent the clinically defined SOZ. **B.** summarises the locations of the electrodes inserted, their labels and the electrodes used for language stimulation are circled in blue and **C.** illustrates language fMRI results during a covert verb generation task.
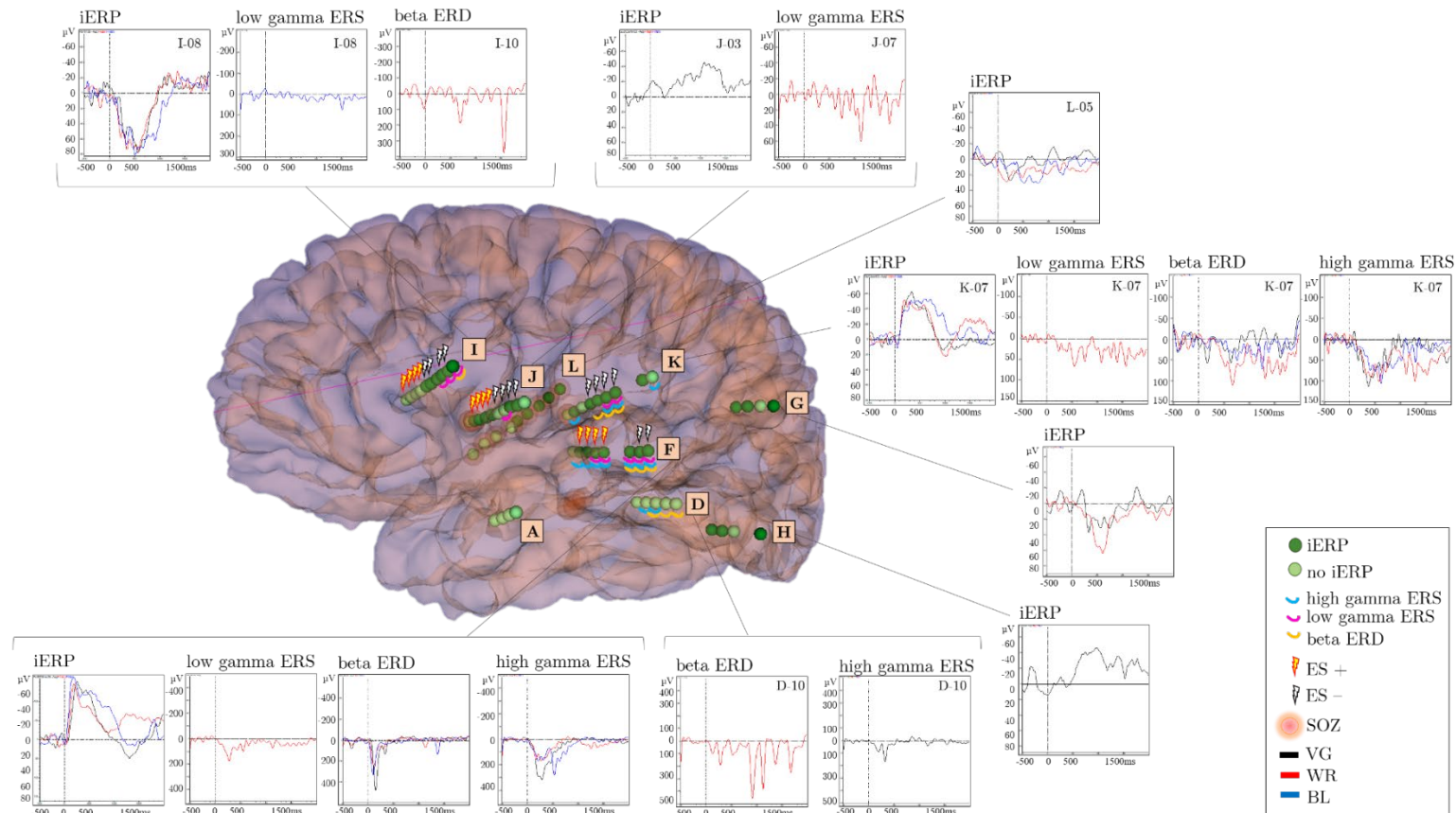
Figure 103. Case 2—Response summary. This summary includes the subset of contacts chosen for this study. Contacts showing iERPs are depicted in dark green and contacts without iERPs in light green. Contacts showing spectral changes are highlighted in either blue (high gamma ERS), pink (low gamma ERS) or yellow (beta ERD). Contacts showing a positive or negative response to electrical stimulation mapping are highlighted (red versus black). Contacts surrounded by red circles represent the clinically defined SOZ. For each electrode, the maximum iERP and/or spectral changes are illustrated.

For this patient's recording 64 contacts were chosen. Reporting results of three tasks (BL, WR and VG) leads to a total number of 192 contacts. Like for the group results reported previously, a higher number of contacts with iERPs was observed compared to contacts showing spectral changes. Furthermore, iERPs were observed in a wider area, while spectral changes were more localised. For clinical electrical language stimulation testing 26 contacts were chosen. Tasks used were an auditory listen and naming task, a picture naming task and reading task. Positive responses were hesitation or auditory hallucinations in response to electrical stimulation. Table 43 summarises the number of contacts showing iERPs and spectral changes and brain regions involved. This summarises activity, which was measured during at least one of the language tasks (see Appendix Figure 134 to Figure 137 for details).

Table 43. Overall occurrence of iERP, spectral changes and electrical stimulation responses for case ID8.

	No of contacts	No of ES+ contacts	No of ES– contacts	Brain regions
iERP	79 (41.2%)	8 (66.7%)	12 (66.7%)	STG_P, SMG, IFG, preC, MTG_A, MTG_P
High gamma ERS	28 (14.6%)	4 (33.3%)	4 (28.6%)	STG_P, SMG, INS_P, MTG_P
Low gamma ERS	11 (5.7%)	2 (16.7%)	7 (50.0%)	STG_P, SMG, IFG, preC
Beta ERD	20 (10.4%)	0 (0.0%)	5 (35.7%)	STG_P, SMG, MTG_P, IFG

For this patient iERPs were most sensitive in predicting ES+ contacts, while beta ERD and high gamma ERS were most specific. Table 44 summarises sensitivity and specificity analysis for the two active tasks word repetition and verb generation. The baseline task was not included in the table as it was a passive listening. Nevertheless, analyses for the passive listening task showed similar results.

Table 44. Relation between ES and iERP/spectral changes—sensitivity and specificity analysis for WR&VG for case ID8.

	iERP	Beta ERD_any	Low gamma ERS_any	High gamma ERS_any
Sensitivity	66.7%	0%	16.7%	33.3%
Specificity	14.3%	64.3%	64.3%	71.4%
PPV	40.0%	0%	28.6%	50.0%
NPV	33.3%	42.8%	47.4%	55.6%

Regarding language activity measured in the ictal onset zone, six contacts used for functional electrical stimulation were part of the seizure onset. Stimulating these contacts during language tasks led to hesitancy in replying to stimuli. Two of these contacts showed robust iERPs and none showed spectral changes.

In summary, this right-handed girl showed left lateralisation for language. Functional electrical stimulation confirmed language-related and essential areas in the left hemisphere and close to the planned resection area. iERPs were most reliable in predicting ES+ contacts. Spectral changes were only seen in a fraction of the stimulation positive contacts.

Case 3 (ID20)

Patient F. was a 14-year and 3 months old, left-handed boy with medication-resistant epilepsy. His seizures started at the age of 11 years and 1 month which were described as "zoning out" and he would have "odd feelings" in addition. His latest Type 1 episodes were auras, where he felt his head "pulsing" and his mind "slipping". His Type 2 seizures presented with increasing throbbing in the head, the inability to speak, grimacing and head drop with eye deviation to the right. These occurred up to seven times per week. Type 3 were bigger seizures, which started like Type 2 seizures and they then progressed with eye blinking or eye deviation upwards and to the right. He showed excessive salivation, lost strength in his legs, showed heavy breathing and shoulder spasms. His speech slurred for some time after the event. These seizures occurred once every ten days, on wakening.

The MRI and PET did not show a focal lesion. Scalp EEG suggested focal seizures with left hemispheric onset, which was close to the midline. However, a precise EEG onset was not found. Therefore, invasive monitoring was offered.

Patient F. was admitted to GOSH Koala ward for a left-sided SEEG implantation. In total, 15 electrodes were implanted. During SEEG monitoring seizure onset was consistently clinically silent. Clinical onset was observed with arousal (when asleep) or eye deviation to right with nystagmus (when awake). Electrographic onset indicated seizure onset in the parietal lobe and near but not directly from the superficial contact of electrode E (parietal lobe). However, areas further posterior were not covered. No seizures were elicited during electrical stimulation of the presumed onset contacts. To investigate language function an fMRI study was done. This resulted in a bilateral language activation. Functional language stimulation of contacts in the Broca's area and subcentral area during invasive monitoring led to dysphasia, feeling in his mouth and/or dysarthria with or without throbbing sensation in his mouth. Furthermore, he reported paraesthesia of his right side of the body and visual disturbances like at the start of his seizures when middle and superficial contacts of electrode E

(parietal lobe) were stimulated. His seizure onset was possibly close to E15–16, however, as there were no electrodes posterior or lateral to this electrode, the exact seizure onset zone could not be determined. Surgical resection was not offered.

For this study, the patient was able to complete six language tasks (BL, WR, VG, PN, CNw and LN). He achieved all points for word repetition, verb generation, picture and colure naming (100%) and reached 95% during the sentence task.

The clinical SEEG implantation regime is summarised in Figure 104. Seven electrodes were included for this study recording. Contacts included in the ictal onset were only partially used for the iERP recording. Contacts F3–5 were included while contacts E12–16 were not. The following Figure 105 illustrate the patient's implantation regime, contacts stimulated during functional electrical stimulation including electrical stimulation responses and iERPs and spectral changes elicited during the auditory word tasks (BL, WR and VG).

A.

B.

Electrode	Label	Contacts	Location
Depth	A	1-12	Left Supramarginal Gyrus
Depth	B	1-8	Left Post Infra Sylvian
Depth	C	1-15	Left Posterior Supramarginal Gyrus
Depth	D	1-12	Left STG
Depth	E	1-18	Left Posterior Oblique – Insula
Depth	(F)	1-10	Left Subcentral
Depth	(G)	1-10	Left Broca
Depth	H	1-10	Left Anterior STG
Depth	I	1-15	Left Middle Hippocampus
Depth	J	1-12	Left Posterior Temporal
Depth	K	1-12	Left TPO
Depth	L	1-18	Left Inferior Parietal
Depth	M	1-12	Left Middle Frontal Gyrus
Depth	N	1-15	Left Orbitofrontal
Depth	(O)	1-10	Left Pre-Broca

C.
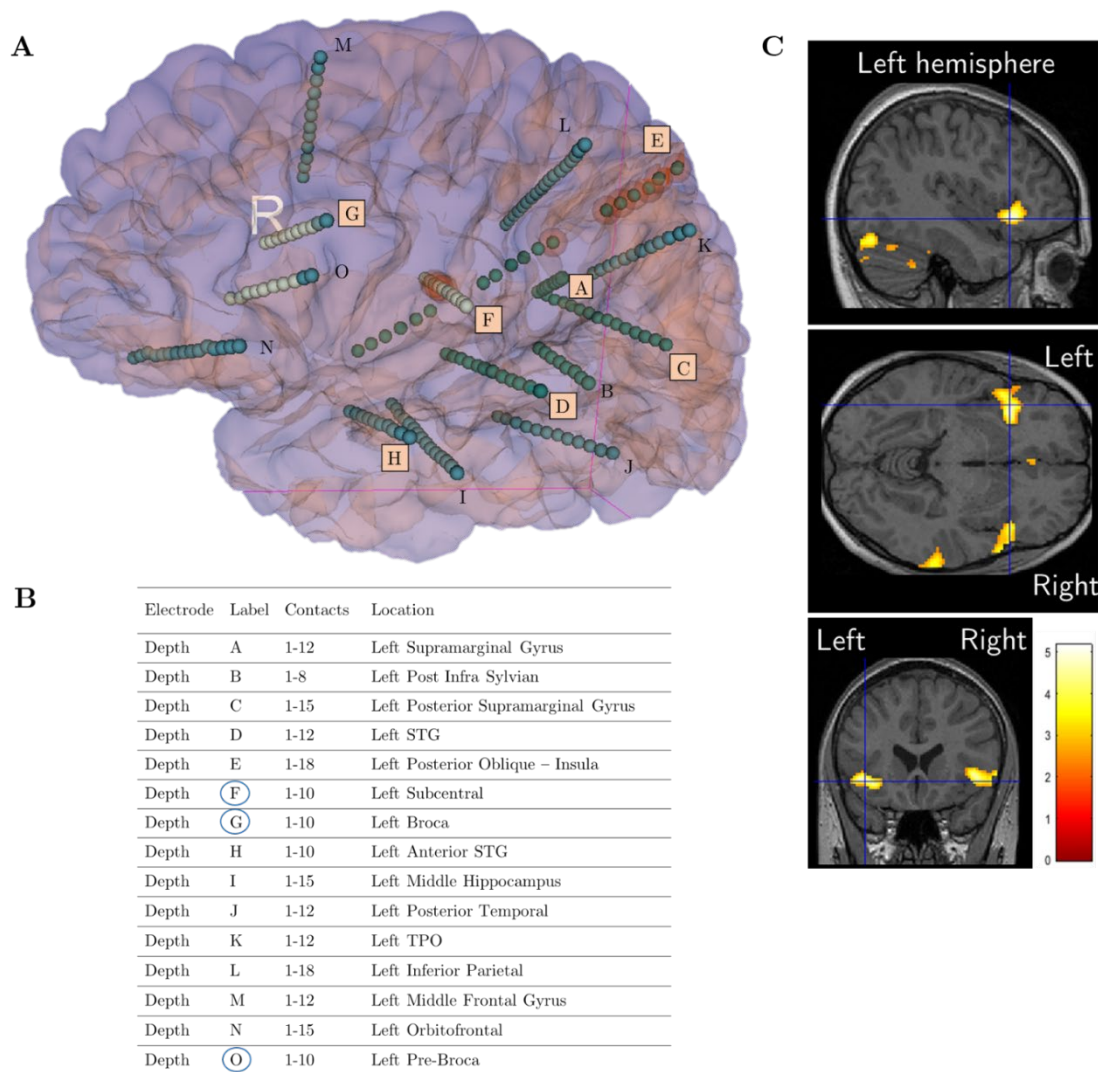
Figure 104. Case 3 (ID20)—SEEG implantation regime summary and fMRI results. A. illustrates all SEEG electrodes implanted, with the ones used for this study highlighted with pink letterboxes. Each blue dot presents a contact. Electrode D, E, F and H show light blue contacts in addition, which highlight contacts used for language stimulation during clinical assessment. Contacts surrounded by red circles represent the clinically defined SOZ. **B.** summarises the locations of the electrodes inserted, their labels and the electrodes used for language stimulation are circled in blue and **C.** illustrates language fMRI results during an overt verb generation task.
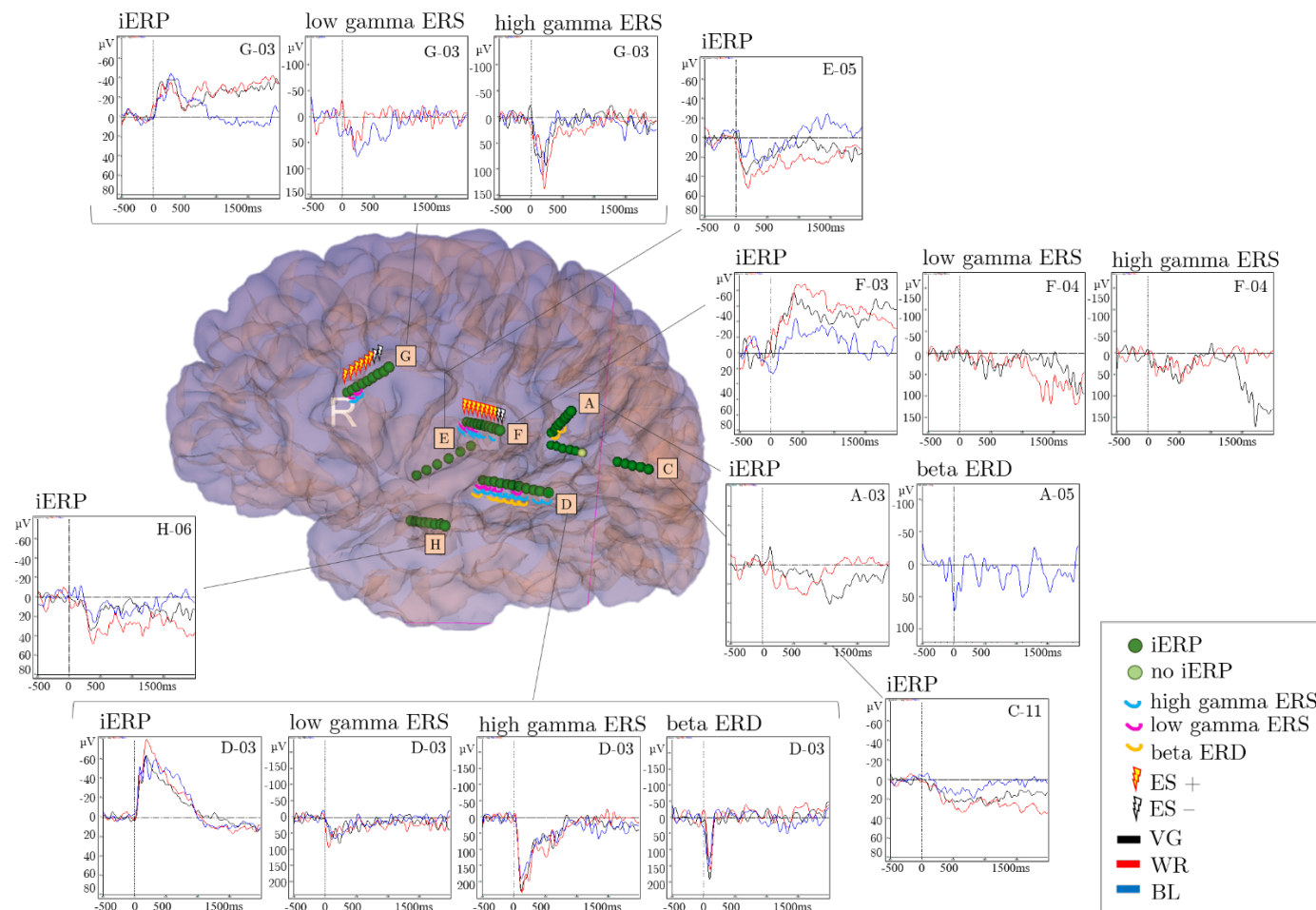
Figure 105. Case 3 (ID20)—Response summary. This summary includes the subset of contacts chosen for this study. Contacts showing iERPs are depicted in dark green and contacts without iERPs in light green. Contacts showing spectral changes are highlighted in either blue (high gamma ERS), pink (low gamma ERS) or yellow (beta ERD). Contacts showing a positive or negative response to electrical stimulation mapping are highlighted (red versus black). For each electrode, the maximum iERP and/or spectral changes are illustrated.

For this patient's recording 64 contacts were chosen. Reporting results of three tasks (BL, WR and VG) leads to a total number of 192 contacts. Like for the group results reported previously, a higher number of contacts with iERPs was observed compared to contacts showing spectral changes. Furthermore, iERPs were observed in a wider area, while spectral changes were more localised. For clinical electrical language stimulation testing 18 contacts were chosen for this study. Tasks chosen were a picture naming task and an auditory word repetition task. Positive responses observed were dysphasia, dysarthria and a feeling in her mouth with or without throbbing in response to electrical stimulation. Electrode O was also used for functional stimulation of this patient, however did not yield any language-related responses. It was not included in the study recording. Table 45 summarises the number of contacts showing iERPs and spectral changes and brain regions involved. This summarises activity, which was measured during at least one of the language tasks (see Appendix Figure 138 and Figure 139 for details).

Table 45. Overall occurrence of iERP, spectral changes and electrical stimulation responses for case ID20.

	No of contacts	No of ES+ contacts	No of ES– contacts	Brain regions
iERP	158 (81.0%)	14 (100%)	4 (100%)	STG_P, STG_A, INS_A, IFG, preC, MFG, MTG_A, INS_P, SMG, SPL
High gamma ERS	37 (19.0%)	7 (50.0%)	1 (25.0%)	STG_P, INS_P, preC, INS_A,
Low gamma ERS	19 (9.7%)	5 (35.8%)	0 (0.0%)	STG_P, INS_P, preC, INS_A,
Beta ERD	14 (7.2%)	0 (0.0%)	0 (0.0%)	STG_P, INS_P, SPL,

For this patient iERPs were most sensitive in predicting ES+ contacts, while beta ERD and low gamma ERS were most specific. Table 46 summarises sensitivity and specificity analysis for the two active tasks word repetition and verb generation. The baseline task was not included in the table as it was a passive

listening. Nevertheless, analyses for the passive listening task showed similar results.

Table 46. Relation between ES and iERP/spectral changes—sensitivity and specificity analysis for WR&VG for case ID20.

	iERP	Beta ERD_any	Low gamma ERS_any	High gamma ERS_any
Sensitivity	100%	0.0%	28.6%	50.0%
Specificity	-	100%	100%	75.0%
PPV	100%	-	100%	87.5%
NPV	-	22.2%	28.6%	30.0%

Regarding language activity measured in the ictal onset zone, only three contacts were included in this study. All these contacts showed robust iERPs during all three language tasks. Stimulating these contacts during language tasks led to dysarthria and a feeling in his mouth with or without throbbing.

In summary, this right-handed boy showed bilateral activation of language. Functional electrical stimulation confirmed language-related and essential areas in the left hemisphere. iERP testing showed language-related activity in more contacts than did electrical stimulation. Spectral changes were only seen in a fraction of the stimulation positive contacts. It is obvious that both analyses add valuable information to localising language areas.

6.4 Discussion

Prior to any surgical resection in epilepsy patients, pre-surgical evaluation is undertaken to delineate the seizure onset zone and eloquent areas to minimise the risk of neurological and cognitive deficits post-surgery. Currently, especially high gamma activity is studied in relation to cognition and its use in predicting post-surgical language outcome. Besides frequency activity, ERPs are a well-known neurophysiological measure to study cognitive processes. Which one of these markers is more sensitive in predicting post-surgical cognitive outcome is a matter of ongoing research. The current study showed that during language processing spectral changes in the beta, low and high gamma band were elicited from perisylvian as well as additional brain regions, however, in number significantly lower than iERP responses. In contrast, speech response activation, studied in a subgroup of patients, was similar for both neurophysiological responses. Brain regions activated during language processing and production were similar using induced versus iERP responses. Furthermore, the majority of contacts measuring spectral changes also showed iERPs (6.4%), while only a few did not (0.5%; contacts measuring only iERPs=50.5%). In addition, the current study presented a preliminary exploration of the relation between ES and ERD/S and iERPs in a subgroup of patients who underwent functional electrical stimulation for language. A weak positive correlation of high ERS– with ES+ and weak negative correlation with beta ERD+ could be shown.

In the following sections, I will discuss the occurrence and localisation of beta ERD, low and high gamma ERS and compare results to iERP data of the previous chapter. Furthermore, I will summarise the concordance of both neurophysiological markers and the relation to electrical stimulation responses and will discuss results in light of the presented case studies.

6.4.1   Region-specific   and   region-   and   task-specific spectral changes and comparison with iERP

Addressing Aim 1 and 2: *Characterise the topography of beta, low- and high-gamma frequency band activity across the sample and characterise the differences and concordance between evoked and induced activity.*

A main result of this work is the overall significantly greater prevalence of iERPs compared to spectral changes, during both auditory and visual tasks. The majority of previous studies have examined gamma ERS only, especially high gamma ERS with one study examining both. Sinai and colleagues (2009) studied the co-occurrence of evoked and induced responses in adult epilepsy patients undergoing extraoperative electrical stimulation for pre-surgical motor and language mapping. The sample size was small with testing six patients and language tasks used were tone and syllable paradigms. They reported induced activity in 12 of 120 electrode sites across patients compared to 28 sites showing evoked responses. Sinai and group sampled from perisylvian brain areas, including the posterior superior and middle temporal gyri, the anterior temporal lobe, the parietal lobe and the inferior frontal lobe. Both electrical changes measured in this study showed a similarly broad distribution, reaching perisylvian and additional brain regions; however, the number of contacts showing induced spectral responses in all sampled brain regions was smaller. They consistently observed broadband spectral changes (40–250 Hz) with the greatest power changes occurring in the high gamma range (around 100 Hz). These findings are generally in line with results of this study. The overall differences between evoked and induced responses described by Sinai and group (2009) could be shown in this study in all three frequency bands—beta ERD, low gamma ERS and high gamma ERS. In addition, this current paediatric study showed that the difference between evoked and induced responses could be observed in more brain regions than described by Sinai and group (2009).

Next, I would like to focus on brain regions involved during auditory and visual tasks. Auditory word tasks yielded the highest amplitude and earliest onset for

all three spectral changes in the posterior STG. This is in agreement with results from iERP analysis of the previous Chapter 5 and previous studies on language-related spectral modulation (N. E. . Crone et al., 2001; Sinai et al., 2005; Towle et al., 2008) and indicates activation of the primary and secondary auditory cortex as well as more posterior temporal auditory areas. Furthermore, like in the previous study, widespread areas were activated, including the supramarginal gyrus and the middle temporal gyrus, which is suggestive of activation in Wernicke's and surrounding areas (Mesulam, Thompson, Weintraub, & Rogalski, 2015; Wernicke, 1874). In addition, the inferior frontal gyrus was highly activated, suggesting the involvement of Broca's area.

During visual tasks, fewer brain regions showed spectral changes, with less frequency activity measured compared to auditory tasks and no task-related differences observed. The inferior temporal gyrus together with the fusiform gyrus showed the highest level of activation during visual tasks. This result ties well with previous studies wherein the so-called baso-lateral temporal language area, which includes the inferior temporal and fusiform gyri, show high engagement during visual word tasks (Edwards et al., 2010; Hart et al., 1998). These patterns are in agreement with iERP results discussed in the preceding chapter. Language-related results of the present study overall confirm previous findings reporting broad-band gamma increases during language tasks, as activity was observed between 30–110Hz (N. E. . Crone et al., 2001; Towle et al., 2008) and beta decreases as ERD was observed between 15–25Hz (Arnal, Wyart, & Giraud, 2011; Fujioka, Trainor, Large, & Ross, 2009).

Following the discussion of the involved brain areas, I would like to reflect on the three frequency bands in more detail. Beta ERD is best known for its role in motor processes, however production of language was also shown to be associated with a decrease in beta activity using scalp EEG and MEG (Pfurtscheller & Lopes da Silva, 2017; S. Weiss & Mueller, 2012). Although it is called desynchronization, it represents an activation of cortical neurons (Steriade, Gloor, Llinás, Lopes da Silva, & Mesulam, 1990) and is described as

a state of maximal readiness to process information (Thatcher, McAlaster, Lester, Horst, & Cantor, 1983). Engel and Fries (2010) showed that beta increased if the current cognitive state had to be maintained and beta decreased once novel or unexpected stimuli had to be processed.

Far more studies examined the role of gamma ERS in language processing and reported that high gamma ERS was superior to low gamma ERS in localising functional brain areas and that it was more robust (Cervenka, Franaszczuk, et al., 2013; N. E. Crone et al., 2011; N. E. Crone, Miglioretti, Gordon, & Lesser, 1998). Hence, it was proposed that high gamma ERS was a more reliable marker of cortical activation (Cervenka, Corines, et al., 2013; Cervenka, Franaszczuk, et al., 2013).

During auditory word processing beta ERD as well as low and high gamma ERS were first observed in the posterior STG (<100ms). This early activity can be interpreted in view of the current proposed framework of language processing with a dorsal and a ventral pathway being responsible for auditory-motor mapping and sound-meaning mapping, respectively (Poeppel & Hickok, 2004). Primarily, as discussed in the previous Chapter 5, the posterior STG is involved in speech perception. In this study, this brain region showed the highest occurrence rate of spectral changes in response to auditory word task for all three frequency bands. Beta ERD followed both the dorsal and the ventral stream showing primary (<100ms), early (100–200ms) and later activation in the supramarginal gyrus, the precentral gyrus and the inferior frontal gyrus as well as in the posterior middle and inferior temporal gyrus and the anterior STG. In contrast, primary and early low and high gamma ERS followed the dorsal route only. Like beta ERD, gamma ERS also showed early activation in the anterior and posterior insula. Only middle and late latency activity in the low and high gamma bands were observed in a few brain regions of the ventral stream, including the posterior middle temporal gyrus, the inferior temporal gyrus and the anterior STG. This study shows that primary and early beta ERD occurs in a wider area compared to gamma ERS, which was more focal. In their review

about beta oscillations Weiss and Mueller (2012) reported that beta synchronises over long distances while gamma was more local. This study furthermore analysed the co-occurrence of the three frequency bands for all contacts and showed that low and high gamma ERS co-occurred more frequently than beta ERD with low and high gamma ERS. This suggests that different cell assemblies in the studied brain regions are oscillating on different frequencies and that including beta ERD can add further knowledge to language processing. In line with my findings Fries (2005, 2015) and Engel and Fries (2010) proposed a balanced interplay of various frequency bands for effective neuronal communication, which I will summarise in a simplified manner here. Alpha band activation was suggested to be the default setting for holding the system stable and flexibly accessible. Attention was associated with theta oscillations. Beta-band activity was associated with maintaining the current sensorimotor or cognitive state, while beta decreased once the system expected change. Once a stimulus was adhered to, stronger higher-frequency gamma band synchronisation was observed. Alpha-beta band activity was conveying top-down information and influencing bottom-up directed gamma-band activity.

Compared to auditory tasks, visual tasks did not elicit primary spectral changes in any frequency band studied (beta ERD, low and high gamma ERS) which was expected as primary visual cortex was not sampled from. Early activity (100–200ms) was observed however. These spectral changes occurred in the same brain regions as during auditory tasks.

The spectral findings of this study partly agree with iERP results from the previous study. There the posterior STG and the posterior insula were involved first during auditory word processing, while in the current study the posterior insula rarely showed early spectral changes. Furthermore, iERP results showed robust activation following both streams, the dorsal and the ventral. In this study, spectral changes were observed in the posterior STG as early as <100ms, while brain regions involved in language perception and integration reported in other studies showed high gamma ERS initially between 200–500ms post-stimulus (N.

E. . Crone et al., 2001; Edwards et al., 2010; Anaïs Llorens et al., 2011; Pei et al., 2011; Towle et al., 2008). Further involved brain regions were similar including the superior temporal sulcus, the left frontal lobe and the peri-rolandic areas. Like in this study, the regions that were found activated, increased as time post-stimulus passed on. These authors observed later activation, occurring between 500–800ms post-stimulus in addition in the supramarginal gyrus and a wider part of the peri-rolandic areas, which is in line with results of this study showing later activation in these areas.

In general, insular beta or gamma changes during language processing were rarely reported by other studies, as most groups in this field used ECoG recordings compared to SEEG recordings and did not sample from deep structures (N. E. . Crone et al., 2001; Edwards et al., 2010; Pei et al., 2011; Towle et al., 2008). To my knowledge, there is no study examining beta ERD and language processing using SEEG. There is one study, which mapped cortical areas responsive to a phonemic fluency task in epilepsy patients admitted for SEEG recording. They analysed frequency changes in the range between 1–250 Hz and demonstrated an increase of beta-gamma frequencies (20–40 Hz) in language regions, especially Broca's area of the dominant hemisphere (Pastori, Francione, Pelle, de Curtis, & Gnatkovsky, 2016). However, studies investigating beta ERD in the context of language processing in patients with SEEG implantation could not be found.

Previous research on language mapping using MEG showed that beta ERD is strongly lateralised during language processing (A. E. Fisher et al., 2008). Recently, several groups using MEG to map language cortex showed that beta ERD can reliably be used to establish language lateralisation in epilepsy surgery patients (Foley et al., 2019; Tierney et al., 2018; Youssofzadeh et al., 2020). The current SEEG results cannot yet be used to indicate the language dominant hemisphere, nor to reliably localise essential language areas.

6.4.2 Speech-response spectral changes and the differences to iERP results

Addressing Aim 3: Characterise speech-response ERS/D and demonstrate differences to iERPs across the sample.

Speech production is a complex process and some of the first neurophysiological studies involved stimulation of speech- and movement-related brain regions and cortical lesion studies (Foerster & Penfield, 1930; Penfield & Boldrey, 1937). Functional neuroimaging studies facilitated the understanding of speech and language associated brain regions. Regions involved in speech production were the inferior frontal gyrus, the anterior insula, the premotor cortex and SMA unilaterally and the primary motor cortex bilaterally. Furthermore, several subcortical areas, such as the posterior pallidum, putamen and the hippocampus are associated with production of speech (Hamamé, Alario, Llorens, Liégeois-Chauvel, & Trébuchon-Da Fonseca, 2014; Price, 2012; Wise, Greene, Büchel, & Scott, 1999). Studying language processing using intracranial EEG resulted in a similar pattern of associated brain regions. At motor speech response onset high gamma activity sustained in similar regions as during language perception and integration, namely the superior temporal gyrus and sulcus, peri-rolandic areas, supramarginal gyrus and inferior frontal gyrus. The inferior frontal gyrus was highly activated prior to response onset during preparation to respond. This activation shifted and decreased with motor speech response onset suggesting not being involved in motor speech response to the same extent as during preparation for speech response (Edwards et al., 2010; Fukuda et al., 2010; Anaïs Llorens et al., 2011; Towle et al., 2008). Crone and colleagues (2001) presented an ECoG case study comparing gamma frequency activation using visual and auditory stimuli during speech production and sign language in an epilepsy patient. The patient was a native English speaker and a professional sign language interpreter, who learned sign language in her adult life. As expected, spoken and signed word production activated different sensorimotor region, tongue and hand region, respectively. Like in the current study, the posterior

331

STG showed the highest and earliest activation during listening to the stimulus, while signed output led to increased activation in the parietal regions compared to speech production. In a subsequent event-related causality analysis investigating functional interactions between brain regions during cognitive processing, the group confirmed their findings and showed in addition that regions with highest high gamma power showed most prominent causal interactions and that electrical stimulation of these contacts led to interference in word production (Korzeniewska, Franaszczuk, Crainiceanu, Kuł, & Crone, 2011).

Results of the current study are in accordance with previous functional imaging and neurophysiology results showing frequency activation in the same brain regions. However, results concerning the extent of spread of different frequency bands in this study were not in line with previously published work. Toyoda and colleagues (2014) showed that low frequency activity in the beta band in response to speech production was more widespread than gamma augmentation (70–110Hz). Differences between the frequency bands in the current study were rare and selective concerning only the postcentral gyrus with increased high gamma activity compared to low gamma activity. No other differences in frequency band patterns were observed. Compared to stimulus-locked activity, where iERP activity was significantly more widespread than that of induced beta and gamma activity, response-related activation was of similar distribution for both neurophysiological responses.

6.4.3 Concordance of evoked and induced language-related activity and the relationship to electrical stimulation responses

Addressing Aim 3: Characterise concordance of iERP and ERS/D topography in a clinical context on an individual case basis.

Evoked ERPs and induced frequency activity was previously mostly investigated separately of each other. The current study mapped the concordance of iERPs and spectral changes. As already discussed before, the majority of contacts measured language-related iERPs and only a small proportion of them showed spectral changes in the three frequency bands. Further analysis showed that most of the brain areas eliciting spectral changes also showed iERPs. During auditory tasks the majority of contacts showed co-occurring gamma ERS and iERPs, while for visual tasks contacts showed higher concordance of iERPs and beta ERD. One of the few studies studying both evoked and induced activity during language processing investigated the basal temporal language area (BTLA) in a patient with epilepsy using invasive EEG recordings (Trébuchon-Da Fonseca et al., 2009). The group showed that BTLA, comprising the fusiform gyrus, parahippocampal gyrus and inferior temporal gyrus was sensitive to auditory and visual language stimuli measuring both neurophysiological changes in a closely circumscribed region of the left BTLA. A further study by Lachaux and co-workers (2005) using both ERPs and gamma band changes in response to visual stimuli showed that both neurophysiological changes were elicited in the same region of the fusiform gyrus. The task included detecting hidden faces in a high-contrast background. This study further showed that morphologically identical ERPs were elicited independent of whether the face was detected by the participant or not. Gamma band activity, however, was shown to be stronger when faces were detected.

The use of iERPs in mapping eloquent areas for pre-surgical evaluation is rare, with only a few groups implementing this method (Trébuchon et al., 2013b). Recently, Lachaux and colleagues (2012) have elaborated on the mechanisms of

iERPs and high frequency activity (HFA, between around 40–150 Hz) with the following conclusions. Both have contrasting mechanisms, where HFA is generated by short lasting synaptic events, depending on synchronisation within a few milliseconds. In contrast, iERPs are generated by long lasting synaptic events, which showed linear summation and a timing varying by tens of milliseconds. Besides the differing frequency content, local field potential generation was different, leading to smaller local field potentials and hence lower amplitudes for HFA and higher amplitudes for iERPs (J.-P. Lachaux et al., 2012). They recommended the use of HFA over iERPs to study neural bases of human cognition with intracranial EEG, stating that for iERPs the underlying direction of the electrical signal—i.e., whether excitatory or inhibitory post-synaptic currents were measured—was unknown. Furthermore, they argued, that iERPs were inferior to HFA due to: 1) their polarity dependence on electrode location, and 2) that when using iERPs one can only rely on the timing and relative amplitude and 3) that iERPs are phase-locked which leads to information reduction in comparison to induced HFA (J.-P. Lachaux et al., 2012).

A few studies on visual perceptual processing compared induced and evoked activity and showed varying results. Fisch and co-workers (2009) reported an increase of gamma power (30–70 Hz) and evoked activity in visual areas of the occipito-temporal cortex observed in response to successful recognition of visual stimuli. Regarding co-occurrence of evoked and induced activity again in response to visual stimuli, Vidal and colleagues (2010) showed only a small spatial overlap (<10%) between gamma band activity, alpha and beta band responses and ERPs. These results are not in line with results presented in this study. However, different modalities were investigated, which might be the reason for the differing results. Another study analysing the co-occurrence of ERPs and gamma band activity in response to a visual paradigm was done by Engel and group (2012). In addition, they included fMRI BOLD signals and showed a tight coupling of gamma power and hemodynamic activity in the peri-calcarine cortex, the fusiform gyrus and the lateral-temporal-occipital cortex. Such a relationship could not be shown for ERP and BOLD signals.

Another body of research focuses on the concordance of gamma band activity and electrical stimulation responses mapping to facilitate the delineation of eloquent cortex. Several groups reported the added value of high gamma activity for localising eloquent areas in patients with epilepsy evaluated for surgical resection (Asano, 2017; Genetti et al., 2015; Kojima et al., 2012; Sinai et al., 2005). Arya and group (2018; 2017, 2015; 2018) investigated high gamma augmentation and its concordance with electrical stimulation results in a paediatric population with drug-resistant epilepsy. They used several language paradigms, including passive listening, picture naming, and spontaneous conversation. Their results showed high specificity, but low sensitivity of high gamma augmentation for language localisation compared to electrical stimulation when using cued language tasks, like picture naming. However, cortical responses to spontaneous conversation showed a higher sensitivity and negative predictive value of high gamma augmentation compared to electrical stimulation. Overall, they argued that the high gamma method could be used to guide electrical stimulation mapping, improve its safety and reduce the time needed. Furthermore, they stated that ECoG mapping of spontaneous language might become a useful clinical tool for language localisation.

To my knowledge, the current study is the first paediatric study analysing language related spectral changes in SEEG data and comparing results to functional electrical stimulation responses. Compared to functional mapping using ECoG, where two-dimensional seizure and functional maps of cortical stimulation responses are compared, electrical stimulation using SEEG does not provide such a map. In contrast, SEEG aims to get information on spatio-temporal dynamics of the seizure and functional networks (Trébuchon & Chauvel, 2016). Due to individual variation in the distribution of language networks language ES testing with SEEG is a challenge (George, Ojemann, Drees, & Thompson, 2020). In addition, stimulating contacts located in different but adjacent brain regions or being located close to white matter tracts leads to stimulation responses that might be hard to interpret (Borchers, Himmelbach, Logothetis, & Karnath, 2012) .

335

The current study presented a preliminary exploration of the relation between ES and ERD/S and iERPs in a subgroup of patients who underwent functional electrical stimulation for language. Only three of the seven patients showed positive electrical stimulation responses. A weak positive correlation of high ERS– with ES+ and weak negative correlation with beta ERD+ could be shown. No relation was observed for low gamma ERS and iERPs. These co-occurrence results are not in line with previous research, as discussed above. Previous studies reported higher sensitivity of high gamma ERS+, especially using spontaneous language (Arya et al., 2015). All of those studies used ECoG recordings. Subdural electrodes have a higher spatial density on the cortex and are thus able to cover a functional area more comprehensibly than SEEG. However, the number of subdural electrodes is generally much lower compared to SEEG electrodes and hence during ECoG a higher proportion of the total number of contacts gets stimulated (Tassi et al., 2016). Hence, current results need to be interpreted in light of the whole number of SEEG contacts implanted, as a high number of SEEG contacts did not get stimulated and did not show ERD/S. Furthermore, functional tasks used for electrical stimulation and the study tasks did not always overlap. Arya and group used different modalities in one study, choosing picture naming for ES and quiet baseline and story listening for high gamma ERS mapping (2018), while in another study they used the same task, open conversation, for both investigations (2015). Both studies argued that high gamma ERS was a specific determinant of ESM language sites and furthermore during the conversation task sensitivity of HGM increased.

6.5 Limitations and consideration

The results of the current study should be interpreted in light of some limitations and practical issues discussed in the following section.

Limitations of this study overlap with the ones of the previous study. Shortly, these included first, the limited number of amplifier channels available for recording spectral changes. In most patients' channels had to be discarded as the

Neuroscan SynAmps[2] was only able to record from 64 channels. I preferentially chose contacts in traditional language areas, the perisylvian regions compared to contacts in other brain regions. This suggests that the findings may underestimate the areas activated by speech perception and speech production.

Second, in some cases I included contacts showing some interictal epileptiform activity, which might have contaminated the gamma band responses.

Third, language lateralisation information was only available for a few patients; hence, conclusions whether spectral changes were observed in areas essential for language could not be made.

Fourth, the group of included patients was heterogeneous. Patients varied in age (5–17 years), some showed lesional and some non-lesional epilepsy, a few underwent prior epilepsy surgery and a few patients were evaluated for language localisation and underwent electrical stimulation mapping for language localisation. Although this study focused on within-patient comparisons, the relatively small number of patients imposes a limitation on the generalizability of results.

To conclude, in this study I recorded and analysed cortical dynamics during speech perception and speech production to gather information about language networks using beta ERD, low gamma ERS and high gamma ERS measured in children and adolescents with SEEG monitoring. As in previous studies and the study presented in Chapter 5, I could show that generators of language-related spectral changes during auditory and visual language stimuli showed a widespread distribution, including cortical and subcortical regions (Bares & Rektor, 2001; Halgren et al., 1995, 1998). The current study furthermore focused on identifying differences between evoked iERPs and induced spectral responses and showed that significantly less induced compared to evoked activity was observed during language perception and processing, but not during speech production. iERPs and spectral changes indicated the same brain regions during language processing and speech production. Contacts showing spectral changes

also showed iERPs in the majority of the contacts included. Contacts showing low and high gamma ERS co-occurred more frequently than low and high gamma ERS with beta ERD. Lastly, comparing contacts used for electrical stimulation and iERP and ERD/S responses showed a weak positive correlation of high gamma ERS– and a weak negative correlation with beta ERD+. The case presentations reported here made clear that this patient population is heterogeneous and language lateralisation or electrical stimulation mapping is still of essence to draw conclusions on language areas being essential and to estimate the risk of language deficits before surgery.

IV OVERALL DISCUSSION

7 Overall Discussion

7.1 Introduction

With 1% of affected children and adolescents, epilepsy is one of the most common neurological diseases in the paediatric population (Russ et al., 2012). Despite the emergence of new antiepileptic drugs about 25-30% of patients progress to drug-resistant epilepsy (Dichter & Brodie, 1996; Picot et al., 2008). For patients with focal epilepsy, epilepsy surgery, including resection and disconnection approaches to remove epileptogenic tissue or disrupt epileptogenic networks provides a safe treatment. Post-surgical outcome is highly dependent on accurate localisation of brain areas generating seizures and functional brain areas. Current recommendations include early referral to pre-surgical assessment (J. H. Cross et al., 2006). Evaluating children and adolescents of different ages and cognitive skills leads to the necessity of finding new methods to aid detection of the seizure onset as well as facilitating methods to delineate eloquent cortex. Current methods to localise functional cortex such as electrical stimulation mapping, fMRI or Wada test require compliance and a certain level of cognitive skills. Furthermore, a recent shift from subdural to SEEG investigations for seizure onset localisation, as epilepsy poses a network disorder, led to the question of how to "map" function compared to subdural electrode studies.

The body of work presented in this thesis attempts to progress understanding of both seizure onset localisation and detection of language cortex. This involved the application of a set of neurophysiological methods, which were recently proposed to improving post-surgical outcomes in adults. While the focus of this thesis is on paediatric epilepsy, the work included in Chapter 2 is a pilot study utilising adult data from the Montreal Neurological Institute and was completed whilst on a fellowship under the supervision of Professor Jean Gotman. The analyses trialled in this adult epilepsy work were then applied to paediatric data in Chapter 3. Besides detecting epileptogenic tissue, the second part of the thesis,

focused on developing tools to improve the detection of language cortex for the use in the pre-surgical evaluation of patients, which is described in Chapter 4–6

.

7.2 PLHG and fast ripples to delineate the seizure onset zone—an adult and a paediatric cohort

7.2.1 Main Findings and clinical implications

1. **Reproducibility of PLHG recruitment.** Both the adult and the paediatric studies, described in Chapter 2 and Chapter 3, respectively, proved that PLHG results, reported by Weiss and colleagues (2015) were reproducible in independent cohorts of patients with drug-resistant epilepsy despite using a different invasive implantation technique, SEEG.

2. **Reproducibility across seizures.** The studies described in Chapter 2 and 3 resulted in PLHG recruitment patterns with good agreement in all three seizures. Hence, the PLHG metric was stable across seizures of a specific type.

3. **Temporal and spatial relationship of PLHG recruitment and ictal sharp activity.** In the adult study in Chapter 2, the occurrence of sharp activity before PLHG recruitment of channels was also considered, because sharp activity is used in clinical practice for visual delineation of the SOZ. Results suggested a greater accordance of PLHG recruitment and ictal sharp activity at the seizure onset rather than during seizure evolution. Furthermore, sharp activity was more widespread across contacts compared to more focal PLHG recruitment. Results suggested a close relationship between the two metrics; however, they arguably capture different aspects of seizure evolution.

4. **PLHG/SOZ overlap was predictive of post-surgical outcome.** For the adult cohort no surgical resection data was available and the independent SOZ definition substituted as a proxy for the likely resection area. PLHG/SOZ

overlap results showed that early PLHG3–7 channels were superior to later appearing PLHG channels in predicting a good post-surgical outcome (Chapter 2). These results were partly confirmed by the paediatric study. Results showed that PLHG/SOZ overlap of PLHG3 channel alone was predictive of post-surgical outcome (Chapter 3).

5. **PLHG classifier accuracy.** For the paediatric cohort resection data was available for analysis of the predictive value of resected PLHG channels on post-surgical outcome (Chapter 3). Contrary to Weiss and colleagues (2015), the results of the paediatric study did not show an improved outcome classification using PLHG1–10 recruitment compared to standard clinical SEEG reporting data.

6. **Fast ripple (FR) classifier accuracy.** Resection of contacts containing fast ripples alone also did not lead to an improvement in post-surgical seizure outcome. Combing fast ripple and SOZ information (S $\cup$ F), however, improved accuracy when comparing paediatric patients with good and poor Engel outcome (Chapter 3).

7. **Combining all three markers was not predictive of post-surgical outcome.** A combination of three measures—PLHG recruitment, SOZ information (derived from standard clinical SEEG reporting) and detection of fast ripples—did not result in an improvement in prediction accuracy compared to using each measure independently (Chapter 3).

The two studies presented in Chapter 2 and 3 demonstrated that the PLHG metric can be implemented effectively using SEEG data of both adult and paediatric cohorts. Comparison of the two studies highlighted the fundamental differences between the two cohorts. First, the number of implanted electrodes varied. For the adult cohort a maximum of nine electrodes were implanted compared to 17 electrodes in the paediatric group. This might be due to diverse aetiology of adult onset epilepsy and epilepsy in children. While adults in general showed higher numbers of acquired pathologies, like mesial temporal sclerosis, brain tumour, stroke and immune related pathologies, children presented with developmental

malformations, genetic and metabolic disorders (Cloppenborg et al., 2019; K. H. Lee, Lee, Seo, Baumgartner, & Westerveld, 2019). Aetiologies in the current studies were in line with previous findings. Furthermore, lesions and SEEG results were more circumscribed in the adult cohort compared to children and adolescents, which was also shown in adult patients having similar brain regions implanted. Five of the eight adult MNI patients underwent selective amygdalohippocampectomy, which all resulted in good outcome (four patients = Engel I, one patient = Engel II). In contrast, in the paediatric cohort surgical procedures were more extensive and showed increased variation. Furthermore, the paediatric cohort included a few patients with previous resections and a few patients where the main aim was of palliative rather than of curative nature, which implied an underlying broad epilepsy network and hence poorer seizure outcome.

As those two studies were the first replication studies using the PLHG metric, one aim was to demonstrate stability of the PLHG metric. This was done by selecting seizures of the same seizure type for analysis. Three seizures with similar focal onsets were used, which was a different proceeding compared to Weiss and colleagues (2015). The group included the first three consecutive seizures, even if they were described as atypical seizures. Testing the stability of the metric was a pivotal aim here to gain confidence in the PLHG metric. Both studies highlighted the good agreement of PLHG recruitment patterns between seizures. Future studies implementing the PLHG metric should include seizures of various seizure types, both typical and atypical seizures to capture a wider seizure network.

As mentioned above, for the MNI adult cohort the clinically defined SOZ was taken as a proxy for the surgical resection. For comparison, the same analysis was also done for the paediatric cohort. Findings of the two studies suggested that the core area, the region initially invaded by the seizure, is of greatest interest for epilepsy surgery compared to late invaded regions when taking the overlap of PLHG and SOZ into account, but not the actual resection information. When

resection information was added to the PLHG and SOZ data for the paediatric cohort, no improvement of prediction accuracy was shown. This must be seen in light of the different aims in the paediatric cohort. As previously mentioned either a curative or a palliative approach was used. This means that although some channels were defined as both SOZ and PLHG recruited they did not get resected. Reasons for non-resection, like localisation in eloquent cortex and their effects need to be studied further. Furthermore, the combination of PLHG and SOZ seemed to be of importance, as SOZ alone was not a good outcome classifier in the paediatric study. This was because the SOZ/Resection overlap did not differ between patients with good compared to poor outcome. This result was not in line with results by Weiss and colleagues (2015) who reported SOZ resection as an effective classifier of seizure outcome.

Fast ripple results of Chapter 3 contributed to the evidence base in this field and again, the seizure onset zone was shown to be of importance for improving outcome prediction. However, FRs were detected in interictal EEG sampling during slow-wave sleep, contrary to PLHG and SOZ information, which was derived from ictal recordings. The paediatric study showed that the combination of FR and SOZ information improved post-surgical outcome, while FR resection alone or SOZ resection alone did not. In line with this, Nevalainen and colleagues (2020) recently argued that failure to observing channels with high FR rates during SEEG is a poor prognostic factor, most likely highlighting poor spatial sampling or multifocal seizure onsets. The present work supports the incorporation of FR detection into the pre-surgical evaluation of children with epilepsy at Great Ormond Street Hospital and in other epilepsy centres.

7.3 iERPs and spectral changes to map language areas

7.3.1 Main Findings

1. **Overall, during auditory and visual tasks a significantly higher number of evoked responses was observed compared to induced spectral responses.** (Chapter 5 and 6)

2. **Auditory word processing.** Chapter 5 and 6 showed the highest level of activation focusing around the perisylvian brain regions. Additional brain regions also showed auditory word related activation, which was true for evoked and induced responses. The earliest activation was observed in the bilateral posterior STG for both evoked and induced responses. Different activation pattern was found in the posterior insula, with iERPs being observed as early as <100ms post stimulus, while frequency changes were observed later in time and occurred less consistently. For iERPs and beta ERD information flow continued along two parallel streams. The dorsal stream, which involved early activation of the supramarginal gyrus, the postcentral gyrus, the precentral and inferior frontal gyrus. Along the ventral stream, early auditory input-related activity was followed by later latency activity in the middle and superior temporal gyri. In contrast, low and high gamma ERS followed the dorsal route only.

3. **Auditory sentence processing.** Chapter 5 reported fewer overall contacts showing iERPs during sentence processing compared to auditory word processing, although cognitive demands increased. However, similar regions were activated by both tasks. One exception was the anterior STG, which did not show any activity during sentence comprehension, but robust word task related activity was observed. This finding was not in line with previous studies reporting that the anterior STG was more sensitive to sentence meaning over word meaning (DeWitt & Rauschecker, 2013b; Scott, Blank, Rosen, & Wise, 2000). However, as discussed in Chapter 5, several factors might have influenced this

negative finding, inter alia the small number of patients sampled from the anterior STG and the increased cognitive abilities necessary for the sentence task compared to the word tasks.

4. **Task specific differences between auditory stimuli.** The passive baseline task elicited the least iERPs and showed morphologically different features regarding peak amplitude, peak latency or shape differences compared to the active word repetition and verb generation tasks. These variations, however, were not region specific. Different iERP activation between word repetition and verb generation tasks was seen in the cingulate gyrus and hippocampus. Higher activation during word repetition was measured in the cingulate gyrus, while the hippocampus showed higher activation during verb generation which is in line with the role of semantic processing during deep memory encoding involving the hippocampus (Vargha-Khadem et al., 1997). (Chapter 5 and 6)

5. **Visual processing.** Perisylvian regions, and in addition, frontal and temporal regions showed activation during visual picture and colour naming. Evoked responses showed regional differences between the two visual tasks while induced responses did not. During colour naming significantly stronger activation was measured in the anterior and posterior insula, while during picture naming significantly higher evoked response amplitudes were observed in the posterior medial temporal gyrus, medial frontal gyrus, inferior frontal gyrus and supramarginal gyrus. Highest induced activity was seen in the inferior temporal gyrus. (Chapter 5 and 6)

6. **Speech response-related activity.** The precentral gyrus followed by the supramarginal gyrus and the posterior STG showed the highest speech response related evoked and induced activity. No differences were found in the response pattern of the three frequency bands. (Chapter 5 and 6)

7. **Left versus right hemisphere.** Chapter 5 reported iERP occurrence for the left and right hemispheres combined. Both hemispheres showed a similar regional iERP occurrence and wave morphology. Some side specific

differences were observed, however: 1) reversed wave polarity in the inferior frontal gyrus, where the left IFG showed a late positivity and the right IFG an earlier negative peak followed by a late positive wave; 2) the right anterior middle temporal gyrus showed an early negative high amplitude component followed by a long lasting positive component, compared to a long lasting positive component in the left hemisphere.

8. **Concordance of frequency activity.** Chapter 6 analysed the co-occurrence of the three frequency bands for all contacts and showed that low and high gamma ERS co-occurred significantly more frequently than beta ERD with low and high gamma ERS.

9. **Concordance of evoked and induced responses.** While the majority of perisylvian contacts showed iERP activity, only a small proportion of those contacts also showed spectral induced responses (mean 12.3% for all tasks combined). In contrast, of those contacts with ERD/S, the majority also showed ERP activity (mean 89.9% for all tasks combined). (Chapter 5 and 6)

10. **Concordance of electrical stimulation responses and evoked and induced responses.** Positive electrical stimulation responses (ES+) were observed in only three of seven patients where this procedure was performed. A weak positive correlation across all contacts of high ERS– with ES+ and weak negative correlation of beta ERD+ with ES+ could be shown. No relation was observed for low gamma ERS and iERPs. (Chapter 6)

Results presented in Chapters 5 and 6 contributed to a more thorough understanding of electrophysiological signature of speech and language processing. I used high spatio-temporal resolution of iERPs and spectral changes to highlight the temporal and spatial course of evoked and induced responses during language processing and production. To my knowledge, these studies are the first to investigate language processing using SEEG in children and adolescents with refractory epilepsy. I demonstrated that SEEG adds knowledge of the contribution of deeper cortical structures, like the cingulate gyrus, the

hippocampus and the insula during speech comprehension and production of language. Due to the increasing clinical use of SEEG investigations, aimed at mapping initiation and propagation of the epileptic networks, studying pre-surgical epilepsy patients opens a new window into brain behaviour interactions. The requirement for SEEG to draw conclusions about functional, eloquent areas will become increasingly important in clinical practice.

The two studies reported here demonstrated how easily these neurophysiological markers could be recorded at the bedside, and how quickly the sampled brain areas can be investigated for involvement in language processing, especially when compared to electrical stimulation mapping. Furthermore, recording iERP and ERS/D did not add any extra burden to the patient and has the potential to minimise the number of contacts needed to be stimulated with ES, which in itself carries the risk of eliciting seizures and after-discharges and might inflict pain.

Neither study shows a clear superiority of one of the two neurophysiological markers, iERPs or spectral changes, in localising language cortex. One caveat is the small number of patients with positive electrical stimulation responses. Differentiating language-related and essential language areas is a challenge for functional mapping of language in pre-surgical evaluation. The location of essential language cortex cannot be reliably inferred from anatomic landmarks or from fMRI or event-related potentials and spectral changes. Towle and colleagues (2008) called language-related, but not essential areas, 'boutique' language processing centres. They argued that disrupting them using electrical stimulation or resecting them during surgery might only lead to deficits observable with in-depth neuropsychological testing, but not during routine clinical observation. They recommended including these 'boutique' areas into the surgical resection, if necessary. Furthermore, Cervenka and co-workers (2013) reported that post-operative decline in naming performance was not predicted by functional electrical language mapping and argued that more sensitive mapping techniques are therefore needed. The EEG markers studied here could be used to pinpoint to brain regions involved in language processing

and therefore guide pre-surgical functional stimulation. One example case study, patient ID2 (p. 344) is a case in point: Electrodes chosen for resection were no tested for language function, although other electrodes outside the resection zone were tested. Post-operatively this patient showed clinically apparent language deficits. Results of this study showed prominent iERPs and beta ERD in the subsequently resected brain regions. This finding emphasized the potential usefulness of spectral changes in aiding localisation of language areas. In this case, this information might not have changed the decision of resecting those brain areas, however, functional risk and prognosis might have been estimated differently.

Overall, the understanding of the effects of epilepsy on language function and re-organisation and to tie this knowledge to surgical planning, specifically when investigating children and adolescents, is of utmost importance. Compared to adult patients, paediatric cohorts often show different characteristics in semiology, aetiology, EEG findings, and treatment approaches. EEG findings in children with temporal lobe epilepsy, for example, are described as more diffuse, complex, and multifocal and surgical resections are often larger compared to adults, which increases the risk of post-operative language deficits (Y. J. Lee & Lee, 2013). Hence, advanced neurophysiological methods to aid localisation of eloquent cortex in paediatric patients are needed to further improve post-surgical cognitive outcomes.

7.4 Future Perspectives

The work presented in the chapters of this thesis covered a broad range of neurophysiological biomarkers (PLHG, sharp activity, FRs, iERPs, ERS/ERD), cognitive and clinical neuroscience questions (language and speech processing and epilepetogenicity of the brain) and investigated an adult and a paediatric cohort with medication-resistant focal epilepsy. Therefore, this work could continue in a number of possible directions in the future, which I will outline here.

7.4.1 Delineation of epileptogenic brain areas

This thesis found the combination of fast ripple and SOZ information critical to improve outcome classification. Further HFO research could take advantage of the unique SEEG paediatric patient cohort. Cognitive task-related data gathered for the second part of this thesis could be used to investigate physiological HFOs and to differentiate between physiological HFOs and pathological HFOs.

Paediatric PLHG results did not seem promising in aiding delineation of epileptogenic cortex. However, the patients included were a heterogeneous group and their investigation with SEEG had both palliative and curative aims. With a bigger cohort and more homogenous subgroups, this biomarker should be investigated further. Furthermore, future research should include all seizure types of a patient and should also trial shorter seizures, as in the current study many patients had to be excluded due to seizure durations being ≤20s (a priori inclusion criterion). This restriction limited the sample and study power and should be considered for further research.

In addition, this thesis only included SEEG patients. A comparison of implantation methods, grids versus depth electrodes, might be a worthwhile endeavour for future studies and shed light on seizure initiation and propagation.

7.4.2 Language mapping for pre-surgical evaluation

One of the aims of future work in the context of language localisation in pre-surgical evaluation is to distinguish between language-related areas and language-essential areas. In this context, comprehensive information of individual language lateralisation is needed and hence fMRI or Wada testing results should be available. This is of importance regarding the analysis of differences in iERPs and ERS/ERD between the language dominant and non-dominant hemispheres. Deciphering the involvement of the left and right hemisphere needs further research. In this context, both patients with typical and atypical language dominance should be studied. In future, evoked or induced responses could be used to lateralise language dominance pre-surgically in children who are unable to perform fMRI or Wada. Furthermore, these findings could guide the use of MEG measures for non-invasive language mapping (Tierney et al., 2018). Due to larger signal to noise ratio beta ERD has been used mostly in MEG studies, however, based on current findings its limitation should be understood.

Replicating electrical stimulation results with an appropriate sample size is needed to prove feasibility of ERS/ERD in pre-surgical SEEG language mapping. Furthermore, evoked and induced responses could be used to guide ES mapping.

Not all patients undergoing invasive EEG implantation are tested for language localisation using electrical stimulation. However, to maximise data collection from this special patient cohort, further non-invasive methods should be incorporated to test feasibility of ERS/ERD or iERPs for language localisation. nTMS was reported to be clinically useful in pre-surgical language mapping (Lefaucheur & Picht, 2016; Tarapore et al., 2013), even in children with extensive cognitive dysfunction (Lehtinen et al., 2018). Furthermore, MEG is increasingly studied in context of cognitive neuroscience, demonstrating that it can be used to localise and lateralise language (Hirata et al., 2010; Pirmoradi, Béland, Nguyen, Bacon, & Lassonde, 2010; Youssofzadeh et al., 2020). Tierney

and group (2018) even presented language lateralisation results using a motion robust wearable MEG system. Combining these methods to strengthen the investigated neurophysiological markers would be useful, especially for pre-surgical evaluation in children.

Ideally, invasive monitoring can be fully avoided in the future. To understand SEEG signals non-invasively, simultaneous SEEG and scalp recording could be performed, even simultaneously with fMRI (Centeno & Carmichael, 2014). This would provide valuable information of task-dependent activity from the depth of the brain and could be translated into surface activity. This would be a step towards non-invasive language mapping.

Finally, SEEG provides a unique window into brain–behaviour interactions to study the functional organisation of speech and language with greater temporal resolution than fMRI and greater spatial resolution than scalp-recorded EEG. Invasive language-related ERP and ERS/ERD data can be used to investigate dynamic functioning and functional connectivity (using coherence or DCM methods) of the language network and individual differences in underlying neural structure and behavioural performance.

APPENDIX

Appendix A—Chapter 2

Independent Component Analysis (ICA) trialled using MNI data

First, an example is presented (see Figure 106 and Figure 107) where using ICA and deleting the first component got rid of the artefact. Next, (see Figure 108 to Figure 113) an example is shown where it was less obvious which components to delete. It was unclear when the threshold is reached where physiological signals were deleted as well.
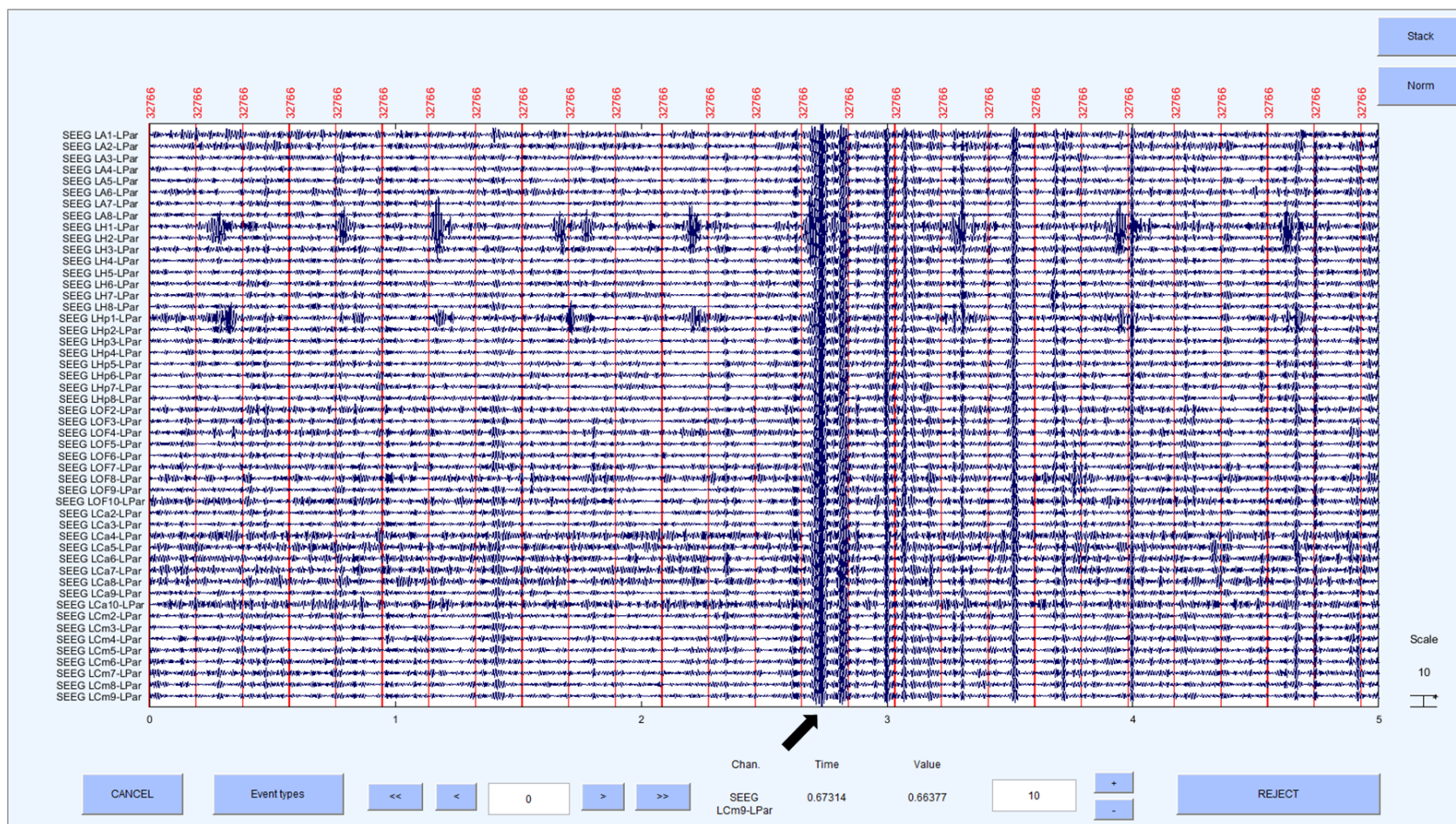
Figure 106. ICA Patient 1, Seizure 1—Original SEEG recording. Second 0–5, where rhythmic artefacts can be seen in all channels throughout the first 5 seconds shown here and very obvious shortly before second 3 starts (marked with black error)
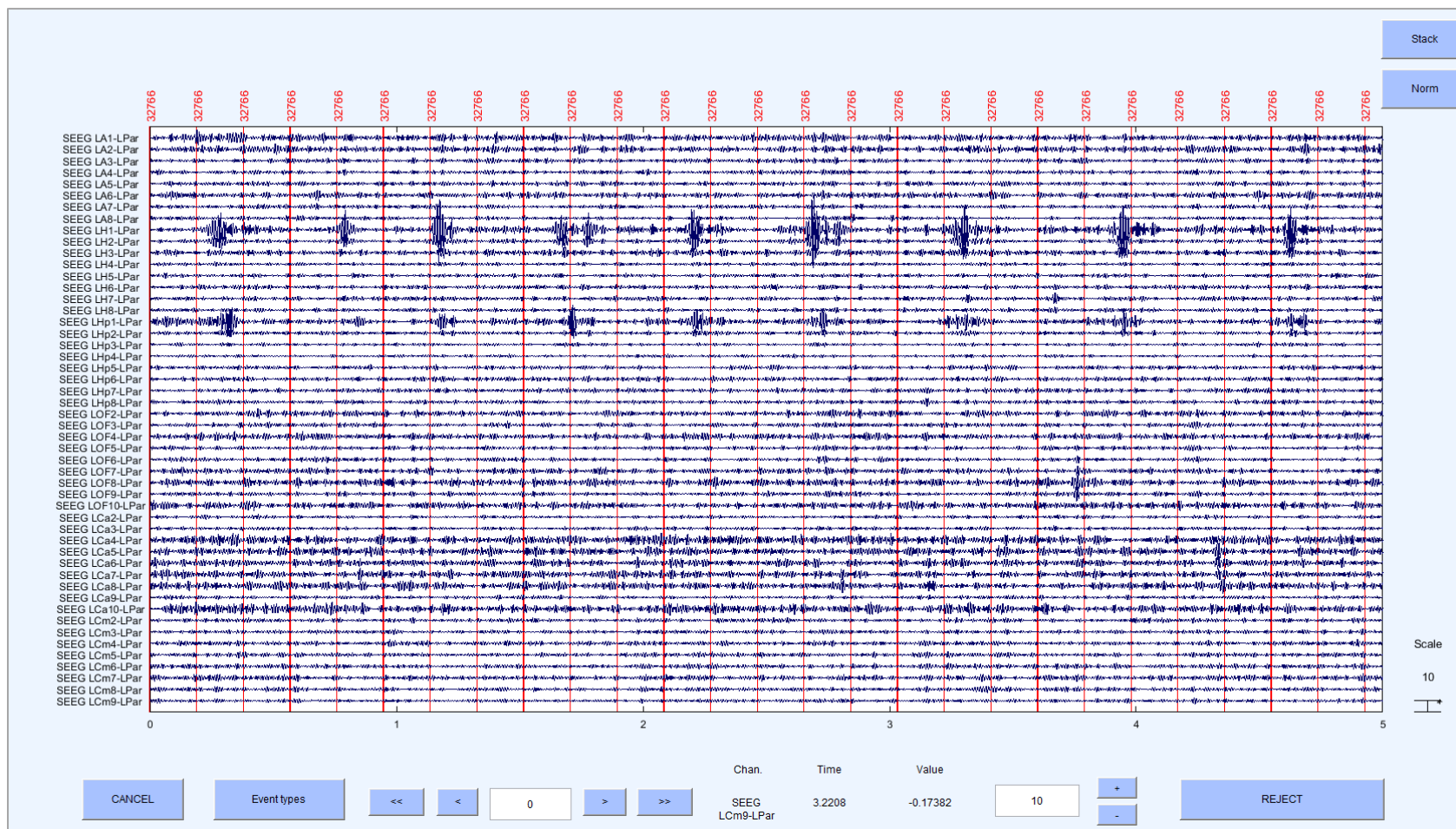
Figure 107. ICA Patient 1, Seizure 1—First component pruned. This eliminated rhythmic artefact seen in original recording.

Figure 108. ICA Patient 3, Seizure 1—Original SEEG recording. Second 5–10, where rhythmic artefacts can be seen in all channels throughout the second 5 seconds presented here.
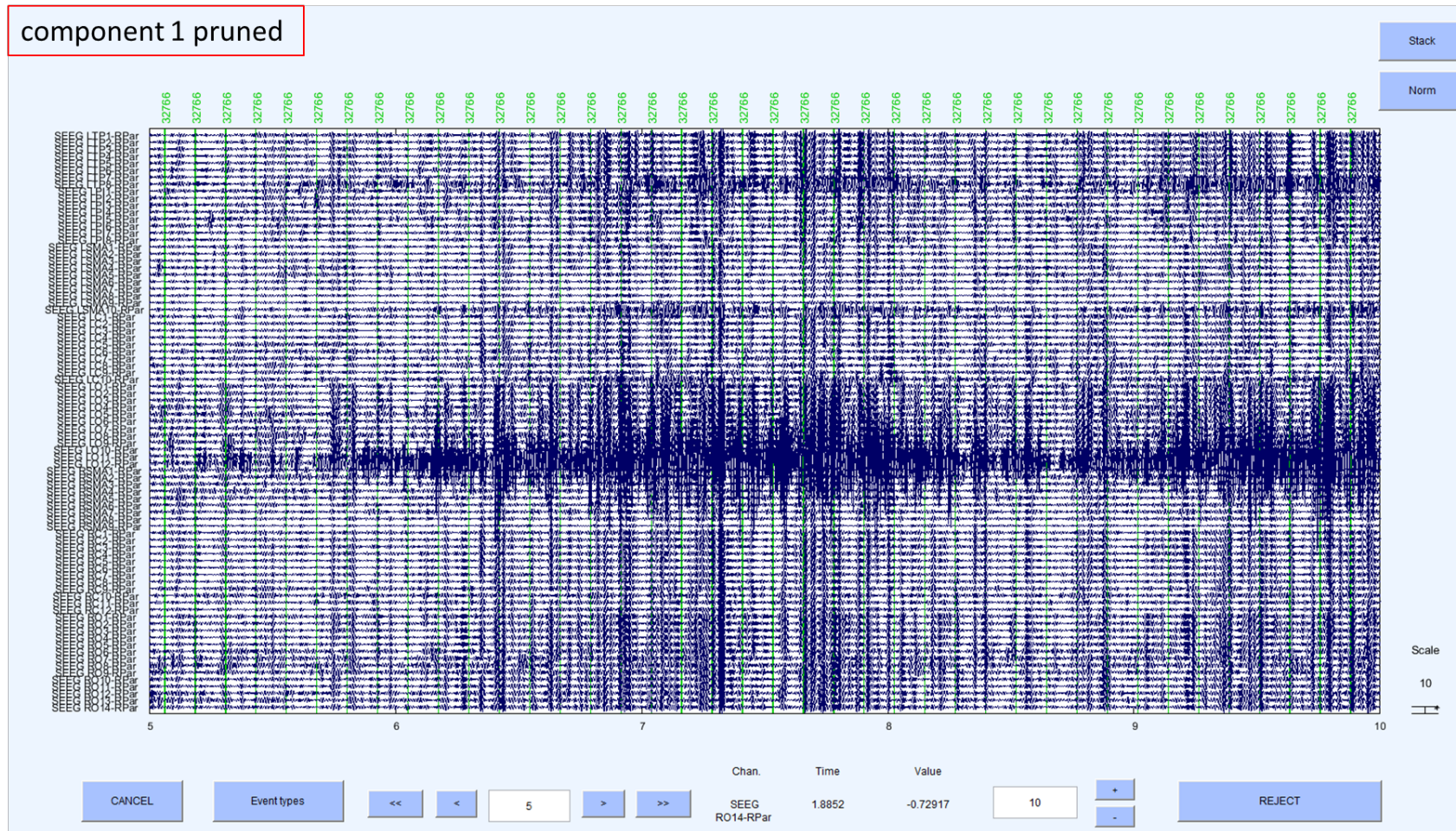
Figure 109. ICA Patient 3, Seizure 1—First component pruned. This only eliminated parts of the artefact seen in original recording.
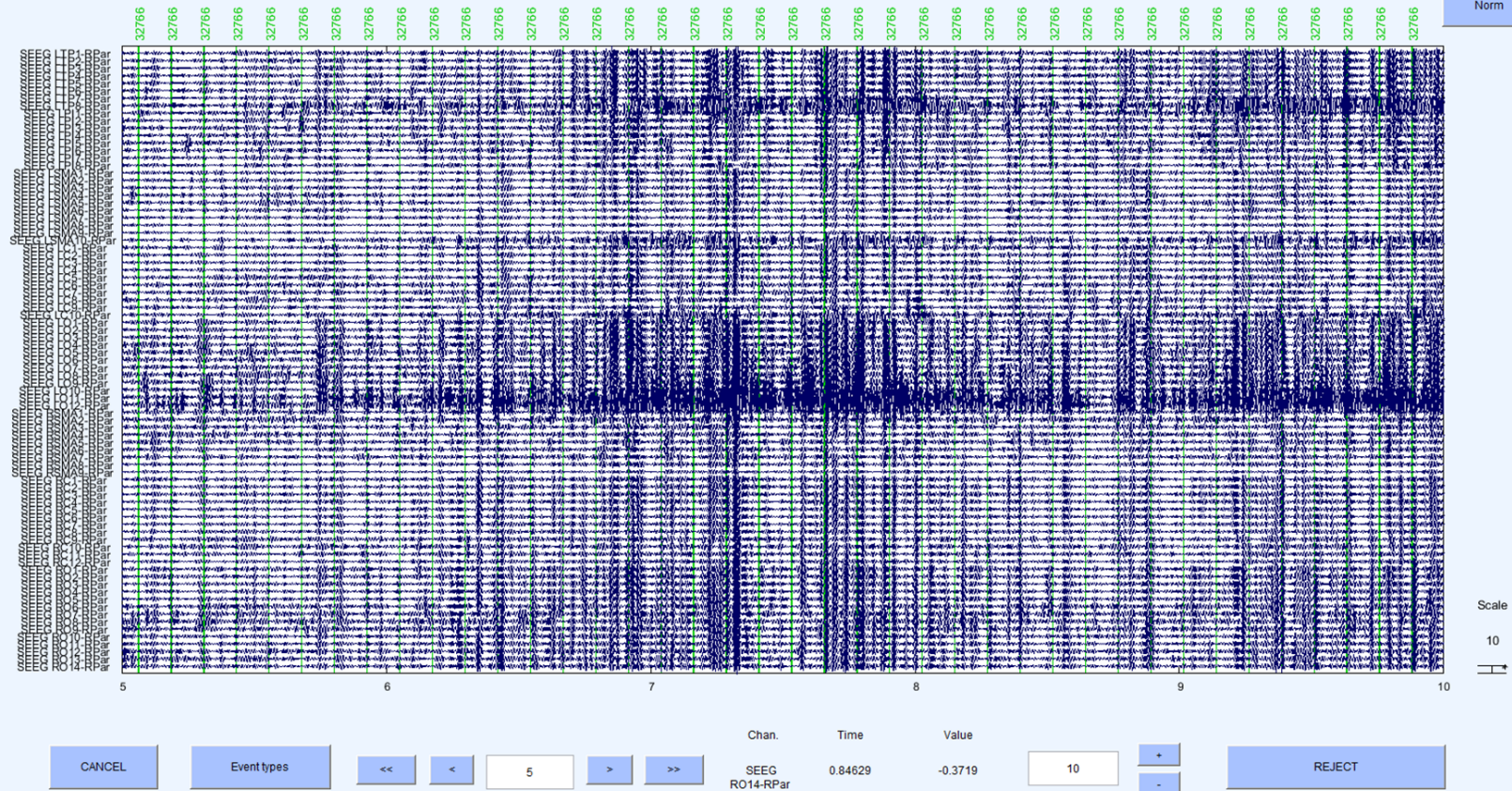
Figure 110. ICA Patient 3, Seizure 1—Independent component (IC) 1 and 2 pruned. This only eliminated parts of the artefact seen in original recording.
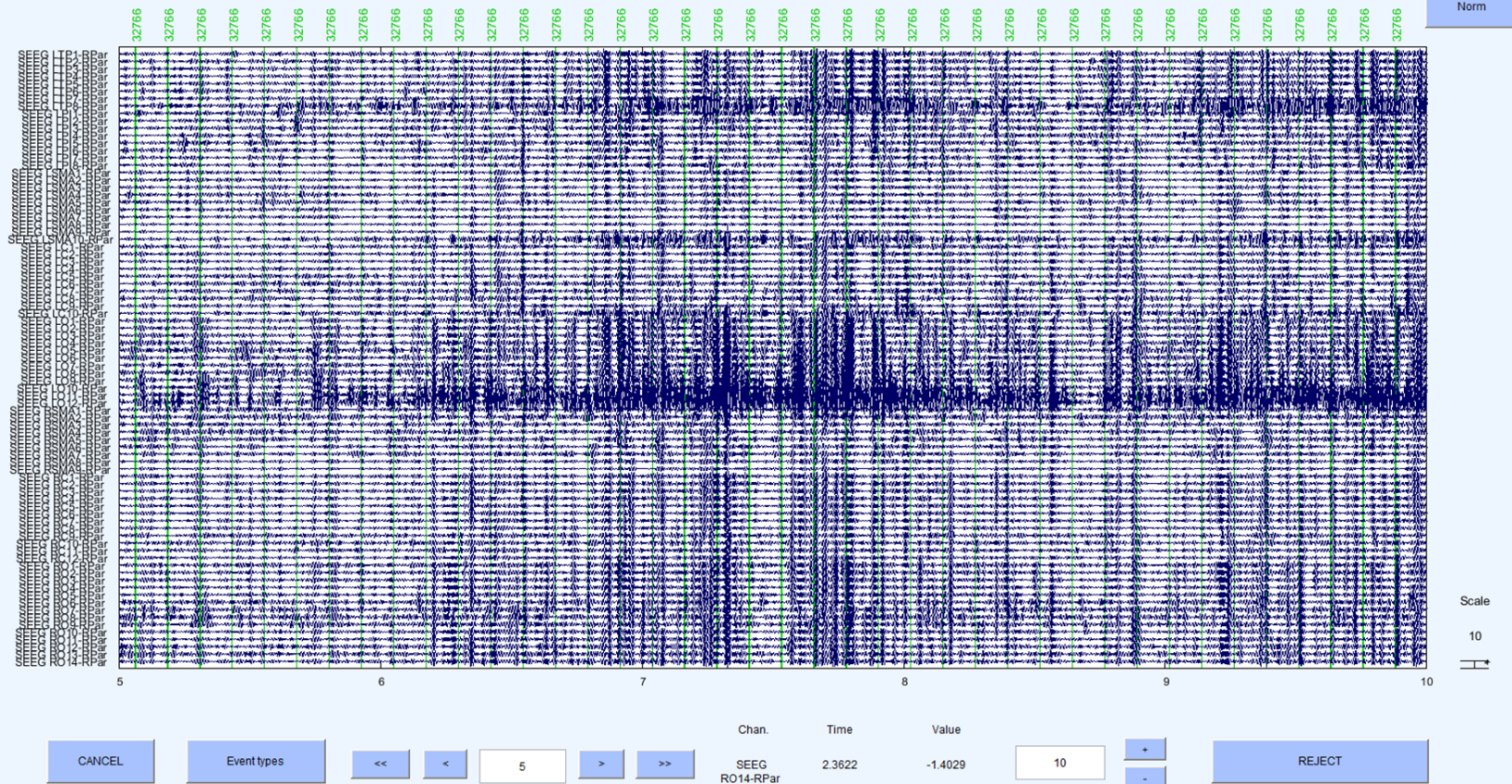
Figure 111. ICA Patient 3, Seizure 1—IC 1 to 3 pruned. This only eliminated parts of the artefact seen in original recording.
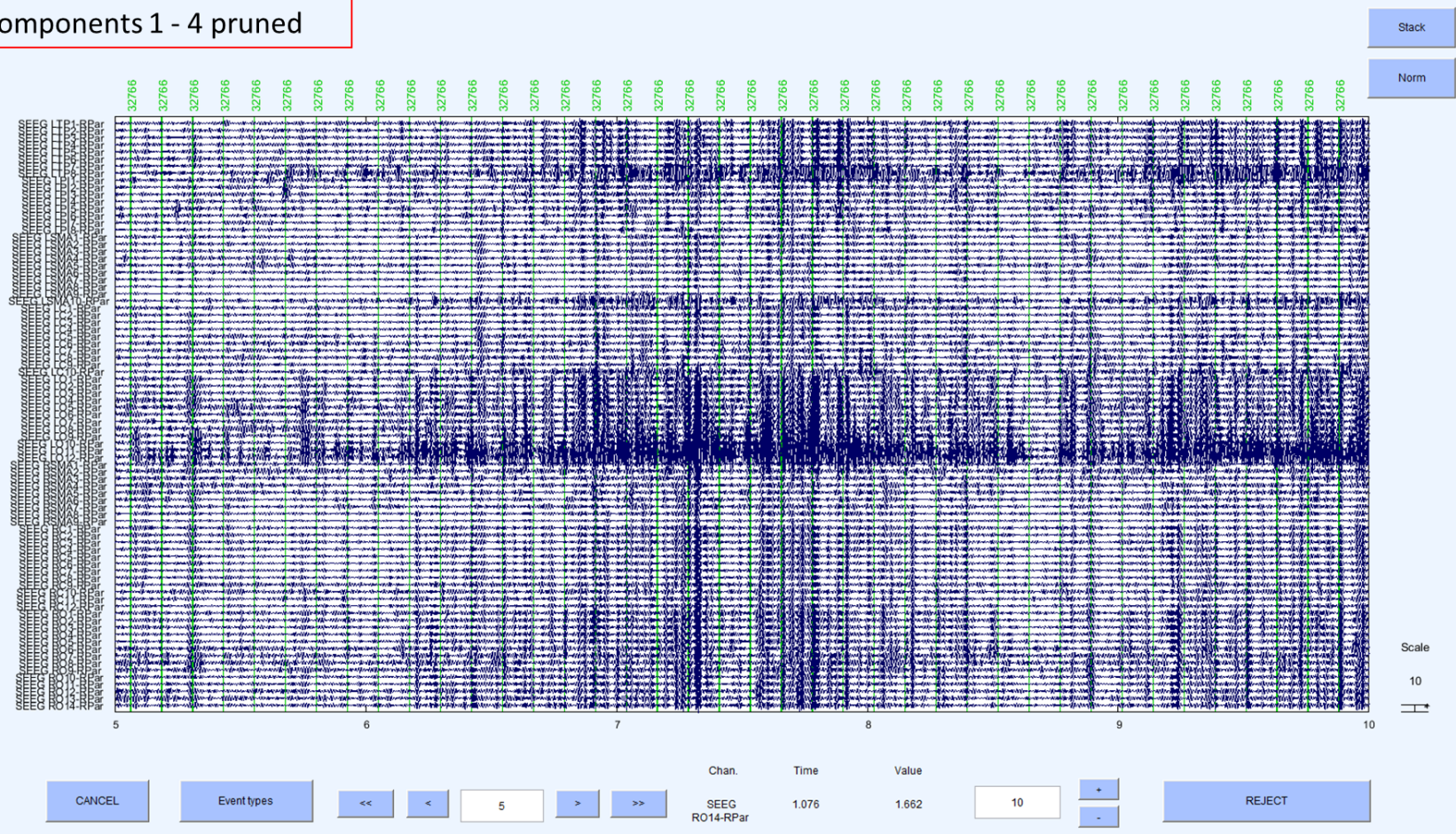
Figure 112. ICA Patient 3, Seizure 1—IC 1 to 4 pruned. This only eliminated parts of the artefact seen in original recording.
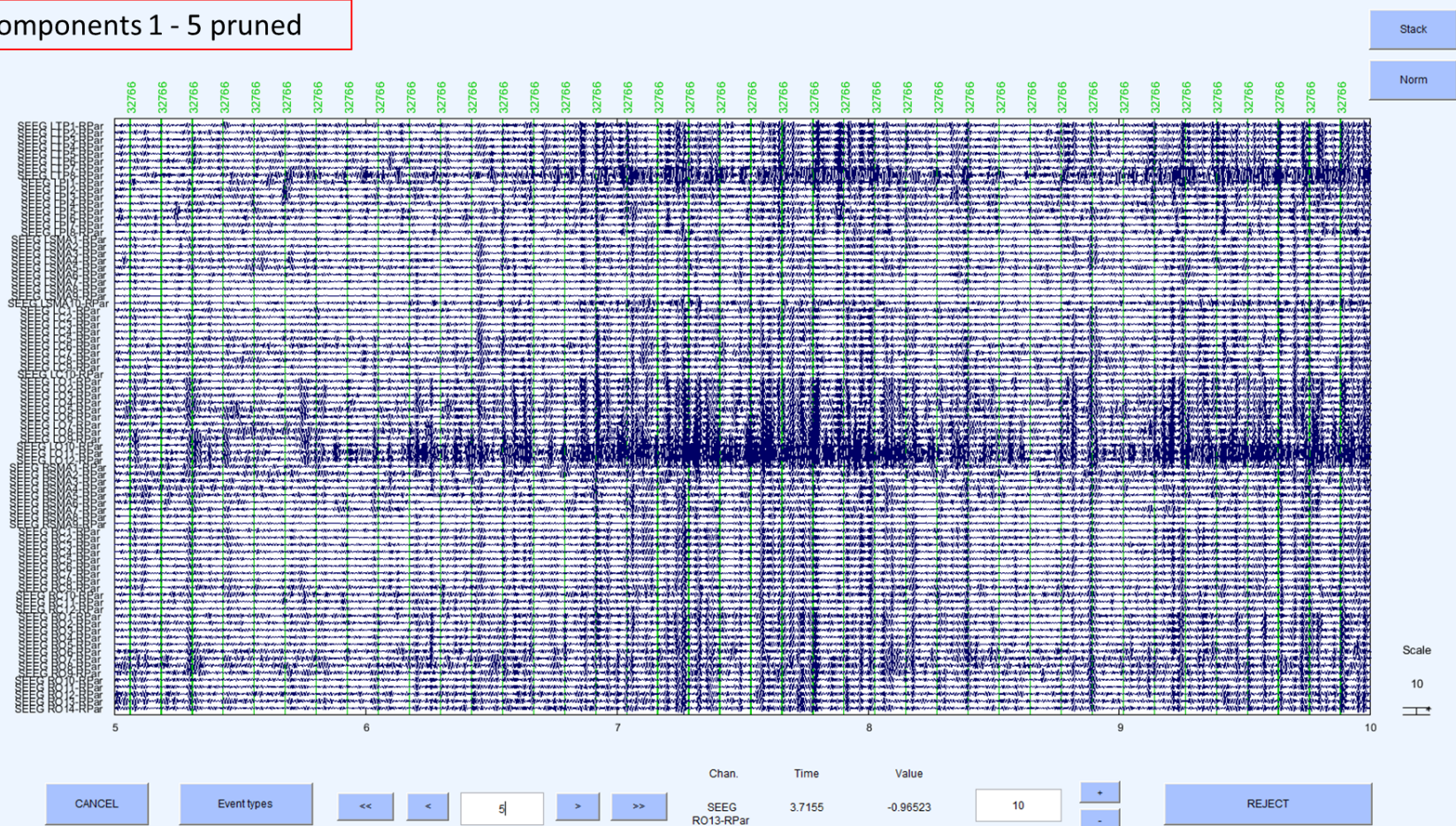
Figure 113. ICA Patient 3, Seizure 1—IC 1 to 5 pruned. This only eliminated parts of the artefact seen in original recording and the boundary to physiological signals is not easy to depict.

SOZ/PLHG overlap (SPO)

This section presents the percentage of SOZ/PLHG overlap (SPO) in patients with good versus poor Engel outcome for PLHG_b (same PLHG recruitment in at least two of the three seizures). Figure 114 illustrates results of a Wilcoxon rank sum test for PLHG_b, assessing whether there was a difference between SPO in patients with good and poor Engel. The boxplot shows percentage of SPO for patients with good and poor Engel outcome. Table 47 presents each patients' Engel outcome, the number of clinically defined SOZ channels, the mean time of recruitment for each patient and the percentage SOZ/PLHG overlap for recruited PLHG channels from 1–10.
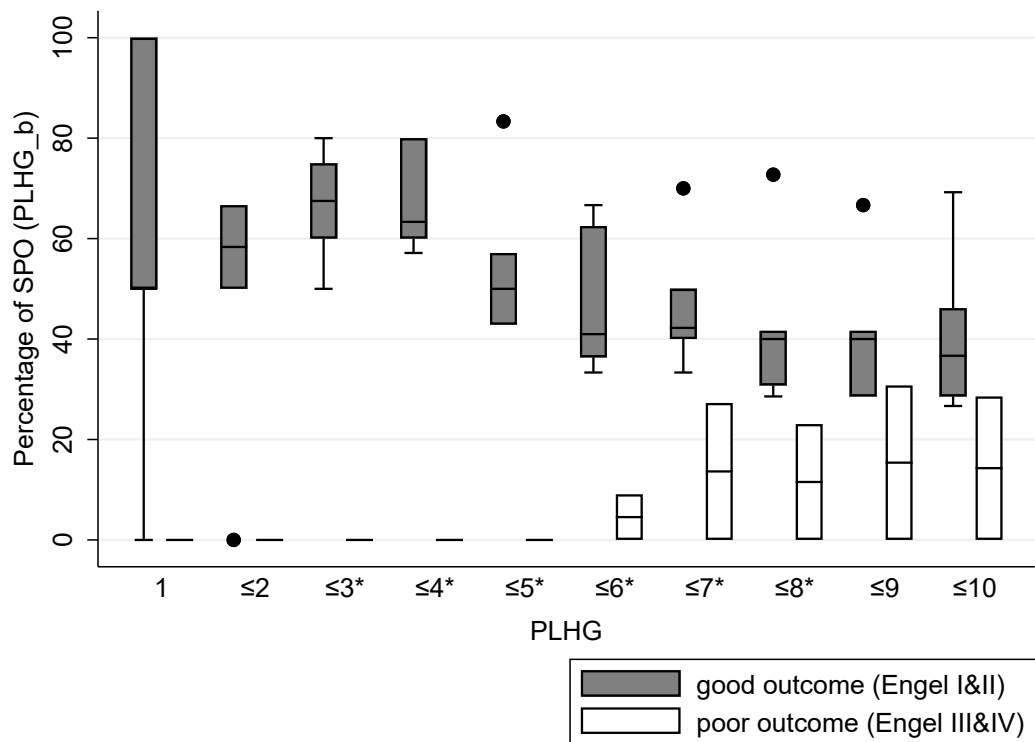
Figure 114. PSO for PLHG_b. Boxplot presenting percentage of PSO for patients with good versus poor Engel outcome from PLHG 1–10 for PLHG_b. Significant difference with p<0.05 is marked with *.

Percentage of SPO of PLHG_b was significantly different between good and poor Engel outcome in PLHG3–8 (n=8, p<0.05, Wilcoxon rank sum test).

Table 47. Percentage of SPO and mean time of PLHG recruitment for each patient (PLHG_b = same PLHG recruitment in at least two of the three seizures).

ID	Engel	SOZ	4 PLHG time	8 PLHG time	SOZ/PLHG overlap (SPO, %)									
					PLHG1	PLHG2	PLHG3	PLHG4	PLHG5	PLHG6	PLHG7	PLHG8	PLHG9	PLHG10
1	III	3	12.2±3.6	18.5±2.5	0.0	0.0	0.0	0.0	0.0	0.0	0.0	0.0	0.0	0.0
2	II	18	8.7±2.2	11.1±3.6	50.0	66.7	**75.0**	66.7	50.0	62.5	50.0	41.7	41.7	46.2
3	I	12	8.3±1.4	26.8±1.8	0.0	0.0	60.0	60.0	42.9	37.5	40.0	40.0	40.0	33.3
4	I	15	8.5±0.4	19.5±5.2	**100.0**	66.7	60.0	60.0	42.9	33.3	40.0	30.8	28.6	28.6
5		27	4.7±1.0	9.2±2.6	-	-	-	-	-	-	-	-	-	-
6	I	12	16.1±7.9	34.6±10.1	50.0	50.0	50.0	57.1	50.0	36.4	33.3	28.6	28.6	26.7
7	I	6	13.7±5.6	44.3±12.5	50.0	50.0	**80.0**	**80.0**	57.1	44.4	44.4	40.0	40.0	40.0
8	III-IV	15	4.6±0.5	7.7±2.6	0.0	0.0	0.0	0.0	0.0	9.1	27.3	23.1	30.8	28.6
9	I	27	13.2±1.3	26.2±4.3	**100.0**	66.7	**75.0**	**80.0**	**83.3**	66.7	**70.0**	**72.7**	66.7	69.2
10		9	90.5±33.5	99.1±27.4	-	-	-	-	-	-	-	-	-	-

Engel: post-operative surgical outcome (J. Engel et al., 1993); SOZ: total number of clinically defined SOZ channels; 4 PLHG time: mean time in seconds until first 4 PLHG recruitment ± SD in seconds; 8 PLHG time: mean time in seconds until first 8 PLHG recruitment ± SD in seconds.

Appendix B—Chapter 3

Artefact_fix (by Dr Richard Rosch)

```matlab
function eeg = artefact_fix(eeg)
cutoff = 10000;

dat = eeg.eeg_data;
mrk = zeros(size(dat,1),size(dat,2));
for r = 1:size(dat,1)
ce  = 0;
for c = 1:size(dat,2)
    if dat(r,c) > cutoff,
    if mrk(r,c-1) > 0
        mrk(r,c) = mrk(r,c-1);
    else
        ce = ce + 1;
        mrk(r,c) = ce;
    end
    end
end

for m = 1:max(mrk(r,:))
    padding     = 100;
    id          = find(mrk(r,:) == m);

    % Linear replacement (doesn't solve it)
    slp         = (dat(r,id(end)+padding) - dat(r,id(1)-padding)) /
(id(end)-id(1) + 2*padding);
    offs        = dat(r,id(1)-padding);
    for k = 1:(id(end)-id(1) + 2*padding)
        dat(r, id(1)-padding + k) = slp*k+offs;
    end

    % smoothed replacement with other data
    %-------------------------------------------------------------
    seglength = id(end) - id(1) + 2*padding + 1;
    segcopy   = dat(r, id(1) - 5000 - seglength : id(1) - 5000 - 1);
    blm       = mean(dat(find(~mrk(r,:))));
    segcopy   = segcopy - mean(segcopy) + blm;

    wini      = id(1)-padding+1:id(end)+padding+1;
    wts       = zeros(1,length(wini));
    wts(1:100)  = linspace(1,0,100);
    wts(end-99:end) = linspace(0,1,100);
    for w = 1:length(wini)
        dat(r,wini(w)) = wts(w)*dat(r,wini(w)) + (1-
wts(w))*segcopy(w);
    end
end

end
eeg.eeg_data = dat;
```

ID1	segment	FR total	FR rejected	FR accepted
	1	3	1	2
	2	2	2	0
	3	2	2	0
	4	12	11	1
	5	23	22	1
	6	11	11	0
	7	14	12	2
	8	17	17	0
	9	11	11	0
	10	16	12	4

ID2	segment	FR total	FR rejected	FR accepted
	1	104	77	27
	2	126	83	43
	3	128	78	50
	4	200	134	66
	5	230	142	88
	6	204	123	81
	7	145	91	54
	8	188	104	84
	9	152	84	68
	10	252	140	112

ID3	segment	FR total	FR rejected	FR accepted
	1	112	102	10
	2	80	74	6
	3	88	76	12
	4	175	154	21
	5	122	107	15
	6	83	77	6
	7	73	66	7
	8	128	111	17
	9	123	99	24
	10	161	137	24

ID4	segment	FR total	FR rejected	FR accepted
	1	98	71	27
	2	11	6	5
	3	23	6	17
	4	23	18	5
	5	126	85	41
	6	19	11	8
	7	88	77	11
	8	22	19	3
	9	8	4	4
	10	24	23	1

ID5	segment	FR total	FR rejected	FR accepted
	1	16	13	3
	2	20	17	3
	3	14	13	1
	4	9	8	1
	5	5	5	0
	6	10	10	0
	7	12	9	3
	8	8	6	2
	9	19	19	0
	10	5	4	1

ID6	segment	FR total	FR rejected	FR accepted
	1	67	44	23
	2	90	45	45
	3	181	156	25
	4	0	0	0
	5	109	62	47
	6	26	11	15
	7	62	33	29
	8	3	3	0
	9	33	17	16
	10	119	51	68

ID7	segment	FR total	FR rejected	FR accepted
	1	23	20	3
	2	23	21	2
	3	34	30	4
	4	25	22	3
	5	32	27	5
	6	51	40	11
	7	37	32	5
	8	49	45	4
	9	37	35	2
	10	16	14	2

ID8	segment	FR total	FR rejected	FR accepted
	1	333	219	114
	2	288	161	127
	3	465	223	242
	4	285	172	113
	5	138	99	39
	6	814	492	322
	7	306	178	128
	8	427	273	154
	9	336	198	138
	10	132	74	58

ID9	segment	FR total	FR rejected	FR accepted
	1	360	97	263
	2	351	84	267
	3	228	95	133
	4	378	199	179
	5	358	89	269
	6	312	69	243
	7	342	85	257
	8	619	153	466
	9	368	106	262
	10	367	114	253

Figure 115. Summary of FR counts for ID1–ID9. FRs were detected using an automatic FR detection algorithm. Each patients' 10 analysed segments are presented, showing total number of FR detected, rejected and accepted ones.

ID10

segment	FR total	FR rejected	FR accepted
1	37	25	12
2	37	25	12
3	31	23	8
4	23	19	4
5	9	9	0
6	11	10	1
7	15	14	1
8	12	10	2
9	23	19	4
10	24	23	1

ID11

segment	FR total	FR rejected	FR accepted
1	31	12	19
2	0	0	0
3	12	5	7
4	26	17	9
5	17	6	11
6	49	20	29
7	2	1	1
8	0	0	0
9	0	0	0
10	29	10	19

ID12

segment	FR total	FR rejected	FR accepted
1	28	116	12
2	11	8	3
3	8	4	4
4	0	0	0
5	20	13	7
6	2	2	0
7	3	0	3
8	3	0	3
9	8	4	4
10	121	43	78

ID13

segment	FR total	FR rejected	FR accepted
1	408	321	87
2	242	79	163
3	355	242	113
4	330	237	93
5	377	286	91
6	281	104	177
7	182	149	33
8	651	316	335
9	453	314	139
10	359	196	163

ID14

segment	FR total	FR rejected	FR accepted
1	0	0	0
2	1	1	0
3	0	0	0
4	2	2	0
5	0	0	0
6	0	0	0
7	1	1	0
8	0	0	0
9	0	0	0
10	7	7	0

ID15

segment	FR total	FR rejected	FR accepted
1	160	75	85
2	70	27	43
3	28	15	13
4	71	43	28
5	30	19	11
6	71	38	33
7	51	38	13
8	84	46	38
9	114	65	49
10	62	38	24

ID16

segment	FR total	FR rejected	FR accepted
1	2472	1019	1453
2	2605	504	2101
3	1619	580	1039
4	1796	927	869
5	1219	550	669
6	1271	721	550
7	1421	753	668
8	2531	552	1979
9	1216	676	540
10	2976	580	2396

ID17

segment	FR total	FR rejected	FR accepted
1	15	14	1
2	28	23	5
3	23	13	10
4	40	26	14
5	19	13	6
6	55	21	34
7	12	11	1
8	17	12	5
9	57	30	27
10	21	12	9

ID18

segment	FR total	FR rejected	FR accepted
1	605	288	317
2	550	287	263
3	1022	494	528
4	900	451	449
5	1154	602	552
6	632	299	333
7	1002	520	482
8	270	127	143
9	993	457	536
10	891	400	491

ID19

segment	FR total	FR rejected	FR accepted
1	0	0	0
2	1	1	0
3	0	0	0
4	0	0	0
5	6	6	0
6	4	4	0
7	5	5	0
8	1	1	0
9	3	3	0
10	0	0	0

Figure 116. Summary of FR counts for ID10–ID18. FRs were detected using an automatic FR detection algorithm. Each patients' 10 analysed segments are presented, showing total number of FR detected, rejected and accepted ones.

Table 48. Example seizures of four patients listing PLHG recruited channels and time of recruitment.

ID3		ID4		ID2		ID14	
PLHG channels	Time	PLHG channels	Time	PLHG channels	Time	PLHG channels	Time
A9-A8	3.0000	S8-S7	3.5996	H4-H3	5.0986	H9-H8	26.0850
A8-A7	3.0000	I4-I3	3.5996	O12-O11	6.2979	H7-H6	26.3848
A7-A6	3.0000	S6-S5	3.5996	I6-I5	7.7969	H8-H7	29.9824
A5-A4	3.0000	S2-S1	3.5996	M12-M11	8.3965	F7-F6	32.0811
A4-A3	3.0000	S7-S6	3.8994	I5-I4	8.3965	Q6-Q5	38.6768
A3-A2	3.0000	S5-S4	4.4990	K17-K16	8.6963	G3-G2	44.6729
B12-B11	3.0000	I6-I5	22.4873	I3-I2	8.9961	Q5-Q4	45.5723
B11-B10	3.0000	I5-I4	24.5859	P2-P1	9.2959	Q8-Q7	45.5723
B10-B9	3.0000	S4-S3	30.5820	I2-I1	9.2959	G5-G4	46.7715
B9-B8	3.0000			Q5-Q4	9.2959	G2-G1	47.3711
B8-B7	3.0000			I4-I3	9.2959	H3-H2	48.2705
B7-B6	3.0000			I8-I7	10.7949	G4-G3	48.5703
B6-B5	3.0000			K18-K17	10.7949	Q7-Q6	49.1699
B5-B4	3.0000			Q15-Q14	10.7949	F6-F5	49.1699
A9-A8	3.0000			Q16-Q15	11.6943	F8-F7	50.0693
C3-C2	3.0000			Q14-Q13	12.2939	H5-H4	50.3691
C2-C1	3.0000			P13-P12	13.1934	Q9-Q8	51.2686
D12-D11	3.0000			P12-P11	14.0928	H4-H3	51.5684
D10-D9	3.0000			P11-P10	14.9922	F5-F4	52.7676
D4-D3	3.0000			K15-K14	15.2920	F10-F9	53.0674
D3-D2	3.0000			E7-E6	16.1914	G14-G13	53.6670
A2-A1	3.2998			J15-J14	16.7910	F4-F3	53.9668
B4-B3	3.5996			Q13-Q12	17.9902	F9-F8	55.4658
D2-D1	3.5996			Q12-Q11	17.9902	M15-M14	55.4658
A6-A5	3.8994			C3-C2	18.2900	F3-F2	60.2627
C7-C6	3.8994			E4-E3	19.1895	K18-K17	65.3594
D11-D10	3.8994			D11-D10	20.0889	Q4-Q3	65.9590
J10-J9	4.4990			E3-E2	20.0889	Q3-Q2	66.5586
E2-E1	5.6982			E2-E1	20.0889	Q2-Q1	66.5586
B2-B1	7.4971			A2-A1	20.3887	G11-G10	66.5586
I4-I3	8.3965			E6-E5	20.3887	P15-P14	66.5586
E3-E2	9.5957			E5-E4	20.3887	P14-P13	66.5586
H11-H10	9.5957			D10-D9	20.6885	P3-P2	66.5586
K12-K11	9.8955			D9-D8	20.9883	P13-P12	66.5586
E4-E3	9.8955			D8-D7	21.2881	Q11-Q10	67.1582
A10-A9	11.9941			D7-D6	21.5879	Q10-Q9	67.1582
K2-K1	12.8936			H7-H6	21.5879	G15-G14	67.4580
ID3		ID4		ID2		ID14	

PLHG channels	Time	PLHG channels	Time	PLHG channels	Time	PLHG channels	Time
K3-K2	13.1934			C5-C4	21.8877	F2-F1	67.4580
F5-F4	14.6924			C9-C8	22.1875	H6-H5	74.9531
E12-E11	14.9922			C2-C1	22.1875	P2-P1	76.4521
G3-G2	14.9922			H8-H7	22.1875	H2-H1	82.1484
I6-I5	15.5918			J12-J11	23.9863		
I2-I1	15.5918			H5-H4	26.6846		
I5-I4	16.1914			D6-D5	26.9844		
I3-I2	16.1914			H6-H5	28.1836		
I15-I14	17.6904			A3-A2	32.6807		
J2-J1	20.3887			D3-D2	32.6807		
F2-F1	21.8877			C8-C7	32.9805		
B3-B2	23.3867			D2-D1	32.9805		
J8-J7	23.3867			P10-P9	33.2803		
G2-G1	24.2861			C4-C3	36.8779		
K11-K10	28.1836			B6-B5	38.0771		
B3-B2	23.3867			C6-C5	38.3770		
J8-J7	23.3867			A4-A3	38.6768		
F4-F3	28.7832			B9-B8	39.2764		
K13-K12	29.6826			C7-C6	39.5762		
J9-J8	31.7813			B10-B9	40.1758		
F3-F2	38.3770			P4-P3	40.1758		
K4-K3	39.8760			D12-D11	41.9746		
G5-G4	45.8721						
F7-F6	50.3691						
C5-C4	53.3672						
I16-I15	56.0654						
I13-I12	58.1641						
C4-C3	60.2627						
E8-E7	66.5586						
I17-I16	69.8564						
I14-I13	72.5547						
E9-E8	74.3535						
G4-G3	76.4521						
K5-K4	78.2510						

One group (ID3, 4) shows some channels being PLHG recruited at the same time increment and very early. The other two patients' seizures (ID2, 14) did not show such an early recruitment. To a later time point, these seizures exhibit recruited channels in the same time increment.

Appendix C—Chapter 4

Signal Processing Unit Circuit

A (light weight), non-intrusive tie clip mono microphone (Prosound, L48AA) was used to record the verbal responses from the participants during testing. The low-level amplitude of the microphone was subsequently processed by an in-house built battery powered amplifier and processing unit (by Alan Worley) to which the output was connected to the one of the SynAmps high level inputs, permitting verbal responses to be time-locked to the on-going ERP data. The high level inputs are galvanically isolated from the electrodes ensuring patient safety.

The small electronic circuit (Figure 117) consisting of a low voltage power amplifier integrated circuit (National Semiconductor, LM 386) was constructed to amplify and filter the microphone signal to ensure it could be processed accurately by the ERP recording system.
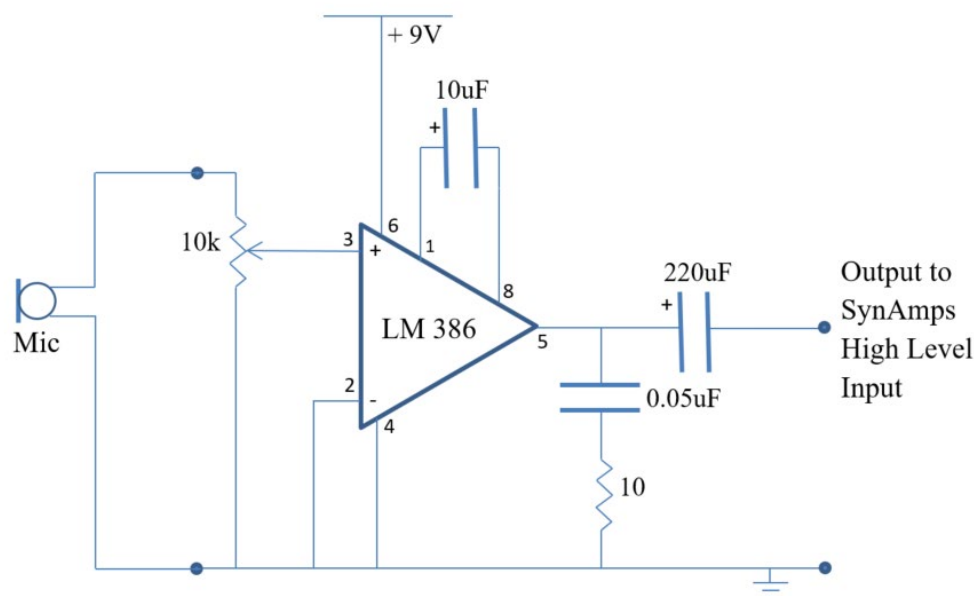
Figure 117. Signal Processing Unit Circuit Schematic.

Appendix D—Chapter 6

Table 49. Wilcoxon rank sum test results comparing iERPs to spectral changes for visual tasks.

	Visual tasks		
	iERP-beta ERD	iERP-low gamma ERS	iERP-high gamma ERS
INS_A	Z=3.6**	Z=3.8**	Z=3.5**
INS_P	Z=2.8**	Z=3.2**	Z=3.1**
IFG	Z=2.5*	Z=3.2**	Z=3.3**
preC	Z=2.8**	Z=2.8**	Z=2.7**
postC	Z=1.2	Z=1.1	Z=0.5
SMG	Z=2.7**	Z=2.6**	Z=2.3*
STG_P	Z=2.6**	Z=2.1*	Z=1.9
MTG_P	Z=1.4	Z=1.9*	Z=1.7
MTG_A	Z=2.4*	Z=2.1*	Z=2.1*

The table summarises Z-scores and significance levels for the comparison of the mean percentage of contacts with iERPs and the mean percentage of contacts showing frequency band activity—beta ERD, low gamma ERS and high gamma ERS for visual tasks (PN, CNw). ** shows a significance level of $p<0.01$ and * shows a significance level of $p<0.05$.

Table 50. Wilcoxon rank sum test results for various frequency band activity comparing tasks.

	Beta				low gamma				high gamma			
	BL-WR	BL-VG	WR-VG	PN-CNw	BL-WR	BL-VG	WR-VG	PN-CNw	BL-WR	BL-VG	WR-VG	PN-CNw
INS_A	Z=-1	Z=-2*	Z=-2	Z=-1	Z=-1	Z=0	Z=2		Z=-1	Z=-1	Z=0	Z=-1
INS_P	Z=-1	Z=-1	Z=1	Z=-1	Z=-1	Z=-1	Z=-1		Z=0	Z=-1	Z=-1	Z=1
IFG	Z=-1	Z=-1	Z=1	Z=0	Z=1	Z=0	Z=-1	Z=-1	Z=-2	Z=-1	Z=-1	Z=0
preC	Z=0	Z=1	Z=1	Z=1	Z=-2	Z=-1	Z=0	Z=0	Z=-1	Z=-1	Z=0	Z=-1
postC	Z=1	Z=-1	Z=-1	Z=-1	Z=-1	Z=0	Z=2	Z=1	Z=-2	Z=2	Z=1	Z=0
SMG	Z=0	Z=0	Z=0	Z=-1	Z=-1	Z=0	Z=0	Z=-1	Z=0	Z=0	Z=0	Z=-1
STG_P	Z=1	Z=1	Z=-1		Z=-2*	Z=-1	Z=1	Z=-1	Z=0	Z=1	Z=1	Z=-1
MTG_A		Z=-1	Z=-1		Z=-1		Z=1	Z=-1	Z=0	Z=0	Z=0	Z=-1
MTG_P	Z=0	Z=-1	Z=-1	Z=0	Z=0	Z=0	Z=0	Z=1	Z=-1	Z=0	Z=0	Z=0

The table summarises Z-scores and significance levels for the comparison of frequency band activity between tasks. * shows a significance level of $p<0.05$. Each auditory word task is compared to all other auditory word tasks. The picture naming task is compared to the colour naming task. A negative Z-score shows that the first task of a pair exhibited less activity, e.g. BL-WR with Z=-2* means that BL task elicited significantly less ($p<0.05$) frequency band activity compared to the WR task. A positive Z-score means the opposite.

Table 51. Wilcoxon rank sum test results for auditory word tasks comparing frequency band activity.

	BL			WR			VG		
	beta- low gamma	beta- high gamma	low gamma- high gamma	beta- low gamma	beta- high gamma	low gamma- high gamma	beta- low gamma	beta- high gamma	low gamma- high gamma
INS_A	Z=-1	Z=-1	Z=0	Z=-1	Z=-1	Z=1	Z=2	Z=1	Z=-1
INS_P	Z=-1	Z=-2*	Z=-1	Z=-1	Z=-1	Z=0	Z=-2*	Z=-2*	Z=0
IFG	Z=0	Z=1	Z=1	Z=1	Z=0	Z=-1	Z=0	Z=0	Z=0
preC	Z=1	Z=1		Z=-1	Z=-1	Z=0	Z=-1	Z=-1	Z=1
postC	Z=0	Z=0	Z=0	Z=-2*	Z=-2*	Z=-1	Z=1	Z=0	Z=0
SMG	Z=0	Z=0	Z=-1	Z=0	Z=-1	Z=-1	Z=0	Z=-1	Z=-1
STG_P	Z=1	Z=-1	Z=-1	Z=-2*	Z=-2*	Z=0	Z=1	Z=0	Z=0
MTG_A				Z=-1		Z=-1	Z=0	Z=1	
MTG_P	Z=0	Z=0	Z=0	Z=0	Z=1	Z=-1	Z=0	Z=1	Z=0

The table summarises Z-scores and significance levels for the comparison of activity between frequency bands for auditory word tasks. * shows a significance level of $p<0.05$. Each frequency band is compared to the two other frequency bands. A negative Z-score shows that the first frequency band listed of a pair exhibited less activity, e.g. beta-low gamma with Z=-2* means that beta ERD showed significantly less ($p<0.05$) spectral changes compared to the low gamma activity. A positive Z-score means the opposite.

Table 52. Wilcoxon rank sum test results for visual naming tasks comparing frequency band activity.

	PN			CNw		
	beta-low gamma	beta-high gamma	low gamma-high gamma	beta-low gamma	beta-high gamma	low gamma-high gamma
INS_A	Z=1	Z=0	Z=-1	Z=1	Z=1	Z=0
INS_P		Z=-1	Z=-1	Z=1	Z=1	
IFG	Z=1	Z=1	Z=0	Z=0	Z=1	Z=1
preC	Z=0	Z=0	Z=0	Z=1	Z=-1	Z=-1
postC	Z=-1	Z=-1	Z=-1	Z=0	Z=-1	Z=-1
SMG		Z=-1	Z=-1	Z=0	Z=0	Z=-1
STG_P	Z=-1	Z=-1	Z=0	Z=-1	Z=-2*	Z=-1
MTG_A				Z=-1	Z=0	Z=0
MTG_P	Z=0	Z=0	Z=0	Z=1	Z=1	Z=-1

The table summarises Z-scores and significance levels for the comparison of activity between frequency bands for visual naming tasks. * shows a significance level of $p<0.05$. Each frequency band is compared to the two other frequency bands. A negative Z-score shows that the first frequency band listed of a pair exhibited less activity, e.g. beta-high gamma with Z=-2* means that beta ERD showed significantly less ($p<0.05$) spectral changes compared to the high gamma activity. A positive Z-score means the opposite.

Table 53. Mean percentage of contacts showing spectral changes and concordance with iERPs.

	% of all contacts					% of ERS/D + iERP					% of ERS/D alone				
	BL	WR	VG	PN	CNw	BL	WR	VG	PN	CNw	BL	WR	VG	PN	CNw
Beta ERD	7.7	12.1	11.1	3.8	7.0	7.1	11.8	10.0	3.2	4.8	0.6	0.3	1.1	0.6	2.2
Low gamma ERS	5.1	11.3	8.7	3.4	2.4	5.1	10.7	8.2	3.0	1.4	0.0	0.6	0.5	0.4	1.0
High gamma ERS	7.7	7.0	11.5	3.8	5.6	7.1	6.4	10.0	3.6	3.6	0.6	0.6	1.5	0.2	2.0

The table summarises mean percentage of contacts showing beta ERD, low gamma ERS and high gamma ERS out of all contacts analysed. Next, mean percentage of contacts showing concordance and mean percentage pf contacts showing only spectral changes is summarised for all three frequency bands and auditory and visual tasks.

Table 54. Wilcoxon rank sum test comparing concordance of iERPs and spectral changes with spectral changes alone.

	conc_iERP&beta– beta ERD	conc_iERP&low gamma– low gamma ERS	conc_iERP&high gamma– high gamma ERS
BL	Z=1.5	Z=3.1**	Z=2.0*
WR	Z=1.7	Z=3.0**	Z=3.2**
VG	Z=1.9	Z=2.6**	Z=1.5
PN	Z=2.2*	Z=1.6	Z=1.7
CNw	Z=0.6	Z=0.7	Z=0.7

The table summarises Z-scores and significance levels for the comparison of the mean percentage of contacts with concordance of iERPs and spectral changes and the mean percentage of contacts showing spectral changes alone for auditory and visual tasks. Frequency bands analysed were beta ERD, low gamma ERS and high gamma ERS. ** shows a significance level of $p<0.01$ and * shows a significance level of $p<0.05$.
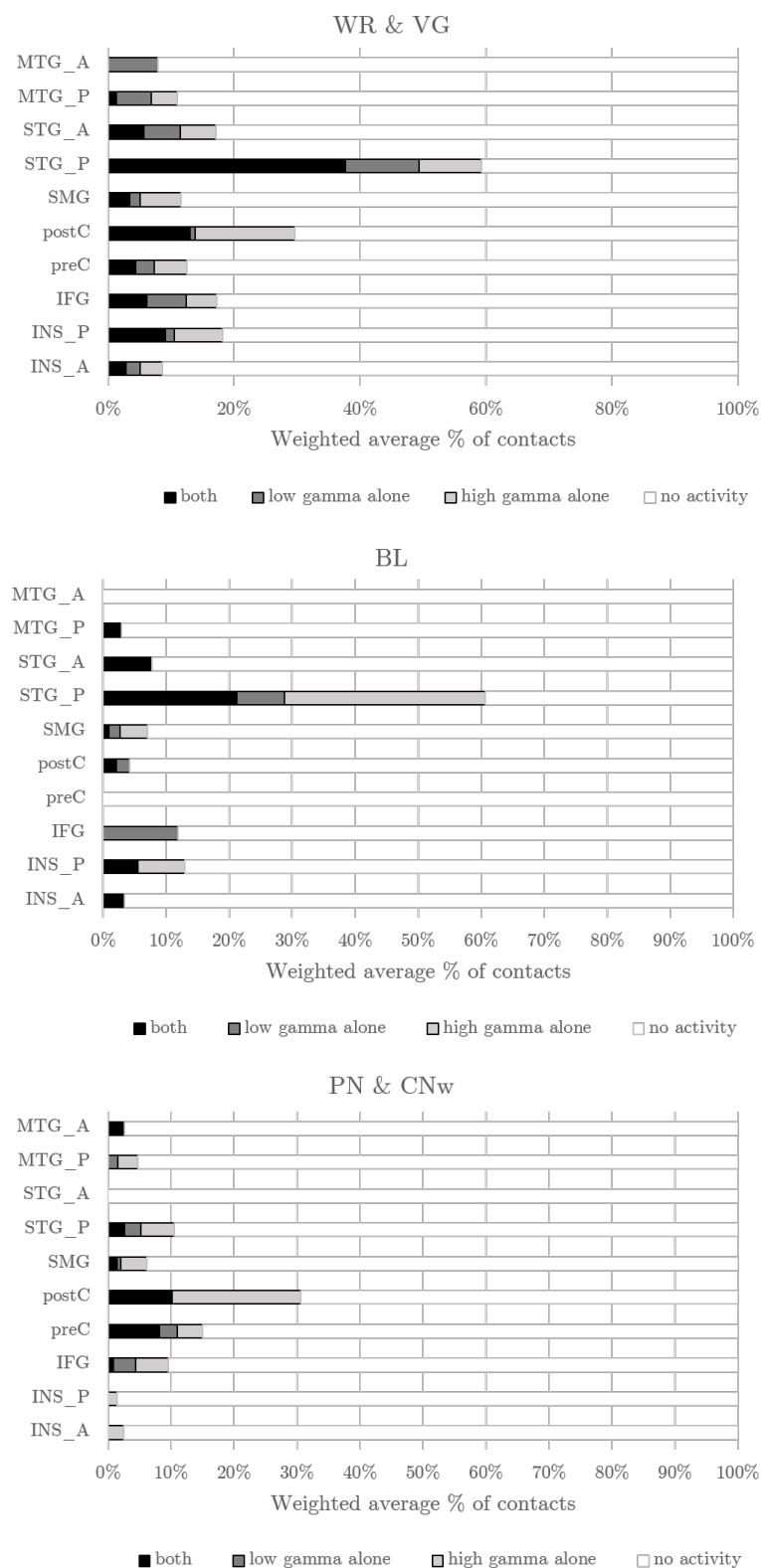
Figure 118. Concordance of region- and task-specific spectral changes comparing low and high gamma ERS. Each graph illustrates the mean percentage of contacts showing either low or high gamma ERS changes alone, spectral changes together or no activity for word repetition and verb generation (WR & VG), the baseline task (BL) or picture naming (PN) and colour naming (CNw).

WR & VG

BL

PN & CNw

Legend (repeated for each graph): ■ both ■ beta alone □ low gamma alone □ no activity
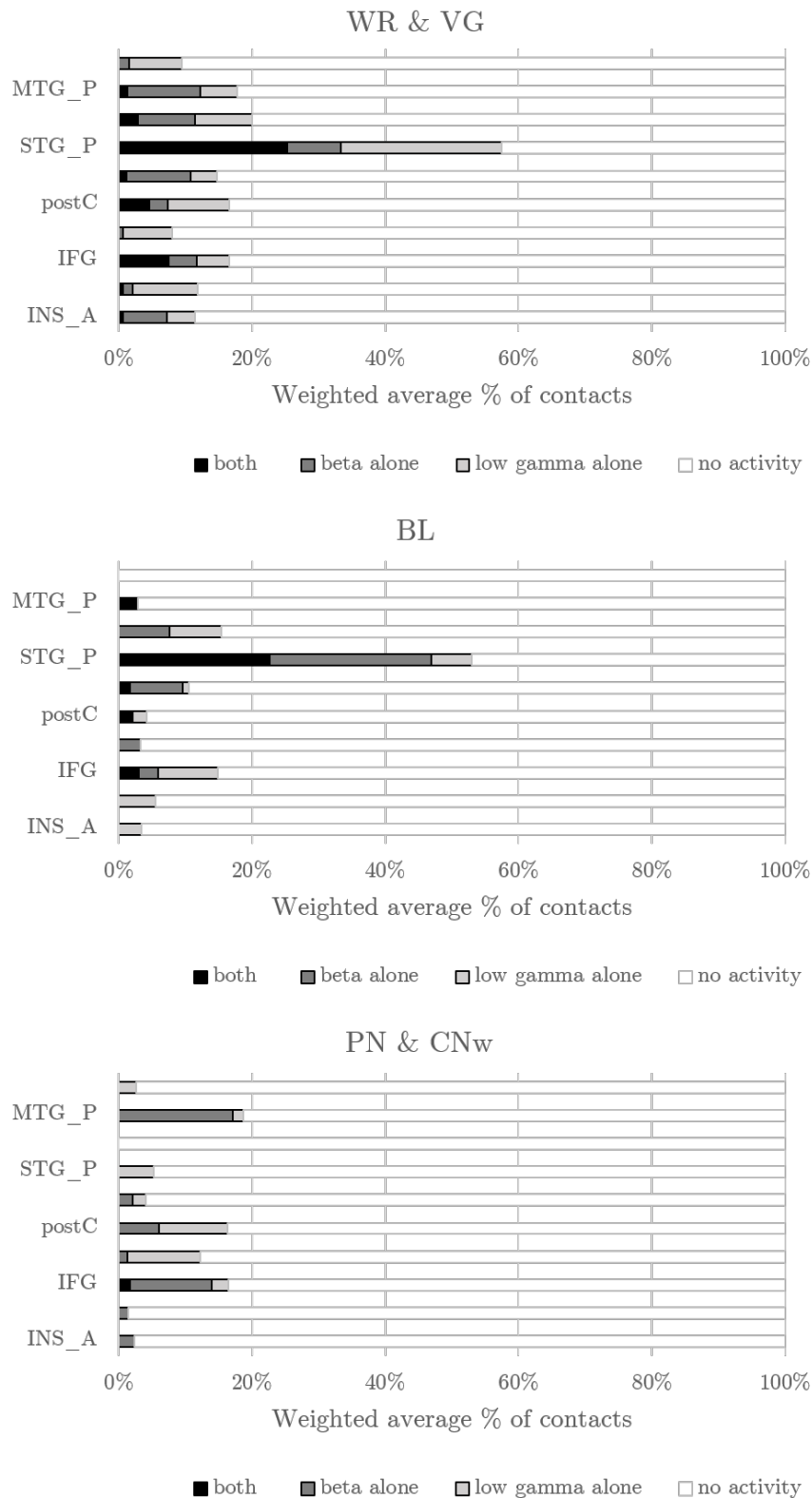
Figure 119. Concordance of region- and task-specific spectral changes comparing beta ERD and low gamma ERS. Each graph illustrates the mean percentage of contacts showing either low or high gamma ERS changes alone, spectral changes together or no activity for word repetition and verb generation (WR & VG), the baseline task (BL) or picture naming (PN) and colour naming (CNw).
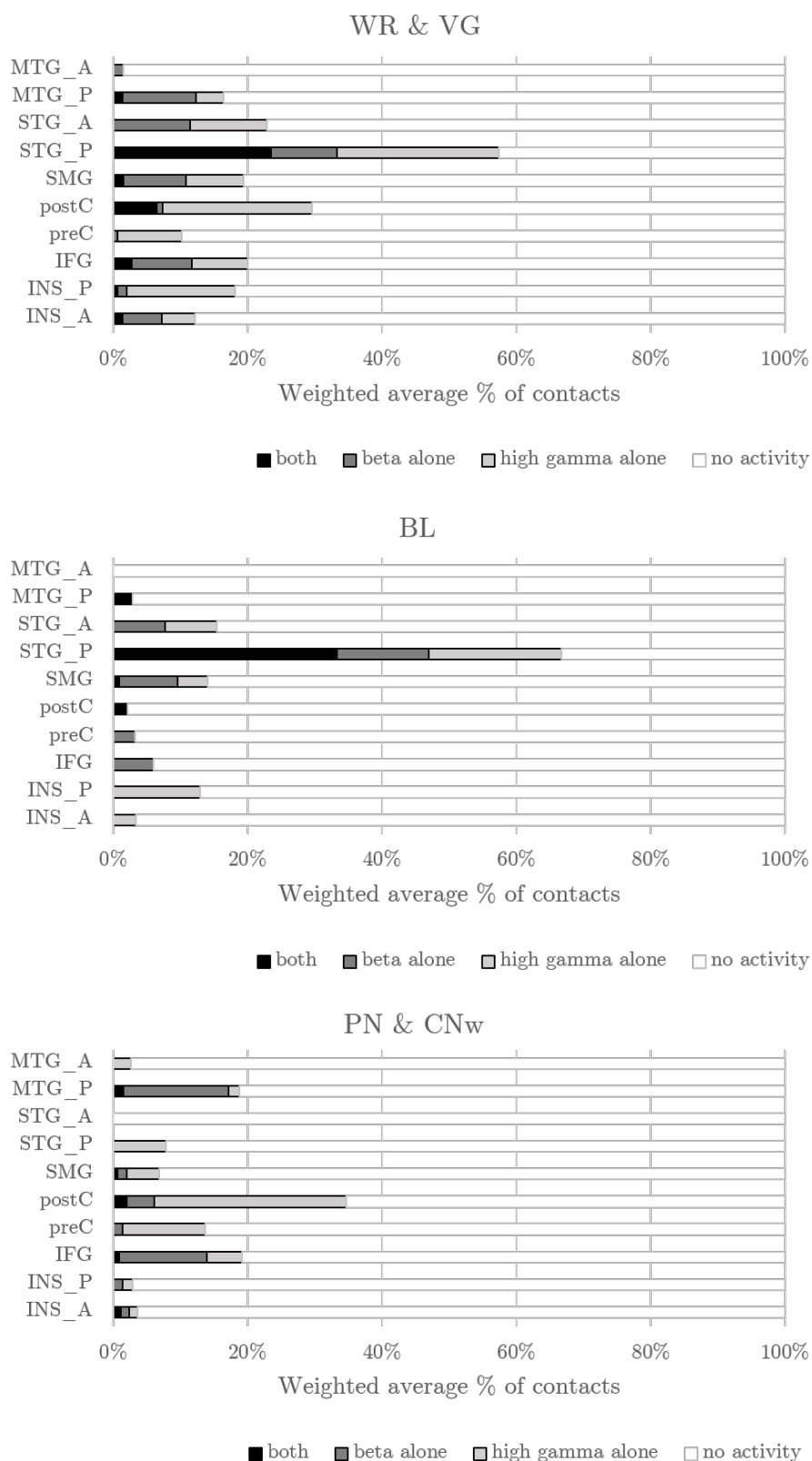
Figure 120. Concordance of region- and task-specific spectral changes comparing beta ERD and high gamma ERS. Each graph illustrates the mean percentage of contacts showing either low or high gamma ERS changes alone, spectral changes together or no activity for word repetition and verb generation (WR & VG), the baseline task (BL) or picture naming (PN) and colour naming (CNw).

377

Table 55. Wilcoxon rank sum test results for speech response induced frequency band activity.

	Speech response – induced		
	beta-low gamma	beta-high gamma	low gamma-high gamma
INS_A	Z=0	Z=1	Z=1
INS_P	Z=0	Z=1	Z=0
IFG	Z=0	Z=-1	Z=-1
preC	Z=1	Z=0	Z=-1
postC	Z=1	Z=0	Z=-2*
SMG	Z=0	Z=0	Z=0
STG_P	Z=1	Z=1	Z=0
MTG_A		Z=-1	Z=-1
SFG	Z=0	Z=0	Z=1
MFG	Z=1	Z=1	Z=1

The table summarises Z-scores and significance levels for the comparison of speech response induced activity between frequency bands. * shows a significance level of $p<0.05$. Each frequency band is compared to the two other frequency bands. A negative Z-score shows that the first frequency band listed of a pair exhibited less activity, e.g. low gamma-high gamma with Z=-2* means that low gamma ERS showed significantly less ($p<0.05$) spectral changes compared to the high gamma ERS. A positive Z-score means the opposite.
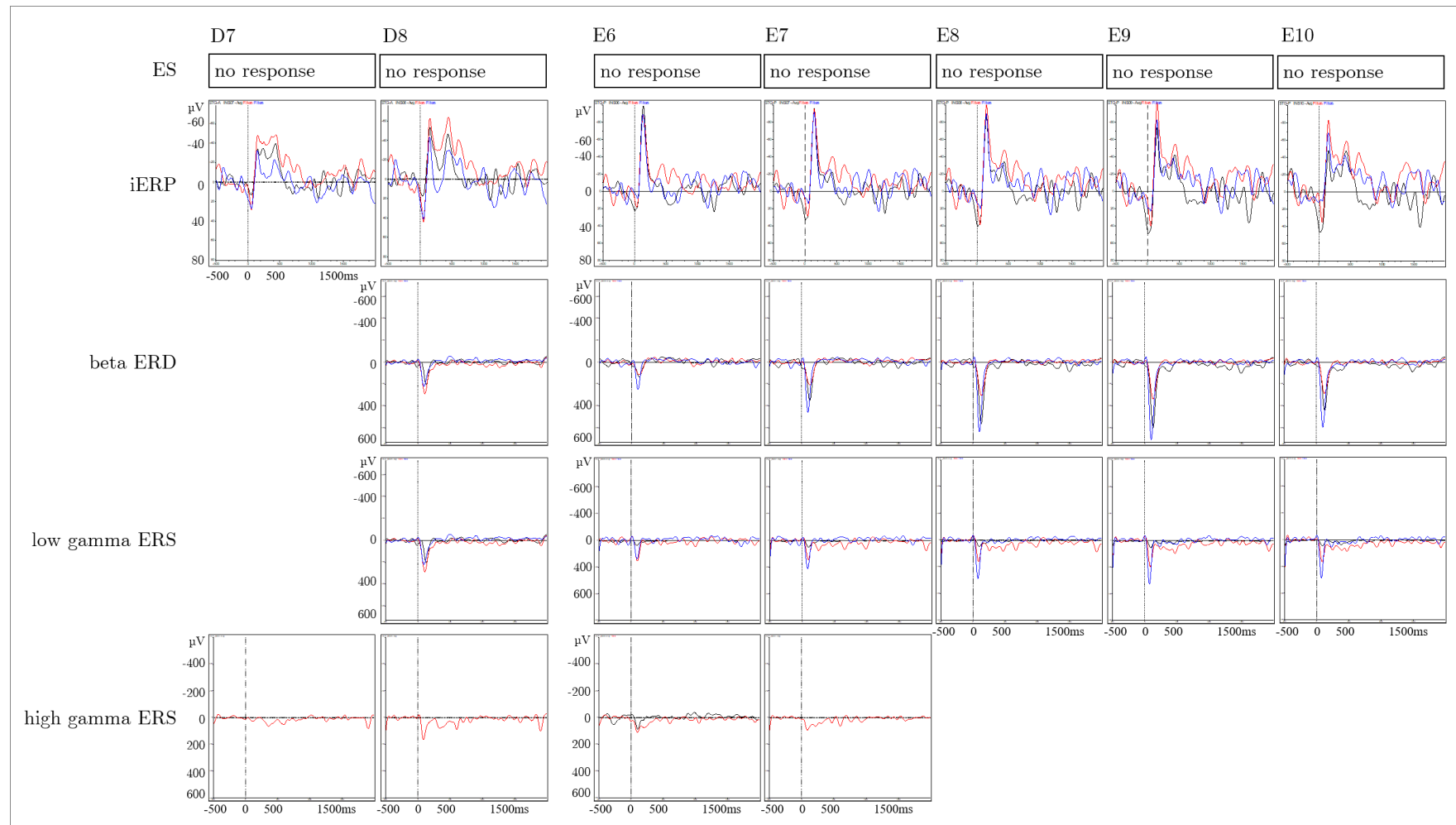
Figure 121. Case 1 (ID2)—contacts used for language stimulation (1). Electrode D (STG to anterior insula) with contacts 7 and 8 and electrode E (STG to posterior insula) with contacts 6,7,8,9,10 are presented. First, language stimulation responses during electrical stimulation are shown for each contact. Next, iERP responses and lastly beta ERD, low and high gamma ERS are presented. Responses during VG are illustrated in black, WR in red and baseline task in blue. Empty spaces indicate no activity measured.
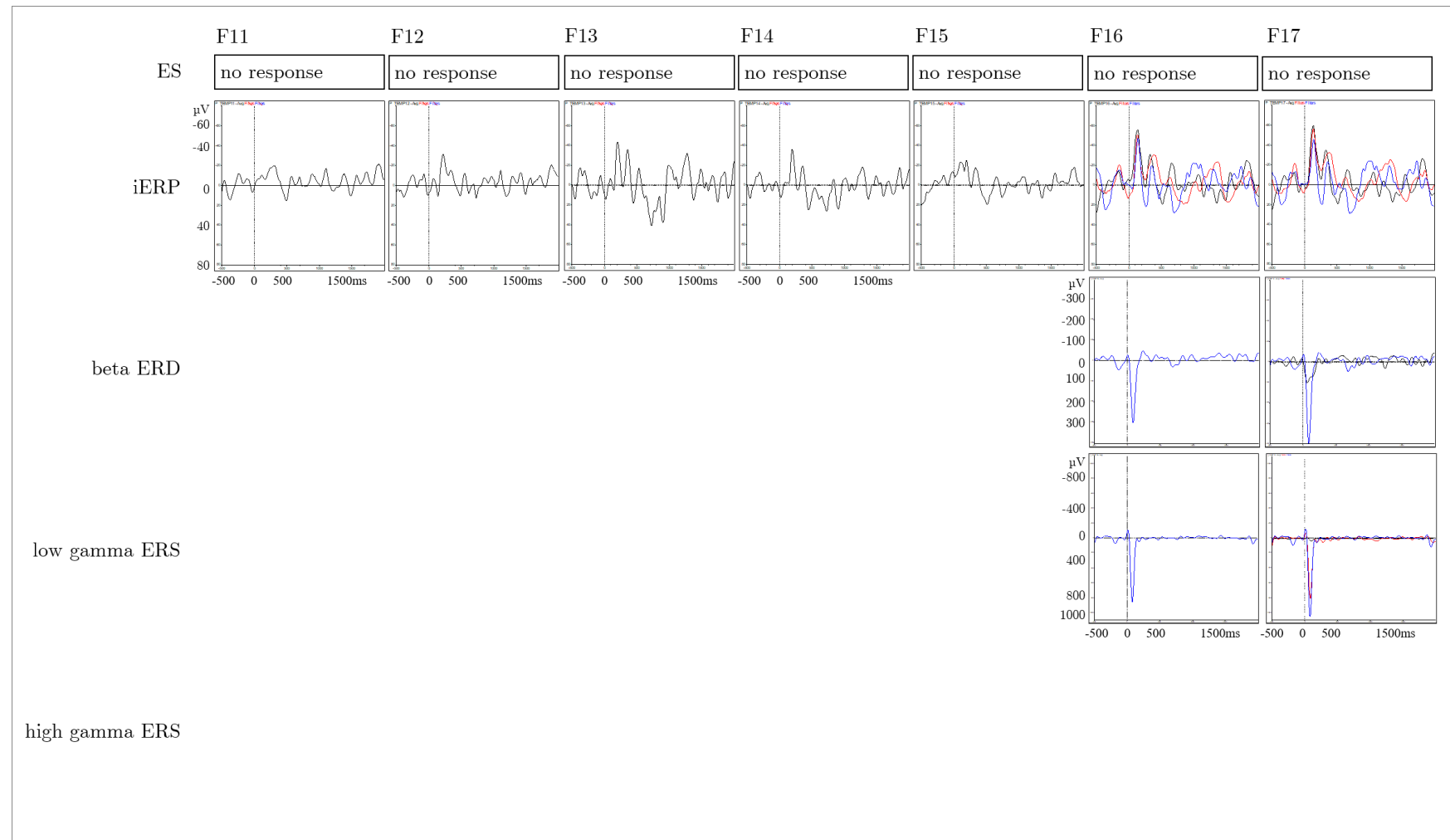
Figure 122. Case 1 (ID2)—contacts used for language stimulation (2). Electrode F (posterior temporal) is presented here with contacts 11–17. First, language stimulation responses during electrical stimulation are presented for each contact. Next, iERP responses and lastly beta ERD, low and high gamma ERS are shown. Responses during VG are illustrated in black, WR in red and baseline task in blue. Empty spaces indicate no activity measured.
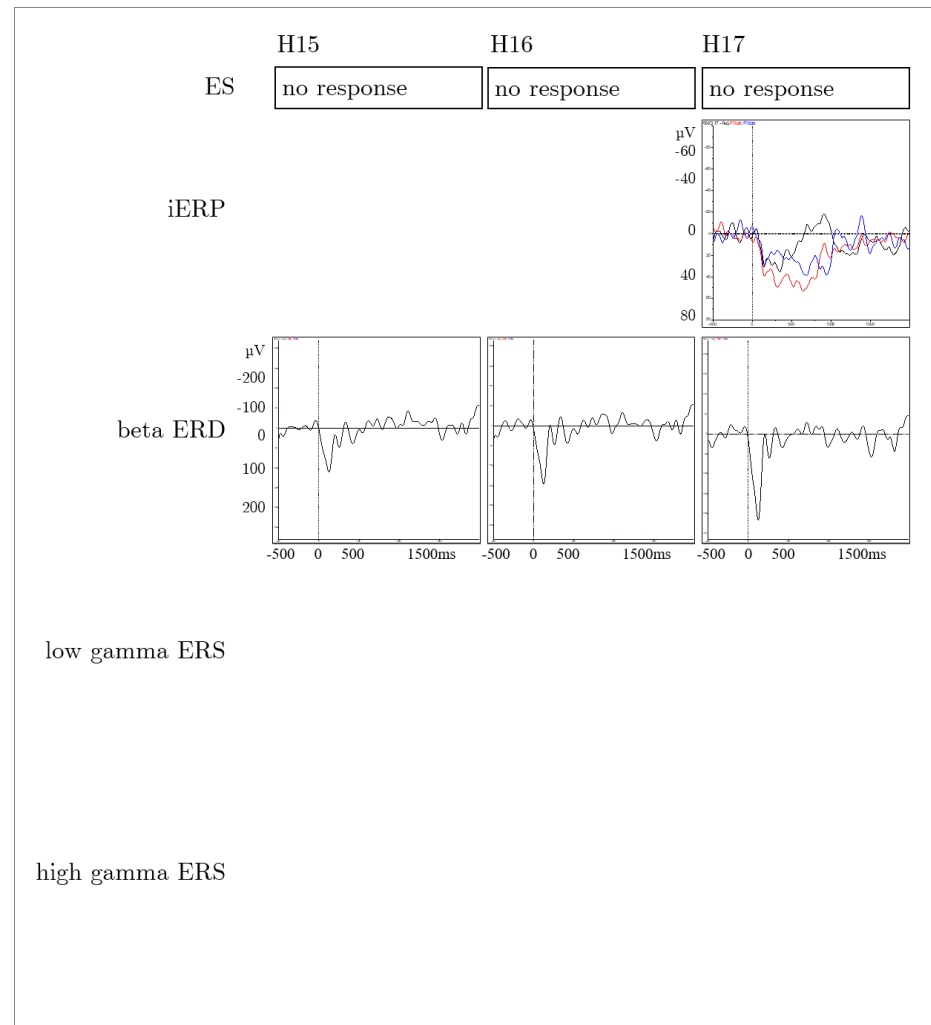
Figure 123. Case 1 (ID2)—contacts used for language stimulation (3). Electrode H (angular) is presented here with contacts 15–17. First, language stimulation responses during electrical stimulation are presented for each contact. Next, iERP responses and lastly beta ERD, low and high gamma ERS are shown. Responses during VG are illustrated in black, WR in red and baseline task in blue. Empty spaces indicate no activity measured.
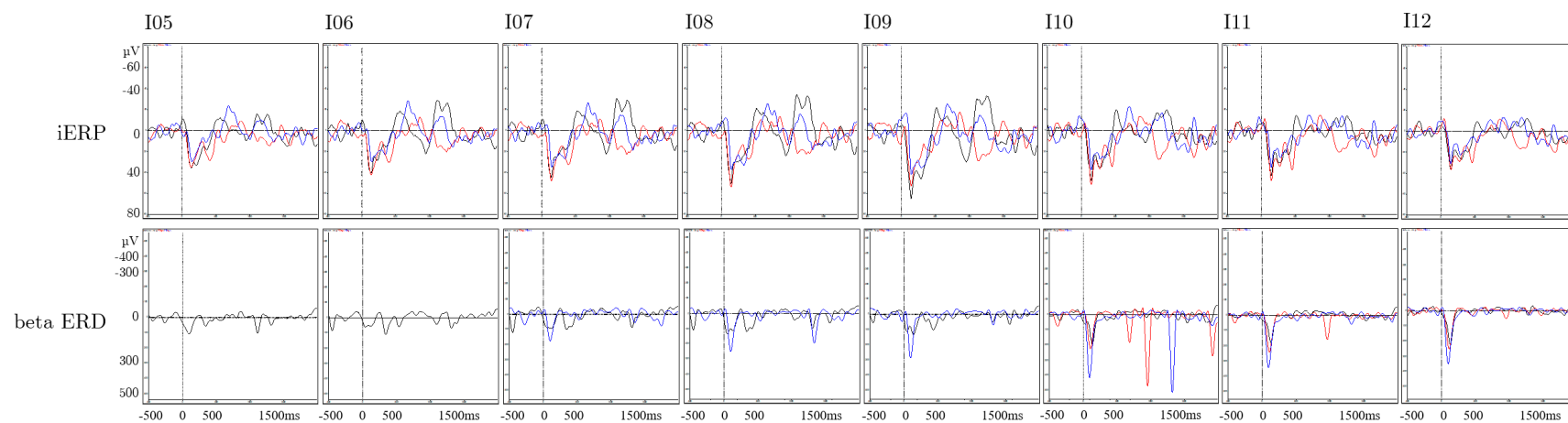
Figure 124. Case 1 (ID2)—contacts included in surgical resection (1). Electrode I (SMG) is presented here with contacts 5–12. First iERP responses and next beta ERD, low and high gamma ERS are shown. Responses during VG are illustrated in black, WR in red and baseline task in blue. Empty spaces indicate no activity measured.

Columns: J05, J06, J07, J08

J07: not recorded from
J08: not recorded from

iERP row axis: µV, -60, -40, 0, 40, 80; x-axis: -500, 0, 500, 1500ms

beta ERD row (J06): µV, -100, -50, 0, 50, 100, 150; x-axis: -500, 0, 500, 1500ms

Rows: iERP, beta ERD, low gamma ERS, high gamma ERS

Figure 125. Case 1 (ID2)—contacts included in surgical resection (2). Electrode J (parietal operculum to posterior insula) is presented here with contacts 5–8. First iERP responses and next beta ERD, low and high gamma ERS are shown. Contacts 7 and 8 were not included in iERP and spectral analysis. Responses during VG are illustrated in black, WR in red and baseline task in blue. Empty spaces indicate no activity measured.

Figure 126. Case 3 (ID8)—contacts used for language stimulation (1). Electrode F (posterior STG to insula) contacts 2–5 and 9–10 were used. First, language stimulation responses during electrical stimulation are presented for each contact. Next, iERP responses and lastly beta ERD, low and high gamma ERS is shown. Responses during VG are illustrated in black, WR in red and baseline task in blue. Empty spaces indicate no activity measured.

Figure 127. Case 3 (ID8)—contacts used for language stimulation (2). Electrode K (parietal operculum) contacts 4–7 were used. First, language stimulation responses during electrical stimulation are presented for each contact. Next, iERP responses and lastly beta ERD, low and high gamma ERS is shown. Responses during VG are illustrated in black, WR in red and baseline task in blue. Empty spaces indicate no activity measured.
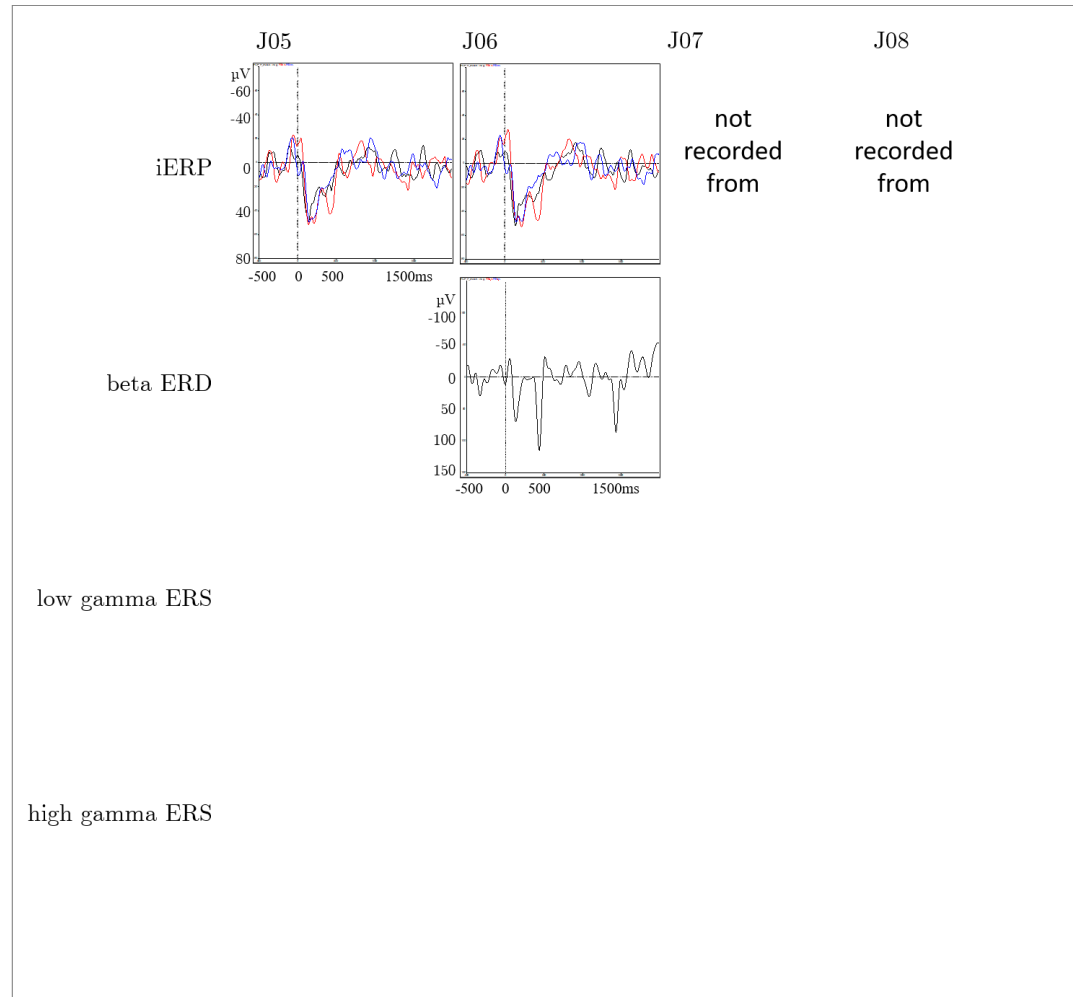
Figure 128. Case 3 (ID8)—contacts used for language stimulation (3). Electrode I (pars triangularis to insula) contacts 1–9 were used. First, language stimulation responses during electrical stimulation are presented for each contact. Next, iERP responses and lastly beta ERD, low and high gamma ERS is shown. Responses during VG are illustrated in black, WR in red and baseline task in blue. Empty spaces indicate no activity measured.
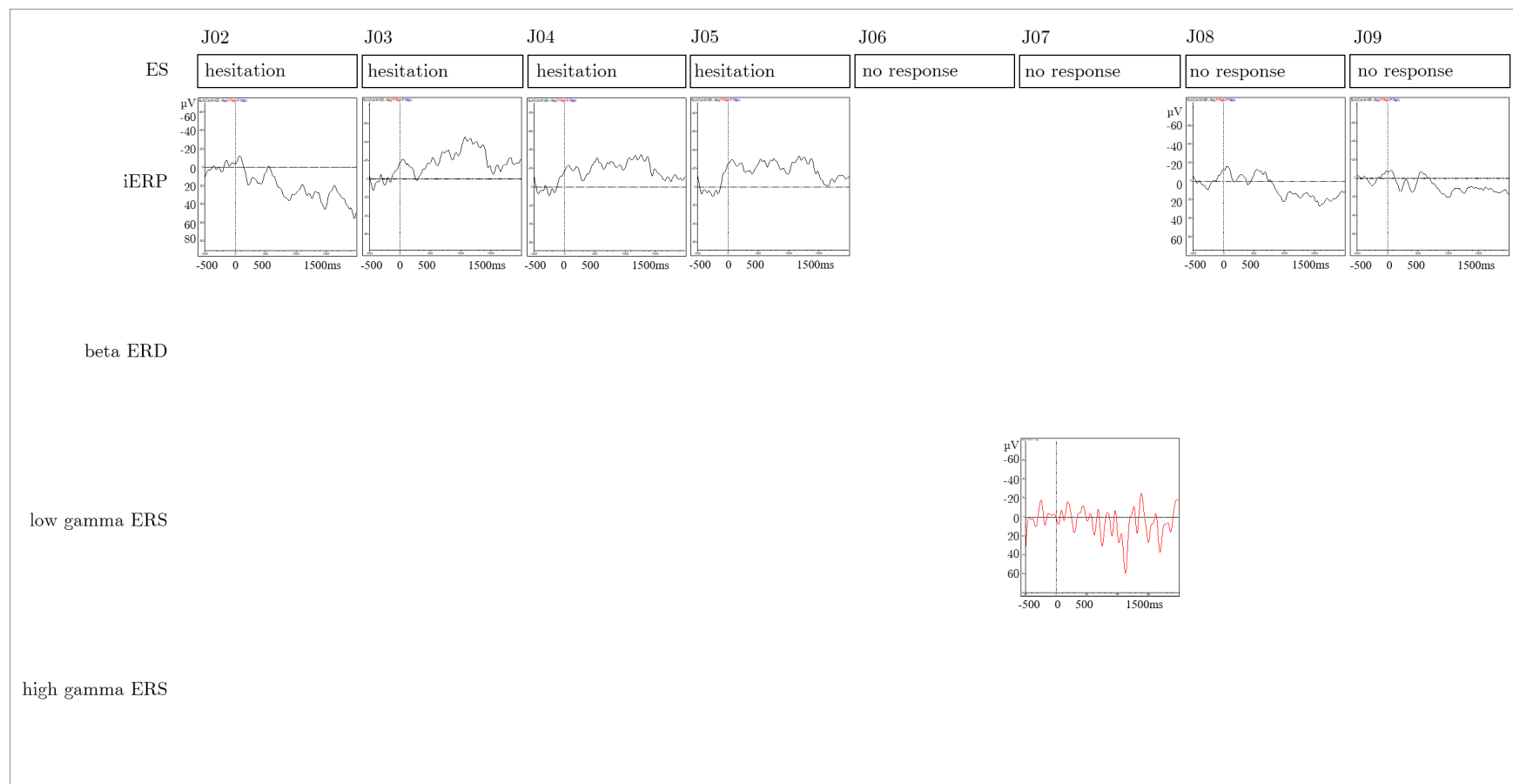
Figure 129. Case 3 (ID8)—contacts used for language stimulation (4). Electrode J (Subcentral to insula) contacts 2–9 were used. First, language stimulation responses during electrical stimulation are presented for each contact. Next, iERP responses and lastly beta ERD, low and high gamma ERS is shown. Responses during VG are illustrated in black, WR in red and baseline task in blue. Empty spaces indicate no activity measured.
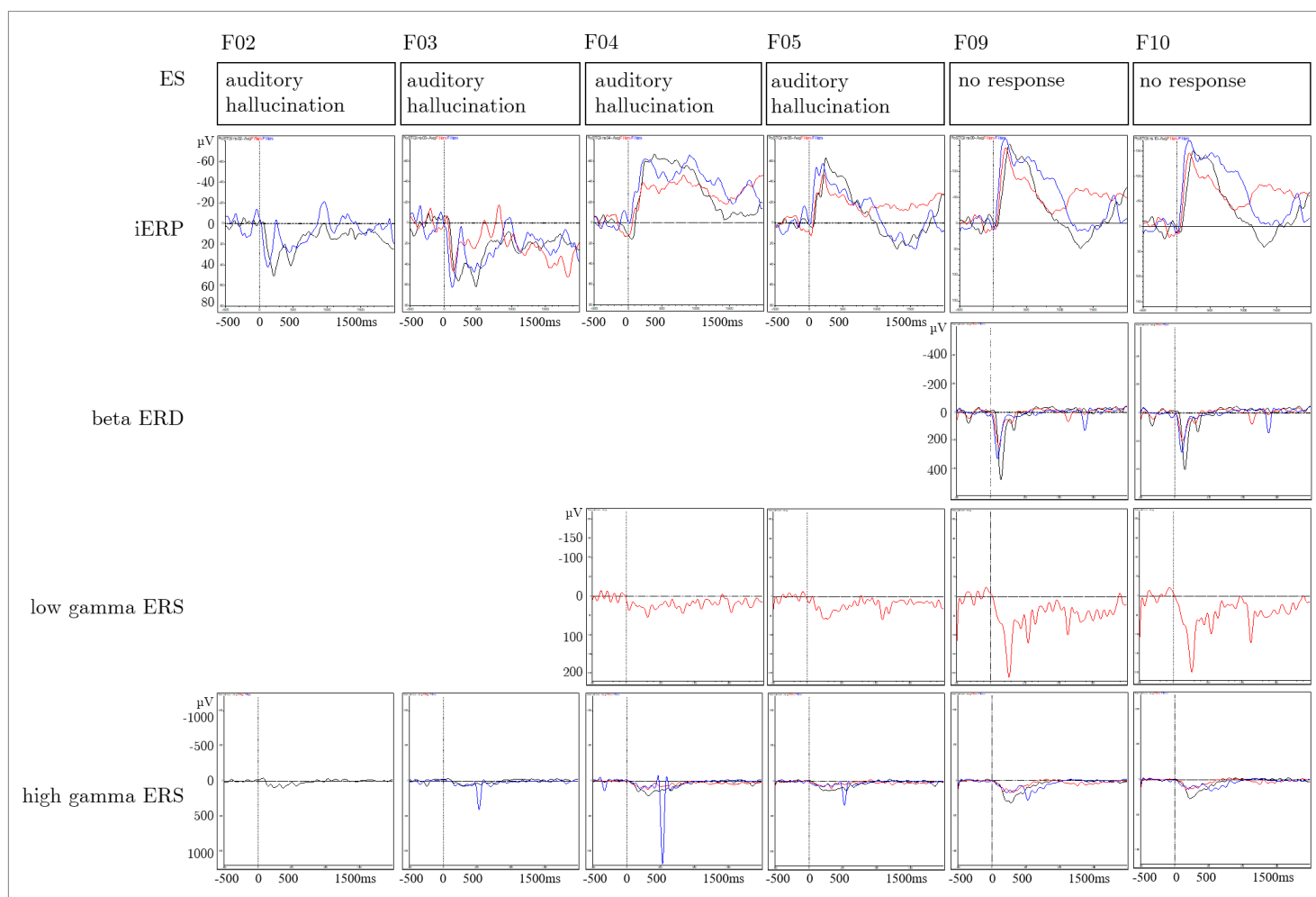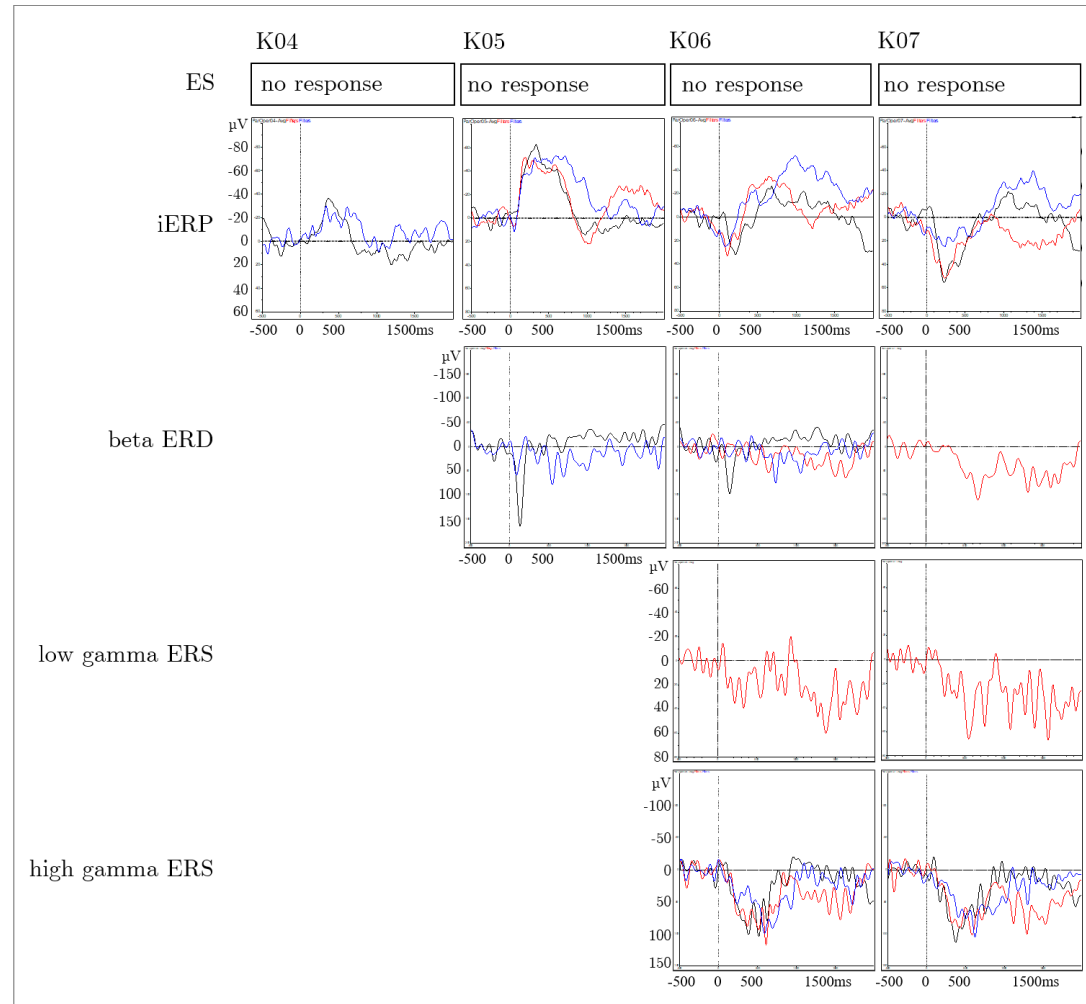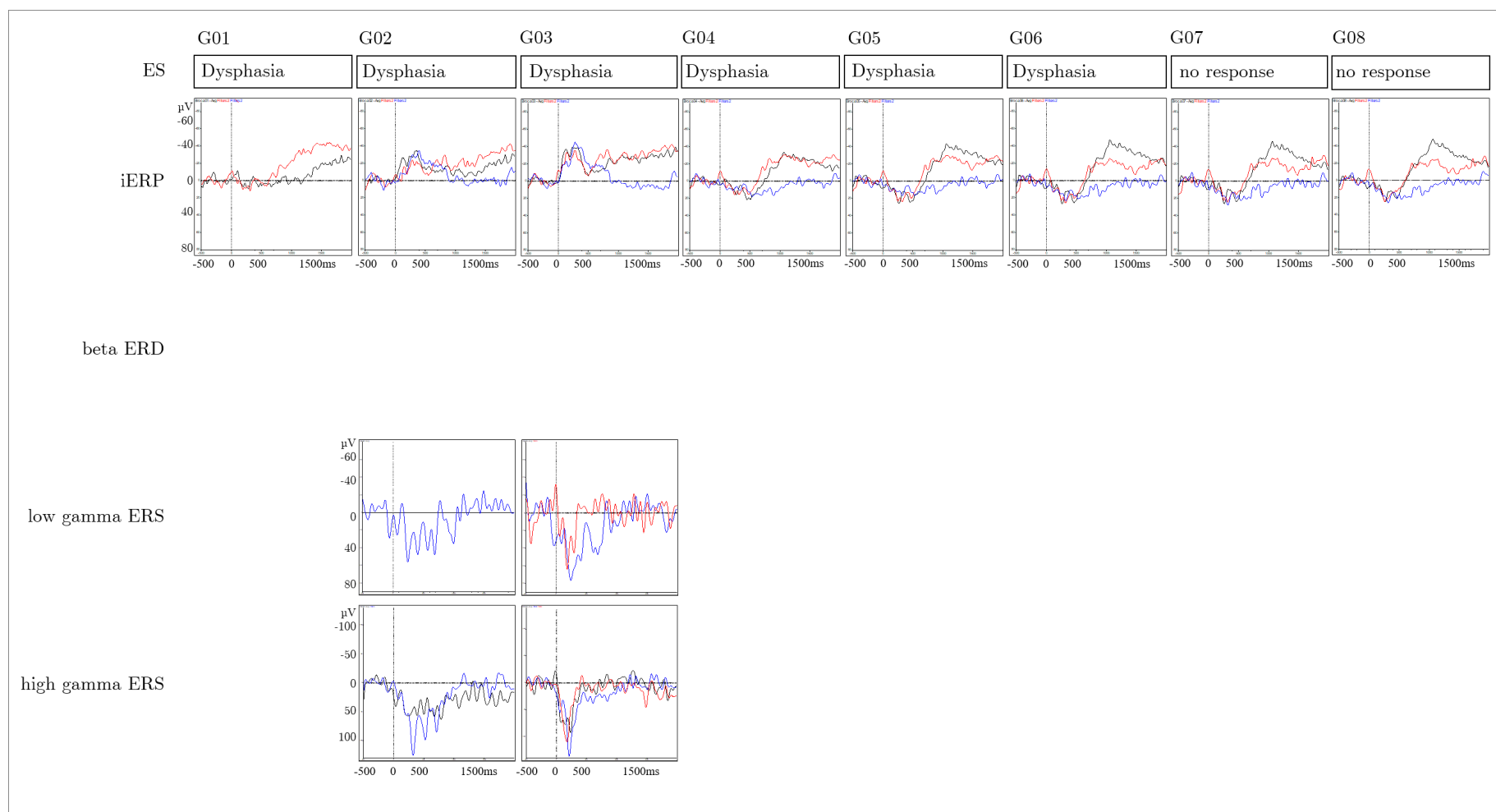
Figure 130. Case 3 (ID20)—contacts used for language stimulation (1). Electrode G (Broca) contacts 1–8 were used. First, language stimulation responses during electrical stimulation are presented for each contact. Next, iERP responses and lastly beta ERD, low and high gamma ERS is shown. Responses during VG are illustrated in black, WR in red and baseline task in blue. Empty spaces indicate no activity measured.
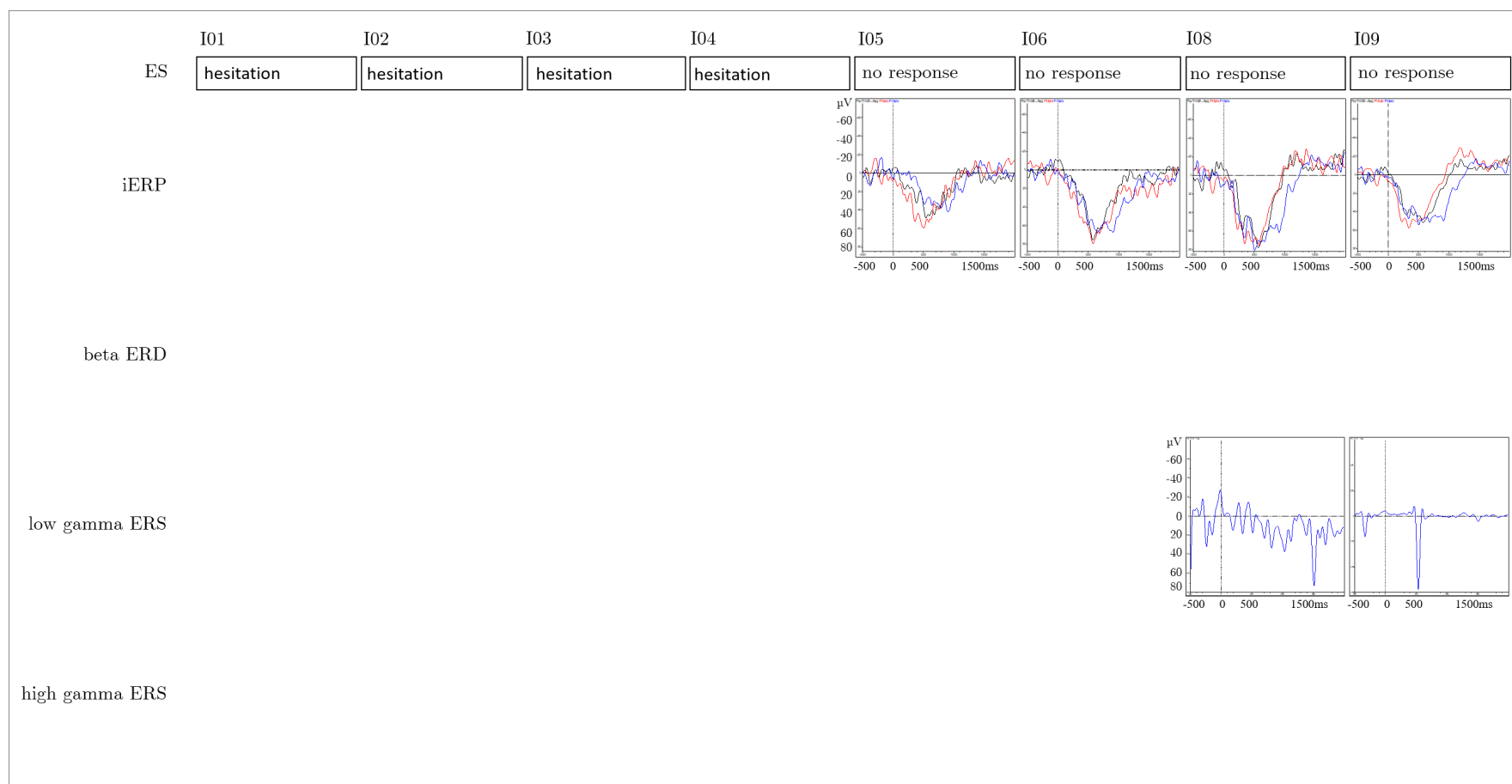
Figure 131. Case 3 (ID20)—contacts used for language stimulation (2). Electrode F (subcentral) contacts 1–10 were used. First, language stimulation responses during electrical stimulation are presented for each contact. Next, iERP responses and lastly beta ERD, low and high gamma ERS is shown. Responses during VG are illustrated in black, WR in red and baseline task in blue. Empty spaces indicate no activity measured.

Case 4 (ID3)

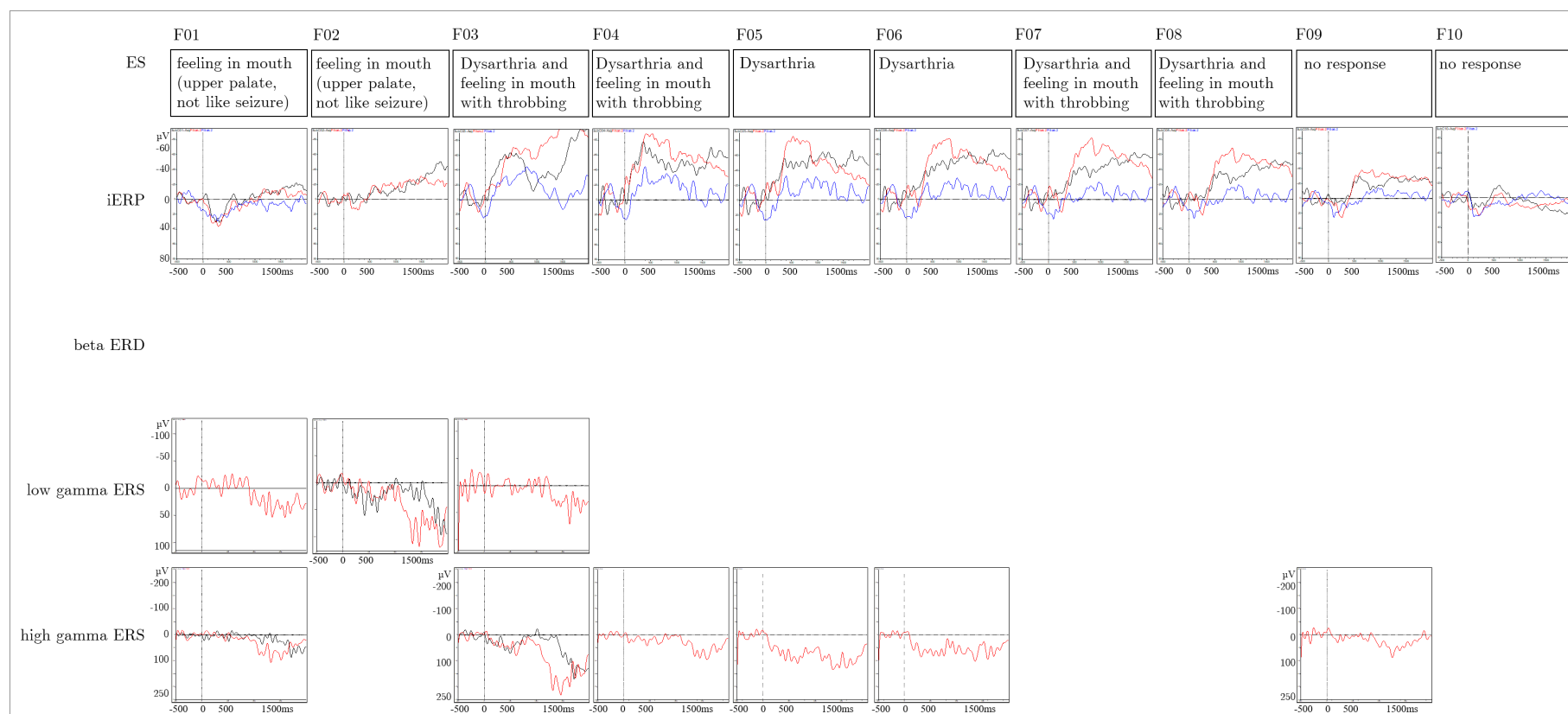Patient ID3 was a 9-year and 9 months old, left-handed girl with medication-resistant epilepsy. Her first seizure occurred at eight months of age. She underwent a left-sided temporo-occipito-parietal disconnection at the age of one and a redo disconnection at the age of eight. Her latest seizures were predominately nocturnal episodes described as gurgling tummy sounds, mild redness of her face, seeking comfort and often being distressed. These episodes occurred 1–2 times per night and lasted up to 40 seconds. Some of her episodes evolved further with left sided (arm/leg) stiffening/hyper-motor movements and the patient reported 'monsters' she was scared about. She had global mild learning difficulties.

MRI results prior to the two disconnection were reported to have a broad malformation of the left hemisphere. Histopathology findings were FCD type 2A with unusual features of inflammation. Post-disconnection MRI results showed a small residual connection with the abnormal left superior temporal gyrus. However, it was not believed its disconnection would yield seizure control, as both previous disconnections did not change the patient's seizure semiology. The scalp EEG lateralised to the left hemisphere and seizure semiology was non-lateralising, however, fear was suggestive of amygdala or insula involvement. Therefore, it was decided to offer an invasive monitoring to define a new surgical target.

Patient ID3 was admitted to GOSH Koala ward for a left-sided SEEG implantation. In total, 12 electrodes were implanted. The invasive EEG showed three distinct electrical patterns with overall similar clinical manifestation with hyper-motor and insular features. It suggested a widespread epileptogenic area extending from S1 (anterior to the previous resection margin, electrode C) and up to the insula (deep contacts of D, K, E, and L). Furthermore, motor stimulation showed positive motor findings for right wrist and fingers (G3–7) and language stimulations yielded results of speech hesitancy over the subcentral area (F2–3, 6–7). Resection would have needed to be extensive and carried a high risk of a motor deficit. Surgical resection was not offered.

For this study, the patient was able to complete three language tasks (BL, WR and VG). She performed best during the word repetition task with 98% followed by the verb generation task with 78%.

The clinical SEEG implantation regime is summarised in Figure 132. A subset of clinically implanted electrodes was included in this study. Certain contacts involved in the seizure onset were included in the iERP recording (contacts from electrodes C, D, E) and others were not (contacts from electrodes K and L). The following Figure 133 illustrates the patient's implantation regime. Contacts stimulated during functional electrical stimulation are highlighted and electrical stimulation responses, iERPs and spectral changes elicited during the auditory word tasks (BL, WR and VG) are illustrated.

Electrode	Label	Contacts	Location
Depth	A	1-10	Left Superior Parietal
Depth	B	1-12	Left Occipital
Depth	C	1-12	Left S1
Depth	D	1-10	Left S2-Insula
Depth	E	1-8	Left Superior Temporal Gyrus-Insula
Depth	F	1-10	Left Subcentral-Insula
Depth	G	1-8	Left M1
Depth	H	1-8	Left Supplementary Motor Cortex
Depth	I	1-15	Left Middle Frontal Gyrus
Depth	J	1-15	Left Inferior Frontal Gyrus
Depth	K	1-18	Left Posterior Insula
Depth	L	1-15	Left Anterior Insula

Figure 132. Case 4 (ID3)—implantation regime summary. A. illustrates the patient's brain images with implanted SEEG electrodes. All electrodes implanted are presented, with the ones used for this study highlighted with pink letterboxes. Each blue dot presents a contact. Electrode F shows light blue contacts in addition, which highlight contacts used for language stimulation during clinical assessment. **B.** illustrates the patients implantation regime, resection area of her previous surgery marked with dark blue stripes, and a presumed residual connection of the previous disconnection circled in white. **C.** summarises the locations of the electrodes inserted, their labels and the electrode used for language stimulation are circled in light blue.

.
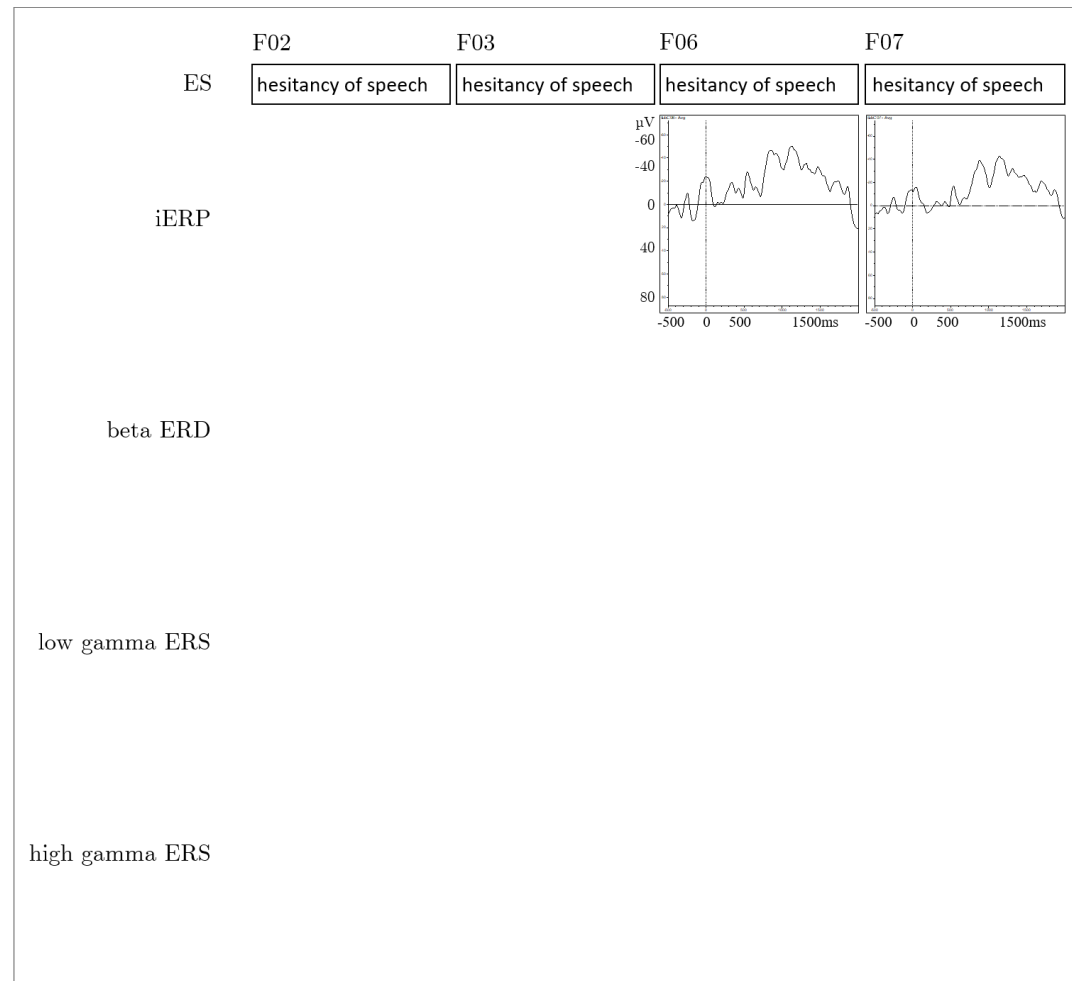
Figure 133. Case 4 (ID3)—contacts used for language stimulation. Electrode F (subcentral to insula) contacts 2,3,6,7 were used. First, language stimulation responses during electrical stimulation are presented for each contact. Next, iERP responses and lastly beta ERD, low and high gamma ERS is shown. Empty spaces indicate no activity measured.

This patient was not suitable for fMRI testing; hence, language lateralisation was unclear. She was left-handed. SEEG implantation was left-sided and ictal and inter-ictal zones were widespread involving possible language-related areas. Language was tested, stimulating electrode F (subcentral to insula), contacts 2–3, 6–7. Speech hesitancy was observed stimulating these pairs of contacts. Only two of these contacts (50.0%) showed robust iERPs and none measured spectral changes in any frequency band. Furthermore, only the verb generation task yielded robust iERPs. This patient was excluded from group analysis as she underwent prior surgery. In general, she showed fewer iERPs (18.0%) compared to the patients included in the group analysis (60.5%) during these three auditory tests. Furthermore, morphology was different. There were no primary components measured and only 1.1% of early components, compared to 14.8% for the group (primary plus early components). Most components elicited were middle latency components with 12.8% compared to 21.0% for the group and again few long latency components with 4.1% compared to 24.7% for the group. The most prominent language-related iERPs were measured in the inferior frontal gyrus, followed by the anterior insula, superior temporal gyrus and superior frontal gyrus. Contacts involved in the ictal onset did not show iERPs. In total, only two contacts showed spectral changes, one showed beta ERD (middle latency activity) and one showed low gamma ERS (late latency activity). Both were located in the inferior frontal gyrus.

In summary, this patient shows few iERPs and hardly any frequency activity. However, when activity was observed it was measured in language related brain regions, which were not involved in the ictal onset. iERP and frequency activity analysis could have been used to give an overview of language-related brain areas. This could have been used to choose contacts for functional electrical stimulation.

Case 5 (ID12)

Patient ID12 was a 6-year and 10 months old, left-handed girl with medication-resistant epilepsy. Her first languages were Portuguese and Spanish and English was her third language. Her first seizure occurred with two months of age. She underwent left frontal resection at the age of 4-years and 2 months. Histology showed FCD type 2a. Four months post-surgery her seizures re-occurred. Her latest events presented from sleep, with usually a single episode. She aroused, her arms elevated and became stiff with jerking movements. She made guttural noise, sat up, cried, looked for her parents and usually had a look of fear. Occasional tongue biting occurred. The average duration of these events were 30 seconds and they occurred 3–4 times a week.

The MRI showed a possible area of residual FCD medially and posteriorly to the resection cavity, in the cortex of the superior frontal gyrus. The most marked areas of hypometabolism in the PET were seen in the region of the left superior temporal gyrus, the left insula extending to left central region and right temporal pole inferiorly. The ictal scalp EEG showed transient changes in the left fronto-parietal region but were not localising. Interictal EEG showed infrequent bursts, which were not definitely localised but showed possible left central maximum. Therefore, invasive monitoring was offered.

Patient ID12 was admitted to GOSH Koala ward for a left-sided SEEG implantation. In total, nine electrodes were implanted. No definite SEEG changes were noted other than slowing in the anterior frontal areas. Stimulation of orbitofrontal contacts reproduced slowing, but no ictal clinical features were elicited. The working hypothesis of the seizure onset zone being posterior to the previous resection was disproved. Functional electrical stimulation suggested motor hand function in F1–2. No language-related brain areas were stimulated. The multidisciplinary team decided to not offer a surgical resection.

For this study, the patient was able to complete six language tasks (BL, WR, VG, LN, PN, CNw) in English. She performed best during the word repetition task with 100% correct responses, followed by the verb generation and colour naming tasks with 86%, picture-naming task with 84% and the sentence task with 30%.

The clinical SEEG implantation regime is summarised in Figure 134. All clinically implanted electrodes were included in this study. Contacts showing slowing during the patient's seizures were included in the iERP recording (A1,2,3,7,8; B1; C5,7,8; E1,3; F3,6; G1,2). The following Figure 135 illustrate the patients implantation regime, contacts stimulated during functional electrical stimulation including electrical stimulation responses, iERPs and spectral changes elicited during the auditory word tasks (BL, WR and VG).

Electrode	Label	Contacts	Location
Depth	A	1-15	Left Orbitofrontal
Depth	B	1-10	Left Broca-Insula
Depth	C	1-10	Left Prefrontal-Cingulate
Depth	D	1-15	Left Posterior Suprafrontal Gyrus
Depth	E	1-10	Left Subcentral
Depth	F	1-8	Left M1
Depth	G	1-5	Left preSMA
Depth	H	1-8	Left Supplementary Motor Cortex
Depth	I	1-12	Left S1
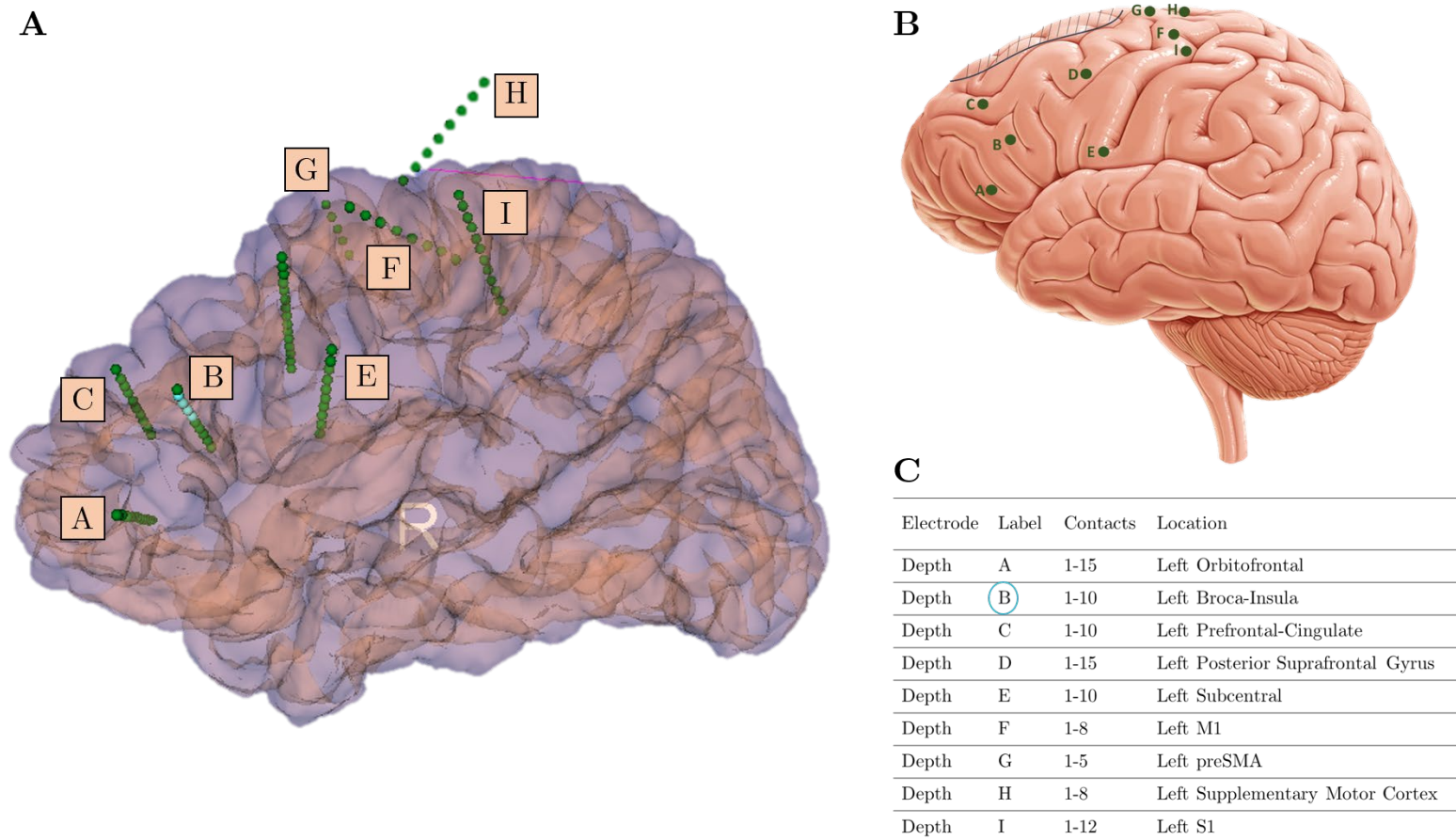
Figure 134. Case 5 (ID12)—implantation regime summary. A. illustrates the patient's brain images with implanted SEEG electrodes made using Slicer. All electrodes implanted were included in the study and are highlighted with pink letterboxes. Each green dot presents a contact. Electrode B shows light blue contacts in addition, which highlight contacts used for language stimulation during clinical assessment. B. illustrates the patient's implantation regime and the resection area of her previous surgery marked with dark blue stripes. C. summarises the locations of the electrodes inserted, their labels and the electrode used for language stimulation is circled in light blue.
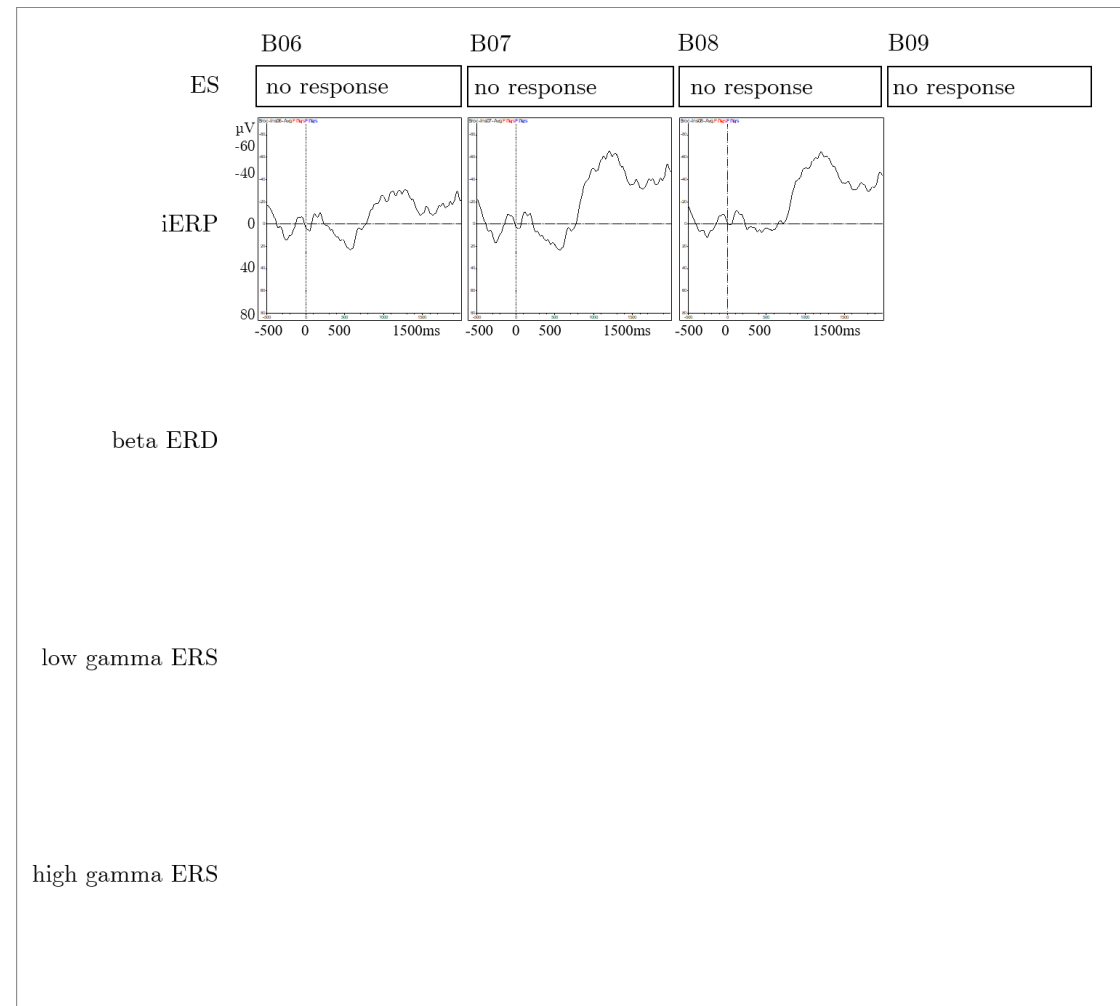
Figure 135. Case 5 (ID12)—contacts used for language stimulation. Electrode B (Broca to insula) contacts 6–9 were used. First, language stimulation responses during electrical stimulation are presented for each contact. Next, iERP responses and lastly beta ERD, low and high gamma ERS are shown. Responses during VG are illustrated in black, WR in red and baseline task in blue. Empty spaces indicate no activity measured.

No fMRI was done in this left-handed patient. Hence, language lateralisation was not clear. Contacts located in Broca's area were stimulated which yielded no responses. Three of these stimulated contacts showed robust iERPs, no spectral changes were observed.

In general, this patient showed fewer iERPs (29.7%) compared to the patients included in the group analysis (60.5%) during these three auditory tests. Furthermore, morphology was different. There were no primary components measured and only 1.5% of early components, compared to 14.8% for the group (primary plus early components). Most components elicited were long latency components with 17.1% compared to 24.7% for the group and 11.3% of middle latency components compared to 21.0% for the group. However, temporal regions showing a high number of iERPs and primary and early components in other patients were not sampled from in this patient. The most prominent language-related iERPs in this patient were observed in the superior frontal gyrus, followed by the orbitofrontal, middle frontal and inferior frontal gyrus. Out of all contacts, 3.1% showed beta ERD which was observed in the anterior insula, inferior frontal gyrus and superior frontal gyrus. 1.0% showed low gamma ERS which was observed in the anterior insula and orbitofrontal region and 2.1% showed high gamma ERS which was seen in the anterior insula, orbitofrontal region and inferior frontal gyrus.

Case 6 (ID19)

Patient ID19 was a 14-year and 5 months old, left-handed boy with medication-resistant epilepsy. His first seizure occurred with 20 months of age. He got a VNS implanted at the age of six years and was seizure free for four years following insertion. His latest seizures presented as episodes of upper limb extension and stiffening with head and shoulder jerks, head dropped to the left, made grunting noises, and could become tremulous. Usually he experienced a warning sign and sought comfort from his parents. His seizures occurred during sleep and on waking, could occur isolated or in clusters of up to 20 on a daily basis. In addition, he had autism spectrum disorder, challenging behaviour and severe learning difficulties.

The MRI showed a left inferior frontal grey-white matter blurring, increased white matter signal in the left temporal pole without any obvious malformation. The left hippocampus was smaller than the right. PET and MEG lateralised to the left hemisphere with an abnormality mainly over the left inferior frontal region and extending into the left temporal and parietal lobes. Scalp EEG and semiology suggested a probable temporal lobe onset, lateralising to the left hemisphere, however, a precise EEG onset was unclear. Therefore, an invasive monitoring was offered.

Patient ID19 was admitted to GOSH Koala ward for a left-sided SEEG implantation. In total, eighteen electrodes were implanted. SEEG recording showed a wide network, with a consistent lead from the orbitofrontal region and the middle frontal gyrus. Functional language stimulation did not lead to obvious interruption. A frontal lobectomy was done, which lead to a seizure outcome of Engel class III. He did not show any language deficits post-surgery.

For this study, the patient was able to complete two language tasks (WR and PN). He performed best during the picture naming task with 80%, followed by the word repetition task with 72%.

The clinical SEEG implantation regime is summarised in Figure 136. Eight electrodes were included for this study recording. Contacts included in the seizure onset were not included in the iERP recording (B5–7, B13–17, C10–11, D10–11). The following

Figure 137 illustrates the patient's implantation regime, contacts stimulated during functional electrical stimulation including electrical stimulation responses and iERPs and spectral changes elicited during the word repetition task.

Electrode	Label	Contacts	Location
Depth	A	1-18	Left Medial Orbitofrontal
Depth	B	1-18	Left Orbitofrontal
Depth	C	1-15	Left SFG-Operculum
Depth	D	1-15	Left Anterior Middle Frontal Gyrus
Depth	E	1-15	Left Posterior Middle Frontal Gyrus
Depth	F	1-12	Left Supplementary Motor Cortex
Depth	G	1-18	Left Anterior Oblique Insula
Depth	H	1-12	Left Subcentral-Insula
Depth	I	1-12	Left Parietal Operculum
Depth	J	1-18	Left Posterior Oblique-Insula
Depth	K	1-12	Left STG-Insula
Depth	L	1-18	Left TPO
Depth	M	1-15	Left Superior Parietal
Depth	N	1-15	Left Occipital
Depth	O	1-12	Left Entorhinal
Depth	P	1-15	Left Amygdala
Depth	Q	1-12	Left Posterior Hippocampus
Depth	R	1-10	Left Broca-Insula

Figure 136. Case 6 (ID19)—implantation regime summary. A. illustrates the patient's brain images with implanted SEEG electrodes. Electrodes included in the study are highlighted with pink letterboxes. Each coloured dot presents a contact. Electrode R shows white contacts in addition, which highlight contacts used for language stimulation during clinical assessment. **B.** illustrates the patient's implantation regime. **C.** summarises the locations of the electrodes inserted, their labels and the electrode used for language stimulations is circled in grey.

	R03	R04	R05	R06	R07	R08
ES	no response	no response	no response	no response	no response	no response
iERP						
beta ERD						
low gamma ERS						
high gamma ERS						
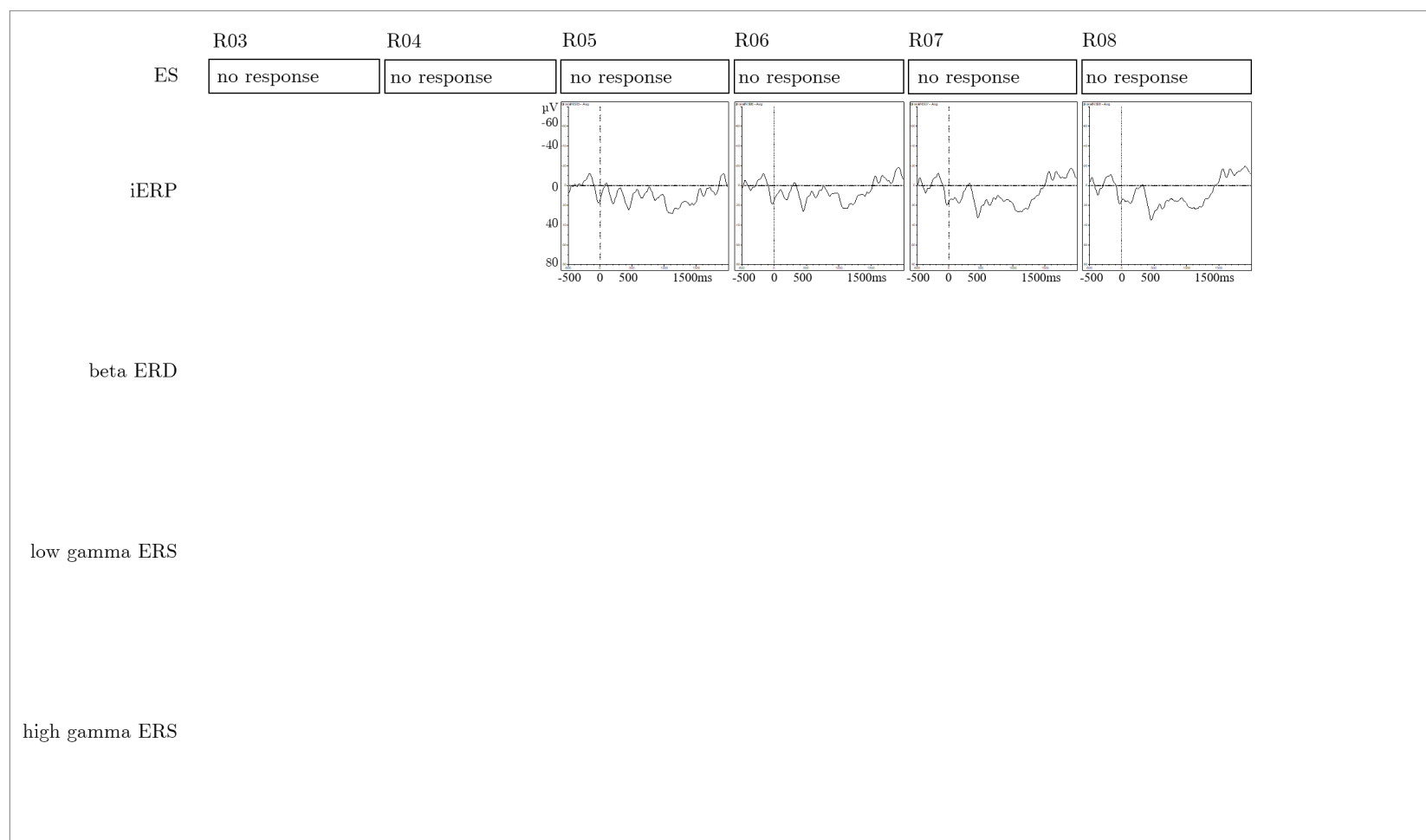
Figure 137. Case 6 (ID19)—contacts used for language stimulation. Electrode R (Broca to insula) contacts 3–8 were used. First, language stimulation responses during electrical stimulation are presented for each contact. Next, iERP responses and lastly beta ERD, low and high gamma ERS is shown. Responses during WR are illustrated in black. Empty spaces indicate no activity measured.

An fMRI investigation was not possible with this patient, hence, language lateralisation was not known. He was left-handed. During the study testing, focussing on the language tasks was hard for this patient and the verb generation and sentence tasks were too difficult for him. Contacts located in Broca's area were stimulated which yielded no responses. However, four of these stimulated contacts showed robust iERPs, no spectral changes were observed.

In general, the number of iERPs observed in this patient (63.1%) was similar to the group average (66.6%) for the word repetition task. Morphology was slightly different. There were no primary components measured however, early components reached 18.5 %, compared with the group average of 12.4% for WR task (primary plus early components). Most components elicited were long latency components with 23.0% compared to 32.4% for the group and 21.5% of middle latency components compared to 21.8% for the group. The most prominent language-related iERPs in this patient were observed in the posterior STG, supramarginal gyrus, posterior insula and inferior frontal gyrus. Out of all contacts, 9.2% showed beta ERD, 7.7% showed low gamma ERS and 4.6% showed high gamma ERS. These spectral changes were observed in the posterior STG and supramarginal gyrus.

A frontal lobectomy, including electrodes B, C and D was done. These electrodes were not involved in this study; hence no conclusion can be drawn regarding these resected contacts.
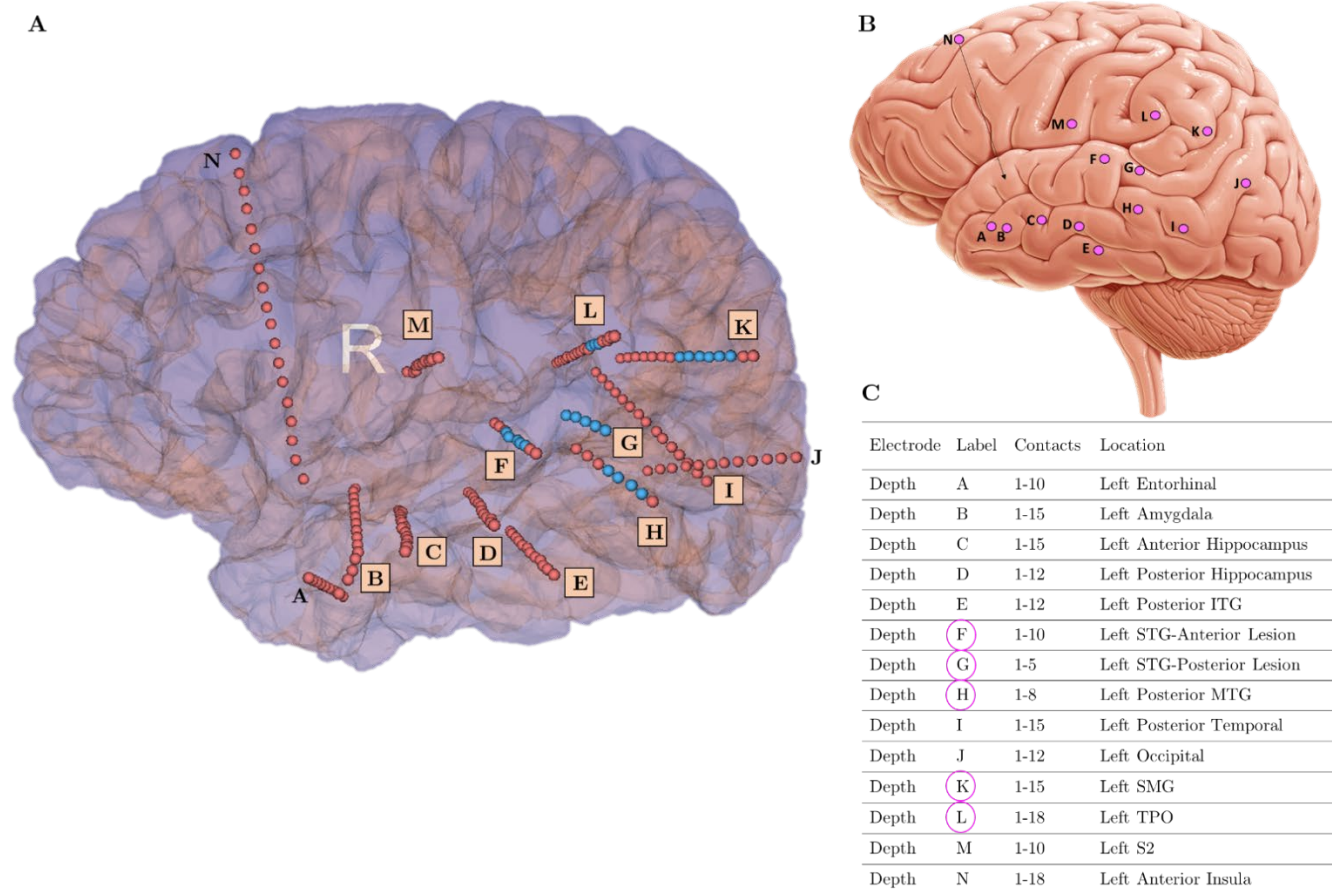
Case 7 (ID100)

Patient ID100 was a 5-year and 2 months old, right-handed girl with medication-resistant epilepsy. She experienced her first seizure at the age of eight weeks. Her latest episodes were subtle, occurred from sleep and were characterised by arousal, restlessness, vocalisation, trembling movements and posturing of the right arm / automatism of the left hand. She verbalised during these events but her voice was "shaky". These seizures lasted between 30 seconds and two minutes. In some of the events she complained of hearing a noise ("what's that noise?", "it was buzzy") or her head felt fuzzy, and she covered her right ear with her right hand. She presented with word finding difficulties and borderline cognitive deficits.

The MRI showed an area of signal abnormality in the posterior part of the inferior portion of the left superior temporal gyrus, suggestive of focal cortical dysplasia. Scalp EEG localised to the temporal regions, most often to the left. Post-ictal slowing consistently lateralised to the left. Clinical features suggested left lateral temporal lobe epilepsy. However, a precise EEG onset was not clear. Therefore, invasive monitoring was offered.

Patient ID100 was admitted to GOSH Koala ward for a left-sided SEEG implantation. In total, fourteen electrodes were implanted. The SEEG suggested a localised epileptogenic zone, possibly corresponding to the main imaging abnormality, involving the superior temporal gyrus, without any involvement posteriorly. The features were suggestive of a FCD 2B involving the left STG. To investigate language function an fMRI study was done. This resulted in a left lateralisation for language. Functional language stimulation of contacts in the posterior and anterior STG yielded no obvious interruption of language. Considering all results, a left temporal lesionectomy was done. The patient is seizure free since surgery. She did not present with deterioration of her language skills post-surgery.

For this study, the patient was able to complete two language tasks (VG and LN). She performed best during the verb generation with 88% of correct answers followed by the sentence task with 60%.

The clinical SEEG implantation regime is summarised in Figure 138. Eleven electrodes were included for this study recording. Contacts included in the ictal onset were used for the iERP recording (F5–8, G1–2, H1, L12–16). The following Figure 139 to Figure 141 illustrate the patient's implantation regime, contacts stimulated during functional electrical stimulation including electrical stimulation responses and iERPs and spectral changes elicited during the verb generation task.

Electrode	Label	Contacts	Location
Depth	A	1-10	Left Entorhinal
Depth	B	1-15	Left Amygdala
Depth	C	1-15	Left Anterior Hippocampus
Depth	D	1-12	Left Posterior Hippocampus
Depth	E	1-12	Left Posterior ITG
Depth	F	1-10	Left STG-Anterior Lesion
Depth	G	1-5	Left STG-Posterior Lesion
Depth	H	1-8	Left Posterior MTG
Depth	I	1-15	Left Posterior Temporal
Depth	J	1-12	Left Occipital
Depth	K	1-15	Left SMG
Depth	L	1-18	Left TPO
Depth	M	1-10	Left S2
Depth	N	1-18	Left Anterior Insula

Figure 138. Case 7 (ID100)—implantation regime summary. A. illustrates the patient's brain images with implanted SEEG electrodes. Electrodes included in the study are highlighted with pink letterboxes. Each coloured dot presents a contact. Electrode L, K, F, G and H show blue contacts in addition, which highlight contacts used for language stimulation during clinical assessment. B. illustrates the patient's implantation regime. C. summarises the locations of the electrodes inserted, their labels and the electrodes used for language stimulation are circled in pink.
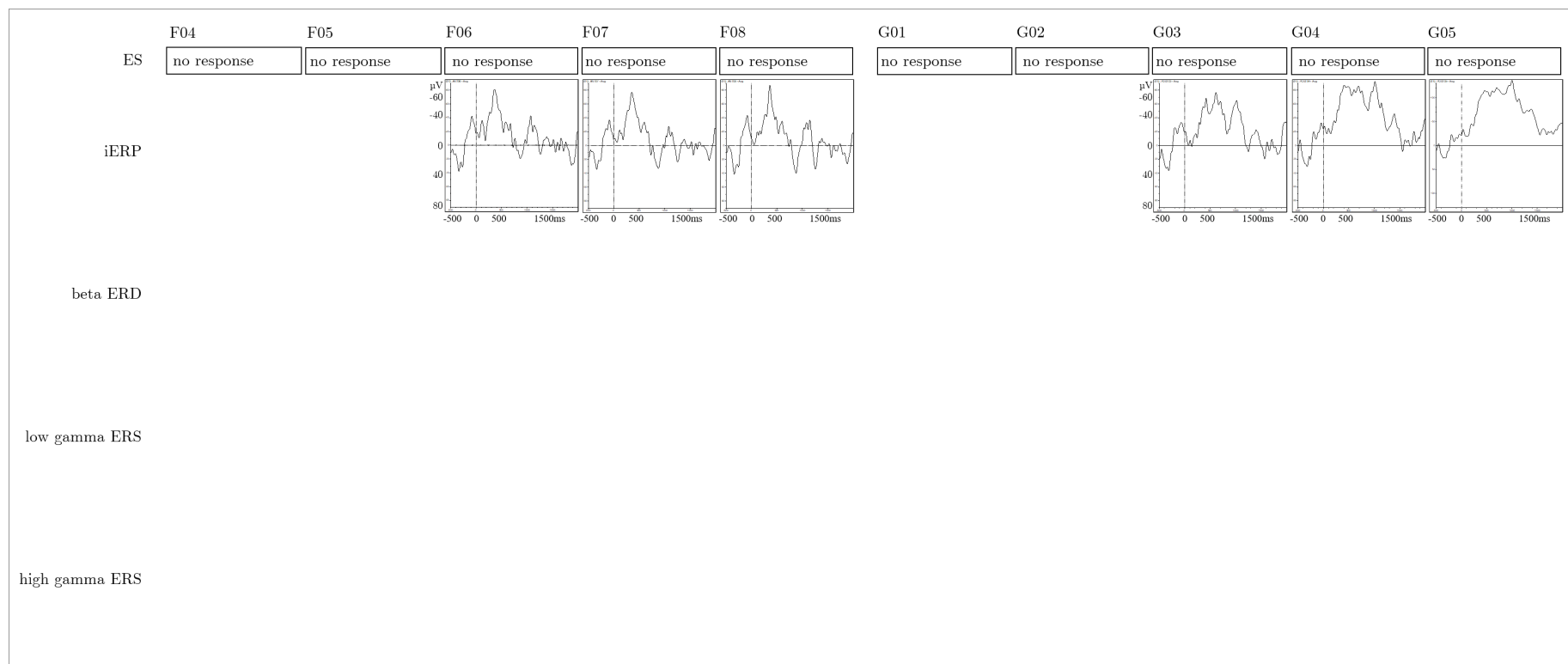
Figure 139. Case 7 (ID100)—contacts used for language stimulation (1). Electrode F (STG to anterior lesion) contacts 4–8 and electrode G (STG to posterior lesion) contacts 1–5 were used. First, language stimulation responses during electrical stimulation are presented for each contact. Next, iERP responses and lastly beta ERD, low and high gamma ERS is shown. Responses during the VG task are illustrated in black. Empty spaces indicate no activity measured.

	H04	H05	H06	H07	L12	L13	L14
ES	no response	no response	no response	no response	no response	no response	no response
iERP			[waveform]		[waveform]		
beta ERD							
low gamma ERS							
high gamma ERS							
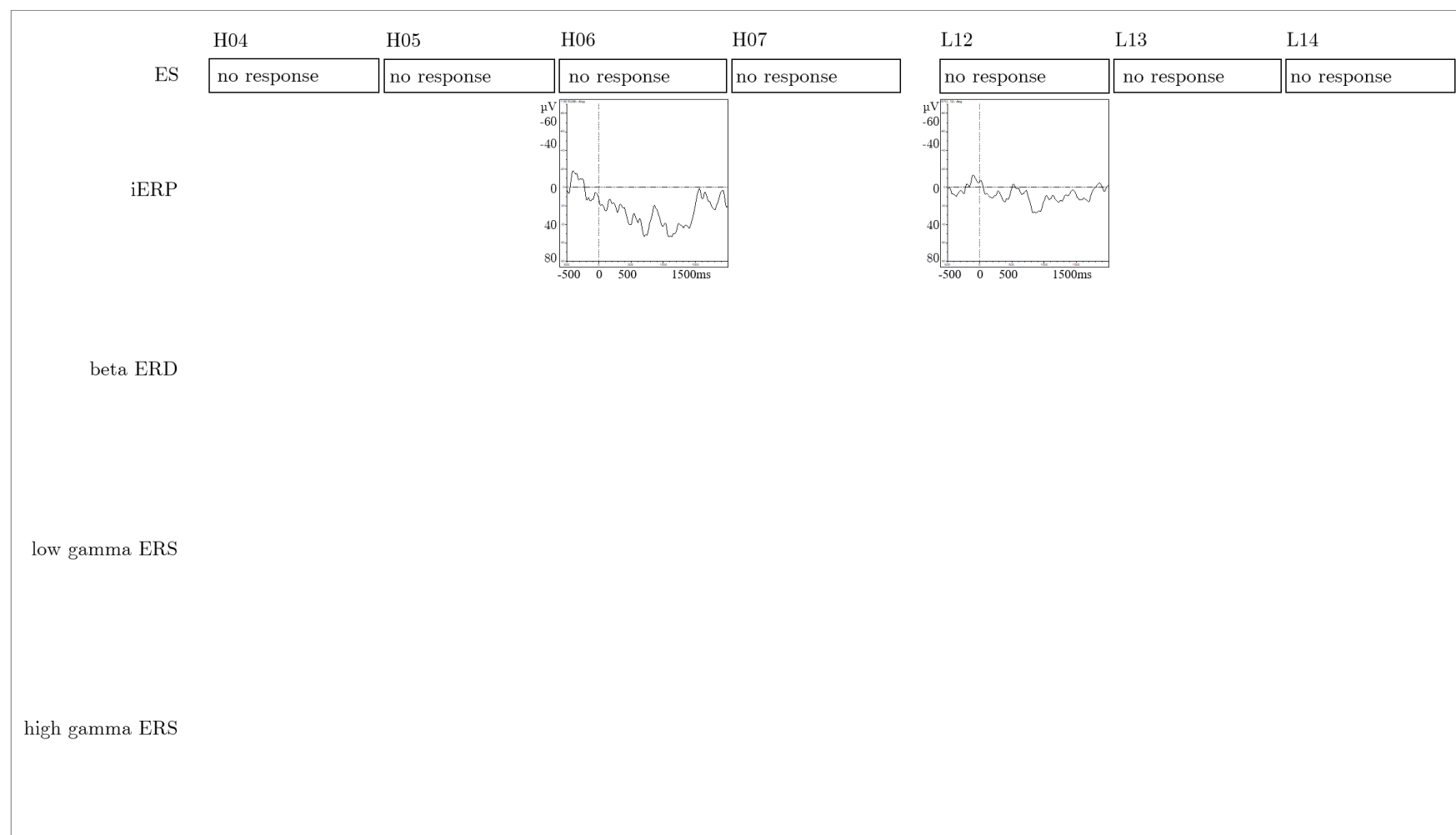
Figure 140. Case 7 (ID100)—contacts used for language stimulation (2). Electrode H (posterior MTG) contacts 4–7 and electrode L (TPO) contacts 12–14 were used. First, language stimulation responses during electrical stimulation are presented for each contact. Next, iERP responses and lastly beta ERD, low and high gamma ERS is shown. Responses during the VG task are illustrated in black. Empty spaces indicate no activity measured.
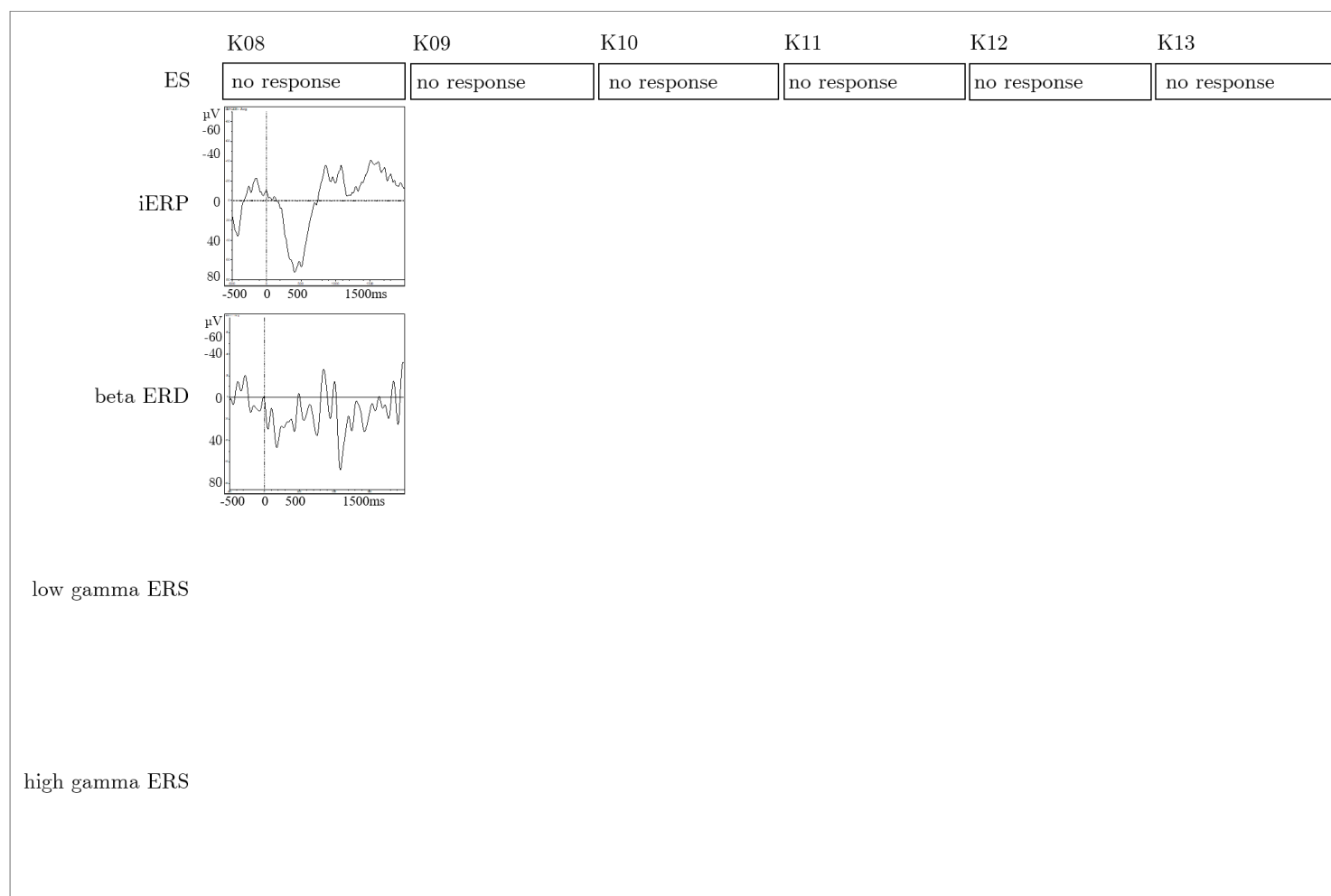
Figure 141. Case 7 (ID100)—contacts used for language stimulation (3). Electrode K (SMG) contacts 8–13 were used. First, language stimulation responses during electrical stimulation are presented for each contact. Next, iERP responses and lastly beta ERD, low and high gamma ERS is shown. Responses during the VG task are illustrated in black. Empty spaces indicate no activity measured.

In general, the number of iERPs observed in this patient (53.1%) was similar to the group average (69.9%) for the verb generation task. Morphology was slightly different. There were no primary components measured and early components reached 4.7 %, compared with the group average of 16.2% for VG task (primary plus early components). Most components elicited were middle latency components with 28.1% compared to 27.5% for the group and 24.0% of long latency components compared to 26.7% for the group. The most prominent language-related iERPs in this patient were observed in the inferior parietal lobule, followed by the posterior and anterior STG. Out of all contacts, 7.8% showed beta ERD, 10.9% showed low gamma ERS and 9.4% showed high gamma ERS. These spectral changes were observed in the inferior parietal lobule, anterior STG and inferior temporal gyrus.

In summary, the fMRI showed a left lateralisation in this right-handed patient. Electrical stimulation did not show any responses. Four of the resected contacts, which were used for functional stimulation showed iERPs, but no langauge deficit during stimulation testing. Post-surgery, the patient did not show deterioration of language skills. This might suggest that the iERPs measured from language-related brain areas, however, not from essential brain regions.

REFERENCES

Adcock, J. E., Wise, R. G., Oxbury, J. M., Oxbury, S. M., & Matthews, P. M. (2003). Quantitative fMRI assessment of the differences in lateralization of language-related brain activation in patients with temporal lobe epilepsy. *NeuroImage*, *18*(2), 423–438. https://doi.org/10.1016/S1053-8119(02)00013-7

Akatsuka, K., Wasaka, T., Nakata, H., Kida, T., & Kakigi, R. (2007). The effect of stimulus probability on the somatosensory mismatch field. *Experimental Brain Research*, *181*(4), 607–614. https://doi.org/10.1007/s00221-007-0958-4

Akiyama, T., McCoy, B., Go, C. Y., Ochi, A., Elliott, I. M., Akiyama, M., … Otsubo, H. (2011). Focal resection of fast ripples on extraoperative intracranial EEG improves seizure outcome in pediatric epilepsy. *Epilepsia*, *52*(10), 1802–1811. https://doi.org/10.1111/j.1528-1167.2011.03199.x

Alkawadri, R., Gaspard, N., Goncharova, I. I., Spencer, D. D., Gerrard, J. L., Zaveri, H., … Hirsch, L. J. (2014). The spatial and signal characteristics of physiologic high frequency oscillations. *Epilepsia*, *55*(12), 1986–1995. https://doi.org/10.1111/epi.12851

Amiri, M., Lina, J.-M. M., Pizzo, F., & Gotman, J. (2016). High Frequency Oscillations and spikes: Separating real HFOs from false oscillations. *Clinical Neurophysiology*, *127*(1), 187–196. https://doi.org/10.1016/j.clinph.2015.04.290

Anwander, A., Tittgemeyer, M., Von Cramon, D. Y., Friederici, A. D., & Knösche, T. R. (2007). Connectivity-based parcellation of Broca's area. *Cerebral Cortex*, *17*(4), 816–825. https://doi.org/10.1093/cercor/bhk034

Aoki, F., Fetz, E. E., Shupe, L., Lettich, E., & Ojemann, G. A. (1999). Increased gamma-range activity in human sensorimotor cortex during performance of visuomotor tasks. *Clinical Neurophysiology*, *110*(3), 524–537. https://doi.org/10.1016/S1388-2457(98)00064-9

Arnal, L. H., Wyart, V., & Giraud, A. L. (2011). Transitions in neural oscillations reflect prediction errors generated in audiovisual speech. *Nature Neuroscience*, *14*(6), 797–801. https://doi.org/10.1038/nn.2810

Arora, J., Pugh, K., Westerveld, M., Spencer, S., Spencer, D. D., & Todd Constable, R. (2009). Language lateralization in epilepsy patients: FMRI validated with the Wada procedure. *Epilepsia*, *50*(10), 2225–2241. https://doi.org/10.1111/j.1528-1167.2009.02136.x

Arya, R., Horn, P. S., & Crone, N. E. (2018). ECoG high-gamma modulation versus electrical stimulation for presurgical language mapping. *Epilepsy and Behavior*, *79*, 26–33. https://doi.org/10.1016/j.yebeh.2017.10.044

Arya, R., Wilson, J. A., Fujiwara, H., Rozhkov, L., Leach, J. L., Byars, A. W., … Rose, D. F. (2017). Presurgical language localization with visual naming associated ECoG high- gamma modulation in pediatric drug-resistant epilepsy. *Epilepsia*, *58*(4), 663–673. https://doi.org/10.1111/epi.13708

Arya, R., Wilson, J. A., Fujiwara, H., Vannest, J., Byars, A. W., Rozhkov, L., … Holland, K. D. (2018). Electrocorticographic high-gamma modulation with passive listening paradigm for pediatric extraoperative language mapping. *Epilepsia*, *59*(January), 792–801. https://doi.org/10.1111/epi.14029

Arya, R., Wilson, J. A., Vannest, J., Byars, A. W., Greiner, H. M., Buroker, J., … Rose, D. F. (2015). Electrocorticographic language mapping in children by high-gamma synchronization during spontaneous conversation: Comparison with conventional electrical cortical stimulation. *Epilepsy Research*, *110*, 78–87. https://doi.org/10.1016/j.eplepsyres.2014.11.013

Asano, E. (2017). High-frequency oscillations are under your control. Don't chase all of them. *Clinical Neurophysiology*, *128*(5), 841–842. https://doi.org/10.1016/j.clinph.2017.02.003

Astheimer, L., Janus, M., Moreno, S., & Bialystok, E. (2014). Electrophysiological measures of attention during speech perception predict metalinguistic skills in children. *Developmental Cognitive Neuroscience*, *7*, 1–12. https://doi.org/10.1016/j.dcn.2013.10.005

Audacity Team. (2018). Audacity(R): Free Audio Editor and Recorder [Computer application]. The name Audacity® is a registered trademark of Dominic Mazzoni. Retrieved from https://audacityteam.org/

Axmacher, N., Elger, C. E., & Fell, J. (2008). Ripples in the medial temporal lobe are relevant for human memory consolidation. *Brain*, *131*(7), 1806–1817. https://doi.org/10.1093/brain/awn103

Bagshaw, A. P., Jacobs, J., Levan, P., Dubeau, F., & Gotman, J. (2009). Effect of sleep stage on interictal high-frequency oscillations recorded from depth macroelectrodes in patients with focal epilepsy. *Epilepsia*, *50*(4), 617–628. https://doi.org/10.1111/j.1528-1167.2008.01784.x

Baldeweg, T., & Boyd, S. (2007). Clinical Neurophysiology. In *Rutter's Child and Adolescent Psychiatry*.

Barba, C., Cross, J. H., Braun, K., Cossu, M., Klotz, K. A., De Masi, S., … Guerrini, R. (2020). Trends in pediatric epilepsy surgery in Europe between 2008 and 2015: Country-, center-, and age-specific variation. *Epilepsia*, *61*(2), 216–227. https://doi.org/10.1111/epi.16414

Bares, M., & Rektor, I. (2001). Basal ganglia involvement in sensory and cognitive processing. A depth electrode CNV study in human subjects. *Clinical Neurophysiology*, *112*(11), 2022–2030. https://doi.org/10.1016/S1388-2457(01)00671-X

Baud, M. O., Perneger, T., Rácz, A., Pensel, M. C., Elger, C., Rydenhag, B., … Seeck, M. (2018). European trends in epilepsy surgery. *Neurology*, *91*(2), e96–e106. https://doi.org/10.1212/WNL.0000000000005776

Benke, T., Köylü, B., Visani, P., Karner, E., Brenneis, C., Bartha, L., … Willmes, K. (2006). Language lateralization in temporal lobe epilepsy: A comparison between fMRI and the Wada test. *Epilepsia*, *47*(8), 1308–1319. https://doi.org/10.1111/j.1528-1167.2006.00549.x

Berg, A. T., Berkovic, S. F., Brodie, M. J., Buchhalter, J., Cross, J. H., Van Emde Boas, W., … Scheffer, I. E. (2010). Revised terminology and concepts for organization of seizures and epilepsies: Report of the ILAE Commission on Classification and Terminology, 2005-2009. *Epilepsia*, *51*(4), 676–685. https://doi.org/10.1111/j.1528-1167.2010.02522.x

Berg, A. T., Zelko, F. A., Levy, S. R., & Testa, F. M. (2012). Age at onset of epilepsy, pharmacoresistance, and cognitive outcomes: A prospective cohort study. *Neurology*, *79*(13), 1384–1391. https://doi.org/10.1212/WNL.0b013e31826c1b55

Berger, H. (1929). Das Elektrenkephalogramm des Menschen. *Archiv Für Psychiatrie Und Nervenkrankheiten*, *87*(1), 527–570. https://doi.org/10.1007/BF01496966

Berger, H. (1969). On the electroencephalogram of man. *Electroencephalography and Clinical Neurophysiology*, *Supplement*(28), 37.

Bikson, M., Fox, J. E., & Jefferys, J. G. R. (2003). Neuronal Aggregate Formation Underlies Spatiotemporal Dynamics of Nonsynaptic Seizure Initiation. *Journal of Neurophysiology*, *89*(4), 2330–2333. https://doi.org/10.1152/jn.00764.2002

Binder, J. R., Frost, J. A., Hammeke, T. A., Cox, R. W., Rao, S. M., & Prieto, T. (1997). Human brain language areas identified by functional magnetic resonance imaging. *Journal of Neuroscience*, *17*(1), 353–362. https://doi.org/10.1523/jneurosci.17-01-00353.1997

Binder, J. R., Tong, J. Q., Pillay, S. B., Conant, L. L., Humphries, C. J., Raghavan, M., … Swanson, S. J. (2020). Temporal lobe regions essential for preserved picture naming after left temporal epilepsy surgery. *Epilepsia*. https://doi.org/10.1111/epi.16643

Blumcke, I., Spreafico, R., Haaker, G., Coras, R., Kobow, K., Bien, C. G., … Avanzini, G. (2017). Histopathological findings in brain tissue obtained during epilepsy surgery. *New England Journal of Medicine*, *377*(17), 1648–1656. https://doi.org/10.1056/NEJMoa1703784

Boatman, D., Lesser, R. P., & Gordon, B. (1995). Auditory speech processing in the left temporal lobe: An electrical interference study. *Brain and Language*. https://doi.org/10.1006/brln.1995.1061

Borchers, S., Himmelbach, M., Logothetis, N., & Karnath, H.-O. (2012). Direct electrical stimulation of human cortex - the gold standard for mapping brain functions? *Nature Reviews. Neuroscience*, *13*(1), 63–70. https://doi.org/10.1038/nrn3140

Bowman, J., Dudek, F. E., & Spitz, M. (2012). Epilepsy. *Relations Industrielles*, *67*(I), 171. https://doi.org/10.7202/1009082ar

Bragin, A., Engel, J., Wilson, C., Fried, I., & Mathern, G. (1999). Hippocampal and entorhinal cortex high-frequency oscillations (100-500 Hz) in human epileptic brain and in kainic acid-treated rats with chronic seizures. *Epilepsia*, *40*(2), 127–137. https://doi.org/10.1111/j.1528-1157.1999.tb02065.x

Bragin, A., Engel, J., Wilson, C. L., Vizentin, E., & Mathern, G. W. (1999). Electrophysiologic analysis of a chronic seizure model after unilateral hippocampal KA injection. *Epilepsia*, *40*(9), 1210–1221.

https://doi.org/10.1111/j.1528-1157.1999.tb00849.x

Bragin, A., Mody, I., Wilson, C. L., & Engel, J. (2002). Local generation of fast ripples in epileptic brain. *The Journal of Neuroscience : The Official Journal of the Society for Neuroscience*, *22*(5), 2012–2021. https://doi.org/22/5/2012 [pii]

Bragin, A., Wilson, C. L., & Engel, J. (2003). Spatial Stability over Time of Brain Areas Generating Fast Ripples in the Epileptic Rat, *44*(9), 1233–1237.

Bragin, A., Wilson, C. L., & Engel, Jj. (2000). Chronic epileptogenesis requires development of a network of pathologically interconnected neuron clusters: a hypothesis. *Epilepsia*, *Suppl 6*, 144–152.

Brázdil, M., Chlebus, P., Mikl, M., Pažourková, M., Krupa, P., & Rektor, I. (2005). Reorganization of language-related neuronal networks in patients with left temporal lobe epilepsy - An fMRI study. *European Journal of Neurology*, *12*(4), 268–275. https://doi.org/10.1111/j.1468-1331.2004.01127.x

Broca, P. (1865). Sur le siège de la faculté du langage articulé. *Bulletins de La Societe d'Anthropologie de Paris*, *6*(1), 377–393.

Brodie, M., & Kwan, P. (2002). Staged approach to epilepsy management. *Neurology*, *58*(8 Suppl 5), 2–8. Retrieved from http://n.neurology.org/content/58/8_suppl_5/S2.long

Bruder, J., Dümpelmann, M., Lachner Piza, D., Mader, M., Schulze-Bonhage, A., & Jacobs-Le Van, J. (2017). Physiological Ripples Associated with Sleep Spindles Differ in Waveform Morphology from Epileptic Ripples. *International Journal of Neural Systems*, *27*(07), 1750011/1-15. https://doi.org/10.1142/s0129065717500113

Buzsáki, G. (2006). *Rhythms of the brain*. Oxford University Press. https://doi.org/10.1093/acprof:oso/9780195301069.001.0001

Buzsáki, G., Horváth, Z., Urioste, R., Hetke, J., & Wise, K. (1992). High-frequency network oscillation in the hippocampus. *Science (New York, N.Y.)*, *256*(5059), 1025–1027. https://doi.org/10.1126/science.1589772

Buzsaki, G., Penttonen, M., Nadasdy, Z., & Bragin, A. (1996). Pattern and inhibition-dependent invasion of pyramidal cell dendrites by fast spikes in the hippocampus in vivo. *Proceedings of the National Academy of Sciences*, *93*(18), 9921–9925. https://doi.org/10.1073/pnas.93.18.9921

Canolty, R. T., & Knight, R. T. (2010). The Functional Role of Cross-frequency coupling. *Trends in Cognitive Sciences*, *14*(11), 506–515. https://doi.org/10.1016/j.tics.2010.09.001.The

Carrie, J. R. G. (1972). A hybrid computer technique for detecting sharp EEG transients. *Electroencephalography and Clinical Neurophysiology*, *33*(3), 336–338. https://doi.org/10.1016/0013-4694(72)90163-0

Catani, M., Jones, D. K., & Ffytche, D. H. (2005). Perisylvian language networks of the human brain. *Annals of Neurology*, *57*(1), 8–16. https://doi.org/10.1002/ana.20319

Centeno, M., & Carmichael, D. W. (2014). Network connectivity in epilepsy: Resting

state fMRI and EEG-fMRI contributions. *Frontiers in Neurology, 5 JUL*(July). https://doi.org/10.3389/fneur.2014.00093

Cervenka, M. C., Boatman-Reich, D. F., Ward, J., Franaszczuk, P. J., & Crone, N. E. (2011). Language Mapping in Multilingual Patients: Electrocorticography and Cortical Stimulation During Naming. *Frontiers in Human Neuroscience, 5*(February), 1–15. https://doi.org/10.3389/fnhum.2011.00013

Cervenka, M. C., Corines, J., Boatman-Reich, D. F., Sheng, X., Franaszczuk, P. J., & Crone, N. E. (2013). Electrocorticographic functional mapping identifies human cortex critical for auditory and visual naming. *NeuroImage, 69*, 267–276. https://doi.org/10.1016/j.neuroimage.2012.12.037.Electrocorticographic

Cervenka, M. C., Franaszczuk, P. J., Crone, N. E., Hong, B., Caffo, B. S., Bhatt, P., … Boatman-Reich, D. (2013). Reliability of early cortical auditory gamma-band responses. *Clinical Neurophysiology, 124*(1), 70–82. https://doi.org/10.1016/j.clinph.2012.06.003

Cheng, X., Schafer, G., & Riddel, P. M. (2014). Immediate auditory repetition of Words and Nonwords: An ERP study of lexical and sublexical processing. *PLoS ONE, 9*(3). https://doi.org/10.1371/journal.pone.0091988

Cho, J. R., Koo, D. L., Joo, E. Y., Seo, D. W., Hong, S. C., Jiruska, P., & Hong, S. B. (2014). Resection of individually identified high-rate high-frequency oscillations region is associated with favorable outcome in neocortical epilepsy. *Epilepsia, 55*(11), 1872–1883. https://doi.org/10.1111/epi.12808

Chrobak, J. J., & Buzsáki, G. (1996). High-Frequency Oscillations in the Output Networks of the Hippocampal-Entorhinal Axis of the Freely Behaving Rat. *The Journal of Neuroscience, 16*(9), 3056–3066. https://doi.org/10.1523/jneurosci.0640-09.2009

Cloppenborg, T., May, T. W., Blümcke, I., Fauser, S., Grewe, P., Hopf, J. L., … Bien, C. G. (2019). Differences in pediatric and adult epilepsy surgery: A comparison at one center from 1990 to 2014. *Epilepsia, 60*(2), 233–245. https://doi.org/10.1111/epi.14627

Conrad, E. C., Tomlinson, S. B., Wong, J. N., Oechsel, K. F., Shinohara, R. T., Litt, B., … Marsh, E. D. (2020). Spatial distribution of interictal spikes fluctuates over time and localizes seizure onset. *Brain, 143*(2), 554–569. https://doi.org/10.1093/brain/awz386

Cooper, R. J., Atkinson, R. J., Clark, R. A., & Michie, P. T. (2013). Event-related potentials reveal modelling of auditory repetition in the brain. *International Journal of Psychophysiology, 88*(1), 74–81. https://doi.org/10.1016/j.ijpsycho.2013.02.003

Cooper, R., Winter, A. L., Crow, H. J., & Walter, W. G. (1965). Comparison of subcortical, cortical and scalp activity using chronically indwelling electrodes in man. *Electroencephalography and Clinical Neurophysiology, 18*(3), 217–228. https://doi.org/10.1016/0013-4694(65)90088-X

Cormack, F., Cross, H. J., Isaacs, E., Harkness, W., Wright, I., Vargha-Khadem, F., & Baldeweg, T. (2007). The Development of Intellectual Abilities in Pediatric Temporal Lobe Epilepsy. *Epilepsia, 48*(1), 201–204.

https://doi.org/10.1111/j.1528-1167.2006.00904.x

Corsi-Cabrera, M., Velasco, F., del Río-Portilla, Y., Armony, J. L., Trejo-Martínez, D., Guevara, M. A., & Velasco, A. L. (2016). Human amygdala activation during rapid eye movements of rapid eye movement sleep: an intracranial study. *Journal of Sleep Research*, *25*(5), 576–582. https://doi.org/10.1111/jsr.12415

Cossu, M., Cardinale, F., Castana, L., Nobili, L., Sartori, I., & Lo Russo, G. (2006). Stereo-EEG in children. *Child's Nervous System*, *22*(8), 766–778. https://doi.org/10.1007/s00381-006-0127-2

Crépon, B., Navarro, V., Hasboun, D., Clemenceau, S., Martinerie, J., Baulac, M., … Le Van Quyen, M. (2010). Mapping interictal oscillations greater than 200 Hz recorded with intracranial macroelectrodes in human epilepsy. *Brain*, *133*(1), 33–45. https://doi.org/10.1093/brain/awp277

Creutzfeldt, O., Ojemann, G., & Lettich, E. (1989a). Neuronal activity in the human lateral temporal lobe - I. Responses to speech. *Experimental Brain Research*, *77*(3), 451–475. https://doi.org/10.1007/BF00249600

Creutzfeldt, O., Ojemann, G., & Lettich, E. (1989b). Neuronal activity in the human lateral temporal lobe - II. Responses to the subjects own voice. *Experimental Brain Research*, *77*(3), 476–489. https://doi.org/10.1007/BF00249601

Croft, L. J. (2014). *Neuroimaging Investigations of Language to Aid Paediatric Neurosurgical Decision Making*. *PQDT - UK & Ireland*. Retrieved from https://login.dist.lib.usu.edu/login?url=https://search.proquest.com/docview/1780 287316?accountid=14761%0Ahttp://xz6kg9rb2j.search.serialssolutions.com?ctx _ver=Z39.88-2004&ctx_enc=info:ofi/enc:UTF-8&rfr_id=info:sid/ProQuest+Dissertations+%26+Theses+Global

Crone, N. (1998). Functional mapping of human sensorimotor cortex with electrocorticographic spectral analysis. II. Event-related synchronization in the gamma band. *Brain*, *121*(12), 2301–2315. https://doi.org/10.1093/brain/121.12.2301

Crone, N. E. ., Boatman, D., Gordon, B., & Hao, L. (2001). Induced electrocorticographic gamma activity during auditory perception. *Clinical Neurophysiology*, *112*(4), 565–582. https://doi.org/10.1016/S1388-2457(00)00545-9

Crone, N. E., Hao, L., Hart, J., Boatman, D., Lesser, R. P., Irizarry, R., & Gordon, B. (2001). Electrocorticographic gamma activity during word production in spoken and sign language. *Neurology*, *57*(11), 2045–2053. https://doi.org/10.1212/WNL.57.11.2045

Crone, N. E., Korzeniewska, A., & Franaszczuk, P. J. (2011). Cortical gamma responses: Searching high and low. *International Journal of Psychophysiology*, *79*(1), 9–15. https://doi.org/10.1016/j.ijpsycho.2010.10.013

Crone, N. E., Miglioretti, D. L., Gordon, B., & Lesser, R. P. (1998). Functional mapping of human sensorimotor cortex with electrocorticographic spectral analysis. II. Event-related synchronization in the gamma band. *Brain : A Journal of Neurology*, *121 (Pt 1*, 2301–2315. https://doi.org/10.1093/brain/121.12.2301

Crone, N. E., Miglioretti, D. L., Gordon, B., Sieracki, J. M., Wilson, M. T., Uematsu, S., & Lesser, R. P. (1998). Functional mapping of human sensorimotor cortex with electrocorticographic spectral analysis I . Alpha and beta event-related desynchronization, 2271–2299.

Crone, N. E., Sinai, A., & Korzeniewska, A. (2006). High-frequency gamma oscillations and human brain mapping with electrocorticography. *Progress in Brain Research*, *159*(06), 275–295. https://doi.org/10.1016/S0079-6123(06)59019-3

Cross, H. J. (2016). The role and limits of seizure semiology. In *Pediatric Epilepsy Surgery* (pp. 3–6). Surrey: Éditions John Libbey Eurotext.

Cross, J. H., Jayakar, P., Nordli, D., Delalande, O., Duchowny, M., Wieser, H. G., … Mathern, G. W. (2006). Proposed criteria for referral and evaluation of children for epilepsy surgery: Recommendations of the subcommission for pediatric epilepsy surgery. *Epilepsia*, *47*(6), 952–959. https://doi.org/10.1111/j.1528-1167.2006.00569.x

Csicsvari, J., Hirase, H., Czurko, A., Mamiya, A., & Buzsaki, G. (1999). Fast network oscillations in the hippocampal CA1 region of Buhl, E.H. (2001). Differential expression of synaptic and nonsynapthe behaving rat. *Journal of Neuroscience*, *19*, RC20.

Curio, G., Mackert, B., Burghoff, M., Neumann, J., Nolte, G., Scherg, M., & Marx, P. (1997). Somatotopic source arrangement of 600 Hz oscillatory magnetic fields at the human primary somatosensory hand cortex. *Neuroscience Letters*, *234*(2–3), 131–134.

D'Argenzio, L., Colonnelli, M. C., Harrison, S., Jacques, T. S., Harkness, W., Scott, R. C., & Cross, J. H. (2012). Seizure outcome after extratemporal epilepsy surgery in childhood. *Developmental Medicine and Child Neurology*, *54*(11), 995–1000. https://doi.org/10.1111/j.1469-8749.2012.04381.x

Davis, H., Davis, P. A., Loomis, A. L., Hervey, E. N., & Hobart, G. (1939). Electrical reactions of the human brain to auditory stimulation during sleep. *Journal of Neurophysiology*, *2*, 500–514. Retrieved from http://ezproxy.lib.uh.edu/login?url=http://search.ebscohost.com/login.aspx?direct=true&db=psyh&AN=1940-01706-001&site=ehost-live

Davis, P. A. (1939). Effects of accoustic stimuli on the waking human brain. *Journal of Neurophysiology*, *2*(6), 494–499.

De Haan, M., & Carver, L. (2013). Development of brain networks for visual social-emotional information processing in infancy. In *The infant mind: Origins of the social brain* (pp. 123–145).

De Tisi, J., Bell, G. S., Peacock, J. L., McEvoy, A. W., Harkness, W. F., Sander, J. W., & Duncan, J. S. (2011). The long-term outcome of adult epilepsy surgery, patterns of seizure remission, and relapse: A cohort study. *The Lancet*, *378*(9800), 1388–1395. https://doi.org/10.1016/S0140-6736(11)60890-8

Delorme, A., Mullen, T., Kothe, C., Akalin Acar, Z., Bigdely-Shamlo, N., Vankov, A., & Makeig, S. (2011). EEGLAB, SIFT, NFT, BCILAB, and ERICA: New tools for advanced EEG processing. *Computational Intelligence and Neuroscience*, *Article*

ID, 12 pages. https://doi.org/10.1155/2011/130714

Démonet, J. F., Thierry, G., & Cardebat, D. (2005). Renewal of the neurophysiology of language: Functional neuroimaging. *Physiological Reviews*, *85*(1), 49–95. https://doi.org/10.1152/physrev.00049.2003

Detre, J. A. (2004). fMRI: Applications in Epilepsy. *Epilepsia*, *45*(s4), 26–31. https://doi.org/10.1111/j.0013-9580.2004.04006.x

Devlin, J. T., & Watkins, K. E. (2007). Stimulating language: Insights from TMS. *Brain*, *130*(3), 610–622. https://doi.org/10.1093/brain/awl331

DeWitt, I., & Rauschecker, J. P. (2013a). Wernicke's area revisited: Parallel streams and word processing. *Brain and Language*, *127*(2), 181–191. https://doi.org/10.1016/j.bandl.2013.09.014

DeWitt, I., & Rauschecker, J. P. (2013b). Wernicke's area revisited: Parallel streams and word processing. *Brain and Language*, *127*(2), 181–191. https://doi.org/10.1016/j.bandl.2013.09.014

Dichter, M. A., & Brodie, M. J. (1996). New Antiepileptic Drugs. *New England Journal of Medicine*, *334*(24), 1583–1590. https://doi.org/10.1056/NEJM199606133342407

Diehl, B., & Lüders, H. O. (2000). Temporal lobe epilepsy: when are invasive recordings needed? *Epilepsia*, *41 Suppl 3*(5), S61–S74.

Dzhala, V. I. (2004). Mechanisms of Fast Ripples in the Hippocampus. *Journal of Neuroscience*, *24*(40), 8896–8906. https://doi.org/10.1523/JNEUROSCI.3112-04.2004

Edwards, E., Nagarajan, S. S., Dalal, S. S., Canolty, R. T., Kirsch, H. E., Barbaro, N. M., & Knight, R. T. (2010). Spatiotemporal imaging of cortical activation during verb generation and picture naming. *NeuroImage*, *50*(1), 291–301. https://doi.org/10.1016/j.neuroimage.2009.12.035

Edwards, E., Soltani, M., Deouell, L. Y., Berger, M. S., & Knight, R. T. (2005). High Gamma Activity in Rresponse to Deviant Aauditory Stimuli Recorded Directly from Human Cortex. *Journal of Neurophysiology*, *94*(6), 4269–4280. https://doi.org/10.1152/jn.00324.2005

Engel, A. K., & Fries, P. (2010). Beta-band oscillations-signalling the status quo? *Current Opinion in Neurobiology*, *20*(2), 156–165. https://doi.org/10.1016/j.conb.2010.02.015

Engel, J. (1993a). Update on surgical treatment of the epilepsies. *Neurology*, *43*, 1612–1617.

Engel, J. (1993b). Update on surgical treatment of the epilepsies Summary of The Second International Palm Desert Conference on the Surgical Treatment of the Epilepsies (1992). *Neurology*, *43*(8), 1612–1617.

Engel, J., Van Ness, P. C., Rasmussen, T., & Ojemann, J. G. (1993). Outcome with respect to epileptic seizures. In E. J. Jr (Ed.), *Surgical treatment of the epilepsies* (2nd ed., pp. 609–621). New York: Raven Press.

Engel, Jerome, Bragin, A., Staba, R., & Mody, I. (2009). High-frequency oscillations: What is normal and what is not? *Epilepsia*, *50*(4), 598–604. https://doi.org/10.1111/j.1528-1167.2008.01917.x

Engel, Jerome, McDermott, M. P., Wiebe, S., Langfitt, J. T., Stern, J. M., Dewar, S., … Kieburtz, K. (2012). Early surgical therapy for drug-resistant temporal lobe epilepsy: a randomized trial. *JAMA : The Journal of the American Medical Association*, *307*(9), 922–930. https://doi.org/10.1001/jama.2012.220

Engell, A. D., Huettel, S., & McCarthy, G. (2012). The fMRI BOLD signal tracks electrophysiological spectral perturbations, not event-related potentials. *NeuroImage*, *59*(3), 2600–2606. https://doi.org/10.1016/j.neuroimage.2011.08.079

Fedorov, A., Beichel, R., Kalpathy-Cramer, J., Finet, J., Fillion-Robin, J., Pujol, S., … Kikinis, R. (2012). 3D Slicer as an Image Computing Platform for the Quantitative Imaging Network. *Magn Resson Imaging*, *30*(9), 1323–1341. https://doi.org/10.1016/j.mri.2012.05.001.3D

Fell, J., Ludowig, E., Rosburg, T., Axmacher, N., & Elger, C. E. (2008). Phase-locking within human mediotemporal lobe predicts memory formation. *NeuroImage*, *43*(2), 410–419. https://doi.org/10.1016/j.neuroimage.2008.07.021

Fisch, L., Privman, E., Ramot, M., Harel, M., Nir, Y., Kipervasser, S., … Malach, R. (2009). Neural "Ignition": Enhanced Activation Linked to Perceptual Awareness in Human Ventral Stream Visual Cortex. *Neuron*, *64*(4), 562–574. https://doi.org/10.1016/j.neuron.2009.11.001

Fisher, A. E., Furlong, P. L., Seri, S., Adjamian, P., Witton, C., Baldeweg, T., … Thai, N. J. (2008). Interhemispheric differences of spectral power in expressive language: A MEG study with clinical applications. *International Journal of Psychophysiology*, *68*(2), 111–122. https://doi.org/10.1016/j.ijpsycho.2007.12.005

Fisher, R. S. (2014). How Can We Identify Ictal and Interictal Abnormal Activity? *Adv Exp Med Biol*, *813*, 3–23. https://doi.org/10.1007/978-94-017-8914-1

Fisher, R. S., Acevedo, C., Arzimanoglou, A., Bogacz, A., Cross, J. H., Elger, C. E., … Wiebe, S. (2014). ILAE Official Report: A practical clinical definition of epilepsy. *Epilepsia*, *55*(4), 475–482. https://doi.org/10.1111/epi.12550

Fisher, R. S., Cross, J. H., French, J. A., Higurashi, N., Hirsch, E., Jansen, F. E., … Zuberi, S. M. (2017). Operational classification of seizure types by the International League Against Epilepsy: Position Paper of the ILAE Commission for Classification and Terminology. *Epilepsia*, *58*(4), 522–530. https://doi.org/10.1111/epi.13670

Flinker, A., Korzeniewska, A., Shestyuk, A. Y., Franaszczuk, P. J., Dronkers, N. F., Knight, R. T., & Crone, N. E. (2015). Redefining the role of Broca's area in speech. *Proceedings of the National Academy of Sciences*, *112*(9), 201414491. https://doi.org/10.1073/pnas.1414491112

Foerster, O., & Penfield, W. (1930). The structural basis of traumatic epilepsy and results of radical operations. *Brain*, *53*, 99–119.

Foffani, G., Uzcategui, Y. G., Gal, B., & Menendez de la Prida, L. (2007). Reduced Spike-Timing Reliability Correlates with the Emergence of Fast Ripples in the Rat Epileptic Hippocampus. *Neuron*, *55*(6), 930–941. https://doi.org/10.1016/j.neuron.2007.07.040

Foley, E., Cross, J. H., Thai, N. J., Walsh, A. R., Bill, P., Furlong, P., … Seri, S. (2019). MEG Assessment of Expressive Language in Children Evaluated for Epilepsy Surgery. *Brain Topography*, *32*(3), 492–503. https://doi.org/10.1007/s10548-019-00703-1

Fonseca, A. T. Da, Guedj, E., Alario, F. X., Laguitton, V., Mundler, O., Chauvel, P., & Liegeois-Chauvel, C. (2009). Brain regions underlying word finding difficulties in temporal lobe epilepsy. *Brain*, *132*(10), 2772–2784. https://doi.org/10.1093/brain/awp083

Forster, M. T., Hattingen, E., Senft, C., Gasser, T., Seifert, V., & Szelényi, A. (2011). Navigated transcranial magnetic stimulation and functional magnetic resonance imaging: Advanced adjuncts in preoperative planning for central region tumors. *Neurosurgery*, *68*(5), 1317–1324. https://doi.org/10.1227/NEU.0b013e31820b528c

Frauscher, B., von Ellenrieder, N., Zelmann, R., Doležalová, I., Minotti, L., Olivier, A., … Gotman, J. (2018). Atlas of the normal intracranial electroencephalogram: neurophysiological awake activity in different cortical areas. *Brain*, (March), 1–15. https://doi.org/10.1093/brain/awy035

Frauscher, B., von Ellenrieder, N., Zelmann, R., Rogers, C., Nguyen, D. K., Kahane, P., … Gotman, J. (2018). High-Frequency Oscillations in the Normal Human Brain, 1–12. https://doi.org/10.1002/ana.25304

Frey, S., Campbell, J. S. W., Pike, G. B., & Petrides, M. (2008). Dissociating the human language pathways with high angular resolution diffusion fiber tractography. *Journal of Neuroscience*, *28*(45), 11435–11444. https://doi.org/10.1523/JNEUROSCI.2388-08.2008

Fried, I., Ojemann, G. A., & Fetz, E. E. (1981). Language-Related Potentials Specific to Human Language Cortex. *Science*, *212*(4492), 353–356.

Friederici, A. D. (2012). The cortical language circuit: From auditory perception to sentence comprehension. *Trends in Cognitive Sciences*, *16*(5), 262–268. https://doi.org/10.1016/j.tics.2012.04.001

Friederici, A. D., Bahlmann, J., Heim, S., Schubotz, R. I., & Anwander, A. (2006). The brain differentiates human and non-human grammars: Functional localization and structural connectivity. *Proceedings of the National Academy of Sciences of the United States of America*, *103*(7), 2458–2463. https://doi.org/10.1073/pnas.0509389103

Friederici, A. D., & Gierhan, S. M. E. (2013). The language network. *Current Opinion in Neurobiology*, *23*(2), 250–254. https://doi.org/10.1016/j.conb.2012.10.002

Friederici, A. D., Wang, Y., Herrmann, C. S., Maess, B., & Oertel, U. (2000). Localization of early syntactic processes in frontal and temporal cortical areas: A magnetoencephalographic study. *Human Brain Mapping*, *11*(1), 1–11. https://doi.org/10.1002/1097-0193(200009)11:1<1::AID-HBM10>3.0.CO;2-B

Fries, P. (2005). A mechanism for cognitive dynamics: neuronal communication through neuronal coherence. *Trends in Cognitive Science*, *9*(10), 474–480.

Fries, P. (2015). Rhythms For Cognition: Communication Through Coherence. *Neuron*, *88*(1), 220–235. https://doi.org/10.1016/j.neuron.2015.09.034.Rhythms

Fu, C. H. Y., Morgan, K., Suckling, J., Williams, S. C. R., Andrew, C., Vythelingum, G. N., & McGuire, P. K. (2002). A Functional Magnetic Resonance Imaging Study of Overt Letter Verbal Fluency Using a Clustered Acquisition Sequence: Greater Anterior Cingulate Activation with Increased Task Demand. *NeuroImage*, *17*(2), 871–879. https://doi.org/10.1006/nimg.2002.1189

Fujioka, T., Trainor, L. J., Large, E. W., & Ross, B. (2009). Beta and gamma rhythms in human auditory cortex during musical beat processing. *Annals of the New York Academy of Sciences*, *1169*(August), 89–92. https://doi.org/10.1111/j.1749-6632.2009.04779.x

Fujiwara, H., Greiner, H. M., Lee, K. H., Holland-Bouley Katherine D., Hee, S. J., Mangano, F. T., … Rose, D. F. (2012). Resection of ictal high-frequency oscillations leads to favorable surgical outcome in pediatric epilepsy. *Epilepsia*, *53*(9), 1607–1617. https://doi.org/10.1016/j.biotechadv.2011.08.021.Secreted

Fukuda, M., Rothermel, R., Juhász, C., Nishida, M., Sood, S., & Asano, E. (2010). Cortical gamma-oscillations modulated by listening and overt repetition of phonemes. *NeuroImage*, *49*(3), 2735–2745. https://doi.org/10.1016/j.neuroimage.2009.10.047

Galanopoulou, A. S., & Moshé, S. L. (2011). In search of epilepsy biomarkers in the immature brain: goals, challenges and strategies. *Biomarkers in Medicine*, *5*(5), 615–628. https://doi.org/10.2217/bmm.11.71.In

Galantucci, S., Tartaglia, M. C., Wilson, S. M., Henry, M. L., Filippi, M., Agosta, F., … Gorno-Tempini, M. L. (2011). White matter damage in primary progressive aphasias: A diffusion tensor tractography study. *Brain*, *134*(10), 3011–3029. https://doi.org/10.1093/brain/awr099

Ganesan, K., Appleton, R., & Tedman, B. (2006). EEG departments in Great Britain : A survey of practice. https://doi.org/10.1016/j.seizure.2006.02.021

Gascoigne, M. B., Smith, M. Lou, Barton, B., Webster, R., Gill, D., & Lah, S. (2018). Accelerated long-term forgetting and behavioural difficulties in children with epilepsy. *Cortex*, *110*, 92–100. https://doi.org/10.1016/j.cortex.2018.03.021

Genetti, M., Tyrand, R., Grouiller, F., Lascano, A. M., Vulliemoz, S., Spinelli, L., … Michel, C. M. (2015). Comparison of high gamma electrocorticography and fMRI with electrocortical stimulation for localization of somatosensory and language cortex. *Clinical Neurophysiology*, *126*(1), 121–130. https://doi.org/10.1016/j.clinph.2014.04.007

George, D. D., Ojemann, S. G., Drees, C., & Thompson, J. A. (2020). Stimulation Mapping Using Stereoelectroencephalography: Current and Future Directions. *Frontiers in Neurology*, *11*(May), 1–7. https://doi.org/10.3389/fneur.2020.00320

Gholipour, T., Koubeissi, M. Z., & Shields, D. C. (2020). Stereotactic electroencephalography. *Clinical Neurology and Neurosurgery*, *189*(December

2019), 105640. https://doi.org/10.1016/j.clineuro.2019.105640

Gloor, P. (1975). Contributions of electroencephalography and electrocorticography to the neurosurgical treatment of the epilepsies. *Advances in Neurology*, *8*, 59–105.

Goldman, J., Becker, M. L., Jones, B., Clements, M., & Leeder, J. S. (2011). Development of biomarkers to optimize pediatric patient management: What makes children different? *Biomarkers in Medicine*, *5*(6), 781–794. https://doi.org/10.2217/bmm.11.96

Grenier, F., Timofeev, I., & Steriade, M. (2001). Focal synchronization of ripples (80-200 Hz) in neocortex and their neuronal correlates. *Journal of Neurophysiology*, *86*(4), 1884–1898.

Grenier, F., Timofeev, I., & Steriade, M. (2003). Neocortical very fast oscillations (ripples, 80-200 Hz) during seizures: intracellular correlates. *Journal of Neurophysiology*, *89*(2), 841–852. https://doi.org/10.1152/jn.00420.2002

Greve, D. N., & Fischl, B. (2009). Accurate and Robust Brain Image Alignment using Boundary-based Registration. *Neuroimage*, *48*(1), 63–72. https://doi.org/10.1016/j.neuroimage.2009.06.060.Accurate

Haegelen, C., Perucca, P., Châtillon, C.-E., Andrade-Valença, L., Zelmann, R., Jacobs, J., … Gotman, J. (2013). High frequency oscillations, extent of surgical resection, and surgical outcome in drug resistant focal epilepsy. *Epilepsia*, *54*(5), 848–857. https://doi.org/10.1111/epi.12075

Haenschel, C., Baldeweg, T., Croft, R. J., Whittington, M., & Gruzelier, J. (2000). Gamma and beta frequency oscillations in response to novel auditory stimuli: A comparison of human electroencephalogram (EEG) data with in vitro models. *Proceedings of the National Academy of Sciences*, *97*(13), 7645–7650. https://doi.org/10.1073/pnas.120162397

Haglund, M. M., Berger, M. S., Shamseldin, M., Lettich, E., & Ojemann, G. A. (1994). Cortical Localization of Temporal Lobe Language Sites in Patients with Gliomas. *Neurosurgery*, *34*(4), 567–56.

Halgren, E., Baudena, P., Clarke, J., Heit, G., Ligeois, C., Chauvel, P., & Musolino, A. (1995). Intracerebral potentials to rare target and distractor auditory and visual stimuli . I . Superior temporal plane and parietal lobe, *94*, 191–220.

Halgren, E., & Marinkovic, K. (1995). Neurophysiological networks integrating human emotions. In *The cognitive neurosciences*. The MIT Press.

Halgren, E., Marinkovic, K., & Chauvel, P. (1998). Generators of the late cognitive potentials in auditory and visual oddball tasks. *Electroencephalography and Clinical Neurophysiology*, *106*(2), 156–164. https://doi.org/10.1016/S0013-4694(97)00119-3

Hamamé, C. M., Alario, F. X., Llorens, A., Liégeois-Chauvel, C., & Trébuchon-Da Fonseca, A. (2014). High frequency gamma activity in the left hippocampus predicts visual object naming performance. *Brain and Language*, *135*, 104–114. https://doi.org/10.1016/j.bandl.2014.05.007

Hamberger, M. J., Seidel, W. T., Mckhann, G. M., Perrine, K., & Goodman, R. R. (2005). Brain stimulation reveals critical auditory naming cortex. *Brain*, *128*(11),

2742–2749. https://doi.org/10.1093/brain/awh621

Hamberger, Marla J. (2007). Cortical language mapping in epilepsy: A critical review. *Neuropsychology Review*, *17*(4), 477–489. https://doi.org/10.1007/s11065-007-9046-6

Hart, J., Crone, N. E., Lesser, R. P., Sieracki, J., Miglioretti, D. L., Hall, C., … Gordon, B. (1998). Temporal dynamics of verbal object comprehension. *Proceedings of the National Academy of Sciences of the United States of America*, *95*(11), 6498–6503. https://doi.org/10.1073/pnas.95.11.6498

Hashimoto, I. (2000). High-Frequency Oscillations of Somatosensory Evoked Potentials and Fields. *Journal of Clinical Neurophysiology*, *17*(3), 309–320.

Helmstaedter, C., Kurthen, M., Linke, D. B., & Elger, C. E. (1997). Patterns of language dominance in focal left and right hemisphere epilepsies: Relation to MRI findings, EEG, sex, and age at onset of epilepsy. *Brain and Cognition*, *33*(2), 135–150. https://doi.org/10.1006/brcg.1997.0888

Hermann, B., Jones, J., Dabbs, K., Allen, C. A., Sheth, R., Fine, J., … Seidenberg, M. (2007). The frequency, complications and aetiology of ADHD in new onset paediatric epilepsy. *Brain*, *130*(12), 3135–3148. https://doi.org/10.1093/brain/awm227

Hermann, B., Jones, J., Sheth, R., Dow, C., Koehn, M., & Seidenberg, M. (2006). Children with new-onset epilepsy: Neuropsychological status and brain structure. *Brain*, *129*(10), 2609–2619. https://doi.org/10.1093/brain/awl196

Herrmann, B., Maess, B., Hahne, A., Schröger, E., & Friederici, A. D. (2011). Syntactic and auditory spatial processing in the human temporal cortex: An MEG study. *NeuroImage*, *57*(2), 624–633. https://doi.org/10.1016/j.neuroimage.2011.04.034

Hickok, G. (2009). The Functional Neuroanatomy of Language Gregory. *Phys Life Rev*, *6*(3), 121–143. https://doi.org/10.1038/jid.2014.371

Hirata, M., Goto, T., Barnes, G., Umekawa, Y., Yanagisawa, T., Kato, A., … Yoshimine, T. (2010). Language dominance and mapping based on neuromagnetic oscillatory changes: comparison with invasive procedures. *Journal of Neurosurgery*, *112*(3), 528–538. https://doi.org/10.3171/2009.7.JNS09239

Höller, Y., Kutil, R., Klaffenböck, L., Thomschewski, A., Höller, P. M., Bathke, A. C., … Trinka, E. (2015). High-frequency oscillations in epilepsy and surgical outcome. A meta-analysis. *Frontiers in Human Neuroscience*, *9*(October), 1–14. https://doi.org/10.3389/fnhum.2015.00574

Hope, T. M. H., Prejawa, S., Jones, P. O., Oberhuber, M., Seghier, M. L., Green, D. W., & Price, C. J. (2014). Dissecting the functional anatomy of auditory word repetition. *Frontiers in Human Neuroscience*, *8*, 1–17. https://doi.org/10.3389/fnhum.2014.00246

Howard, M. A., Volkov, I. O., Mirsky, R., Garell, P. C., Noh, M. D., Granner, M., … Brugge, J. F. (2000). Auditory cortex on the human posterior superior temporal gyrus. *The Journal of Comparative Neurology*, *416*(1), 79–92. https://doi.org/10.1002/(sici)1096-9861(20000103)416:1<79::aid-cne6>3.0.co;2-2

Hua, K., Oishi, K., Zhang, J., Wakana, S., Yoshioka, T., Zhang, W., … Mori, S. (2009). Mapping of functional areas in the human cortex based on connectivity through association fibers. *Cerebral Cortex*, *19*(8), 1889–1895. https://doi.org/10.1093/cercor/bhn215

Hussain, S. A., Mathern, G. W., Hung, P., Weng, J., Sankar, R., & Wu, J. Y. (2017). Intraoperative fast ripples independently predict postsurgical epilepsy outcome: Comparison with other electrocorticographic phenomena. *Epilepsy Research*, *135*, 79–86. https://doi.org/10.1016/j.eplepsyres.2017.06.010.Intraoperative

Hussain, S. A., Mathern, G. W., Sankar, R., & Wu, J. Y. (2016). Prospective and "live" fast ripple detection and localization in the operating room: Impact on epilepsy surgery outcomes in children. *Epilepsy Research*, *127*, 344–351. https://doi.org/10.1016/j.eplepsyres.2016.09.017

Ibarz, J. M., Foffani, G., Cid, E., Inostroza, M., & Menendez de la Prida, L. (2010). Emergent Dynamics of Fast Ripples in the Epileptic Hippocampus. *Journal of Neuroscience*, *30*(48), 16249–16261. https://doi.org/10.1523/JNEUROSCI.3357-10.2010

Ijff, D. M., & Aldenkamp, A. P. (2013). Cognitive side-effects of antiepileptic drugs in children. In *Handbook of Clinical Neurology* (1st ed., Vol. 111, pp. 707–718). Elsevier B.V. https://doi.org/10.1016/B978-0-444-52891-9.00073-7

Ille, S., Sollmann, N., Hauck, T., Maurer, S., Tanigawa, N., & Obermueller, T. (2015). Combined noninvasive language mapping by navigated transcranial magnetic stimulation and functional MRI and its comparison with direct cortical stimulation. *Journal of Neurosurgery*, *123*(July), 1–14. https://doi.org/10.3171/2014.9.JNS14929.Disclosure

Indefrey, P. (2011). The spatial and temporal signatures of word production components: A critical update. *Frontiers in Psychology*, *2*(OCT), 1–16. https://doi.org/10.3389/fpsyg.2011.00255

Jacobs, J., Asano, E., Otsubo, H., Wu, J., Zijlmans, M., Mohamed, I., … Gotman, J. (2012). High-frequency oscillations (HFOs) in clinical epilepsy. *Progress in Neurobiology*, *98*(3), 302–315. https://doi.org/10.1016/j.biotechadv.2011.08.021.Secreted

Jacobs, J., Banks, S., Zelmann, R., Zijlmans, M., Jones-Gotman, M., & Gotman, J. (2016). Spontaneous ripples in the hippocampus correlate with epileptogenicity and not memory function in patients with refractory epilepsy. *Epilepsy and Behavior*, *62*, 258–266. https://doi.org/10.1016/j.yebeh.2016.05.025

Jacobs, J., LeVan, P., Chander, R., Hall, J., Dubeau, F., & Gotman, J. (2008). Interictal high-frequency oscillations (80-500 Hz) are an indicator of seizure onset areas independent of spikes in the human epileptic brain. *Epilepsia*, *49*(11), 1893–1907. https://doi.org/10.1111/j.1528-1167.2008.01656.x

Jacobs, J., Levan, P., Chtillon, C. D., Olivier, A., Dubeau, F., & Gotman, J. (2009). High frequency oscillations in intracranial EEGs mark epileptogenicity rather than lesion type. *Brain*, *132*(4), 1022–1037. https://doi.org/10.1093/brain/awn351

Jacobs, J., Wu, J., Perucca, P., Zelmann, R., Mader, M., Dubeau, F., … Gotman, J. (2018). Removing high-frequency oscillations A prospective multicenter study on

seizure outcome, 1–14. https://doi.org/10.1212/WNL.0000000000006158

Jacobs, J., Zijlmans, M., Zelmann, R., Chatillon, C., Hall, J., Olivir, A., … Gotman, J. (2010a). High-Frequency Electroencephalographic Oscillations Correlate With Outcome of Epilepsy Surgery. *Annals of Neurology*, *67*(2), 209–220. https://doi.org/10.1002/ana.21847

Jacobs, J., Zijlmans, M., Zelmann, R., Chatillon, C., Hall, J., Olivir, A., … Gotman, J. (2010b). High-Frequency Electroencephalographic Oscillations Correlate With Outcome of Epilepsy Surgery. *Annals of Neurology*, *67*(2), 209–220. https://doi.org/10.1016/j.clinph.2011.06.006.A

Janecek, J. K., Swanson, S. J., Sabsevitz, D. S., Hammeke, T. A., Manoj, R., Rozman, M., & Binder, J. R. (2013). Language Lateralization by fMRI and Wada Testing in 229 Epilepsy Patients: Rates and Predictors of Discordance. *Epilepsia*, *54*(2), 314–322. https://doi.org/10.1038/jid.2014.371

Jayakar, P., Nordli, D., & Snead, O. C. (2016). The role and limits of surface EEG and source imaging. In John Libbey Eurotext (Ed.), *Pediatric Epilepsy Surgery* (pp. 7–24). Surrey.

JEC. (2011). Joint Epilepsy Council: National incidence and prevelance of epilepsy. Retrieved from http://www.epilepsyscotland.org.uk/pdf/Joint_Epilepsy_Council_Prevalence_and_Incidence_September_11_(3).pdf

Jenkinson, M., Bannister, P., Brady, M., & Smith, S. (2002). Improved optimization for the robust and accurate linear registration and motion correction of brain images. *NeuroImage*, *17*, 825–841. https://doi.org/10.1016/S1053-8119(02)91132-8

Jenkinson, M., & Smith, S. (2001). A global optimisation method for robust affine registration of brain images. *Medical Image Analysis*, *5*, 143–156. https://doi.org/10.1016/S1361-8415(01)00036-6

Jensen, O., & Colgin, L. L. (2007). Cross-frequency coupling between neuronal oscillations. *Trends in Cognitive Sciences*, *11*(7), 7–9.

Jung, J., Mainy, N., Kahane, P., Minotti, L., Hoffmann, D., Bertrand, O., & Lachaux, J. P. (2008). The neural bases of attentive reading. *Human Brain Mapping*, *29*(10), 1193–1206. https://doi.org/10.1002/hbm.20454

Jung, W., Pacia, S., & Devinsky, R. (1999). Neocortical temporal lobe epilepsy: intracranial EEG features and surgical outcome. *Journal of Clinical Neurophysiology*, *16*(5), 419–425.

Kalcher, J., & Pfurtscheller, G. (1995). Discrimination between phase-locked and non-phase-locked event- related {EEG} activity. *Electroencephalogr. Clin. Neurophysiol.*, *94*(5), 381–384.

Kamada, K., Sawamura, Y., Takeuchi, F., Kuriki, S., Kawai, K., Morita, A., & Todo, T. (2007). Expressive and receptive language areas determined by a non-invasive reliable method using functional magnetic resonance imaging and magnetoencephalography. *Neurosurgery*, *60*(2), 296–305. https://doi.org/10.1227/01.NEU.0000249262.03451.0E

Katz, J. S., Abel, T. J., & Abel, T. J. (2019). Stereoelectroencephalography Versus Subdural Electrodes for Localization of the Epileptogenic Zone : What Is the Evidence ? *Neurotherapeutics*, *16*, 59–66.

Keenan, N., & Sadlier, L. G. (2015). Paediatric EEG provision in New Zealand: a survey of practice. *The New Zealand Medical Journal*, *128*, 1411–1427. Retrieved from https://www.nzma.org.nz/journal/read-the-journal/all-issues/2010-2019/2015/vol-128-no-1411-27-mar-2015/6479

Kerber, K., Dümpelmann, M., Schelter, B., Le Van, P., Korinthenberg, R., Schulze-Bonhage, A., & Jacobs, J. (2014). Differentiation of specific ripple patterns helps to identify epileptogenic areas for surgical procedures. *Clinical Neurophysiology*, *125*(7), 1339–1345. https://doi.org/10.1016/j.clinph.2013.11.030

Kim, D. W., Kim, H. K., Lee, S. K., Chu, K., Chung, C. K., Kim, K., … Chung, K. (2010). Extent of neocortical resection and surgical outcome of epilepsy : Intracranial EEG analysis. *Epilepsia*, *51*(6), 1010–1017. https://doi.org/10.1111/j.1528-1167.2010.02567.x

Koessler, L., Benar, C., Maillard, L., Badier, J. M., Vignal, J. P., Bartolomei, F., … Gavaret, M. (2010). Source localization of ictal epileptic activity investigated by high resolution EEG and validated by SEEG. *NeuroImage*, *51*(2), 642–653. https://doi.org/10.1016/j.neuroimage.2010.02.067

Kojima, K., Brown, E. C., Rothermel, R., Carlson, A., Fuerst, D., Matsuzaki, N., … Asano, E. (2013). Clinical significance and developmental changes of auditory-language-related gamma activity. *Clinical Neurophysiology*, *124*(5), 857–869. https://doi.org/10.1016/j.clinph.2012.09.031

Kojima, K., Brown, E. C., Rothermel, R., Carlson, A., Matsuzaki, N., Shah, A., … Asano, E. (2012). Multimodality language mapping in patients with left-hemispheric language dominance on Wada test. *Clinical Neurophysiology*, *123*(10), 1917–1924. https://doi.org/10.1016/j.clinph.2012.01.027

Korzeniewska, A., Franaszczuk, P. J., Crainiceanu, C. M., Kuł, R., & Crone, N. E. (2011). Dynamics of large-scale cortical interactions at high gamma frequencies during word production: Event related causality (ERC) analysis of human electrocorticography (ECoG). *NeuroImage*, *56*(4), 2218–2237. https://doi.org/10.1016/j.neuroimage.2011.03.030

Koshino, Y., & Niedermeyer, E. (1975). Enhancement of Rolandic mu-rhythm by pattern vision. *Electroencephalography and Clinical Neurophysiology*, *28*(5), 535–538.

Krauss, G. L., Fisher, R., Plate, C., Hart, J., Uematsu, S., Gordon, B., & Lesser, R. P. (1996). Cognitive effects of resecting basal temporal language areas. *Epilepsia*, *37*(5), 476–483. https://doi.org/10.1111/j.1528-1157.1996.tb00594.x

Krieg, S. M., Sabih, J., Bulubasova, L., Obermueller, T., Negwer, C., Janssen, I., … Ringel, F. (2014). Preoperative motor mapping by navigated transcranial magnetic brain stimulation improves outcome for motor eloquent lesions. *Neuro-Oncology*, *16*(9), 1274–1282. https://doi.org/10.1093/neuonc/nou007

Krieg, S. M., Sollmann, N., Tanigawa, N., Foerschler, A., Meyer, B., & Ringel, F. (2016). Cortical distribution of speech and language errors investigated by visual

object naming and navigated transcranial magnetic stimulation. *Brain Structure and Function*, *221*(4), 2259–2286. https://doi.org/10.1007/s00429-015-1042-7

Kutsy, R. L., Farrell, D. F., & Ojemann, G. A. (1999). Ictal Patterns of Neocortical Seizures Monitored with Intracranial Electrodes : Correlation with Surgical Outcome. *Epilpesia*, *40*(3), 257–266.

Kwan, P., Arzimanoglou, A., Berg, A. T., Brodie, M. J., Hauser, W. A., Mathern, G., … French, J. (2010). Definition of drug resistant epilepsy: Consensus proposal by the ad hoc Task Force of the ILAE Commission on Therapeutic Strategies. *Epilepsia*, *51*(6), 1069–1077. https://doi.org/10.1111/j.1528-1167.2009.02397.x

Lachaux, J.-P., Axmacher, N., Mormann, F., Halgren, E., & Crone, N. E. (2012). High-frequency neural activity and human cognition: Past, present and possible future of intracranial EEG research. *Progress in Neurobiology*, *98*(3), 279–301. https://doi.org/10.1016/j.pneurobio.2012.06.008

Lachaux, J. P., George, N., Tallon-Baudry, C., Martinerie, J., Hugueville, L., Minotti, L., … Renault, B. (2005). The many faces of the gamma band response to complex visual stimuli. *NeuroImage*, *25*(2), 491–501. https://doi.org/10.1016/j.neuroimage.2004.11.052

Lau, E. F., Phillips, C., & Poeppel, D. (2008). A cortical network for semantics: (De)constructing the N400. *Nature Reviews Neuroscience*, *9*(12), 920–933. https://doi.org/10.1038/nrn2532

Lee, K. H., Lee, Y.-J., Seo, J. H., Baumgartner, J. E., & Westerveld, M. (2019). Epilepsy Surgery in Children versus Adults. *Journal of Korean Neurosurgical Society*, *62*(3), 328–335. https://doi.org/10.3340/jkns.2019.0026

Lee, Y. J., & Lee, J. S. (2013). Temporal lobe epilepsy surgery in children versus adults: From etiologies to outcomes. *Korean Journal of Pediatrics*, *56*(7), 275–281. https://doi.org/10.3345/kjp.2013.56.7.275

Lefaucheur, J. P., & Picht, T. (2016). The value of preoperative functional cortical mapping using navigated TMS. *Neurophysiologie Clinique*, *46*(2), 125–133. https://doi.org/10.1016/j.neucli.2016.05.001

Lehtinen, H., Mäkelä, J. P., Mäkelä, T., Lioumis, P., Metsähonkala, L., Hokkanen, L., … Gaily, E. (2018). Language mapping with navigated transcranial magnetic stimulation in pediatric and adult patients undergoing epilepsy surgery: Comparison with extraoperative direct cortical stimulation. *Epilepsia Open*, *3*(2), 224–235. https://doi.org/10.1002/epi4.12110

Lesser, R. P., Crone, N. E., & Webber, W. R. S. (2011). Using subdural electrodes to assess the safety of resections. *Epilepsy and Behavior*, *20*(2), 223–229. https://doi.org/10.1016/j.yebeh.2010.08.022

Lettori, D., Battaglia, D., Sacco, A., Veredice, C., Chieffo, D., Massimi, L., … Guzzetta, F. (2008). Early hemispherectomy in catastrophic epilepsy. A neuro-cognitive and epileptic long-term follow-up. *Seizure*, *17*(1), 49–63. https://doi.org/10.1016/j.seizure.2007.06.006

Liebenthal, E., Binder, J. R., Spitzer, S. M., Possing, E. T., & Medler, D. A. (2005). Neural substrates of phonemic perception. *Cerebral Cortex*, *15*(10), 1621–1631.

https://doi.org/10.1093/cercor/bhi040

Liégeois-Chauvel, C., Musolino, A., Badier, J. M., Marquis, P., & Chauvel, P. (1994). Evoked potentials recorded from the auditory cortex in man: evaluation and topography of the middle latency components. *Electroencephalography and Clinical Neurophysiology/ Evoked Potentials*, *92*(3), 204–214. https://doi.org/10.1016/0168-5597(94)90064-7

Liégeois-Chauvel, C., Trébuchon-Dafonseca, A., Marquis, P., & Chauvel, P. (2003). Presurgical Assessment of the Epilepsies with Clinical Neurophysiology and Functional Imaging. In F. R. and H. O. Lüders (Ed.), *Handbook of Clinical Neurophysiology* (Vol. 3, pp. 305–316). Chapter 2.22: Elsevier B.V. https://doi.org/10.1016/S1567-4231(03)03023-5

Liégeois, F., Connelly, A., Cross, J. H., Boyd, S. G., Gadian, D. G., Vargha-Khadem, F., & Baldeweg, T. (2004). Language reorganization in children with early-onset lesions of the left hemisphere: An fMRI study. *Brain*, *127*(6), 1229–1236. https://doi.org/10.1093/brain/awh159

Liégeois, F., Connelly, A., Salmond, C. H., Gadian, D. G., Vargha-Khadem, F., & Baldeweg, T. (2002). A direct test for lateralization of language activation using fMRI: Comparison with invasive assessments in children with epilepsy. *NeuroImage*, *17*(4), 1861–1867. https://doi.org/10.1006/nimg.2002.1327

Light, G. A., Williams, L. E., Minow, F., Sprock, J., Rissling, A., Sharp, R., … Braff, D. L. (2010). Electroencephalography (EEG) and Event-Related Potentials (ERP's) with Human Participants. *Current Protocols in Neuroscience*, *Chapter 6*, Unit 6.2524. https://doi.org/10.1002/0471142301.ns0625s52.Electroencephalography

Llorens, A., Dubarry, A. S., Trébuchon, A., Chauvel, P., Alario, F. X., & Liégeois-Chauvel, C. (2016). Contextual modulation of hippocampal activity during picture naming. *Brain and Language*, *159*, 92–101. https://doi.org/10.1016/j.bandl.2016.05.011

Llorens, Anaïs, Trébuchon, A., Liégeois-Chauvel, C., & Alario, F. X. (2011). Intra-cranial recordings of brain activity during language production. *Frontiers in Psychology*, *2*(DEC), 1–12. https://doi.org/10.3389/fpsyg.2011.00375

Luck, S. J. (2014). A Broad Overview of the Event-Related Potential Technique. In *An Introduction to the Event-Related Potential Technique* (2nd ed., pp. 1–34). MIT Press. https://doi.org/10.1007/s10409-008-0217-3

Luders, H. (2008). *Textbook of Epilepsy Surgery*. London: Informa, Ltd.

Lüders, H. O., Najm, I., Nair, D., Widdess-Walsh, P., & Bingman, W. (2006). The epileptogenic zone: General principles. *Epileptic Disorders*, *8*(SUPPL. 2), 1–9.

Mainy, N., Jung, J., Baciu, M., Kahane, P., Schoendorff, B., Minotti, L., … Lachaux, J. P. (2008). Cortical dynamics of word recognition. *Human Brain Mapping*, *29*(11), 1215–1230. https://doi.org/10.1002/hbm.20457

Makeig, S. (1993). Auditory event-related dynamics of the EEG spectrum and effects of exposure to tones. *Electroencephalography and Clinical Neurophysiology*, *86*, 283–293. https://doi.org/10.1109/20.42276

Malmgren, K., & Edelvik, A. (2017). Long-term outcomes of surgical treatment for epilepsy in adults with regard to seizures, antiepileptic drug treatment and employment. *Seizure*, *44*, 217–224. https://doi.org/10.1016/j.seizure.2016.10.015

Maratos, E. J., Allan, K., & Rugg, M. D. (2000). Recognition memory for emotionally negative and neutral words: An ERP study. *Neuropsychologia*, *38*(11), 1452–1465. https://doi.org/10.1016/S0028-3932(00)00061-0

Martino, J., de Witt Hamer, P. C., Vergani, F., Brogna, C., de Lucas, E. M., Vázquez-Barquero, A., … Duffau, H. (2011). Cortex-sparing fiber dissection: An improved method for the study of white matter anatomy in the human brain. *Journal of Anatomy*, *219*(4), 531–541. https://doi.org/10.1111/j.1469-7580.2011.01414.x

Matsumoto, A., Brinkmann, B. H., Matthew Stead, S., Matsumoto, J., Kucewicz, M. T., Marsh, W. R., … Worrell, G. (2013). Pathological and physiological high-frequency oscillations in focal human epilepsy. *Journal of Neurophysiology*, *110*(8), 1958–1964. https://doi.org/10.1152/jn.00341.2013

Mehvari-Habibabadi, J., Basiratnia, R., Moein, H., Zare, M., Barakatain, M., Aghakhani, Y., & Tabrizi, N. (2017). Prognostic value of ictal onset patterns in postsurgical outcome of temporal lobe epilpesy. *Iranian Journal of Neurology*, *16*(4), 185–191.

Mesulam, M. M., Thompson, C. K., Weintraub, S., & Rogalski, E. J. (2015). The Wernicke conundrum and the anatomy of language comprehension in primary progressive aphasia. *Brain*, *138*(8), 2423–2437. https://doi.org/10.1093/brain/awv154

Miller, K. J., Shenoy, P., Miller, J. W., Rao, R. P. N., & Ojemann, J. G. (2007). Real-time functional brain mapping using electrocorticography, *37*, 504–507. https://doi.org/10.1016/j.neuroimage.2007.05.029

Miller, K. J., Sorensen, L. B., Ojemann, J. G., & Nijs, M. den. (2007). ECoG observations of power-law scaling in the human cortex, *1*, 1–4. Retrieved from http://arxiv.org/abs/0712.0846

Moerel, M., De Martino, F., & Formisano, E. (2014). An anatomical and functional topography of human auditory cortical areas. *Frontiers in Neuroscience*, *8*(8 JUL), 1–14. https://doi.org/10.3389/fnins.2014.00225

Mohanraj, R., & Brodie, M. (2006). Diagnosing refractory epilepsy : response to sequential treatment. *European Journal of Neurology*, *13*, 277–282. https://doi.org/10.1111/j.1468-1331.2006.01215.x

Molholm, S., Sehatpour, P., Mehta, A. D., Shpaner, M., Gomez-Ramirez, M., Ortigue, S., … Foxe, J. J. (2006). Audio-visual multisensory integration in superior parietal lobule revealed by human intracranial recordings. *Journal of Neurophysiology*, *96*(2), 721–729. https://doi.org/10.1152/jn.00285.2006

Morán, M. A., Mufson, E. J., & Mesulam, M. -M. (1987). Neural inputs into the temporopolar cortex of the rhesus monkey. *Journal of Comparative Neurology*, *256*(1), 88–103. https://doi.org/10.1002/cne.902560108

Nagasawa, T., Juhász, C., Rothermel, R., Hoechstetter, K., Sood, S., & Asano, E. (2012). Spontaneous and visually driven high-frequency oscillations in the

occipital cortex: Intracranial recording in epileptic patients. *Human Brain Mapping*, *33*(3), 569–583. https://doi.org/10.1002/hbm.21233

Nagasawa, T., Juhász, C., Rothermel, R., Hoechstetter, K., Sood, S., Asano, E., … Asano, S. (2012). Spontaneous and visually-driven high-frequency oscillations in the occipital cortex: Intracranial recording in epileptic patients. *Human Brain Mapping*, *33*(3), 569–583. https://doi.org/10.1002/hbm.21233.

Najm, I., Jehi, L., Palmini, A., Gonzalez-Martinez, J., Paglioli, E., & Bingaman, W. (2013). Temporal patterns and mechanisms of epilepsy surgery failure. *Epilepsia*, *54*(5), 772–782. https://doi.org/10.1111/epi.12152

Narizzano, M., Arnulfo, G., Ricci, S., Toselli, B., Tisdall, M., Canessa, A., … Cardinale, F. (2017). SEEG assistant: a 3DSlicer extension to support epilepsy surgery. *BMC Bioinformatics*, *18*, 18–124. https://doi.org/10.1186/s12859-017-1545-8

Neuper, C., & Pfurtscheller, G. (2001). Evidence for distinct beta resonance frequencies in human EEG related to specific sensorimotor cortical areas. *Clinical Neurophysiology*, *112*(11), 2084–2097. https://doi.org/10.1016/S1388-2457(01)00661-7

Nevalainen, P., von Ellenrieder, N., Klimeš, P., Dubeau, F., Frauscher, B., & Gotman, J. (2020). Association of fast ripples on intracranial EEG and outcomes after epilepsy surgery. *Neurology*, *95*(16).

Ngugi, A. K., Bottomley, C., Kleinschmidt, I., Sander, J. W., & Newton, C. R. (2010). Estimation of the burden of active and life-time epilepsy: A meta-analytic approach. *Epilepsia*, *51*(5), 883–890. https://doi.org/10.1111/j.1528-1167.2009.02481.x

Nonoda, Y., Miyakoshi, M., Ojeda, A., Makeig, S., Juh??sz, C., Sood, S., … Blackman, M. R. (2016). Interictal high-frequency oscillations generated by seizure onset and eloquent areas may be differentially coupled with different slow waves. *Clinical Neurophysiology*, *127*(6), 2489–2499. https://doi.org/10.1016/j.clinph.2016.03.022

Northam, G. B., Adler, S., Eschmann, K. C. J., Chong, W. K., Cowan, F. M., & Baldeweg, T. (2018). Developmental conduction aphasia after neonatal stroke. *Annals of Neurology*, *83*(4), 664–675. https://doi.org/10.1002/ana.25218

Ogawa, S., Menon, R., Tank, D., Kim, S., Merkle, H., Ellermann, J., & Ugurbilt, K. (1993). Functional brain mapping by blood oxygenation level-dependent. *Biophys*, *64*(3), 803–812.

Oh, A., Duerden, E. G., & Pang, E. W. (2014). The role of the insula in speech and language processing. *Brain and Language*, *135*(416), 96–103. https://doi.org/10.1016/j.bandl.2014.06.003

Ojemann, G a. (1979). Individual variability in cortical localization of language. *Journal of Neurosurgery*, *50*(2), 164–169. https://doi.org/10.3171/jns.1979.50.2.0164

Ojemann, George, Ojemann, J., Lettich, E., & Berger, M. (2008). Cortical language localization in left, dominant hemisphere. An electrical stimulation mapping

investigation in 117 patients. 1989. *Journal of Neurosurgery*, *108*(2), 411–421. https://doi.org/10.3171/JNS/2008/108/2/0411

Okanishi, T., Akiyama, T., Tanaka, S.-I. I., Mayo, E., Mitsutake, A., Boelman, C., … Otsubo, H. (2014). Interictal high frequency oscillations correlating with seizure outcome in patients with widespread epileptic networks in tuberous sclerosis complex. *Epilepsia*, *55*(10), 1602–1610. https://doi.org/10.1111/epi.12761

Parkinson, G. M. (2002). High incidence of language disorder in children with focal epilepsies. *Developmental Medicine and Child Neurology*, *44*(8), 533–537. https://doi.org/10.1017/S0012162201002511

Pascual-Leone, A., GAtes, J. R., & Dhuna, A. (1991). Induction of Speech Arrest and Counting Errors With Rapid-Rate Transcranial Magnetic Stimulation. *Neurology*, *41*(5), 697–702.

Pastori, C., Francione, S., Pelle, F., de Curtis, M., & Gnatkovsky, V. (2016). Fluency tasks generate beta-gamma activity in language-related cortical areas of patients during stereo-EEG monitoring. *Brain and Language*, *163*, 50–56. https://doi.org/10.1016/j.bandl.2016.09.006

Patterson, K., Nestor, P. J., & Rogers, T. T. (2007). Where do you know what you know? The representation of semantic knowledge in the human brain. *Nature Reviews Neuroscience*, *8*(12), 976–987. https://doi.org/10.1038/nrn2277

Pei, X., Leuthardt, E. C., Gaona, C. M., Brunner, P., Wolpaw, J. R., & Schalk, G. (2011). Spatiotemporal dynamics of electrocorticographic high gamma activity during overt and covert word repetition. *NeuroImage*, *54*(4), 2960–2972. https://doi.org/10.1016/j.neuroimage.2010.10.029

Pellegrino, G., Hedrich, T., Chowdhury, R., Hall, J. A., Lina, J. M., Dubeau, F., … Grova, C. (2016). Source localization of the seizure onset zone from ictal EEG/MEG data. *Human Brain Mapping*, *37*(7), 2528–2546. https://doi.org/10.1002/hbm.23191

Penfield, W., & Boldrey, E. (1937). Somatic motor and sensory representation in the cerebral cortex of man as studied by electric stimulation. *Brain*, *60*, 389–443.

Penfield, W., & Jasper, H. (1954). *Epilepsy and the Functional Anatomy of the Human Brain*. Boston: Little and Brown.

Penny, W. D., Duzel, E., Miller, K. J., & Ojemann, J. G. (2008). Testing for nested oscillation. *Journal of Neuroscience Methods*, *174*(1), 50–61. https://doi.org/10.1016/j.jneumeth.2008.06.035

Pfurtscheller, G. (1977). Graphical display and statistical evaluation of event-related desynchronization (ERD). *Electroencephalography and Clinical Neurophysiology*, *43*(5), 757–760.

Pfurtscheller, G. (1992). Event-related synchronization (ERS): an electrophysiological correlate of cortical areas at rest. *Electroencephalography and Clinical Neurophysiology*, *83*, 62–69. https://doi.org/10.1016/0013-4694(92)90133-3

Pfurtscheller, G. (2001). Functional brain imaging based on ERD/ERS. *Vision Research*, *41*(10–11), 1257–1260. https://doi.org/10.1016/S0042-6989(00)00235-2

Pfurtscheller, G., & Aranibar, A. (1977). Event-related cortical desynchronisation detected by power measurements of scalp EEG. *Electroencephalography and Clinical Neurophysiology*, (42), 817–826.

Pfurtscheller, G., & Aranibar, A. (1977). Event-related cortical desynchronization detected by power measurements of scalp EEG. *Electroencephalography and Clinical Neurophysiology*, *42*(6), 817–826.

Pfurtscheller, G., & Aranibar, A. (1979). Evaluation of event-related desynchronization (ERD) preceding and following voluntary self-paced movement. *Electroencephalogr Clin Neurophysio*, *46*(2), 138–146. https://doi.org/10.1016/0013-4694(79)90063-4

Pfurtscheller, G., & Lopes da Silva, F. H. (2017). EEG Event-Related Desynchronization and Event-Related Synchronization Author(s): In D. L. Schomer & F. H. Lopes da Silva (Eds.), *Niedermeyer's Electroencephalography : Basic Principles , Clinical Applications and Related Fields (7 ed.)* (7th ed., pp. 1–34). Oxford University Press. https://doi.org/10.1093/med/9780190228484.001.0001

Pfurtscheller, G., & Lopes, F. H. (1999). Event-related EEG / MEG synchronization and desynchronization : basic principles. *Clinical Neurophysiology*, *110*, 1842–1857. https://doi.org/10.1016/S1388-2457(99)00141-8

Picot, M. C., Baldy-Moulinier, M., Daurès, J. P., Dujols, P., & Crespel, A. (2008). The prevalence of epilepsy and pharmacoresistant epilepsy in adults: A population-based study in a Western European country. *Epilepsia*, *49*(7), 1230–1238. https://doi.org/10.1111/j.1528-1167.2008.01579.x

Pirmoradi, M., Béland, R., Nguyen, D. K., Bacon, B. A., & Lassonde, M. (2010). Language tasks used for the presurgical assessment of epileptic patients with MEG. *Epileptic Disorders*, *12*(2), 97–108. https://doi.org/10.1684/epd.2010.0314

Podkorytova, I., Hoes, K., & Lega, B. (2016). Stereo-Encephalography Versus Subdural Electrodes for Seizure Localization. *Neurosurgery Clinics of North America*, *27*(1), 97–109. https://doi.org/10.1016/j.nec.2015.08.008

Poeppel, D., Emmorey, K., Hickok, G., & Pylkkänen, L. (2012). Towards a new neurobiology of language. *J Neurosci*, *23*(7), 14125–14131. https://doi.org/10.1523/JNEUROSCI.3244-12.2012.Towards

Poeppel, D., & Hickok, G. (2004). Towards a new functional anatomy of language. *Cognition*, *92*(1–2), 1–12. https://doi.org/10.1016/j.cognition.2003.11.001

Prasad, A., Pacia, S. V., Vazquez, B., Doyle, W. K., & Devinsky, O. (2003). Extent of ictal origin in mesial temporal sclerosis patients monitored with subdural intracranial electrodes predicts outcome. *Journal of Clinical Neurophysiology*, *20*(4), 243–248. https://doi.org/10.1097/00004691-200307000-00003

Price, C. J. (2012). A review and synthesis of the first 20years of PET and fMRI studies of heard speech, spoken language and reading. *NeuroImage*, *62*(2), 816–847. https://doi.org/10.1016/j.neuroimage.2012.04.062

Prpić, N. (2015). Language processing – role of inferior parietal lobule. *Gyrus*, *3*(3), 173–176. https://doi.org/10.17486/gyr.3.1037

Pulsifer, M. B., Brandt, J., Salorio, C. F., Vining, E. P. G., Carson, B. S., & Freeman, J. M. (2004). The Cognitive Outcome of Hemispherectomy in 71 Children. *Epilepsia*, *45*(3), 243–254. https://doi.org/10.1111/j.0013-9580.2004.15303.x

Radüntz, T., Scouten, J., Hochmuth, O., & Meffert, B. (2015). EEG artifact elimination by extraction of ICA-component features using image processing algorithms. *Journal of Neuroscience Methods*, *243*, 84–93. https://doi.org/10.1016/j.jneumeth.2015.01.030

Ray, S., Niebur, E., Hsiao, S. S., Sinai, A., & Crone, N. E. (2008). High-frequency gamma activity (80-150 Hz) is increased in human cortex during selective attention. *Clinical Neurophysiology*, *119*(1), 116–133. https://doi.org/10.1016/j.clinph.2007.09.136

Rektor, I., Kaňovský, P., Bareš, M., Brázdil, M., Streitová, H., Klajblová, H., … Daniel, P. (2003). A SEEG study of ERP in motor and premotor cortices and in the basal ganglia. *Clinical Neurophysiology*, *114*(3), 463–471. https://doi.org/10.1016/S1388-2457(02)00388-7

Remedios, R., Logothetis, N. K., & Kayser, C. (2009). An auditory region in the primate insular cortex responding preferentially to vocal communication sounds. *Journal of Neuroscience*, *29*(4), 1034–1045. https://doi.org/10.1523/JNEUROSCI.4089-08.2009

Ries, S. K., Dronkers, N. F., & Knight, R. T. (2016). Choosing words: left hemisphere, right hemisphere, or both? Perspective on the lateralization of word retrieval. *Ann N Y Acad Sci*, *1369*(1), 111–131. https://doi.org/10.1016/j.physbeh.2017.03.040

Roehri, N., Pizzo, F., Lagarde, S., Lambert, I., Nica, A., McGonigal, A., … Bénar, C.-G. G. (2017). High-frequency oscillations are not better biomarkers of epileptogenic tissues than spikes. *Annals of Neurology*, *83*(1), 84–97. https://doi.org/10.1002/ana.25124

Rosenow, F., & Lüders, H. (2001). Presurgical evaluation of epilepsy. *Brain : A Journal of Neurology*, *124*(Pt 9), 1683–1700. https://doi.org/10.4103/1817-1745.40593

Rösler, J., Niraula, B., Strack, V., Zdunczyk, A., Schilt, S., Savolainen, P., … Picht, T. (2014). Language mapping in healthy volunteers and brain tumor patients with a novel navigated TMS system: Evidence of tumor-induced plasticity. *Clinical Neurophysiology*, *125*(3), 526–536. https://doi.org/10.1016/j.clinph.2013.08.015

Ryvlin, P., Cross, J. H., & Rheims, S. (2014). Epilepsy surgery in children and adults. *The Lancet Neurology*, *13*(11), 1114–1126. https://doi.org/10.1016/S1474-4422(14)70156-5

Sakpichaisakul, K., Byars, A. W., Horn, P. S., Aungaroon, G., Greiner, H. M., Mangano, F. T., … Arya, R. (2020). Neuropsychological outcomes after pediatric epilepsy surgery: Role of electrical stimulation language mapping. *Seizure*, *80*(June), 183–191. https://doi.org/10.1016/j.seizure.2020.06.029

Sanai, N., Mirzadeh, Z., & Berger, M. S. (2008). Functional outcome after language mapping for glioma resection. *The New England Journal of Medicine*, *358*(1), 18–27. https://doi.org/10.1056/NEJMoa067819

Sarubbo, S., De Benedictis, A., Maldonado, I. L., Basso, G., & Duffau, H. (2013).

Frontal terminations for the inferior fronto-occipital fascicle: Anatomical dissection, DTI study and functional considerations on a multi-component bundle. *Brain Structure and Function*, *218*(1), 21–37. https://doi.org/10.1007/s00429-011-0372-3

Saur, D., Kreher, B. W., Schnell, S., Kümmerera, D., Kellmeyera, P., Vrya, M. S., … Weiller, C. (2008). Ventral and dorsal pathways for language. *Proceedings of the National Academy of Sciences of the United States of America*, *105*(46), 18035–18040. https://doi.org/10.1073/pnas.0805234105

Scheffer, I. E., Berkovic, S., Capovilla, G., Connolly, M. B., French, J., Guilhoto, L., … Zuberi, S. M. (2017). ILAE classification of the epilepsies: Position paper of the ILAE Commission for Classification and Terminology. *Epilepsia*, *58*(4), 512–521. https://doi.org/10.1111/epi.13709

Schevon, C. A., Weiss, S. A., McKhann, G. J., Goodman, R. R., Yuste, R., Emerson, R. G., & Trevelyan, A. J. (2012). Evidence of an inhibitory restraint of seizure activity in humans. *Nature Communications*, *3*, 1060. https://doi.org/10.1038/ncomms2056

Schomaker, J., & Talsma, D. (2009). The Relationship between Response Time and the Strength of Top-Down Attentional Control: An ERP Study. *Journal of European Psychology Students*, *1*(1), 2. https://doi.org/10.5334/jeps.ab

Scott, S., Blank, C. C., Rosen, S., & Wise, R. J. S. (2000). Identification of a pathway for intelligible speech in the left temporal lob. *Brain*, *123*(Pt 12), 2400–2406.

Shibasaki, H., & Hallett, M. (2006). What is the Bereitschaftspotential? *Clinical Neurophysiology*, *117*(11), 2341–2356. https://doi.org/10.1016/j.clinph.2006.04.025

Siapas, A. G., & Wilson, M. A. (1998). Coordinated interactions between hippocampal ripples and cortical spindles during slow-wave sleep. *Neuron*, *21*, 1123–1128.

Sills, G. J. (2013). Classical mechanisms of action of antiepileptic drugs. In H. Potschka & H. Lerche (Eds.), *Therapeutic Targets and Perspectives in the Pharmacological Treatment of Epilepsy* (pp. 62–65). Bremen: UNI-MED Verlag. https://doi.org/10.1016/j.yebeh.2015.08.030

Sinai, A., Bowers, C., Crainiceanu, C., Boatman, D., Gordon, B., Lesser, R., … Crone, N. E. (2005). Electrocorticographic high gamma activity versus electrical cortical stimulation mapping of naming. *Brain*, *128*(7), 1556–1570. https://doi.org/10.1093/brain/awh491

Sinai, A., Crone, N. E., Wied, H. M., Franaszczuk, P. J., Miglioretti, D., & Boatman-Reich, D. (2009). Intracranial mapping of auditory perception: Event-related responses and electrocortical stimulation. *Clinical Neurophysiology*, *120*(1), 140–149. https://doi.org/10.1016/j.clinph.2008.10.152

Skirrow, C., Cross, H. J., Cormack, F., Harkness, W., Vargha-Khadem, F., & Baldeweg, T. (2011). Long-term intellectual outcome after temporal lobe surgery in childhood. *Neurology*, *76*(15), 1330–1337. https://doi.org/10.1212/WNL.0b013e31821527f0

Skirrow, C., Cross, H. J., Harrison, S., Cormack, F., Harkness, W., Coleman, R., …

Baldeweg, T. (2015). Temporal lobe surgery in childhood and neuroanatomical predictors of long-term declarative memory outcome. *Brain*, *138*, 80–93. https://doi.org/10.1093/brain/awu313

Spanedda, F., Cendes, F., & Gotman, J. (1997). Relations Between EEG Seizure Morphology, Interhemispheric Spread, and Mesial Temporal Atrophy in Bitemporal Epilepsy. *Epilepsia*, *38*(12), 1300–1314.

Staba, R. J., Frighetto, L., Behnke, E. J., Mathern, G. W., Fields, T., Bragin, A., … Engel, J. (2007). Increased fast ripple to ripple ratios correlate with reduced hippocampal volumes and neuron loss in temporal lobe epilepsy patients. *Epilepsia*, *48*(11), 2130–2138. https://doi.org/10.1111/j.1528-1167.2007.01225.x

Staba, R. J., Wilson, C. L., Bragin, A., & Fried, I. (2002). Quantitative analysis of high-frequency oscillations (80-500 Hz) recorded in human epileptic hippocampus and entorhinal cortex. *Journal of Neurophysiology*, *88*(4), 1743–1752. https://doi.org/10.1152/jn.2002.88.4.1743

Staba, R. J., Wilson, C. L., Bragin, A., Jhung, D., Fried, I., & Engel, J. (2004). High-frequency oscillations recorded in human medial temporal lobe during sleep. *Annals of Neurology*, *56*(1), 108–115. https://doi.org/10.1002/ana.20164

Stafstrom, C. E., & Carmant, L. (2015). Seizures and epilepsy: An overview for neuroscientists. *Cold Spring Harbor Perspectives in Medicine*, *5*(6), 1–18. Retrieved from http://perspectivesinmedicine.org/content/5/6/a022426.full.pdf%5Cnhttp://ovids p.ovid.com/ovidweb.cgi?T=JS&PAGE=reference&D=emed13&NEWS=N&AN =2015098874

Stefan, H., & Trinka, E. (2017). Magnetoencephalography (MEG): Past, current and future perspectives for improved differentiation and treatment of epilepsies. *Seizure*, *44*, 121–124. https://doi.org/10.1016/j.seizure.2016.10.028

Steinmetz, H., Furst, G., & Freund, H. J. (1990). Variation of perisylvian and calcarine anatomic landmarks within stereotaxic proportional coordinates. *American Journal of Neuroradiology*, *11*(6), 1123–1130.

Steinschneider, M., Liegeois-Chauvel, C., & Brugge, J. F. (2011). Auditory Evoked Potentials and Their Utility in the Assessment of Complex Sound Processing. In J. A. Winer & C. E. Schreiner (Eds.), *The Auditory Cortex* (pp. 535–559). Springer Science+Business Media. https://doi.org/10.1007/978-1-4419-0074-6

Steriade, M., Gloor, P., Llinás, R. R., Lopes da Silva, F. H., & Mesulam, M.-M. (1990). Basic mechanisms of cerebral rhythmic activities. *Electroencephalography and Clinical Neurophysiology*, *76*, 481–508.

Sullivan, M. D., Janus, M., Moreno, S., Astheimer, L., & Bialystok, E. (2014). Early stage second-language learning improves executive control: Evidence from ERP. *Brain and Language*, *139*, 84–98. https://doi.org/10.1016/j.bandl.2014.10.004

Sung, C., Muller, V., Jones, J. E., & Chan, F. (2014). Vocational rehabilitation service patterns and employment outcomes of people with epilepsy. *Epilepsy Research*, *108*(8), 1469–1479. https://doi.org/10.1016/j.eplepsyres.2014.06.016

Takahashi, S., Vajkoczy, P., & Picht, T. (2013). Navigated transcranial magnetic

stimulation for mapping the motor cortex in patients with rolandic brain tumors. *Neurosurgical Focus*, *34*(4), E3. https://doi.org/10.3171/2013.1.FOCUS133

Talairach, J., & Bancaud, J. (1973). Stereotaxic approach to epilepsy: methodology of anatomo-functional stereotaxic investigations. *Prog Neurol Surg*, *5*, 297–354.

Talairach, J., & Bancaud, J. (1974). New approach to the neurosurgery of epilepsy: stereotaxic methodology and therapeutic results, 1: introduction and history. *Neurochirurgie*, *20*, 1–240.

Tallon-Baudry, C., & Bertrand, O. (1999). Oscillatory gamma activity in humans and its role in object representation. *Trends in Cognitive Sciences*, *3*(4), 151–162. https://doi.org/10.1016/S1364-6613(99)01299-1

Tarapore, P. E., Findlay, A. M., Honma, S. M., Mizuiri, D., Houde, J. F., Berger, M. S., & Nagarajan, S. S. (2013). Language mapping with navigated repetitive TMS: Proof of technique and validation. *NeuroImage*, *82*, 260–272. https://doi.org/10.1016/j.neuroimage.2013.05.018

Tassi, L., Jayakar, P., Pieper, T., & Kahane, P. (2016). Intracranial EEG recordings and electrical stimulation. In *Pediatric Epilepsy Surgery* (pp. 61–75). Editions John Libbey Eurotext.

Taylor, M. J., & Baldeweg, T. (2002). Application of EEG, ERP and intracranial recordings to the investigation of cognitive functions in children. *Developmental Science*, *5*(3), 318–334. https://doi.org/10.1111/1467-7687.00372

Téllez-Zenteno, J. F., & Hernández-Ronquillo, L. (2012). A Review of the Epidemiology of Temporal Lobe Epilepsy. *Epilepsy Research and Treatment*, *2012*, 1–5. https://doi.org/10.1155/2012/630853

Téllez-Zenteno, J. F., Ronquillo, L., Moien-Afshari, F., & Wiebe, S. (2010). Surgical outcomes in lesional and non-lesional epilepsy: A systematic review and meta-analysis. *Epilepsy Research*, *89*(2–3), 310–318. https://doi.org/10.1016/j.eplepsyres.2010.02.007

Terra-Bustamante, V. C., Inuzuka, L. M., Fernandes, R. M. F., Escorsi-Rosset, S., Wichert-Ana, L., Alexandre, V., … Sakamoto, A. C. (2007). Outcome of hemispheric surgeries for refractory epilepsy in pediatric patients. *Child's Nervous System*, *23*(3), 321–326. https://doi.org/10.1007/s00381-006-0212-6

Tharwat, A. (2018). Independent component analysis: An introduction. *Applied Computing and Informatics*, 1–15. https://doi.org/10.1016/j.aci.2018.08.006

Thatcher, R. W., McAlaster, R., Lester, M. L., Horst, R. L., & Cantor, D. S. (1983). Hemispheric EEG asymmetries related to cognitive functioning in children. *Cognitive Processing in the Right Hemisphere*, 125–146.

Thom, M., Mathern, G. W., Cross, J. H., & Bertram, E. H. (2010). Mesial temporal lobe epilepsy: How do we improve surgical outcome? *Annals of Neurology*, *68*(4), 424–434. https://doi.org/10.1002/ana.22142

Tierney, T. M., Holmes, N., Meyer, S. S., Boto, E., Roberts, G., Leggett, J., … Barnes, G. R. (2018). Cognitive neuroscience using wearable magnetometer arrays: Non-invasive assessment of language function. *NeuroImage*, *181*, 513–520. https://doi.org/10.1016/j.neuroimage.2018.07.035

Tomson, T., & Steinhoff, B. J. (2012). Principles of drug treatment in adults. *Handbook of Clinical Neurology*, *108*, 683–698. https://doi.org/10.1016/B978-0-444-52899-5.00022-8

Towle, V. L., Yoon, H. A., Castelle, M., Edgar, J. C., Biassou, N. M., Frim, D. M., … Kohrman, M. H. (2008). ECoG gamma activity during a language task: Differentiating expressive and receptive speech areas. *Brain*, *131*(8), 2013–2027. https://doi.org/10.1093/brain/awn147

Toyoda, G., Brown, E. C., Matsuzaki, N., Kojima, K., Nishida, M., & Asano, E. (2014). Electrocorticographic correlates of overt articulation of 44 English phonemes: Intracranial recording in children with focal epilepsy. *Clinical Neurophysiology*, *125*(6), 1129–1137. https://doi.org/10.1016/j.clinph.2013.11.008

Traub, R. D. (2003). Fast Oscillations and Epilepsy. *Epilepsy Currents / American Epilepsy Society*, *3*(3), 77–79. https://doi.org/10.1046/j.1535-7597.2003.03301.x

Trébuchon-Da Fonseca, A., Bénar, C., Bartoloméi, F., Régis, J., Démonet, J., Chauvel, P., & Liégeois-Chauvel, C. (2009). Electrophysiological study of the basal temporal language area: A convergence zone between language perception and production networks. *Clinical Neurophysiology*, *120*(3), 539–550. https://doi.org/10.1016/j.clinph.2008.12.042

Trébuchon, A., & Chauvel, P. (2016). Electrical Stimulation for Seizure Induction and Functional Mapping in Stereoelectroencephalography. *Journal of Clinical Neurophysiology*, *33*(6), 511–521. https://doi.org/10.1097/WNP.0000000000000313

Trébuchon, A., Démonet, J. F., Chauvel, P., & Liégeois-Chauvel, C. (2013a). Ventral and dorsal pathways of speech perception: An intracerebral ERP study. *Brain and Language*, *127*(2), 273–283. https://doi.org/10.1016/j.bandl.2013.04.007

Trébuchon, A., Démonet, J. F., Chauvel, P., & Liégeois-Chauvel, C. (2013b). Ventral and dorsal pathways of speech perception: An intracerebral ERP study. *Brain and Language*, *127*(2), 273–283. https://doi.org/10.1016/j.bandl.2013.04.007

Trevelyan, A. J., Sussillo, D., Watson, B. O., & Yuste, R. (2006). Modular propagation of epileptiform activity: evidence for an inhibitory veto in neocortex. *The Journal of Neuroscience : The Official Journal of the Society for Neuroscience*, *26*(48), 12447–12455. https://doi.org/10.1523/JNEUROSCI.2787-06.2006

Tuxhorn, I. (2010). Extra-operative and Intra-operative Electrical Stimulation. In *Pediatric Epilepsy Surgery: Preoperative Assessment and Surgical Treatment* (pp. 41–52). Stuttgart, New York, Delhi: Thieme Verlagsgruppe.

Urrestarazu, E., Chander, R., Dubeau, F., & Gotman, J. (2007). Interictal high-frequency oscillations (10-500 Hz) in the intracerebral EEG of epileptic patients. *Brain*, *130*(9), 2354–2366. https://doi.org/10.1093/brain/awm149

Urrestarazu, E., Jirsch, J. D., LeVan, P., Hall, J., & Gotman, J. (2006). High-frequency intracerebral EEG activity (100-500 Hz) following interictal spikes. *Epilepsia*, *47*(9), 1465–1476. https://doi.org/10.1111/j.1528-1167.2006.00618.x

Usui, N., Terada, K., Baba, K., Matsuda, K., Nakamura, F., Usui, K., … Inoue, Y. (2010). Very high frequency oscillations (over 1000Hz) in human epilepsy.

Clinical Neurophysiology, *121*(11), 1825–1831. https://doi.org/10.1016/j.clinph.2010.04.018

Usui, N., Terada, K., Baba, K., Matsuda, K., Nakamura, F., Usui, K., … Inoue, Y. (2011). Clinical significance of ictal high frequency oscillations in medial temporal lobe epilepsy. *Clinical Neurophysiology*, *122*(9), 1693–1700. https://doi.org/10.1016/j.clinph.2011.02.006

van 't Klooster, M. A., Leijten, F. S. S., Huiskamp, G., Ronner, H. E., Baayen, J. C., van Rijen, P. C., … Zijlmans, M. (2015). High frequency oscillations in the intra-operative ECoG to guide epilepsy surgery ("The HFO Trial"): study protocol for a randomized controlled trial. *Trials*, *16*(1), 422. https://doi.org/10.1186/s13063-015-0932-6

van 't Klooster, M. A., van Klink, N. E. C., Zweiphenning, W. J. E. M., Leijten, F. S. S., Zelmann, R., Ferrier, C. H., … Zijlmans, M. (2017). Tailoring epilepsy surgery with fast ripples in the intraoperative electrocorticogram. *Annals of Neurology*, *81*(5), 664–676. https://doi.org/10.1002/ana.24928

van Klink, N. E. C., van 't Klooster, M. A., Zelmann, R., Leijten, F. S. S., Ferrier, C. H., Braun, K. P. J., … Zijlmans, M. (2014). High frequency oscillations in intra-operative electrocorticography before and after epilepsy surgery. *Clinical Neurophysiology*, *125*(11), 2212–2219. https://doi.org/10.1016/j.clinph.2014.03.004

van Klink, N., Frauscher, B., Zijlmans, M., & Gotman, J. (2016). Relationships between interictal epileptic spikes and ripples in surface EEG. *Clinical Neurophysiology*, *127*(1), 143–149. https://doi.org/10.1016/j.clinph.2015.04.059

Van Schooneveld, M. M. J., & Braun, K. P. J. (2013). Cognitive outcome after epilepsy surgery in children. *Brain & Development*, *35*(8), 721–729. https://doi.org/10.1016/j.braindev.2013.01.011

Vargha-Khadem, F., Gadian, D. G., Watkins, K. E., Connelly, A., Van Paesschen, W., & Mishkin, M. (1997). Differential effects of early hippocampal pathology on episodic and semantic memory. *Science*, *277*(5324), 376–380. https://doi.org/10.1126/science.277.5324.376

Vargha-Khadem, F., O'Gorman, A. M., & Watters, G. V. (1985). Aphasia and handedness in relation to hemispheric side, age at injury and severity of cerebral lesion during childhood. *Brain*, *108*(3), 677–696. https://doi.org/10.1093/brain/108.3.677

Vidal, J. R., Ossandón, T., Jerbi, K., Dalal, S. S., Minotti, L., Ryvlin, P., … Lachaux, J. P. (2010). Category-specific visual responses: An intracranial study comparing gamma, beta, alpha, and ERP response selectivity. *Frontiers in Human Neuroscience*, *4*(November). https://doi.org/10.3389/fnhum.2010.00195

Vigliocco, G., Vinson, D. P., Druks, J., Barber, H., & Cappa, S. F. (2011). Nouns and verbs in the brain: A review of behavioural, electrophysiological, neuropsychological and imaging studies. *Neuroscience and Biobehavioral Reviews*, *35*(3), 407–426. https://doi.org/10.1016/j.neubiorev.2010.04.007

Vigneau, M., Beaucousin, V., Hervé, P. Y., Duffau, H., Crivello, F., Houdé, O., … Tzourio-Mazoyer, N. (2006). Meta-analyzing left hemisphere language areas:

Phonology, semantics, and sentence processing. *NeuroImage*, *30*(4), 1414–1432. https://doi.org/10.1016/j.neuroimage.2005.11.002

Vingerhoets, G. (2006). Cognitive effects of seizures. *Seizure*, *15*(4), 221–226. https://doi.org/10.1016/j.seizure.2006.02.012

von Stein, A. U., & Sarnthein, J. (2000). Different frequencies for different scales of cortical integration: from local gamma to long range alpha/theta synchronization. *International Journal of Psychophysiology*, *38*, 301–313. https://doi.org/10.1016/S0167-8760(00)00172-0

Wada, J., & Rasmussen, T. (1960). Intracarotid injection of sodium amytal for the lateralization of cerebral speech dominance. *Neurosurgery*, *17*, 266−282.

Wang, S., Wang, I. Z., Bulacio, J. C., Mosher, J. C., Gonzalez-Martinez, J., Alexopoulos, A. V., … So, N. K. (2013). Ripple classification helps to localize the seizure-onset zone in neocortical epilepsy. *Epilepsia*, *54*(2), 370–376. https://doi.org/10.1111/j.1528-1167.2012.03721.x

Wang, Y., Fifer, M. S., Korzeniewska, A., Cervenka, M. C., Boatman-reich, D. F., & Crone, N. E. (2016). Spatial-temporal functional mapping of language at the bedside with electrocorticography. *Neurology*, *86*, 1181–1189.

Weiller, C., Musso, M., Rijntjes, M., & Saur, D. (2009). Please don't underestimate the ventral pathway in language. *Journal of Cognitive Neuroscience*, *2213*, 369–370. https://doi.org/10.1162/jocn.2009.21300

Weiss-Croft, L. J., & Baldeweg, T. (2015). Maturation of language networks in children: A systematic review of 22years of functional MRI. *NeuroImage*, *123*, 269–281. https://doi.org/10.1016/j.neuroimage.2015.07.046

Weiss, S. A., Banks, G. P., McKhann, G. M., Goodman, R. R., Emerson, R. G., Trevelyan, A. J., & Schevon, C. A. (2013). Ictal high frequency oscillations distinguish two types of seizure territories in humans. *Brain*, *136*, 3796–3808. https://doi.org/10.1093/brain/awt276

Weiss, S. A., Lemesiou, A., Connors, R., Banks, G. P., McKhann, G. M., Goodman, R. R., … Schevon, C. A. (2015). Seizure localization using ictal phase-locked high gamma: A retrospective surgical outcome study. *Neurology*, *84*(23), 2320–2328. https://doi.org/10.1212/WNL.0000000000001656

Weiss, S. A., Orosz, I., Salamon, N., Moy, S., Wei, L., Van't Klooster, M. A., … Staba, R. J. (2016). Ripples on spikes show increased phase-amplitude coupling in mesial temporal lobe epilepsy seizure-onset zones. *Epilepsia*, *57*(11), 1916–1930. https://doi.org/10.1111/epi.13572

Weiss, S., & Mueller, H. M. (2012). " Too many betas do not spoil the broth ": the role of beta brain oscillations in language processing, *3*(June), 1–15. https://doi.org/10.3389/fpsyg.2012.00201

Wendling, F., Badier, J. M., Chauvel, P., & Coatrieux, J. L. (1997). A methods to quantify invariant information in depth-recorded epileptic seizures. *Electroencephalography and Clinical Neurophysiology*, *102*(6), 472–485. https://doi.org/10.1016/S0013-4694(96)96633-3

Wernicke, C. (1874). *Der Aphasische Syndromkomplex*. Breslau: Cohn and Weigert.

Whitney, C., Weis, S., Krings, T., Huber, W., Grossman, M., & Kircher, T. (2009). Activity during Intrinsic Word Production. *Journal of Cognitive Neuroscience, 21*(4), 697–712. https://doi.org/10.1162/jocn.2009.21056.Task-dependent

Wiebe, S., Blume, W. T., Girvin, J. P., & Eliasziw, M. (2001). A Randomized , Controlled Trial of Surgery for Temporal-Lobe Epilepsy. *Nature Reviews. Neurology*, *345*(5), 311–318. https://doi.org/10.1056/NEJM200108023450501

Wise, R. J. S., Greene, J., Büchel, C., & Scott, S. K. (1999). Brain regions involved in articulation. *The Lancet*, *353*, 1057–1061. https://doi.org/10.1016/S0140-6736(98)07491-1

Woods, R. P., Dodrill, C. B., & Ojemann, G. A. (1988). Brain injury, handedness, and speech lateralization in a series of amobarbital studies. *Annals of Neurology*, *23*(5), 510–518. https://doi.org/10.1002/ana.410230514

Worrell, G. A., Parish, L., Cranstoun, S. D., Jonas, R., Baltuch, G., & Litt, B. (2004). High-frequency oscillations and seizure generation in neocortical epilepsy. *Brain*, *127*(7), 1496–1506. https://doi.org/10.1093/brain/awh149

Wu, J. Y., Sankar, R., Lerner, J. T., Matsumoto, J. H., Vinters, H. V., & Mathern, G. W. (2010). Removing interictal fast ripples on electrocorticography linked with seizure freedom in children. *Neurology*, *75*(19), 1686–1694. https://doi.org/10.1212/WNL.0b013e3181fc27d0

Yamazoe, T., von Ellenrieder, N., Khoo, H. M., Huang, Y. H., Zazubovits, N., Dubeau, F., & Gotman, J. (2019). Widespread interictal epileptic discharge more likely than focal discharges to unveil the seizure onset zone in EEG-fMRI. *Clinical Neurophysiology*, *130*(4), 429–438. https://doi.org/10.1016/j.clinph.2018.12.014

Yang, L., Wilke, C., Brinkmann, B., Worrell, G. A., & He, B. (2011). Dynamic imaging of ictal oscillations using non-invasive high-resolution EEG. *NeuroImage*, *56*(4), 1908–1917. https://doi.org/10.1016/j.neuroimage.2011.03.043

Youssofzadeh, V., Stout, J., Ustine, C., Gross, W. L., Conant, L. L., Humphries, C. J., … Raghavan, M. (2020). *Mapping language from MEG beta power modulations during auditory and visual naming. NeuroImage* (Vol. 220). Elsevier Inc. https://doi.org/10.1016/j.neuroimage.2020.117090

Zelmann, R., Jacobs, J., Zijlmans, M., Dubeau, F., & Gotman, J. (2012). A comparison between detectors of high frequency oscillations. *Clinical Neurophysiology*, *123*(1), 106–116. https://pubmed.ncbi.nlm.nih.gov/21763191/

Zijlmans, M., Huiskamp, G. M., Cremer, O. L., Ferrier, C. H., Van Huffelen, A. C., & Leijten, F. S. S. (2012). Epileptic high-frequency oscillations in intraoperative electrocorticography: The effect of propofol. *Epilepsia*, *53*(10), 1799–1809. https://doi.org/10.1111/j.1528-1167.2012.03650.x

Zijlmans, M., Worrell, G. A., Dümpelmann, M., Stieglitz, T., Barborica, A., Heers, M., … Le Van Quyen, M. (2017). How to record high-frequency oscillations in epilepsy: A practical guideline. *Epilepsia*, *58*(8), 1305–1315. https://doi.org/10.1111/epi.13814